VNIVERSITAT DE VALÈNCIA

Facultad de Química

Departamento de Química Orgánica

Programa de Doctorado en Química

con Mención de Excelencia

Synthesis of novel fluorinated building blocks and α-helix peptidomimetics

Tesis Doctoral

Daniel Mark Sedgwick

Dirigida por:

Prof. Santos Fustero Lardiés

Dr. Pablo Barrio Fernández

Valencia

Septiembre 2018

D. Santos Fustero Lardiés, Catedrático de Química Orgánica de la Universitat de València, y **D. Pablo Barrio Fernández**, Investigador Doctor Senior de la Universitat de València,

CERTIFICAN:

Que la presente Tesis Doctoral, titulada "**Synthesis of novel fluorinated building blocks and α-helix peptidomimetics**", ha sido realizada bajo su dirección en el Departamento de Química Orgánica de la Universitat de València, por el licenciado en Química **D. Daniel Mark Sedgwick**, y autorizan su presentación para que sea calificada como Tesis Doctoral.

Valencia, Septiembre 2018

Fdo. Santos Fustero Lardiés

Fdo. Pablo Barrio Fernández

List of abbreviations

[M]	metal complex
[O]	oxidant
Å	ångströms
Ac	acetyl
AIBN	azobisisobutyronitrile
AIDS	acquired immunodeficiency syndrome
aq	aqueous
Ar	aryl
atm	atmospheres
AZT	azidothymidine
$B_2(pin)_2$	bis(pinacolato)diboron
Bn	benzyl
Boc	*tert*-butyloxycarbonyl
br	broad
Bu	butyl
Bz	benzoyl
ca.	*circa*
CAN	cerium ammonium nitrate
cat.	catalytic amount
CC_{50}	half maximal cytotoxic concentration
CM	cross metathesis
CNS	central nervous system
COD	cyclooctadiene
Conv.	conversion
Cy	cyclohexyl
δ	chemical shift
d	doublet
dba	dibenzylideneacetone
DBU	1,8-diazobicyclo[5.4.0]undec-7-ene
DCE	1,2-dichloroethane
DCM	dichloromethane
DFT	density functional theory
DHQ	dihydroquinine
DHQD	dihydroquinidine
DIBAL-H	diisobutyl aluminium hydride
DMAP	4-dimethylaminopyridine
DME	1,2-dimethoxyethane
DMF	*N,N*-dimethyl formamide
DMPU	*N,N'*-dimethylpropyleneurea
DMSO	dimethyl sulfoxide
DNA	deoxyribonucleic acid
DOS	diversity-oriented synthesis
dppf	1,1'-bis(diphenylphosphino)-ferrocene
dr	diastereomeric ratio
DTBM	3,5-di-*tert*-butyl-4-methoxy phenyl
e.g.	for example
EC_{50}	half maximal effective concentration
ee	enantiomeric excess
equiv	equivalents
er	enantiomeric ratio
ESI	electrospray ionisation
Et	ethyl
EWG	electron-withdrawing group
FDA	food and drug administration
FG	functional group
g	grams
gem	geminal
h	hours
HAART	highly active antiretroviral therapy
HBTU	hexafluorophosphate benzotriazole tetramethyl uronium

Hept	Heptyl
HIV	human immunodeficiency virus
HMDS	hexamethyldisilazane
HMPA	hexamethylphosphoramide
HMTA	hexamethylenetetramine
HPLC	high-performance liquid chromatography
HRMS	high-resolution mass spectrometry
hv	photon of light
Hz	Hertz
i.e.	in other words
***i*-Pr**	isopropyl
IC_{50}	half maximal inhibitory concentration
IR	infrared
L	ligand
LA	lewis acid
LDA	lithium diisopropylamide
LRMS	low-resolution mass spectrometry
m	*meta*
M	molar
m	multiplet
***m*-CPBA**	*meta*-chloroperoxybenzoic acid
MALDI	matrix-assisted laser desorption/ionisation
Me	methyl
mg	milligram
min	minutes
mmol	millimole
ml	millilitre
mp	melting point
Ms	mesyl, methanesulfonyl
MS	molecular sieves
MTBE	methyl *tert*-butyl ether
MTIP	myosin-tail domain interacting protein
mw	microwave irradiation
MyoA	myosin A
N	normal
NBS	*N*-bromosuccinimide
NFSI	*N*-fluorobenzenesulfonimide
NME	new molecular entity
NMO	*N*-methylmorpholine *N*-oxide
NMR	nuclear magnetic resonance
NNRTI	non-nucleoside reverse transcriptase inhibitor
NRTI	nucleoside reverse transcriptase inhibitor
NtRTI	nucleotide reverse transcriptase inhibitor
Nu	nucleophile
o	*ortho*
°C	degrees Celsius
p	*para*
PCC	pyridinium chlorochromate
PDB	protein database
PET	positron emission tomography
Ph	phenyl
PMB	*para*-methoxybenzyl
PMP	*para*-methoxyphenyl
ppm	parts per million
Py	pyridine
q	quartet
QTOF	quadrupole time-of-flight

r.t.	room temperature
RCEYM	ring-closing enyne metathesis
RCM	ring-closing metathesis
Rev	regulator of expression of virion proteins
R_F	fluorine-containing substituent
R_f	retention factor
RNA	ribonucleic acid
RRE	Rev response element
R_T	retention time
s	singlet
sat	saturated
SM	starting material
t	triplet
***t*-Bu**	*tert*-butyl
TBAF	tetrabutylammonium fluoride
TBS	*tert*-butyl dimethyl silyl
Tf	trifluoromethanesulfonyl
TFA	trifluoroacetic acid
THF	tetrahydrofuran
TLC	thin-layer chromatography
TMS	trimethyl silyl
TOCSY	total correlation spectroscopy
TOF	time of flight
Tol	*p*-tolyl
Ts	tosyl, toluenesulfonyl
TS	transition state
TXCA	trihaloisocyanuric acid
UV	ultraviolet
WHO	world health organisation

Index

0.0. Abstract.

At its heart, the present PhD thesis is based on the premise of two important areas in modern organic chemistry: firstly, the development of new methodologies to incorporate fluorine into organic molecules; and secondly, the design and synthesis of small molecules with high therapeutic potential (Scheme 0.0).

The work presented in the first three chapters will therefore focus on the incorporation of fluorine into organic molecules and the synthesis of fluorinated building blocks. In each chapter, we aim to obtain biologically relevant small molecules containing fluorine atoms or fluorinated groupings. The introduction of fluorine is a commonly used method in drug discovery to fine-tune the properties of drug candidates and therefore, given the scarcity of fluorine-containing molecules in natural sources, new synthetic methods towards new fluorinated scaffolds represent an important goal for organic chemists. On the other hand, the fourth and final chapter will explore the possibilities of novel *p*-terphenyl structures as peptidomimetics to exploit important biological targets.

In this context, the present PhD thesis will have the following structure.

Chapter 1. *Synthesis of enantioenriched 1-amino-1,2-dihydronaphthalenes.*

This work builds upon past efforts in our research group in the area of diversity oriented synthesis, utilising *ortho*-bromobenzaldehyde as a common precursor. In this study, we will synthesise an unprecedented fluorinated scaffold containing a trifluoromethyl group, during which we will explore the effect of fluorinated groups during the ring-closing metathesis reaction (RCM).

Chapter 2. *Synthesis of 1,2-fluorohydrins via 1,2-difunctionalisation of olefins.*

This chapter focuses on simplicity and practicality. Fluorohydrins are an important class of fluorinated organic molecules; fludrocortisone was the first fluorinated drug to obtain FDA approval. Their synthesis has traditionally relied on the opening of epoxides, but in this chapter we will bypass this intermediate to form fluorohydrins directly from olefins, one of the most widely available and inexpensive classes of chemical.

Chapter 3. *Synthesis and reactivity of β-fluorovinyl sulfones.*

In this chapter we will develop methodologies for the stereodivergent synthesis of both (*E*)- and (*Z*)-β-fluorovinyl sulfones, a scarcely studied structure with potential as a fluorinated building block. We will also explore the reactivity of these structures.

Chapter 4. *Synthesis and biological evaluation of novel p-terphenyls as α-helix mimetics.*

The work described in this chapter is part of a long-term project within our research group, in collaboration with J. Gallego (UCV) and J. Alcamí (ISCIII). We found that *p*-terphenyls can be used to mimic the α-helix in the Rev protein of HIV-1. In this way, these small molecules are able to inhibit the replication of the virus. This chapter will build upon this work, exploring different structures and substitution patterns in order to learn more about the structure-activity relationship of these compounds, as well as designing a new derivative to tackle a protein-protein interaction that is key in the parasitic cycle of malaria.

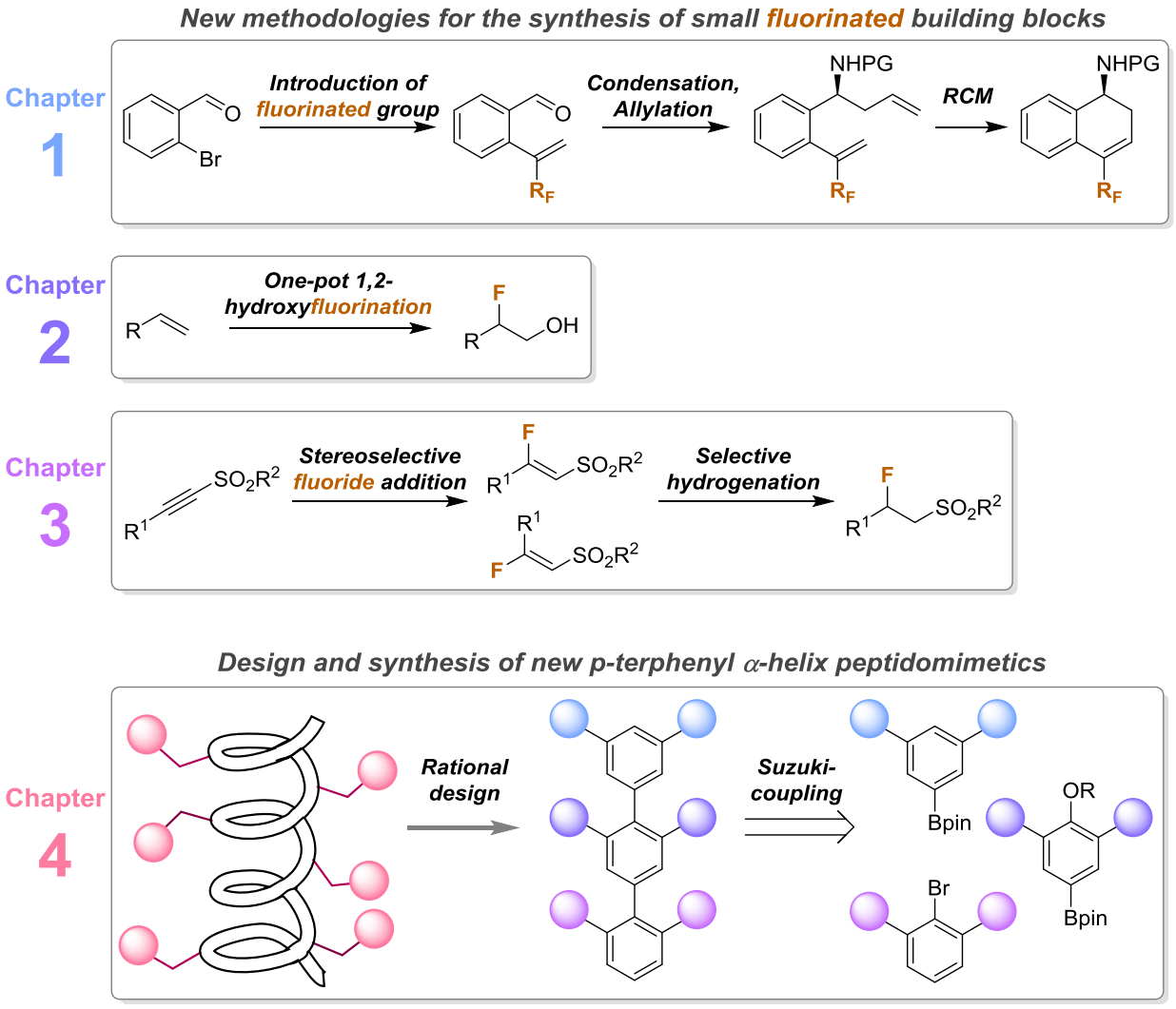

Scheme 0.0. General objectives.

0.0. Resum.

La present tesi doctoral està basada en dues àrees importants de la química orgánica moderna: en primer lloc, el desenvolupament de noves metodologies per la incorporació de flúor a molècules orgàniques; i en segon lloc, el disseny i síntesi de molècules menudes amb un gran potencial terapèutic (Esquema 0.0).

El treball presentat en els capítols 1 al 3 s'enfocarà a la incorporació del flúor en molècules orgàniques i la síntesi de *building blocks* fluorats. Cada capítol té com a objectiu l'obtenció d'una classe de molècula orgánica fluorada diferent. La introducció del flúor és un mètode utilitzat sovint per modificar les propietats de candidats a nous fàrmacs. Per tant, i degut a la manca de fonts naturals que continguen àtoms de flúor, el desenvolupament de noves metodologies per l'obtenció d'estructures fluorades representa una meta important per als químics orgànics. D'una altra banda, al quart capítol s'exploraran les possibilitats de noves estructures terfeníliques com peptidomimètics que interaccionen amb dianes biològiques importants.

En aquest context, el present document tindrà la següent estructura.

0.0. Resumen.

La presente tesis doctoral está basada en dos áreas importantes de la química orgánica moderna: en primer lugar, el desarrollo de nuevas metodologías para la incorporación de flúor en moléculas orgánicas; y en segundo lugar, el diseño y síntesis de moléculas pequeñas con un gran potencial terapéutico (Esquema 0.0).

El trabajo presentado en los capítulos 1 al 3 se basará en la incorporación del flúor en moléculas orgánicas y la síntesis de *building blocks* fluorados. Cada capítulo tiene como objetivo la síntesis de una clase de molécula orgánica fluorada diferente. La introducción del flúor es un método utilizado habitualmente para modificar las propiedades de candidatos de nuevos fármacos. Por tanto, y dada la escasez de fuentes naturales que contienen átomos de flúor, el desarrollo de nuevas metodologías para la obtención de estructuras fluoradas representa una meta importante para los químicos orgánicos. Por otro lado, en el cuarto capítulo se explorarán las posibilidades de nuevas estructuras terfenílicas como peptidomiméticos que interactúan con dianas biológicas importantes.

En este contexto, el presente documento tendrá la siguiente estructura.

Capítol 1. *Síntesi d'1-amino-1,2-dihidronaftalens enantioenriquits.*

Aquest treball és una extensió d'esforços previs del nostre grup d'investigació a l'àrea de la síntesi orientada a la diversitat, a la qual s'utilitza *orto*-brombenzaldehíd com a precursor comú. Més específicament, en aquest estudi se sintetitzaran molècules fluorades sense precedent a la literatura química, i a més s'exploraran els efectes dels grups fluorats durant les reaccions de metàtesi de tancament d'anell.

Capítol 2. *Síntesi de 1,2-fluorhidrines mitjançant la 1,2-difunctionalització d'olefines.*

Aquest capítol té com a objectiu la practicitat. Les fluorhidrines representen una classe de compostos orgànics importants; la Fludrocortisona va ser el primer fàrmac fluorat aprovat per la FDA. Tradicionalment, la síntesi d'aquesta estructura s'ha basat en l'obertura d'epòxids, però en aquest treball es tindrà com a objectiu l'obtenció de l'estructura desitjada directament a partir d'olefines, una de les classes de compostos químics més abundants i barats.

Capítol 3. *Síntesi i reactivitat de β-fluorovinilsulfones.*

Dins d'aquest capítol es desenvoluparan metodologies per a la síntesi estereodivergent d'(*E*)- i (*Z*)-β-fluorovinilsulfones, una estructura poc estudiada amb potencial com a

Capítulo 1. *Síntesis de 1-amino-1,2-dihidronaftalenos enantioenriquecidos.*

Este trabajo es una extensión de esfuerzos previos en nuestro grupo de investigación en el área de la síntesis orientada a la diversidad, en la que se utiliza el *orto*-bromobenzaldehído como precursor común. Más específicamente, este estudio se centrará en la síntesis de moléculas fluoradas inéditas en la literatura química, y además se explorarán los efectos de los grupos fluorados durante las reacciones de metátesis de cierre de anillo.

Capítulo 2. *Síntesis de 1,2-fluorhidrinas mediante 1,2-difuncionalización de olefinas.*

Este capítulo tiene como meta la practicidad. Las fluorhidrinas representan una clase de compuestos orgánicos importantes; la Fludrocortisona fue el primero fármaco fluorado aprobado por la FDA. Tradicionalmente, la síntesis de esta estructura ha sido dominada por la apertura de epóxidos, pero en este estudio se tendrá como objetivo la obtención del producto deseado directamente a partir de olefinas, una de las clases de compuestos químicos más abundantes y baratos.

Capítulo 3. *Síntesis y reactividad de β-fluorovinilsulfonas.*

Dentro de este capítulo se desarrollarán métodos para la síntesis estereodivergente de (*E*)- y (*Z*)-β-fluorovinilsulfonas, una estructura muy poca estudiada con potencial como

precursor de molècules fluorades més complexes. A més a més, s'explorarà la reactivitat d'aquests nous derivats.

Capítol 4. *Síntesi i avaluació biológica de nous* p-*terfenils com mimètics de proteïnes amb forma d'α-hèlix.*

El treball descrit a aquest capítol forma part d'un projecte de llarg termini dins del nostre grup d'investigació, en col·laboració amb els profesors J. Gallego (UCV) i J. Alcamí (ISCIII). S'ha descobert que els *p*-terfenils es poden utilitzar per mimetitzar l'α-hèlix de la proteína Rev del VIH-1. D'aquesta manera els terfenils són capaços d'inhibir la replicació del virus. Aquest capítol aprofundeix en l'esmentat estudi, i explora noves estructures i patrons de substitució per tal d'aclarir més quant a la relació estructura-activitat d'aquests derivats. A més a més, es durà a terme la síntesi d'un nou terfenil amb la fi d'inhibir una interacció proteïna-proteïna clau en el cicle vital de la malaltia parasitària de la malària.

precursor de moléculas fluoradas más complejas. Además, se explorará la reactividad de estos nuevos derivados.

Capítulo 4. *Síntesis y evaluación biológica de nuevos* p-*terfenilos como miméticos de proteínas con forma de α-hélice.*

El trabajo descrito en este capítulo forma parte de un proyecto de largo plazo dentro de nuestro grupo de investigación, en colaboración con los profesores J. Gallego (UCV) y J. Alcamí (ISCIII). Se ha descubierto que los *p*-terfenilos se pueden utilizar para mimetizar la α-hélice de la proteína Rev del VIH-1. De esta manera, los terfenilos son capaces de inhibir la replicación del virus. Este capítulo profundiza en dicho estudio, y explora nuevas estructuras y patrones de sustitución para esclarecer más acerca de la relación estructura-actividad de estos derivados. Además, se llevará a cabo la síntesis de un nuevo terfenilo con el fin de inhibir una interacción proteína-proteína clave en el ciclo vital de la enfermedad parasitaria de la malaria.

Chapter 1

Synthesis of fluorinated benzo-fused bicyclic homoallylic amines

1.0. Objectives.

Given the background of our research group in the asymmetric allylation of *tert*-butanesulfinyl imines and the synthesis of di- and tetrahydronaphthalene scaffolds, in this work we aimed to study the effects of different fluorinated groups in this synthetic route.

This would include the synthesis of a variety of benzaldehyde-derived sulfinimines with a fluorinated olefin in the *ortho* position, which would serve as a handle to then carry out the ring-closing metathesis reaction. The main fluorinated group on which this chapter will focus is the trifluoromethyl group.

Given the scarcity of this class of fluorinated dihydronaphthalenes in the literature, and the importance of both fluorine chemistry and the dihydronaphthalene skeleton in industrial settings, the resulting enantioenriched 1-amino-1,2-dihydronaphthalenes could represent interesting targets.

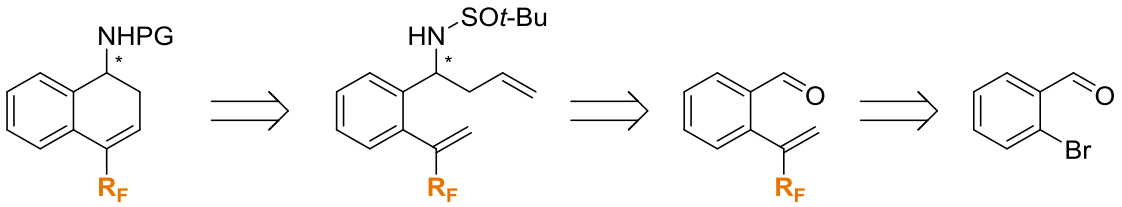

1.1. Introduction.

1.1.1. The use of N-tert-butanesulfinyl imines in the synthesis of enantioenriched homoallylic amines.

Asymmetric synthesis has become a fundamental area of organic chemistry in recent years since the realisation that chemistry is three-dimensional, just like the world around us.[1] Although the concept of chirality has been understood for more than a century, its underlying importance in many fields was not fully appreciated until the infamous thalidomide disaster in the 1960s.[2] Of course, in this specific example the teratogenic side-effects could not have been avoided even administering the enantiopure drug due to racemisation *in vivo*. However, we as chemists are now aware of the drastic differences in biological activity that a pair of enantiomers can have, and there are now many more restrictions and requirements that new drugs must pass in order to gain approval.

This has led to a global research effort to develop methods of obtaining a single enantiomer in organic synthesis; so-called asymmetric synthesis. There are currently several viable ways to achieve this: 1) use of chiral catalysts; 2) use of diastereomeric resolving agents to preferentially crystallise one enantiomer over the other; 3) use of the "chiral pool"; and the most relevant to this work, 4) use of chiral auxiliaries.

The use of chiral auxiliaries depends on the facile addition of a chiral group, which can then be used to infer chirality into a different part of the molecule, and its subsequent removal. This essentially allows the introduction of a wide variety of functional groups in an enantioselective manner, without leaving a trace on the final product.[3]

One such example is the use of *tert*-butylsulfinamide **1.1**, a chiral auxiliary developed by Ellman and co-workers in 1997[4] that has seen increased use in the past decade for a number of reasons: its simple synthesis has permitted wide commercial availability at accessible prices; easy preparation of versatile *N-tert*-butanesulfinyl imines **1.2** *via* condensation of **1.1** with the corresponding aldehyde or ketone (Scheme 1.1); the formal positive charge on the sulphur atom augments the electrophilicity of the resulting imines, increasing their reactivity towards a range of nucleophiles; the *N-tert*-butanesulfinyl group is a potent directing group, due to its bulk and coordinating ability; and lastly, the sulfinyl moiety can be quantitatively removed in acidic conditions. These chiral imine intermediates have been used to

[1] U. Meierhenrich, *Amino acids and the Asymmetry of Life,* Springer, Berlin, 2008.
[2] S. W. Smith, *Toxicol. Sci.*, 2009, **110**, 4-30.
[3] Y. Gnas and F. Glorius, *Synthesis*, 2006, **12**, 1899-1930.
[4] G. Liu, D. A. Cogan and J. A. Ellman, *J. Am. Chem. Soc.*, 1997, **119**, 9913-9914.

synthesise a wide range of enantioenriched amines, which represent important motifs in the pharmaceutical and agrochemical industries, as well as in natural product synthesis and biochemical research.

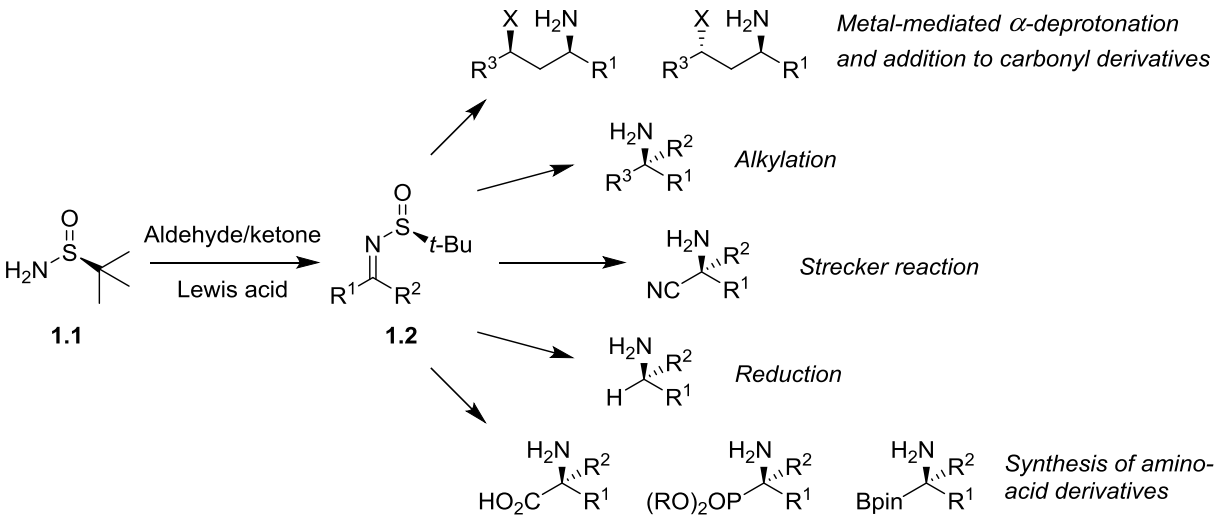

Scheme 1.1. The use of *tert*-butylsulfinamide in the asymmetric synthesis of amines.

Despite the wide variety of nucleophiles that have been successfully added to sulfinyl imines **1.2**,[5] this chapter will focus specifically on the 1,2-allylation of *N-tert*-butanesulfinyl imines. The first examples were disclosed by Ellman *et al.* in 1999 in a report dealing with the addition of organolithium and Grignard reagents to *N-tert*-butanesulfinyl aldimines and ketimines, including the addition of allylmagnesium bromide **1.3**; the addition took place with high yields and diastereoselectivities using DCM at -78 °C (Scheme 1.2).[6]

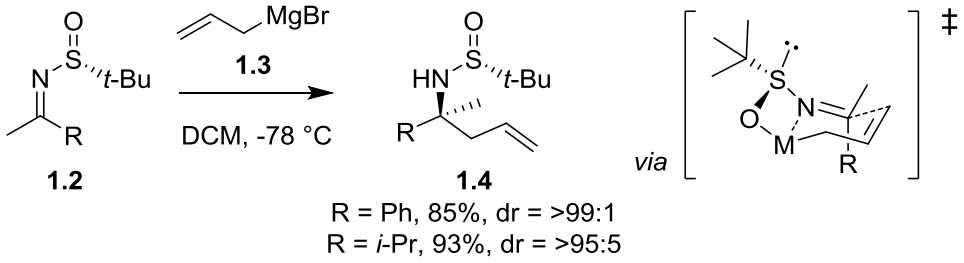

Scheme 1.2. The first addition of allylmagnesium bromide 1.3 to *N-tert*-butanesulfinyl ketimines.

[5] M. T. Robak, M. A. Herbage and J. A. Ellman, *Chem. Rev.*, 2010, **110**, 3600-3740.
[6] D. A. Cogan, G. Liu and J. Ellman, *Tetrahedron*, 1999, **55**, 8883-8904.

Since then a plethora of reports have surfaced utilising variants of the allylation reaction: in the asymmetric synthesis of natural products[7] and biologically relevant compounds;[8] with different metals such as boron,[9] zinc,[7d, 10] and indium;[11] and even in cascade reactions.[12]

In terms of the mechanism, the results obtained by Ellman *et al.* in the above example support a closed chair-like transition state (Scheme 1.2), such as those proposed by Hua and co-workers in their study with the related *N*-*p*-toluenesulfinyl imines.[13] In this way, the metal centre interacts with both the nitrogen atom of the imine and the oxygen atom of the sulfinyl group, activating the imine as well as forcing the sulfinyl group into a rigid conformation, thereby improving the directing ability of the bulky *tert*-butyl substituent. The superior results observed in the allylation reaction compared to the addition of other organometallic species have been attributed to the formation of this rigid six-membered transition state. This was later reinforced by studies carried out by Xu, Lin and co-workers, who observed different stereochemistry in the products depending on the conditions used in the reaction (Table 1.1).[10] These authors used zinc as the metal of choice, stating that the higher reactivity compared with indium-based reagents allowed milder reaction conditions—the reactions were all carried out at room temperature.

[7] a) M. B. Bertrand and J. P. Wolfe, *Org. Lett.*, 2006, **8**, 2353-2356. b) Y. Nishikawa, M. Kitajima, N. Kogure and H. Takayama, *Tetrahedron*, 2009, **65**, 1608-1617. c) R. S. Grainger and E. J. Welsh, *Angew. Chem. Int. Ed.*, 2007, **46**, 5377-5380. d) M. Liu, X.-W. Sun, M.-H. Xu and G.-Q. Lin, *Chem. Eur. J.*, 2009, **15**, 10217-10224.

[8] X.-Z. Wang and T. R. Burke Jr., *Synlett*, 2004, **3**, 0469-0472.

[9] a) S.-W. Li and R. A. Batey, *Chem. Commun.*, 2004, 1382-1383. b) Y.-S. Zhao, Q. Liu, P. Tian, J.-C. Tao and G.-Q. Lin, *Org. Biomol. Chem.*, 2015, **13**, 4174-4178.

[10] X.-W. Sun, M.-H. Xu and G.-Q. Lin, *Org. Lett.*, 2006, **8**, 4979-4982.

[11] a) F. Foubelo and M. Yus, *Tetrahedron: Asymmetry*, 2004, **15**, 3823-3825. b) X.-W. Sun, M. Liu, M.-H. Xu and G.-Q. Lin, *Org. Lett.*, 2008, **10**, 1259-1262. c) J. C. González-Gómez, F. Foubelo and M. Yus, *Synlett*, 2008, **18**, 2777-2780. d) M. Medjahdi, J. C. González-Gómez, F. Foubelo and M. Yus, *J. Org. Chem.*, 2009, **74**, 7859-7865.

[12] a) I. R. Cooper, R. Grigg, W.-S. MacLachlan, M. Thornton-Pett and V. Sridharan, *Chem. Commun.*, 2002, 1372-1373. b) I. R. Cooper, R. Grigg, M.-J. Hardie, W.-S. MacLachlan, M. Thornton-Pett, V. Sridharan and W. A. Thomas, *Tetrahedron Lett.*, 2003, **44**, 2283-2285.

[13] D. H. Hua, S. W. Miao, J. S. Chen and S. Iguchi, *J. Org. Chem*., 1991, **56**, 4-6.

Table 1.1. Condition-controlled stereoselectivity inversion.

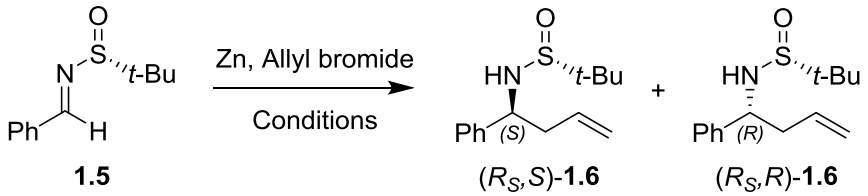

1.5 (R_S,S)-**1.6** (R_S,R)-**1.6**

Entry	Solvent	Additive (equiv)	Time (h)	Yield **1.6** (%)	dr
1	THF	None	0.5	99	90:10
2	THF	$In(OTf)_3$ (1.3)	10	93	**98:2**
3	THF	HMPA (2)	1	99	53:47
4	HMPA	None	1	99	26:74
5	HMPA	H_2O (10 µL)	12	97	**1:99**

Standard reaction conditions: Reactions carried out with 0.25 mmol **1.5** and 0.5 mmol Zn and allyl bromide at r.t. in 5 ml solvent.

The result obtained with THF as a solvent and no additive (entry 1, Table 1.1) is also consistent with *si*-face allylation—resulting in the (*S*)-amine product—through the closed transition state described by Ellman and Hua (Scheme 1.3, **TS-1**). When indium(III) triflate is used as an additive, however, the authors proposed a slightly different transition state (Scheme 1.3, **TS-2**). In this case, the addition of a stronger Lewis acid disrupts the six-membered transition state and forces it open. Nevertheless, the additive binds the sulfinyl oxygen and the imine nitrogen atoms just as in TS-1, once again promoting *si*-face addition. On the other hand, when hexamethylphosphoramide (HMPA) was used as a solvent, the opposite diastereoisomer was obtained. HMPA is strongly coordinating due to the highly polarised P=O bond, and as such is thought to interrupt the coordination of the sulfinyl group to the zinc metal centre by solvating the zinc cation (Scheme 1.3, **TS-3**). With no Lewis acid present, the uncoordinated sulfinyl group would adopt a synperiplanar conformation, this time promoting *re*-face allylation and resulting in the (*R*)-amine product.

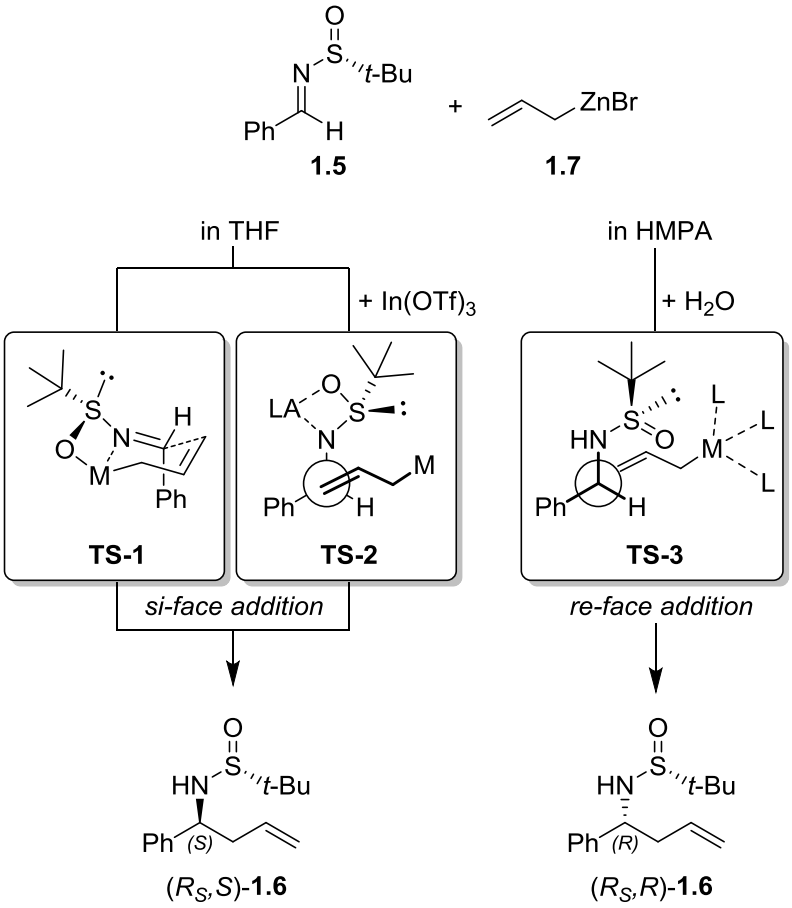

Scheme 1.3. Transition states involved in the stereoselectivity inversion observed by Xu, Lin *et al.*[10]

A similar study was published in 2009 by the same authors, in which the group studied the asymmetric benzoyloxyallylation of *N*-*tert*-butanesulfinyl imines and used this as the key step in the synthesis of natural product (-)-Cytoxazone.[7d]

1.1.2. The ring-closing metathesis reaction and the use of fluorinated olefins.

The term "olefin metathesis" was first used by Calderon, and comes from the Greek word μεταθεση meaning "change of position", reflecting exactly the way a metathesis reaction works; the double bond effectively switches between pairs of carbon atoms during the reaction (Figure 1.1).[14]

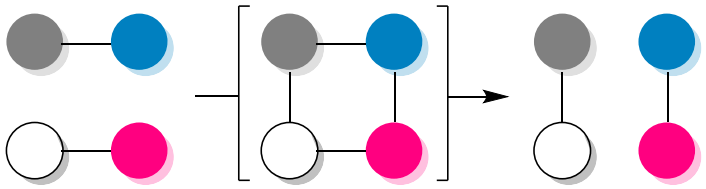

Figure 1.1. A simple view of metathesis reactions.

The reaction was discovered accidentally in 1955 by a DuPont research group,[15] but it was not until later that the reaction took hold as a useful transformation in a synthetic chemist's toolbox due to the impractical catalysts involved: early catalysts based on nickel, tin or molybdenum displaying this activity were neither bench-stable nor viable for large-scale synthesis or commercialisation. Robert Grubbs solved these problems using ruthenium-based catalysts in the 1990s, and was later awarded the Nobel Prize in 2005—along with Yves Chauvin and Richard Schrock—for "the development of the metathesis method in organic synthesis".[16] The first-generation Grubbs catalyst was first described in 1995. The second-generation catalyst, developed in 1999, boasts improved stability towards air and moisture, due to the replacement of one tricyclohexylphosphine ligand for an *N*-heterocyclic carbene. Also developed in 1999 were the Hoveyda-Grubbs catalysts, which incorporated an *ortho*-isopropoxy group into the benzylidene ligand, replacing the second phosphine ligand. These catalysts offer greater thermal stability, despite being slower to initiate the reaction (Figure 1.2).[17]

[14] N. Calderon, H. Y. Chen and K. W. Scott, *Tetrahedron*, 1967, **34**, 3327-3329.

[15] a) A. W. Anderson and N. G. Merckling, U. S. Patent 2721198, October 18, 1955. b) W. L. Truett, D. R. Johnson, I. M. Robinson and B. A. Montague, *J. Am. Chem. Soc.*, 1960, **82**, 2337-2340.

[16] a) Y. Chauvin, *Angew. Chem. Int. Ed.*, 2006, **45**, 3741-3747. b) R. R. Schrock, *Angew. Chem. Int. Ed.*, 2006, **45**, 3748-3759. c) R. H. Grubbs, *Angew. Chem. Int. Ed.*, 2006, **45**, 3760-3765.

[17] For an extensive review on metathesis catalysts, see: G. C. Vougioukalakis and R. H. Grubbs, *Chem. Rev.*, 2010, **110**, 1746-1787.

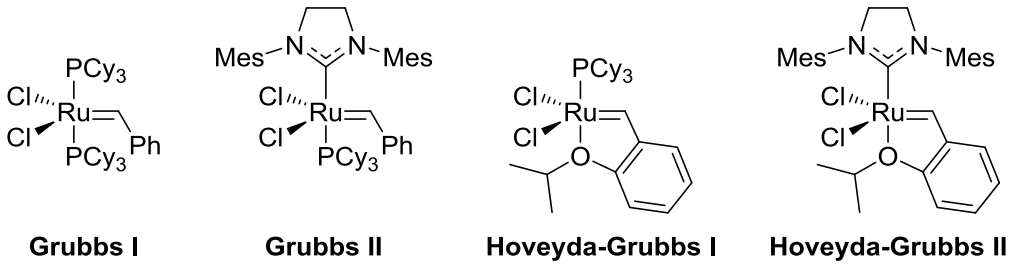

Figure 1.2. Selected ruthenium-based metathesis catalysts.

In the past 20 years, since the mass commercialisation of these catalysts, metathesis reactions have become fundamental to synthetic chemists. Several classes of the reaction have been described: a) ring-opening metathesis (ROM); b) ring-opening metathesis polymerisation (ROMP); c) ring-closing metathesis (RCM); d) cross metathesis (CM); e) acyclic diene metathesis (ADMET); and other variations including alkynes (Scheme 1.4).

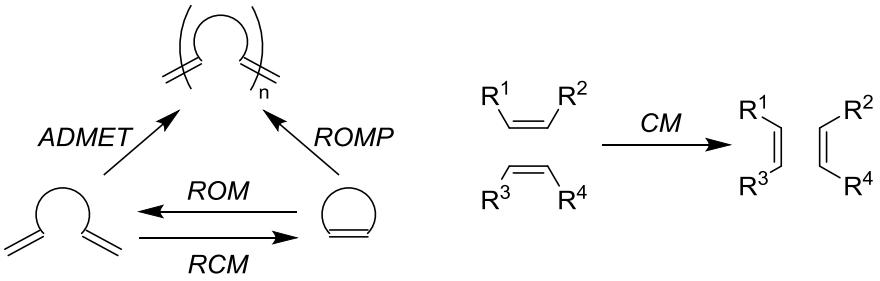

Scheme 1.4. Summary of metathesis reactions.

In terms of this chapter, the most important of these is ring-closing metathesis. RCM reactions have gained popularity due to their potential to provide easy access to medium and large-sized rings,[18] as well as heterocycles,[19] motifs that feature heavily in natural products, pharmaceuticals, and medically relevant compounds. For example, in 2005 a group from Boehringer Ingelheim described the scale-up of the synthesis of 15-membered macrocyclic protease inhibitor **1.9** active against hepatitis C, in which they obtained an 83% yield and 90% purity on a 400 kg scale (Scheme 1.5).[20]

[18] L. Yet, *Chem. Rev.*, 2000, **100**, 2963-3007.
[19] a) A. Deiters and S. F. Martin, *Chem. Rev.*, 2004, **104**, 2199-2238. b) I. Nakamura and Y. Yamamoto, *Chem. Rev.*, 2004, **104**, 2127-2198.
[20] T. Nicola, M. Brenner, K. Donsbach and P. Kreye, *Org. Process Res. Dev.*, 2005, **27**, 513-515.

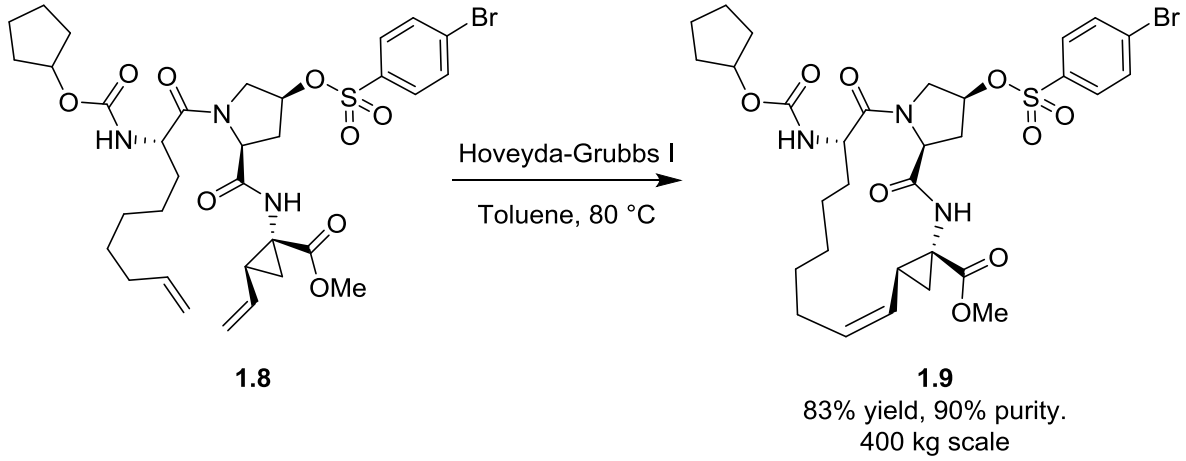

Scheme 1.5. Industrial application of the ring-closing metathesis reaction.

On a more relevant note, various forms of metathesis reaction have also been applied successfully to fluorinated substrates containing fluorinated groups both away from and directly attached to the olefin in question.[21] The first examples were described just a few months apart in 2003-2004 by the groups of Brown,[22] Haufe,[23] and Rutjes.[24] In the vast majority of cases, the reactions required high temperatures in order to take place, immediately differentiating them from analogous reactions involving non-fluorinated substrates.

Brown and co-workers described the synthesis of a range of fluorinated cyclic sulfamides **1.11** that bear a resemblance to known HIV protease inhibitors, obtaining high yields in all cases (Scheme 1.6).

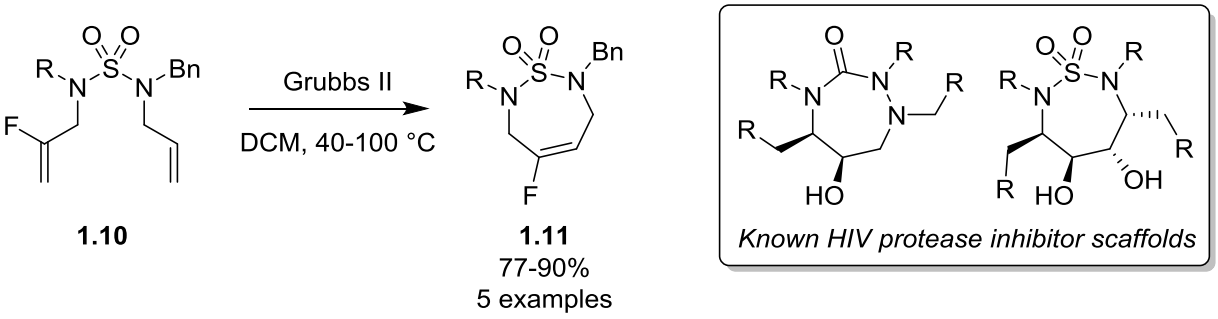

Scheme 1.6. RCM strategy to synthesise HIV protease-like fluoroalkene containing sulfamides.

[21] For an extensive review on metathesis reactions using fluorinated substrates, see: S. Fustero, A. Simón-Fuentes, P. Barrio and G. Haufe, *Chem. Rev.*, 2015, **115**, 871-930.
[22] S. S. Salim, R. K. Bellingham, V. Satcharoen and R. C. D. Brown, *Org. Lett.*, 2003, **5**, 3403-3406.
[23] M. Marhold, A. Buer, H. Hiemstra, J. H. van Maarseveen and G. Haufe, *Tetrahedron Lett.*, 2004, **45**, 57-60.
[24] V. de Matteis, F. L. van Delft, R. de Gelder, J. Tiebes and F. P. J. T. Rutjes, *Tetrahedron Lett.*, 2004, 959-963.

Haufe *et al.* found that fluorinated acrylate derivatives **1.12** and related compounds were the most suitable substrates due to the more electron-deficient nature of the double bond. The authors therefore focused their efforts on the synthesis of fluorinated unsaturated lactams **1.13** (Scheme 1.7).

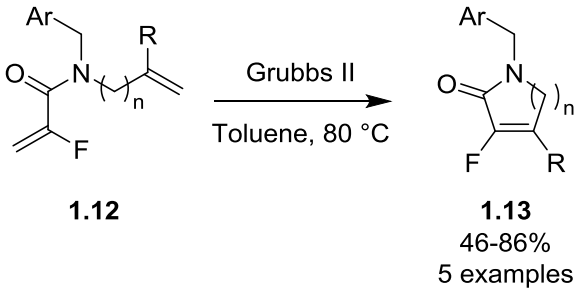

1.12 **1.13**
46-86%
5 examples

For Ar = Ph, R = H, n = 1 reaction occurred at r.t.
No reaction occurred when n = 3, 4.

Scheme 1.7. Synthesis of fluorinated γ- and δ-lactams *via* RCM of fluoroalkenes.

Rutjes and co-workers, on the other hand, explored a more diverse scope of the reaction, including trifluoromethylated olefins. Several interesting observations arise when comparing the results of the three reports, in that many substrates that were unsuccessful for trifluoromethyl-containing olefins were in fact successful for fluoroolefins, and *vice versa*. Various unsaturated chloro- and trifluoromethylated five-membered rings could be obtained in high yields with this strategy, whereas the synthesis of trifluoromethylated unsaturated γ-lactams was unsuccessful; the opposite was true for the related monofluorinated substrates. Similarly, the synthesis of trifluoromethylated piperidines failed using this method, whilst their monofluorinated analogues could be obtained in high yields (Scheme 1.8). However, this could be due to the incompatibility of the more basic benzyl protecting group with the catalyst, since a later publication by Rutjes detailed the successful synthesis of other trifluoromethylated piperidines with less basic nitrogen functionalities.[25]

[25] V. de Matteis, F. L. van Delft, H. Jakobi, S. Lindell, J. Tiebes and F. P. J. T. Rutjes, *J. Org. Chem.*, 2006, **71**, 7527-7532.

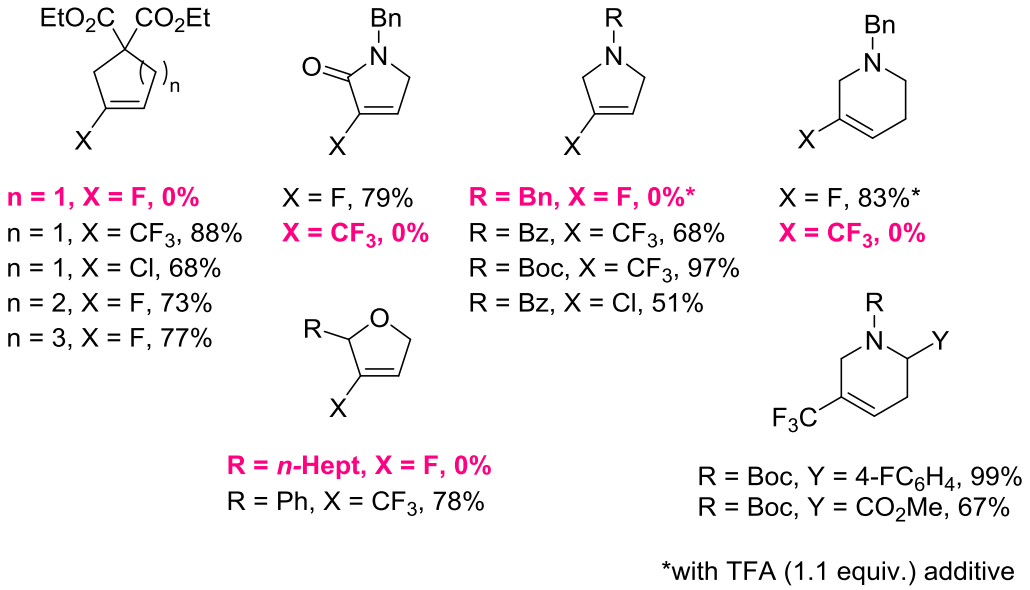

Scheme 1.8. A selection of results from Brown,[22] Haufe,[23] and Rutjes[24, 25] showcasing the differences in reactivity between trifluoromethyl and fluoroalkenes.

The RCM reaction has also seen other advances in recent years: Haufe *et al.* later applied this methodology to the synthesis of a selection of bicyclic lactams and lactones;[26] and Marquez *et al.* applied it to the synthesis of fluorinated pyrroles;[27] and Couve-Bonnaire *et al.* applied the reaction to the synthesis of fluorinated heterocycles including an oxaza bond.[28]

[26] M. Marhold, C. Stillig, R. Fröhlich and G. Haufe, *Chem. Eur. J.*, 2014, **20**, 5777-5785.
[27] T. J. Cogswell, C. S. Donald and R. Marquez, *Org. Biomol. Chem.*, 2016, **14**, 183-190.
[28] D. Guérin, I. Dez, A.-C. Gaumont, X. Pannecoucke and S. Couve-Bonnaire, *C. R. Chimie*, 2018, **21**, 740-748.

1.1.3. The asymmetric allylation/RCM strategy towards enantioenriched cyclic homoallylic amines.

In 2007, Grainger and Welsh described the synthesis of a natural product, (-)-Aphanorphine **1.21**,[7c] using the allylation of *N*-*tert*-butanesulfinyl imines as the key step to introduce the desired chiral information. In this example, the authors used an interesting strategy involving the asymmetric allylation followed by a ring-closing metathesis (RCM) reaction between the newly added allyl group and a second double bond that was already present in the substrate (Scheme 1.9).

The authors achieved an elegant synthesis of the natural product, starting with the condensation of (*R*)-*tert*-butylsulfinamide (*R*)-**1.1** with the simple aldehyde **1.14** to form the corresponding imine **1.15** in a high yield. Following this, the authors added Grignard reagent **1.16** to the imine, affording the resulting enantioenriched sulfinylamine **1.17**. Here, the authors state that they were unable to separate the diastereoisomers and so continued with the synthesis using the mixture. After *N*-methylation, the authors carried out a RCM reaction to construct the six-membered ring present in the final product. Acid-catalysed methanolysis of the sulfinyl protecting group gave the free amine **1.20**, which could be recrystallised to furnish the enantiomerically pure (*R*)-**1.20**. From there, the desired product **1.21** was synthesised in 9 more steps, giving a total of 15 steps.

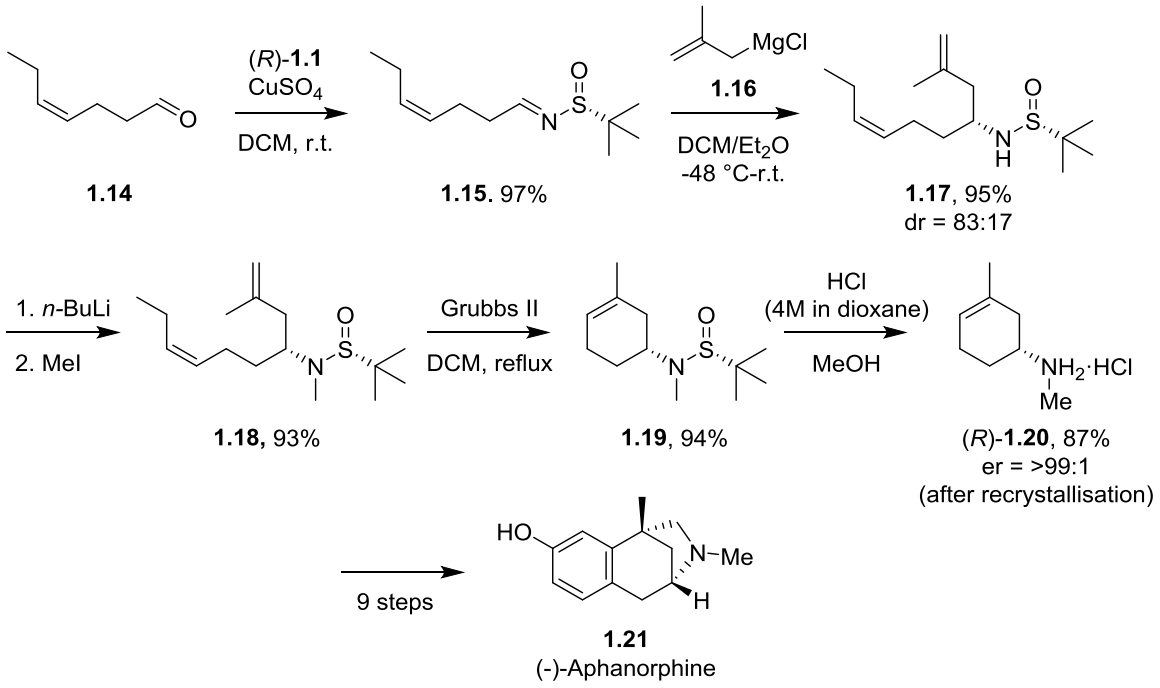

Scheme 1.9. Total synthesis of (-)-Aphanorphine by Grainger and Welsh.[7c]

This same allylation/RCM strategy has been employed by our group in several other publications. The first of these dealt with the asymmetric synthesis of fluorinated cyclic α-aminoesters.[29] In this case, imines **1.22** were used, bearing the methyl ether of (*R*)-phenylglycinol as the chiral auxiliary rather than *N-tert*-butylsulfinamide (Scheme 1.10). The allylation with the corresponding allylzinc bromide took place with high diastereoselectivity, due to the cyclic transition state in which the methoxy group of the chiral auxiliary coordinates to the zinc metal centre.

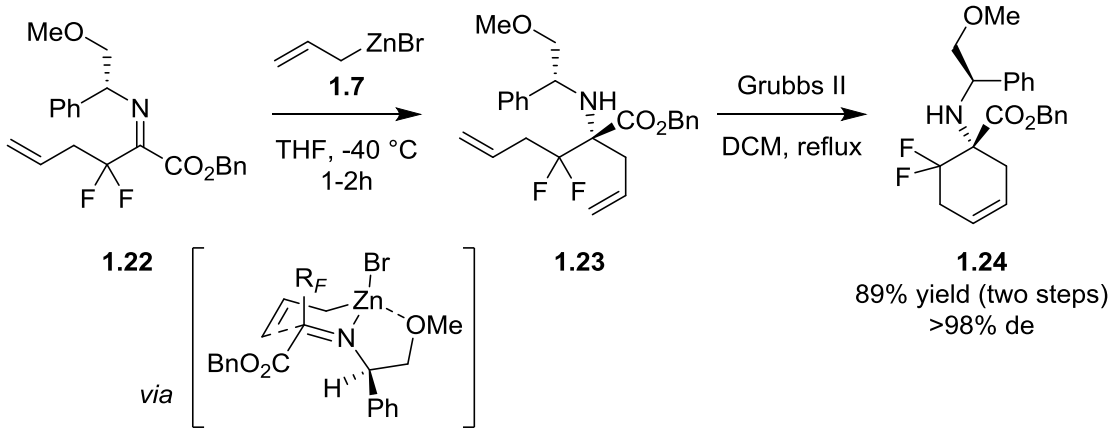

Scheme 1.10. Synthesis of fluorinated cyclic α-aminoesters *via* allylation/RCM strategy.

A second example in 2013 saw the asymmetric synthesis of pyrazole-based bicyclic peptidomimetics.[30] In this case the *N-tert*-butanesulfinyl imine **1.25** was used for the diastereoselective allylation reaction, affording both diastereoisomers by using the suitable conditions: indium-based addition to obtain the (*S*)-amine product (conditions ***i***, Scheme 1.11);[11d] and zinc-based addition in HMPA/water for the opposite (*R*)-amine (conditions ***ii***, Scheme 1.11).[10] Unfortunately, following the allylation step, the ring-closing metathesis was unsuccessful with the sulfinyl protecting group on the amine. Therefore, given that an alanine residue was present in the desired final products, the sulfinyl protecting group was exchanged for the Boc-protected alanine chain. The resulting product **1.27** was a suitable substrate for the key ring-closing metathesis reaction, paving the way to potential peptidomimetics **1.29**.

[29] S. Fustero, M. Sánchez-Roselló, V. Rodrigo, C. del Pozo, J. F. Sanz-Carvera and A. Simón, *Org. Lett.*, 2006, **8**, 4129-4132.

[30] S. Fustero, R. Román, A. Asensio, M. A. Maestro, J. L. Aceña and A. Simón-Fuentes, *Eur. J. Org. Chem.*, 2013, 7164-7174.

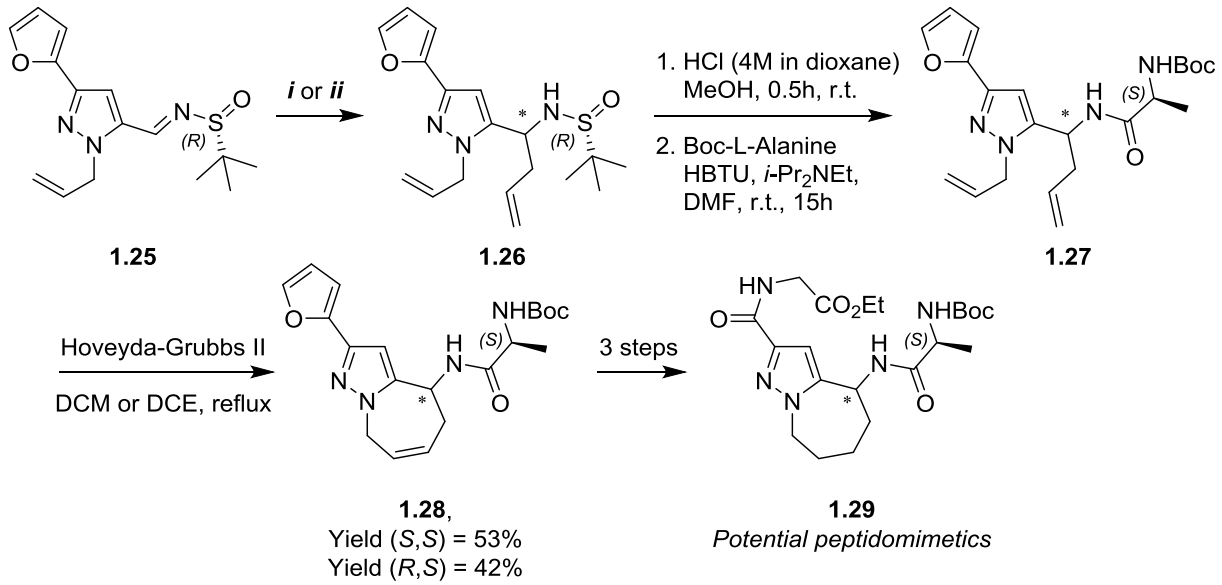

1.25 **1.26** **1.27**

1.28,
Yield (*S*,*S*) = 53%
Yield (*R*,*S*) = 42%

1.29
Potential peptidomimetics

i. Allyl bromide, In, sat. NaBr (aq.), r.t., 4 days: 50% yield, dr = >99:1 (R_S,*S*):(R_S,*R*). ***ii.*** Allyl bromide, Zn, HMPA, H_2O, r.t., 15h: 58% yield, dr = 1:>99 (R_S,*S*):(R_S,*R*).

Scheme 1.11. Synthesis of both diastereoisomers of bicyclic homoallylic amines through the use of varying asymmetric allylation conditions.

Marquez and co-workers also reported the use of the allylation/RCM strategy in the synthesis of α,β-unsaturated-δ-lactams (Scheme 1.12).[31] However, these authors used a *p*-methoxybenzyl protecting group on the starting imine **1.30**, resulting in racemic products. Following this, the unsaturated lactams **1.33** were successfully hydrogenated to **1.34** with almost complete diastereoselectivity.

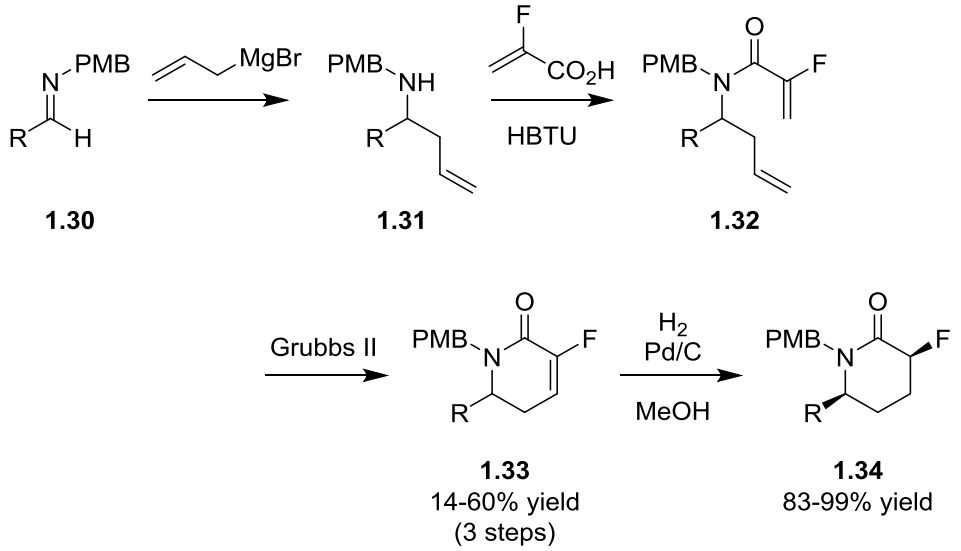

1.30 **1.31** **1.32**

1.33
14-60% yield
(3 steps)

1.34
83-99% yield

Scheme 1.12. Construction of fluorinated δ-lactams.

[31] T. J. Cogswell, C. S. Donald, D.-L. Long and R. Marquez, *Org. Biomol. Chem.*, 2015, **13**, 717-728.

1.1.4. Di- and tetrahydronaphthalenes; a privileged class of compounds.

Dihydronaphthalenes are often used as precursors for the related tetrahydronaphthalene—or tetralin—scaffold, and therefore represent interesting synthetic targets. Tetralins are a privileged substructure in pharmaceuticals and natural products; many FDA-approved drugs contain the tetralin core or are derived from tetralin-based natural products (Figure 1.3).[32]

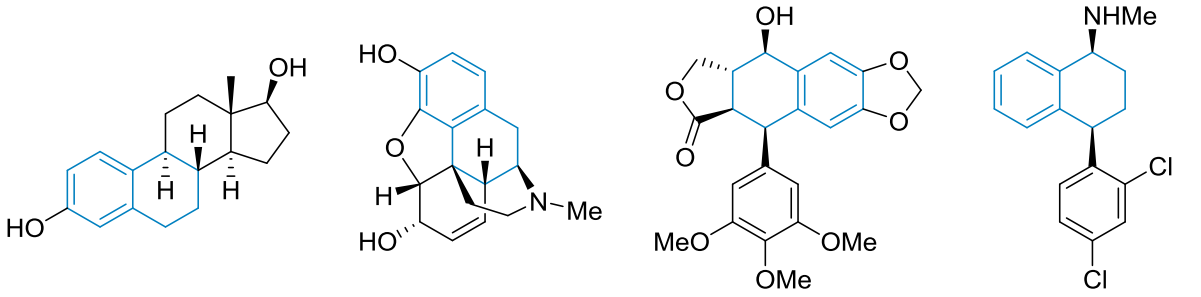

Oestradiol
Major oestrogen hormone and widely used medication

Morphine
Prototypical opioid and structural basis of many painkillers

Podophyllotoxin
Natural antiviral, derivatives used in anticancer drugs

Sertraline
Selective serotonin uptake inhibitor antidepressant

Figure 1.3. Tetralin-derived drugs and natural products.

The dihydronaphthalene scaffold itself is extremely scarce in FDA-approved drugs, although some examples of bioactive compounds do exist that are based on this structure. For example, a conformationally restricted analogue of amphetamine, 2-amino-1,2-dihydronaphthalene (2-ADN), was proven to be a potent CNS stimulant (Figure 1.4, a).[33] In contrast, the corresponding tetrahydronaphthalene analogue was shown to be much less active.

In addition, several dihydronaphthalene derivatives of podophyllotoxin have been proven to have potent anticancer activity. In particular, **I** and **II** display high cytotoxicity and selectivity against HT-29 cancer cell lines (Figure 1.4, b).[34]

[32] a) K. Huhl, *Climacteric*, 2005, **8**, 3-63. b) M. Waldhoer, S. E. Bartlett and J. L. Whistler, *Annu. Rev. Biochem.*, 2004, **73**, 953-990. c) A. Janecka, J. Fichna and T. Janecki, *Curr. Top. Med. Chem*., 2004, **4**, 1-17. d) H. Xu, M. Lv and X. Tian, *Curr. Med. Chem.*, 2009, **16**, 327-349. e) G. Macqueen, L. Born and M. Steiner, *CNS Drug Rev.*, 2001, **7**, 1-24.

[33] B. A. Hathaway, D. E. Nichols, M. B. Nichols and G. K. W. Yim, *J. Med. Chem.*, 1982, **25**, 535-538.

[34] M. A. Castro, J. M. M. del Corral, M. Gordaliza, P. A. Garcia, M. A. Gomez-Zurita, M. D. Garcia-Gravalos, J. de la Iglesia-Vicente, C. Gajate, F. An, F. Mollinedo and A. S. Feliciano, *J. Med. Chem*., 2004, **47**, 1214-1222.

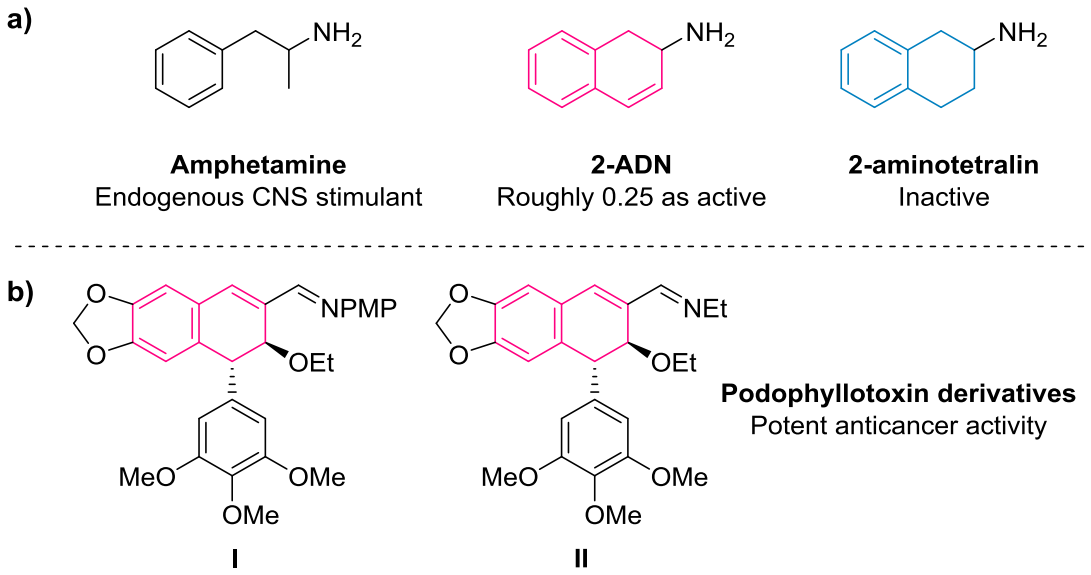

Figure 1.4. a) Structure of amphetamine and derivatives. b) Structure of dihydronaphthalene-based derivatives of podophyllotoxin with anticancer activity.

Furthermore, dihydronaphthalenes have proved key intermediates in the synthesis of opioid derivatives codeine and dihydroisocodeine (Figure 1.5).[35]

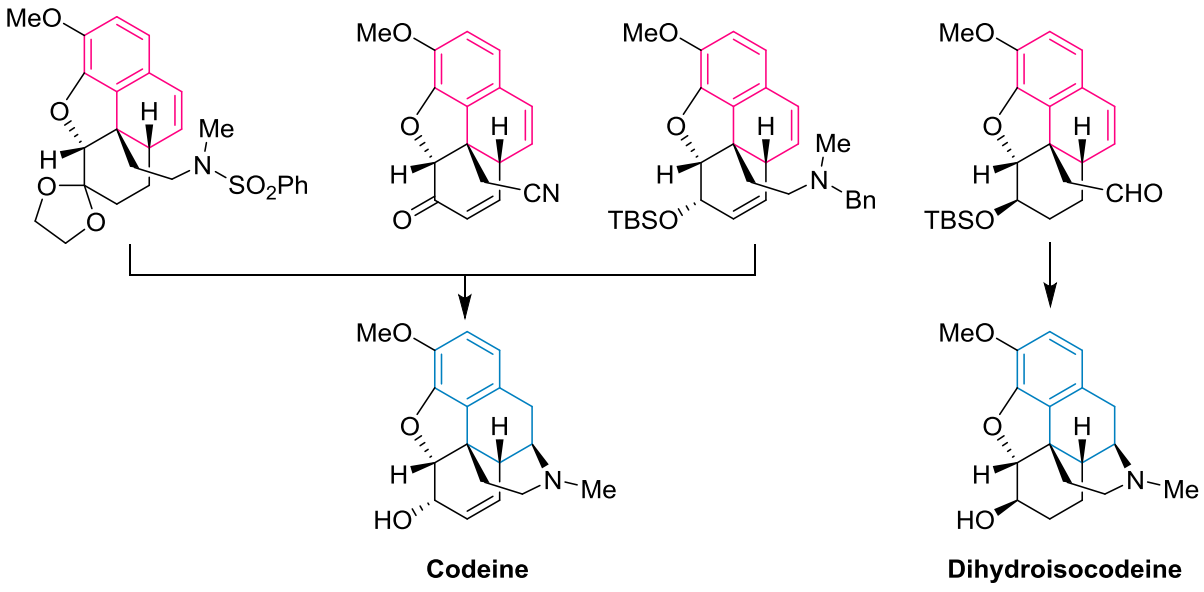

Figure 1.5. Dihydronaphthalene intermediates used in the synthesis of opioids.

[35] L. Quilin and Z. Hongbin, *Chin. J. Org. Chem.*, 2017, **37**, 1629-1652.

Examples of dihydronaphthalenes containing an amine substituent mainly consist of those with the amine in the C2 position; the related 1-amino-1,2-dihydronaphthalenes are much less common, especially enantioenriched versions. However, there are several examples of their synthesis using the asymmetric catalytic ring opening of azabenzonorbornadienes **1.35**. This strategy was originally developed by Lautens,[36] and has since been used to synthesise 1,2-aminoalcohols **1.36**, 1,2-diamines **1.37**,[36, 37] 1-amino[38] **1.38** and 1-amino-2-alkyl-1,2-dihydronaphthalenes **1.39** (Scheme 1.13).[39]

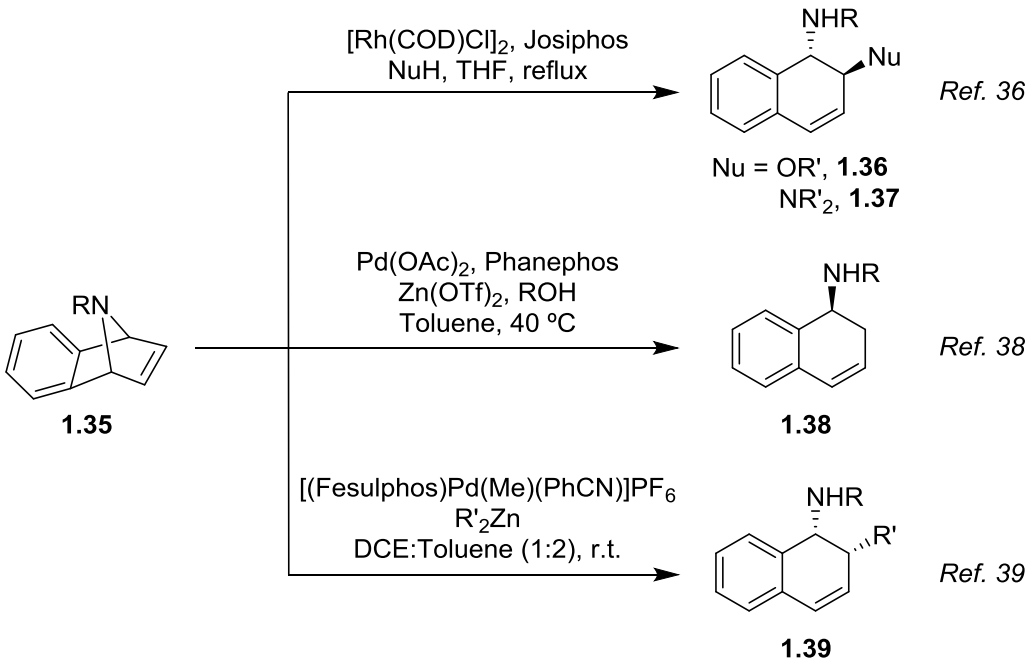

Scheme 1.13. Synthesis of 1-amino-1,2-dihydronaphthalenes using the catalytic ring opening of azabenzonorbornadienes.

[36] M. Lautens, K. Fagnou and T. Rovis, *J. Am. Chem. Soc.*, 2000, **122**, 5650-5651.

[37] a) Y.-H. Cho, V. Zunic, H. Senboku, M. Olsen and M. Lautens, *J. Am. Chem. Soc.*, 2006, **128**, 6837-6846. b) Y.-H. Cho, A. Fayol and M. Lautens, *Tetrahedron: Asymmetry*, 2006, **17**, 416-427.

[38] F. Yang, J. Chen, J. Xu, F. Ma, Y. Zhou, M. V. Shinde and B. Fan, *Org. Lett.*, 2016, **18**, 4832-4835.

[39] S. Cabrera, R. Gómez Arrayás and J. C. Carretero, *Angew. Chem. Int. Ed.*, 2004, **43**, 3944-3947.

1.2. Background.

Our research group has been active in this field of research over the past decade, as seen previously. As well as cyclohexenes[29] and pyrazole-based bicycles,[30] we have also studied the synthesis of di- and tetrahydronaphthalenes using the asymmetric allylation/RCM strategy.

The first example explored the application of this protocol to obtain a range of 1-amino-1,2-dihydronaphthalene products, as well as its use in the synthesis of Sertraline and its derivatives: an antidepressant originally developed by Pfizer under the trade name Zoloft (Scheme 1.14).[32e, 40]

In this study, our group studied the possibility of combining these reactions into a one-pot process. This type of method has become popular in recent years, since in an industrial setting, synthetic chemists must deal with environmental and economic issues to make the process as cheap and sustainable as possible; the use of one-pot processes is one way to help alleviate these problems, since there is no need to purify after each reaction and therefore the added waste from chromatography or solvents is not generated.

The one-pot process developed included three steps: condensation, allylation, and ring-closing metathesis. Since all three reactions were fairly clean and produced few by-products, the main challenge was finding a suitable solvent and the compatibility between allylzinc bromide and the ruthenium-based catalyst used in the RCM step. Fortunately, the one-pot procedure proceeded well in THF, affording the corresponding dihydronaphthalene in an 85% yield and excellent diastereoselectivity starting from 2-vinylbenzaldehyde **1.40** (Scheme 1.14). Dihydronaphthalene **1.41** was then taken forward to synthesise **1.42**, an intermediate in Chandrasekhar's total synthesis of Sertraline.[41]

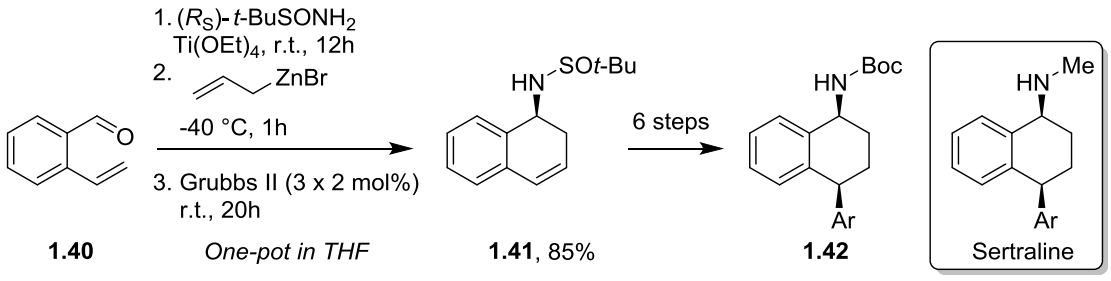

Scheme 1.14. One-pot procedure towards the synthesis of Sertraline.

[40] S. Fustero, R. Lázaro, L. Herrera, E. Rodríguez, N. Mateu and P. Barrio, *Org. Lett.*, 2013, **15**, 3770-3773.
[41] S. Chandrasekhar and M. V. Reddy, *Tetrahedron*, 2000, **56**, 1111-1114.

The ring closing metathesis reaction is not limited to the simple coupling of two olefins; ring-closing enyne metathesis (RCEYM) is also a well-established transformation involving the coupling of an alkene and an alkyne, resulting in 1,3-dienes. This process was also explored by our group in the context of the synthesis of dihydronaphthalene derivatives, giving rise to a related allylation/RCEYM procedure (Scheme 1.15).[42] In this way, a small library of dihydronaphthalenes **1.45** was synthesised in good yields.

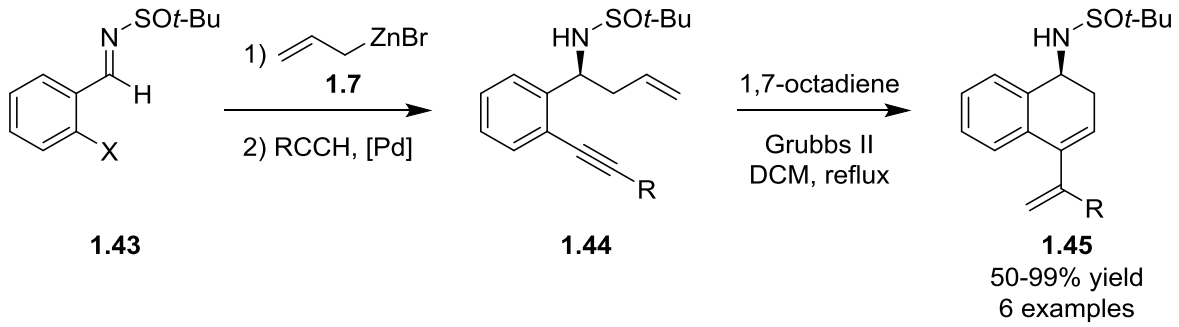

Scheme 1.15. RCEYM strategy towards functionalised dihydronaphthalenes.

In a separate study, our group also studied the same methodology on substrates with an *ortho*-(α-fluoro)vinyl group.[43] In accordance to the previous examples involving RCM of fluorinated olefins, this reaction required high temperatures to proceed. Nonetheless, both the allylation and RCM reactions took place in high yields, resulting in enantioenriched fluorinated dihydronaphthalenes **1.48** (Scheme 1.16).

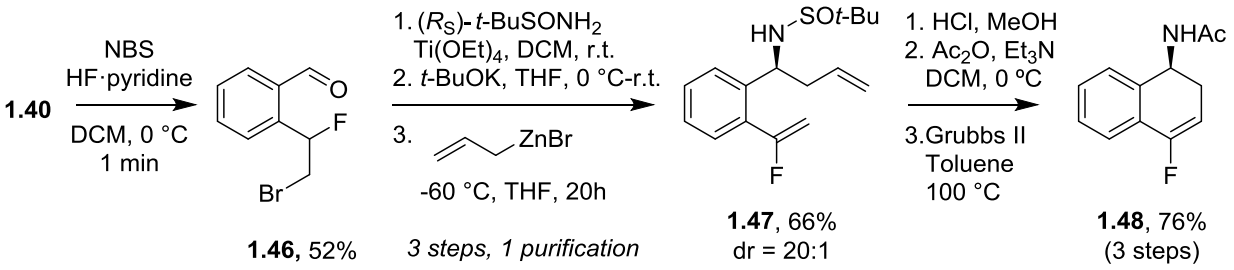

Scheme 1.16. Allylation/RCM sequence using pendant vinyl fluorides.

[42] R. Lázaro, P. Barrio, C. Finamore, R. Román and S. Fustero, *Struct. Chem.*, 2017, **28**, 445-452.
[43] R. Lázaro, R. Román, D. M. Sedgwick, G. Haufe, P. Barrio and S. Fustero, *Org. Lett.,* 2016, **18**, 948-951.

1.3. Results and discussion.

In accordance with the objectives described in Section 1.0, the first step would be the construction of *ortho*-trifluoromethylvinyl benzaldehyde and related substrates with other fluorinated groups in the same position, in order to proceed to the condensation/allylation/RCM procedure and obtain the desired enantioenriched amino dihydronaphthalenes.

In this context, in 2014 Valdés and co-workers described a fairly general method to add the 1,1,1-trifluoropropene group onto aromatic rings *via* palladium-catalysed coupling between aryl bromides and trifluoromethylated tosylhydrazone **1.49** (Scheme 1.17).[44]

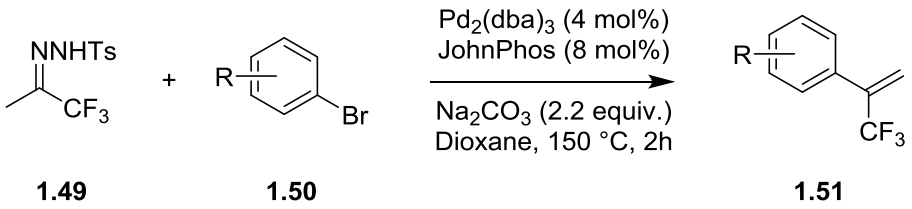

Scheme 1.17. Synthesis of trifluoromethyl styrenes *via* coupling of tosylhydrazones and aryl bromides.

With regards to the mechanism, the authors proposed a catalytic cycle that starts with the oxidative addition of the aryl bromide to the palladium to give intermediate **I** (Scheme 1.18). Following this, the carbene species formed by the liberation of elemental nitrogen from diazo intermediate **II** coordinates to the palladium metal centre to form intermediate **III**. From there, migratory insertion of the carbene ligand and β-hydride elimination from the methyl group originating from **1.49** affords **1.51**.

This method represented a step forward with regards to the introduction of this fluorinated group in aromatic substrates; although other methods did exist they usually required harsher conditions and more complex starting materials.[45]

[44] A. Jiménez-Aquino, J. A. Vega, A. A. Trabanco and C. Valdés, *Adv. Synth. Catal.*, 2014, **356**, 1079-1084.

[45] a) B. Jiang and Y. Xu, *J. Org. Chem.*, 1991, **56**, 7336-7340. b) G.-Q. Shi, X.-H. Huang and F. Hong, *J. Org. Chem.*, 1996, **61**, 3200-3204. c) B. Jiang, Q.-F. Wang, C.-G. Yang and M. Xu, *Tetrahedron Lett.*, 2001, **42**, 4083-4085. d) O. Kobayashi, D. Uraguchi and T. Yamakawa, *J. Fluorine Chem.*, 2009, **130**, 591-594.

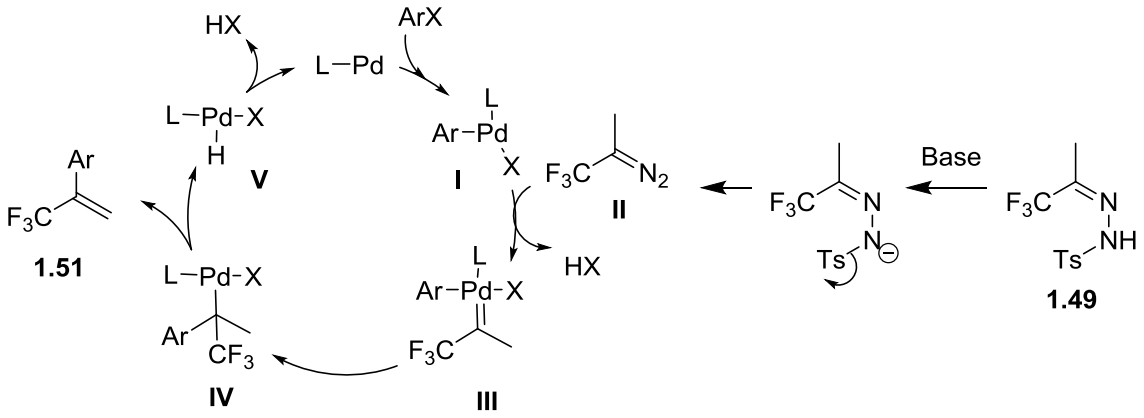

Scheme 1.18. Proposed mechanism for the formation of α-trifluoromethyl styrenes.

The reaction was shown to be functional group tolerant, and the authors obtained α-trifluoromethyl styrenes containing an array of functionalities on the aromatic ring. However, the reaction had never been carried out with an aldehyde in the *ortho* position, as we required for our planned synthetic route.

Nonetheless, we first proceeded to synthesise trifluoromethylated tosylhydrazone **1.49** through condensation between 1,1,1-trifluoromethylacetone **1.52** and tosylhydrazine **1.53**, giving a good yield of the corresponding bench-stable tosylhydrazone after recrystallisation (Scheme 1.19).

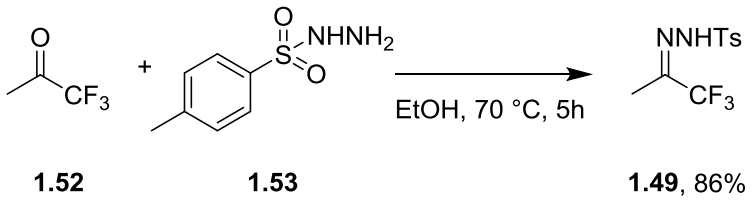

Scheme 1.19. Synthesis of trifluoromethylated building block tosylhydrazone 1.49.

We then attempted the coupling of **1.49** with *ortho*-bromobenzaldehyde **1.54**, but found that this substrate was incompatible with the conditions described by Valdés *et al.* Nevertheless, after a short optimisation we were able to obtain the desired aldehyde **1.55** in a good 73% yield by changing the solvent to THF and using a lower temperature in a microwave oven (Scheme 1.20).

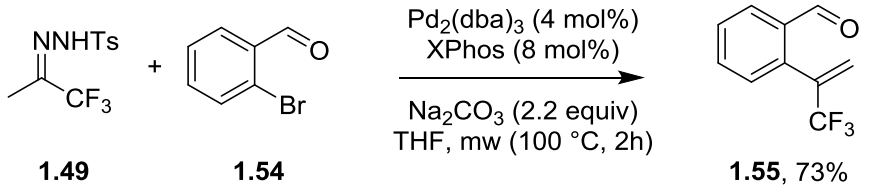

1.49 **1.54** **1.55**, 73%

Scheme 1.20. Synthesis of trifluoromethylated *ortho*-vinyl benzaldehydes 1.55.

Using this method, we were able to synthesise a small library of trifluoromethylated substrates (Table 1.2). Here, it was important for the reaction to proceed to completion; the starting benzaldehydes and the products had a very similar retention factor on silica gel, making the separation very difficult. Furthermore, the products were unstable and relatively volatile, so purification had to be carried out in solvents with low boiling points—mixtures of hexane and diethyl ether—and the products were used immediately in the next step.

Table 1.2. Scope of the palladium-catalysed coupling reaction to introduce the trifluoromethylvinyl moiety.

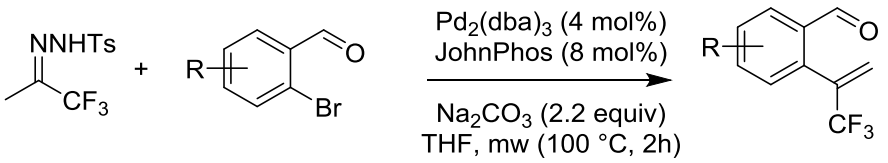

1.49 **1.54** **1.55**

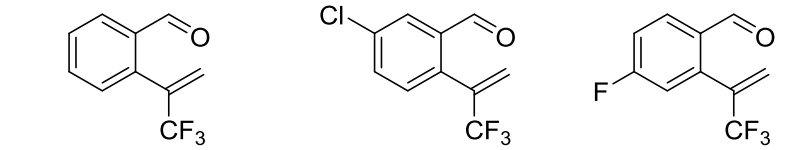

1.55a, 73% **1.55b**, 69% **1.55c**, 59%

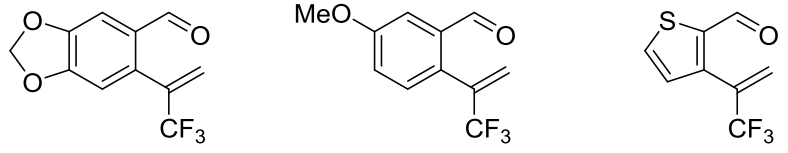

1.55d, 71% **1.55e**, 73% **1.55f**, 94%

After obtaining a range of trifluoromethylated substrates, we then decided to synthesise derivatives with other fluorinated groups. Given that we had now optimised the coupling reaction using trifluoromethylated tosylhydrazones, we decided to apply the same strategy to the synthesis of other fluorinated derivatives. Therefore, starting with the corresponding fluorinated ketones we planned to form the tosylhydrazones and couple them with *o*-bromobenzaldehyde **1.54**. However, we found that

mono-fluoroacetone was far too expensive to be used as a starting material, and so we turned to the corresponding sulfonyl derivatives—since the sulfone group could be removed through treatment with magnesium leaving the free (di)fluoromethyl group, as described by Gouverneur *et al.*[46]

In this context, we found that such tosylhydrazones could be prepared with a two-step reaction sequence: the addition of (di)fluoromethyl phenyl sulfone **1.56** to ethyl acetate, followed by condensation of the resulting ketone **1.57** with tosylhydrazide **1.53** (Scheme 1.21). We found that the addition of difluoromethyl phenyl sulfone **1.56a** to ethyl acetate had to be carried out at -98 °C (in a bath of ethanol/liquid nitrogen) rather than the standard -78 °C, potentially due to the instability of the intermediate anion. Furthermore, these addition reactions were more successful when the base was added to the mixture of ethyl acetate and the sulfone (Barbier-like conditions), rather than first forming the intermediate anion and then adding the electrophile. Again, this was most likely due to the instability of the intermediate anions.

After preparing the fluorinated tosylhydrazones, we attempted the coupling reaction. Unfortunately, we did not observe the desired derivatives **1.55** in any case; the result was generally a complex mixture, and the crude NMR spectra contained no sign of the desired products. Changing the reaction conditions (lower temperatures and reaction times due to possible decomposition, higher catalyst loading etc.) was also unsuccessful.

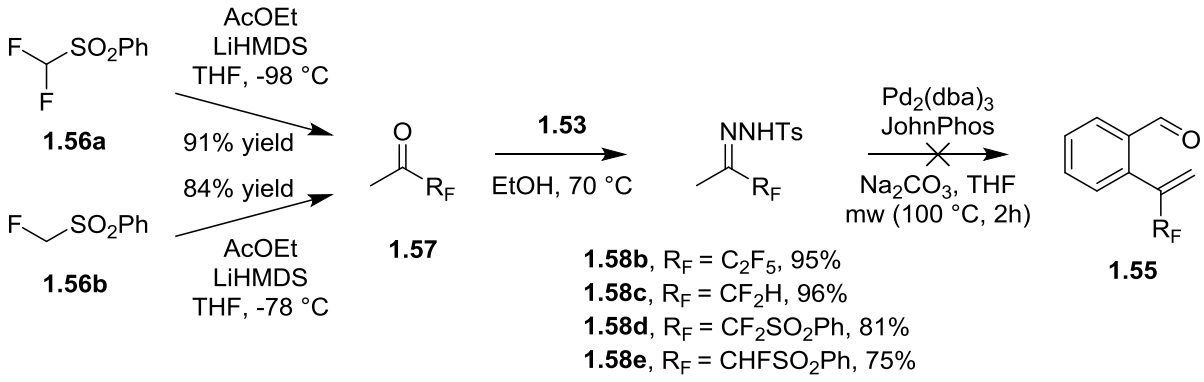

Scheme 1.21. Synthesis of fluorinated tosylhydrazones 1.58 and failed couplings towards 1.55.

Therefore, we decided to follow Gouverneur *et al.*, taking their report as a starting point to synthesise the other products we had in mind. In this context, we first attempted a palladium-catalysed cross-coupling between boronic acid **1.59** and vinyl bromide **1.60** to introduce the pentafluoroethyl group. Here, it is worth mentioning that this reaction has not been carried out before, and other studies often

[46] J. Walkowiak, T. Martinez del Campo, B. Ameduri and V. Gouverneur, *Synthesis*, 2010, **11**, 1883-1890.

lack the pentafluoroethyl group, instead focusing on the related and more common trifluoromethyl substituent. Fortunately, the reaction was a success, and we obtained the desired pentafluoroethyl-bearing compound **1.55g**, although we found this compound to be even more unstable than the trifluoromethylated analogues (**1.55a-f**) and were unfortunately unable to obtain acceptable NMR spectra (Scheme 1.22). However, using the compound in the next reaction immediately after purification we were able to continue the synthesis.

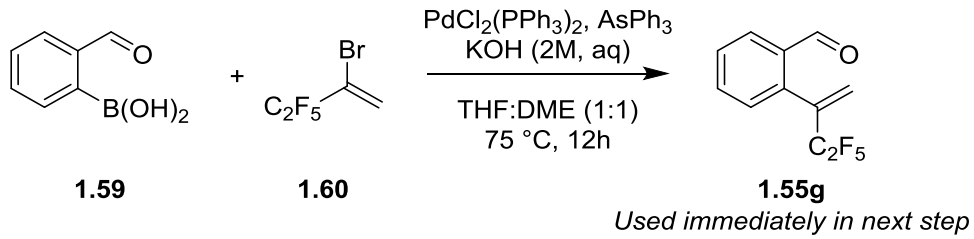

Scheme 1.22. Synthesis of pentafluoroethyl-containing substrate 1.55g.

Following this, we turned our attention to the (di)fluoromethyl-bearing aldehydes. Given that Gouverneur and co-workers had described a route to synthesise α-difluoromethylstyrene, we started with an analogous route with an acetal-protected aldehyde in the *ortho* position—we reasoned that a reactive aldehyde in the *ortho* position could interfere with several steps in the synthetic sequence. This route started with the introduction of a ketone group into the commercial substrate **1.61**, followed by the addition of the corresponding sulfone to form alcohol intermediate **1.63**.[47] From there, we attempted the dehydration to give the final acetal-protected aldehyde **1.64**, but the reaction was unsuccessful in all conditions tested, resulting in complex mixtures (Scheme 1.23).

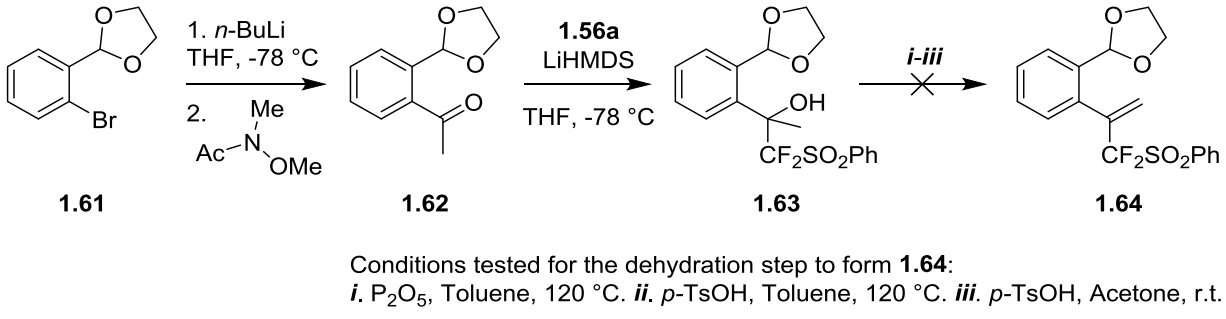

Scheme 1.23. First attempted synthetic route towards (di)fluoromethanesulfonyl-bearing substrates.

[47] G. K. S. Prakash, J. Hu, Y. Wang and G. A. Olah, *Eur. J. Org. Chem.*, 2005, **11**, 2218-2223.

In light of these results, a second route was designed in which the aldehyde group was to be incorporated in the final step. This route started with the direct addition of difluoromethyl phenyl sulfone **1.56a** to *o*-bromobenzaldehyde **1.54** to form alcohol **1.65**, which was then oxidised to ketone **1.66**. The oxidation step caused certain problems. Reaction with pyridinium di- and chlorochromate, as well as with manganese(II) oxide all failed to proceed to completion, which was problematic given the difficulty in separating the ketone product from the alcohol starting material by column chromatography. Eventually, we found that using Jones' reagent ($CrO_3 \cdot H_2SO_4$) in dichloroethane in the microwave oven at 70 °C forced the reaction to complete, and afforded desired ketone **1.66** in high yields. This intermediate was then used in a Wittig reaction to form the C—C double bond. Interestingly, when *t*-BuOK was used as the base in this step, the Wittig product was not formed. Instead, we observed a cleavage of the ketone—CF_2SO_2Ph bond. The final step was then the introduction of the aldehyde in the *ortho* position, but unfortunately this reaction did not take place in any of the conditions tested (Scheme 1.24).

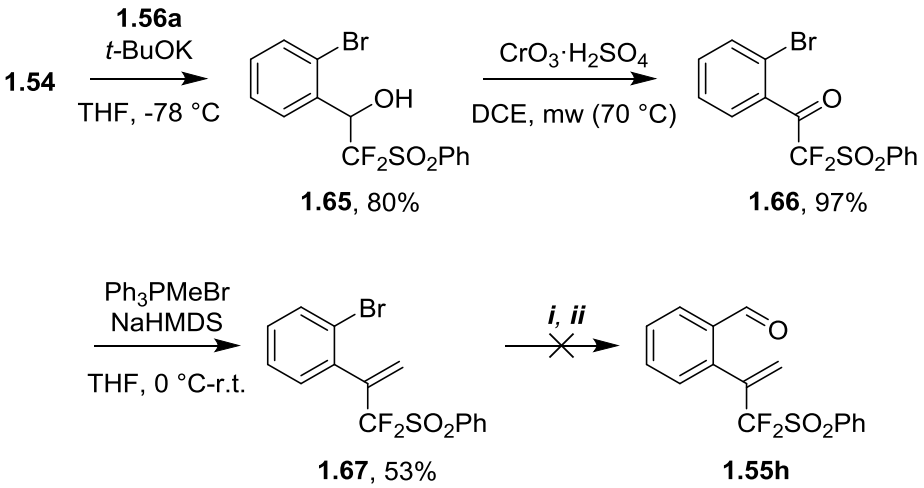

Scheme 1.24. Second attempted route towards (di)fluoromethanesulfonyl-bearing substrates.

We therefore resorted to a longer reaction sequence starting with the formylation of commercial compound **1.61** using *n*-BuLi and DMF (Scheme 1.25). From there, the desired fluoroalkyl phenyl sulfone—we attempted this route with both the mono- and difluoro derivatives—was introduced *via* nucleophilic addition to the aldehyde to form alcohol **1.69**, which was then oxidised to the corresponding ketone. In this case, this was carried out with Dess-Martin periodinane, due to the suspected sensitivity of the acetal protecting group to acidic conditions, such as those arising from the

use of Jones' reagent. Nonetheless, the separation of alcohol and ketone was much more simple here than in the previous route, and therefore it was less important for the reaction to proceed to completion. A simple Wittig reaction with methyltriphenylphosphonium bromide produced the desired C—C double bond, and subsequent deprotection of the aldehyde group provided **1.55h**.

The synthesis of the monofluorinated derivative was unsuccessful using this synthetic route; **1.70b** was incompatible with the Wittig reaction to form **1.71b**, likely due to the acidic proton in the α-position with respect to the sulfone group.

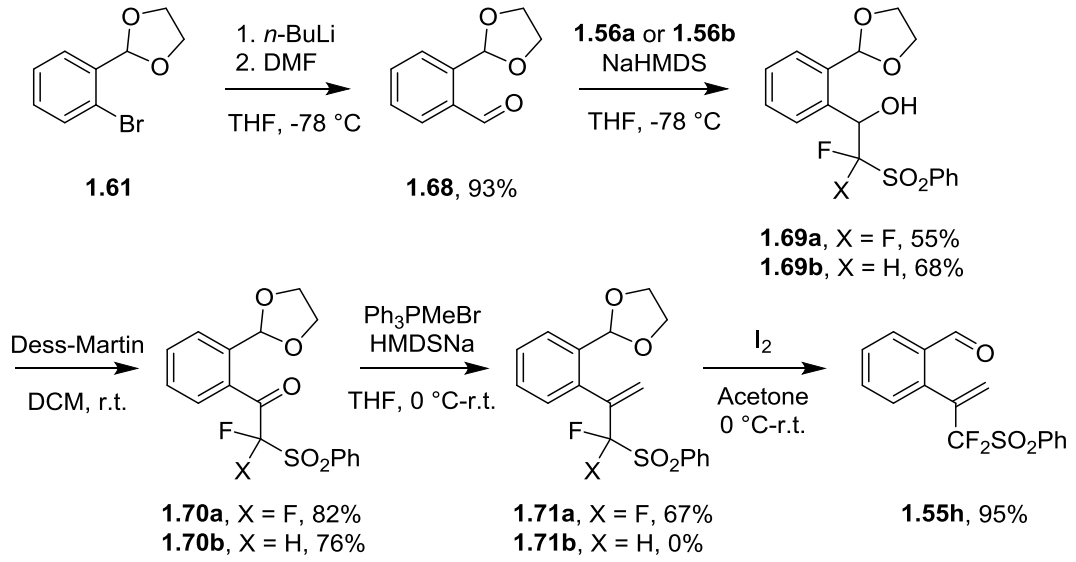

Scheme 1.25. Synthesis of difluoromethyl-containing substrate 1.55h.

Furthermore, in order to later study the effect of the fluorinated groups on the reaction sequence, we synthesised two non-fluorinated derivatives containing the methyl and ethyl ester substituents. To this end, we first chose to study α-methyl analogue **1.55i** since this was the simplest change we could make to remove fluorine. Secondly, we chose the ethyl ester **1.55j** given the electron-withdrawing nature of this substituent, which would mimic the electronic properties of the trifluoromethylated olefins without containing fluorine atoms in the structure. These were synthesised *via* analogous routes to those already seen for the synthesis of the fluorinated derivatives. Methyl-bearing **1.55i** was synthesised by palladium-catalysed cross-coupling between 2-bromobenzaldehyde **1.54** and boronate **1.72** (Scheme 1.26, a). On the other hand, ethyl ester-bearing **1.55j** was synthesised by a three-step sequence, starting with the addition of the organolithiate derived from **1.61** to diethyl oxalate. Wittig methylenation of the thus obtained ketoester and deprotection of the acetal rendered the final product in an overall moderate yield (Scheme 1.26, b).

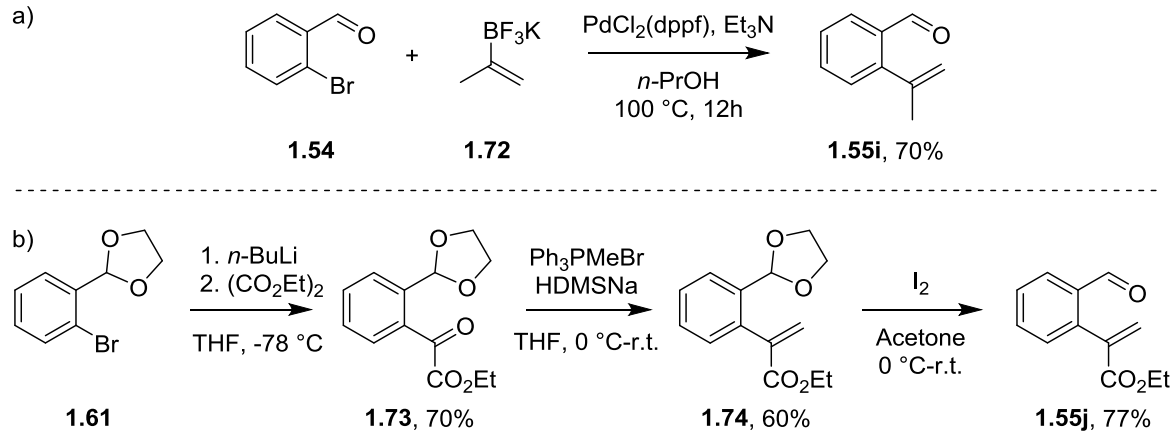

Scheme 1.26. Synthesis of non-fluorinated derivatives for comparison.

With the 2-vinylbenzaldehyde derivatives in hand, we formed the corresponding *N-tert*-butanesulfinyl imines uneventfully, despite obtaining only moderate yields in several cases, potentially due to the instability of the aldehyde starting materials. In the case of **1.75g** (see Scheme 1.22), it is worth noting that the yield represents both the coupling and the condensation steps, due to the difficulties in isolating the aldehyde starting material (Table 1.3).

Table 1.3. Results of the condensation reaction to form the corresponding *N-tert*-butanesulfinyl imines

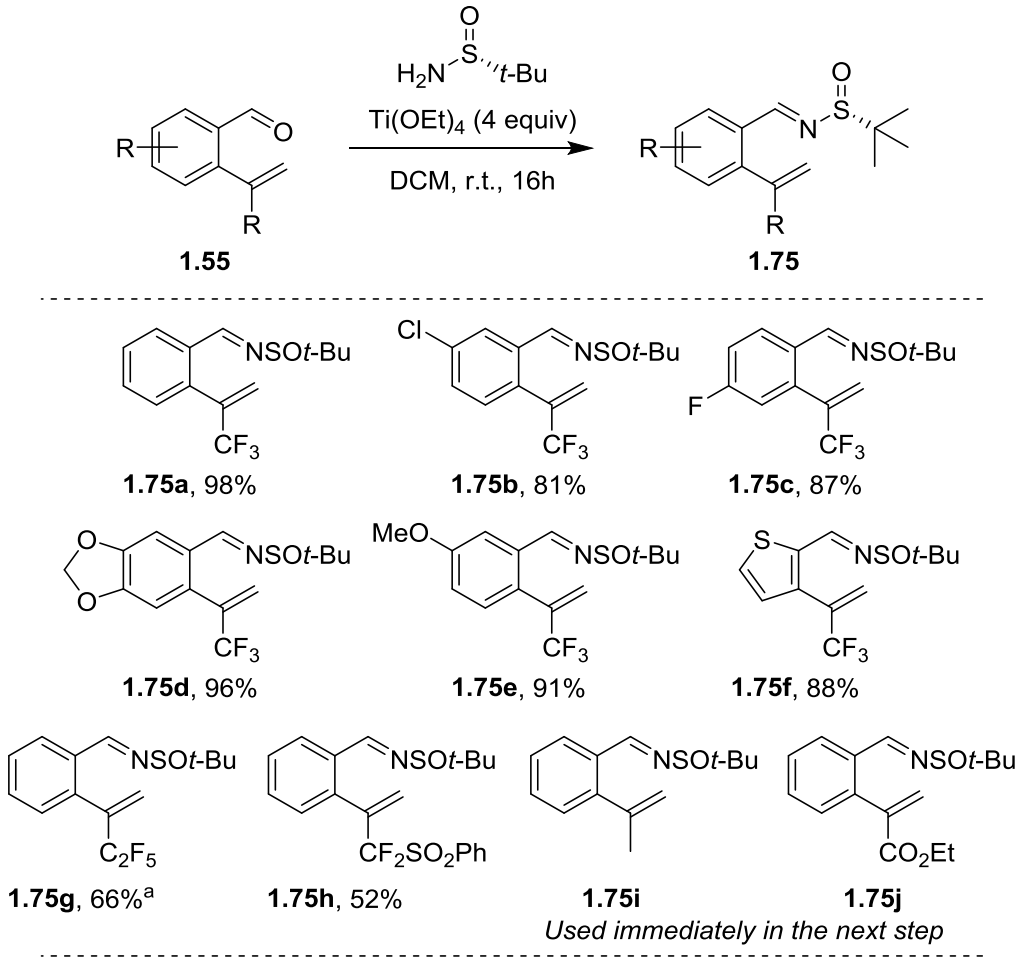

[a] Yield corresponds to the total yield including both the synthesis of **1.55g** and the condensation depicted here.

From there, the next step was the diastereoselective allylation reaction using allylzinc bromide **1.7**. For this step, we used the same conditions that had been previously developed in our group.[43] The yield of the allylation (or crotylation) reaction was high in all cases, except the slightly lower yield observed for thiophene-based **1.76f** (Table 1.4). Additionally, excellent diastereoselectivity was observed in all cases, although incidentally the two non-fluorinated substrates gave slightly lower diastereoselectivities (dr = 10:1 vs. >20:1). The reactions were carried out with both racemic and enantiopure *N-tert*-butanesulfinyl imines, in order to reliably analyse the diastereoisomeric ratio *via* chiral HPLC.

Table 1.4. Diastereoselective allylation and crotylation reaction with *N-tert*-butanesulfinyl imines 1.75.

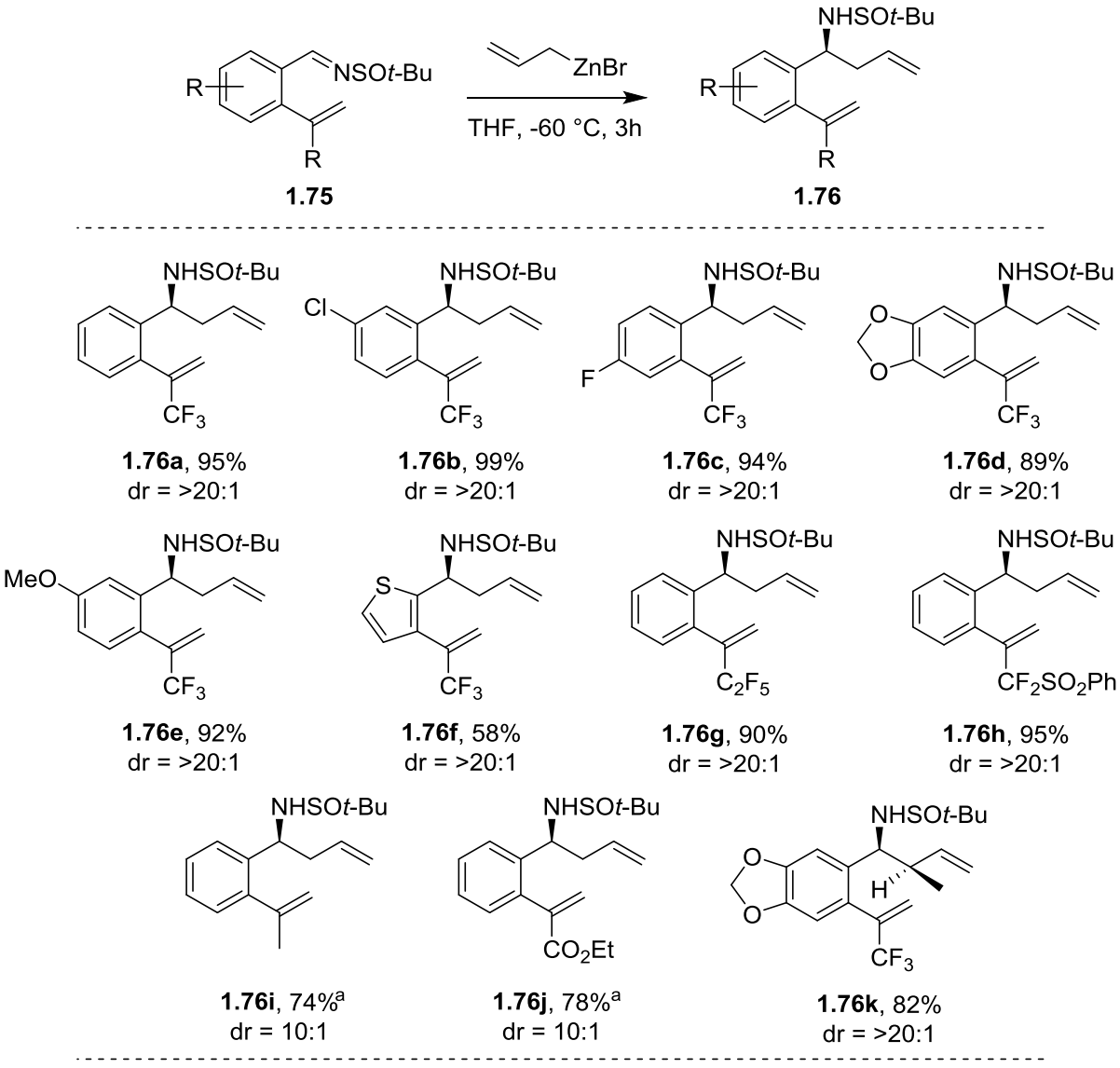

[a] Yields correspond to both the condensation and allylation steps.

The reaction was assumed to take place *via* the same six-membered chair-like transition state demonstrated earlier, resulting in the (*S*)-amine products (Scheme 1.27). This was extrapolated from an earlier study carried out in our research group, in which the absolute stereochemistry of the secondary amine was elucidated *via* X-ray crystallography.[40]

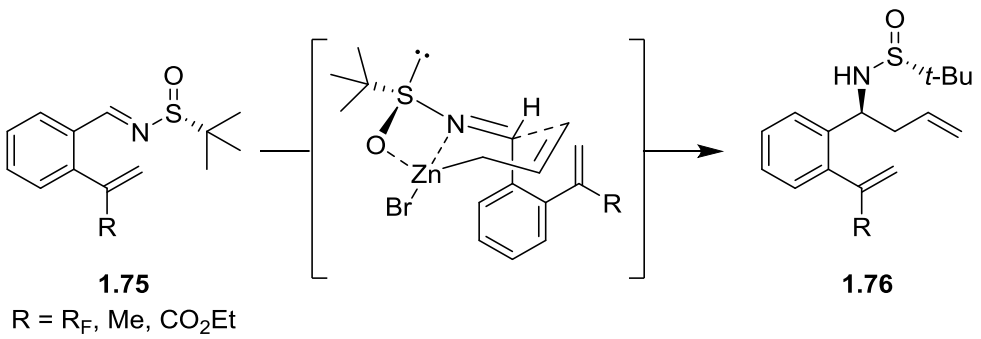

Scheme 1.27. Transition state explaining the stereochemical outcome of the allylation reaction.

In terms of the final step in the sequence, the RCM, we found it necessary to first exchange the *N*-sulfinyl protecting group for the fluorinated substrates to react (as seen previously).[43] Treatment of **1.76** with HCl in methanol quickly and efficiently removed the *N*-*tert*-butanesulfinyl group. Following this, we chose *tert*-butyloxycarbonyl (Boc) and acetyl (Ac) as the new protecting groups due to their ease of introduction (Table 1.5). Fortunately, we observed no decay in optical purity during the exchange of the protecting group.

Table 1.5. Protection group exchange.[a]

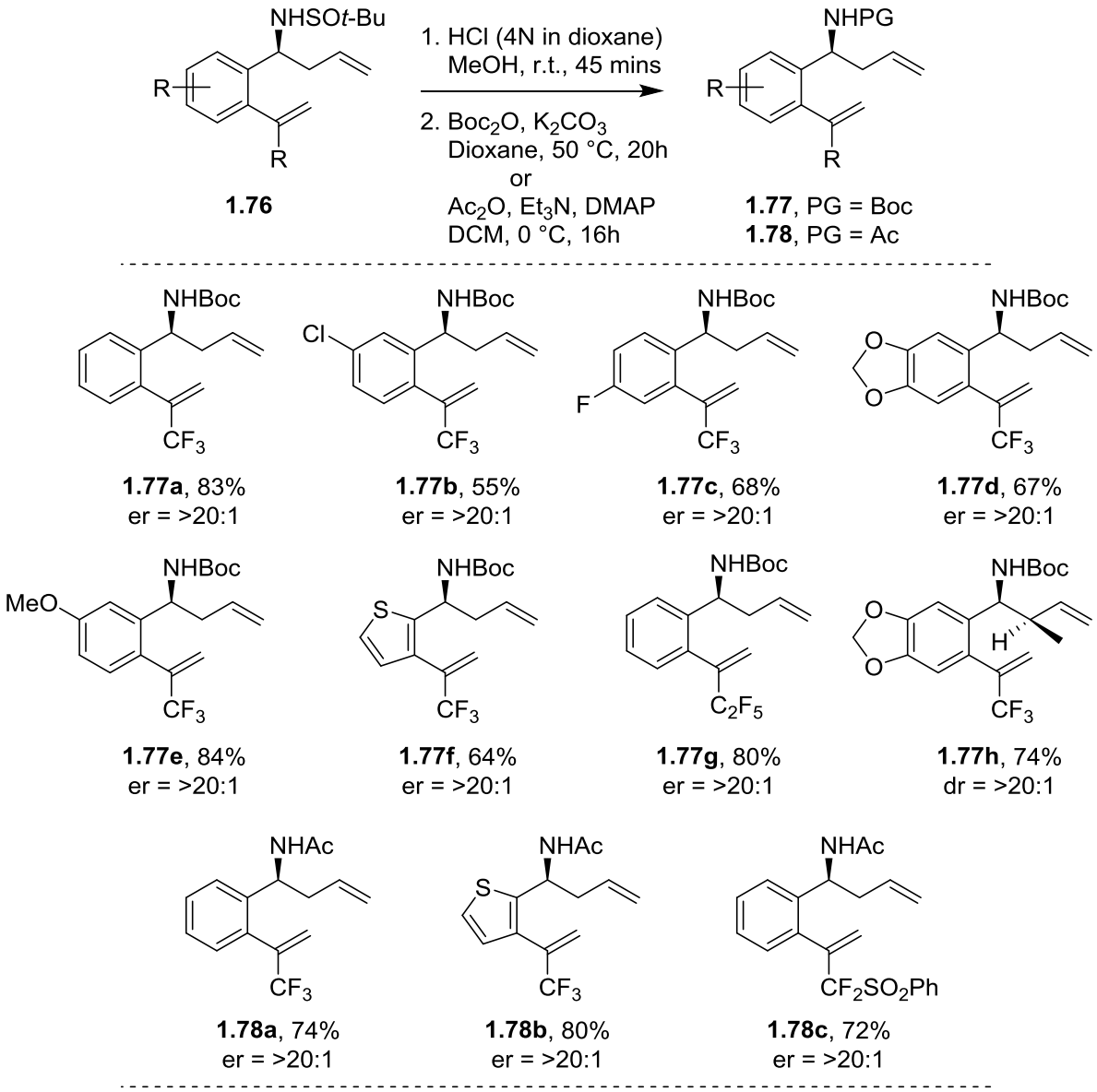

1.76

1.77, PG = Boc
1.78, PG = Ac

1.77a, 83%
er = >20:1

1.77b, 55%
er = >20:1

1.77c, 68%
er = >20:1

1.77d, 67%
er = >20:1

1.77e, 84%
er = >20:1

1.77f, 64%
er = >20:1

1.77g, 80%
er = >20:1

1.77h, 74%
dr = >20:1

1.78a, 74%
er = >20:1

1.78b, 80%
er = >20:1

1.78c, 72%
er = >20:1

[a] Yields correspond to the total yield over both deprotection and reprotection steps.

Once the protecting groups had been exchanged, we tackled the RCM reaction again. Even without the deactivating *N-tert*-butanesulfinyl group, the reaction was not as straightforward as one may think; this was to be expected in part, given the past examples dealing with the RCM of trifluoromethylated olefins.[22-25] The reaction mixture had to be heated to high temperatures for the reaction to take place (Table 1.6). Though the yields were generally low to moderate, the optical purity of the products was maintained, with the exception of the slight decay observed in the thiophene-based products **1.79f** and **1.80b** (er = >20:1 to 18:1) (Table 1.6).

Table 1.6. RCM reaction with stryrenes bearing fluorinated substituents to form dihydronaphthalenes.

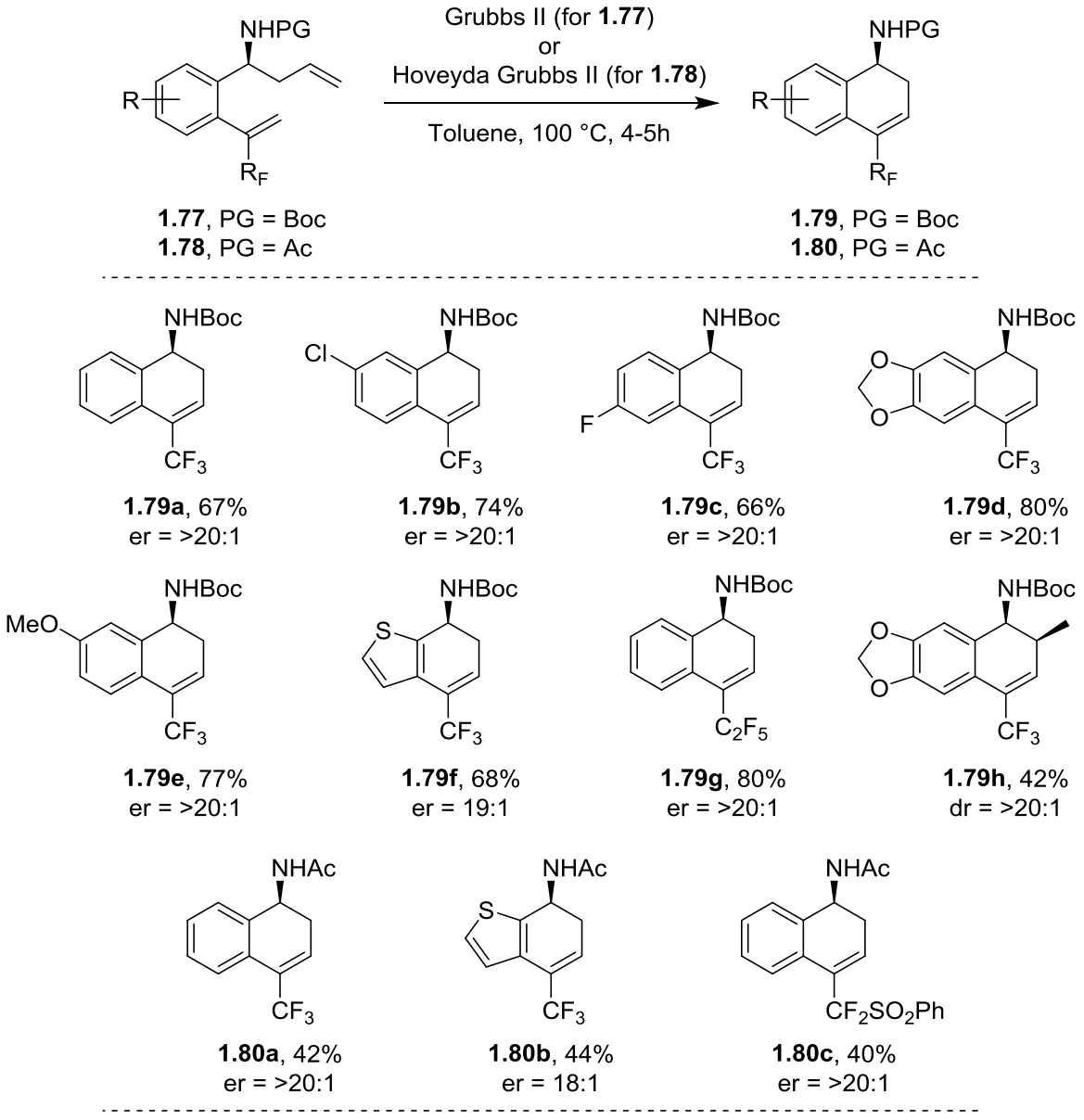

We then carried out the final ring closing metathesis step with the non-fluorinated derivatives **1.76i** and **1.76j**, revealing the dramatic effect of the vinyl substituent. While fluorinated substrates **1.76a-h** bearing the *tert*-butanesulfinyl protecting group had proven unreactive even when forcing the reaction in toluene at high temperatures, non-fluorinated derivatives **1.76i** and **1.76j** were suitable substrates in standard RCM conditions at room temperature, even with the sulfinyl protecting group intact (Scheme 1.28). In particular, it is worth noting the stark difference observed between substrates **1.76a** and **1.76j**; both compounds contain an electron-withdrawing substituent on the olefin and therefore are electronically similar, yet the non-fluorinated **1.76j** was far more reactive than **1.76a**.

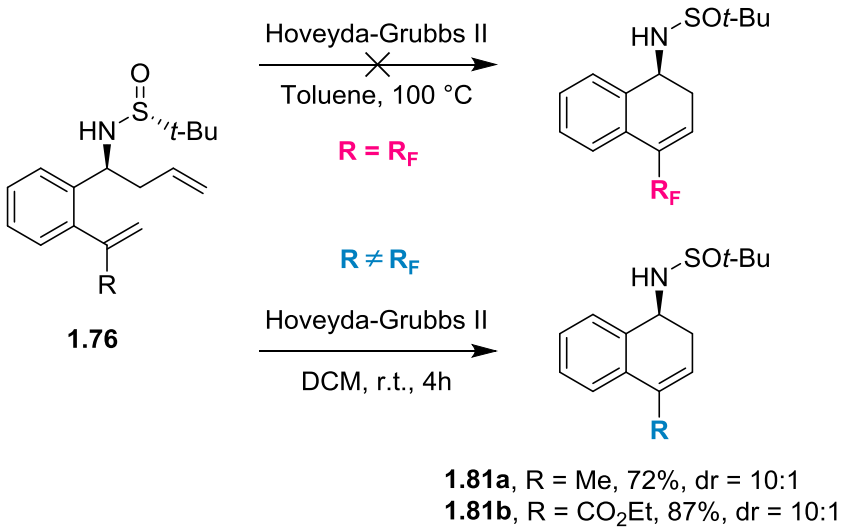

Scheme 1.28. Dramatic effect of fluorinated groups on the RCM reaction.

In summary, a new approach to the synthesis of 1-amino-4-fluoroalkyl-1,2-dihydronaphthalene derivatives from readily available *ortho*-fluoroalkylvinyl benzaldehydes has been developed, with a particular emphasis on those bearing trifluoromethyl substituents. Additionally, we have studied the deactivating effect of such fluoroalkyl substitution on RCM reactions. We can conclude that α-fluoroalkylated styrenes are much less reactive than their corresponding non-fluorinated α- substituted counterparts, and this deactivation is much more pronounced than for common electron-withdrawing groups, such as esters.

1.4. Conclusions.

We have successfully carried out an asymmetric allylation/RCM sequence to synthesise enantioenriched fluorinated 1-amino-1,2-dihydronaphthalenes, using *N-tert*-butylsulfinamide as a chiral auxiliary in order to achieve high diastereoselectivities in the allylation step.

Furthermore, we have studied substituent effects in the RCM reaction; olefins containing fluorinated groups are highly deactivated and must be forced to react at high temperatures, in contrast to comparable non-fluorinated substituents.

The dihydronaphthalene products may find uses in pharmaceutical sciences given the prominence of both fluorine chemistry and the privileged di-/tetrahydronaphthalene scaffold in pharmaceutical sciences.

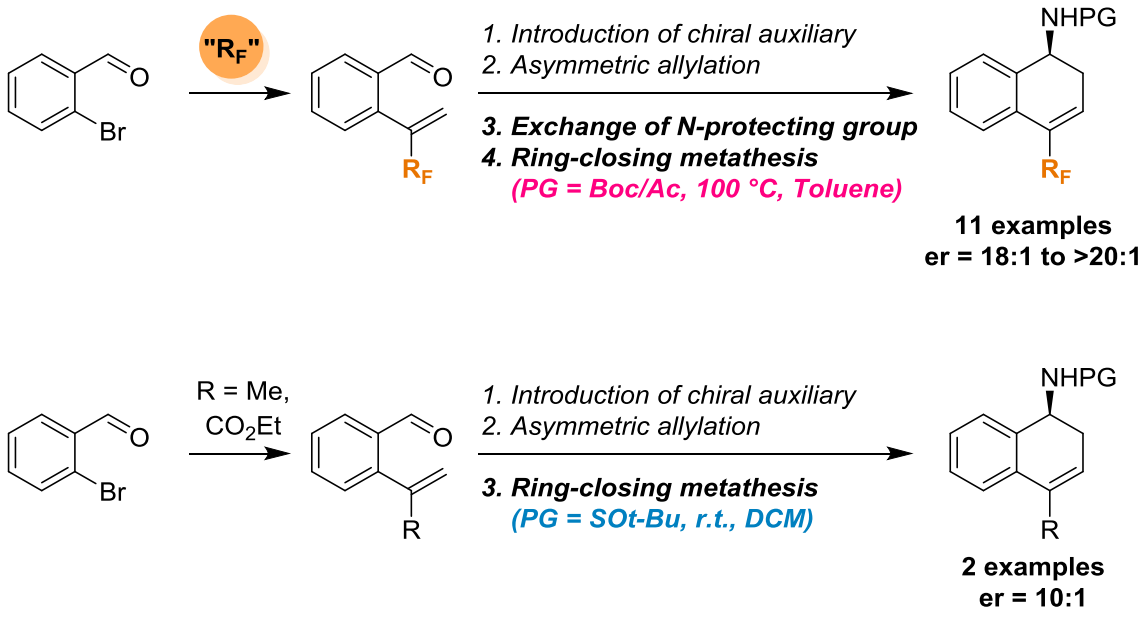

1.5. Experimental section.

Reactions were carried out under a nitrogen atmosphere unless otherwise indicated. Solvents were purified prior to use: THF and toluene were distilled from sodium and DCM from calcium hydride. The reactions were monitored with the aid of TLC on 0.25 mm pre-coated silica-gel plates. The TLC plates were revealed with with UV light and aqueous ceric ammonium molybdate solution or potassium permanganate stain. Flash column chromatography was performed with the indicated solvents on silica gel 60 (particle size: 0.040–0.063 mm). ^{1}H, ^{13}C and ^{19}F NMR spectra were recorded on a 300 MHz spectrometer. Chemical shifts are given in ppm (δ), referenced to the residual proton resonances of the solvents. Coupling constants (*J*) are given in Hertz (Hz). The letters s, d, t, q and m stand for singlet, doublet, triplet, quartet and multiplet respectively. The letters br indicate that the signal is broad.

1.5.1. Synthesis of (2-formyl)-α-trifluoromethyl styrenes.

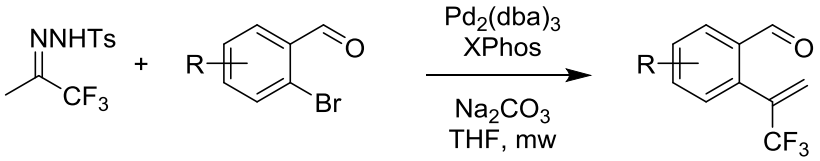

1.49 **1.54** **1.55**

A 5-mL microwave glass vial was charged with $Pd_2(dba)_3$ (4 mol%, 0.07 mmol), Xphos (8 mol%, 0.09 mmol), Na_2CO_3 (2.2 equiv, 2.37 mmol) and *N*-tosylhydrazone **1.49** (1.40 mmol, 1.3 equiv), which was previously prepared from 1,1,1- trifluoromethyl ketone (1 equiv, 22 mmol) and tosylhydrazide (1 equiv, 22 mmol) by heating at 70 °C in EtOH (0.5 M) for 5h and then filtering the precipitate solid at room temperature as a crystalline white solid. The solid reagents were dried together under reduced pressure before being used. THF (0.3 M) and the corresponding *o*-bromobenzaldehyde **1.54** (1.08 mmol) were added. The vial was sealed and the mixture was heated by microwave irradiation at 100 °C for 90 minutes. The reaction mixture was cooled to room temperature, opened, filtered through Celite and concentrated under reduced pressure. The residue obtained was purified by flash column chromatography and used immediately for the next condensation reaction. Due to the instability of the aldehyde products, we were unable to obtain HRMS measurements for some derivatives.

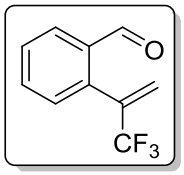

2-(3,3,3-Trifluoro-1-propen-2-yl)benzaldehyde, 1.55a

Flash chromatography of the crude reaction product [*n*-hexane-Et_2O (30:1)] afforded **1.55a** as a yellow oil (73%, 200 mg). The spectroscopic data of **1.55a** are consistent with those described in the literature.[48]

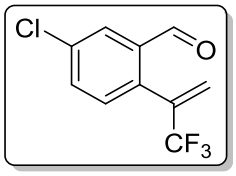

5-Chloro-2-(3,3,3-trifluoro-1-propen-2-yl)benzaldehyde, 1.55b

Flash chromatography of the crude reaction product [*n*-hexane-Et_2O (30:1)] afforded **1.55b** as a yellow oil (69%, 250 mg).

^{1}H NMR ($CDCl_3$, 300 MHz): δ 5.64 (q, *J*= 3.0 Hz, 1H), 6.32 (q, *J*= 3.0 Hz, 1H), 7.36 (dd, *J*= 3.0, 1.5 Hz, 1H), 7.59 (dd, *J*= 8.4, 2.4 Hz, 1H), 7.97 (d, *J*= 3.0 Hz, 1H), 10.07 (s, 1H) ppm.

^{13}C NMR ($CDCl_3$, 75.5 MHz): δ 122.3 (q, *J*= 273.9 Hz, CF_3), 125.6 (q, *J*= 4.7 Hz, C), 128.2 (CH), 132.1 (CH), 133.6 (CH), 134.4 (q, *J*= 30.2 Hz, C), 134.4 (q, *J*= 30.2 Hz, C), 134.7 (C), 136.0 (C), 136.3 (C), 189.4 (C) ppm.

^{19}F NMR ($CDCl_3$, 282.4 MHz): δ -67.5 (s, 3F) ppm.

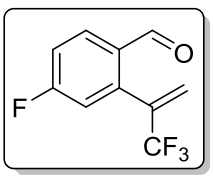

4-Fluoro-2-(3,3,3-trifluoro-1-propen-2-yl)benzaldehyde, 1.55c

Flash chromatography of the crude reaction product [*n*-hexane-Et_2O (30:1)] afforded **1.55c** as a colourless oil (59%, 220 mg).

[48] B. Jiang and Y. Xu, *J. Org. Chem*., 1991, **56**, 7336-7340.

^{1}H NMR ($CDCl_3$, 300 MHz): δ 5.67 (q, *J*= 2.7 Hz, 1H), 6.32 (q, *J*= 3.0 Hz, 1H), 7.12 (dd, *J*= 8.7, 2.4 Hz, 1H), 7.28-7.21 (m, 2H), 8.05 (dd, *J*= 8.7, 5.7 Hz, 1H), 10.05 (s, 1H) ppm.

^{13}C NMR ($CDCl_3$, 75.5 MHz): δ 117.1 (d, *J*= 21.7 Hz, CH), 117.8 (d, *J*= 23.0 Hz, CH), 122.1 (q, *J*=273.8 Hz, CF_3), 125.7 (q, *J*= 4.8 Hz, C), 131.2 (d, *J*= 9.9 Hz, CH), 131.5 (d, *J*= 2.8 Hz, CH), 134.4 (q, *J*= 32.5 Hz, C), 139.1 (d, *J*= 9.4 Hz, CH), 165.2 (d, *J*= 264.2 Hz, CF), 189.0 (C) ppm.

^{19}F NMR ($CDCl_3$, 282.4 MHz): δ -103.15 (m, 1F), -66.4 (s, 3F) ppm.

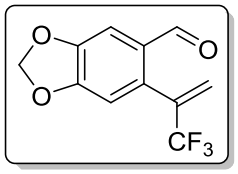

6-(3,3,3-Trifluoro-1-propen-2-yl)benzo[d][1,3]dioxole-5-carbaldehyde, 1.55d

Flash chromatography of the crude reaction product [*n*-hexane-Et_2O (20:1)] afforded **1.55d** as a yellow solid (71%, 200 mg), with a melting point of 74-76 °C.

^{1}H NMR ($CDCl_3$, 300 MHz): δ 4.74 (q, *J*= 1.2 Hz, 1H), 5.22 (s, 2H), 5.41 (q, *J*= 1.5 Hz, 1H), 5.94 (s, 1H), 6.56 (s, 1H), 9.06 (s, 1H) ppm.

^{13}C NMR ($CDCl_3$, 75.5 MHz): δ 102.4 (CH_2), 106.7 (CH), 110.6 (CH), 125.3 (q, *J*= 273.8 Hz, CF_3), 125.7 (q, *J*= 4.8 Hz, C), 130.4 (C), 133.5 (C), 134.6 (q, *J*= 31.9 Hz, CH_2), 149.0 (C), 152.1 (C), 189.0 (C) ppm.

^{19}F NMR ($CDCl_3$, 282.4 MHz): δ -67.6 (s, 3F) ppm.

HRMS (EI) calcd. for $C_{11}H_8F_3O_3$ [$M+H^+$]: 245.0420, found: 245.0416.

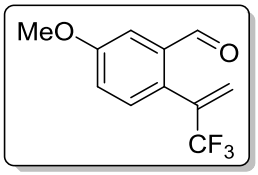

5-Methoxy-2-(3,3,3-trifluoro-1-propen-2-yl)benzaldehyde, 1.55e

Flash chromatography of the crude reaction product [*n*-hexane-Et_2O (20:1)] afforded **1.55e** as a yellow oil (73%, 300 mg).

^{1}H NMR ($CDCl_3$, 300 MHz): δ 3.88 (s, 3H), 5.58 (q, *J*= 1.2 Hz, 1H), 6.37 (q, *J*= 1.5 Hz, 1H), 7.16 (dd, *J*= 8.7, 3.0 Hz, 1H), 7.32 (d, *J*= 8.7 Hz, 1H), 7.48 (d, *J*= 3.0 Hz, 1H), 10.08 (s, 1H) ppm.

^{13}C NMR ($CDCl_3$, 75.5 MHz): δ 55.6 (CH_3), 111.0 (CH), 120.9 (CH), 122.5 (q, *J*= 273.9 Hz, CF_3), 125.3 (q, *J*= 4.8 Hz, CH_2), 129.3 (CH), 131.9 (CH), 134.9 (q, *J*= 32.1 Hz, C), 136.1 (C), 160.3 (C), 190.7 (C) ppm.

^{19}F NMR ($CDCl_3$, 282.4 MHz): δ -67.6 (s, 3F) ppm.

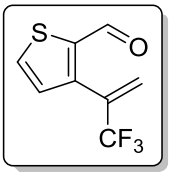

3-(3,3,3-Trifluoro-1-propen-2-yl)thiophene-2-carbaldehyde, 1.55f

Flash chromatography of the crude reaction product [*n*-hexane-Et_2O (20:1)] afforded **1.55f** as a yellow oil (94%, 500 mg).

^{1}H NMR ($CDCl_3$, 300 MHz): δ 5.74 (q, *J*= 1.5 Hz, 1H), 6.27 (q, *J*= 1.5 Hz, 1H), 7.16-7.19 (m, 1H), 7.72 (dd, *J*= 4.8, 1.2 Hz, 1H), 9.85 (d, *J*= 1.5 Hz, 1H) ppm.

^{13}C NMR ($CDCl_3$, 75.5 MHz): δ 122.1 (q, *J*= 273.8 Hz, CF_3), 126.1 (q, *J*= 5.1 Hz, CH_2), 129.5 (C), 131.9 (q, *J*= 32.5 Hz, C), 134.1 (C), 141.4 (C), 142.2 (C), 182.9 (C) ppm.

^{19}F NMR ($CDCl_3$, 282.4 MHz): δ -67.0 (s, 3F) ppm.

HRMS (EI) calcd. for $C_8H_6F_3OS$ [$M+H^+$]: 207.0086, found: 207.0081.

1.5.2. Synthesis of **1.55g**.

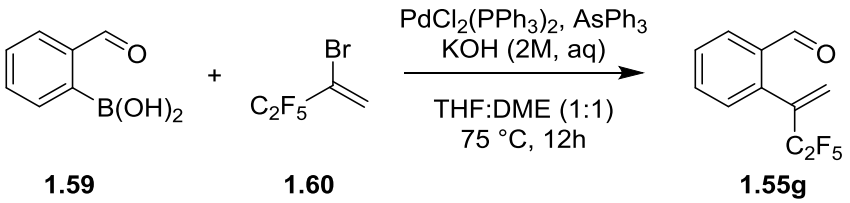

1.59 **1.60** **1.55g**

To a solution of **1.60** (1.3 equiv, 0.87 mmol) in THF:DME (1:1, 2 ml) and aq. 2 M KOH (1.3 ml), phenylboronic acid **1.59** (1 equiv, 0.67 mmol), $PdCl_2(PPh_3)_2$ (3 mol%, 0.02 mmol), and $AsPh_3$ (15 mol% equiv, 0.1 mmol) were added under an inert atmosphere in a sealed tube. The mixture was stirred at 75 °C for 12h. The mixture was cooled to room temperature, water (5 ml) was added, and the mixture was extracted with Et_2O (2 × 10 ml). The combined organic layers were washed with brine and dried over anhydrous sodium sulphate. The solvent was removed and the crude residue was used immediately in the next condensation reaction.

1.5.3. Synthetic route towards **1.55h**.

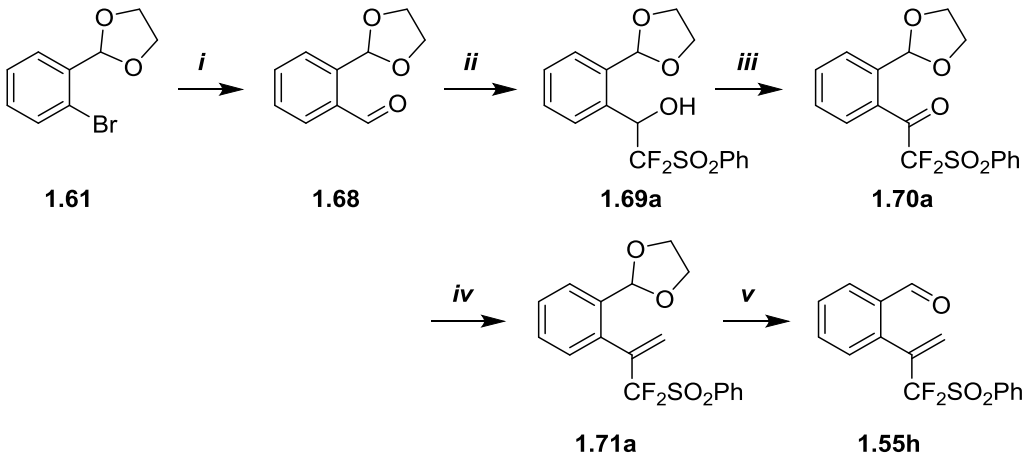

1.61 **1.68** **1.69a** **1.70a** **1.71a** **1.55h**

i. Formylation reaction. In a round-bottomed flask, 2-bromobenzaldehyde ethylene acetal **1.61** (5 mmol, 1 equiv) was dissolved in anhydrous THF (25 ml) and cooled to -78 °C. Then a solution of *n*-BuLi (2.6 M in hexane, 7.5 mmol, 1.5 equiv) was added dropwise and stirred for 1h at the same temperature. Then, *N*,*N*-dimethyl formamide (7.5 mmol, 1.5 equiv) was added dropwise and the reaction mixture was allowed to warm up to 0 °C. The reaction was quenched with a saturated solution of ammonium chloride and the mixture was extracted with diethyl ether. The organic phase was

subsequently washed with brine, dried over anhydrous sodium sulfate, and the solvent was evaporated *in vacuo.* No further purification was necessary.

ii. Sulfone addition. The crude reaction mixture from the previous step (883 mg, 4.96 mmol) was dissolved in THF (24 ml), and $PhSO_2CF_2H$ (0.9 ml, 5.95 mmol) was added, and the mixture was cooled to -78 °C. At this temperature, LiHMDS (1M in THF, 6.5 ml, 6.5 mmol) was added dropwise and the mixture was stirred for 15h. Saturated aqueous ammonium chloride was then added at -78 °C and the residue was brought to room temperature and extracted with diethyl ether. The combined organic layers were dried over $MgSO_4$ and the solvent was evaporated under reduced pressure. Flash chromatography of the crude reaction mixture [*n*-hexane-EtOAc (4:1)] afforded **1.69a** as a colourless oil (55%, 1.2 g).

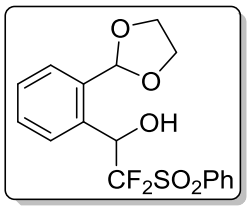

1-[2-(1,3-Dioxolan-2-yl)phenyl]-2,2-difluoro-2-(phenylsulfonyl)-1-ethanol, 1.69a.

^{1}H NMR ($CDCl_3$, 300 MHz): δ 3.63 (br, 1H), 4.00-4.07 (m, 2H), 4.12-4.20 (m, 2H), 5.95 (s, 1H), 6.22 (d, *J*= 22.5 Hz, 1H), 7.35-7.42 (m, 2H), 7.55-7.62 (m, 3H), 7.71-7.76 (m, 2H), 8.02 (d, *J*= 7.5 Hz, 2H) ppm.

^{13}C NMR ($CDCl_3$, 75.5 MHz): δ 65.1 (CH_2), 65.2 (CH_2), 66.2 (dd, *J*= 27.2, 18.4 Hz, CH), 102.1 (CH), 120.7 (dd, *J*= 299.9, 289.4 Hz, CF_2), 126.9 (CH), 128.8 (CH), 128.9 (CH), 129.2 (CH), 129.5 (CH), 130.7 (CH), 132.9 (C), 139.0 (C), 135.4 (CH), 135.8 (C) ppm.

^{19}F NMR ($CDCl_3$, 282.4 MHz): δ -119.1 (ddd, *J*= 238.3 Hz, 22.6, 1.9 Hz, 1F), -103.0 (d, *J*= 238.3 Hz, 1F).

HRMS (EI) calcd. for $C_{17}H_{20}F_2NO_5S$ [M+NH_4^+]: 388.1025, found: 388.1025.

iii. Oxidation reaction. To a solution of **1.69a** (626 mg, 1.69 mmol) in DCM (17 ml), $NaHCO_3$ (20 mg) and Dess-Martin periodinane were added (907 mg, 2.03 mmol) at room temperature. The reaction mixture was stirred at room temperature for 2h and was then filtered through Celite and the filtrate was washed with water and saturated aq. $NaHCO_3$. The combined organic layers were dried over anhydrous sodium sulphate and the solvent was evaporated under reduced pressure. The crude product was purified by column chromatography [hexane:EtOAc (4:1)] to afford **1.70a** as a colourless oil (82%, 520 mg).

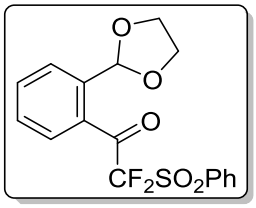

1-[2-(1,3-Dioxolan-2-yl)phenyl]-2,2-difluoro-2-(phenylsulfonyl)-1-ethanone, 1.70a

^{1}H NMR ($CDCl_3$, 300 MHz): δ 3.74-3.82 (m, 2H), 3.85-3.93 (m, 2H), 6.12 (s, 1H), 7.50-7.55 (m, 3H), 7.60-7.69 (m, 3H), 7.76-7.81 (m, 1H), 7.99-8.02 (m, 2H) ppm.

^{13}C NMR ($CDCl_3$, 75.5 MHz): δ 64.5 (CH_2), 101.5 (CH), 114.7 (t, *J*= 303.4 Hz, CF_2), 126.9 (CH), 127.9 (CH), 129.0 (CH), 129.3 (CH), 130.9 (CH), 131.5 (CH), 132.8 (C), 133.1 (C), 135.8 (CH), 138.6 (C), 190.2 (t, *J*= 25.2 Hz, C) ppm.

^{19}F NMR ($CDCl_3$, 282.4 MHz): δ -105.5 (s, 2F) ppm.

HRMS (EI) calcd. for $C_{17}H_{18}F_2O_5SN$ [M+NH_4^+]: 386.0874, found: 386.0870.

iv. Wittig methylenation. Ketone **1.70a** was subjected to the same conditions as described previously for Wittig methylenation (*see ii. Wittig methylenation, Section 1.6.3*).

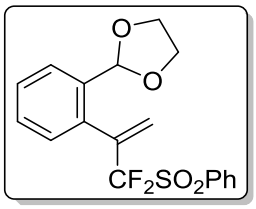

2-{2-[3,3-Difluoro-3-(phenylsulfonyl)-1-propen-2-yl]phenyl}-1,3-dioxolane, 1.71a

Flash chromatography [*n*-hexane-EtOAc (6:1)] afforded **1.71a** as a colourless oil (67%, 235 mg).

^{1}H NMR ($CDCl_3$, 300 MHz): δ 3.97-4.16 (m, 4H), 5.88 (s, 1H), 5.96 (t, *J*= 0.9 Hz, 1H), 6.37 (t, *J*= 1.5 Hz, 1H), 7.37-7.46 (m, 3H), 7.55-7.60 (m, 2H), 7.65-7.75 (m, 2H), 7.97 (d, *J*= 7.20 Hz, 2H) ppm.

^{13}C NMR ($CDCl_3$, 75.5 MHz): δ 65.4 (CH_2), 101.5 (CH), 120.4 (t, *J*= 288.3 Hz, CF_2), 126.8 (CH), 128.7 (CH), 128.9 (CH), 129.1 (CH), 129.95 (t, *J*= 6.8 Hz, CH_2), 130.3 (CH), 130.8 (CH), 132.9 (C), 133.8 (C), 134.6 (t, *J*= 22.1 Hz, C), 135.1 (CH), 136.7 (C) ppm.

^{19}F NMR ($CDCl_3$, 282.4 MHz): δ -97.7 (br, 2F; CF_2) ppm.

HRMS (EI) calcd. for $C_{18}H_{20}F_2O_4SN$ [M+NH_4^+]: 384.1081, found: 384.1076.

v. Acetal deprotection. Wittig product **1.71a** was subjected to the same conditions as described previously for Wittig methylenation (*see iii. Acetal deprotection, Section 1.6.3*).

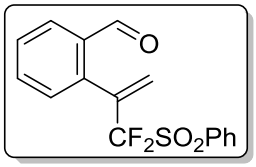

2-[3,3-Difluoro-3-(phenylsulfonyl)-1-propen-2-yl]benzaldehyde, 1.55h

Flash chromatography [*n*-hexane-EtOAc (7:1)] afforded **1.55h** as a white solid (95%, 260 mg) with a melting point of 120-122 °C.

^{1}H NMR ($CDCl_3$, 300 MHz): δ 5.91 (t, *J*= 0.9 Hz, 1H), 6.42 (t, *J*= 1.5 Hz, 1H), 7.54-7.60 (m, 5H), 7.72-7.78 (m, 1H), 7.94-7.99 (m, 3H), 10.18 (s, 1H) ppm.

^{13}C NMR ($CDCl_3$, 75.5 MHz): δ 120.1 (t, *J*= 288.9 Hz, CF_2), 129.1 (CH), 129.3 (CH), 129.4 (CH), 130.2 (t, *J*= 6.8 Hz, CH_2), 130.8 (CH), 131.7 (CH), 132.6 (C), 133.5 (CH), 134.4 (t, *J*= 22.3 Hz, C), 135.0 (C), 135.4 (CH), 136.9 (C), 191.3 (C) ppm.

^{19}F NMR ($CDCl_3$, 282.4 MHz): δ -99.3 (s, 2F) ppm.

HRMS (EI) calcd. for $C_{16}H_{16}F_2O_3SN$ [M+NH_4^+]: 340.0819, found: 340.0814.

*1.5.4. Synthesis of **1.55i**.*

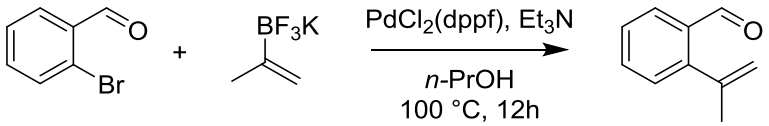

1.54 **1.72** **1.55i**

A solution of potassium isopropenyltrifluoroborate **1.72** (237 mg, 1.6 mmol), $PdCl_2$(dppf).CH_2Cl_2 (21 mg, 0.03 mmol), *o*-bromobenzaldehyde **1.54** (237 mg, 1.28 mmol), and Et_3N (0.2 ml, 1.4 mmol) in *n*-PrOH (20 ml) was heated at 100 °C under a N_2 atmosphere for 13h. Then the mixture was cooled to room temperature, and diluted with water (10 ml) followed by extraction with diethyl ether (20 ml). The ethereal layer was washed with brine (10 ml) and dried over anhydrous sodium sulphate. The solvent was removed *in vacuo*, and the crude product was purified by flash column chromatography

(hexane/DCM 30:1) affording 2-(1-propen-2-yl)benzaldehyde **1.55i** (130 mg, 0.9 mmol, 70%), whose spectroscopic data were consistent with those described in the literature.[49] This product was used immediately for the next condensation reaction.

1.5.5. Synthetic route towards ***1.55j***.

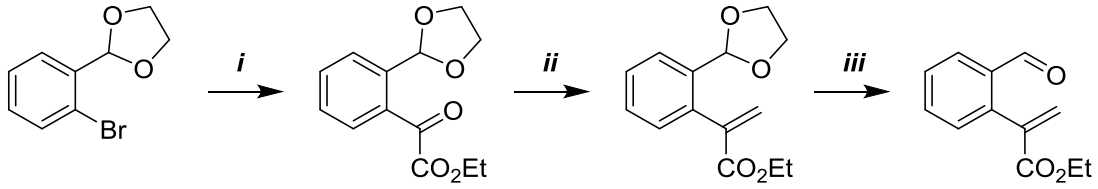

1.61 **1.73** **1.74** **1.55j**

i. Addition of diethyl oxalate. *n*-BuLi (2.5 M in *n*-hexane, 1.24 mmol, 0.5 ml) was added slowly to a solution of 2-bromobenzaldehyde ethylene acetal **1.61** (1.12 mmol, 0.2 ml) in anhydrous THF (10 ml) at -78 °C. After stirring for 1h, diethyloxalate (1.24 mmol, 0.17 ml) was added to the mixture at -78 °C. The mixture was stirred for 3h, and was subsequently quenched through addition of saturated aqueous NH_4Cl. The mixture was extracted with Et_2O and the combined organic layers were washed with brine, dried over anhydrous sodium sulphate, and concentrated under vacuum. The residue was purified by flash chromatography [*n*-hexane: Et_2O (7:1)] to afford **1.73** (188 mg, 70%), whose spectroscopic data are consistent with those described in the literature.[50]

ii. Wittig methylenation. NaHMDS (1 M in toluene, 1.4 ml, 0.822 mmol) was added dropwise to a suspension of methyl triphenylphosphonium chloride (294 mg, 0.822 mmol) in THF (4 ml) at 0 °C under nitrogen atmosphere. The resulting mixture was stirred at this temperature for 45 mins, after which a solution of **1.73** (525 mg, 0.685 mmol) in THF (4 ml) was slowly added. The reaction mixture was stirred at room temperature until **1.73** was no longer detectable by TLC (approximately 12h). The reaction mixture was then hydrolysed with a saturated solution of NH_4Cl (3 ml) and extracted with EtOAc (3 × 10 mL). The organic layer was washed with brine (2 × 5 ml), dried over anhydrous sodium sulphate, and concentrated *in vacuo* to give a yellow oil, which was purified by means of column chromatography on silica gel [*n*-hexane-EtOAc (10:1)] to afford ethyl 2-[2-(1,3-dioxolan-2-yl)phenyl]acrylate as a colourless oil (60%, 120 mg).

[49] S. Basak, D. Mal, *Tetrahedron*, 2016, **72**, 1758-1772.
[50] K. Tanaka, M. Katsurada, F. Ohno, Y. Shiga and M. Oda, *J. Org. Chem.*, 2000, **65**, 432-437.

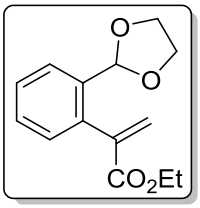

Ethyl 2-[2-(1,3-dioxolan-2-yl)phenyl]acrylate, 1.74

^{1}H NMR (CD_3OD, 300 MHz): δ 1.24 (t, *J*= 7.2 Hz, 3H), 3.91-3.93 (m, 2H), 4.00-4.03 (m, 2H), 4.19 (q, *J*= 7.2 Hz, 2H), 5.70 (d, *J*= 2.0 Hz, 1H), 5.71 (s, 1H), 6.45 (d, *J*= 2.0 Hz, 1H), 7.15-7.18 (m, 1H), 7.35-7.38 (m, 2H), 7.53-7.56 (m, 1H) ppm.

^{13}C NMR (CD_3OD, 75.5 MHz): δ 14.5 (CH_3), 62.2 (CH_2), 64.4 (CH_2), 102.9 (CH), 127.7 (CH), 128.1 (CH_2), 128.9 (CH), 129.4 (CH), 131.4 (CH), 137.4 (C), 138.0 (C), 143.1 (C), 168.2 (C) ppm.

HRMS (EI) calcd. for $C_{14}H_{17}O_4$ [$M+H^+$]: 249.1121, found: 249.1114.

iii. Acetal deprotection. To a solution of the previous product (420 mg, 1.15 mmol) in acetone (6 ml) at 0 °C, I_2 (one bead) was added and the mixture was stirred at this temperature for 5h. After this time, the solvent was removed under reduced pressure and the residue was purified by flash chromatography [*n*-hexane-EtOAc (7:1)] affording **1.55j** as a colourless oil (77%, 150 mg), whose spectroscopic data are consistent with those described in the literature.[51]

[51] a) S. W. Youn, H. S. Song and J. H. Park, *Org. Lett*., 2014, **16**, 1028. b) T. Minami, T. Isonaka and Y. Okada, J. Ichikawa, *J. Org. Chem*., 1993, **58**, 7009-7015.

1.5.6. Synthesis of tert-butanesulfinyl imines.

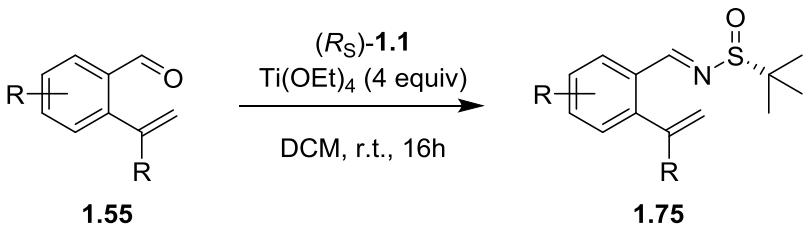

A solution of the corresponding aldehyde **1.55** (5 mmol, 1.0 equiv) and $Ti(OEt)_4$ (5.0 equiv) in anhydrous DCM (0.1 M) was stirred for 5 minutes at room temperature. To the resulting solution, (*R*)-*N*-*tert*-butanesulfinamide **1.1** was added, and the mixture was stirred at room temperature for 12h. After this time, saturated aqueous $NaHCO_3$ was added until white titanium salts precipitated. The suspension was filtered through a short pad of Celite, washing with small portions of DCM. The filtrate was extracted with ethyl acetate and the combined organic layers were washed with brine, dried over anhydrous sodium sulphate, and concentrated under vacuum. The residue was purified by flash chromatography to afford imines **1.75**. Neither of the non-fluorinated products **1.75i** or **1.75j** required further purification and were used immediately in the following allylation step.

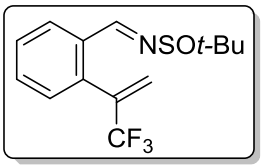

(R_S-*E*)-**2-Methyl-*N*-[2-(3,3,3-trifluoro-1-propen-2-yl)benzylidene]propane-2-sulfinamide, 1.75a**

Flash chromatography of the crude reaction product [*n*-hexane-Et_2O (5:1)] afforded **1.75a** as a yellow oil (98%, 525 mg). $[\alpha]_D^{25}$ = -13.9 (c 1.0; $CHCl_3$).

^{1}H NMR ($CDCl_3$, 300 MHz): δ 1.25 (s, 9H), 5.56 (q, *J*= 1.2 Hz, 1H), 6.25 (q, *J*= 1.5 Hz, 1H), 7.36-7.39 (m, 1H), 7.50-7.53 (m, 2H), 8.10-8.13 (m, 1H), 8.71 (s, 1H) ppm.

^{13}C NMR ($CDCl_3$, 75.5 MHz): δ 22.6 (CH_3), 57.9 (C), 122.5 (q, *J*= 274.3 Hz, CF_3), 124.9 (q, *J*= 5.0 Hz, CH_2), 128.4 (CH), 129.3 (CH), 130.5 (CH), 131.6 (CH), 132.9 (C), 135.6 (C), 135.9 (q, *J*= 31.7 Hz, C), 160.8 (CH) ppm.

^{19}F NMR ($CDCl_3$, 282.4 MHz): δ -67.3 (s, 3F) ppm.

HRMS (EI) calcd. for $C_{14}H_{17}F_3NOS$ [$M+H^+$]: 304.0977, found: 304.0982.

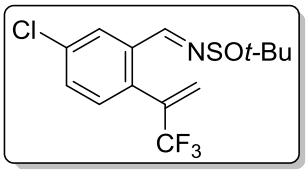

(*R*$_S$-*E*)-***N*-[5-Chloro-2-(3,3,3-trifluoro-1-propen-2-yl)benzylidene]-2-methylpropane-2-sulfinamide, 1.75b**

Flash chromatography of the crude reaction product [*n*-hexane-Et_2O (5:1)] afforded **1.75b** as a pale yellow solid (81%, 400 mg), with a melting point of 49-51 °C. $[\alpha]_D^{25}$ = -85.1 (c 1.0; $CHCl_3$).

^{1}H NMR ($CDCl_3$, 300 MHz): δ 1.25 (s, 9H), 5.57 (q, *J*= 3.0 Hz, 1H), 6.28 (q, *J*= 3.0 Hz, 1H), 7.33 (d, *J*= 9.0 Hz, 1H), 7.48 (dd, *J*= 8.4, 2.4 Hz, 1H), 8.08 (d, *J*= 3.0 Hz, 1H), 8.63 (s, 1H) ppm.

^{13}C NMR ($CDCl_3$, 75.5 MHz): δ 22.6 (CH_3), 58.2 (C), 122.3 (q, *J*= 271.8 Hz, CF_3), 125.7 (q, *J*= 4.0 Hz, CH_2), 125.7 (C), 128.1 (CH), 131.6 (CH), 131.8 (CH), 133.7 (C), 134.4 (C), 135.8 (C), 134.9 (q, *J* =31.9 Hz, C), 159.6 (CH) ppm.

^{19}F NMR ($CDCl_3$, 282.4 MHz): δ -67.4 (s, 3F) ppm.

HRMS (EI) calcd. for $C_{14}H_{16}F_3NOS$ [M+H$^+$]: 338.0588, found: 228.0582.

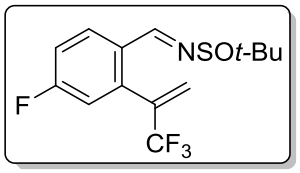

(*R*$_S$-*E*)-***N*-[4-Fluoro-2-(3,3,3-trifluoro-1-propen-2-yl)benzylidene]-2-methylpropane-2-sulfinamide, 1.75c**

Flash chromatography of the crude reaction product [*n*-hexane-Et_2O (5:1)] afforded **1.75c** as a white solid (87%, 425 mg) with a melting point of 46-48 °C. $[\alpha]_D^{25}$ = -116.94 (c 1.0; $CHCl_3$).

^{1}H NMR ($CDCl_3$, 300 MHz): δ 1.24 (s, 9H), 5.60 (q, *J*= 1.20 Hz, 1H), 6.29 (q, *J*= 1.5 Hz, 1H), 7.09 (dd, *J*= 8.7, 2.4 Hz, 1H), 7.18-7.25 (m, 1H), 8.14 (dd, *J*= 9.0, 6.0 Hz, 1H), 8.64 (s, 1H) ppm.

^{13}C NMR ($CDCl_3$, 75.5 MHz): δ 22.4 (CH_3), 57.8 (C), 117.0 (d, *J*= 21.7 Hz, CH), 117.8 (d, *J*= 20.7 Hz, CH), 122.2 (q, *J*= 273.8 Hz, CF_3), 125.6 (q, *J*= 5.1 Hz, CH_2), 129.4 (q, *J*= 5.0 Hz, C), 131.3 (d, *J*= 9.9 Hz, CH), 131.5 (d, *J*= 2.8 Hz, CH), 134.6 (q, *J*= 31.9 Hz, C), 137.6 (d, *J*= 8.9 Hz, C), 159.5 (CH), 164.1 (d, *J*= 256.7 Hz, CF) ppm.

^{19}F NMR ($CDCl_3$, 282.4 MHz): δ -67.3 (s, 3F), -106.7 (s, 1F) ppm.

HRMS (EI) calcd. for $C_{14}H_{16}F_4NOS$ [M+H$^+$]: 322.0883, found: 322.0875.

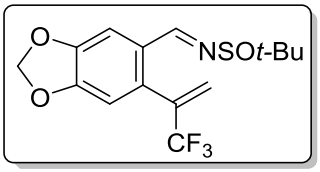

(R_S-*E*)-**2-Methyl-*N*-{[6-(3,3,3-trifluoro-1-propen-2-yl)benzo[d][1,3]dioxol-5-yl] methylene}propane-2-sulfinamide, 1.75d**

Flash chromatography of the crude reaction product [*n*-hexane-Et_2O (5:1)] afforded 4d as a white solid (96%, 300 mg) with a melting point of 58-60 °C. $[\alpha]_D^{25}$ = -50.3 (c 1.0; $CHCl_3$).

^{1}H NMR ($CDCl_3$, 300 MHz): δ 1.23 (s, 9H), 5.55 (q, *J*= 1.5 Hz, 1H), 6.07 (d, *J*= 1.2 Hz, 1H), 6.08 (d, *J*= 1.2 Hz, 1H), 6.25 (q, *J*= 1.2 Hz, 1H), 6.81 (s, 1H), 7.58 (s, 1H), 8.57 (s, 1H) ppm.

^{13}C NMR ($CDCl_3$, 75.5 MHz): δ 22.5 (CH_3), 57.7 (C), 102.1 (CH_2), 107.0 (CH), 109.7 (CH), 122.4 (q, *J*= 274.0 Hz, CF_3), 125.5 (q, *J*= 4.7 Hz, CH_2), 128.0 (C), 131.4 (C), 134.9 (q, *J*= 31.5 Hz, C), 148.8 (C), 150.6 (C), 159.8 (C) ppm.

^{19}F NMR ($CDCl_3$, 282.4 MHz): δ -67.4 (s, 3F) ppm.

HRMS (EI) calcd. for $C_{15}H_{17}F_3NO_3S$ [M+H$^+$]: 348.0876, found: 348.0876.

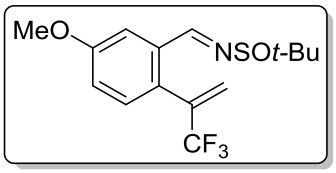

(R_S-*E*)-***N*-[5-Methoxy-2-(3,3,3-trifluoro-1-propen-2-yl)benzylidene]-2-methyl propane-2-sulfinamide, 1.75e.**

Flash chromatography of the crude reaction product [*n*-hexane-Et_2O (5:1)] afforded **1.75e** as a colourless oil (91%, 350 mg). $[\alpha]_D^{25}$ = -80.1 (c 1.0; $CHCl_3$).

^{1}H NMR ($CDCl_3$, 300 MHz): δ 1.21 (s, 9H), 3.83 (s, 3H), 5.48 (d, *J*= 1.5 Hz, 1H), 6.19 (d, *J*= 1.5 Hz, 1H), 7.02 (dd, *J*= 8.4, 2.7 Hz, 1H), 7.26 (d, *J*= 8.7 Hz, 1H), 7.58 (d, *J*= 2.7 Hz, 1H), 8.64 (s, 1H) ppm.

^{13}C NMR ($CDCl_3$, 75.5 MHz): δ 22.4 (CH_3), 55.3 (CH_3), 57.8 (C), 112.0 (CH), 118.1 (CH), 122.5 (q, *J*= 274.0 Hz, CF_3), 120.7 (C), 125.0 (q, *J*= 4.7 Hz, CH_2), 131.5 (CH), 134.0 (C), 134.0 (q, *J*= 31.5 Hz, C), 135.4 (q, *J*= 31.5 Hz, C), 159.5 (C), 160.0 (C), 160.7 (C) ppm.

^{19}F NMR ($CDCl_3$, 282.4 MHz): δ -67.0 (s, 3F) ppm.

HRMS (EI) calcd. for $C_{15}H_{19}F_3NO_2S$ [M+H$^+$]: 334.1108, found: 334.1093.

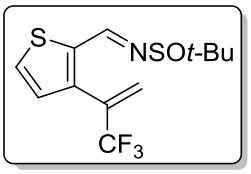

(*R*$_S$-*E*)-**2-Methyl-*N*-{[5-(3,3,3-trifluoro-1-propen-2-yl)benzo[b]thiophen-6-yl]methylene}propane-2-sulfinamide, 1.75f**

Flash chromatography of the crude reaction product [*n*-hexane-Et_2O (5:1)] afforded **1.75f** as a yellow oil (88%, 315 mg). $[\alpha]_D^{25}$ = -55.0 (c 1.0; $CHCl_3$).

^{1}H NMR ($CDCl_3$, 300 MHz): δ 1.24 (s, 9H), 5.64 (q, *J*= 1.5 Hz, 1H), 6.22 (q, *J*= 1.5 Hz, 1H), 7.13-7.16 (m, 1H), 7.55 (dd, *J*= 5.4, 1.2 Hz, 1H), 8.63 (s, 1H) ppm.

^{13}C NMR ($CDCl_3$, 75.5 MHz): δ 22.5 (CH_3), 58.2 (C), 120.4 (C), 125.7 (q, *J*= 5.1 Hz, CH_2), 129.1 (CH), 131.4 (CH), 131.9 (q, *J*= 32.2 Hz, C), 138.5 (C), 139.2 (C), 154.2 (CH) ppm.

^{19}F NMR ($CDCl_3$, 282.4 MHz): δ -66.9 (s, 3F) ppm.

HRMS (EI) calcd. for $C_{12}H_{15}F_3NOS_2$ [M+H$^+$]: 310.0542, found: 310.0545.

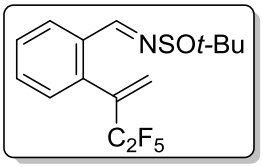

(*R*$_S$-*E*)-**2-Methyl-*N*-[2-(3,3,4,4,4-pentafluoro-1-buten-2-yl)benzylidene]propane-2-sulfinamide, 1.75g**

Flash chromatography of the crude reaction product [*n*-hexane-Et_2O (5:1)] afforded **1.75g** as a colourless oil (66%, 100 mg). $[\alpha]_D^{25}$ = - 60.2 (c 1.0; $CHCl_3$).

^{1}H NMR ($CDCl_3$, 300 MHz): δ 1.23 (s, 9H), 5.71 (br, 1H), 6.28 (br, 1H), 7.30-7.33 (m, 1H), 7.47-7.50 (m, 2H), 8.09-8.12 (m, 1H) ppm.

^{13}C NMR ($CDCl_3$, 75.5 MHz): δ 22.5 (CH_3), 57.8 (C), 113.1 (tq, *J*= 255.4, 38.1 Hz, CF_2), 119.1 (qt, *J*= 286.9, 38.1 Hz, CF_3), 127.9 (t, *J*= 7.6 Hz, CH_2), 128.4 (CH), 129.3 (CH), 130.8 (CH), 131.5 (CH), 132.9 (C), 135.4 (t, *J*= 23.1 Hz, C), 139.9 (C), 160.8 (CH) ppm.

^{19}F NMR ($CDCl_3$, 282.4 MHz): δ -114.4 (q, *J*= 57.8 Hz, 2F), -83.0 (t, *J*= 2.0 Hz, 3F) ppm.

HRMS (EI) calcd. for $C_{15}H_{17}F_5NOS$ [M+H$^+$]: 354.0946, found: 354.0948.

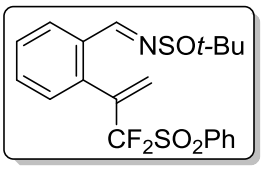

(*R*$_S$-*E*)-***N*-[2-(3,3-Difluoro-3-phenylsulfonyl-1-propen-2-yl)benzylidene]-2-methylpropane-2-sulfinamide, 1.75h**

Flash chromatography of the crude reaction product [*n*-hexane-EtOAc (5:1)] afforded **1.75h** as a colourless oil (52%, 120 mg). $[\alpha]_D^{25}$ = - 16.3 (c 1.0; $CHCl_3$).

^{1}H NMR ($CDCl_3$, 300 MHz): δ 1.21 (s, 9H), 5.86 (t, *J*= 0.9 Hz, 1H), 6.32 (t, *J*= 1.5 Hz, 1H), 7.47-7.61 (m, 5H), 7.70-7.76 (m, 1H), 7.95-8.06 (m, 3H), 8.71 (s, 1H) ppm.

^{13}C NMR ($CDCl_3$, 75.5 MHz): δ 22.5 (CH_3), 57.8 (C), 120.18 (t, *J*= 289.1 Hz, CF_2), 128.7 (CH), 129.2 (*C*H), 129.3 (CH), 129.9 (t, *J*= 6.7 Hz, CH_2), 130.8 (CH), 131.7 (CH), 132.7 (C), 133.0 (C), 135.2 (t, *J*= 22.3 Hz, C), 135.3 (CH), 136.1 (C), 161.3 (CH) ppm.

^{19}F NMR ($CDCl_3$, 282.4 MHz): δ -99.8 (br s, 1F), -98.3 (br s, 1F) ppm.

HRMS (EI) calcd. For $C_{20}H_{22}F_2NO_3S_2$ [M+H$^+$]: 426.1005, found: 426.1000.

1.5.7. General procedure for the asymmetric allylation/crotylation reaction.

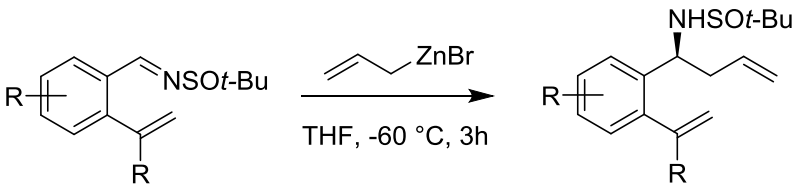

1.75 **1.76**

A 1 M solution of allylzinc/crotylzinc bromide in THF was prepared by stirring allyl/crotyl bromide (1.0 equiv) and activated Zn (3.0 equiv) in anhydrous THF (1 M) at 55 °C. This freshly prepared solution (1.1 equiv, 0.55 mmol) was then added to a solution of imine **1.75** (1.0 equiv, 0.5 mmol) in THF (0.1 M) at -60 °C. After stirring for 3h at -60 °C the reaction mixture was quenched with saturated aqueous NH_4Cl and extracted with EtOAc. Flash column chromatography afforded compounds **1.76**.

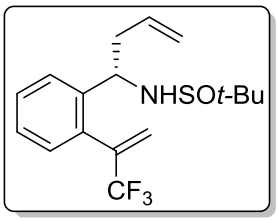

(R_S)-2-Methyl-*N*-{(*S*)-1-[2-(3,3,3-trifluoro-1-propen-2-yl)phenyl]-3-buten-1-yl} propane-2-sulfinamide, 1.76a

Flash chromatography of the crude reaction product [*n*-hexane-EtOAc (5:1)] afforded **1.76a** as a colourless oil (95%, 250 mg). $[\alpha]_D^{25}$ = - 225.8 (c 1.0; $CHCl_3$).

^{1}H NMR ($CDCl_3$, 300 MHz): δ 1.09 (s, 9H), 2.24-2.50 (m, 2H), 3.69 (br, 1H), 4.54-4.59 (m, 1H), 5.10-5.16 (m, 2H), 5.66 (d, *J*= 3.0 Hz, 1H), 5.62-5.76 (m, 1H), 6.14 (q, *J*= 3.0 Hz, 1H), 7.17-7.22 (m, 2H), 7.33-7.41 (m, 2H) ppm.

^{13}C NMR ($CDCl_3$, 75.5 MHz): δ 22.6 (CH_3), 43.1 (CH_2), 52.4 (CH), 55.6 (C), 119.4 (CH_2), 122.8 (q, *J*= 271.8 Hz, CF_3), 124.2 (q, *J*= 4.9 Hz, CH_2), 127.2 (CH), 127.7 (CH), 129.1 (CH), 129.9 (CH), 133.3 (C), 134.5 (CH), 136.6 (q, *J*= 31.1 Hz, C), 140.8 (C) ppm.

^{19}F NMR ($CDCl_3$, 282.4 MHz): δ -67.5 (s, 3F) ppm.

HRMS (EI) calcd. for $C_{17}H_{23}F_3NOS$ [M+H$^+$]: 346.1447, found: 346.1437.

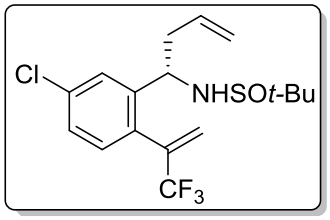

(R_S)-*N*-{(*S*)-1-[5-Chloro-2-(3,3,3-trifluoro-1-propen-2-yl)phenyl]-3-buten-1-yl}-2-methylpropane-2-sulfinamide, 1.76b

Flash chromatography of the crude reaction product [*n*-hexane-EtOAc (5:1)] afforded **1.76b** as a colourless oil (99%, 230 mg). $[\alpha]_D^{25}$ = - 57.5 (c 1.0; $CHCl_3$).

^{1}H NMR ($CDCl_3$, 300 MHz): δ 1.18 (s, 9H), 2.27-2.36 (m, 1H), 2.49-2.57(m, 1H), 3.76 (s, 1H), 4.60 (ddd, *J*= 6.0, 3.0, 0.5 Hz, 1H), 5.19-5.25 (m, 2H), 5.68-5.81 (m, 2H), 6.23 (dd, *J*= 3.0, 3.0 Hz, 1H), 7.18 (d, *J*= 9.0 Hz, 1H), 7.26-7.29 (m, 1H), 7.45 (d, *J*= 3.0 Hz, 1H) ppm.

^{13}C NMR ($CDCl_3$, 75.5 MHz): δ 22.5 (CH_3), 42.9 (CH_2), 52.2 (CH), 55.8 (C), 119.8 (CH_2), 122.5 (q, *J*= 203.8 Hz, CF_3), 124.8 (q, *J*= 4.8 Hz, CH_2), 127.5 (CH), 128.1 (CH), 131.3 (CH), 131.6 (C), 133.9 (CH), 135.7 (q, *J*= 31.5 Hz, C), 142.9 (C) ppm.

^{19}F NMR ($CDCl_3$, 282.4 MHz): δ -67.5 (s, 3F) ppm.

HRMS (EI) calcd. for $C_{17}H_{22}ClF_3NOS$ [M+H$^+$]: 380.1057, found: 380.1053.

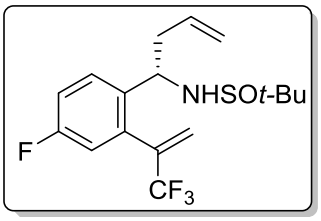

(R_S)-*N*-{(*S*)-1-[4-Fluoro-2-(3,3,3-trifluoro-1-propen-2-yl)phenyl]-3-buten-1-yl}-2-methylpropane-2-sulfinamide, 1.76c.

Flash chromatography of the crude reaction product [*n*-hexane-EtOAc (4:1)] afforded **1.76c** as colourless oil (94%, 265 mg). $[\alpha]_D^{25}$ = - 103.4 (c 1.0; $CHCl_3$).

^{1}H NMR ($CDCl_3$, 300 MHz): δ 1.15 (s, 9H), 2.27-2.38 (m, 1H), 2.46-2.52 (m, 1H), 3.75 (s, 1H), 4.57 (ddd, *J*= 5.7, 3.9, 1.5 Hz, 1H), 5.16-5.21 (m, 2H), 5.66-5.80 (m, 2H), 6.22 (q, *J*= 1.2 Hz, 1H), 6.93 (dd, *J*= 9.3, 2.7 Hz, 1H), 7.09 (dt, *J*= 8.4, 3.0 Hz, 1H), 7.43 (dd, *J*= 5.7, 2.2 Hz, 1H) ppm.

^{13}C NMR ($CDCl_3$, 75.5 MHz): δ 22.5 (CH_3), 43.1 (CH_2), 51.8 (CH), 55.6 (C), 116.4 (d, *J*= 10.1 Hz, CH), 116.7 (d, *J*= 11.0 Hz, CH), 119.5 (CH_2), 122.6 (q, *J*= 273.6 Hz, CF_3), 124.7 (q, *J*= 4.8 Hz, CH_2), 129.7 (q, *J*= 8.4 Hz, CH), 134.16 (*C*H), 135.0 (d, *J*= 8.0 Hz, C), 135.4 (q, *J*= 31.3 Hz, C), 136.6 (d, *J*= 3.1 Hz, C), 161.1 (d, *J*= 249.1 Hz, CF) ppm.

^{19}F NMR ($CDCl_3$, 282.4 MHz): δ -114.8 (ddd, *J*= 9.0, 8.2, 5.6 Hz, 1F), -67.5 (s, 3F) ppm.

HRMS (EI) calcd. for $C_{17}H_{22}F_4NOS$ [M+H$^+$]: 364.1353, found: 364.1345.

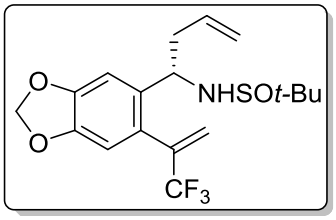

(*R*$_S$)-**2-Methyl-*N*-{(*S*)-1-[6-(3,3,3-trifluoro-1-propen-2-yl)benzo[d][1,3]dioxol-5-yl]-3-buten-1-yl}propane-2-sulfinamide, 1.76d**

Flash chromatography of the crude reaction product [*n*-hexane-EtOAc (4:1)] afforded **1.76d** as a colourless oil (89%, 225 mg). $[\alpha]_D^{25}$ = -61.6 (c 1.0; $CHCl_3$).

^{1}H NMR ($CDCl_3$, 300 MHz): δ 1.17 (s, 9H), 2.24-2.38 (m, 1H), 2.44-2.51 (m, 3H), 3.72 (s, 1H), 4.54 (ddd, *J*= 9.6, 3.9, 1.5 Hz, 1H), 5.15-5.21 (m, 2H), 5.67-5.77 (m, 2H), 5.98 (dd, *J*= 6.0, 1.2 Hz, 2H), 6.18 (q, *J*= 1.2 Hz, 1H), 6.67 (s, 1H), 6.88 (s, 1H) ppm.

^{13}C NMR ($CDCl_3$, 75.5 MHz): δ 22.5 (CH_3), 43.1 (CH_2), 52.3 (CH), 55.5 (C), 101.4 (CH_2), 107.2 (CH), 109.4 (CH), 119.3 (CH_2), 122.8 (q, *J*= 273.3 Hz, CF_3), 124.6 (q, *J*= 4.6 Hz, CH_2), 134.4 (C), 134.6 (CH), 135.0 (q, *J*= 31.2 Hz, C), 136.6 (C), 145.6 (C), 148.5 (C) ppm.

^{19}F NMR ($CDCl_3$, 282.4 MHz): δ -67.6 (s, 3F) ppm.

HRMS (EI) calcd. for $C_{18}H_{23}F_3NO_3S$ [M+H$^+$]: 390.1345, found: 390.1356.

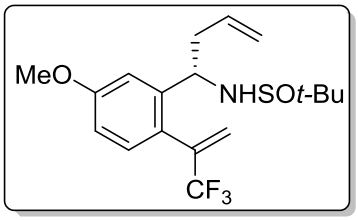

(R_S)-*N*-{(*S*)-1-[5-Methoxy-2-(3,3,3-trifluoro-1-propen-2-yl)phenyl]-3-buten-1-yl}-2-methylpropane-2-sulfinamide, 1.76e

Flash chromatography of the crude reaction product [*n*-hexane-EtOAc (4:1)] afforded **1.76e** as a white solid (92%, 280 mg), with a melting point of 60-62 °C. $[\alpha]_D^{25}$ = - 91.7 (c 1.0; $CHCl_3$).

^{1}H NMR ($CDCl_3$, 300 MHz): δ 1.18 (s, 9H), 2.28-2.40 (m, 1H), 2.50-2.57 (m, 1H), 3.73 (br, 1H), 3.81 (s, 3H), 4.60 (ddd, *J*= 9.6, 3.9, 1.8 Hz, 1H), 5.17-5.23 (m, 2H), 5.69 (q, *J*= 1.5 Hz, 1H), 5.71-5.83 (m, 1H), 6.19 (q, *J*= 1.2 Hz, 1H), 6.84 (dd, *J*= 8.4, 2.7 Hz, 1H), 6.98 (d, *J*= 2.7 Hz, 1H), 7.16 (d, *J*= 9.0 Hz, 1H) ppm.

^{13}C NMR ($CDCl_3$, 75.5 MHz): δ 22.5 (CH_3), 43.1 (CH), 52.5 (CH_2), 55.1 (CH_3), 55.6 (C), 112.9 (CH), 112.8 (CH), 119.4 (CH_2), 122.9 (q, *J*= 273.8 Hz, CF_3), 124.4 (q, *J*= 4.0 Hz, CH_2), 125.5 (C), 131.1 (CH), 134.4 (CH), 135.9 (q, *J*= 31.1 Hz, C), 142.4 (C), 160.0 (C) ppm.

^{19}F NMR ($CDCl_3$, 282.4 MHz): δ -67.7 (s, 3F) ppm.

HRMS (EI) calcd. for $C_{18}H_{25}F_3NO_2S$ [$M+H^+$]: 376.1553, found: 376.1560.

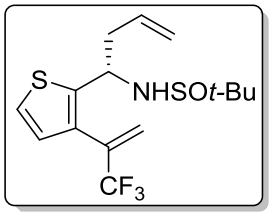

(R_S)-2-Methyl-*N*-{(*S*)-1-[5-(3,3,3-trifluoro-1-propen-2-yl)benzo[b]thiophen-6-yl]-3-buten-1-yl}propane-2-sulfinamide, 1.76f

Flash chromatography of the crude reaction product [*n*-hexane-EtOAc (4:1)] afforded **1.76f** as a colourless oil (58%, 450 mg). $[\alpha]_D^{25}$ = - 75.7 (c 1.0; $CHCl_3$).

^{1}H NMR ($CDCl_3$, 300 MHz): δ 1.20 (s, 9H), 2.42-2.53 (m, 1H), 2.57-2.64 (m, 1H), 3.79 (s, 1H), 4.78-4.83 (m, 1H), 5.16-5.22 (m, 2H), 5.78-5.80 (m, 1H), 5.64-5.77 (m, 1H), 6.12 (q, *J*= 1.5 Hz, 1H), 6.93 (dd, *J*= 5.4, 1.2 Hz, 1H), 7.28 (d, *J*= 4.8 Hz, 1H) ppm.

^{13}C NMR ($CDCl_3$, 75.5 MHz): δ 22.9 (CH_3), 44.9 (CH_2), 50.9 (CH), 55.8 (C), 117.2 (C), 119.8 (C), 120.2 (CH_2), 124.3 (q, *J*= 5.1 Hz, CH_2), 125.2 (CH), 128.2 (CH), 132.5 (q, *J*= 31.6 Hz, C), 133.9 (CH), 145.2 (C) ppm.

^{19}F NMR ($CDCl_3$, 282.4 MHz): δ -67.3 (s, 3F) ppm.

HRMS (EI) calcd. for $C_{15}H_{21}F_3NOS_2$ [M+H$^+$]: 352.1011, found: 52.1008.

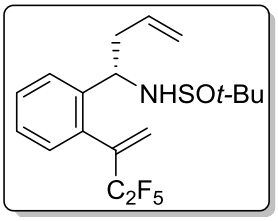

(*R*$_S$)-2-Methyl-*N*-{(*S*)-1-[2-(3,3,4,4,4-pentafluoro-1-buten-2-yl)phenyl]-3-buten-1-yl}propane-2-sulfinamide, 1.76g

Flash chromatography of the crude reaction product [*n*-hexane-EtOAc (5:1)] afforded **1.76g** as a white solid (90%, 180 mg), with a melting point of 59-61 °C. $[\alpha]_D^{25}$ = - 90.2 (c 1.0; $CHCl_3$).

^{1}H NMR ($CDCl_3$, 300 MHz): δ 1.15 (s, 9H), 2.32-2.40 (m, 1H), 2.51-2.58 (m, 1H), 3.78 (br, 1H), 4.56-4.61 (m, 1H), 5.17-5.24 (m, 2H), 5.50-5.83 (m, 1H), 5.88 (s, 1H), 6.23 (s, 1H), 7.17-7.19 (m, 1H), 7.24-7.30 (m, 1H), 7.36-7.47 (m, 2H) ppm.

^{13}C NMR ($CDCl_3$, 75.5 MHz): δ 22.5 (CH_3), 42.9 (CH_2), 52.6 (CH), 55.6 (C), 108.8-125.0 (C_2F_5), 119.4 (CH_2), 127.1 (CH), 127.6 (t, *J*= 7.7 Hz, CH_2), 127.7 (CH), 129.1 (CH), 130.1 (CH), 133.8 (C), 134.5 (CH), 140.9 (C) ppm.

^{19}F NMR ($CDCl_3$, 282.4 MHz): δ -112.8 (d, *J*= 181.3 Hz, 2F), -82.7 (s, 3F) ppm.

HRMS (EI) calcd. for $C_{18}H_{23}F_5OSN$ [M+H$^+$]: 396.1415, found: 396.1422.

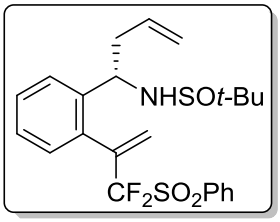

(*R*$_S$)-*N*-{(*S*)-1-[2-(3,3-Difluoro-3-(phenylsulfonyl)-1-propen-2-yl)phenyl]-3-buten-1-yl}-2-methylpropane-2-sulfinamide , 1.76h

Flash chromatography of the crude reaction product [*n*-hexane-EtOAc (2:1)] afforded **1.76h** as a colourless oil (95%, 100 mg). $[\alpha]_D^{25}$ = - 66.1 (c 1.0; $CHCl_3$).

^{1}H NMR ($CDCl_3$, 300 MHz): δ 1.16 (s, 9H), 2.30-2.41 (m, 1H), 2.61-2.65 (m, 1H), 3.79 (br s, 1H), 4.64-4.68 (m, 1H), 5.14-5.21 (m, 2H), 5.69-5.83 (m, 1H), 6.06 (br, 1H), 6.42 (t, *J*= 1.5 Hz, 1H), 7.18-7.47 (m, 4H), 7.57-7.62 (m, 2H), 7.72-7.77 (m, 1H), 7.99 (d, *J*= 7.5 Hz, 2H) ppm.

^{13}C NMR ($CDCl_3$, 75.5 MHz): δ 22.6 (CH_3), 42.9 (CH_2), 52.8 (CH), 55.6 (C), 119.2 (CH_2), 120.5 (t, *J*= 287.7 Hz, CF_2), 125.3 (C), 127.1 (CH), 127.5 (CH), 128.2 (CH), 129.0 (CH), 129.2 (CH), 130.5 (t, *J*= 6.2 Hz, CH_2), 130.6 (CH), 130.9 (CH), 132.9 (C), 134.8 (CH), 135.2 (CH), 140.8 (C) ppm.

^{19}F NMR ($CDCl_3$, 282.4 MHz): δ -99.9 (d, *J*= 219.1 Hz, 1F; CF*F*), -94.8 (d, *J*= 205.6 Hz, 1F; C*F*F) ppm.

HRMS (EI) calcd. for $C_{23}H_{28}F_2NO_3S_2$ [M+H$^+$]: 468.1469, found: 468.1468.

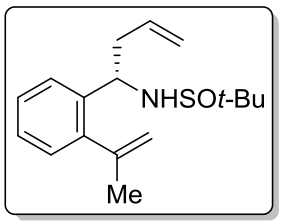

(R_S)-2-Methyl-*N*-{(*S*)-1-[2-(1-propen-2-yl)phenyl] -3-buten-1-yl}propane-2-sulfinamide, 1.76i

Flash chromatography of the crude reaction product [*n*-hexane-EtOAc (8:1)] afforded **1.76i** as a colourless oil (74% from **1.55i**, 100 mg). $[\alpha]_D^{25}$ = - 88.8 (c 1.0; $CHCl_3$).

^{1}H NMR ($CDCl_3$, 300 MHz): δ 1.11 (s, 9H), 2.04 (s, 3H), 2.27-2.55 (m, 2H), 3.59 (br, 1H), 4.66 (br, 1H), 4.81 (s, 1H), 5.08-5.12 (m, 2H), 5.18 (s, 1H), 5.59-5.74 (m, 1H), 7.04 (d, *J*= 7.0 Hz, 1H), 7.16-7.19 (m, 2H), 7.30 (d, *J*= 7.1 Hz, 1H) ppm.

^{13}C NMR ($CDCl_3$, 75.5 MHz): δ 22.5 (CH_3), 25.7 (CH_3), 43.8 (CH_2), 52.5 (CH), 55.5 (C), 115.8 (CH_2), 118.9 (CH_2), 127.0 (CH), 127.1 (CH), 128.1 (C), 134.6 (CH), 138.2 (C), 143.9 (C), 144.7 (C) ppm.

HRMS (EI) calcd. for $C_{17}H_{26}NOS$ [M+H$^+$]: 292.1730, found: 292.1722.

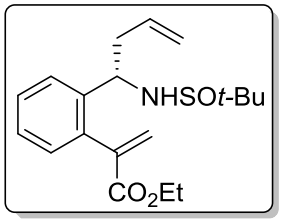

(R_S)-Ethyl 2-{2-[(1*S*)-1-[(*tert*-butylsulfinyl)amino]-3-buten-1-yl]phenyl}acrylate, 1.76j

Flash chromatography of the crude reaction product [*n*-hexane-EtOAc (3:1)] afforded **1.76j** as colourless oil (78% from **1.55j**, 39 mg). $[\alpha]_D^{25}$ = - 99.8 (c 1.0; $CHCl_3$).

^{1}H NMR ($CDCl_3$, 300 MHz): δ 1.16 (s, 9H), 1.27 (t, *J*= 8.5 Hz, 3H), 2.29-2.40 (m, 1H), 2.56-2.63 (m, 1H), 3.70 (br, 1H), 4.18-4.29 (m, 2H), 4.47-4.52 (m, 1H), 5.13-5.18 (m, 2H), 5.63-5.77 (m, 1H), 5.81 (d, *J*= 1.5 Hz, 1H), 6.61 (d, *J*= 1.5 Hz, 1H), 7.12 (dd, *J*= 7.5, 1.7 Hz, 1H), 7.27-7.28 (m, 1H), 7.31-7.37 (m, 1H), 7.44 (dd, *J*= 8.0, 1.7 Hz, 1H) ppm.

^{13}C NMR ($CDCl_3$, 75.5 MHz): δ 14.1 (CH_3), 22.6 ($3CH_3$), 42.8 (CH_2), 52.9 (CH), 55.6 (C), 61.3 (CH_2), 119.1 (CH_2), 126.9 (CH), 127.1 (CH), 128.2 (CH), 129.8 (CH), 129.9 (CH_2), 134.5 (CH), 137.0 (C), 139.9 (C), 140.4 (C), 166.4 (C) ppm.

HRMS (EI) calcd. for $C_{19}H_{28}F_3NO_3S$ [M+H$^+$]: 350.1784, found: 350.1793.

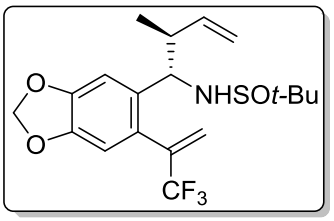

(*R*$_S$)-**2-Methyl-*N*-{(*1S*,*2S*)-2-methyl-1-[6-(3,3,3-trifluoro-1-propen-2-yl)benzo[d] [1,3]dioxol-5-yl]-3-buten-1-yl}propane-2-sulfinamide, 1.76k**

Flash chromatography of the crude reaction product [*n*-hexane-EtOAc (3:1)] afforded **1.76k** as a colourless oil (82%, 133 mg). $[\alpha]_D^{25}$ = - 71.1 (c 1.0; $CHCl_3$).

^{1}H NMR ($CDCl_3$, 300 MHz): δ 0.75 (d, *J*= 6.9 Hz, 3H), 1.15 (s, 9H), 2.28-2.41 (m, 1H), 3.98 (s, 1H), 4.21 (dd, *J*= 9.3, 0.9 Hz, 1H), 5.17-5.25 (m, 2H), 5.63-5.75 (m, 1H), 5.93 (d, *J*= 1.2 Hz, 1H), 5.99 (dd, *J*= 4.5, 1.5 Hz, 2H), 6.21 (q, *J*= 1.5 Hz, 1H), 6.72 (d, *J*= 0.9 Hz, 1H), 6.82 (s, 1H) ppm.

^{13}C NMR ($CDCl_3$, 75.5 MHz): δ 16.9(CH_3), 22.6 ($3CH_3$), 47.5 (CH), 55.6 (C), 56.4 (CH), 101.5 (CH_2), 107.4 (CH), 108.9(CH), 117.7(CH_2), 121.1 (q, *J*= 273.3 Hz, CF_3), 124.6 (C), 125.6 (q, *J*= 4.9 Hz, CH_2), 132.9 (C), 135.6 (q, *J*= 30.7 Hz, C), 146.7 (C), 141.6 (CH), 148.5 (C) ppm.

^{19}F NMR ($CDCl_3$, 282.4 MHz): δ -65.5 (s, 3F) ppm.

HRMS (EI) calcd. for $C_{19}H_{25}F_3NO_3S$ [M+H$^+$]: 404.1502, found: 404.1523.

1.5.8. General procedure for protecting group exchange.

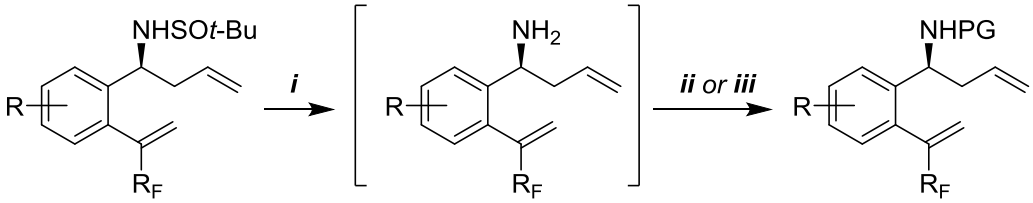

1.76

1.77, PG = Boc
1.78, PG = Ac

i. Removal of the chiral auxiliary. Hydrogen chloride (2.9 mmol, 4.0 equiv, 4M in 1,4-dioxane) was added to a solution of the corresponding sulfinyl amine (0.73 mmol, 1.0 equiv) in MeOH (1 M) at room temperature. After 45 minutes the deprotection was complete and the solution was concentrated to dryness. The residue was re-dissolved in DCM (5 ml) and 2M NaOH was added and extracted three times with DCM. The combined organic layers were dried over anhydrous sodium sulphate. Solvents were removed under reduced pressure and the crude reaction mixture was used in the next protection step without further purification.

ii. N-Boc-protection. The crude deprotection product was dissolved in anhydrous 1,4-dioxane (0.2 M) and treated with K_2CO_3 (1.8 mmol, 2.5 equiv) and di-*tert*-butyl dicarbonate (Boc_2O) (0.9 mmol, 1.1 equiv), and the resulting mixture was stirred at 50 °C overnight. The suspension was then filtered through a short pad of Celite and washed with small portions of ethyl acetate. Solvents were removed under reduced pressure and the residue was purified by means of flash chromatography on silica gel affording the desired product.

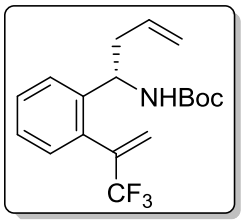

***tert*-Butyl** (*S*)-**{1-[2-(3,3,3-trifluoro-1-propen-2-yl)phenyl]-3-buten-1-yl}carbamate, 1.77a**

Flash chromatography of the crude reaction product [*n*-hexane-Et_2O (30:1)] afforded **1.77a** as a white solid (83%, 100 mg), with a melting point of 30-32 °C. $[\alpha]_D^{25}$ = - 18.5 (c 1.0; $CHCl_3$).

^{1}H NMR ($CDCl_3$, 300 MHz): δ 1.39 (s, 9H), 2.41-2.47 (m, 2H), 4.78 (br, 1H), 4.92 (br, 1H), 5.04- 5.12 (m, 2H), 5.60-5.74 (m, 2H), 6.20 (d, *J*= 3.0 Hz, 1H), 7.25-7.38 (m, 2H) ppm.

^{13}C NMR ($CDCl_3$, 75.5 MHz): δ 28.3 (CH_3), 41.0 (CH_2), 50.4 (CH), 50.5 (CH), 79.4 (C), 118.8 (CH_2), 122.9 (q, *J*= 271.8 Hz, CF_3), 124.4 (q, *J*= 2.2 Hz, CH_2), 125.9 (CH), 126.8 (CH), 129.2 (CH), 130.1 (CH), 132.5 (C), 134.0 (CH), 141.5 (C), 154.7 (C) ppm.

^{19}F NMR ($CDCl_3$, 282.4 MHz): δ -67.0 (s, 3F) ppm.

HRMS (EI) calcd. for $C_{18}H_{23}F_3NO_2$ [M+H$^+$]: 342.1675, found: 342.1673.

HPLC (Chiralcel OD-H, 98:2 hexane/*i*-PrOH, 1 ml min^{-1}, 240 nm) R_T (major) = 5.00 min, R_T (minor) = 4.56 min.

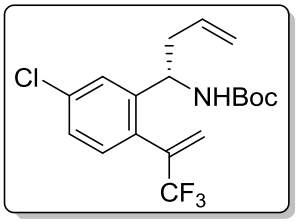

***tert*-Butyl (*S*)-{1-[5-chloro-2-(3,3,3-trifluoro-1-propen-2-yl)phenyl]-3-buten-1-yl} carbamate, 1.77b**

Flash chromatography of the crude reaction product [*n*-hexane-Et_2O (30:1)] afforded **1.77b** as a colourless oil (55%, 90 mg). $[\alpha]_D^{25}$ = - 38.2 (c 1.0; $CHCl_3$).

^{1}H NMR ($CDCl_3$, 300 MHz): δ 1.40 (s, 9H), 2.30-2.48 (m, 2H), 4.83-4.89 (m, 2H), 5.09-5.14 (m, 2H), 5.60-5.71 (m, 1H), 5.74 (br, 1H), 6.23 (d, *J*= 1.5 Hz, 1H), 7.18 (d, *J*= 9.0 Hz, 1H), 7.23 (dd, *J*= 9.0, 3.0 Hz, 1H), 7.35 (d, *J*= 3.0 Hz, 1H) ppm.

^{13}C NMR ($CDCl_3$, 75.5 MHz): δ 28.3 (CH_3), 40.9 (CH_2), 50.5 (d, *J*= 1.4 Hz, CH), 79.7 (C), 118.6 (CH_2), 122.7 (q, *J*= 273.8 Hz, CF_3), 125.2 (q, *J*= 4.7 Hz, CH_2), 126.3 (CH), 127.0 (CH), 130.7 (C), 131.3 (CH), 133.5 (CH), 135.2 (C), 135.7 (C), 143.9 (C), 154.7 (C) ppm.

^{19}F NMR ($CDCl_3$, 282.4 MHz): δ -66.9 (s, 3F) ppm.

HRMS (EI) calcd. for $C_{14}H_{15}ClF_3NO_2$ [M-(*t*-Bu)+H$^+$]: 320.0660, found: 320.0658.

HPLC (Chiralcel OD-H, 98:2 hexane/*i*-PrOH, 1 ml min^{-1}, 240 nm) R_T (major) = 4.01 min, R_T (minor) = 4.24 min.

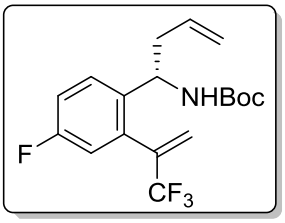

***tert*-Butyl (*S*)-{1-[4-fluoro-2-(3,3,3-trifluoro-1-propen-2-yl)phenyl]-3-buten-1-yl} carbamate, 1.77c**

Flash chromatography of the crude reaction product [*n*-hexane-Et_2O (20:1)] afforded **1.77c** as a pale yellow oil (68%, 105 mg). $[\alpha]_D^{25}$ = - 12.2 (c 1.0; $CHCl_3$).

^{1}H NMR ($CDCl_3$, 300 MHz): δ 1.38 (s, 9H), 2.37-2.46 (m, 2H), 4.81-4.89 (m, 2H), 5.04-5.11 (m, 2H), 5.58-5.22 (m, 1H), 5.78 (br, 1H), 6.23 (d, *J*= 1.5 Hz, 1H), 6.95 (dd, *J*= 9.3, 2.7 Hz, 1H), 7.07 (dd, *J*= 8.1, 2.7 Hz, 1H), 7.33 (dd, *J*= 8.7, 3.4 Hz, 1H) ppm.

^{13}C NMR ($CDCl_3$, 75.5 MHz): δ 28.3 (CH_3), 41.0 (CH_2), 50.1 (CH), 75.5 (C), 116.2 (d, *J*= 21.0 Hz, CH), 116.7 (d, *J*= 22.1 Hz, CH), 118.3 (CH_2), 122.7 (q, *J*= 273.9 Hz, CF_3), 125.0 (d, *J*= 2.0 Hz, CH), 127.7 (d, *J*= 83.3 Hz, CH), 133.7 (CH), 134.2 (C), 135.5 (d, *J*= 31.5 Hz, C), 137.6 (d, *J*= 3.1 Hz, C), 154.7 (C), 160.9 (d, *J*= 271.8 Hz, CH) ppm.

^{19}F NMR ($CDCl_3$, 282.4 MHz): δ -115.7 (ddd, *J*= 14.4, 8.5, 5.6 Hz, 1F), -66.9 (s, 3F) ppm.

HRMS (EI) calcd. for $C_{18}H_{22}F_4NO_2$ [$M+H^+$]: 360.1581, found: 360.1573.

HPLC (Chiralcel OD-H, 99.5:0.5 hexane/*i*-PrOH, 1 ml min^{-1}, 240 nm) R_T (major) = 8.96 min, R_T (minor) = 9.82 min.

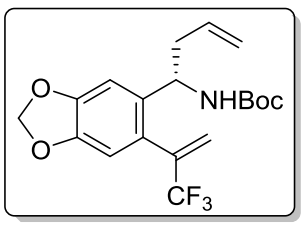

***tert*-Butyl (*S*)-{1-[6-(3,3,3-trifluoro-1-propen-2-yl)benzo[d][1,3]dioxol-5-yl]-3-buten-1-yl} carbamate, 1.77d**

Flash chromatography of the crude reaction product [*n*-hexane-Et_2O (10:1)] afforded **1.77d** as a colourless oil (67%, 120 mg). $[\alpha]_D^{25}$ = - 19.2 (c 1.0; $CHCl_3$).

^{1}H NMR ($CDCl_3$, 300 MHz): δ 1.25 (s, 9H), 2.25 (t, *J*= 6.9 Hz, 2H), 4.63-4.70 (m, 2H), 4.89-4.97 (m, 2H), 5.45-5.57 (m, 2H), 5.83 (s, 2H), 6.04 (d, *J*= 1.5 Hz, 1H), 6.55 (s, 1H), 6.68 (s, 1H) ppm.

^{13}C NMR ($CDCl_3$, 75.5 MHz): δ 28.3 (CH_3), 41.1 (CH_2), 50.7 (CH), 79.4 (C), 101.4 (CH_2), 105.9 (CH), 109.7 (CH), 118.0 (CH_2), 122.9 (q, *J*= 279.3 Hz, CF_3), 124.7 (q, *J*= 2.3 Hz, CH_2), 124.7 (C), 125.6 (C), 133.9 (CH), 135.8 (C), 136.3 (C), 146.7 (C), 148.4 (C), 154.7 (C) ppm.

^{19}F NMR ($CDCl_3$, 282.4 MHz): δ -66.1 (s, 3F) ppm.

HRMS (EI) calcd. for $C_{19}H_{23}F_3NO_4$ [M+H$^+$]: 386.1574, found: 386.1580.

HPLC (Chiralpak IC, 98:2 hexane/*i*-PrOH, 1 ml min^{-1}, 240 nm) R_T (major) = 7.46 min, R_T (minor) = 6.65 min.

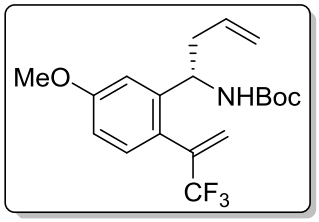

***tert*-Butyl** (*S*)**-{1-[5-methoxy-2-(3,3,3-trifluoro-1-propen-2-yl)phenyl]-3-buten-1-yl} carbamate, 1.77e**

Flash chromatography of the crude reaction product [*n*-hexane-Et_2O (10:1)] afforded **1.77e** as a colourless oil (84%, 105 mg). $[\alpha]_D^{25}$ = - 26.3 (c 1.0; $CHCl_3$).

^{1}H NMR ($CDCl_3$, 300 MHz): δ 1.39 (s, 9H), 2.34- 2.50 (m, 2H), 3.81 (s, 3H), 4.81-4.90 (m, 2H), 5.04-5.12 (m, 2H), 5.60-5.74 (m, 2H), 6.17 (d, *J*= 1.5 Hz, 1H), 6.79 (dd, *J*= 8.4, 2.7 Hz, 1H), 6.88 (d, *J*= 2.7 Hz, 1H), 7.16 (d, *J*= 8.1 Hz, 1H) ppm.

^{13}C NMR ($CDCl_3$, 75.5 MHz): δ 28.3 (CH_3), 40.9 (CH_2), 50.7 (CH), 55.2 (CH_3), 79.4 (C), 111.8 (CH), 118.0 (CH_2), 122.9 (q, *J*= 268.8 Hz, CF_3), 124.5 (q, *J*= 3.5 Hz, CH_2), 124.7 (C), 131.2 (CH), 134.0 (CH), 136.2 (d, *J*= 28.8 Hz, C), 143.1 (C), 154.7 (C), 160.1 (C) ppm.

^{19}F NMR ($CDCl_3$, 282.4 MHz): δ -66.1 (s, 3F) ppm.

HRMS (EI) calcd. for $C_{19}H_{25}F_3NO_3$ [M+H$^+$]: 372.1781, found: 372.1783.

HPLC (Chiralpak IC, 98:2 hexane/*i*-PrOH, 1 ml min^{-1}, 240 nm) R_T (major) = 6.67 min, R_T (minor) = 5.74 min.

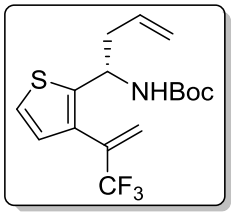

***tert*-Butyl (*S*)-{1-[3-(3,3,3-trifluoro-1-propen-2-yl)thiophen-2-yl]-3-but-3-en-1-yl} carbamate, 1.77f**

Flash chromatography of the crude reaction product [*n*-hexane-Et_2O (20:1)] afforded **1.77f** as a colourless oil (64%, 160 mg). $[\alpha]_D^{25}$ = - 4.5 (c 1.0; $CHCl_3$).

^{1}H NMR ($CDCl_3$, 300 MHz): δ 1.41 (s, 3H), 2.47-2.58 (m, 2H), 4.82 (s, 1H), 5.07-5.13 (m, 3H), 5.63-5.72 (m, 1H), 5.76 (s,1H), 6.12 (d, *J*= 1.2 Hz), 6.96 (dd, *J*= 5.1, 0.9 Hz, 1H), 7.20 (d, *J*= 5.4 Hz, 1H) ppm.

^{13}C NMR ($CDCl_3$, 75.5 MHz): δ 28.3 (CH_3), 42.0 (CH_2), 48.6 (CH), 79.8 (C), 118.6 (CH_2), 122.1 (q, *J*= 267.0 Hz, CF_3), 123.1 (CH), 123.8 (CH_2), 128.2 (CH), 130.7 (C), 133.2 (CH), 146.1 (C), 154.6 (C) ppm.

^{19}F NMR ($CDCl_3$, 282.4 MHz): δ -66.7 (s, 3F) ppm.

HRMS (EI) calcd. for $C_{16}H_{21}F_3NO_2S$ $[M+H^+]$: 348.1240, found: 348.1249.

HPLC (Chiralpcel OD-H, 98:2 hexane/*i*-PrOH, 1 ml min^{-1}, 240 nm) R_T (major) = 4.68 min, R_T (minor) = 4.37 min.

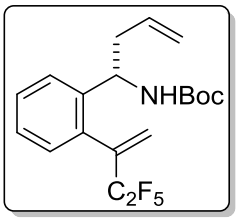

***tert*-Butyl (*S*)-{1-[2-(3,3,4,4,4-pentafluoro-1-buten-2-yl)phenyl]-3-buten-1-yl} carbamate, 1.77g**

Flash chromatography of the crude reaction product [*n*-hexane-Et_2O (10:1)] afforded **1.77g** as a colourless oil (80%, 80 mg). $[\alpha]_D^{25}$ = - 19.0 (c 1.0; $CHCl_3$).

^{1}H NMR ($CDCl_3$, 300 MHz): δ 1.32 (s, 9H), 2.38-2.40 (m, 2H), 4.69 (br, 1H), 4.79 (br, 1H), 4.96-5.02 (m, 2H), 5.56-5.64 (m, 1H), 5.75 (s, 1H), 6.14 (s, 1H), 7.11-7.13 (m, 1H), 7.16-7.20 (m, 1H), 7.28-7.33 (m, 2H) ppm.

^{13}C NMR ($CDCl_3$, 75.5 MHz): δ 28.3 (CH_3), 41.1 (CH_2), 50.8 (CH), 79.3 (C), 112.5 (tq, *J*= 251.1, 39.4 Hz, CF_2), 117.9 (CH_2), 119.4 (qt, *J*= 287.7, 36.6 Hz, CF_3), 125.9 (CH), 126.8 (CH), 127.7 (CH_2), 129.2 (CH), 130.3 (CH), 133.1 (C), 134.1 (CH), 135.9 (C), 154.6 (C) ppm.

^{19}F NMR ($CDCl_3$, 282.4 MHz): δ -112.7 (br, 2F), -82.9 (s, 3F) ppm.

HRMS (EI) calcd. for $C_{19}H_{23}F_5NO_2$ [M+H$^+$]: 392.1643, found: 392.1637.

HPLC (Chiralcel OD-H, 98:2 hexane/*i*-PrOH, 1 ml min^{-1}, 240 nm) R_T (major) = 4.68min, R_T (minor) = 4.28 min.

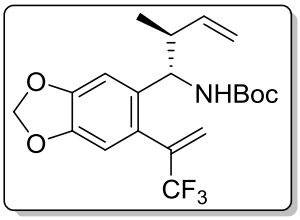

***tert*-Butyl {(*1S,2S*)-2-methyl-1-[6-(3,3,3-trifluoro-1-propen-2-yl)benzo[d][1,3] dioxol-5-yl]-3-buten-1-yl}carbamate, 1.77h**

Flash chromatography of the crude reaction product [*n*-hexane-Et_2O (10:1)] afforded **1.77h** as a colourless oil (74%, 95 mg). $[\alpha]_D^{25}$ = - 39.8 (c 1.0; $CHCl_3$).

^{1}H NMR ($CDCl_3$, 300 MHz): δ 0.89 (d, *J*= 6.9 Hz, 3H), 1.38 (s, 9H), 2.44 (dd, *J*= 21.0, 13.8 Hz, 1H), 4.7 (s, 2H), 5.11-5.04 (m, 2H), 5.83-5.71 (m, 2H), 5.96 (dd, *J*= 3.3, 1.2 Hz, 2H), 6.19 (s, 1H), 6.72 (s, 1H), 6.76 (s, 1H) ppm.

^{13}C NMR ($CDCl_3$, 75.5 MHz): δ 17.2 (CH_3), 21.5 (CH), 28.3 (CH_3), 43.9 (CH), 54.7 (CH), 79.2 (C), 101.4 (CH_2), 106.2 (CH), 109.5 (CH), 116.4 (CH_2), 122.9 (q, *J*= 274.3 Hz, CF_3), 124.7 (C), 125.4 (CH_2), 128.4 (C), 135.3 (C), 146.2 (C), 148.3 (C), 154.7 (C) ppm.

^{19}F NMR ($CDCl_3$, 282.4 MHz): δ -66.4 (s, 3F) ppm.

HRMS (EI) calcd. for $NaC_{20}H_{24}F_3NO_4$ [M+Na$^+$]: 422.1550, found: 422.1561.

HPLC (Chiralpak IC, 98:2 hexane/*i*-PrOH, 1 ml min^{-1}, 240 nm) R_T (major) = 6.50 min, R_T (minor) = 5.97 min.

iii. N-Acetyl-protection. The crude residue from the chiral auxiliary deprotection was re-dissolved in anhydrous DCM (8 ml), and Ac_2O (1.2 mmol, 1.5 equiv), Et_3N (1.62 mmol, 2 equiv) and

DMAP (0.162 mmol, 0.8 equiv) were successively added at room temperature. The mixture was stirred at room temperature for 16h. At this time, the reaction was quenched with aqueous NH_4Cl and extracted with ethyl acetate. The combined organic layers were dried over anhydrous sodium sulphate. The solvent was removed under reduced pressure and the residue was purified by means of flash chromatography on silica gel.

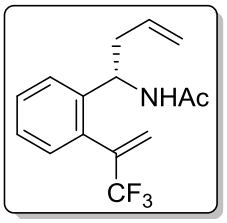

(*S*)-***N*-{1-[2-(3,3,3-Trifluoro-1-propen-2-yl)phenyl]-3-buten-1-yl}acetamide, 1.78a**

Flash chromatography of the crude reaction product [*n*-hexane-EtOAc (2:1)] afforded **1.78a** as a colourless oil (74%, 90 mg). $[\alpha]_D^{25}$ = - 41.7 (c 1.0; $CHCl_3$).

^{1}H NMR ($CDCl_3$, 300 MHz): δ 1.90 (s, 3H), 2.43-2.48 (m, 2H), 5.02-5.09 (m, 2H), 5.15-5.22 (m, 1H), 5.60-5.73 (m, 1H), 5.76 (dd, *J*= 1.3, 1.3 Hz, 1H), 5.98 (d, *J*= 7.3 Hz, 1H), 6.19 (dd, *J*= 1.5, 1.5 Hz, 1H), 7.23-7.28 (m, 2H), 7.32-7.37 (m, 2H) ppm.

^{13}C NMR ($CDCl_3$, 75.5 MHz): δ 23.1 (CH_3), 40.5 (CH_2), 49.5 (CH), 118.0 (CH_2), 123.2 (q, *J*= 275.5 Hz, CF_3), 124.6 (q, *J*= 6.0 Hz, CH_2), 126.0 (CH), 126.9 (CH), 129.1 (CH), 130.1 (CH), 132.7 (C), 134.1 (CH), 136.1 (q, *J*= 34.0 Hz, C), 141.1 (C) ppm.

^{19}F NMR ($CDCl_3$, 282.4 MHz): δ -67.0 (s, 3F) ppm.

HRMS (EI) calcd. for $C_{15}H_{17}F_3NO$ [M+H$^+$]: 284.1257, found: 284.1253.

HPLC (Chiralcel OD-H, 95:5 hexane/*i*-PrOH, 1 ml min^{-1}, 240 nm) R_T (major) = 9.52 min, R_T (minor) = 8.12 min.

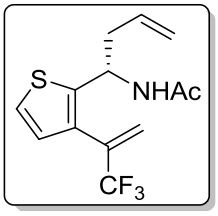

(*S*)-***N*-{1-[3-(3,3,3-Trifluoro-1-propen-2-yl)thiophen-2-yl]-3-buten-1-yl}acetamide, 1.78b**

Flash chromatography of the crude reaction product [*n*-hexane-EtOAc (2:1)] afforded **1.78b** as a colourless oil (80%, 190 mg). $[\alpha]_D^{25}$ = - 28.7 (c 1.0; $CHCl_3$).

^{1}H NMR ($CDCl_3$, 300 MHz): δ 7.18 (d, *J*= 5.2 Hz, 1H), 6.93 (dd, *J*= 5.2, 1.1 Hz, 1H), 6.26 (d, *J*= 6.9 Hz, 1H), 6.09 (dd, *J*= 1.5, 1.3 Hz, 1H), 5.77 (dd, *J*= 1.5, 1.3 Hz), 5.59-5.73 (m, 1H), 5.4 (q, *J*= 7.5 Hz, 1H), 5.11-5.03 (m, 2H), 2.62-2.44 (m, 2H), 1.02 (s, 3H) ppm.

^{13}C NMR ($CDCl_3$, 75.5 MHz): δ 22.9 (CH_3), 41.6 (CH_2), 47.7 (CH), 118.5 (CH_2), 122.8 (q, *J*= 275.5 Hz, CF_3), 123.2 (CH), 123.9 (q, *J*= 5.5 Hz, CH_2), 128.1 (CH), 131.0 (C), 132.8 (q, *J*= 32.9 Hz, C), 133.2 (CH), 145.1 (C), 169.1 (C) ppm.

^{19}F NMR ($CDCl_3$, 282.4 MHz): δ -67.2 (s, 3F) ppm.

HRMS (EI) calcd. for $C_{13}H_{15}F_3NOS$ [M+H$^+$]: 290.0821, found: 290.0831.

HPLC (Chiralcel OD-H, 95:5 hexane/*i*-PrOH, 1 ml min^{-1}, 240 nm) R_T (major) = 9.00 min, R_T (minor) = 8.14 min.

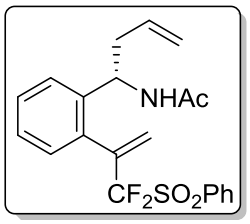

(*S*)-***N*-(1-{2-[3,3-Difluoro-3-(phenylsulfonyl) -1-propen-2-yl]phenyl}-3-buten-1-yl) acetamide, 1.78c**

Flash chromatography of the crude reaction product [*n*-hexane-EtOAc (1:1)] afforded **1.78c** as a colourless oil (72%, 90 mg). $[\alpha]_D^{25}$ = - 14.5 (c 1.0; $CHCl_3$).

^{1}H NMR ($CDCl_3$, 300 MHz): δ 1.90 (s, 3H), 2.49-2.54 (m, 2H), 5.02-5.19 (m, 3H), 5.61-5.74 (m, 2H), 6.06 (br, 1H), 6.41 (br, 1H), 7.27-7.42 (m, 3H), 7.47-7.49 (m, 1H), 7.57-7.62 (m, 2H), 7.71-7.77 (m, 1H), 7.99 (d, *J*= 7.8 Hz, 2H) ppm.

^{13}C NMR ($CDCl_3$, 75.5 MHz): δ 23.2 (CH_3), 31.5 (CH_2), 40.6 (CH_2), 50.0 (CH), 117.9 (CH_2), 120.5 (t, *J*= 172.8 Hz, CF_2), 125.8 (CH), 127.0 (CH), 129.1 (CH), 129.2 (CH), 130.7 (C), 130.9 (CH), 132.9 (C), 133.6 (C), 134.2 (CH), 135.2 (CH), 141.2 (C), 169.0 (C) ppm.

^{19}F NMR ($CDCl_3$, 282.4 MHz): δ -99.7 (s, 1F), -93.1 (s, 1F) ppm.

HRMS (EI) calcd. for $C_{21}H_{22}F_2NO_3S$ [M+H$^+$]: 406.1288, found: 406.1284.

Unfortunately, we were unable to separate the enantiomers of this compound using chiral HPLC. However, the final compound in the reaction sequence (**1.80c**) was successfully analysed and was found to have an er of >20:1.

1.5.9. General procedure for the RCM reaction.

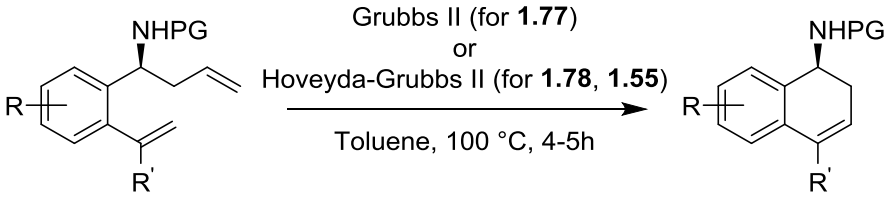

1.77, PG = Boc
1.78, PG = Ac
1.55, PG = SO*t*-Bu, R' = Me, CO_2Et

1.79, PG = Boc
1.80, PG = Ac
1.81, PG = SO*t*-Bu, R' = Me, CO_2Et

To a solution of the corresponding homoallylamine (0.4 mmol, 1.0 equiv) in toluene (for R'= R_F) or DCM (for R'= CH_3, CO_2Et) (8 ml, 0.05M), 2nd generation Grubbs catalyst (Grubbs II) (0.02 mmol, 5 mol%) (for **1.77**) or 2nd generation Hoveyda-Grubbs catalyst [Hoveyda-Grubbs II] (0.02 mmol, 5 mol%) (for **1.78** and **1.55i-j**) was added. The reaction mixture was stirred approximately 4h at 100 °C (for R'= R_F) or room temperature (for R'= CH_3, CO_2Et). After that time, the reaction mixture was concentrated under vacuum and purified by means of flash chromatography on silica gel.

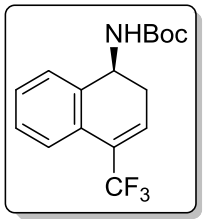

***tert*-Butyl** (*S*)-**[4-(trifluoromethyl)-1,2-dihydronaphthalen-1-yl] carbamate, 1.79a**

Flash chromatography of the crude reaction product [*n*-hexane-Et_2O (20:1)] afforded **1.79a** as a white solid (67%, 80 mg), with a melting point of 39-41 °C. $[\alpha]_D^{25}$ = - 16.3 (c 1.0; $CHCl_3$).

^{1}H NMR ($CDCl_3$, 300 MHz): δ 1.45 (s, 9H), 2.66 (br, 2H), 4.79-4.94 (m, 2H), 6.64-6.67 (m, 1H), 7.32-7.35 (m, 2H), 7.37-7.40 (m, 1H), 7.45-7.47 (m, 1H) ppm.

^{13}C NMR ($CDCl_3$, 75.5 MHz): δ 28.5 (CH_3), 29.6 (CH_2), 47.2 (CH), 79.8 (C), 123.3 (q, *J*= 273.1 Hz, CF_3), 124.6 (CH), 127.4 (C), 127.6 (CH), 128.3 (CH), 129.6 (q, *J*= 5.8 Hz, CH), 125.6 (C), 135.3 (C), 154.9 (C) ppm.

^{19}F NMR ($CDCl_3$, 282.4 MHz): δ -64.3 (s, 3F) ppm.

HRMS (EI) calcd. for $C_{16}H_{19}F_3NO_2$ [M+H$^+$]: 314.1362, found: 314.1347.

HPLC (Chiralcel OD-H, 99.5:0.5 hexane/*i*-PrOH, 1 ml min^{-1}, 240 nm) R_T (major) = 17.92 min, R_T (minor) = 16.40 min.

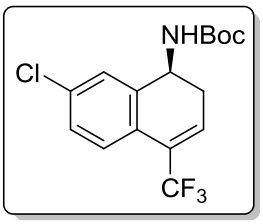

***tert*-Butyl** (*S*)**-[7-chloro-4-(trifluoromethyl)-1,2-dihydronaphthalen-1-yl] carbamate, 1.79b**

Flash chromatography of the crude reaction product [*n*-hexane- Et_2O (20:1)] afforded **1.79b** as a white solid (74%, 75 mg), with a melting point 85-87 °C. $[\alpha]_D^{25}$ = - 3.43 (c 1.0; $CHCl_3$).

^{1}H NMR ($CDCl_3$, 300 MHz): δ 1.46 (s, 9H), 2.60-2.65 (m, 2H), 4.80-4.92 (m, 2H), 6.64-6.68 (m, 2H), 7.27-7.31 (m, 1H), 7.36 (d, *J*= 1.8 Hz, 1H), 7.39 (d, *J*= 2.0 Hz, 1H) ppm.

^{13}C NMR ($CDCl_3$, 75.5 MHz): δ 28.3 (CH_3), 29.5 (CH_2), 47.1 (CH), 80.1 (C), 123.1 (q, *J*= 277.8 Hz, CF_3), 125.9 (CH), 127.4 (CH), 127.7 (C), 128.3 (CH), 129.9 (q, *J*= 5.0 Hz, CH), 134.7 (C), 137.4 (C), 154.9 (C) ppm.

^{19}F NMR ($CDCl_3$, 282.4 MHz): δ -64.5 (s, 3F) ppm.

HRMS (EI) calcd. for $C_{16}H_{18}ClF_3NO_2$ [$M+H^+$]: 348.0973, found: 348.0975.

HPLC (Chiralcel OD-H, 99:1 hexane/*i*-PrOH, 1 ml min^{-1}, 240 nm) R_T (major) = 13.45 min, R_T (minor) = 11.37 min.

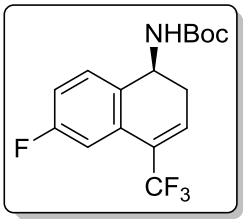

***tert*-Butyl** (*S*)**-[6-fluoro-4-(trifluoromethyl)-1,2-dihydronaphthalen-1-yl] carbamate, 1.79c**

Flash chromatography of the crude reaction product [*n*-hexane-Et_2O (20:1)] afforded **1.79c** as a colourless oil (66%, 60 mg). $[\alpha]_D^{25}$ = - 16.2 (c 1.0; $CHCl_3$).

^{1}H NMR ($CDCl_3$, 300 MHz): δ 1.44 (s, 9H), 2.57-2.74 (m, 2H), 4.76-4.91 (m, 2H), 6.72 (t, *J*= 3.3 Hz, 2H), 7.01 (ddd, *J*= 10.8, 8.4, 2.7 Hz, 1H), 7.15-7.19 (m, 1H), 7.40 (dd, *J*= 8.4, 5.7 Hz, 1H) ppm.

^{13}C NMR ($CDCl_3$, 75.5 MHz): δ 28.3 (CH_3), 29.8 (CH_2), 46.5 (CH), 79.9 (C), 111.8 (d, *J*= 2.2 Hz, CH), 112.2 (CH), 115.4 (CH), 115.7 (CH), 123.0 (q, *J*= 277.8 Hz, CF_3), 127.9 (q, *J*= 24.5 Hz, C), 129.2 (q, *J*= 7.6 Hz, C), 131.0 (C), 154.8 (C), 162.4 (d, *J*= 241.6 Hz, CF) ppm.

^{19}F NMR ($CDCl_3$, 282.4 MHz): δ -64.6 (s, 3F), -113.2 (dd, *J*= -15.2, 9.0 Hz, 1F) ppm.

HRMS (EI) calcd. for $C_{16}H_{18}F_4NO_2$ [M+H$^+$]: 332.1312, found: 332.1310.

HPLC (Chiralcel OD-H, 99:1 hexane/*i*-PrOH, 1 ml min^{-1}, 240 nm) R_T (major) = 12.44 min, R_T (minor) = 11.69 min.

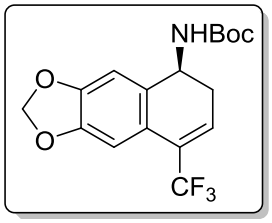

***tert*-Butyl** (*S*)-**[8-(trifluoromethyl)-5,6-dihydronaphtho[2,3-d][1,3]dioxol-5-yl] carbamate, 1.79d**

Flash chromatography of the crude reaction product [*n*-hexane-Et_2O (5:1)] afforded **1.79d** as a colourless oil (80%, 58 mg). $[\alpha]_D^{25}$ = - 2.05 (c 1.0; $CHCl_3$).

^{1}H NMR ($CDCl_3$, 300 MHz): δ 1.44 (s, 9H), 2.54-2.68 (m, 2H), 4.62-4.64 (m, 1H), 4.77 (s, 1H), 5.97 (s, 2H), 6.53-6.56 (m, 1H), 6.89 (s, 1H), 6.96 (s, 1H) ppm.

^{13}C NMR ($CDCl_3$, 75.5 MHz): δ 28.4 (CH_3), 29.6 (CH_2), 47.3 (CH), 79.8 (CH), 101.4 (CH_2), 105.4 (CH), 108.5 (C), 123.3 (q, *J*= 277.8 Hz, CF_3), 127.5 (q, *J*= 5.7 Hz, CH), 128.0 (C), 128.4 (C), 130.1 (C), 147.5 (C), 147.6 (C), 154.8 (C) ppm.

^{19}F NMR ($CDCl_3$, 282.4 MHz): δ -63.9 (s, 3F) ppm.

HRMS (EI) calcd. for $C_{17}H_{19}F_3NO_4$ [M+H$^+$]: 358.1261, found: 258.1259.

HPLC (Chiralpak IC, 98:2 hexane/*i*-PrOH, 1 ml min^{-1}, 240 nm) R_T (major) = 12.93 min, R_T (minor) = 9.66 min.

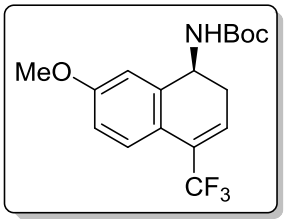

***tert*-Butyl** (*S*)-**[7-methoxy-4-(trifluoromethyl)-1,2-dihydronaphthalen-1-yl] carbamate, 1.79e**

Flash chromatography of the crude reaction product [*n*-hexane-Et_2O (7:1)] afforded **1.79e** as a white solid (77%, 53 mg), with a melting point of 80-82 °C. $[\alpha]_D^{25}$ = - 5.44 (c 1.0; $CHCl_3$)

^{1}H NMR ($CDCl_3$, 300 MHz): δ 1.45 (s, 9H), 2.61 (br, 2H), 3.83 (s, 3H), 4.78-4.86 (m, 2H), 6.49-6.52 (m, 1H), 6.84 (dd, *J*= 8.7, 2.7 Hz, 1H), 6.94 (d, *J*= 2.7 Hz, 1H), 7.40 (dd, *J*= 8.7, 1.8 Hz, 1H) ppm.

^{13}C NMR ($CDCl_3$, 75.5 MHz): δ 28.4 (CH_3), 29.6 (CH_2), 47.6 (CH), 55.4 (CH_3), 79.8 (C), 79.8 (C), 113.3 (CH), 120.3 (C), 123.4 (q, *J*= 273.0 Hz, CF_3), 126.1 (CH), 126.7 (C), 128.2 (d, *J*= 29.8 Hz, C), 137.4 (C), 154.9 (C), 159.9 (C) ppm.

^{19}F NMR ($CDCl_3$, 282.4 MHz): δ -63.9 (s, 3F) ppm.

HRMS (EI) calcd. for $C_{17}H_{21}F_3NO_3$ [M+H$^+$]: 344.1468, found: 344.1460.

HPLC (Chiralpak IC, 98:2 hexane/*i*-PrOH, 1 ml min^{-1}, 240 nm) R_T (major) = 10.54 min, R_T (minor) = 7.88 min.

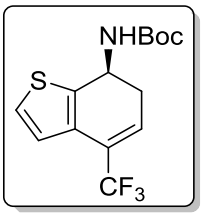

***tert*-Butyl** (*S*)-**[4-(trifluoromethyl)-6,7-dihydrobenzo[b]thiophen-7-yl] carbamate, 1.79f**

Flash chromatography of the crude reaction product [*n*-hexane-Et_2O (12:1)] afforded **1.79f** as a yellow solid (68%, 99 mg), with a melting point of 81-83 °C. $[\alpha]_D^{25}$ = - 35.4 (c 1.0; $CHCl_3$).

^{1}H NMR ($CDCl_3$, 300 MHz): δ 1.44 (s, 9H), 2.74-2.84 (m, 2H), 4.90 (br, 1H), 5.17-5.94 (m, 1H), 6.38-6.42 (m, 1H), 7.06 (dd, *J*= 5.4, 1.8 Hz), 7.24 (d, *J*= 5.1 Hz) ppm.

^{13}C NMR ($CDCl_3$, 75.5 MHz): δ 28.7 (CH_3), 31.5 (CH_2), 44.1 (CH), 80.0 (C), 117.6 (C), 121.2 (C), 124.3 (CH), 125.3 (CH), 125.5 (CH), 129.3 (C), 137.5 (C), 154.5 (C) ppm.

^{19}F NMR ($CDCl_3$, 282.4 MHz): δ -66.6 (s, 3F) ppm.

HRMS (EI) calcd. for $C_{14}H_{17}F_3NO_2S$ [M+H$^+$]: 320.0927, found: 320.0922.

HPLC (Chiralpak IC, 98:2 hexane/*i*-PrOH, 1 ml min^{-1}, 240 nm) R_T (major) = 8.08 min, R_T (minor) = 7.04 min.

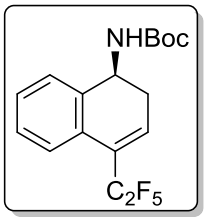

***tert*-Butyl** (*S*)**-[4-(perfluoroethyl)-1,2-dihydronaphthalen-1-yl] carbamate, 1.79g**

Flash chromatography of the crude reaction product [*n*-hexane-Et_2O (15:1)] afforded **1.79g** as a colourless oil (80%, 20 mg). $[\alpha]_D^{25}$ = - 15.8 (c 1.0; $CHCl_3$).

^{1}H NMR ($CDCl_3$, 300 MHz): δ 1.46 (s, 9H), 2.64-2.66 (m, 2H), 4.74-4.77 (m, 1H), 4.85-4.92 (m, 1H), 6.68 (t, *J*= 6.03 Hz, 1H), 7.30-7.33 (m, 2H), 7.38-7.41 (m, 1H), 7.50-7.53 (m, 1H) ppm.

^{13}C NMR ($CDCl_3$, 75.5 MHz): δ 28.4 (CH_3), 29.9 (CH_2), 47.4 (CH), 79.9 (C), 113.5-121.6 (C_2F_5), 125.4 (CH), 127.4 (CH), 127.9 (C), 128.2 (CH), 128.9 (CH), 133.3 (t, *J*= 10.0 Hz, CH), 135.7 (C), 154.9 (C) ppm.

^{19}F NMR ($CDCl_3$, 282.4 MHz) δ -111.2 (q, *J*= 285 Hz, 2F), -83.3 (s, 3F) ppm.

HRMS (EI) calcd. for $NaC_{17}H_{18}F_5NO_2$ [M+Na$^+$]: 386.1150, found: 386.1138.

HPLC (Chiralpak IC, 98:2 hexane/*i*-PrOH, 1 ml min^{-1}, 240 nm) R_T (major) = 8.20 min, R_T (minor) = 7.37 min.

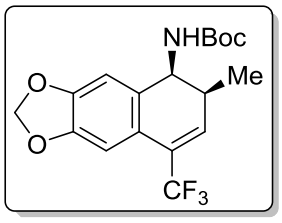

***tert*-Butyl [**(*5S,6S*)**-6-methyl-8-(trifluoromethyl)-5,6-dihydronaphtho[2,3-d][1,3] dioxol-5-yl] carbamate, 1.79h**

Flash chromatography of the crude reaction product [*n*-hexane-Et_2O (20:1)] afforded **1.79h** as a white solid (42%, 30 mg), with a melting point of 135-137 °C. $[\alpha]_D^{25}$ = - 32.5 (c 1.0; $CHCl_3$).

^{1}H NMR ($CDCl_3$, 300 MHz): δ 1.2 (d, *J*= 7.2 Hz), 1.44 (s, 9H), 2.74 (s, 1H), 4.62-4.64 (m, 1H), 4.77 (s, 1H), 5.97 (s, 2H), 6.28-6.29 (m, 1H), 6.89 (s, 1H), 6.96 (s, 1H) ppm.

^{13}C NMR ($CDCl_3$, 75.5 MHz): δ 14.2 (CH_3), 28.3 (CH_3), 32.2 (CH), 51.5 (CH), 79.7 (C), 101.4 (CH_2), 105.3 (CH), 108.6 (CH), 120.6 (C), 123.3 (q, *J*= 277.8 Hz, CF_3), 127.7 (q, *J*= 29.6 Hz, C), 131.2 (C), 133.8 (q, *J*= 8.2 Hz, CH), 147.5 (C), 147.7 (C), 155.3 (C) ppm.

^{19}F NMR ($CDCl_3$, 282.4 MHz): δ -64.3 (s, 3F) ppm.

HRMS (EI) calcd. for $C_{18}H_{21}F_3NO_4$ [M+H$^+$]: 372.1417, found: 372.1402.

HPLC (Chiralpak IC, 98:2 hexane/*i*-PrOH, 1 ml min^{-1}, 240 nm) R_T (major) = 9.49 min, R_T (minor) = 7.44 min.

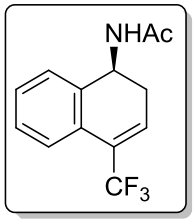

(*S*)-***N*-[4-(Trifluoromethyl)-1,2-dihydronaphthalen-1-yl]acetamide, 1.80a**

Flash chromatography of the crude reaction product [*n*-hexane-EtOAc (2:1)] afforded **1.80a** as a colourless oil (42%, 54 mg). $[\alpha]_D^{25}$ = - 2.0 (c 1.0; $CHCl_3$).

^{1}H NMR ($CDCl_3$, 300 MHz): δ 1.96 (s, 3H), 2.58-2.79 (m, 2H), 5.19-5.25 (m, 1H), 5.71 (br, 1H), 6.64-6.68 (m, 1H), 7.32-7.39 (m, 3H), 7.48-7.51 (m, 1H) ppm.

^{13}C NMR ($CDCl_3$, 75.5 MHz): δ 23.4 (CH_3), 29.2 (CH_2), 45.8 (CH), 123.5 (q, *J*= 271.1 Hz, CF_3), 124.7 (q, *J*= 2.2 Hz, CH), 127.4 (C), 128.1 (CH), 128.6 (CH), 129.1 (CH), 129.7 (q, *J*= 6.2 Hz, CH), 134.6 (C), 169.2 (C) ppm.

^{19}F NMR ($CDCl_3$, 282.4 MHz): δ -64.3 (s, 3F) ppm.

HRMS (EI) calcd. for $C_{13}H_{13}F_3NO$ [M+H$^+$]: 256.0944, found: 256.0956.

HPLC (Chiralcel OD-H, 95:5 hexane/*i*-PrOH, 1 ml min^{-1}, 240 nm) R_T (major) = 19.70 min, R_T (minor) = 15.40 min.

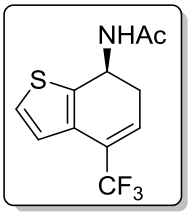

(*S*)-***N*-[4-(Trifluoromethyl)-6,7-dihydrobenzo[b]thiophen-7-yl]acetamide, 1.80b**

Flash chromatography of the crude reaction product [*n*-hexane-EtOAc (4:1)] afforded **1.80b** as a white solid (44%, 65 mg), with a melting point of 133-135 °C. $[\alpha]_D^{25}$ = - 6.5 (c 1.0; $CHCl_3$).

^{1}H NMR ($CDCl_3$, 300 MHz): δ 1.94 (s, 3H), 2.74-2.78 (m, 2H), 5.33-5.40 (m, 1H; C*H*), 5.96 (d, *J*= 9.3 Hz, 1H; N*H*), 6.39-6.42 (m, 1H; C*H*), 7.08 (dd, *J*= 5.1, 1.8 Hz, 1H; C*H*), 7.26 (d, *J*= 5.1 Hz, 1H; C*H*) ppm.

^{13}C NMR ($CDCl_3$, 75.5 MHz): δ 23.1 (CH_3), 30.7 (CH_2), 42.1 (CH), 122.5 (q, *J*= 268.4 Hz, CF_3), 123.9 (CH), 124.7 (C), 125.1 (q, *J*= 4.4 Hz, CH), 125.2 (CH), 126.1 (q, *J*= 32.4 Hz, C), 129.6 (C), 136.6 (C), 169.1 (C) ppm.

^{19}F NMR ($CDCl_3$, 282.4 MHz): δ -66.5 (s, 3F) ppm.

HRMS (EI) calcd. for $C_{11}H_{11}F_3NOS$ [$M+H^+$]: 262.0508, found: 262.0505.

HPLC (Chiralcel OD-H, 95:5 hexane/*i*-PrOH, 1 ml min^{-1}, 240 nm) R_T (major) = 20.20 min, R_T (minor) = 18.17 min.

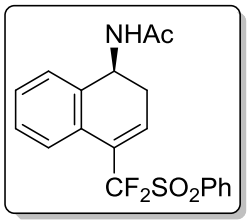

(*S*)-***N*-{4-[Difluoro(phenylsulfonyl)methyl]-1,2-dihydronaphthalen-1-yl}acetamide, 1.80c**

Flash chromatography of the crude reaction product [*n*-hexane-EtOAc (3:1)] afforded **1.80c** as a white solid (40%, 15 mg), with a melting point of 70-72 °C. $[\alpha]_D^{25}$ = - 7.45(c 1.0; $CHCl_3$).

^{1}H NMR ($CDCl_3$, 300 MHz): δ 1.94 (s, 3H), 2.57-2.63 (m, 1H), 2.79-2.86 (m, 1H), 5.19 (m, 1H), 6.13 (d, *J*= 8.1 Hz, 1H), 6.75-6.77 (m, 1H), 7.32-7.35 (m, 3H), 7.63-7.81 (m, 4H), 7.99-8.02 (m, 2H) ppm.

^{13}C NMR ($CDCl_3$, 75.5 MHz): δ 23.3 (CH_3), 29.9 (CH_2), 46.2 (CH), 122.3 (t, *J*= 288.4 Hz, CF_2), 126.1 (t, *J*= 19.4 Hz, C) 126.3-126.4 (C+CH), 127.8 (CH), 128.4 (CH), 129.1 (CH), 129.3 (CH), 130.7 (2CH), 132.9 (C), 135.1 (CH), 135.3 (CH), 136.5 (t, *J*= 10.0 Hz, C), 169.4 (C) ppm.

^{19}F NMR ($CDCl_3$, 282.4 MHz): δ 96.3 (dd, *J*= 229.0, 5.1 Hz), 99.2 (d, *J*= 228.7 Hz) ppm.

HRMS (EI) calcd. for $C_{19}H_{18}F_2NO_3S$ [M+H$^+$]: 378.0970, found: 378.0955.

HPLC (Chiralcel ODH, 80:20 hexane/*i*-PrOH, 1 ml min^{-1}, 240 nm) R_T (major) = 9.73 min, R_T (minor) = 8.45 min.

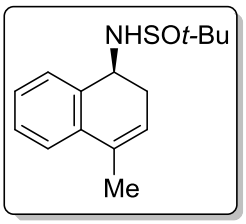

(R_S)-**2-Methyl-*N*-[(*S*)-4-methyl-1,2-dihydronaphthalen-1-yl]propane-2-sulfinamide, 1.81a**

Flash chromatography of the crude reaction product [*n*-hexane-EtOAc (2:1)] afforded **1.81a** as a colourless oil (72%, 25 mg). $[\alpha]_D^{25}$ = - 6.8 (c 1.0; $CHCl_3$).

^{1}H NMR ($CDCl_3$, 300 MHz): δ 1.14 (s, 9H), 2.04 (s, 3H), 2.50-2.71 (m, 2H), 3.36 (d, *J*= 9.0 Hz, 1H), 4.37-4.44 (m, 1H), 5.78 (br, 1H), 7.20-7.34 (m, 4H) ppm.

^{13}C NMR ($CDCl_3$, 75.5 MHz): δ 19.1 (CH_3), 22.6 (CH_3), 32.6 (CH_2), 55.0 (CH), 56.1 (C), 122.1 (CH), 123.4 (CH), 126.7 (CH), 127.2 (CH), 127.9 (CH), 132.2 (C), 134.9 (C), 135.9 (C) ppm.

HRMS (EI) calcd. for $C_{15}H_{22}NOS$ [M+H$^+$]: 264.1417, found: 264.1412.

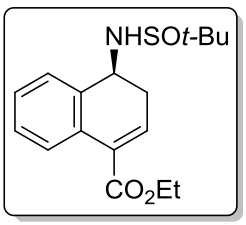

(R_S)-**Ethyl-(*4S*)-4-[(*tert*-butylsulfinyl)amino]-3,4-dihydronaphthalene-1-carboxylate, 1.81b**

Flash chromatography of the crude reaction product [*n*-hexane-EtOAc (1:1)] afforded **1.81b** as a colourless oil (87%, 15 mg). $[\alpha]_D^{25}$ = - 4.2 (c 1.0; $CHCl_3$).

^{1}H NMR ($CDCl_3$, 300 MHz): δ 1.18 (s, 9H), 1.40 (t, *J*= 7.0 Hz, 3H), 2.78-2.83 (m, 2H), 3.34 (d, *J*= 9.2 Hz, 1H), 4.32 (q, *J*= 7.0 Hz, 2H), 4.44-4.51 (m, 1H), 7.07-7.10 (m, 1H), 7.29-7.40 (m, 3H), 7.89 (d, *J*= 7.5 Hz, 1H) ppm.

^{13}C NMR ($CDCl_3$, 75.5 MHz): δ 14.2 (CH_3), 22.6 ($3CH_3$), 32.6 (CH_2), 54.1 (CH), 56.3 (C), 60.8 (CH_2), 126.7 (CH), 126.9 (CH), 128.1 (CH), 128.2 (CH), 130.0 (C), 130.7 (C), 135.6 (CH), 135.8 (C), 165.9 (C) ppm.

HRMS (EI) calcd. for $C_{17}H_{24}NO_3S$ [$M+H^+$]: 322.1471, found: 322.1473.

Chapter 2

A simple route to 1,2-fluorohydrins via 1,2-difunctionalisation of olefins

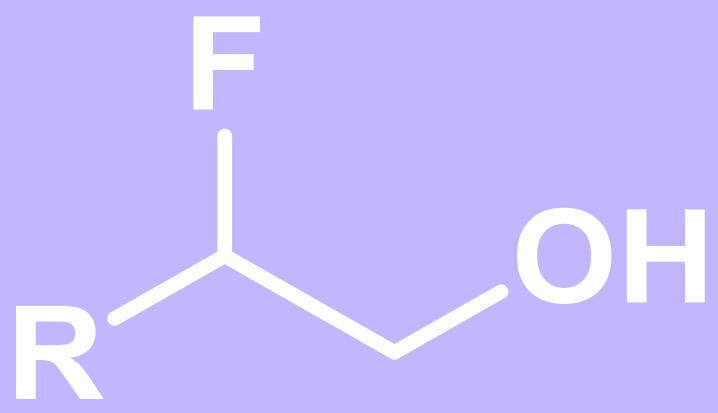

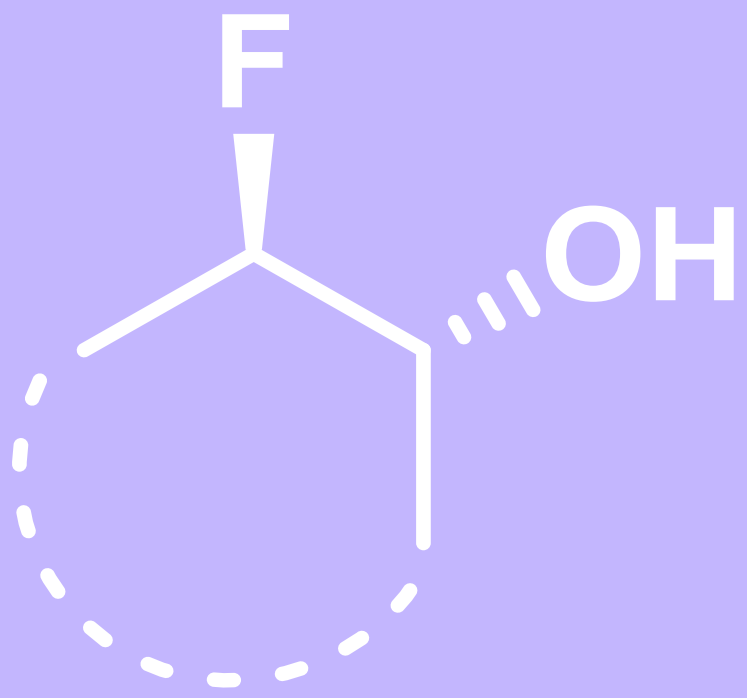

2.0. Objectives.

In this chapter we will study the possibility of a one-pot procedure for the synthesis of fluorohydrins from olefin starting materials, whereby the epoxidation and subsequent opening with HF is carried out in the same reaction sequence. To this end, the compatibility of *m*-CPBA and HF·amine reagents will need to be assured in terms of this transformation. The regioselectivity will also be studied.

This work was developed in collaboration with the group of G.B. Hammond, and a part of the scope of this project was carried out in the University of Louisville (Kentucky, USA) during a short placement (July-October 2017).

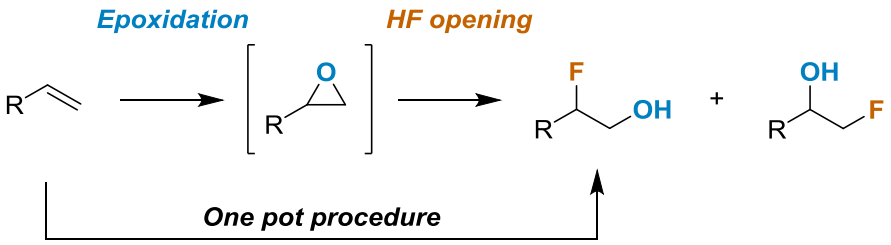

2.1. Introduction.

2.1.1. Olefin 1,2-difunctionalisation.

The 2001 Nobel Prize in Chemistry was partly awarded to Barry Sharpless "for his work on chirally catalysed oxidation reactions"; a testament to his emblematic asymmetric epoxidation and 1,2-dihydroxylation of olefins, and to the utility of olefin 1,2-difunctionalisation in general.[52] The 1,2-difunctionalisation of olefins is a powerful transformation in organic chemistry, allowing us to rapidly build molecular complexity at the expense of a double bond. Not only that, but olefins are ideal starting blocks for many organic synthetic routes, due to the following characteristics.

- They are among the cheapest and most abundant organic starting material containing useful functional groups.
- They are often tolerant of a great variety of transformations throughout a synthetic route, and can be "revealed" at will through the addition of heteroatoms.
- They are usually prochiral, providing an escape from "flatland" as well as facile access to the chiral world.[53]

Aside from hydrogenation or halogenation processes—which in themselves could be classed as formal 1,2-difunctionalisation of olefins—perhaps the first example of this illustrious transformation was the dihydroxylation of olefins reported in the 1930s by Criegee.[54] This osmium-based transformation was for years a purely stoichiometric transformation due to a lack of viable catalytic alternatives. This was clearly not ideal, given the toxicity and cost of osmium tetroxide. Criegee did, however, observe an accelerating effect when pyridine was added to the reaction media—this would later be crucial to Sharpless' studies into this transformation (Scheme 2.1, a).

Later, in the 1970s, VanRheenen and co-workers at the Upjohn Company developed the so-called Upjohn dihydroxylation, in which a tertiary amine oxide additive permitted the use of catalytic amounts of osmium tetroxide (Scheme 2.1, b).[55]

[52] K. B. Sharpless, *Angew. Chem. Int. Ed.*, 2002, **41**, 2024-2032.
[53] F. Lovering, J. Bikker and C. Humblet, *J. Med. Chem.*, 2009, **52**, 6752-6756.
[54] a) R. Criegee, *Justus Liebigs Ann. Chem.*, 1936, **522**, 75-96. b) R. Criegee, *Angew. Chem.*, 1937, **50**, 153-155. c) R. Criegee, *Angew. Chem.*, 1938, **51**, 519-520.
[55] V. VanRheenen, R. C. Kelly and D. Y. Cha, *Tetrahedron Lett.*, 1976, **23**, 1973-1976.

These studies formed the basis of Sharpless' seminal advances in the 1980s, when the group successfully developed an asymmetric version of the *cis*-dihydroxylation of alkenes using catalytic osmium tetroxide in conjunction with a cinchona alkaloid ligand to induce chirality and *N*-methylmorpholine *N*-oxide (NMO) as a terminal oxidant to regenerate the active osmium tetroxide (Scheme 2.1, c).[56]

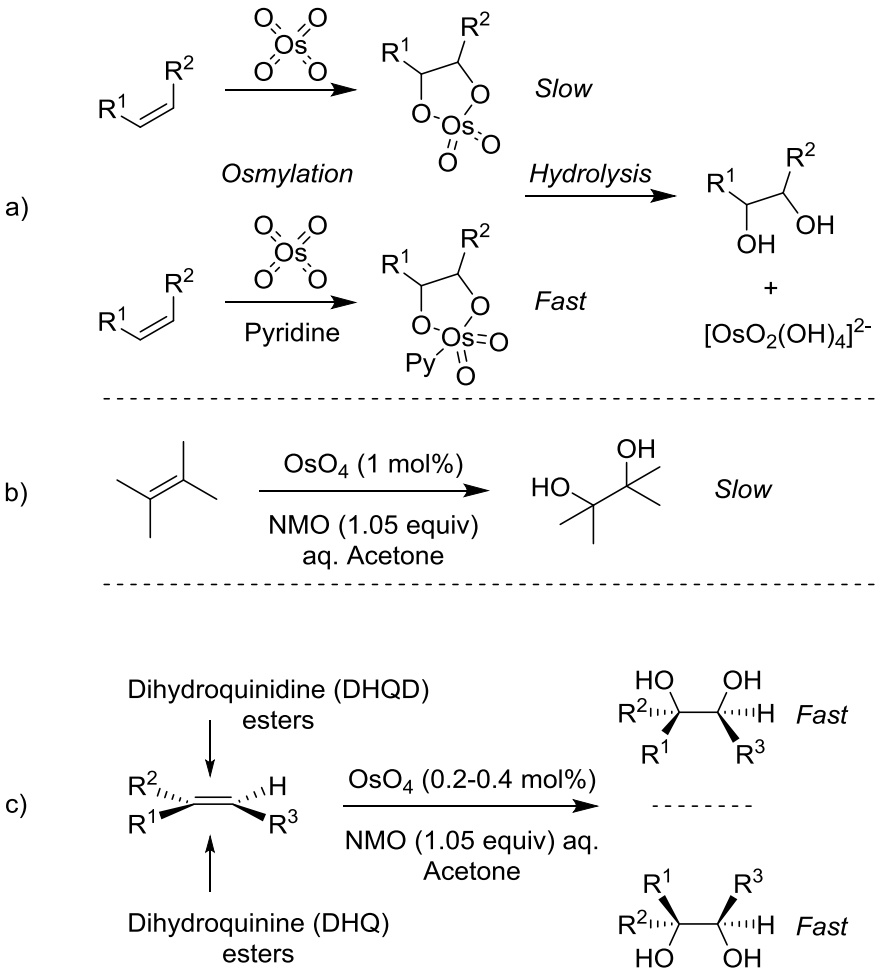

Scheme 2.1. a) The first dihydroxylation sequence developed by Criegee, highlighting the rate-enhancing effect observed when pyridine was present in the reaction media. b) The Upjohn dihydroxylation, the first efficient catalytic version of the transformation. c) Sharpless' first asymmetric catalytic variant, the rate of which is also enhanced by the quinuclidine-based ligand.

Interestingly, the cinchona alkaloid chiral ligands granted the perfect balance between binding strength of the two species present in the catalytic cycle; it binds strongly enough to osmium tetroxide to

[56] a) S. G. Hentges and K. B. Sharpless, *J. Am. Chem. Soc.*, 1980, **102**, 4263-4265. b) E. N. Jacobsen, I. Markó, W. S. Mungall, G. Schröder and K. B. Sharpless, *J. Am. Chem. Soc.*, 1988, **110**, 1968-1970.

accelerate the rate of the asymmetric reaction, and is labile enough to be cleaved from the osmate ester for the catalytic cycle to continue at a fast rate. This phenomenon, termed "ligand-accelerated catalysis" by Sharpless himself, is also responsible for negating the uncatalysed reaction which leads to the racemic product. However, another catalytic cycle was later found to be acting in unison with the NMO co-oxidant. This was later rectified and a refined version was developed using the solid potassium osmate salt along with potassium ferricyanide as the co-oxidant. This advance allowed the group to develop the so-called AD-mix (AD being an abbreviation of *asymmetric dihydroxylation*), a commercially available mixture containing all the required components—that is, potassium osmate, potassium ferricyanide, potassium carbonate and the corresponding cinchona alkaloid present as a phthalazine adduct—in the correct ratio, permitting scientists around the world to carry out this sophisticated transformation by simply adding 1.4 g of AD-mix to 1 mmol of olefin.[57]

This transformation was also extended to the 1,2-hydroxylamination of olefins, again by Sharpless and co-workers.[58] This can be achieved through the addition of an imide precursor, usually a mixture of an *N*-chlorosodiocarbamate or an *N*-halosulfonamide such as chloramine-T, and of course the osmium catalyst and ligand (Scheme 2.2).

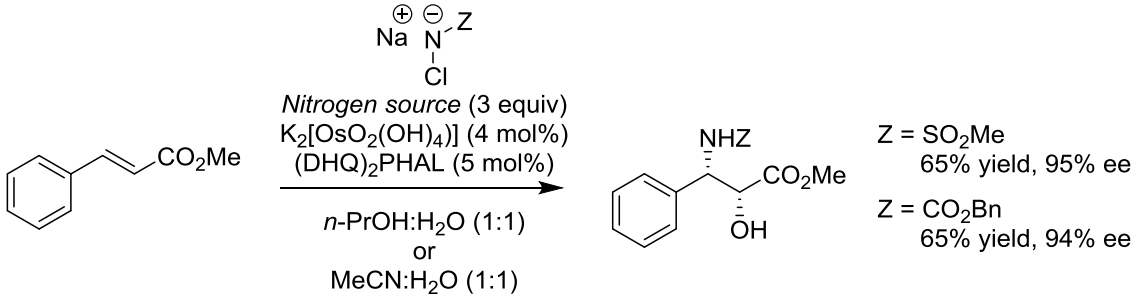

Scheme 2.2. Representative examples of olefin 1,2-hydroxyamination developed by Sharpless.

Since these early examples, there have been many advances in this field including 1,2-dicarbofunctionalisations,[59] 1,2-carboheterofunctionalisations,[60] and new 1,2-

[57] H. C. Kolb, M. S. VanNieuwenhze and K. B. Sharpless, *Chem. Rev.*, 1994, **94**, 2483-2547.

[58] a) K. B. Sharpless, D. W. Patrick, L. K. Truesdale and S. A. Biller, *J. Am. Chem. Soc.*, 1975, **97**, 2305-2307. b) E. Herranz, S. A. Biller and K. B. Sharpless, *J. Am. Chem. Soc.*, 1978, **100**, 3596-3598. For a review on the 1,2-hydroxyamination of alkenes see: J. A. Bodkin and M. D. McLeod, *J. Chem. Soc., Perkin Trans. 1.*, 2002, 2733-2746.

[59] For selected recent examples see: a) X. Tang and A. Studer, *Angew. Chem. Int. Ed.*, 2018, **57**, 814-817. b) Z. Kuang, K. Yang and Q. Song, *Org. Lett.*, 2017, **19**, 2702-2705. c) R. K. Dhungana, B. Shrestha, R. Thapa-Magar, P. Basnet and R. Giri, *Org. Lett.*, 2017, **19**, 2154-2157.

[60] For selected recent examples see: a) J. Cheng, Y. Cheng, J. Xie and C. Zhu, *Org. Lett.*, 2018, **19**, 6452-6455. b) Y.-Y. Liu, X.-H. Yang, R.-J. Song, S. Luo and J.-H. Li, *Nature Commun.*, 2017, **8**, Article number: 14720, DOI: 10.1038/ncomms14720.

diheterofunctionalisations.[61] Thus, given the large volume of work available in this area, this section will focus on selected examples that incorporate fluorine into the final product. Of course, one of the earliest and most emblematic examples of this class of difunctionalisation is the halofluorination reaction first described by Olah and co-workers, using *N*-halosuccinimide in conjunction with their own HF·pyridine reagent (Scheme 2.3).[62] This reaction can also be carried out using other halogen sources, such as elemental bromine or iodine with a silver nitrate additive, or trihaloisocyanuric acids—the latter proving the most sustainable and atom economical, since the cyanuric acid precipitate can be halogenated and reused.[63] In terms of the mechanism, the reaction first involves the formation of a halonium cation intermediate, which is then opened by the nucleophilic fluoride present in the HF·pyridine solution in a regioselective manner to form the Markovnikov product.[64]

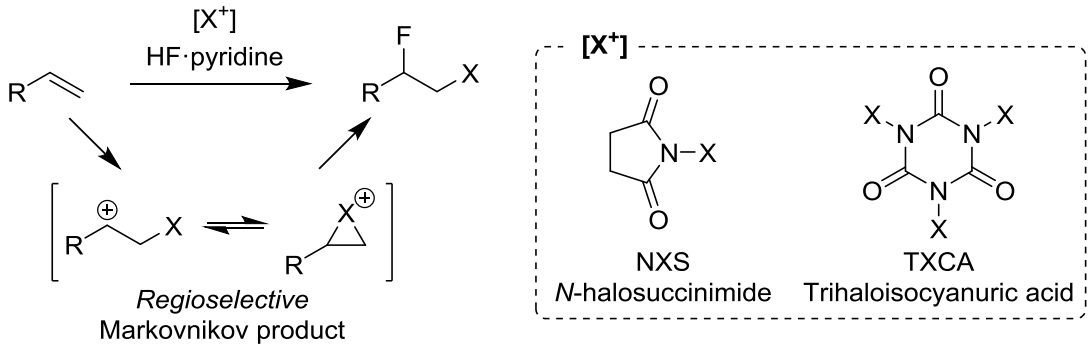

Scheme 2.3. Halofluorination using electrophilic halogen sources and Olah's reagent.

More recent examples of olefin 1,2-difunctionalisations incorporating a fluorine substituent into the final product were reported by Liu *et al.* through the years 2009-2016.[65] This group developed a high-valent palladium catalytic cycle using strong iodine(III) oxidant **2.1** combined with silver(I) fluoride as the source of nucleophilic fluorine. In this context, the authors suggest a mechanism by which the 5-aminopent-1-ene starting materials undergo aminopalladation to form six-membered ring **I**. From there, the palladium(II) centre is oxidised to palladium(IV) by **2.1** and AgF. The R—F bond in the final piperidine product is then formed *via* reductive elimination from **II** (Scheme 2.4, a).[66] Curiously, when

[61] For selected recent examples see: a) Y. Yang, R.-J. Song, X.-H. Ouyang, C.-Y. Wang, J.-H. Li and S. Luo, *Angew. Chem. Int. Ed.*, 2017, **56**, 7916-7919. b) X. Sun, X. Li, S. Song, Y. Zhu, Y.-F. Liang and N. Jiao, *J. Am. Chem. Soc.*, 2015, **137**, 6059-6066. c) J. L. Jat, M. P. Paudyal, H. Gao, Q.-L. Xu, M. Yousufuddin, D. Devarajan, D. H. Ess, L. Kürti and J. R. Falck, *Science*, 2014, **343**, 61-65.

[62] a) G. A. Olah, M. Nojima and I. Kerekes, *Synthesis*, 1973, **1973**, 780-783. b) G. A. Olah, J. T. Welch, Y. D. Vankar, M. Nojima, I. Kerekes and J. A. Olah, *J. Org. Chem.*, 1979, **44**, 3872-3881.

[63] L. T. C. Crespo, R. da S. Ribeiro, M. C. S. de Mattos and P. M. Esteves, *Synthesis*, 2010, **14**, 2379-2382.

[64] M. Lübke, R. Skupin and G. Haufe, *J. Fluorine Chem.*, 2000, **102**, 125-133.

[65] G. Yin, X. Mu and G. Liu, *Acc. Chem. Res.*, 2016, **49**, 2413-2423.

[66] T. Wu, G. Yin and G. Liu, *J. Am. Chem. Soc.*, 2009, **131**, 16354-16355.

N-tosyl amines were used the six-membered *endo* product was observed, whereas when the amine protecting group was changed to a strongly-chelating carbamate the 5-*exo* product was observed (Scheme 2.4, b).[67] This methodology was also applied to the total synthesis of fluorinated derivatives of both Swainsonine and Febrifugine by the same authors in 2016, highlighting the usefulness of this practical procedure in the preparation of **2.2**, a common intermediate towards both natural product analogues (Scheme 2.4, c).[68] In 2012, the same transformation was reported by Meng, Li *et al.* using metal-free reaction conditions.[69]

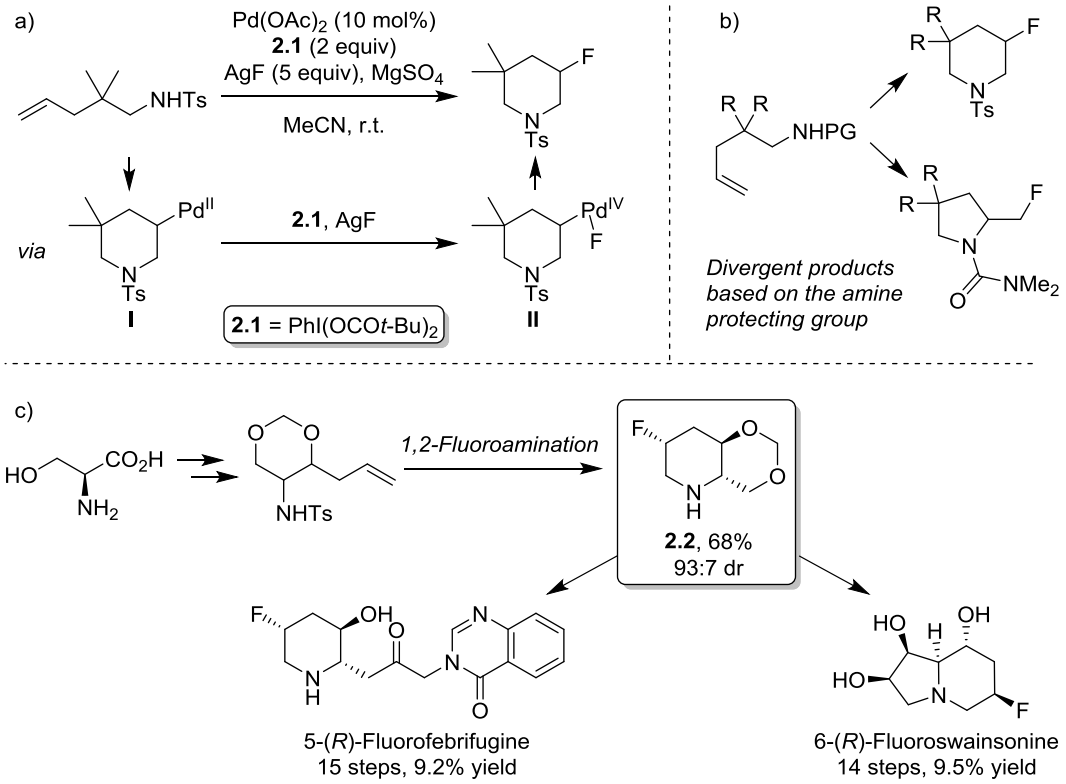

Scheme 2.4. a) Intramolecular 1,2-aminofluorination mechanism. b) Stereodivergent products depending on the amine protecting group. c) 1,2-Aminofluorination in the synthesis of natural product analogues.

Similar transformations have been described using carboxylic acids with an unactivated olefin in a remote position, mainly based on electrophilic lactonisations without requiring a metal promoter.[70] For example, in 2014 Rueping *et al*. described the use of 2-vinylbenzoic acids as substrates for this type of

[67] T. Wu, J. Cheng, P. Chen and G. Liu, *Chem. Commun.*, 2013, **49**, 8707-8709.

[68] L. Wu, P. Chen and G. Liu, *Org. Lett.*, 2016, **18**, 960-963.

[69] Q. Wang, W. Zhong, X. Wei, M. Ning, X. Meng and Z. Li, *Org. Biomol. Chem.*, 2012, **10**, 8566-8569.

[70] a) M. Sawaguchi, S. Hara, T. Fukuhara and N. Yoneda, *J. Fluorine Chem.*, 2000, **104**, 277-280. b) L. F. Lourie, Y. A. Serguche, G. V. Shevchenko, M. V. Ponomarenko, A. N. Chernega, E. B. Rusanov and J. A. K. Howard, *J. Fluorine Chem.*, 2006, **127**, 377-385. c) Y. A. Serguchev, L. F. Lourie, M. V. Ponomarenko, E. B. Rusanov and N. V. Ignat'ev, *Tetrahedron Lett.*, 2011, **52**, 5166-5169.

transformation (Scheme 2.5).[71] To this end, they employed a phase-transfer strategy by which Selectfluor was gradually introduced into the apolar media by anion exchange with a sodium carbonate additive. Stuart and co-workers then developed another version of this transformation using a hypervalent fluoroiodine reagent, in this case not limited to 2-vinylbenzoic acid derivatives.[72]

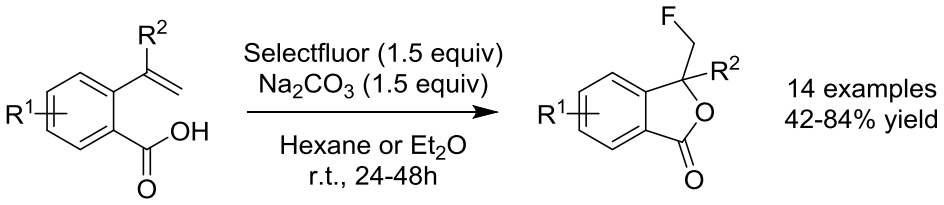

Scheme 2.5. Selectfluor-mediated fluorolactonisation of 2-vinylbenzoic acids derivatives.

All previous examples of this approach with *electrophilic* fluorine sources afforded exclusively the 5-*exo* lactonisation, however, in 2016 Jacobsen reported the first example of this transformation using a *nucleophilic* fluoride source to afford the 6-*endo* lactones, and in an enantioselective manner.[73] To this end, the authors employed aryl iodide **2.3** bearing a chiral C_2 axis as the catalyst—this species would undergo oxidation by *m*-CPBA and subsequent fluorination by HF·pyridine would produce the active hypervalent fluoroiodine complex responsible for the fluorolactonisation (Scheme 2.6). These conditions were first reported by Shibata *et al.* in the development of an aminofluorination protocol.[74]

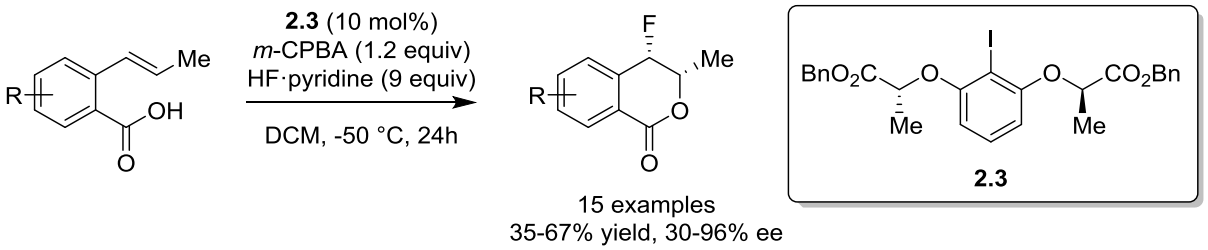

Scheme 2.6. Enantioselective fluorolactonisation developed by Jacobsen *et al.*

However, many of the aforementioned transformations are intramolecular, and are therefore limited to defined substrate classes. Therefore, searching for ways to improve the scope of 1,2-

[71] D. Parmar, M. Sudan Maji and M. Rueping, *Chem. Eur. J.*, 2014, **20**, 83-86.
[72] G. C. Geary, E. G. Hope and A. M. Stuart, *Angew. Chem. Int. Ed.*, 2015, **54**, 14911-14914.
[73] E. M. Woerly, S. M. Banik and E. N. Jacobsen, *J. Am. Chem. Soc.*, 2016, **138**, 13858-13861.
[74] S. Suzuki, T. Kamo, K. Fukushi, T. Hiramatsu, E. Tokunaga, T. Dohi, Y. Kita and N. Shibata, *Chem. Sci.*, 2014, **5**, 2754-2760.

difunctionalisations involving the introduction of fluorine into the final product—and based on their own observations that iodonium species formed between iodine(III) reagents and olefins undergo oxidative addition with palladium species[75]—in 2017 Liu and co-workers described the palladium-catalysed fluorocarbonylation of unactivated olefins, affording β-fluorocarboxylic acid derivatives (Scheme 2.7).[76] Interestingly, the palladium catalysed process ends with either the acyl fluoride or the carboxylic acid from adventitious acetate or fluoride ions in the media. Therefore, the authors quenched with a nucleophile such as methanol, water or amine to converge the two intermediate products into the single desired ester, carboxylic acid or amide respectively.

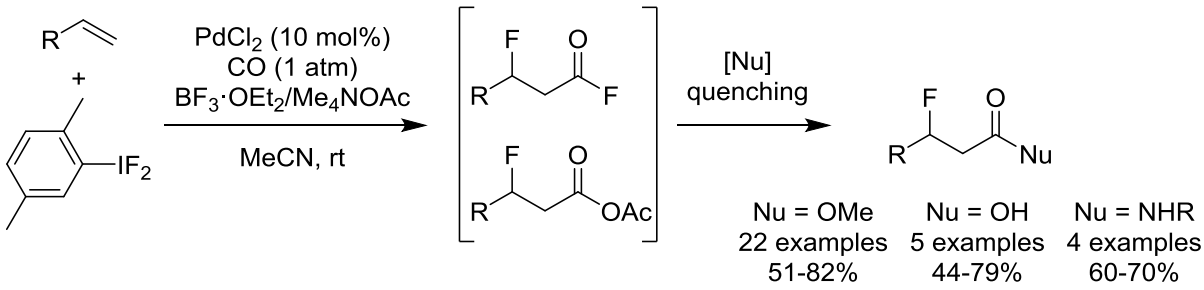

Scheme 2.7. Synthesis of β-fluorocarbonyl derivatives *via* 1,2-difunctionalisation of olefins.

More recently, in 2016 several advances in 1,2-difluorination reactions were described. Building on the stoichiometric procedure reported by Hara, Yoneda and co-workers using iodoarene difluorides in combination with 5HF·Et_3N,[77] Jacobsen[78] and Gilmour[79] presented protocols in which the iodoarene can be used catalytically to provide high yields and, in Jacobsen's examples, high enantioselectivities (Scheme 2.8, a). Furthermore, Jacobsen and co-workers were able to obtain different products depending on whether the favoured reaction pathway involved anchimeric assistance from a neighbouring amide group (affording 1,2-difluorinated products **2.5**) or migration of the aryl substituent (affording 1,1-difluorinated products **2.6**). Gilmour also provided a similar protocol using the simple *p*-iodotoluene as the catalyst, giving rise to racemic 1,2-difluorinated products (Scheme 2.8, b).

[75] M. Li, F. Yu, X. Qi, P. Chen and G. Liu, *Angew. Chem. Int. Ed.*, 2016, **55**, 13843-13848.
[76] X. Qi, F. Yu, P. Chen and G. Liu, *Angew. Chem. Int. Ed.*, 2017, **56**, 12692-12696.
[77] S. Hara, J. Nakahigashi, K. Ishi-i, M. Sawaguchi, H. Sakai, T. Fukuhara and N. Yoneda, *Synlett.*, 1998, 495-496.
[78] a) S. M. Banik, J. W. Medley and E. N. Jacobsen, *J. Am. Chem. Soc.*, 2016, **138**, 5000-5003. b) S. M. Banik, J. W. Medley and E. N. Jacobsen, *Science*, 2016, **353**, 51-54.
[79] I. G. Molnár and R. Gilmour, *J. Am. Chem. Soc.*, 2016, **138**, 5004-5007.

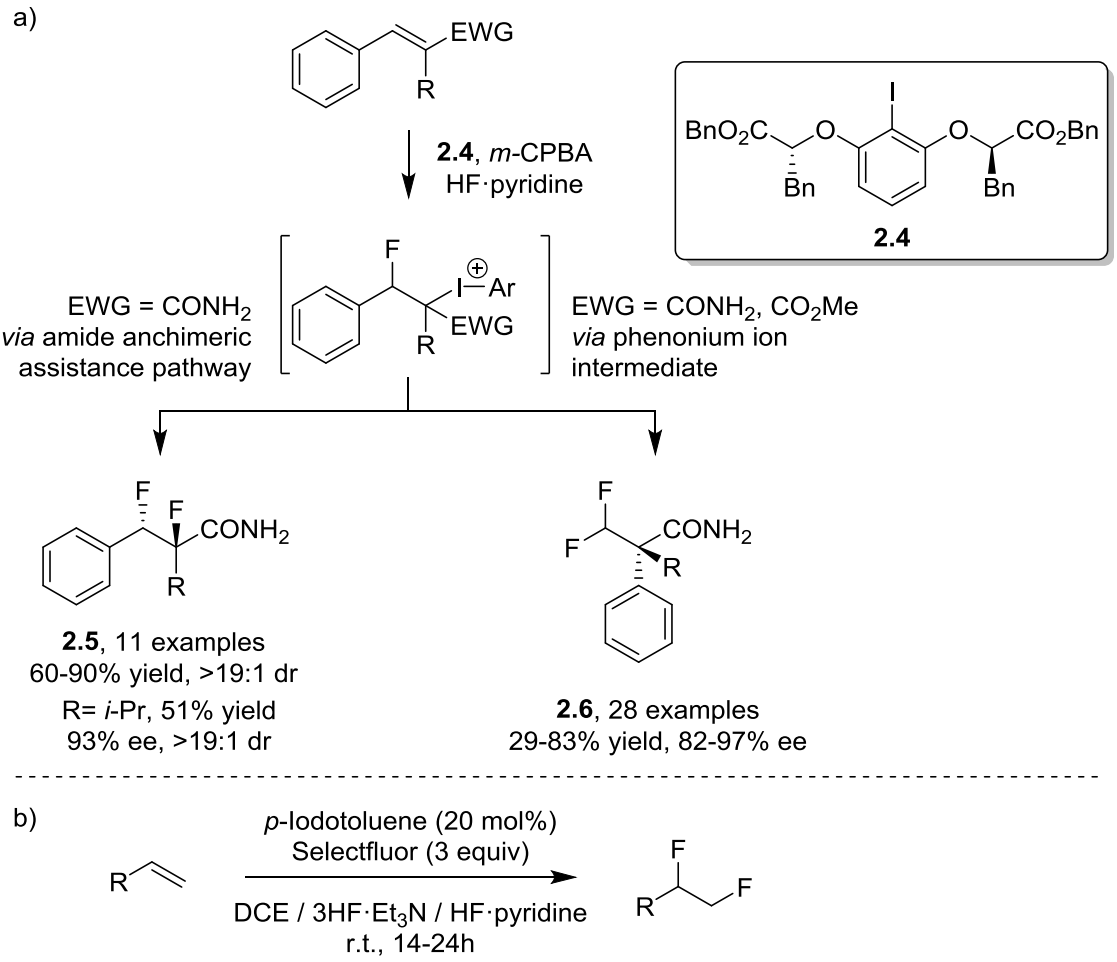

Scheme 2.8. Difluorinations developed by Jacobsen and Gilmour.

2.1.2. Fluorohydrins.

The first fluorine-containing drug to reach the market, Fludrocortisone, contains a fluorohydrin moiety and resulted in a decisive drive for research in this field (Figure 2.1). The discovery of this compound came about when in the 1950s Fried and Sabo observed that the introduction of a halogen into the cortisol skeleton increased its bioactivity, and that the activity was inversely proportional to the size of the halogen.[80] In this sense, the presence of the fluorine atom was shown to increase the activity 10-fold for glucocorticoid and up to 800-fold for mineralocorticoid receptors. Fludrocortisone is primarily administered as the acetate prodrug which is hydrolysed *in vivo*, and is generally used to replace aldosterone (the main compound in the mineralocorticoid class of hormones) in patients suffering maladies that cause hormone imbalances.

Other fluorinated steroid-based drugs have also been approved for use as anti-inflammatories, such as Fluticasone propionate and Difluprednate (Figure 2.1).[81] The latter was proven to have increased topical potency due to the fluorine substituents in positions C6 and C9, whereas the C21 acetate and C17 butyrate groups improve the lipophilicity and anti-inflammatory activity, respectively.[82]

Since then, other drugs containing the fluorohydrin subunit have been introduced into the market with varying therapeutic uses. For example, Sofosbuvir is an anti-viral drug that was approved by the FDA in 2013 for use in the treatment of hepatitis C (Figure 2.1).[83] This compound is also a prodrug, first requiring metabolism in the liver to hydrolyse the ester and the phosphoramide groups, as well as subsequent phosphorylation to afford the active triphosphate form.

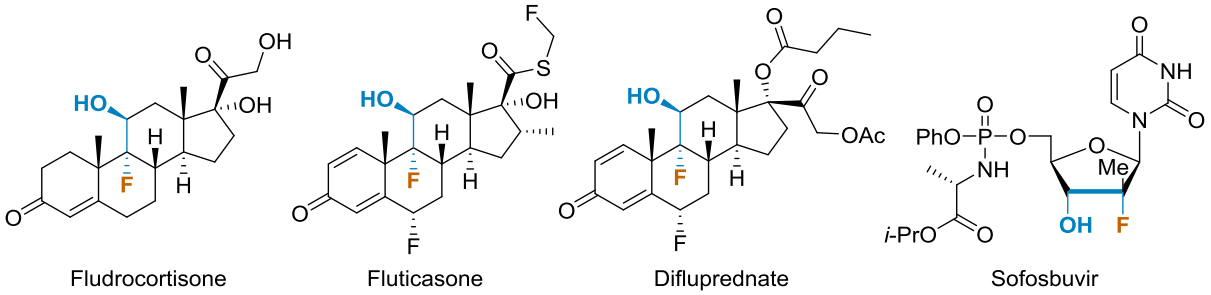

Figure 2.1. Steroid-based drugs containing a fluorohydrin moiety, and Sofosbuvir, a more recent anti-viral agent used against hepatitis C.

[80] J. Fried and E. F. Sabo, *J. Am. Chem. Soc.*, 1954, **76**, 1455-1456.
[81] K. N. Jamal and D. G. Callanan, *Clin. Opthal.*, 2009, **3**, 381-390.
[82] M. Korenfeld, *Expert Rev. Ophthamol.*, 2008, **3**, 619-625.
[83] a) A. Yancey, A. Armbruster and S. Tackett, *J. Pharm. Tech.*, 2015, **31**, 29-37. b) A. Fung, Z. Jin, N. Dyatkina, G. Wang, L. Beigelman and J. Deval, *Antimicrob. Agents Chemother.*, 2014, **58**, 3636-3645.

The synthesis of fluorohydrins has been dominated by the opening of epoxides with nucleophilic fluoride sources, among which HF·amine reagents stand out for their atom economy and practicality. The synthesis of fluorohydrins has been described at length in the chemical literature.[84]

The opening of terminal epoxides with fluoride sources generally follows the standard rules for this type of transformation: the fluoride attacks the most substituted carbon in acidic reaction conditions due to an S_N1 type mechanism, resulting in the terminal alcohol; and the least substituted carbon in basic reaction conditions due to an S_N2 type mechanism, resulting in the terminal fluoride. However, with HF·amine reagents the situation is not always as straightforward as it may seem, given the competing nature of the acidic HF and the basic hydrogen-bond donor. Haufe and Sattler studied the regioselectivity of this opening using **2.7** as the model substrate, finding that 9HF·pyridine typically favours the formation of **2.8** through an S_N1 type mechanism whereas $3HF{\cdot}Et_3N$ shows little selectivity (Scheme 2.9).[85] These results can be shifted towards the formation of the opposite regioisomer through the addition of extra base, essentially lowering the concentration of HF and leading to more basic reaction conditions. Nevertheless, this seems slightly unnecessary since similar results are obtained through the simple treatment of the epoxide with an inorganic fluoride salt, such as KHF_2 (Scheme 2.9, a). Furthermore, since the reaction between the epoxide and Olah's reagent generally takes place *via* an S_N1 type mechanism, the presence of proximal heteroatoms can alter the regioselectivity of the process (Scheme 2.9, b)

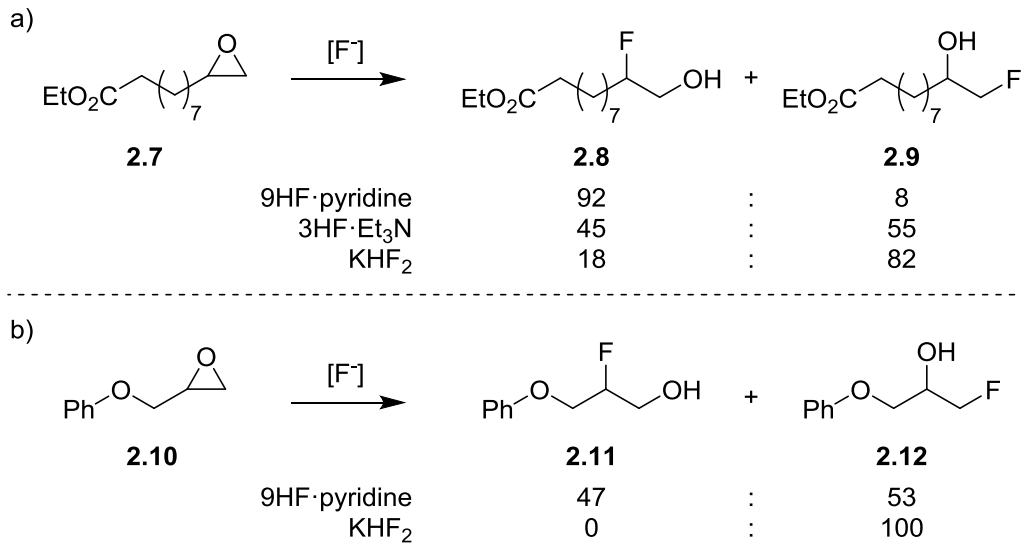

Scheme 2.9. Regioselectivity observed with the opening of epoxides with varying fluoride sources.

[84] For an extensive review on the synthesis of fluorohydrins, see: a) G. Haufe, *J. Fluorine Chem*., 2004, **125**, 875-894. For a review on transition-metal catalysed processes, including the opening of epoxides with fluoride, see: b) C. Hollingworth and V. Gouverneur, *Chem. Commun.*, 2012, **48**, 2929-2942.

[85] A. Sattler and G. Haufe, *J. Fluorine Chem.*, 1994, **69**, 185-190.

2.2. Background.

Several reports have been published regarding the 1,2-hydroxyfluorination of olefins. However, to the best of our knowledge, none of these have involved the use of HF·amine reagents—although Jouannetaud *et al.* employed HF·SBF_5 superacid to produce cinchona-derived fluorohydrins in 2006.[86] This reaction, however, was unselective and the authors obtained complex mixtures of products in most cases.

In this context, the vast majority use Selectfluor as an electrophilic fluorine source. For example, in the years 2004 and 2013 the groups of Stavber[87] and Singh,[88] respectively, reported facile procedures involving the use of Selectfluor in an aqueous medium for the 1,2-hydroxyfluorination of alkenes. However, these were both limited to aromatic derivatives, and both afforded the corresponding terminal fluorides (Scheme 2.10).

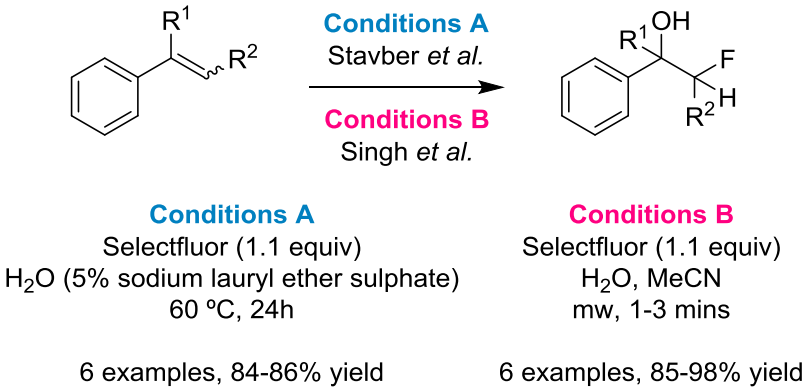

Scheme 2.10. The use of Selectfluor and water in the 1,2-hydroxyfluorination of olefins.

Furthermore, in 2012 Davies and co-workers achieved the regio- and diastereoselective synthesis of fluorohydrins starting from allylamines **2.13**.[89] The authors developed a one-pot epoxidation-ring opening sequence using *m*-CPBA and HBF_4 as the fluoride source, obtaining moderate yields and high diastereomeric excesses in almost all cases (99:1 dr in most cases). In addition, they were able to selectively produce one diastereoisomer or the other depending on the amount of tetrafluoroboric acid

[86] V. Chagnault, M.-P. Jouannetaud, J.-C. Jacquesya and J. Marrot, *Tetrahedron*, 2006, **62**, 10248-10254.
[87] G. Stavber, M. Zupan, M. Jereb and S. Stavber, *Org. Lett.,* 2004, **6**, 4973-4976.
[88] A. Kumar, T. V. Singh and P. Venugopalan, *J. Fluorine Chem.*, 2013, **150**, 72-77.
[89] A. J. Cresswell, S. G. Davies, J. A. Lee, M. J. Morris, P. M. Roberts and J. E. Thomson, *J. Org. Chem.*, 2012, **77**, 7262-7281.

(Scheme 2.11). With just two equivalents of tetrafluoroboric acid, a hydrogen bond is established between the amine group and the *m*-CPBA during the epoxidation step, delivering the epoxide group to the same face as the amine to afford **2.14**. However, when excess tetrafluoroboric acid is used, this is disrupted since the amine is completely protonated throughout the reaction, and the epoxide is delivered to the other face due to steric interactions, affording **2.15** instead.

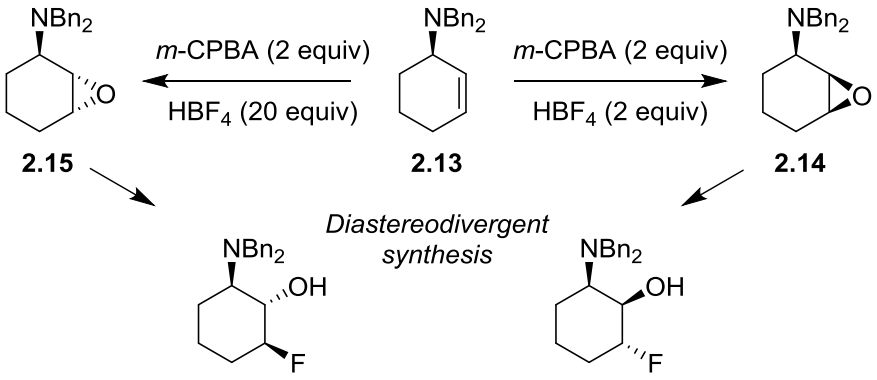

Scheme 2.11. Diastereodivergent synthesis of fluorohydrins using allylic amine starting materials.

Most recently, in 2017 Xu, Tang and co-workers reported a silver-catalysed hydroxyfluorination procedure.[90] The authors employed a mixture of AgOTf and $Sm(OTf)_3$ as the catalyst and promoter, a complex $PhNO_2/H_2O/MeNO_2$ solvent mixture and Selectfluor as the fluorine source (Scheme 2.12). The reaction is limited to the use of styrenes **2.16** as substrates, due to the radical pathway proposed by the authors. Nonetheless, for styrenes the reaction shows a wide scope and functional group compatibility, as well as being the first to selectively achieve the fluoride substituent in an internal position from a procedure of this kind.

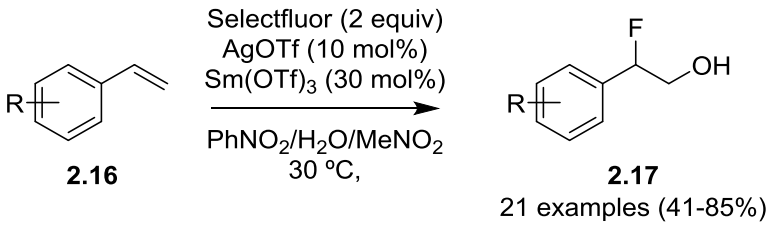

Scheme 2.12. Ag-catalysed radical 1,2-hydroxyfluorination of styrenes.

[90] Y. Li, X. Jiang, C. Zhao, X. Fu, X. Xu and P. Tang, *ACS Catal.*, 2017, **7**, 1606-1609.

In addition, the authors carried out a number of experiments to shed some light on the reaction mechanism. These included the use of a radical inhibitor, a radical trapping agent, performing the reaction under strict oxygen exclusion and isotopic labelling. All of these experiments suggested that a radical chain or a single-electron transfer mechanism may be operating. Supported by DFT calculations, the following reaction mechanism was proposed (Scheme 2.13). After complexation to styrene **2.16**, the corresponding silver species **II** is oxidised by Selectfluor rendering a silver(II) intermediate complex **III**, which in turn oxidises the styrene ligand to the corresponding radical cation **IV**, regenerating the silver(I) active catalyst **I**. The styrene radical cation **IV** then reacts with water affording the key benzylic radical **V**, which is subsequently fluorinated by Selectfluor affording products **2.17**. Interestingly, theoretical calculations showed that radical cation **VI** obtained as a by-product may preferentially promote the Ag(I)/Ag(II) oxidation step over Selectfluor. Hence, after the first catalytic cycle using Selectfluor as the oxidant (Route A), Route B would be operating (Scheme 2.13).

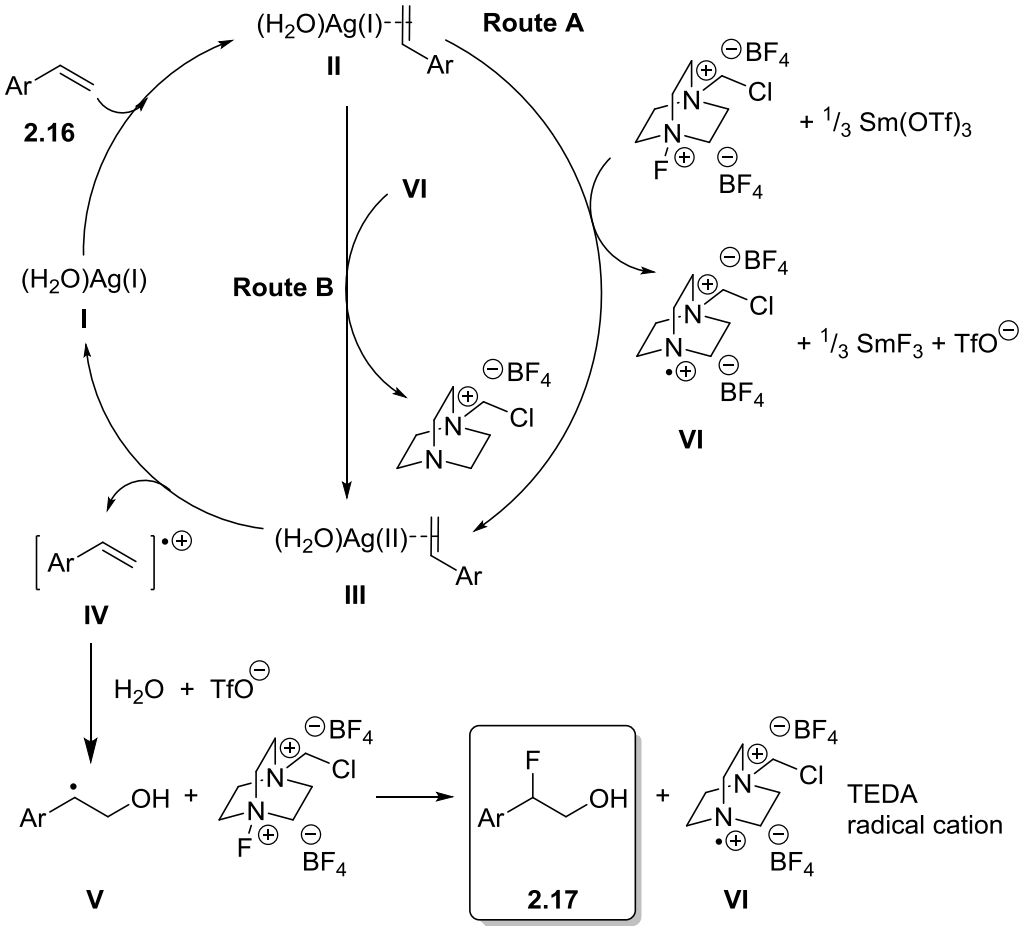

Scheme 2.13. Mechanism of 1,2-hydroxyfluorination of styrenes described by Xu, Tang *et al.*

2.3. Results and discussion.

2.3.1. Development of a one-pot hydroxyfluorination procedure.

To begin this work, we first analysed the possibility of the one pot procedure using styrene as the model substrate with a combination of *m*-CPBA and HF·amine, given that these were decided to be the most standard and practical reagents for both of the necessary transformations (Table 2.1). To our delight, the desired fluorohydrin was obtained in a decent yield and regioselectivity. This showed that the reagents were indeed compatible; the epoxidation was possible in acidic conditions in the presence of HF, and the subsequent opening took place without complications.

We first studied the necessary equivalents of the two reagents, and quickly found that a large excess of HF compared to *m*-CPBA was necessary for the reaction to proceed to completion (entries 1-5, Table 2.1). We also studied the delay in HF addition, first allowing a period of time for the epoxidation step before the subsequent ring opening (entries 5-8, Table 2.1). However, we observed no significant advantage to this. Therefore, we opted to add all the reactants at the beginning in the search for maximum simplicity and practicality.

Oddly, no reaction was obtained when using $3HF{\cdot}Et_3N$ as the fluoride source (entry 10, Table 2.1). This could perhaps be due to incompatibility of *m*-CPBA with triethylamine, since the intermediate epoxide was not observed and only the starting styrene was recuperated.

No significant difference was observed between HF·pyridine and HF·DMPU (entries 8-9 and 13-14, Table 2.1) and so we decided to continue the study using HF·pyridine, given the lower cost of this reagent. Similarly, dichloromethane was preferred to chloroform due to the lower environmental cost (entry 9 vs. 14, Table 2.1).

A small amount of the regioisomer with the fluorine in the terminal position was observed in all cases, although the major product was the desired **2.19**; all conditions tested showed a selectivity of around 5:1 - 7:1 (**2.19**:**2.20**) (Table 2.1).

Hence, the optimum conditions taken forward were the use of two equivalents of *m*-CPBA, seven equivalents of HF·pyridine, in dichloromethane at 0 °C and with simultaneous addition of all reagents from the onset (entry 14, Table 2.1).

Table 2.1. Optimisation of our one-pot 1,2-difunctionalisation procedure towards fluorohydrins.

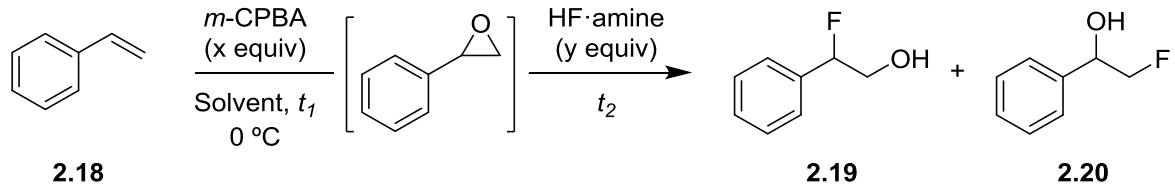

2.18 **2.19** **2.20**

Entry	Solvent	x	y	t_1 (h)	t_2 (h)	amine	Yield **2.19** (%)[a, b]
1	$CHCl_3$	1.1	2.2	1	5	DMPU	32
2	$CHCl_3$	1.2	2.4	1	5	DMPU	44
3	$CHCl_3$	1.5	3	1	5	DMPU	48
4	$CHCl_3$	2	4	1	5	DMPU	55
5	$CHCl_3$	2	7	1	5	DMPU	76
6	$CHCl_3$	2	7	4	18	DMPU	77
7	$CHCl_3$	2	7	0.5	5	DMPU	75
8	$CHCl_3$	2	7	0	5	DMPU	75
9	$CHCl_3$	2	7	0	5	pyridine	74
10	$CHCl_3$	2	7	0	5	Et_3N	-[c]
11	DCM	1.1	7	0.5	6	DMPU	40
12	DCM	2	7	1	4	DMPU	75
13	DCM	2	7	0	5	DMPU	76
14	DCM	2	7	0	5	pyridine	75

[a] Determined through ^{1}F NMR using fluorobenzene as an internal standard. [b] Yield is given as a mixture of regioisomers (a small amount of **2.20** was always observed, although **2.19** was always the major product). [c] No reaction observed.

A slight inconvenience was the formation of small amounts of **2.21** resulting from the opening of the intermediate epoxide with *m*-chlorobenzoic acid, although this could be separated by simple flash column chromatography. The acidic media presumably activates the epoxide to a state in which this relatively poor nucleophile is able to open the epoxide ring (Scheme 2.14). Of course, given the situations seen previously, the exact reaction mechanism might be far more complex and will be studied in more detail in turn. The formation of this side product could be avoided in a stepwise synthesis; however, any economic loss resulting from the small drop in product yield would presumably be offset by the practicality of the one pot procedure.

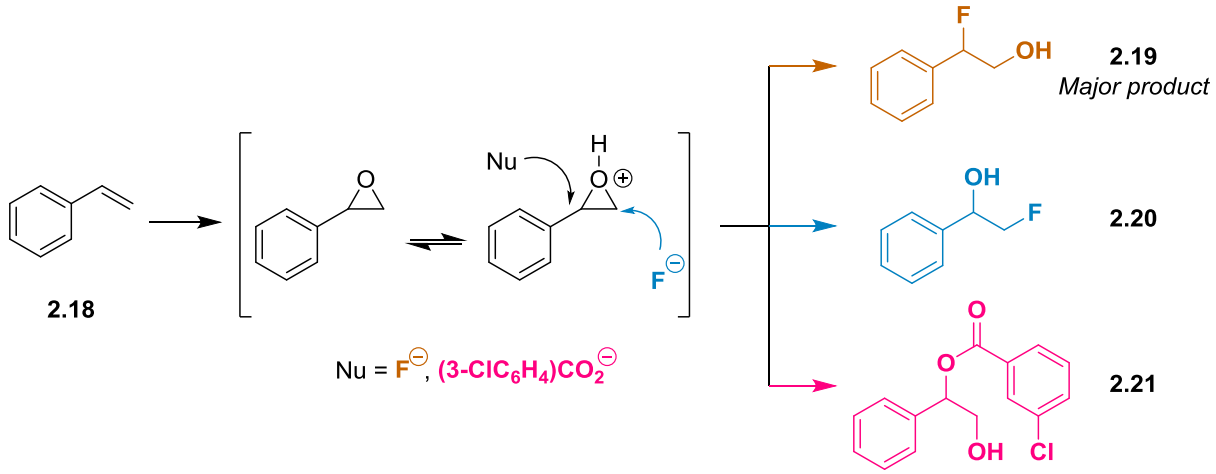

Scheme 2.14. The origin of side product 2.21.

With the optimum conditions in hand, we selected a range of olefins to study the scope of our one-pot 1,2-hydroxyfluorination protocol. We first studied several styrene derivatives with varying substituents on the aromatic ring (Table 2.2).

Table 2.2. Scope of aromatic substrates.[a]

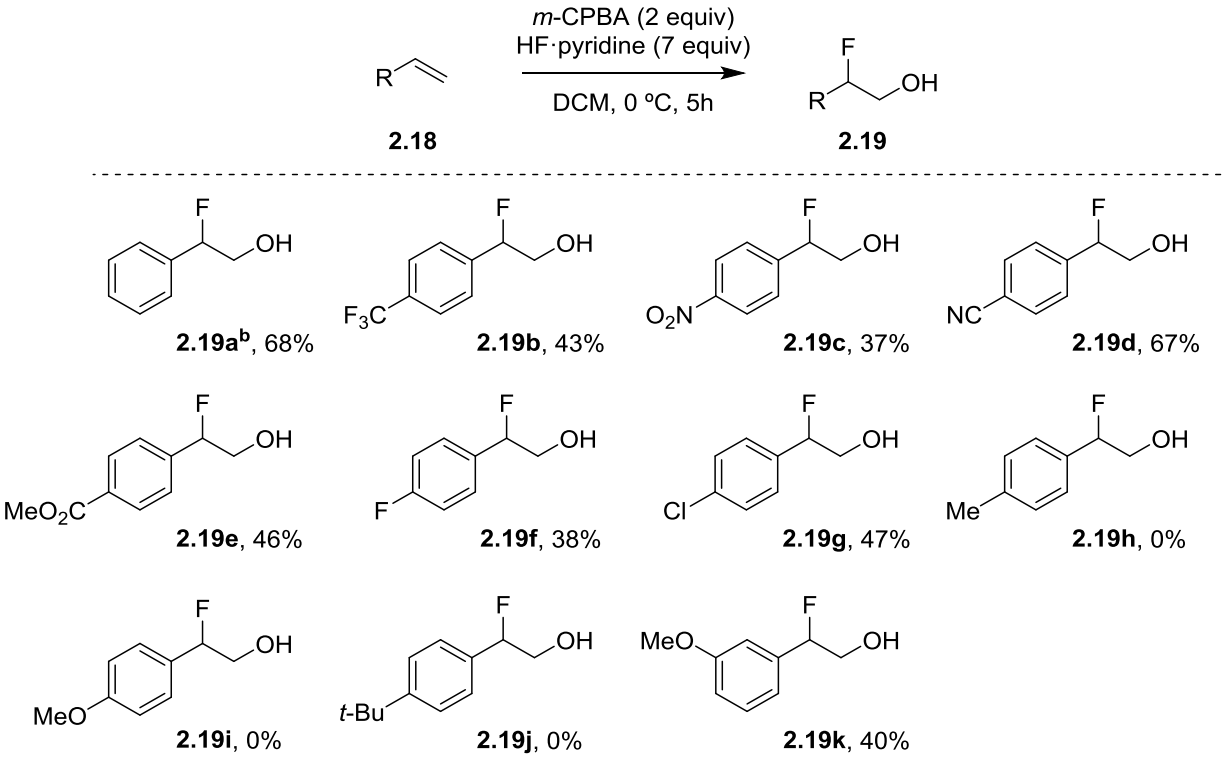

[a] Isolated yields. [b] The reaction was also carried out on a 10 mmol scale with a yield of 53%.

The reaction proved to be fairly tolerant of electron-withdrawing substituents: styrene derivatives bearing trifluoromethyl, nitro, nitrile, ester, fluorine and chlorine substituents in the *para* position (**2.19a**-**g**, Table 2.2) all resulted in moderate to good yields, bearing in mind that these yields take into account two steps (a global yield of 50% corresponds to roughly 70% yield in each of the two reactions).

Electron-donating substituents such as methoxy groups in the *para* position hampered the reaction and the main species identified in the crude mixture was the intermediate epoxide, possibly due to its lower electrophilicity (**2.19i**, Table 2.2). Interestingly, *m*-methoxystyrene gave rise to the desired fluorohydrin in a moderate yield (**2.19k**, Table 2.2), confirming that electronic effects were hampering the formation of the products in the case of **2.19i**—the negative inductive effect of the methoxy group overrides the resonance effect when in the *meta* position, acting as an electron-withdrawing group although the aromatic ring itself is electron-rich. Oddly, neither *p*-methylstyrene nor *p*-*tert*-butyl styrene resulted in the corresponding fluorohydrin products **2.19h** and **2.19j**, despite being only slightly electron-donating.

We next decided to explore aliphatic alkenes to set our methodology apart from those seen in previously reported 1,2-hydroxyfluorinations of alkenes, which have all been limited to aromatic derivatives. To this end, we chose allylbenzene derivatives, dodecene and cycloalkenes as suitable substrates. In order to begin to explore the reaction mechanism, we selected methylcyclohexene **2.18r** and 1,2-dimethylcyclohexene **2.18s** as substrates; if the reaction were to proceed through the prior opening of the epoxide and formation of a carbocation intermediate, the more substituted derivatives could give rise to higher yields and/or regioselectivities due to the facile opening of the epoxide and stabilisation of the positively-charged intermediate.

Therefore, we first had to synthesise **2.18s**. This was done *via* addition of methyllithium to 2-methylcyclohexanone to form alcohol **2.22** and subsequent iodine-mediated dehydration (Scheme 2.15).[91] This strategy afforded the isomeric olefins **2.18s** and **2.23** in a 5:1 ratio. Since we were unable to separate these two isomers by neither column chromatography nor distillation, we used the 5:1 mixture in the hydroxyfluorination reaction.

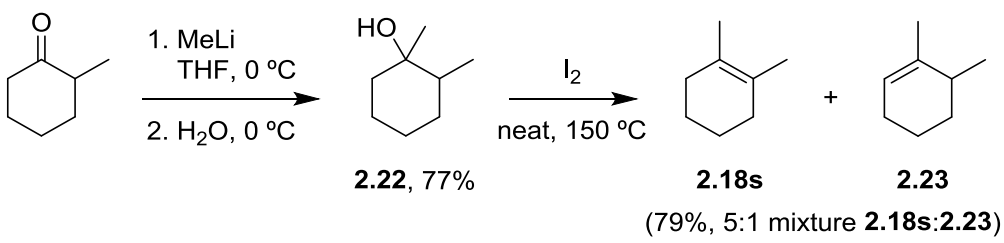

Scheme 2.15. Synthesis of dimethylcyclohexene 2.18s.

[91] N. G. Léonard and P. J. Chirik, *ACS Catal.*, 2018, **8**, 342-348.

Table 2.3. Reaction scope of aliphatic substrates.[a]

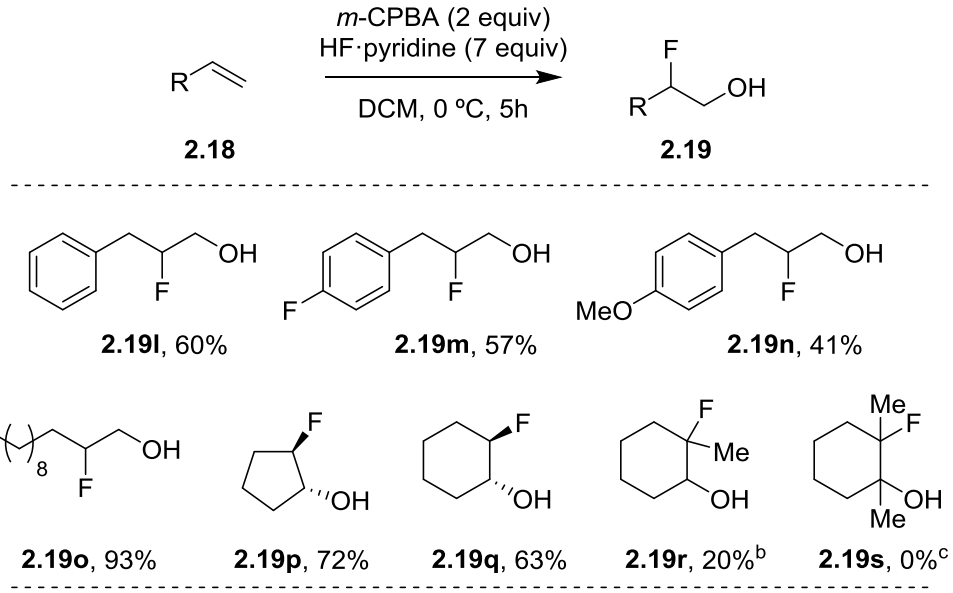

[a] Isolated yields. [b] Inseparable 3:1 *cis*:*trans* mixture. [c] 5:1 mixture of **2.18s** and **2.23** used as the starting material.

The results were generally good: the desired fluorohydrins were formed in moderate yields in most cases. In contrast to our expected results, the more substituted alkenes **2.18r** and **2.18s** gave lower yields. However, in the crude mixture we were able to identify mostly the starting alkene, and therefore we concluded that the problem arose due to the first epoxidation step rather than the opening with HF.

On the other hand, allylbenzene and derivatives **2.18l-n** all gave rise to desired fluorohydrins **2.19l-n** in moderate to good yields (a global yield of 60% corresponds with an average of 77% yield for both steps), concordant with the assumption that electronic effects had hampered the reaction in the case of certain styrene derivatives. Fluorohydrin **2.19o** derived from dodecene gave excellent results, and unsubstituted cyclopentene **2.18p** and cyclohexene **2.18q** also resulted in good yields.

Encouraged by these results, we turned our attention to more challenging substrates that could be useful in the life sciences (Table 2.4). In this sense, we decided that cholesterol could be an interesting substrate choice, given that the fluorohydrin product would bear a certain resemblance to Fludrocortisone and Difluprednate (fluorohydrin-containing drugs currently on the market, refer to Section 2.1.2). The reaction proceeded well, and the product **2.19t** was formed in high selectivity to give a high 76% yield as a 3.5:1 mixture of inseparable diastereoisomers. We were able to speculate the major product in this mixture since cholesterol is reported to undergo epoxidation with *m*-CPBA in a 4:1 isomeric ratio, favouring the α isomer.[92]

[92] M. Poirot and De Medina, Int. Pat., 2003-FR1248, April 18, 2003.

Similarly, the use of glucal **2.18u** in our protocol could result an analogue of fluorodeoxyglucose—the F^{18} version of which is a commonly used radiopharmaceutical in PET imaging.[93] Unfortunately, glucal did not react under the reaction conditions, possibly due to the hydroxyl groups—we had not confirmed the compatibility with hydroxyl groups in the previous studies of the reaction scope—or due to the enol-ether nature of the double bond. We therefore tested tri-*O*-benzyl-D-glucal **2.18v** but, disappointingly, this also resulted in no reaction.

Table 2.4. Use of biologically relevant substrates in our 1,2-hydroxyfluorination reaction.

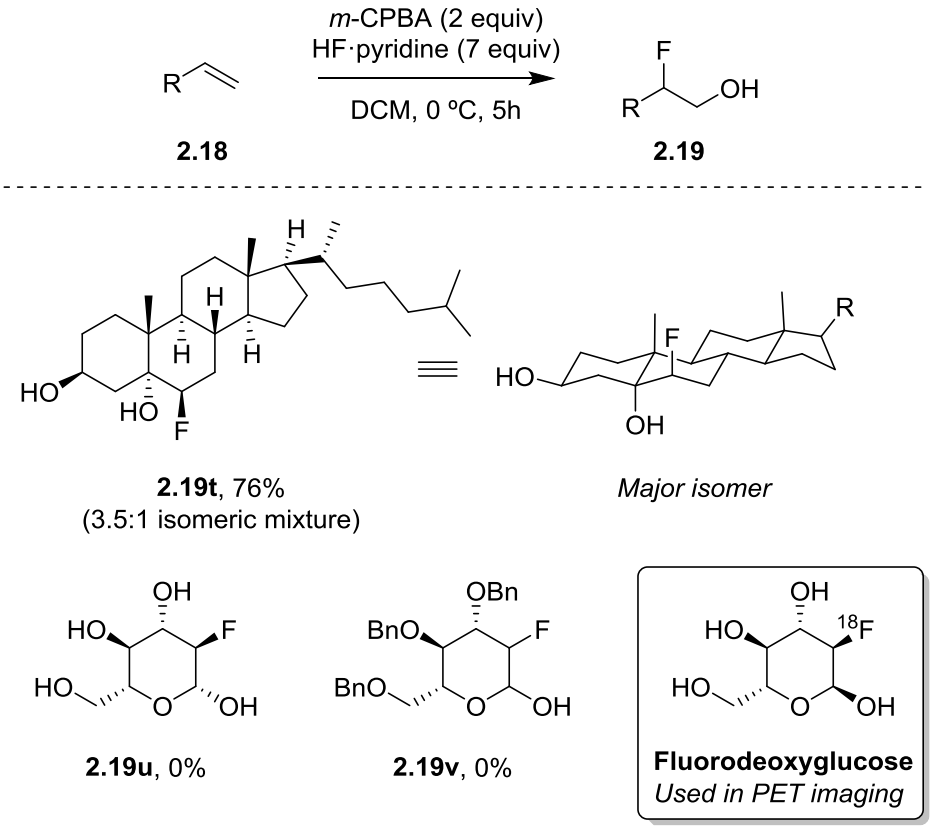

[93] a) P. Som, H. L. Atkins, D. Bandoypadhyay, J. S. Fowler, A. R. MacGregor, K. Matsui, Z. H. Oster, D. F. Sacker, C. Y. Shlue, H. Turner, C.-N. Wan, A. P. Wolf and S. V. Zabinski, *J. Nucl. Med.*, 1980, **21**, 670-675. b) A. Newberg, A. Alavi and M. Reivich, *Sem. Nucl. Med.*, 2002, **32**, 13-34.

2.3.2. Stereochemical studies.

The ultimate goal for this strategy would be the development of an enantioselective version. However, the development of such a protocol would require us to first understand the reaction mechanism entirely, and given the previously discussed background of this transformation we were aware of the complex situation that could arise. Despite giving rise to the product of an S_N1 type reaction pathway, it seemed unlikely that the epoxide fully opens to form the carbocation intermediate.

In a recent report, Hammond, Xu *et al.* described the regio- and stereoselective ring-opening of aziridines **2.24** with HF·DMPU which, incidentally, was developed by the same group a few years earlier.[94, 95] They originally reasoned that the increased acidity of HF·DMPU compared to other HF·amine reagents may be beneficial both for controlling the regioselectivity of the opening by favouring the nucleophilic attack at the most substituted carbon (Markovnikov regioselectivity) and for increasing the reactivity. Hence, they found that the treatment of *N*-tosylaziridines **2.24** with 7.5 equivalents of HF·DMPU in DCE at room temperature for 18-24 hours led to the formation of the corresponding β-fluoroamines **2.25** in good to excellent yields and excellent regioselectivities in most cases (Scheme 2.16).

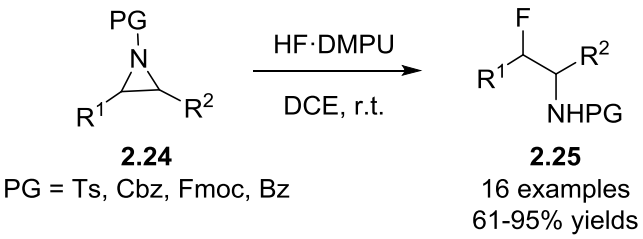

Scheme 2.16. Regio- and stereoselective ring-opening of *N*-tosylaziridines by HF·DMPU.

In addition, the authors studied the stereochemical outcome when bicyclic **2.24a** and, more interestingly, chiral non-racemic aziridines **2.24b-d** were used as substrates (Scheme 2.17). Firstly, complete inversion was observed for bicyclic aziridines **2.24a**, affording exclusively the corresponding *trans*-products **2.25a** (Scheme 2.17, Eq. a). On the other hand, the study with chiral non-racemic substrates shed more light onto the complex stereochemical scenario observed (Scheme 2.17, Eq. b-d). Purely aliphatic aziridine **2.24b** afforded the corresponding fluoroamine **2.25b** with complete inversion

[94] O. E. Okoromoba, Z. Li, N. Robertson, M. S. Mashuta, U. R. Couto, C. F. Tormena, B. Xu and G. B. Hammond, *Chem. Commun*., 2016, **52**, 13353-13356.
[95] O. E. Okoromoba, J. Han, G. B. Hammond and B. Xu, *J. Am. Chem. Soc.*, 2014, **136**, 14381-14384.

of configuration, similar to that observed in equation a, supporting an S_N2 mechanism. A similar proposal had been made by Schlosser *et al.* in 1990, referencing a "conveyer-belt" type mechanism to explain the contradictory results observed in the opening of epoxides with Olah's reagent—the reaction appeared to take neither an S_N1 nor S_N2 pathway, given the inversion of stereochemistry yet the internal attack of the fluoride ion. Given the polymer-like structure of HF·pyridine even in solution, Schlosser and co-workers suggested that a chain of H—F hydrogen bonds formed a ring around the epoxide, stabilising the positive charges that built up and fixing a defined stereochemical outcome (Figure 2.2).[96]

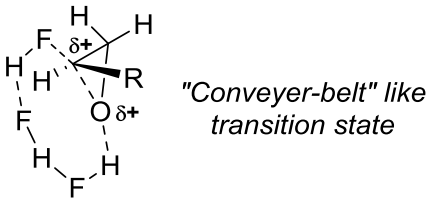

Figure 2.2. Conveyer-belt like transition state proposed by Schlosser *et al.*

On the other hand, phenyl substituted aziridine **2.24c** racemised upon opening. The authors rationalised this result with the extra stabilisation of the positive charge in the benzylic position (**TS-1**, Scheme 2.17), resulting in a quasi-S_N1 type mechanism. Finally, the most striking result was obtained when benzyl substituted substrate **2.24d** was used; fluoroamine **2.25d** was obtained in high ee, although with almost complete retention of configuration. The authors explain this unexpected stereochemical outcome with neighbouring group participation, by which the adjacent phenyl ring would stabilise the intermediate carbocation, following an S_Ni type mechanism. DFT calculations support this proposal and suggest a hydrogen bond directed delivery of the fluoride anion from the same face the nitrogen atom is placed, resulting in a quasi-S_Ni transition state (**TS-2**, Scheme 2.17).

[96] H. Suga, T. Hamatani and M. Schlosser, *Tetrahedron*, 1990, **46**, 4247-4254.

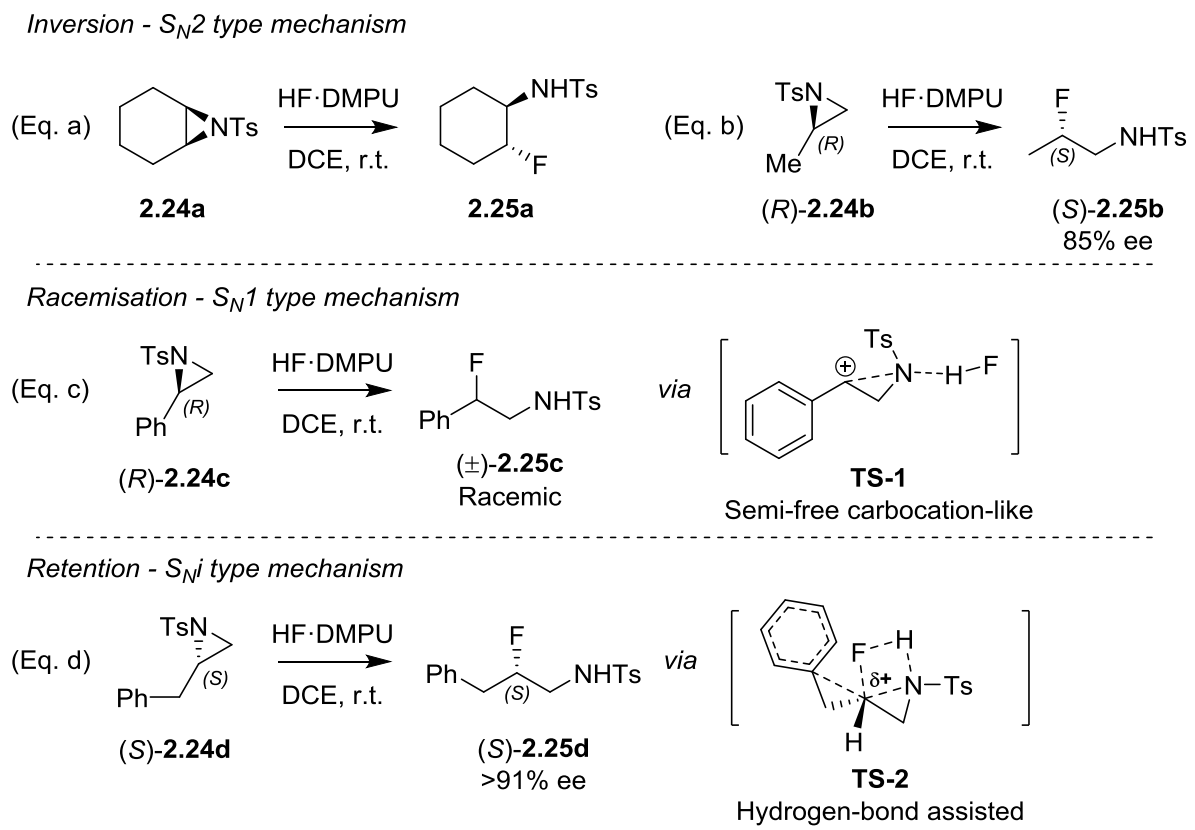

Scheme 2.17. Study on the stereochemical outcome of the ring-opening of aziridines by HF·DMPU.

Given these precedents, we first studied the use of *cis*- and *trans*-stilbene in our one pot hydroxyfluorination protocol. Since the two processes are stereospecific—that is, epoxidation is *syn* specific, and the opening usually takes place in an *anti* manner—well-defined products should be obtained.

Unexpectedly, we found that although the *trans* isomer did indeed afford exclusively the *anti* fluorohydrin product, the *cis* isomer furnished a 1:1 ratio of *syn* and *anti* diastereoisomers. We attributed this observation to the fact that *cis*-stilbene oxide would be less stable due to steric repulsions between the two phenyl groups in close proximity, thereby promoting the prior opening of the epoxide, forming a carbocation intermediate and giving rise to a 1:1 mixture of products (Scheme 2.18).

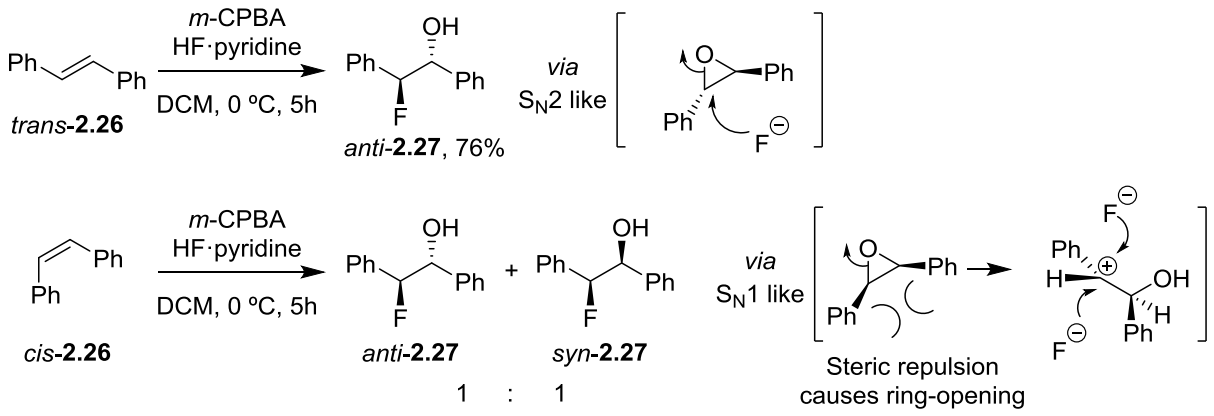

Scheme 2.18. Stereochemical outcomes using *cis*- and *trans*-stilbene.

These results made us question if the stereochemical outcome would be the same for epoxides as that obtained by Hammond, Xu *et al.* in the case of aziridines. Therefore, we next studied the opening of enantiomerically-enriched epoxides with both HF·DMPU and HF·pyridine. Given the poor UV-absorption spectra of the fluorohydrin products, we had to first convert the products to the corresponding naphthoyl esters to measure the enantiomeric excess *via* HPLC (Scheme 2.19). As we expected, we observed a large degree of racemisation upon treatment of the commercially available (*R*)-styrene oxide **2.28** with HF·pyridine and almost complete racemisation with HF·DMPU, concordant with the acidity of each of the two HF reagents. Furthermore, the addition of an external base did not improve the situation significantly.

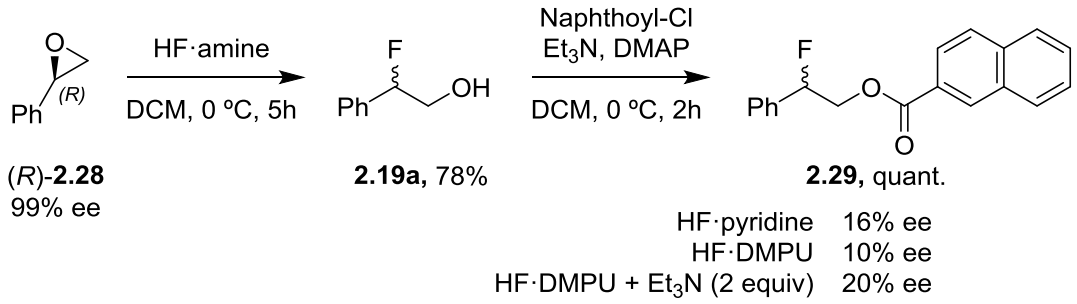

Scheme 2.19. Significant racemisation upon opening of styrene oxide with HF·amine reagents.

We had expected this outcome, and refused to be disheartened by the poor enantiomeric excesses obtained. We then turned to aliphatic derivatives, since these should be opened by HF·amine reagents with inversion *via* an S_N2 like pathway and, more importantly, conservation of the optical purity. Therefore, we synthesised (*S*)-dodecene oxide **2.30**, treated it with HF·amine reagents, and formed the

2-naphthoyl ester for analysis by HPLC.[97] To our delight, and as we hoped, we found that the product was formed in good yield and the enantioselectivity of the starting epoxide was maintained (Scheme 2.20).

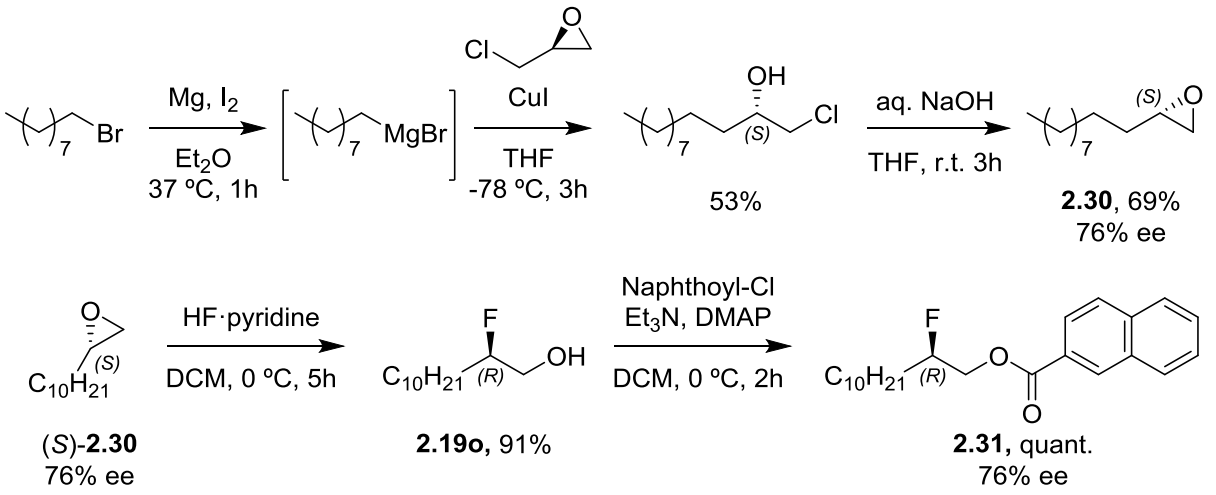

Scheme 2.20. Synthesis and analysis of an aliphatic enantioenriched epoxide in the ring-opening reaction with HF·pyridine.

These results must be taken into account for the development of an enantioselective version of this protocol. Furthermore, we would also need to study the compatibility of enantioselective epoxidation conditions with the HF·amine reagents; some options include the Sharpless asymmetric epoxidation,[52] or the use of the Jacobsen[98] or Shi catalysts.[99]

[97] F. Derosa, S. Karve and M. Heartlein, Int. Pat., 2015200465, 2015.
[98] W. Zhang, J. L. Loebach, S. R. Wilson and E. N. Jacobson, *J. Am. Chem. Soc.*, 1990, **112**, 2801-2803.
[99] Y. Shi, *Acc. Chem. Res.*, 2004, **37**, 488-496.

2.4. Conclusions.

We have developed a simple, metal-free and practical one pot protocol for the 1,2-hydroxyfluorination of olefins. The procedure is robust, showing compatibility with a variety of functional groups and proceeding in good yields and regioselectivities even under air and used-as-received solvents.

Furthermore, we have built upon past examples of this type of transformations, opening up the possibility of one pot procedures from aliphatic alkenes. This class of substrates was lacking from the previously reported hydroxyfluorination reactions.

Finally, we have studied the stereoselective implications of the opening of epoxides with HF·amine reagents, and we have found that an enantioselective one pot procedure could be possible for aliphatic alkenes, pending compatibility studies with HF·amine reagents and asymmetric catalysts for enantioselective epoxidation.

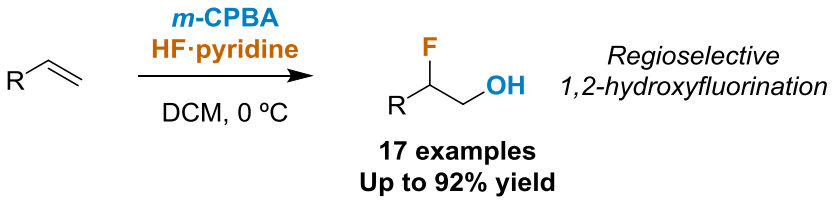

2.5. Experimental section.

Reactions were carried out under atmospheric conditions. DCM was used without further purification. The reactions were monitored with the aid of TLC on 0.25 mm pre-coated silica-gel plates. Visualization was carried out with UV light and aqueous ceric ammonium molybdate solution or potassium permanganate stain. Flash column chromatography was performed with the indicated solvents on silica gel 60 (particle size: 0.040–0.063 mm). ^{1}H, ^{13}C and ^{19}F NMR spectra were recorded on a 300 MHz spectrometer. Chemical shifts are given in ppm (δ), referenced to the residual proton resonances of the solvents. Coupling constants (*J*) are given in Hertz (Hz). The letters m, s, d, t, and q stand for multiplet, singlet, doublet, triplet, and quartet respectively. The letters br indicate that the signal is broad. HPLC analyses were performed using either a JASCO PU-2089 Plus chromatographer equipped with an MD-2010 detector or an Agilent 1100 series instrument equipped with a refraction index detector using chiral stationary columns from Daicel. IR spectra were recorded in a Thermo Scientific FTIR spectrometer Nicolet iS10.

2.5.1. General procedure for the 1,2-hydroxyfluorination of olefins.

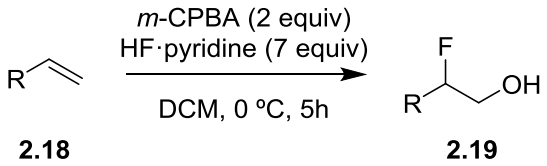

2.18 **2.19**

A 5-ml polypropylene vial was charged with *m*-CPBA 77% w/w (90 mg, 0.4 mmol, 2 equiv). DCM (2 ml) was added and the resulting suspension was cooled in an ice bath. The corresponding olefin (0.2 mmol) was then added followed by HF·pyridine 70% w/w (36 µL, 1.4 mmol, 7 equiv). The reaction mixture was stirred for 5h, then quenched by the addition of ice and a spatula tip of $KHSO_3$, and stirred for a further 30 minutes whilst warming to room temperature. The reaction mixture was then extracted with DCM (3 x 5 ml), and the combined organic layers dried over anhydrous sodium sulphate, filtered and concentrated under reduced pressure. The crude mixture was purified by flash chromatography using appropriate mixtures of hexanes and ethyl acetate as the eluent (for low molecular weight derivatives pentane/diethyl ether mixtures were used due to their high volatility).

Compounds **2.19a-g**, **2.19l-r** and both *anti*- and *syn*-**2.27** have been previously described, and their spectroscopic data were concordant with those reported in the literature.

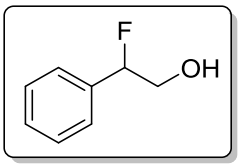

2-Fluoro-2-phenylethanol, 2.19a

Flash chromatography of the crude reaction product [*n*-hexane-AcOEt (2:1)] afforded **2.19a** as a colourless oil (68%, 19 mg). This reaction was also carried out on a 10 mmol scale (1.04 g styrene) following an otherwise identical procedure, obtaining the title compound in 53% yield.[90]

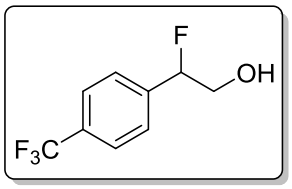

2-Fluoro-2-(4-(trifluoromethyl)phenyl)ethanol, 2.19b

Flash chromatography of the crude reaction product [*n*-hexane-AcOEt (2:1)] afforded **2.19b** as a colourless oil (43%, 18 mg).

^{1}H NMR (300 MHz, $CDCl_3$): δ 1.96 (dd, *J*= 7.7, 5.5 Hz, 1H), 3.95–3.74 (m, 2H), 5.56 (ddd, *J*= 48.3, 6.2, 3.8 Hz, 1H), 7.40 (d, *J*= 8.0 Hz, 1H), 7.59 (d, *J*= 8.4 Hz, 2H) ppm.

^{13}C NMR (75.5 MHz, $CDCl_3$): δ 66.3 (d, *J*= 24.1 Hz), 93.9 (d, *J*= 174.0 Hz), 123.9 (q, *J*= 272.2 Hz), 125.6 (q, *J*= 3.6 Hz), 125.9 (d, *J*= 7.5 Hz), 130.9 (q, *J*= 32.3 Hz), 140.3, (d, *J*= 20.0 Hz) ppm.

^{19}F NMR (282 MHz, $CDCl_3$): δ -62.74 (s, 3F), -189.98 (ddd, 1F, *J*= 48.6, 27.0, 21.8 Hz).

HRMS (EI) calcd. for $NaC_9H_8F_4O$ [M+Na^+]: 231.0403, found: 231.0396.

IR (neat, ν_{max}, cm^{-1}): 3338, 2360, 1623, 1418, 1323, 1256, 1164, 1113, 1066, 1017, 880, 841, 765, 698.

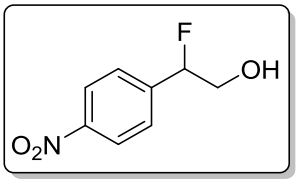

2-Fluoro-2-(4-nitrophenyl)ethanol, 2.19c

Flash chromatography of the crude reaction product [*n*-hexane-AcOEt (2:1)] afforded **2.19c** as a colourless oil (37%, 14 mg).[90]

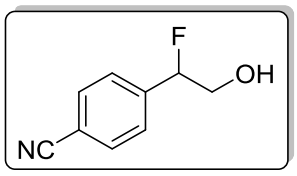

2-Fluoro-2-(4-cyanophenyl)ethanol, 2.19d

Flash chromatography of the crude reaction product [*n*-hexane-AcOEt (2:1)] afforded **2.19d** as a colourless oil (67%, 22 mg).[90]

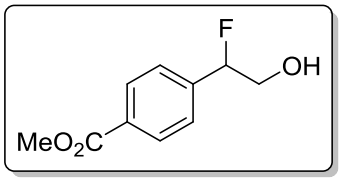

Methyl 4-(1-fluoro-2-hydroxyethyl)benzoate, 2.19e

Flash chromatography of the crude reaction product [*n*-hexane-AcOEt (2:1)] afforded **2.19e** as a colourless oil (46%, 17 mg).[90]

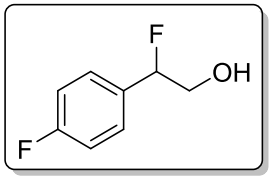

2-Fluoro-2-(4-fluorophenyl)ethanol, 2.19f

Flash chromatography of the crude reaction product [*n*-hexane-AcOEt (2:1)] afforded **2.19f** as a colourless oil (38%, 12 mg).[90]

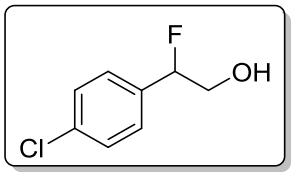

2-Fluoro-2-(4-chlorophenyl)ethanol, 2.19g

Flash chromatography of the crude reaction product [*n*-hexane-AcOEt (2:1)] afforded **2.19g** as a colourless oil (47%, 16 mg). [90]

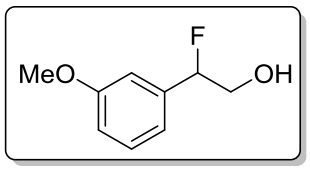

2-Fluoro-2-(3-methoxyphenyl)ethanol, 2.19k

Flash chromatography of the crude reaction product [*n*-hexane-AcOEt (2:1)] afforded **2.19k** as a colourless oil (40%, 14 mg).

^{1}H NMR ($CDCl_3$, 300 MHz): δ 1.92 (br s, OH), 3.75 (s, 3H), 3.93–3.77 (m, 2H), 5.47 (ddd, *J*= 48.7, 7.5, 3.3 Hz, 1H), 6.86–6.72 (m, 3H), 7.30–7.19 (m, 1H) ppm.

^{13}C NMR (75.5 MHz , $CDCl_3$): δ 55.2, 66.5 (d, *J*= 24.4 Hz), 94.6 (d, *J*= 172.8 Hz), 111.2 (d, *J*= 7.7 Hz), 114.2, 117.8 (d, *J*= 7.1 Hz), 129.7, 137.8 (d, *J*= 19.8 Hz), 159.7 ppm.

^{19}F NMR (282 MHz, $CDCl_3$): δ -187.89 (ddd, *J*= 48.9, 29.4, 19.5 Hz).

HRMS (EI) calcd. for $NaC_9H_{11}FO_2$ [M+Na^+]: 193.0635, found: 193.0637.

IR (neat, ν_{max}, cm^{-1}):3667, 2938, 1587, 1490, 1456, 1435, 1255, 1157, 854, 780, 735, 696.

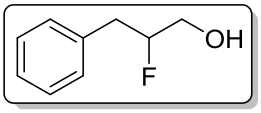

2-Fluoro-3-phenylpropanol, 2.19l

Flash chromatography of the crude reaction product [n-hexane-AcOEt (2:1)] afforded **2.19l** as a colourless oil (60%, 19 mg).[100]

IR (neat, ν_{max}, cm^{-1}): 3370, 3029, 2931, 1719, 1496, 1455, 1257, 1050, 903, 836, 746, 700.

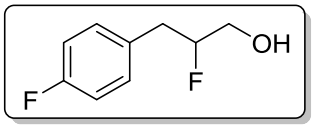

2-Fluoro-3-(4-fluorophenyl)propanol, 2.19m

Flash chromatography of the crude reaction product [n-hexane-AcOEt (2:1)] afforded **2.19m** as a colourless oil (57%, 20 mg).[100]

IR (neat, ν_{max}, cm^{-1}): 3369, 2935, 1718, 1602, 1510, 1258, 1222, 1159, 1052, 818, 750.

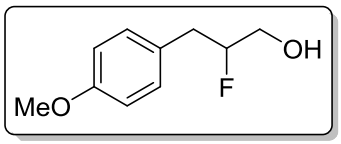

2-Fluoro-3-(4-methoxyphenyl)propanol, 2.19n

Flash chromatography of the crude reaction product [n-hexane-AcOEt (2:1)] afforded **2.19n** as a white solid (41%, 15 mg).[100]

IR (neat, ν_{max}, cm^{-1}): 3358, 2916, 2838, 1717, 1614, 1587, 1511, 1436, 1302, 1244, 1176, 1111, 1091, 1070, 1023, 886, 809, 749, 717.

[100] F. Luo, P. Wang and Y. Gong, *Tetrahedron Lett.*, 2010, **51**, 1693-1695.

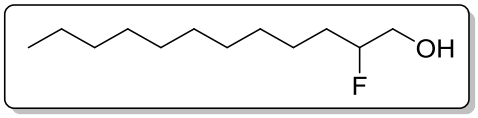

2-Fluorododecan-1-ol, 2.19o

Flash chromatography of the crude reaction product [n-hexane-AcOEt (2:1)] afforded **2.19o** as a waxy solid (93%, 38 mg).[101]

HPLC (Chiralcel AY-H, 95:5 hexane/*i*-PrOH, 1 mL min^{-1}, 240 nm) R_T (major) = 10.41 min, R_T (minor) = 11.27 min.

IR (neat, ν_{max}, cm^{-1}): 3461, 2917, 2849, 1456, 1378, 1261, 1101, 965, 860, 827, 719, 628, 622, 616, 611, 605.

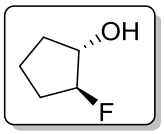

***trans*-2-Fluorocyclopentanol, 2.19p**

Flash chromatography of the crude reaction product [n-pentane-Et2O (1:1)] afforded **2.19p** as a colourless oil (72%, 15 mg).[102]

IR (neat, ν_{max}, cm^{-1}): 3331, 2963, 1084, 1035, 877.

This reaction was also conducted at the 2 mmol scale using the following procedure: A 5-mL polypropylene vial was charged with *m*-CPBA 77% w/w (900 mg, 4 mmol, 2 equiv). DCM (20 ml) was added and the resulting suspension was cooled in an ice bath. Finally, cyclopentene (2 mmol) was added followed by HF·pyridine 70% w/w (360 µL, 14 mmol, 7 equiv). The reaction mixture was stirred for 5h, then quenched by the addition of ice and a spatula of $KHSO_3$ and stirred for a further 30 minutes whilst warming to room temperature. The reaction mixture was then extracted with DCM (3 x 20 ml), and the combined organic layers dried over anhydrous sodium sulphate, filtered and concentrated under reduced pressure with the bath of the rotary evaporator at 0 °C. The residue was purified by kugelrohr distillation (35 °C, 15 mmHg), affording **2.19p** as a colourless liquid (126 mg, 61%).

[101] H. Yoshino, K. Nomura, S. Matsubara, K. Oshima, K. Matsumoto, R. Hagiwara and Y. Ito, *J. Fluorine Chem.* 2004, **125**, 1127-1129.
[102] D. F. Shellhamer, A. A. Briggs, B. M. Miller, J. M. Prince, D. H. Scott and V. L. Heasley, *J. Chem. Soc. Perkin Trans. 2* 1996, 973-977.

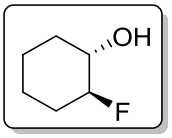

***trans*-2-Fluorocyclohexanol, 2.19q**

Flash chromatography of the crude reaction product [*n*-pentane-Et_2O (1:1)] afforded **2.19q** as a colourless oil (63%, 15 mg).[101]

IR (ν_{max}, cm^{-1}): 3567, 2934, 2862, 2360, 1734, 1559, 1456, 1099, 1015, 842, 669, 616.

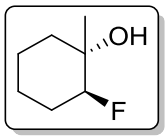

***trans*-Fluoro-2-methylcyclohexanol, 2.19r**

Flash chromatography of the crude reaction product [*n*-pentane-Et_2O (1:1)] afforded **2.19r** as a colourless oil (20%, 5 mg).[101]

IR (neat, ν_{max}, cm^{-1}): 3545, 2929, 2858, 2360, 1716, 1670, 1575, 1448, 1333, 1297, 1262, 1164, 1145, 1092, 1072, 999, 948, 889, 807, 749, 717, 686.

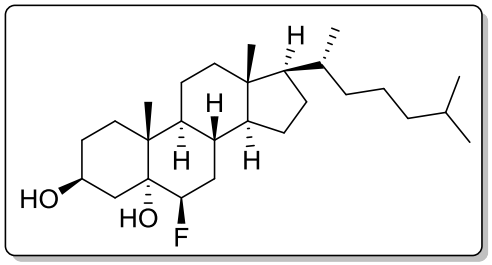

(3*S*,5*R*,6*R*,8*S*,9*S*,10*R*,13*R*,14*S*,17*R*)-**6-Fluoro-10,13-dimethyl-17-((*R*)-6-methylheptan-2-yl)hexadecahydro-5*H*-cyclopenta[α]phenanthrene-3,5-diol, 2.19t**

Flash chromatography of the crude reaction product [*n*-hexane-AcOEt (2:1)] afforded **2.19t** as a white solid (76%, 14 mg), with a melting point of 200-203 °C.

^{1}H NMR (300 MHz, $CDCl_3$): δ 0.79 (d, *J*= 6.6 Hz, 3H), 0.80 (d, *J*= 6.6 Hz, 3H), 0.83 (d, *J*= 6.5 Hz, 3H), 1.83 – 0.95 (m, 34H), 2.12 – 1.87 (m, 2H), 4.00 (tt, *J*= 10.6, 5.4 Hz, 1H), 4.18 (dt, *J*= 49.2, 2.8 Hz, 1H) ppm.

^{13}C NMR ($CDCl_3$, 75.5 MHz): δ 15.9 (s), 16.0 (s), 18.6 (s), 21.0 (s), 22.5 (s), 22.8 (s), 23.8 (s), 23.9 (s), 27.9 (s), 28.1 (s), 30.3 (s), 30.7 (s), 31.7 (s), 32.0 (s), 34.8 (s), 35.7 (s), 36.1 (s), 38.1 (d, *J*= 2.0 Hz), 39.4 (s), 39.8 (s), 40.3 (s), 42.7 (s), 45.3 (s), 56.0 (d, *J*= 23.2 Hz), 67.2 (s), 74.6 (d, *J*= 21.1 Hz), 95.3 (d, *J*= 178.9 Hz) ppm.

^{19}F NMR ($CDCl_3$, 282.4 MHz): δ -184.8 (m).

HRMS (EI) calcd. for $C_{27}H_{50}NO_2$ [M-HF+NH_4^+]: 420.3836, found: 420.3829.

IR (neat, ν_{max}, cm^{-1}): 3416, 2936, 2866, 1467, 1375, 1017, 959, 862, 800, 603.

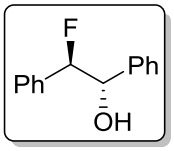

(1*R**,2*S**)-**2-Fluoro-1,2-diphenylethanol, *anti*-2.27**

Flash chromatography of the crude reaction product [*n*-hexane-AcOEt (2:1)] afforded *anti*-**2.27** as a white solid (76%, 33 mg).[90]

Chapter 3

The synthesis and reactivity of fluorovinyl sulfones

3.0. Objectives.

The main objective of this project was to synthesise the scarcely studied β-fluorovinyl sulfones. Basing our objectives on the literature available at the time, we proposed their synthesis should be relatively straightforward taking advantage of the intrinsic electrophilicity of the corresponding alkynyl sulfones.

Furthermore, given that this class of compounds had not been described in the literature, we planned to study the reactivity of such compounds; nucleophilic additions, cycloadditions, hydrogenations and coupling reactions were all potentially well-suited to this class of compounds. In this way, the synthesised β-fluorovinyl sulfones could be used as fluorinated building blocks to produce more complex fluorinated structures.

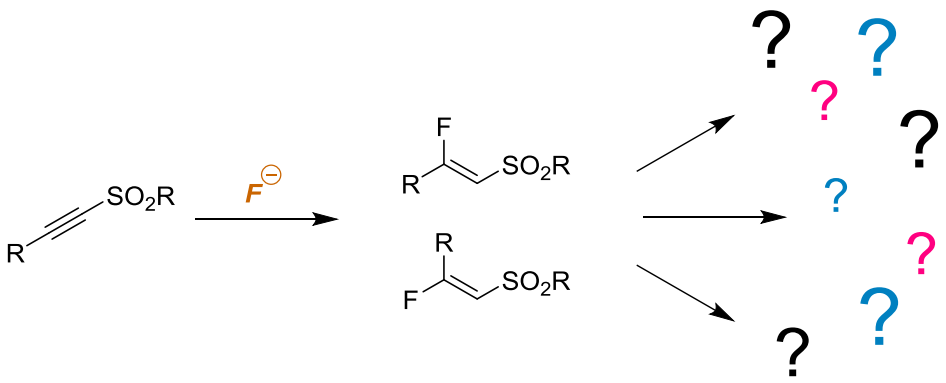

3.1. Introduction.

3.1.1. Previous syntheses of fluorovinyl sulfones and related compounds.

We began this venture after finding that this class of compounds was scarce in the chemical literature; although several methods had been described for the synthesis of α-fluorovinyl sulfones,[103, 104] still none existed with the fluorine in the β position. We therefore decided to focus on the β isomers. However, during the preparation of this work in mid-2017, two separate reports were published detailing the synthesis of β-fluorovinyl sulfones.[105, 106]

Related compounds with electron withdrawing groups, such as esters and ketones, had been described—although still overwhelmingly in their α-fluorinated isomer. Traditionally, the formation of compounds of this type has been dominated by the elimination of HX from carefully chosen starting materials (Scheme 3.1).[107] However, this approach is hindered by the availability of the specific starting materials for each desired product. It is also worth noting that early examples are often limited to compounds arising from either fluoroethylenes or polyfluorinated starting materials, for lack of selective and practical fluorinating agents; this is somewhat less of a problem nowadays. Nonetheless, both mono- and difluorinated acrylates and ketones have been synthesised in this way (Scheme 3.1). Archibald and co-workers reported an interesting example in 1990, consisting in the addition of 1,1-difluoroethene **3.1** to acyl chlorides **3.2**, followed by triethylamine-mediated elimination of HCl from intermediate **3.3**, finally furnishing the desired Friedel-Crafts like products 2,2-difluorovinyl ketones **3.4**, as well as acrylates **3.6** after the regioselective Baeyer-Villiger oxidation (Scheme 3.1).[105]

[103] G. K. S. Prakash, S. Chacko, H. Vaghoo, N. Shao, L. Gurung, T. Mathew and G. A. Olah, *Org. Lett.,* 2009, **11**, 1127–1130.

[104] a) M. He, A. K. Ghosh and B. Zajc, *Synlett*, 2008, **7**, 999–1004. b) S. K. Mandal, A. K. Ghosh, R. Kumar and B. Zajc, *Org. Biomol. Chem*., 2012, **10**, 3164-3167.

[105] X. Zeng, S. Liu, G. B. Hammond and B. Xu, *Chem. Eur. J.*, 2017, **23**, 11977–11981.

[106] C. D. McCune, M. L. Beio, J. M. Sturdivant, R. de la Salud-Bea, B. M. Darnell and D. B. Berkowitz, *J. Am. Chem. Soc.*, 2017, **139**, 14077–14089.

[107] T. G. Archibald and K. Baum, *J. Org. Chem.*, 1990, **55**, 3562-3565.

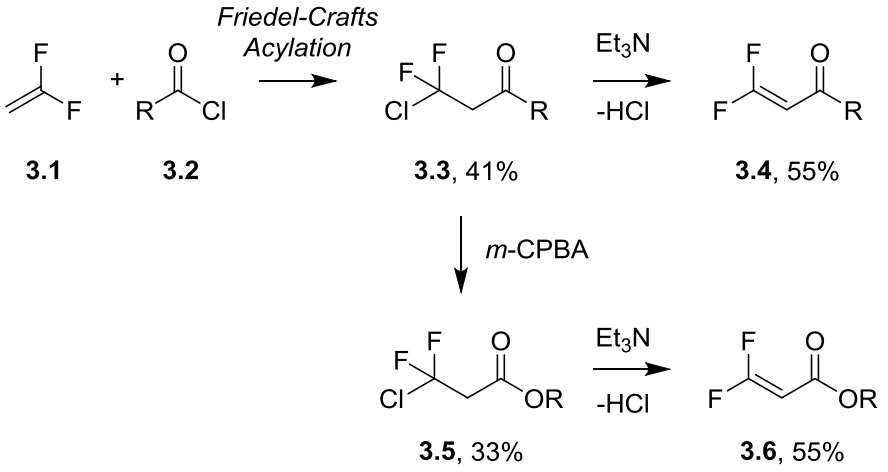

Scheme 3.1. Synthesis of β,β-difluoro-α,β-unsaturated ketones and acrylates *via* HX elimination.

Nguyen and Wakselman were particularly active in this area in the 1980s and 90s, and successfully synthesised β-fluoro-α,β-unsaturated esters **3.10** (Scheme 3.2) and carboxylic acids **3.14**, as well as related α-fluoro-α,β-ketones and allylic alcohols.[108]

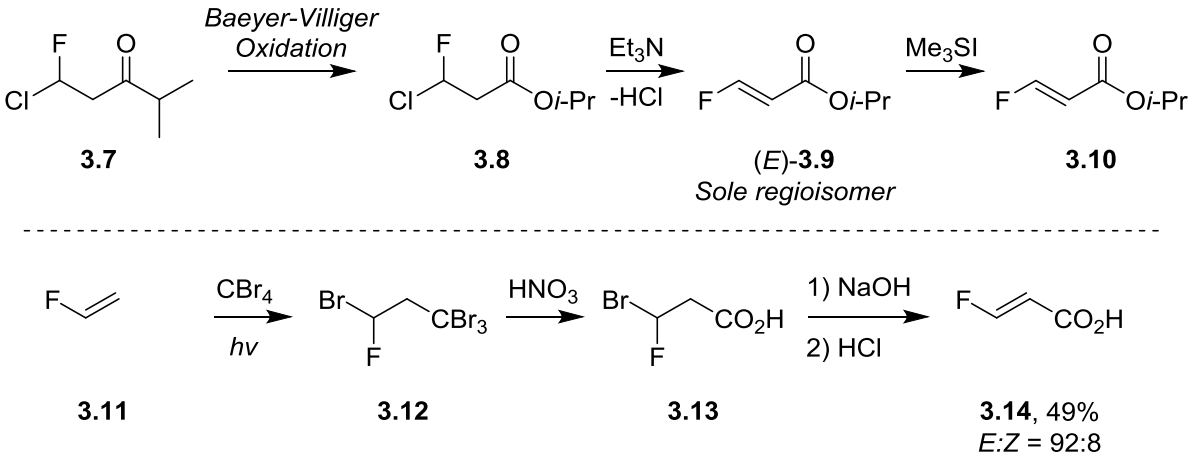

Scheme 3.2. Past examples of fluorinated α,β-unsaturated carbonyl compounds.

The development of new fluorinating reagents in turn resulted in several new—or perhaps better said, updated—methodologies for the synthesis of conjugated vinyl fluorides, using more sophisticated fluorinated starting materials or reagents to give access to a wider scope of target compounds. For

[108] a) H. Molines, and C. Wakselman, *J. Fluorine Chem.*, 1984, **25**, 447-451. b) T. Nguyen, J. Leroy and C. Wakselman, *J. Org. Chem.*, 1993, **58**, 3772-3774. c) T. Nguyen and C. Wakselman, *J. Org. Chem.*, 1989, **54**, 5640-5642. d) A. Ohmori, S. Takaki, T. Kitahara, Eur. Pat. 136668, 1985. e) H. Molines, T. Nguyen and C. Wakselman, *Synthesis*, 1985, **8**, 755-756.

example, in 1985, McCarthy, Peet *et al.* described the first fluoro-Pummerer rearrangement, utilising DAST as an alternative to acetic anhydride in the traditional Pummerer rearrangement (Scheme 3.3).[109a] They later applied this to the synthesis of vinyl fluoride-containing nucleoside mechanism-based inhibitors of *S*-adenosyl-L-homocysteine hydrolase, an enzyme responsible for the hydrolysis of *S*-adenosylhomocysteine into L-homocysteine and adenosine.[109b] In 1990, Krishnan and Sampson applied this new methodology to the synthesis of β-fluoroacrylonitriles **3.19** and acrylates **3.20** (Scheme 3.3).[109c]

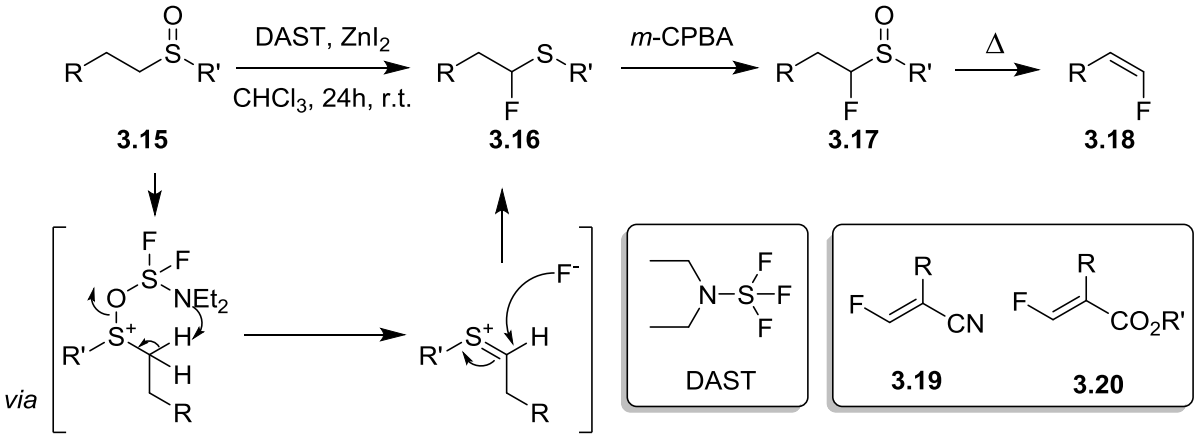

Scheme 3.3. The fluoro-Pummerer rearrangement and its application to the synthesis of β-fluoroacrylonitriles and acrylates.

The wider availability of fluorinated small molecules permitted the application of more traditional olefin syntheses to obtain fluorinated analogues. Many of these have been successfully applied or adapted accordingly to the synthesis of α-fluoro-α,β-unsaturated carbonyls and related compounds. These are the Wittig, Julia, Peterson and related olefinations,[104, 110, 111, 112, 113, 114] as well as Knoevenagel-like

[109] a) J. R. McCarthy, N. P. Peet, M. E. LeTourneau and M. Inbasekaran, *J. Am. Chem. Soc.*, 1985, **107**, 735–737. b) E. T. Jarvi, J. R. McCarthy, S. Mehdi, D. P. Matthews, M. L. Edwards, N. J. Prakash, T. L. Bowlin, P. S. Sunkara and P. Bey, *J. Med. Chem.*, 1991, **34**, 647-656. c) G. Krishnan and G. Sampson, *Tetrahedron Lett.*, 1990, **31**, 5609-5612. d) For a review on fluoro-Pummerer rearrangements see: V. Hugenberg and G. Haufe, *J. Fluorine Chem.*, 2012, **143**, 238-262.

[110] a) Y. Suzuki and M. Sato, *Tetrahedron Lett.* 2004, **45**, 1679–1681. b) For a review of fluorinated phosphonium ylides and their reactivity, see: D. J. Burton, Z.-Y. Yang and W. Qiu, *Chem. Rev.*, 1996, **96**, 1641−1715.

[111] D. Chevrie, T. Lequeux and J.-C. Pommelet, *Org. Lett.*, 1999, **1**, 1539-1541.

[112] a) S. Sano, T. Ando, K. Yokoyama and Y. Nagao, *Synlett*, 1998, **7**, 777-779. b) S. Sano, K. Saito and Y. Nagao, *Tetrahedron Lett.*, 2003, **44**, 3987-3990. c) C. Grison, S. Genève, E. Halbin and P. Coutrot, *Tetrahedron*, 2001, **57**, 4902-4923.

[113] a) A. K. Ghosh, S. Banerjee, S. Sinha, S. B. Kang and B. Zajc, *J. Org. Chem.*, 2009, **74**, 3689-3697. b) E. Pfund, C. Lebargy, J. Rouden and T. Lequeux, *J. Org. Chem*., 2007, **72**, 7871-7877. c) B. Zajc and R. Kumar, *Synthesis*, 2010, **11**, 1822-1836.

[114] a) N. Asakura, Y. Usuki and H. Iio, *J. Fluorine Chem.*, 2003, **124**, 81-88. b) J. T. Welch and R. W. Herbert, *J. Org. Chem*., 1990, **55**, 4782-4784.

reactions,[103, 115] which all formally involve the addition of a fluoromethylene anion to a carbonyl compound followed by an elimination to form the double bond. Of these methods, the Peterson, Julia, Knoevenagel-like and Horner-Wadsworth-Emmons (HWE) methods have been used to synthesise α-fluorovinyl sulfones (Scheme 3.4).[116]

Unfortunately, many of these procedures suffer from poor stereoselectivity,[110, 114] the need for metal catalysts,[112a, 116] or the use of complex or expensive starting materials. Furthermore, all of these only provide access to the vinyl fluorides with the fluorine in the α position relative to the functional group.

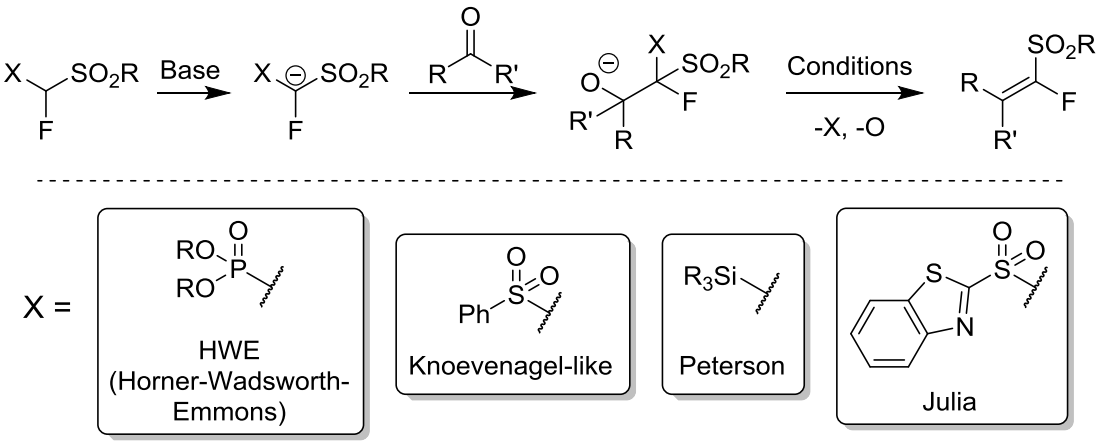

Scheme 3.4. Compilation of reactions involving a fluorinated carbon-acid/carbonyl addition-elimination for the synthesis of α-fluorovinyl sulfones.

Methods to synthesise the related β isomers are much less common. In this context, the vast majority of the literature deals with the addition of the fluoride ion to electron-deficient alkynes. Nevertheless, the simplest ester of this type, ethyl (*Z*)-3-fluoropropenoate (*Z*)-**3.22**, can be synthesised *via* Wittig reaction with ethyl oxylate **3.21** as shown by Patrick *et al.* in 2011,[117] following the methodology described by Burton *et al.* back in 1985 (Scheme 3.5).[118] For the opposite stereoisomer however, the authors did use the nucleophilic addition of fluoride to ethyl propiolate **3.23**, obtaining the desired ethyl (*E*)-3-fluoropropenoate (*E*)-**3.22**, albeit in a low yield.

[115] a) J. Qian, W. Yi, M. Lv and C. Cai, *Synlett*, 2015, **26**, 127–132. b) T. Kitazume and N. Ishikawa, *Chem. Lett.*, 1981, 1259-1260.

[116] For other examples of addition-elimination procedures to form the desired compounds, see: a) M. Inbasekaran, N. P. Peet, J. R. McCarthy and M. E. LeTourneau, *J. Chem. Soc., Chem. Commun*., 1985, 678-679. b) T. Ishihara and M. Kuroboshi, *Chem. Lett.*, 1987, 1145-1148. c) G. Lemonnier, L. Zoute, G. Dupas, J.-C. Quirion and P. Jubault, *J. Org. Chem.*, 2009, **74**, 4124-4131.

[117] T. B. Patrick, J. Neumann and A. Tatro, *J. Fluorine Chem*., 2011, **132**, 779–782.

[118] D. G. Cox, N. Gurusamy and D. J. Burton, *J. Am. Chem. Soc.*, 1985, **107**, 2811-2812.

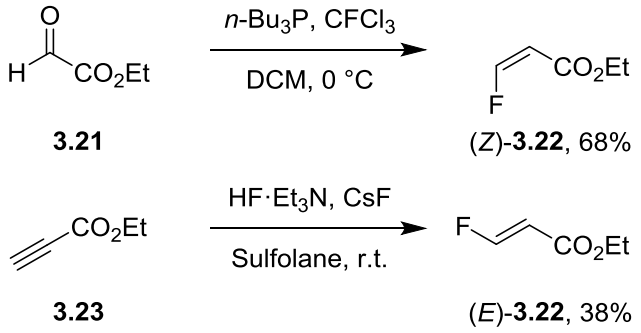

Scheme 3.5. Synthesis of ethyl (*E*)- and (*Z*)-3-fluoropropenoate 3.22.

There are several precedents for the addition of fluoride to electron-deficient alkynes such as these, although many suffer from low yields or low/uncontrollable stereoselectivity.[119] Interestingly, Cousseau *et al*. saw a reverse in selectivity with 2-decynenitrile **3.24** when using a polymer-bound version of the fluoride nucleophile (Scheme 3.6). Nonetheless, the *Z* isomers were the major product in the vast majority of cases. This can be explained by considering the reaction mechanism; after addition of the fluoride ion, the negative charge on the intermediate species would be most stable the furthest possible away from the electronegative fluorine atom, resulting in the *trans*-addition of HF across the alkyne.

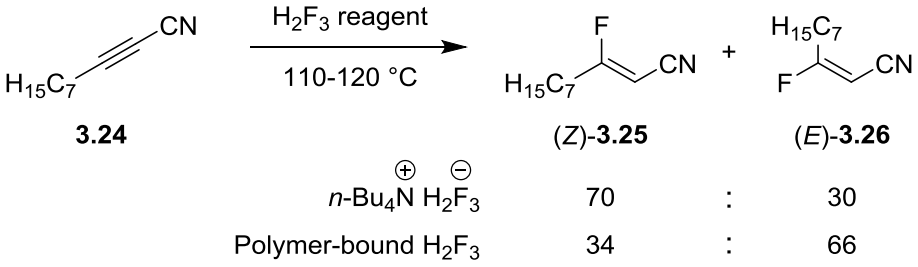

Scheme 3.6. Reverse in selectivity when using the polymer-bound dihydrogen trifluoride reagent with 2-decynenitrile.

Later, in 2012 Jiang *et al.* described an efficient method for the hydrofluorination of electron deficient alkynes, albeit using a relatively expensive nucleophilic fluoride reagent: silver(I) fluoride.[120] To achieve this, the authors simply heated a mixture of the alkyne and AgF in MeCN:H_2O (20:1) at 80 °C for ten hours, obtaining the desired compounds in good to excellent yields (Scheme 3.7). The

[119] a) P. Albert and J. Cousseau, *J. Chem. Soc., Chem. Commun.,* 1985, 961-962. b) A. Gorgues, D. Stéphan and J. Cousseau, *J. Chem. Soc., Chem. Commun.,* 1989, 1493-1493.
[120] Y. Li, X. Liu, D. Ma, B. Liu and H. Jiang, *Adv. Synth. Catal*., 2012, **354**, 2683-2688.

stereoselectivities varied greatly (4:1–99:1), though always in favour of the *Z* isomer corresponding to the *trans*-hydrofluorination.

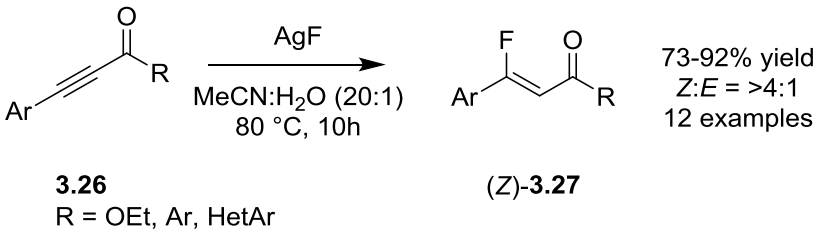

Scheme 3.7. Hydrofluorination of electon-deficient alkynes to form (*Z*)-β-fluorochalcones.

Following this, in 2017 Sun, Gong and co-workers described the synthesis of the same β-fluoroalkenyl carbonyl products starting from the corresponding β-chloro derivatives.[121] This reaction consists in the elimination of HCl to form the corresponding alkynyl carbonyl compound, and from there the same addition of nucleophilic fluoride.

The remainder of this section will look specifically at the synthesis of fluorovinyl sulfones. The fluoro-Pummerer rearrangement following the development of DAST permitted the facile synthesis of a simple fluorinated sulfone building block, fluoromethyl phenyl sulfone **3.30**, which the McCarthy group exploited throughout the 1980s and 90s.[116a, 122, 123] The α-protons are fairly acidic in this compound; sulfones are strongly electron-withdrawing, and the resulting anion is stabilised through resonance. Therefore, treatment of **3.30** with *n*-BuLi forms the corresponding carbanion, which then reacts with an aldehyde to give the corresponding α-fluoro-β-hydroxy sulfone **3.31**. Upon treatment with methanesulfonyl chloride, elimination of H_2O from the molecule results in the desired α-fluorovinyl sulfone, **3.32** (Scheme 3.8).

[121] J. Zhang, L. Liu, J. Duan, L. Gu, B. Chen, T. Sun and Y. Gong, *Adv. Synth. Catal.*, 2017, **359**, 4348-4358.
[122] J. R. McCarthy, D. P. Matthews, M. L. Edwards, D. M. Stemerick and E. T. Jarvi, *Tetrahedron Lett.*, 1990, **31**, 5449-5452.
[123] a) J. R. McCarthy, E. W. Huber, T.-B. Le, F. M. Laskovics and D. P. Matthews, *Tetrahedron*, 1996, **52**, 45-58. b) J. R. McCarthy, D. P. Matthews, D. M. Stemerick, E. W. Huber, P. Bey, B. J. Lippert, R. D. Snyder and P. S. Sunkara, *J. Am. Chem. Soc.,* 1991, **113**, 7439-7440.

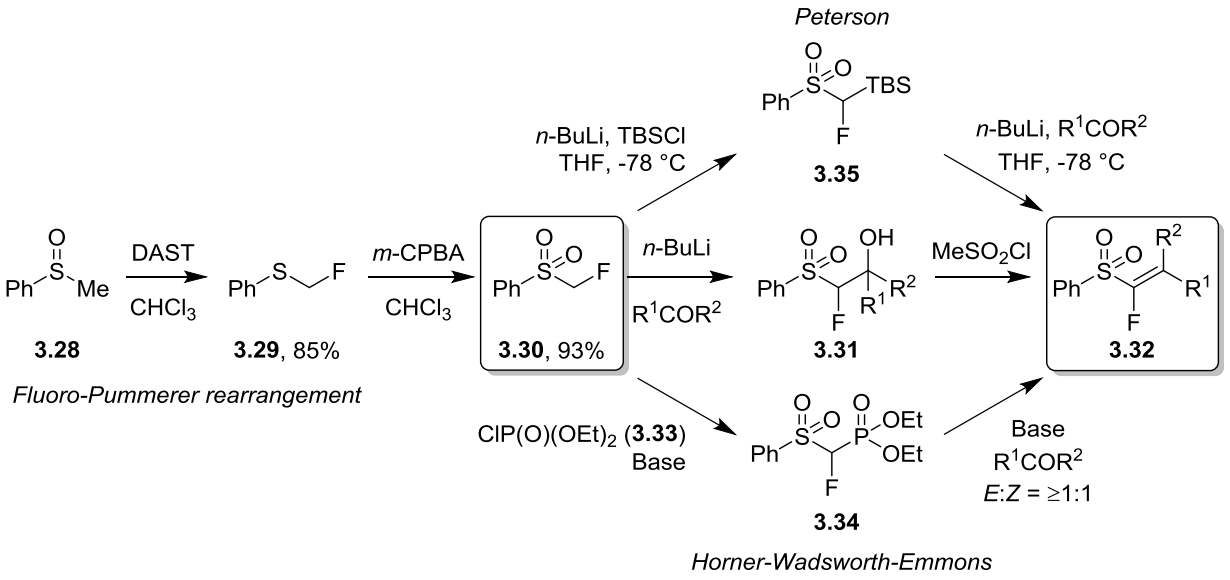

Scheme 3.8. The use of fluorinated building block fluoromethyl phenyl sulfone in the synthesis of α-fluorovinyl sulfones 3.32 *via* HWE reactions reported by McCarthy *et al.*,[116a, 122, 123] and Peterson olefinations reported by Usuki *et al.*[114a]

The group later turned to modified Horner-Wadsworth-Emmons reactions, again starting from fluorinated building block **3.30** (Scheme 3.8).[122] Treatment of **3.30** with diethyl chlorophosphate **3.33** and base forms **3.34**, a suitable reagent for the HWE reaction. Reaction of **3.34** with base and a carbonyl compound then results in the corresponding α-fluorovinyl sulfone, albeit in relatively poor *E*/*Z* selectivity. The same authors have used this method to introduce a terminal vinyl fluoride moiety into nucleoside mechanism-based inhibitors of ribonuclease diphosphate reductase, an enzyme which transforms ribonucleotides into deoxyribonucleotides.[123] Berkowitz *et al.* also used the HWE approach to synthesise and develop terminal vinyl fluoride containing amino acids as mechanism-based inhibitors of pyridoxal phosphate dependent enzymes, such as amino acid decarboxylases.[124]

Usuki and co-workers disclosed the synthesis of various α-fluorovinyl sulfones using a Peterson olefination in 2003 (Scheme 3.8).[114a] This reaction showed higher *E*/*Z* selectivity than the previous examples, although still moderate. The preference for the formation of the *E* isomer is thought to be due to no more than steric effects in the intermediate. It is worth noting that these reactions resulted in slightly higher yields when carried out in a one-pot manner without isolating the intermediate **3.35**. Furthermore, the *E*/*Z* selectivities were mostly unaffected.

[124] D. B. Berkowitz, R. de la Salud-Bea and W.-J. Jiang, *Org. Lett.*, 2004, **6**, 1821-1824.

Wnuk and co-workers also used this same approach but with the addition of slightly more sophisticated versions of **3.34**, using a 2-pyridinyl or 2-pyrimidinyl sulfone rather than the simpler phenyl.[125] This was synthesised by mixing 2-mercaptopyridine with diethyl (chloromethyl)phosphonate followed by oxidation of the resulting sulphide, and subsequent fluorination with Selectfluor to give **3.38**. The actual Horner-Wadsworth-Emmons reaction was carried out in the standard manner, resulting in high yields of **3.39** and high *E*/*Z* selectivities when aromatic aldehydes were used (>19:1). Unfortunately, for aliphatic aldehydes the *E*/*Z* selectivity was a meagre 2:1 (Scheme 3.9).

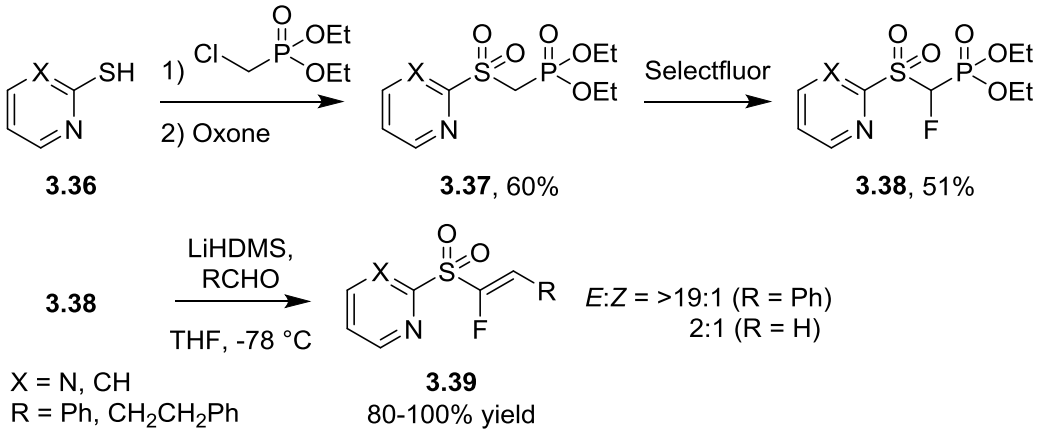

Scheme 3.9. Synthesis of α-fluorovinyl 2-pyridyl and 2-pyrimidinyl sulfones *via* HWE reaction.

The Julia olefination was applied to the synthesis of α-fluorovinyl sulfones in 2008 by Zajc and co-workers.[104a] This procedure relied on the successful synthesis of fluorinated disulfone **3.43**, during which the authors encountered certain problems with chemoselectivity; the fluorination of the central methylene group can result in both the mono- and difluorinated product (Scheme 3.10). Interestingly, this method resulted in the opposite *E*/*Z* selectivity for the products, in most cases giving the *Z* isomer as the major product.

[125] S. F. Wnuk, P. I. Garcia Jr. and Z. Wang, *Org. Lett.*, 2004, **6**, 2047-2049.

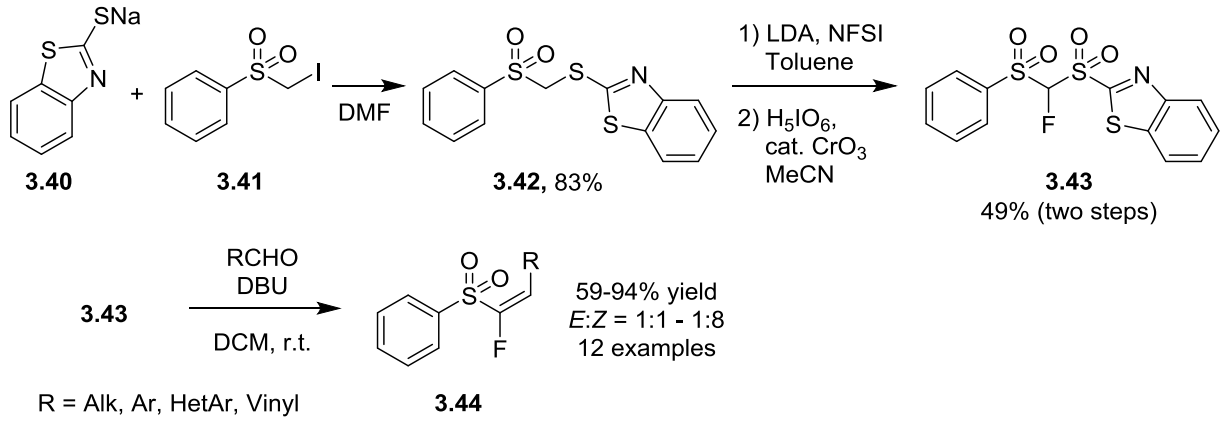

Scheme 3.10. The application of the Julia olefination to the synthesis of α-fluorovinyl sulfones.

Prakash and co-workers also described a simple and effective route to α-fluorovinyl sulfones starting from the simple and commercially available compound fluorobis(phenylsulfonyl)methane **3.45** (Scheme 3.13).[103] In this reaction, **3.45** is alkylated using a simple mixture of caesium carbonate and a benzyl, propargyl or allyl halide. The subsequent elimination of $PhSO_2X$ provides the corresponding (*E*)-α-fluorovinyl sulfones **3.46**.

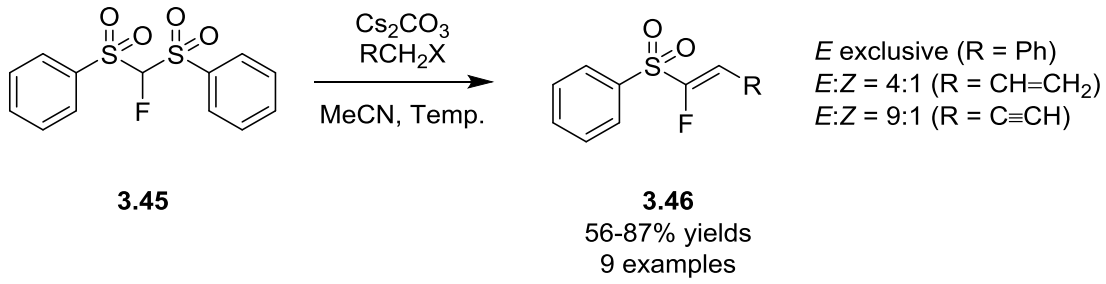

Scheme 3.13. Synthesis of (*E*)-α-fluorovinyl sulfones by Prakash *et al.*[103]

3.1.2. The chemistry of vinyl sulfones.

The synthetic utility of vinyl sulfones in organic chemistry is well-established. The strongly electron-withdrawing character of the sulfone group renders the double bond highly electron deficient, allowing it to react in a wide array of chemical processes. Traditionally, vinyl sulfones have been viewed as excellent substrates for Michael additions and cycloaddition reactions, although over the past few decades the rapidly advancing field of organic chemistry has given rise to ever more sophisticated processes. A brief overview of earlier reactions covered in the literature can be seen below (Scheme 3.12).[126] However, the reactions covered in more detail in this section will be limited to those deemed more important to the development of this project, due to the great volume of work available in this area.

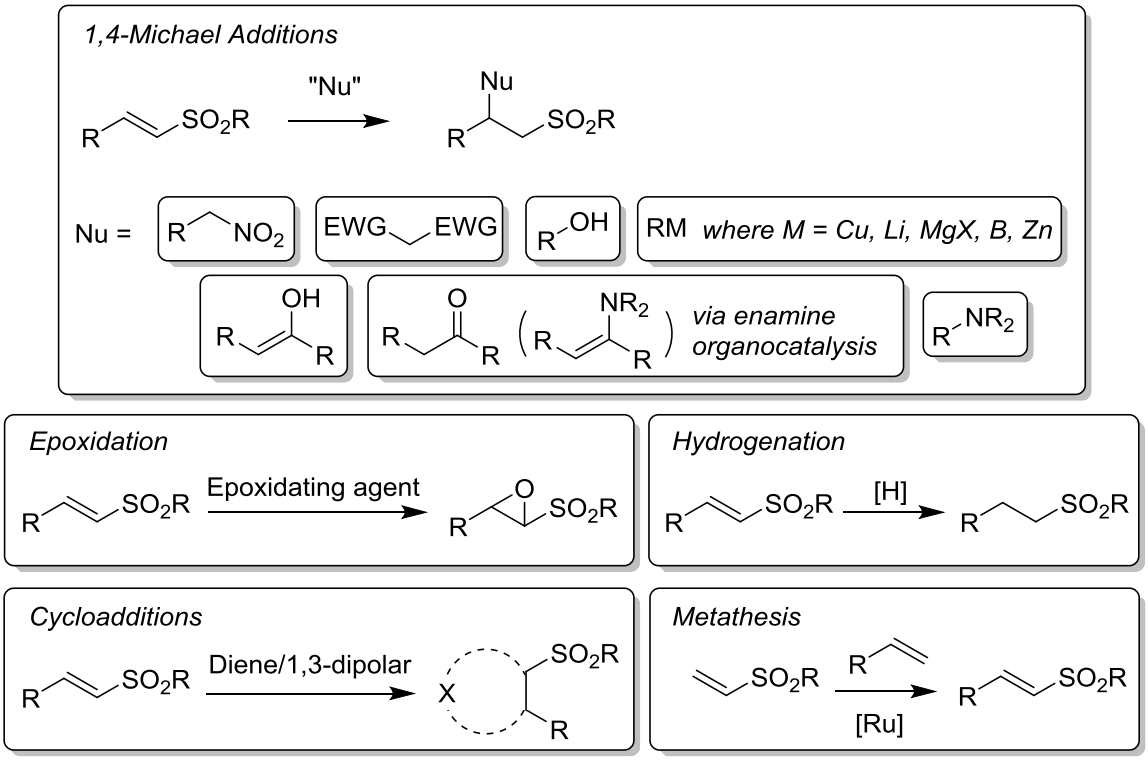

Scheme 3.12. General reactions of vinyl sulfones.[126]

[126] For earlier reviews on the chemistry of vinyl sulfones, see: a) N. S. Simpkins, *Tetrahedron*, 1990, **46**, 6951-6984. b) D. C. Meadows and J. Gervay-Hague, *Med. Res. Rev.*, 2006, **26**, 793-814. c) A.-N. R. Alba, X. Companyó and R. Rios, *Chem. Soc. Rev.*, 2010, **39**, 2018-2033. For a review on their synthesis see: Y. Fang, Z. Luo and X. Xu, *RSC Adv.*, 2016, **6**, 59661-59676.

3.1.2.1. Transition metal catalysed reactions.

In 2004, Carretero and co-workers reported the first example of the asymmetric conjugate addition of carbon nucleophiles to α,β-unsaturated sulfones **3.47** (Scheme 3.13).[127] However, the reaction heavily relied on the coordinating ability of the 2-pyridyl substitution on the sulfone; no reaction occurred with the standard phenyl substitution. The authors attributed this to the ability of the pyridine ring to coordinate to the metal catalysts used, thereby directing the reaction to take place at the double bond (Scheme 3.13). Furthermore, not only did no reaction occur with the phenyl substitution on the sulfone, but little to no reaction was observed for other nitrogen-based directing groups, highlighting the special geometry and electronic properties provided by the 2-pyridyl group. With the optimised conditions, the authors successfully added a range of arylboronic acids to α,β-unsaturated 2-pyridyl sulfones in high yields and good enantioselectivities, using the combination of a rhodium catalyst and the chiral ligand Chiraphos, **3.49**.

In subsequent studies Carretero *et al.* disclosed the application of the same catalytic system to the addition of alkenyl boronic acids to similar substrates,[128, 129] and more recently a Fujiwara-Moritani / intramolecular Michael addition sequence rendering densely functionalised indanes.[130]

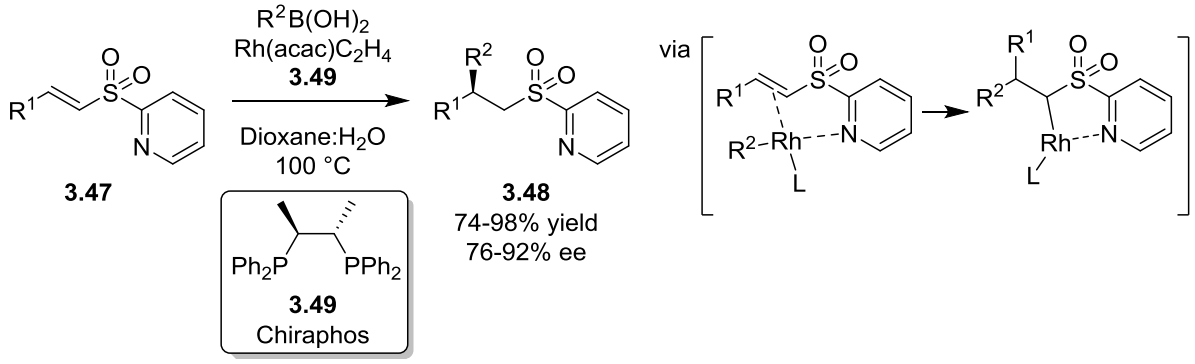

Scheme 3.13. Addition of boronic acids to α,β-unsaturated 2-pyridyl sulfones by Carretero *et al.*[127-129]

Several other reports were published in the past decade involving 1,4-additions to vinyl 2-pyridyl sulfones, albeit using different conditions. Firstly, Charette, Bechara and co-workers reported the use of a copper-BINAP system to catalyse the addition of dialkyl zinc reagents to α,β-unsaturated 2-pyridyl

[127] P. Mauleón and J. C. Carretero, *Org. Lett.*, 2004, **6**, 3195-3198.
[128] P. Mauleón and J. C. Carretero, *Chem. Commun.*, 2005, 4961-4963.
[129] P. Mauleón, I. Alonso, M. Rodríguez Rivero and J. C. Carretero, *J. Org. Chem.*, 2007, **72**, 9924-9935.
[130] P. D. Legarda, A. García-Rubia, R. Goméz Arrayás and J. C. Carretero, *Adv. Synth. Catal.*, 2016, **358**, 1065-1072.

sulfones (Scheme 3.14, Method 1).[131] This was followed by a publication from Feringa *et al.* just a few months later, in which they carried out the same transformation using Grignard reagents instead of zinc-based nucleophiles (Scheme 3.14, Method 2),[132] and a second by Feringa in 2010 using very similar conditions to Charette, but with monodentate ligand **3.52** rather than BINAP **3.50** (Scheme 3.14, Method 3).[133] All three procedures were fairly robust, resulting in high yields and high enantioselectivities in most cases.

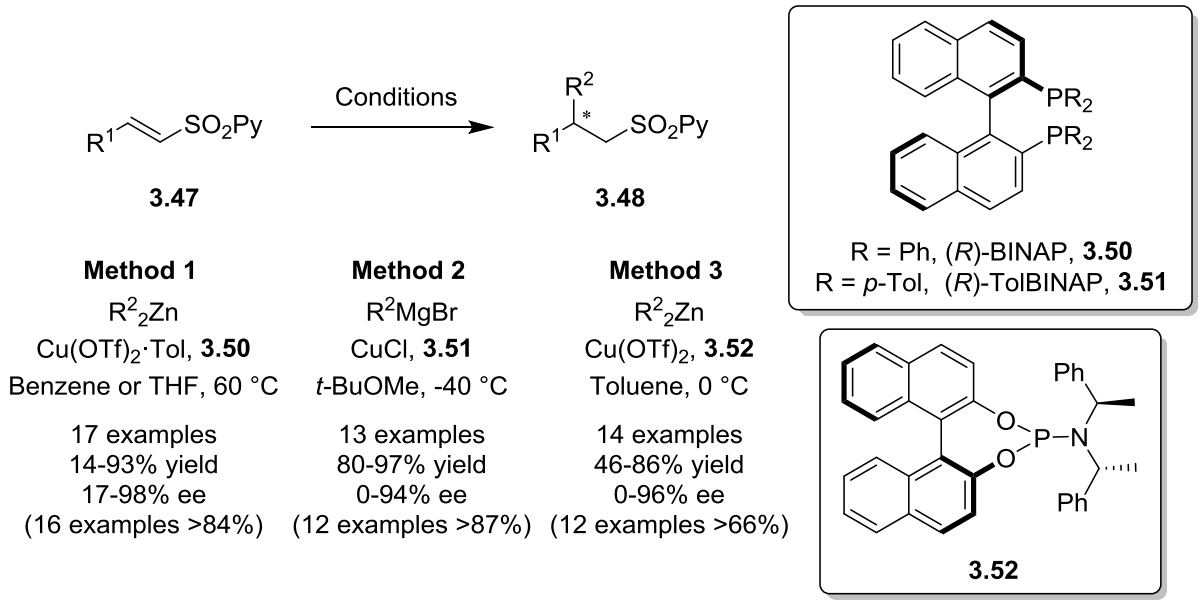

Scheme 3.14. Other methods for the addition of organometallics to α,β-unsaturated 2-pyridyl sulfones.

Following this work with 2-pyridyl sulfones, there was still a lack of methods to carry out similar reactions in a more generic way, i.e. without relying on the coordinating ability of the pyridyl group. In 2012, Nishimura, Hayashi and co-workers overcame this challenge using a rhodium-based catalyst in conjunction with a diferrocenyl ligand **3.56** (Scheme 3.15).[134] This system showed excellent reactivity and successfully added a range of arylboronic acids to the β position of α,β-unsaturated sulfones in high enantioselectivites. Careful ligand choice was important here, as more common asymmetric ligands such as BINAP resulted in *cine* substitution; addition in β, followed by elimination of the adjacent sulfone group upon release of the rhodium catalyst to give the corresponding terminal olefin **3.54** (Scheme 3.15). The same authors later showed that these same conditions can also be used for the

[131] J.-N. Desrosiers, W. S. Bechara and A. B. Charette, *Org. Lett.*, 2008, **10**, 2315-2318.
[132] P. H. Bos, A. J. Minnaard and B. L. Feringa, *Org. Lett.*, 2008, **10**, 4219-4222.
[133] P. H. Bos, B. Maciá, M. A. Fernández-Ibáñez, A. J. Minnaard and B. L. Feringa, *Org. Biomol. Chem.*, 2010, **8**, 47-49.
[134] T. Nishimura, Y. Takiguchi and T. Hayashi, *J. Am. Chem. Soc.*, 2012, **134**, 9086-9089.

addition of cyclopropyl boronic acids to afford β-cyclopropyl sulfones **3.55**.[135] The reaction could be extended to α,β-unsaturated ketones, esters and nitro compounds, with similarly high yields and enantioselectivities.

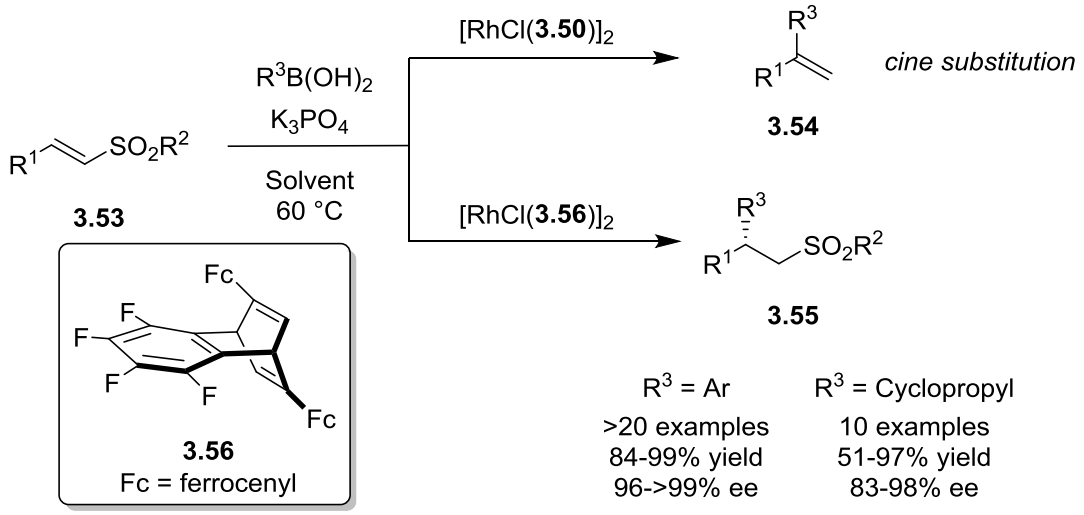

Scheme 3.15. Asymmetric addition of aryl and cyclopropyl boronic acids to α,β-unsaturated sulfones.

Additionally, other functionalities besides carbon nucleophiles have been introduced into the β position by means of transition metal catalysis. In 2011, Carretero *et al.* successfully carried out the borylation of vinyl sulfones that, after subsequent oxidation, afforded β-hydroxy sulfones **3.57** in high yields and enantioselectivities (Scheme 3.16).[136] In this case, both phenyl and 2-pyridyl sulfones gave good results, and the most effective catalytic system was copper(I) chloride with either the Josiphos **3.58** or Taniaphos **3.59** ligands—both ferrocene-based diphosphine ligands—with relatively high catalytic loadings of 10 mol%. On the other hand, Duan and co-workers successfully described the enantioselective addition of diarylphosphines both to vinyl sulfonic esters and vinyl trifluoromethyl sulfones.[137]

[135] R. Takechi and T. Nishimura, *Chem. Commun.*, 2015, **51**, 8528-8531.
[136] A. L. Moure, R. Gómez Arrayás and J. C. Carretero, *Chem. Commun.*, 2011, **47**, 6701-6703.
[137] J. Lu, J. Ye and W.-L. Duan, *Org. Lett.*, 2013, **15**, 5016-5019.

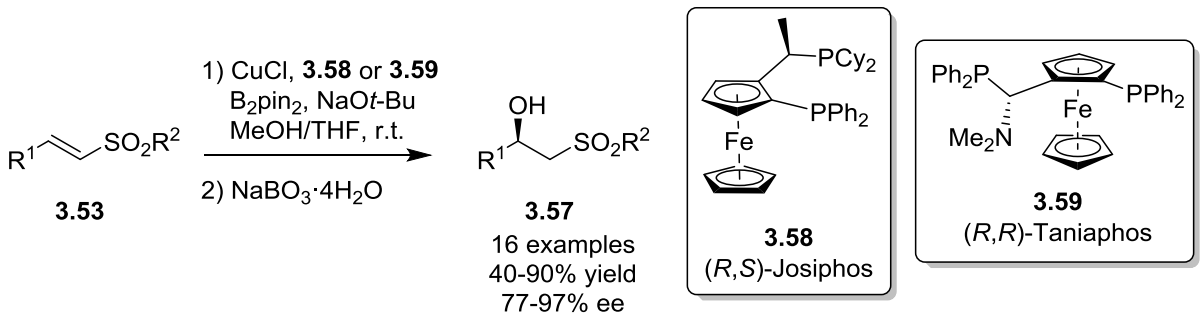

Scheme 3.16. Asymmetric borylation/oxidation sequence by Carretero *et al.*[136]

Vinyl sulfones, although originally deemed challenging coupling partners due to their strongly coordinating character, have also been used successfully in Heck reactions.[138] Gillingham *et al.* demonstrated the use of sulfoxides, sulfides and sulfones as Heck-coupling partners to aryl halides and triflates, through the use of the exceptionally active and very bulky catalyst $Pd[(Pt\text{-}Bu)_3]_2$, resulting in high yields and stereoselectivities (Scheme 3.17).

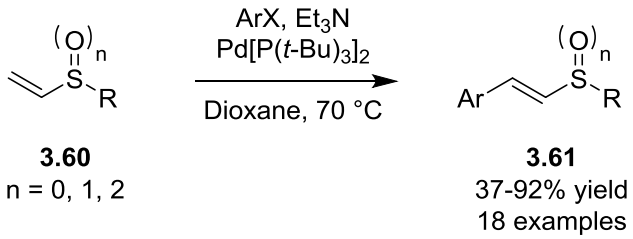

Scheme 3.17. Stereoselective Heck reactions using vinyl sulphides, sulfoxides and sulfones.

[138] D. G. Bachmann, C. C. Wittwer and D. G. Gillingham, *Adv. Synth. Catal.*, 2013, **355**, 3703-3707.

3.1.2.2. Organocatalytic reactions.

In contrast to the examples seen thus far, vinyl sulfones have also been used successfully in organocatalytic processes. For instance, in 2013 Dou and Lu disclosed an thiourea-catalysed asymmetric addition of fluorinated oxindoles **3.63** to vinyl (bis)sulfones **3.62**, to produce the corresponding fluorinated oxindole adducts **3.67** (Scheme 3.18).[139] One year later, Jiang *et al.* published a report focusing on the addition of oxazolones **3.64** catalysed by related thiourea **3.66**. The authors demonstrated how these products could be transformed into **3.69**, a useful precursor towards enantioenriched monofluorinated bioactive molecules (Scheme 3.18).[140]

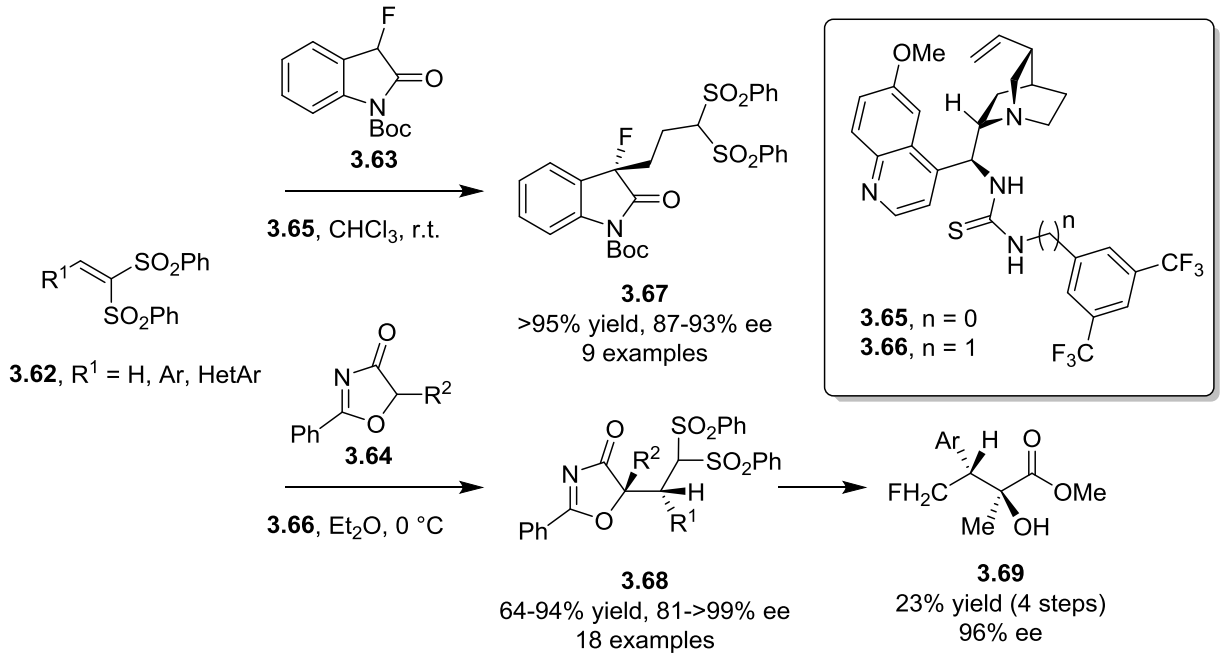

Scheme 3.18. Organocatalysed nucleophilic additions to vinyl (bis)sulfones.

Along with phenyl and pyridyl sulfones, recently a "second generation" class of sulfone substrates (**3.70**) has emerged carrying a substituted tetrazole group, which has been used to exert a greater degree of stereocontrol, as well as augmented reactivity. Cid and co-workers recently demonstrated the high reactivity of these new sulfones in Michael additions with a wide variety of nucleophiles including amines, malonates, alkoxides, thiols and more, as well as in cycloadditions with dienes,

[139] X. Dou and Y. Lu, *Org. Biomol. Chem.*, 2013, **11**, 5217-5221.
[140] Q. Liu, B. Qiao, K. F. Chin, C.-H. Tan and Z. Jiang, *Adv. Synth. Catal.,* 2014, **356**, 3777-3783.

nitrones, nitrile oxides and azides; the latter occurred with concomitant loss of the sulfone group as previously seen.[141]

Simlandy and Mukherjee used this new class of sulfones in a thia-Michael/Julia-Kocienski cascade reaction to obtain enantioenriched 2*H*-thiochromenes **3.72** (Scheme 3.19).[142] This reaction starts with the condensation of 2-mercaptobenzaldehyde **3.71** with Jørgensen's diarylprolinol silyl ether catalyst. From there, the thiol group adds to the β position of the vinyl sulfone to form the sulfide intermediate in an enantioselective manner, and a Julia-Kocienski olefination between the α-carbon and the free aldehyde affords the final thiochromene.

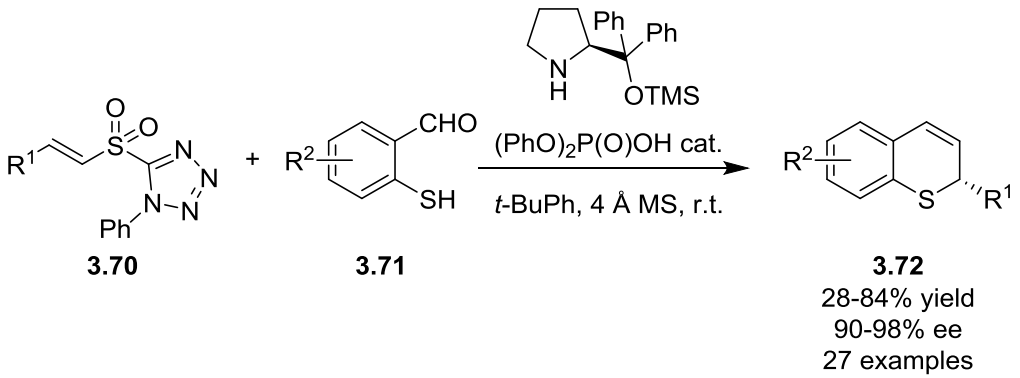

Scheme 3.19. Enantioselective cascade reaction to form 2*H*-thiochromenes 3.72.

[141] E. Rodrigo, I. Alonso, J. L. García Ruano and M. B. Cid, *J. Org. Chem.*, 2016, **81**, 10887-10899.
[142] A. K. Simlandy and S. Mukherjee, *J. Org. Chem.*, 2017, **82**, 4851-4858.

3.1.2.3. Cycloaddition reactions.

On the other hand, cycloadditions have also been a longstanding reaction for vinyl sulfones, due to their electron deficient-character making them excellent dienophiles.[126] Aside from coupling with standard dienes,[143] there are also many reports that utilise vinyl sulfones in other classes of cycloadditions. For example, Shanmugam and co-workers reported a [3+2]-1,3-dipolar cycloaddition with isatin-derived azomethine ylides **3.74** to form dispiropyrrolidine bisoxindoles **3.75** (Scheme 3.20).[144]

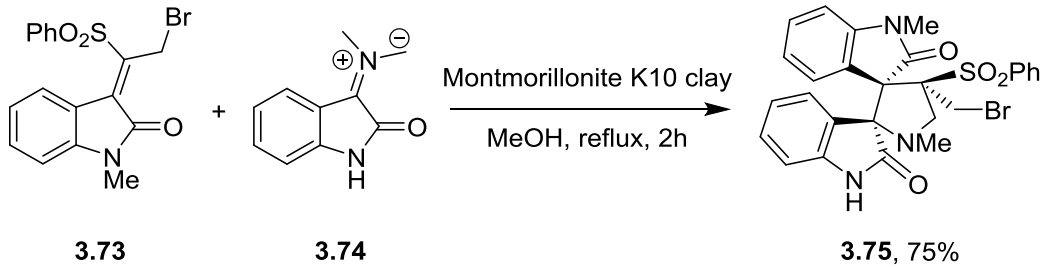

3.73 **3.74** **3.75**, 75%

Scheme 3.20. Cycloaddition between isatin-derived azomethine and vinyl sulfone dipolarophile.

Azides have also been used, however in these cases the sulfone is often eliminated *in situ* in an aromatisation process after the cycloaddition has taken place.[145] Pathak and co-workers have been very active in this area over the past few years, and have disclosed several cycloaddition reactions between azides and vinyl sulfones.[145a-d] In 2014, the group published two reports dealing with this area. Perhaps the most interesting is a three-component reaction involving a nucleophilic substitution between sodium azide and an alkyl halide, followed by a cycloaddition between the resulting azide and vinyl sulfone **3.76**, affording triazoles **3.77** in high yields and regioselectivities (Scheme 3.21). The same authors have also carried out extensive studies into the potential of these cycloaddition reactions in carbohydrate chemistry, as a way to introduce triazole groups into sugar molecules, or to couple two sugar molecules together to produce triazole-linked disaccharides **3.78** (Scheme 3.21).

[143] a) V. Lysiak, A. Ratajczak, A. Mencel, K. Jarzembek and J. Polanski, *Bioorg. Med. Chem.*, 2005, **13**, 671-675. b) P. Zhao and C. M. Beaudry, *Angew. Chem. Int. Ed.*, 2014, **53**, 10500-10503.

[144] P. Shanmugam, B. Viswambharan, K. Selvakumar and S. Madhavan, *Tetrahedron Lett.*, 2008, **49**, 2611-2615.

[145] a) S. Dey, D. Datta and T. Pathak, *Synlett*, 2011, **17**, 2521-2524. b) A. Kayet and T. Pathak, *J. Org. Chem,* 2013, **78**, 9865-9875. c) S. Dey and T. Pathak, *RSC Adv.*, 2014, **4**, 9275-9278. d) D. Sahu, S. Dey, T. Pathak and B. Ganguly, *Org. Lett.*, 2014, **16**, 2100-2103. e) C. Hager, R. Miethchen and H. Reinke, *J. Fluorine Chem.*, 2000, **104**, 135-142.

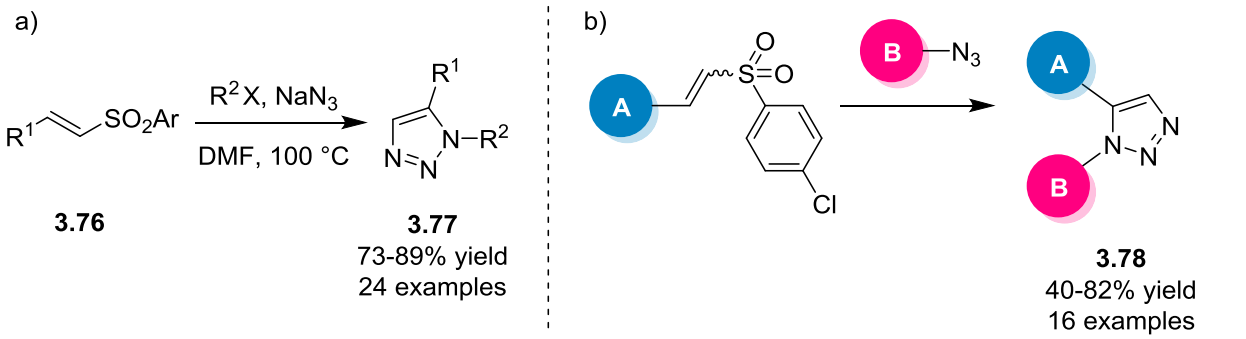

Scheme 3.21. a) Cycloaddition reaction between azides and vinyl sulfones with concomitant loss of the sulfone group. b) Application to carbohydrate chemistry, where A and B are distinct sugar molecules functionalised with a vinyl sulfone and an azide respectively.

In 2013, Wulff and co-workers reported the synthesis of complex tricyclic compounds **3.81** *via* 1,3-dipolar cycloaddition between cyclic vinyl sulfones **3.79** and pyrazolidinone-derived azomethine imines **3.80** (Scheme 3.22, a).[146] Good yields were obtained, albeit with a relatively small scope; the authors found that certain combinations of bulkier substrates hindered the reaction. Following this, in 2014 Namboothiri *et al.* reported another 1,3-dipolar cycloaddition, this time using diazosulfone dipoles **3.83** (Scheme 3.22, b).[147] In this case, the sulfone group in the dipolarophile **3.82** was also eliminated *in situ*, along with the ketone group originating from **3.83**. The reactions proceeded in mild conditions—at 0 °C and 15 minutes of reaction time—to give pyrazoles **3.84** in high yields and regioselectivities.

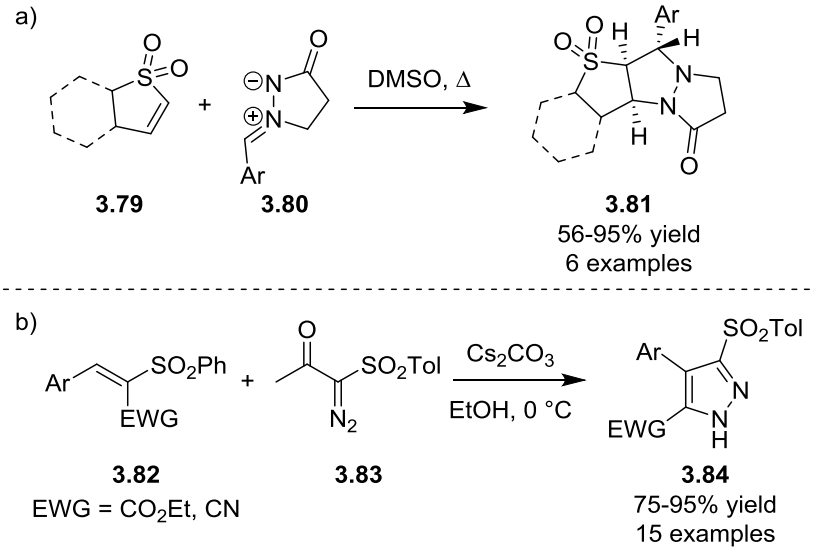

Scheme 3.22. Further examples of 1,3-dipolar cycloaddition reactions with vinyl sulfone dipolarophiles.

[146] S. S. Y. Wong, M. G. Brant, C. Barr, A. G. Oliver and J. E. Wulff, *Bellstein J. Org. Chem.*, 2013, **9**, 1419-1425.
[147] R. Kumar, D. Nair and I. N. N. Namboothiri, *Tetrahedron,* 2014, **70**, 1794-1799.

3.1.2.4. Hydrogenation reactions.

Heterogeneous hydrogenation was discovered by Sabatier at the beginning of the 20th century,[148] and later in the 1960s Wilkinson and co-workers at Monsanto developed the first homogeneous catalyst precursor, $[(PPh_3)_3RhCl]$.[149] Since then, countless new catalysts and reactions have been developed, converting hydrogenation reactions into some of the most important in organic chemistry; they are highly atom economical, cheap, usually require very low catalyst loadings, and lend themselves well to industrial settings.[150] Despite this, vinyl sulfones have lagged behind their ester or carboxylic acid counterparts.

Since the first asymmetric homogeneous hydrogenation was described for the synthesis of L-DOPA in the 1970s[151] there have been many reports on the homogeneous hydrogenation of plenty of other α,β-unsaturated carbonyl compounds, although few examples exist for the related sulfones. Several standard heterogeneous methods have been described,[152] including a recent patent and a report on the hydrogenation of an intermediate towards the synthesis of Eletriptan hydrobromide, a selective agonist of 5-HT_1 receptors.[153] In addition, Alper and Cho described a homogeneous procedure using a palladium catalyst pre-activated with oxygen that was capable of hydrogenating a variety of vinyl sulfones,[154] and Toru *et al.* reported a radical addition of alkyl halides followed by reduction by Bu_3SnH.[155] Other older publications detailed the diastereoselective hydrogenation with a homogeneous rhodium catalyst,[156] or the hydrogenation of vinyl sulfones containing a second coordinating group such as a carboxylic acid or an ester in the β position.[157] Although important advances, they were still insufficient compared to the advances made in the asymmetric hydrogenation of other substrates, given that they still relied on specific substrates containing another functional group to direct the stereoselectivity.

---

[148] E.K. Rideal, *Biogr.Mem. R. Soc.,* 1942, **4**, 63–66.

[149] a) J. F. Young, J. A. Osborne, H. Jardine and G. Wilkinson, *Chem. Commun.*, 1965, 131. b) J. A. Osborn, F. H. Jardine, J. F. Young and G. Wilkinson, *J. Chem. Soc. A.,* 1966, **0**, 1711–1732.

[150] D. J. Ager, A. H. M. de Vries and J. G. de Vries, *Chem. Soc. Rev.*, 2012, **41**, 3340-3380

[151] W. S. Knowles, *Angew. Chem. Int. Ed*., 2002,**41**, 1998–2007.

[152] a) Y. Jiang and T.-P. Loh, *Chem. Sci.*, 2014, **5**, 4939-4943. b) B. C. Ranu, S. K. Guchhait and K. Ghosh, *J. Org. Chem.*, 1998, **63**, 5250-5251.

[153] a) U. S. Kumar, V. R. Sankar, M. M. Rao, T. S. Jaganathan and R. B. Reddy, *Org. Process. Res. Dev.*, 2012, **16**, 1917-1920. b) S. B. Bhirud, P. S. Johar, E. Sharma, R. Prajapaty and C. K. Gupta, Int. Pat. 004811, 2012.

[154] a) I. S. Cho and H. Alper, *J. Org. Chem.*, 1994, **59**, 4027-4028. b) I. S. Cho and H. Alpar, *J. Mol. Catal. A: Chem.*, 1995, **106**, 7-10.

[155] a) N. Mase, Y. Watanabe and T. Toru, *Tetrahedron Lett.*, 1999, **40**, 2797-2800. b) N. Mase, Y. Watanabe, T. Toru, T. Kakamoto and T. Hagiwara, *J. Org. Chem.*, 2000, **65**, 7083-7090.

[156] D. Ando, C. Bevan, J. M. Brown and D. W. Price, *J. Chem. Soc., Chem. Commun.*, 1992, 592-594.

[157] J. M. Paul and C. Palmer, U.S. Pat. 6,274,758, 2001.

In 1997, Pfaltz *et al.* described the first hydrogenation reaction using a chiral version of Crabtree's homogeneous iridium-based catalyst using chiral phosphinooxazoline (PHOX) N,P-ligands (Figure 3.1),[158] increasing the visibility of iridium-based catalysts in hydrogenation contexts; until then, their rhodium-based counterparts had seen far more use.

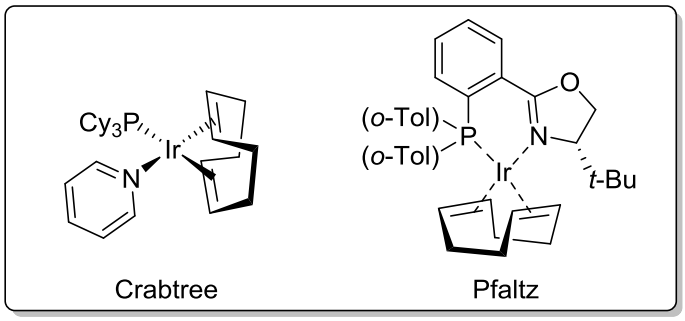

Figure 3.1. Crabtree's homogeneous Ir-based catalyst and Pfaltz's asymmetric Ir-PHOX version.

Over the past few decades, both the Pfaltz[159] and Andersson[160] groups have been active in developing new chiral iridium-based catalysts of this type to be used in enantioselective hydrogenation reactions, and in 2012 the Andersson group took up the challenge of developing a general catalytic system for the asymmetric hydrogenation of sulfone substrates.[161] The authors focused on cyclic allylic sulfones, although they also successfully hydrogenated a variety of vinyl sulfones (*E*)-**3.85** with high yields and enantioselectivities (Scheme 3.23). Several ligands were tested in order to achieve high enantioselectivities for all substrates, but eventually complex **3.87** was found to be the best performing and most general. Subsequently, these saturated products were subjected to the Ramberg-Bäcklund rearrangement—one of the most important transformations for this class of saturated sulfones—to produce chiral allylic compounds **3.88**. Later, in 2014, the group published a second report on this reaction, this time comparing the reactivity of the *E* and *Z* isomers and different *S*-substitutions on the

[158] a) R. Crabtree, *Acc. Chem. Res.*, 1979, **12**, 331-337. b) P. Schnider, G. Koch, R. Prétôt, G. Wang, F. M. Bonen, C. Krüger and A. Pfaltz, *Chem. Eur. J.*, 1997, **3**, 887.

[159] a) D. Rageot, D. H. Woodmansee, B. Pugin and A. Pfaltz, *Angew. Chem. Int. Ed.*, 2011, **50**, 9598-9601. b) B. Wüstenberg and A. Pfaltz, *Adv. Synth. Catal.*, 2008, **350**, 174-178. For a review, see: c) A. Pfaltz, J. Blankenstein, R. Hilgraf, E. Hörmann, S. McIntyre, F. Menges, M. Schönleber, S. P. Smidt, B. Wüstenberg and N. Zimmermann, *Adv. Synth. Catal.*, 2003, **345**, 33-43.

[160] For reviews on Andersson's work, see: a) C. Margarita and P. G. Andersson, *J. Am. Chem. Soc.*, 2017, **139**, 1346-1356. b) J. J. Verendel, O. Pàmies, M. Diéguez and P. G. Andersson, *Chem. Rev.*, 2014, **114**, 2130-2169. c) T. L. Church, T. Rasmussen and P. G. Andersson, *Organometallics,* 2010, **29**, 6769-6781. d) K. Källström, I. Muslow and P. G. Andersson, *Chem. Eur. J.,* 2006, **12**, 3194-3200. e) K. Källström, C. Hedberg, P. Brandt, A. Bayer and P. G. Andersson, *J. Am. Chem. Soc.*, 2004, **126**, 14308-14309.

[161] T. Zhou, B. Peters, M. F. Maldonado, T. Govender and P. G. Andersson, *J. Am. Chem. Soc.*, 2012, **134**, 13592-13595.

vinyl sulfone starting materials with the same catalyst (Scheme 3.23).[162] In this study, they found that the *E* and *Z* isomers performed differently under the reaction conditions: although the enantioselectivity remained high, the conversions dropped significantly.

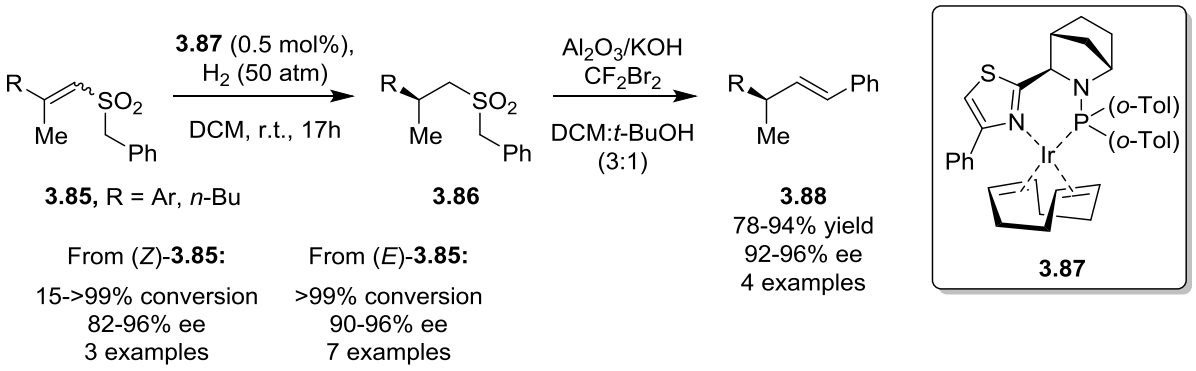

Scheme 3.23. Asymmetric hydrogenation of vinyl sulfones and subsequent Ramberg-Bäcklund rearrangement.

Zhang and co-workers have also been working in this field over the past few years. In 2012, the group published a procedure for the enantioselective hydrogenation of β-amido-α,β-unsaturated sulfones, this time using a rhodium-based catalyst with the Tangphos ligand **3.91** (Scheme 3.24).[163] The authors only used the *Z*-sulfones, perhaps due to the beneficial effects of having two coordinating groups in *cis*, and obtained high yields and enantioselectivities for all the compounds tested.

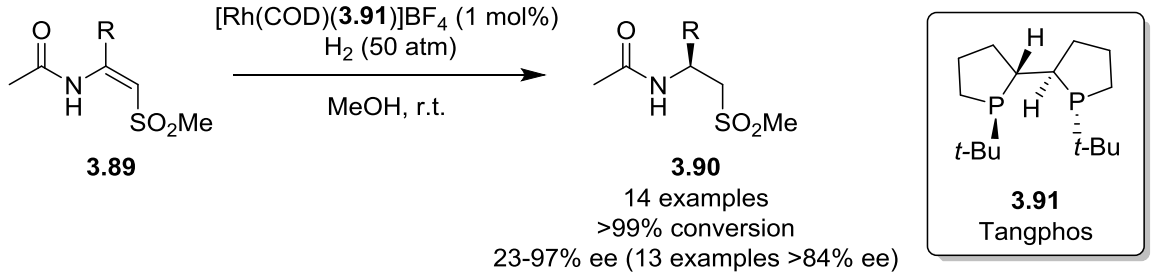

Scheme 3.24. Asymmetric hydrogenation of β-amido-α,β-unsaturated sulfones.

Following this, in 2017 the same authors published a second account of the enantioselective hydrogenation of α-substituted α,β-unsaturated sulfones **3.92** (Scheme 3.25).[164] The authors screened

[162] B. K. Peters, T. Zhou, J. Rujirawanich, A. Cadu, T. Singh, W. Rabten, S. Kerdphon and P. G. Andersson, *J. Am. Chem. Soc.*, 2014, **136**, 16557-16562.
[163] J. Jiang, Y. Wang and X. Zhang, *ACS Catal.*, 2014, **4**, 1570-1573.
[164] L. Shi, B. Wei, X. Yin, P. Xue, H. Lv and X. Zhang, *Org. Lett.*, 2017, **19**, 1024-1027.

several families of ligands, including Josiphos **3.58** and Tangphos **3.91**, with little success. They eventually found that the 3D structure of BINAP and related ligands gave the best enantioselectivities with these substrates, and among them DTBM-Segphos (**3.94**) was the best in generality. Aromatic groups with electron-donating and withdrawing, heteroaromatics, and aliphatic groups were all well tolerated, resulting in high enantioselectivities across the board.

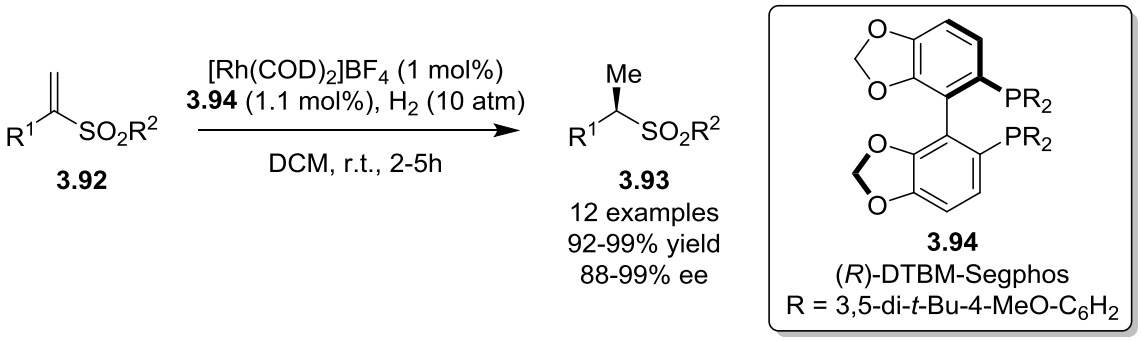

Scheme 3.25. Asymmetric hydrogenation of α-substituted α,β-unsaturated sulfones 3.92.

Although not technically a hydrogenation, Carretero *et al.* also reported the enantioselective reduction of vinyl sulfones using phenylsilane in 2007.[165] Yet again, the authors demonstrated the significance of the 2-pyridyl sulfones; no reaction occurred with substrates **3.95a** lacking this group, whereas yields of >90% were obtained for substrates **3.95b**. A small screening found that BINAP **3.50** or Segphos **3.97**, in conjunction with a copper metal centre, was once again the most efficient system to promote this reaction (Scheme 3.26). With the optimised conditions in hand, the authors proceeded to explore the scope of the reaction and found that the reduction of vinyl sulfones **3.95b** resulted in high yields and moderate to high enantioselectivities for a wide variety of substrates.

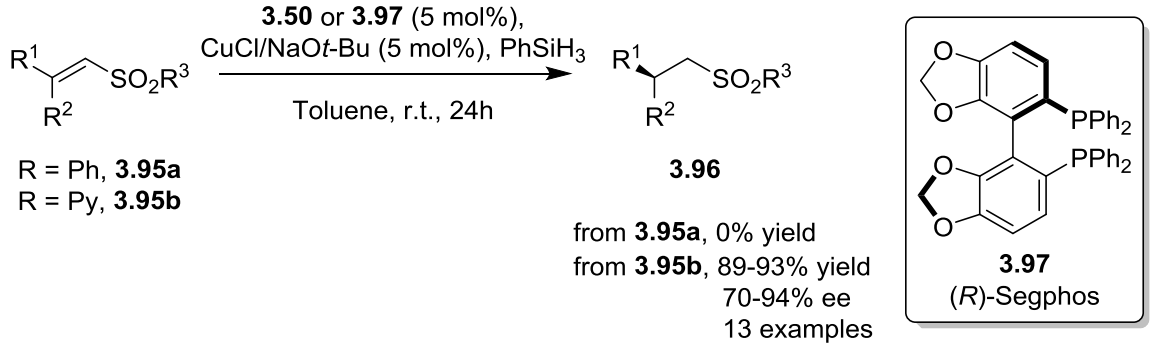

Scheme 3.26. Asymmetric reduction of vinyl sulfones using phenylsilane as the reducing agent.

[165] T. Llamas, R. Gómez Arrayás and J. C. Carretero, *Angew. Chem. Int. Ed.*, 2007, **46**, 3329-3332.

3.1.2.5. Reactions with fluorovinyl sulfones.

Despite remaining a vastly underexplored field several examples of reactions carried out with fluorovinyl sulfones do exist, although the majority of these utilise the α-fluoro isomers. These are mainly desulfonylation reactions (given that fluorovinyl sulfones have been synthesised in the past generally with the intention of later removing the sulfonyl group), a transformation that has been successfully carried out in two ways: 1) prior transformation into the corresponding stannane, and subsequent hydrolysis (this is the only example of downstream chemistry with the β-fluoro derivatives) (Scheme 3.27, a);[106, 124, 166] and 2) treatment with aluminium amalgam (Scheme 3.27, b).[123, 116a]

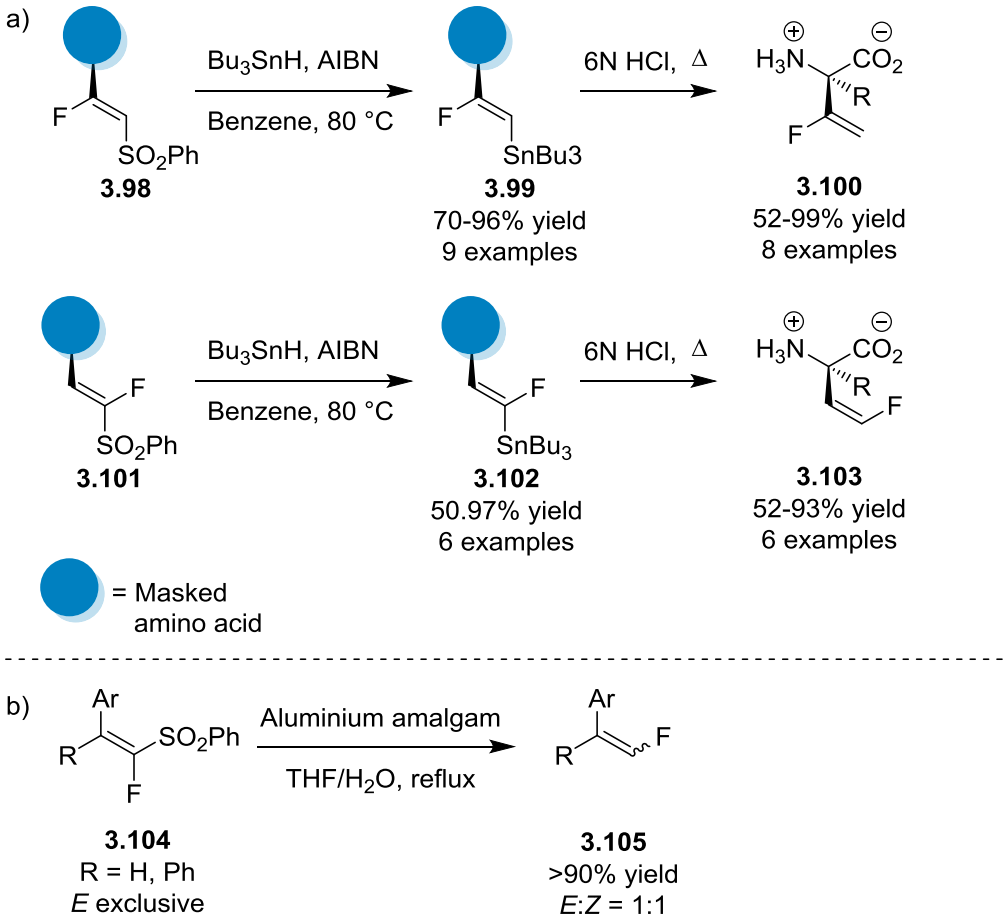

Scheme 3.27. Desulfonylation of fluorovinyl sulfones. a) Prior transformation into stannanes followed by hydrolysis.[106, 124] b) Direct reductive desulfonylation with aluminium amalgam.[116a]

[166] C. Chen, K. Wilcoxen, K. Kim and J. R. McCarthy, *Tetrahedron Lett.*, 1997, **38**, 7677-7680.

In another study, α-fluorovinyl sulfones **3.106** and sulfoxides were used as electrophiles with isocyanoacetates **3.107** with varying success.[167] In very few cases the reactions proceeded to completion, and in many cases mixtures of starting material, addition product **3.108**, fluorinated pyrrole **3.111**, and sulfonyl pyrrole **3.112** were obtained (Scheme 3.28). These products are due to the cascade that is produced after the simple addition product **3.108** is formed. From there, the negative charge resulting from the first Michael addition attacks the carbon of the isocyanate, forming heterocyclic intermediate **3.109**, which then isomerises to **3.110** and either eliminates the sulfonyl group or fluoride to produce **3.111** or **3.112** respectively.

The highest yield of the desired fluorinated pyrrole **3.111** that was achieved was a meagre 35% which, interestingly, was obtained when a cryptand additive was present; in this case the desired fluoropyrrole was the only product. Nevertheless, in most cases the major product was either Michael addition product **3.108** or defluorinated pyrrole **3.112**, along with various side products.

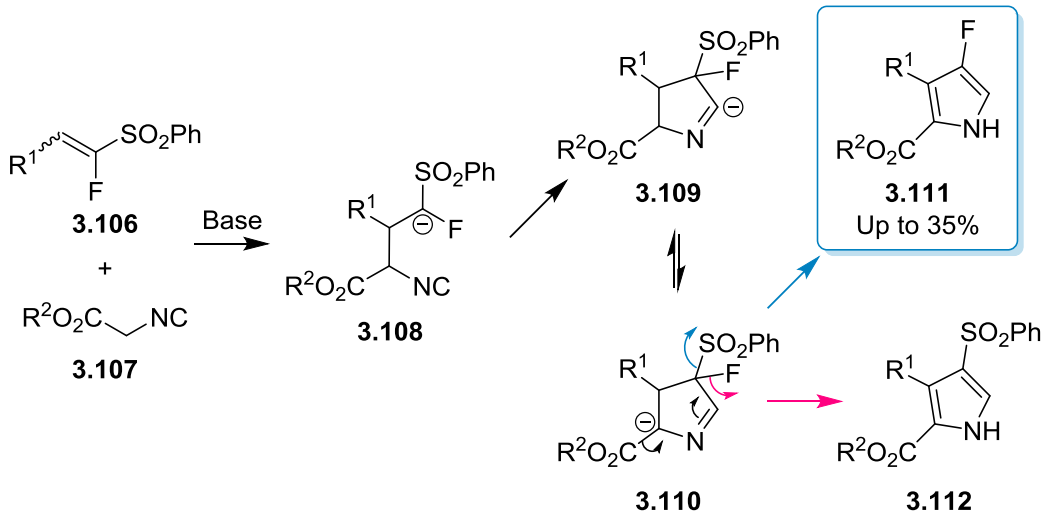

Scheme 3.28. Michael addition of isocyanoacetates to fluorovinyl sulfones as a route to fluorinated pyrroles.[167]

Finally, α-fluorinated vinyl sulfones have been used in a few cycloaddition processes, with varying success. Fluorovinyl sulfone **3.113** was used in dipolar cycloaddition with sodium azide to afford fluorinated triazole **3.114**—an intermediate towards **3.115** which was then used in biological studies as orally active antihypertensives—albeit in a low 15% yield (Scheme 3.29).[168]

[167] H. Uno, K. Sakamoto, T. Tominaga and N. Ono, *Bull. Chem. Soc. Jpn.*, 1994, **67**, 1441-1448.
[168] D. J. Carini, J. V. Duncia, P. E. Aldrich, A. T. Chiu, A. L. Johnson, M. E. Pierce, W. A. Price, J. B. Santella III, G. J. Wells, R. R. Wexler, P. C. Wong, S.-E. Yoo and P. B. M. W. M. Timmermans, *J. Med. Chem.*, 1991, **34**, 2525-2547.

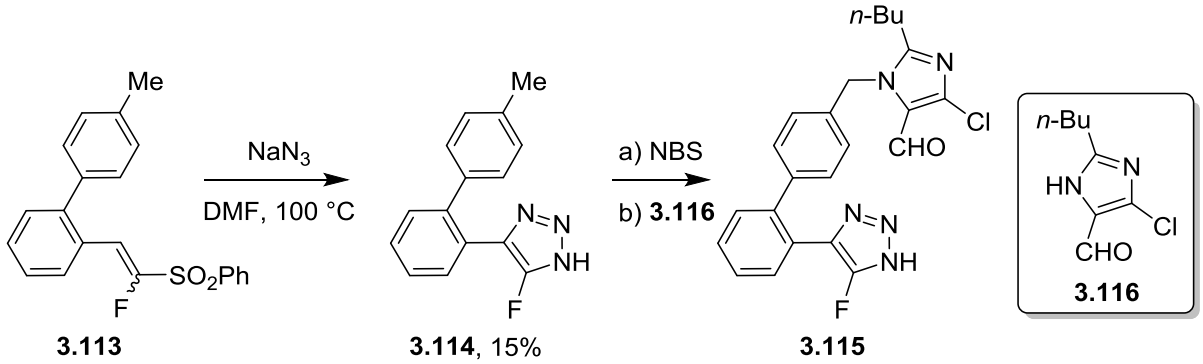

Scheme 3.29. 1,3-Dipolar cycloaddition between sodium azide and fluorovinyl sulfone 3.113.

More recently, in 2008 Haufe *et al.* described the Diels-Alder reaction with various α-fluoro-β-arylvinyl sulfones **3.117** as the dienophiles (Scheme 3.30).[169] The reactions proceeded well, although the fluorovinyl sulfones were fairly unreactive without electron-withdrawing groups on the aryl substituent; the reaction times for the simple phenyl and 4-OMe containing sulfones were 23 and 54 hours respectively. Interestingly, when cyclopentadiene was used as the diene, the *exo* adduct was formed in slight excess, whereas when the diene used was diphenylisobenzofuran, the *endo*-fluoro adduct was formed in excess. Nevertheless, the products were formed in good yields and moderate selectivities.

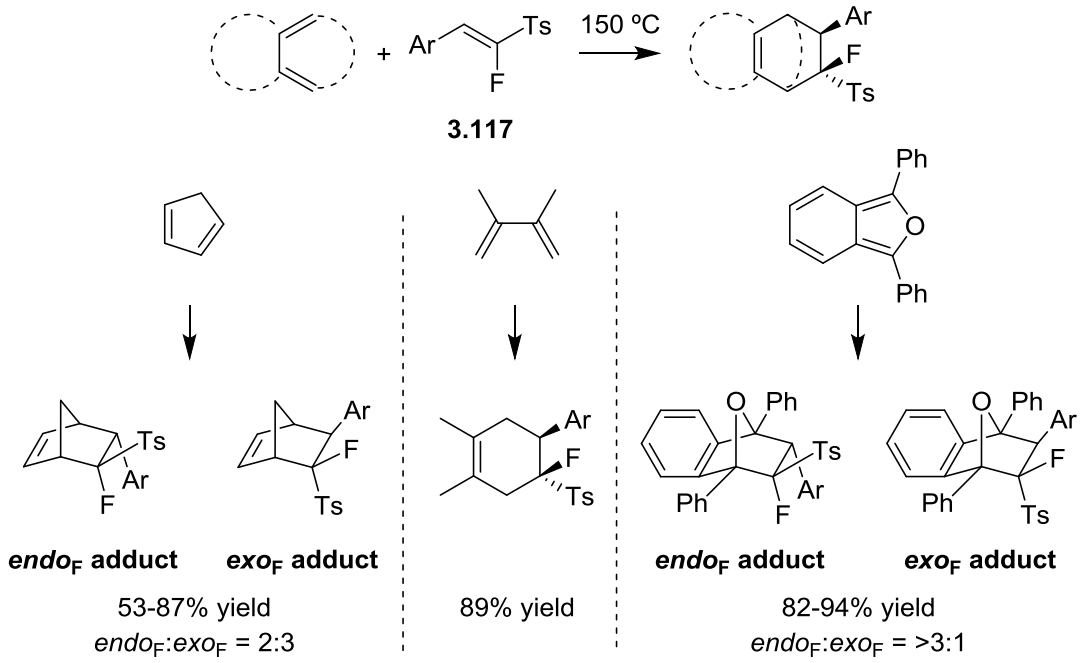

Scheme 3.30. Cycloaddition reactions with fluorovinyl sulfones.

[169] A. V. Shastin, V. G. Nenajdenko, V. M. Muzalevskiy, E. S. Balenkova, R. Fröhlich and G. Haufe, *Tetrahedron*, 2008, **64**, 9725-9732.

3.2. Background.

As mentioned previously, when we embarked on this project, only the α isomers existed in the literature. The following examples of the synthesis of β-fluorovinyl sulfones were published just last year during the development of our own process.

The first example of β-fluorovinyl sulfones came from Hammond, Xu *et al.*,[105] with an elegant gold-catalysed synthesis starting from the corresponding alkynyl sulfones that gave high yields and a wide scope (Scheme 3.31). The authors used a JohnPhos gold bistriflimide catalyst in conjunction with HF·pyridine as the fluoride source. This procedure was based on traditional gold catalysis, by which the gold catalyst activates the triple bond in **3.118**, converting it into a suitable electrophile for attack by the nucleophilic fluoride ion. The catalytic cycle finishes with protodeauration, producing the corresponding β-fluorovinyl sulfone **3.119** and releasing the gold catalyst. The reaction was compatible with various functional groups, including carbonyls, halides and ethers, and gave exclusively the *Z* isomer in all cases.

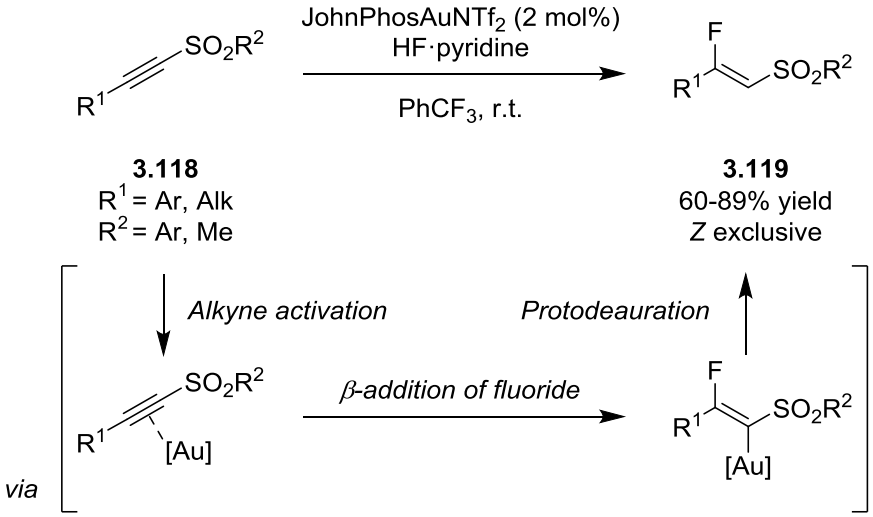

Scheme 3.31. Synthesis of β-fluorovinyl sulfones by Hammond, Xu *et al.*[105]

The second and last example was disclosed by Berkowitz and co-workers.[106] In this report, the authors prepared amino acid derivatives **3.123** with the (1'-fluoro)vinyl group in the quaternary α position, with the same goal as in the aforementioned publication by the same authors: mechanism-based inhibitors for pyridoxal phosphate dependent enzymes.

Berkowitz *et al.* described the synthesis and isolation of the long-elusive β,β-difluorovinyl phenyl sulfone **3.121**, and its use as a fluorinated building block; specifically a (1-fluoro)vinyl cation surrogate.[106] Percy *et al.* had described a potential synthesis and use of **3.121** in 1996, trapping it as a dienophile in a Diels-Alder reaction, although they were unable to isolate it.[170] Nonetheless, Berkowitz achieved the synthesis of this compound by treating β-chloro-β,β-difluoroethyl phenyl sulfone **3.120** with a highly hindered amine base, 2,2,6,6-tetramethylpiperidine, for just 15-20 seconds before immediately isolating the desired β,β-difluorovinyl phenyl sulfone *via* acid work up and distillation. This was then used as an electrophile to synthesise masked amino acid derivatives **3.122** with the (1'-fluoro)vinyl group in the quaternary α position (Scheme 3.32).

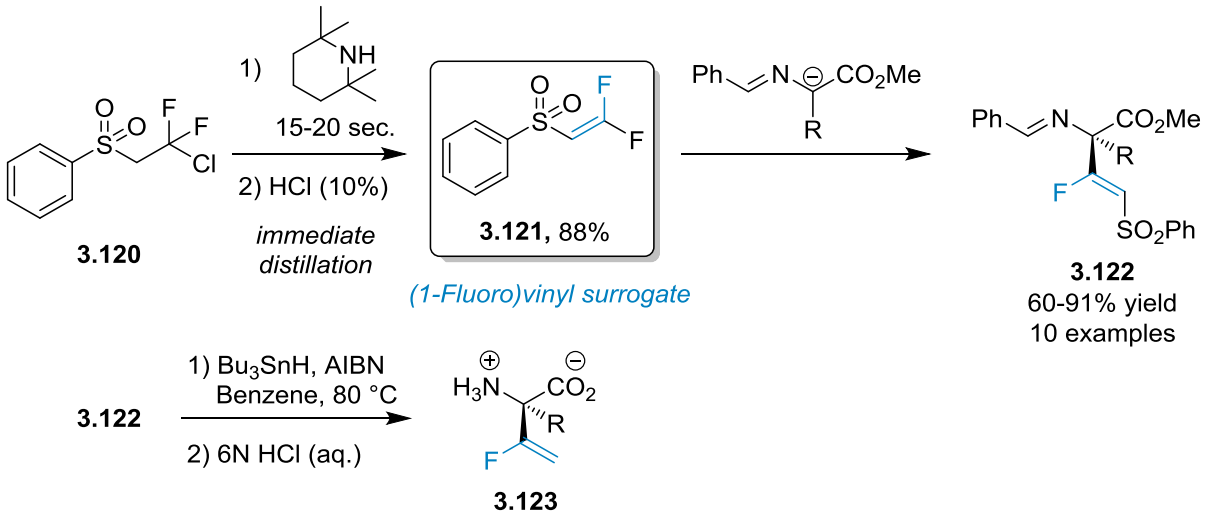

Scheme 3.32. β,β-Difluorovinyl phenyl sulfone 3.121 as a (1-fluoro)vinyl cation surrogate in the synthesis of α-(1'-fluoro)vinyl amino acids for use as mechanism-based inhibitors.

[170] P. J. Crowley, J. M. Percy and K. Stansfield, *Tetrahedron Lett.*, 1996, **37**, 8233-8236.

3.3. Results and discussion.

3.3.1. Synthesis of β-fluorovinyl sulfones.

The starting alkynyl sulfones were synthesised using the methodology described by Nair and co-workers, taking **3.125** as the model substrate.[171] This synthetic route involves cerium(IV) ammonium nitrate (CAN) mediated iodosulfonylation of phenylacetylene to give 2-iodo-2-phenyl-1-tosylethene **3.124**, followed by treatment with K_2CO_3 to eliminate HI, resulting in the desired **3.125** (Scheme 3.33).

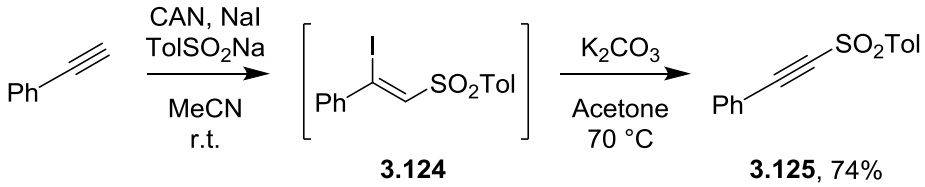

Scheme 3.33. Synthesis of model alkynyl sulfone 3.125.

From there we began to test fluoride sources, and found that treatment of **3.125** with TBAF—one of the most common and least expensive fluoride sources—produced **3.126** *via* addition of fluoride in the β position, albeit in a moderate 43% yield. It's worth noting that the β-fluorovinyl sulfone was formed exclusively as the *Z* stereoisomer, as has been seen by other authors when adding fluoride to ynones or ynals.[120, 121] However, a relatively high quantity of β-keto sulfone **3.127** was also formed in the reaction with TBAF (Scheme 3.34).

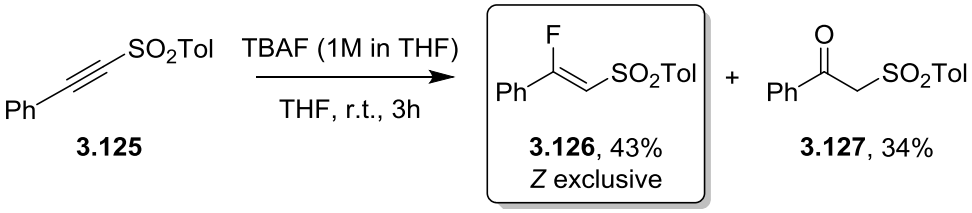

Scheme 3.34. Preliminary tests with TBAF.

Nevertheless, encouraged by the knowledge that it is in fact possible to obtain β-addition using nothing more than the intrinsic electrophilicity of the alkynyl sulfone moiety, we turned to other fluoride

[171] V. Nair, A. Augustine and T. D. Suja, *Synthesis*, 2002, **15**, 2259-2265.

sources in the hope of improving the yield and the chemoselectivity (Table 3.1). We attributed the formation of **3.127** to the addition of residual water present either in the THF, the glassware, or the TBAF solution itself (commercial TBAF solutions contain *ca.* 5% water). Unfortunately, other "drier" fluoride sources such as KF, KHF_2, NaF, TMAF, TBAT, and ZnF_2 all either failed to react or resulted in lower selectivity and yield than the commercial solution of TBAF. Practical elements such as the use of oven-dried glassware, molecular sieves, freshly distilled THF, or a new TBAF solution to ensure the minimum amount of residual water gave similarly disappointing results. Furthermore, the reaction was attempted with more equivalents of TBAF, in order to increase the rate of reaction and force the introduction of fluoride into the structure, but to no avail. On a positive note, neither the α-fluorovinyl sulfone nor the related (*E*)-β-fluorovinyl sulfone was observed in any case.

Table 3.1. Optimisation studies with other sources of fluoride.[a]

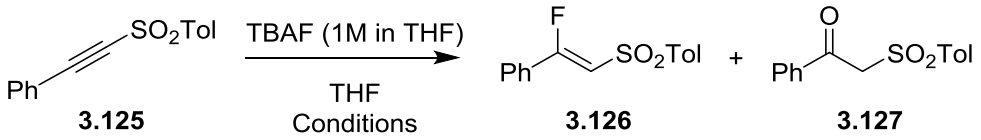

3.125 **3.126** **3.127**

Entry	Equiv TBAF	Additive	T (°C)	Time (h)	Yield **3.126** (%)[c]	**3.126**:**3.127**[d]
1	1.5	-	0	6	45	1:1
2	1.5	-	60	3	38	1:1
3[b]	1.5	-	r.t.	3	31	1:2
4	1.5	4 Å MS	r.t.	3	37	1:1
5	1.5	Na_2SO_4 (2 equiv)	r.t.	3	39	1:1
6	5	-	r.t.	2	41	1:1

[a] All glassware oven-dried and fresh THF and TBAF solution used. [b] Reaction carried out with TBAF (1M in THF) after 24h with 4 Å MS. [c] Isolated yield. [d] Ratio determined by ^{1}H NMR of crude reaction mixture.

Given that these attempts failed to improve the results, we decided to explore the possibility of a metal-catalysed reaction. In this context, Jiang *et al.* and Sun, Gong *et al.* described the use of silver(I) fluoride in the synthesis of β-fluorochalcones, although the silver species was used stoichiometrically in both cases.[172]

[172] a) Y. Li, X. Liu, D. Ma, B. Liu and H. Jiang, *Adv. Synth. Catal.*, 2012, **354**, 2683-2688. b) J. Zhang, L. Liu, J. Duan, L. Gu, B. Chen, T. Sun and Y. Gong, *Adv. Synth. Catal.*, 2017, **359**, 4348-4358.

Zhu *et al.* also published a report on the hydrofluorination of ynamides using silver(I) fluoride as the fluorinating agent in 2014.[173] However, the same authors published a second study in 2016 in which they were able to control the regioselectivity of the hydrofluorination of the same class of ynamide substrates, achieving α-fluoroenamides **3.129** with a silver catalyst (Scheme 3.35, a) and (*Z*)-β-fluoroenamides **3.130** with a copper catalyst (Scheme 3.35, b).[174] However, the regioselectivity seems to be somewhat substrate-dependent rather than purely catalyst-dependent. Submitting ynamides **3.128a** to the copper-catalysed conditions resulted in no reaction; the substitution at the nitrogen atom is critical for the success of the reaction. Curiously, the β-hydrofluorination procedure also resulted in high yields and selectivities when using the $(Ph_3P)_3CuF$ stoichiometrically.

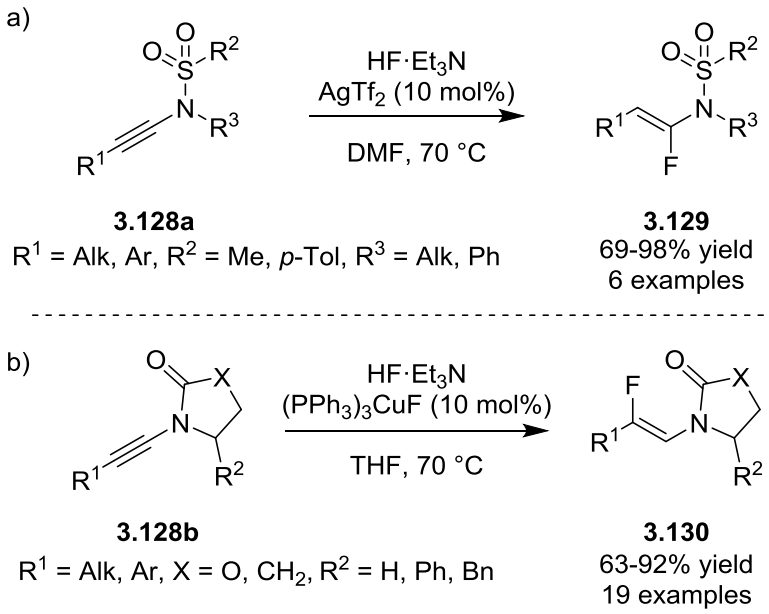

Scheme 3.35. a) α-Hydrofluorination of ynamides using silver catalysis. b) β-Hydrofluorination of ynamides using copper catalysis.

In terms of gold catalysis, the Hammond group recently disclosed a novel HF reagent—HF·DMPU (*N,N*-dimethylpropyleneurea)—and described its use in the gold-catalysed hydrofluorination of alkynes (Scheme 3.36).[175] Amongst the examples was ethyl phenylpropiolate **3.131**, which when treated with JohnPhos gold phthalimide catalyst **[Au]-I** produced the β-fluorinated product, ethyl 3-fluoro-3-phenylacrylate **3.132** in high yield, regioselectivity, and *Z*-stereoselectivity.

[173] J. Che, Y. Li, F. Zhang, R. Zheng, Y. Bai and G. Zhu, *Tetrahedron Lett.*, 2014, **55**, 6240-6242.
[174] G. He, S. Qiu, H. Huang, G. Zhu, D. Zhang, R. Zhang and H. Zhu, *Org. Lett.*, 2016, **18**, 1856-1859.
[175] O. E. Okoromoba, J. Han, G. B. Hammond and B. Xu, *J. Am. Chem. Soc.*, 2014, **136**, 14381-14384.

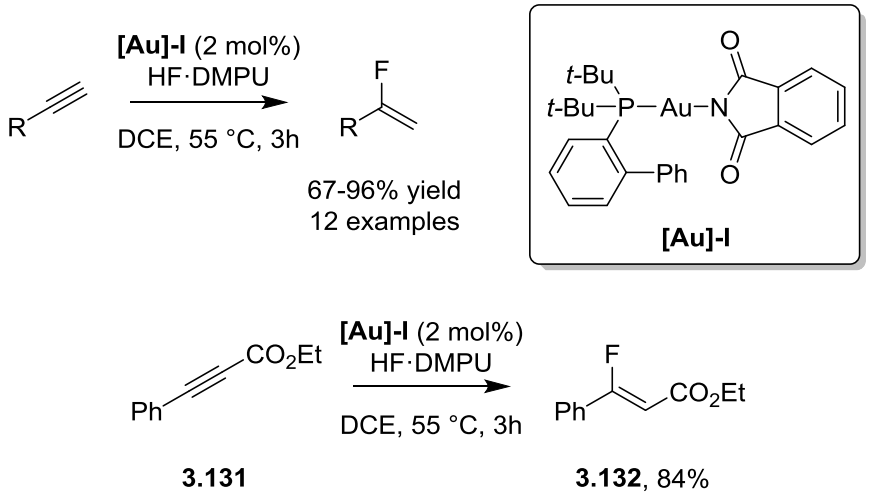

Scheme 3.36. Gold-catalysed hydrofluorination of alkynes reported by Hammond *et al.*

We therefore looked into the reaction between alkynyl sulfone **3.125** and fluorine sources in the presence of a variety of metal catalysts, focusing on those seen in the previously mentioned examples (Table 3.2).

To our surprise, we found that both the (*E*)-β-fluorovinyl sulfone—which is thus far unknown in the chemical literature—and the expected *Z* isomer were formed to a certain degree with both copper and silver catalysts. Interestingly, the *E* isomer was the major product formed only when $3HF{\cdot}Et_3N$ was used in conjunction with copper catalyst $(PPh_3)_3CuF$, whereas changing the HF source to Olah's reagent (HF·pyridine) or HF·DMPU resulted in more of the *Z* isomer. In contrast, the use of both silver and gold resulted in the *Z* isomer as the major product, as seen in the uncatalysed reaction with TBAF (entry 18, Table 3.2). We identified the geometric isomers using the coupling constant in the ^{1}H and ^{19}F NMR spectra; *trans* H—F coupling constants, corresponding to the *Z* isomer, are larger. In this case, we observed coupling constants of 30 Hz and 18 Hz, accounting for the *Z* and *E* isomers respectively (Figure 3.2).

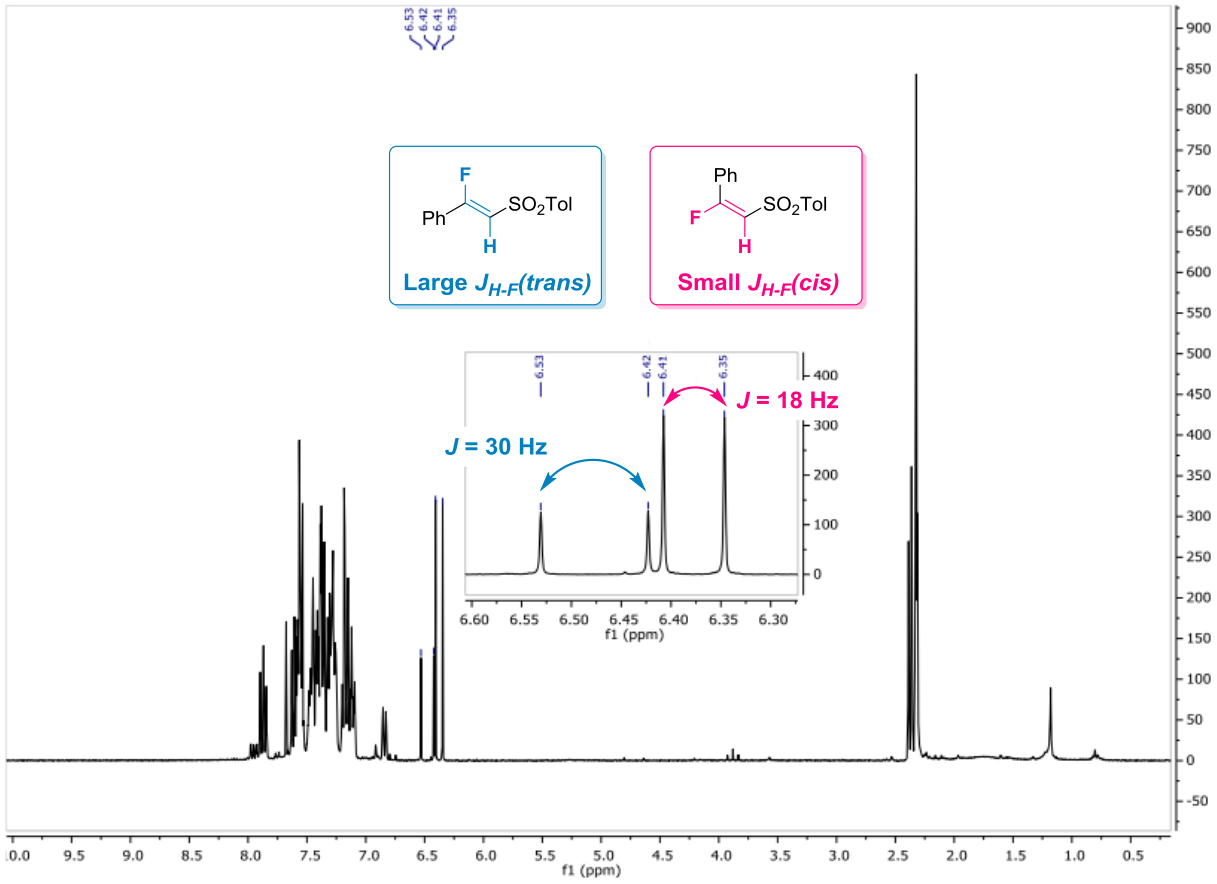

Figure 3.2. Identification of *E* and *Z* isomers based on the H-F coupling constant.

Table 3.2. Exploration of different metal catalysts and HF sources.

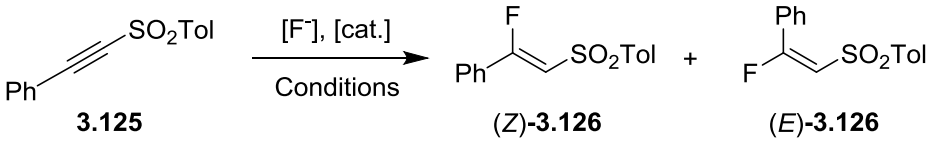

3.125 (*Z*)-**3.126** (*E*)-**3.126**

Entry	[cat.]	F^- source	Solvent	T (°C)	Time (h)	Yield **3.126** (%)	*Z*:*E*
1	$(Ph_3P)_3CuF$	$3HF{\cdot}Et_3N$	THF	70	16	58%	1:2
2	$(Ph_3P)_3CuF$	HF·DMPU	THF	70	16	51%	1:1
3	$(Ph_3P)_3CuF$	HF·Py	THF	70	16	49%	3:1
4	$(Ph_3P)_3CuF$	$3HF{\cdot}Et_3N$	THF	55	20	63%	2:3
5	$(Ph_3P)_3CuF$	$3HF{\cdot}Et_3N$	Dioxane	55	20	58%	1:3
6	$(Ph_3P)_3CuF$	$3HF{\cdot}Et_3N$	Dioxane	70	6	42%	1:3
7	$(Ph_3P)_3CuF$	$3HF{\cdot}Et_3N$	Dioxane	70	20	90%	1:3
8	$Ag(NTf)_2$	$3HF{\cdot}Et_3N$	DMF	70	16	55%	5:1
9	-	AgF	MeCN (aq.)	r.t.	16	-	-
10	Ph_3PAuMe	$3HF{\cdot}Et_3N$	THF	55	6	-	-
11	Ph_3PAuMe	HF·DMPU	DCE	55	6	37%	19:1
12	Ph_3PAuMe	HF·Py	DCE	55	6	44%	12:1
13	Ph_3PAuMe	HF·DMPU	THF	70	16	51%	1:1
14	Ph_3PAuMe	HF·DMPU	DCE	55	20	53%	25:1
15	Ph_3PAuMe	HF·DMPU	DCE	70	6	44%	22:1
16	SPhosAuOTf	HF·DMPU	DCE	55	20	37%	25:1
17	JohnPhosAuCl	HF·DMPU	DCE	55	20	58%	3:1
18	-	TBAF	THF	r.t.	3	43%	99:1

In the end, the best *Z*-selectivity was obtained with with TBAF in THF; although the gold-catalysed reactions gave slightly higher yields and acceptable selectivities (entry 14, Table 3.2), we decided that the metal-free treatment of alkynyl sulfones with just TBAF in THF far outweighed the gold-catalysed procedure in terms of practicality, cost, and sustainability. However, we still had the problem of the formation of β-keto sulfones **3.127**. On the other hand, we had also discovered suitable reaction conditions to favour the formation of the corresponding *E* isomers—this will be developed further later in the chapter, given that these derivatives remain unprecedented in the chemical literature (*vide infra*).

To this end, we decided to run some control experiments to determine the origin of this unwanted side-product (Scheme 3.37). We first treated **3.125** with a mixture of THF:H_2O (10:1), to see if water was a

strong enough nucleophile to add to the β position as we first suspected. However, we found that this was not the case, and no reaction took place. Therefore, we treated the product **3.126** with the same THF:H_2O mixture, to see if the product was a better electrophile and an addition-elimination reaction was responsible for the formation of **3.127**, although this also failed to give a reaction, even after addition of a small amount of TBAF. Finally, we found that addition of one equivalent of lithium hydroxide to the mixture of **3.126** in THF:H_2O resulted in a 1:1:1 mixture of **3.125**, **3.126**, and **3.127**. This suggested that the presence of hydroxide ions promoted both the elimination of HF from the product, as well as the formation of the β-keto sulfone through addition to the alkynyl sulfone starting material. We confirmed this by treating starting alkynyl sulfone **3.125** with lithium hydroxide in aqueous THF, and observing that the β-keto sulfone was indeed formed.

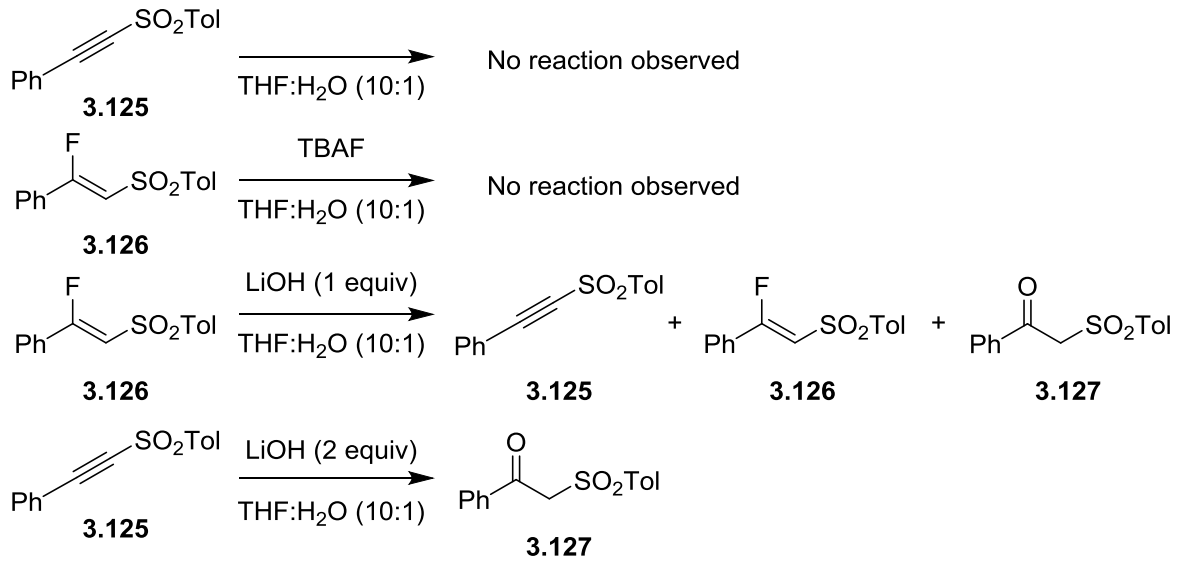

Scheme 3.37. Control experiments to determine the origin of 3.127.

In light of these results, we deduced that the reaction responsible for the formation of β-keto sulfone **3.127** was the addition of the hydroxide ion, and that this species came from the commercial TBAF solution. Since THF-based solutions of TBAF often contain a small amount of water, the basic nature of TBAF means that there would be significant amounts of OH^- present in the media. We therefore took a new approach, and explored the use of acidic additives to the reaction mixture in order to neutralise the hydroxide solution, thereby hindering the formation of the unwanted β-keto sulfones. To our delight, this approach was more successful than the last attempts, and both the yield and selectivity improved greatly with this addition. However, the reaction was also sensitive to the manner in which the TBAF solution was neutralised: the best results were obtained with just one equivalent of NH_4Cl whereas saturated aqueous NH_4Cl solution or stronger acids, such as TsOH, inhibited the reaction (Table 3.3).

Table 3.3. Optimisation using acids to neutralise the TBAF solution.

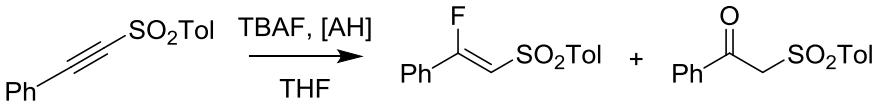

3.125 **3.126** **3.127**

Entry	[AH]	Equiv [AH]	Time (h)	Conv. (%)	**3.126**[c]	**3.126**:**3.127**[e]
1	-	-	3	100	43%	1:1
2	NH_4Cl	1	3	100	73%	13:1
3	NH_4Cl	1.5	20	70	N.D.[d]	10:1
4	NH_4Cl	2	20	56	N.D.[d]	10:1
5	NH_4Cl (sat.)[b]	-	8	0	-	-
6	TsOH	1	8	0	-	-
7[a]	-	-	5	90	N.D.	3:1

[a] TBAF@SiO_2 used instead of TBAF (1M in THF). [b] The solvent used was THF:H_2O/NH_4Cl(sat.) (10:1). [c] Isolated yield. [d] Given the difficulty in separating these compounds (starting **3.125**, **3.126**, and **3.127**) by flash column chromatography, the yield was not determined for these reactions since they did not proceed to completion. [e] The ratio was determined using ^{1}H NMR of the crude reaction mixture.

The reaction was also attempted with TBAF supported on silica gel, since we hypothesised that the acidic nature of silica would offset the basicity of TBAF and prevent the formation of **3.127**. Not only that, but it should contain far less water and therefore less hydroxide ions. Although the selectivity was slightly better than when the standard THF solution was used, the difference was not as drastic as we had hoped (entry 7, Table 3.3).

With these optimised conditions in hand (entry 2, Table 3.3), we sought to explore the scope of the reaction. We therefore synthesised a range of alkynyl sulfones with varied substituents, such as electron-withdrawing and donating aromatic groups, heteroaromatics, and aliphatic groups (Table 3.4). Aside from **3.125g** and **3.125p-u**, these were all synthesised following the same CAN-mediated iodosulfonylation/HI elimination methodology described by Nair *et al.* (refer to Scheme 3.33, from now on referred to as method **A**), starting from the corresponding terminal alkynes.[171] The remaining derivatives were synthesised *via* a second method (denominated method **B**, this will be discussed in more depth on page 163) based on the nucleophilic addition of the terminal alkyne to diphenyl or dimethyl disulphide. The majority of the terminal alkyne starting materials were commercially available, although given the high price of some derivatives we opted to synthesise them ourselves.

Table 3.4. Synthesis of alkynyl sulfones 3.125.

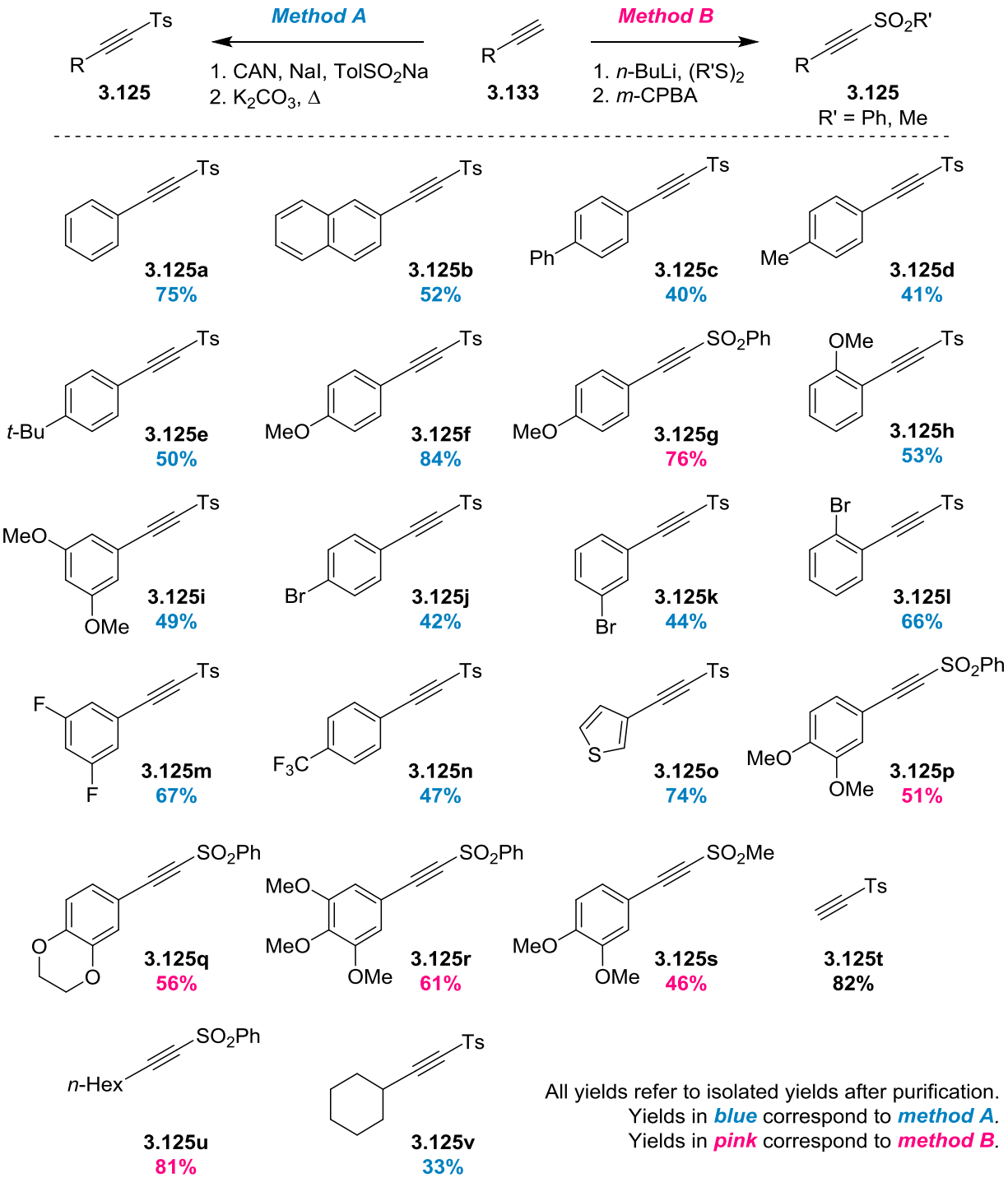

Terminal alkyne **3.133l** containing the *ortho*-bromo substituent (Scheme 3.38) necessary for the synthesis of **3.125l** (Table 3.4) was synthesised through the deprotection of the TMS protected derivative, which we found to be a far cheaper alternative to the expensive terminal alkyne. A simple treatment with potassium carbonate in methanol afforded the desired **3.133l** in a 96% yield.

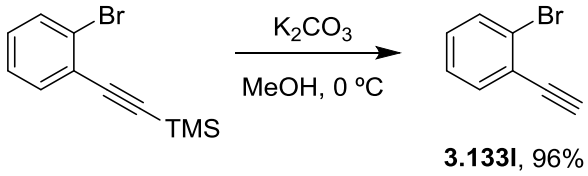

Scheme 3.38. Synthesis of (2-bromophenyl)acetylene 3.133l.

On the other hand, electron-rich alkynes **3.133p-r** (Scheme 3.39) were synthesised using a Corey-Fuchs reaction, starting from the corresponding aldehyde. To this end, the aldehydes were reacted with tetrabromomethane and triphenylphosphine, resulting in the *gem*-dibromoalkene intermediates **3.134**. This was then subjected to a DBU-mediated elimination reaction to afford the desired terminal alkynes **3.133p-r** in high yields.[176]

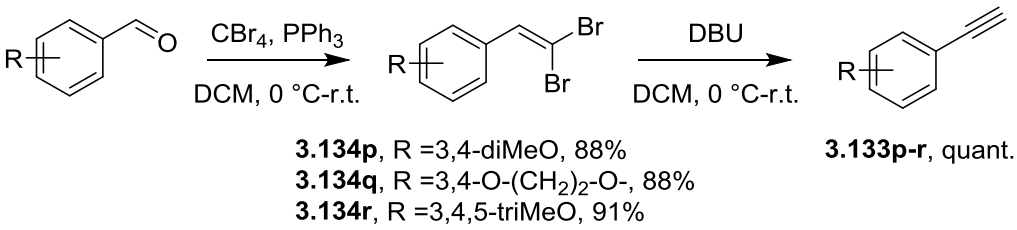

Scheme 3.39. Synthesis of electron-rich terminal alkynes.

After the synthesis of the non-commercial (or expensive) terminal alkynes, the alkynyl sulfones could then be synthesised. Method **A** (Scheme 3.33) was generally inadequate for terminal alkyne substrates bearing methoxy substituents on the aromatic ring; during the first attempt to synthesise compounds **3.125h** and **3.125i** (Table 3.4) *via* method **A** we isolated a mixture consisting mostly of the vinyl iodide intermediate. Furthermore, the retention factors of the intermediate and the final product were very similar in all solvent mixtures tested, and we had to resort to different reaction conditions for the second step to proceed to completion. Eventually we achieved these compounds by using a longer reaction time and a higher temperature (75 °C rather than 60 °C).

[176] a) S. S. Ichake, A. Konala, V. Kavala, C.-W. Kuo and C. F. Yao, *Org. Lett.*, 2017, **19**, 54-57. b) A. K. Morri, Y. Thummala and V. R. Doddi, *Org. Lett.*, 2015, **17**, 4640-4643.

On the other hand, **3.125g**, **3.125p-s** and **3.125u** (Table 3.4) were synthesised *via* method **B**: a two-step sequence consisting in *n*-BuLi mediated addition of the terminal alkyne to phenyl or methyl disulphide, followed by oxidation of the resulting methyl or phenyl sulphide to the corresponding sulfone.[105] During the first step of this reaction with phenyl disulphide, thioanisole was formed as a side product. This was removed either by column chromatography or by high vacuum before the subsequent oxidation step, although this could often be ignored and extra equivalents of *m*-CPBA used in the oxidation step since the resulting phenyl methyl sulfone by-product could usually be separated from the desired alkynyl sulfone (Scheme 3.40).

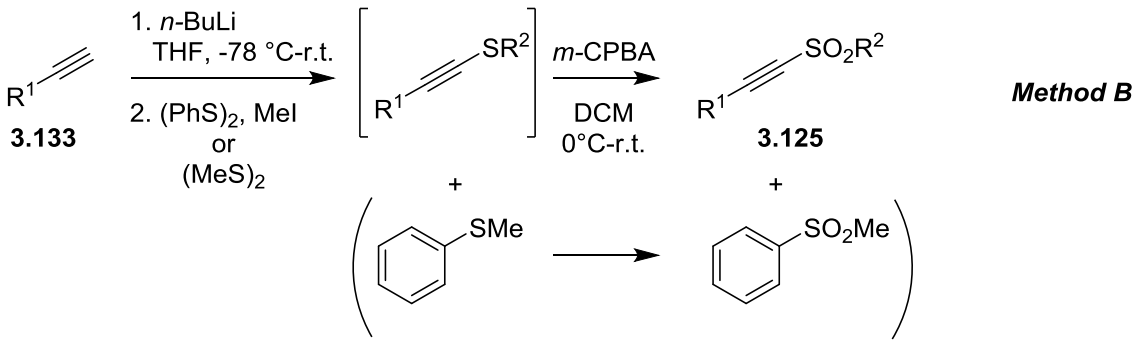

Scheme 3.40. Method B, *n*-BuLi mediated addition of terminal alkyne 3.133 to phenyl or methyl disulfide and subsequent oxidation with *m*-CPBA.

Finally, ethynyl tosyl sulfone **3.125t** was synthesised by aluminium chloride mediated coupling of (bis)trimethylsilylacetylene to afford the TMS-protected sulfone intermediate **3.135** and subsequent deprotection, although this step proved somewhat difficult. Standard procedures such as treatment with potassium carbonate in methanol afforded **3.136**, resulting from the deprotection of the TMS group, followed by addition of two molecules of methanol to the terminal position. In the end, the deprotection was carried out by slowly adding an aqueous solution of sodium fluoride to a solution of **3.135** in methanol at 0 °C (Scheme 3.41).[177] Therefore, we reasoned that treatment of **3.135** with TBAF could proceed similarly, resulting in 2,2-difluoroethyl tosyl sulfone **3.137**. However, this was not the case, although the likely high instability of this compound means that it could have been formed and lost during the course of the reaction.

[177] J. R. Sommer, A. H. Shelton, A. Parthasarathy, I. Ghiviriga, J. R. Reynolds and K. S. Schanze, *Chem. Mater.*, 2011, **23**, 5296-5304.

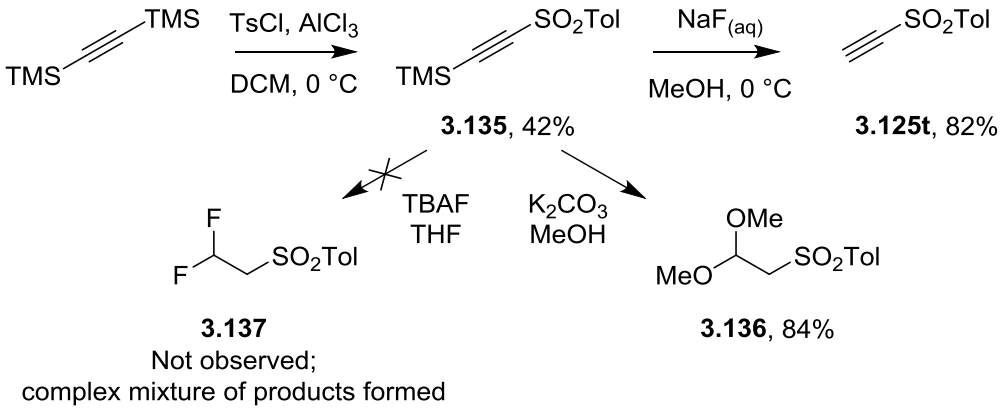

Scheme 3.41. Problems with the removal of the TMS protecting group; unexpected formation of 3.136 and attempts to form 3.137 under analogous conditions.

After the successful synthesis of our library of alkynyl sulfones **3.125**, we tested them with our metal-free fluorination procedure (Table 3.5). To our delight, a range of neutral and electron-donating groups were well-tolerated (**3.126a-i**, Table 3.5). However, electron-withdrawing groups resulted in slightly lower yields and selectivities. Bromine-containing substrates **3.125j** and **3.125k** gave moderate yields and selectivities, and fluorinated substrates **3.125m** and **3.125n** resulted in lower yields and selectivities. Substrates **3.125h** and **3.125l** with substitutions in the *ortho* position failed to react (Table 3.5), possibly due to steric effects.

Interestingly, methyl sulfone **3.125s** reacted well in just one hour and the corresponding ketone was not observed. This suggests that the less electrophilic methanesulfonyl alkyne was unreactive towards hydroxide ions in the reaction media, resulting purely in the desired fluorovinyl sulfone **3.126s** (Table 3.5).

Unfortunately, terminal fluorovinyl sulfone **3.126t** was not observed; in fact, when TBAF was added to ethynyl tolyl sulfone **3.125t** the mixture fumed and a black paste was formed almost immediately, even at low temperatures (Table 3.5).

Table 3.5. Scope of the hydrofluorination reaction with TBAF and NH_4Cl.

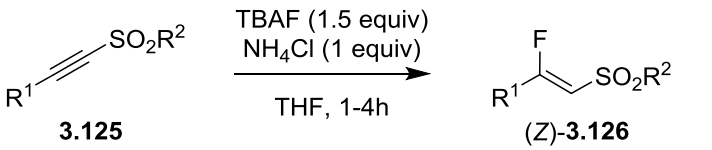

3.125 (*Z*)-**3.126**

Yield%[a] (**3.126**:**3.127**)[b]

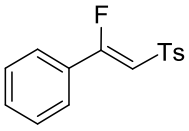

(*Z*)-**3.126a**
72% (91:9)

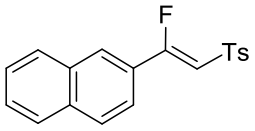

(*Z*)-**3.126b**
69% (91:9)

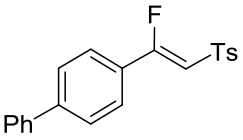

(*Z*)-**3.126c**
72% (91:9)

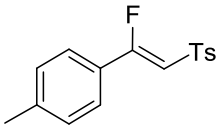

(*Z*)-**3.126d**
67% (96:4)

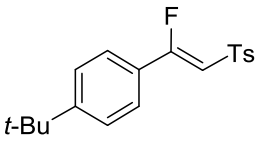

(*Z*)-**3.126e**
67% (90:10)

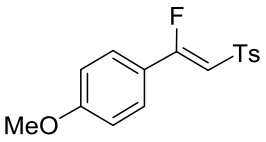

(*Z*)-**3.126f**
71% (93:7)

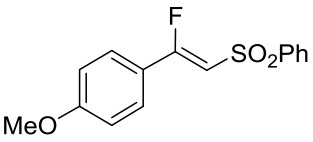

(*Z*)-**3.126g**
72% (93:7)

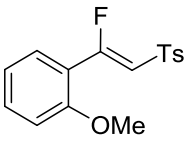

(*Z*)-**3.126h**
0%[c]

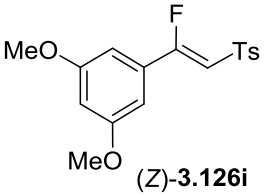

(*Z*)-**3.126i**
70% (95:5)

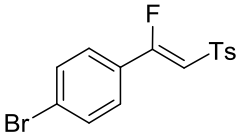

(*Z*)-**3.126j**
63% (84:16)

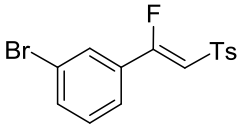

(*Z*)-**3.126k**
60% (80:20)

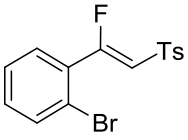

(*Z*)-**3.126l**
0%[c]

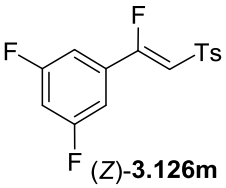

(*Z*)-**3.126m**
30% (67:33)

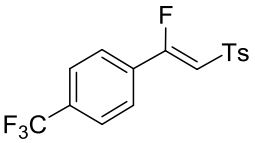

(*Z*)-**3.126n**
28% (72:28)

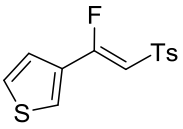

(*Z*)-**3.126o**
70% (94:6)

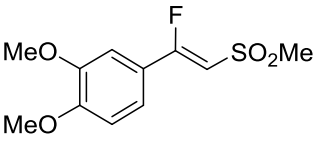

(*Z*)-**3.126s**
86% (>99:1)

(*Z*)-**3.126t**
0%[d]

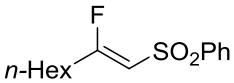

(*Z*)-**3.126u**
0%[e]

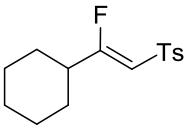

(*Z*)-**3.126v**
0%[e]

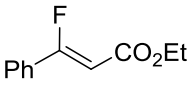

(*Z*)-**3.132**[f]
50% (>99:1)
from **3.131**

[a] Isolated yield. [b] Determined by ^1H NMR (see experimental section). [c] No reaction, starting material recuperated. [d] Violent exothermic reaction, product not detected (see text). [e] Corresponding allene formed (see text). [f] Reaction carried out at 60 °C over 16h.

Aliphatic substrates **3.125u** and **3.125v** were also unsuccessful, this time due to the rapid formation of the corresponding allenyl sulfone, **3.138**.[178] We attributed this to the presence of a hydrogen atom in the γ position, which could be deprotonated in the basic reaction conditions (Scheme 3.42).

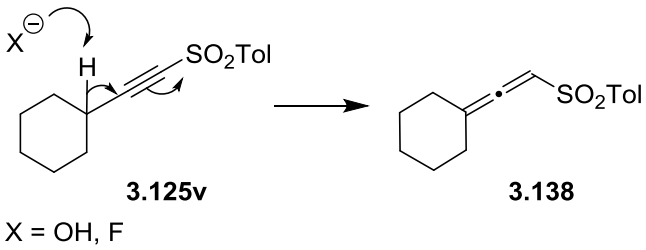

3.125v **3.138**

X = OH, F

Scheme 3.42. Speculative mechanism for the formation of the sulfonyl allene derivative from aliphatic alkynyl sulfones.

The related ethyl phenylpropiolate was also shown to be a suitable substrate, and the corresponding ethyl β-fluoro-β-phenylacrylate **3.132** was also obtained in moderate yield (Table 3.5). The ester was less reactive in our optimised reaction conditions, and the mixture had to be heated for the reaction to proceed. Even after 24 hours at 60 °C full conversion was still not achieved, although the product was still obtained in a synthetically useful 50% yield.

[178] S. E. Denmark, M. A. Harmata and K. S. White, *J. Org. Chem.*, 1987, **52**, 4031-4042.

We then turned our attention to the E isomers. Thankfully, the metal-catalysed processes that had given rise to this geometric isomer avoided the formation of the unwanted β-keto sulfone **3.127** and other side products; here, the main difficulty was improving the selectivity. Having previously obtained the best results with $(PPh_3)_3CuF$ and $3HF{\cdot}Et_3N$ (entries 5-7, Table 3.2), we resumed our search for the optimum conditions here. Unfortunately, we had problems reproducing these reactions. The catalyst was originally prepared following a procedure described by Chaudhuri *et al.* in 2000, a somewhat awkward procedure containing several steps (**Cat1**) (Scheme 3.43, a).[179] After several failed attempts to recreate an active catalyst using this method, we turned to a different solution and followed a simpler synthesis described by Szabó *et al.* (**Cat2**) (Scheme 3.43, b).[180]

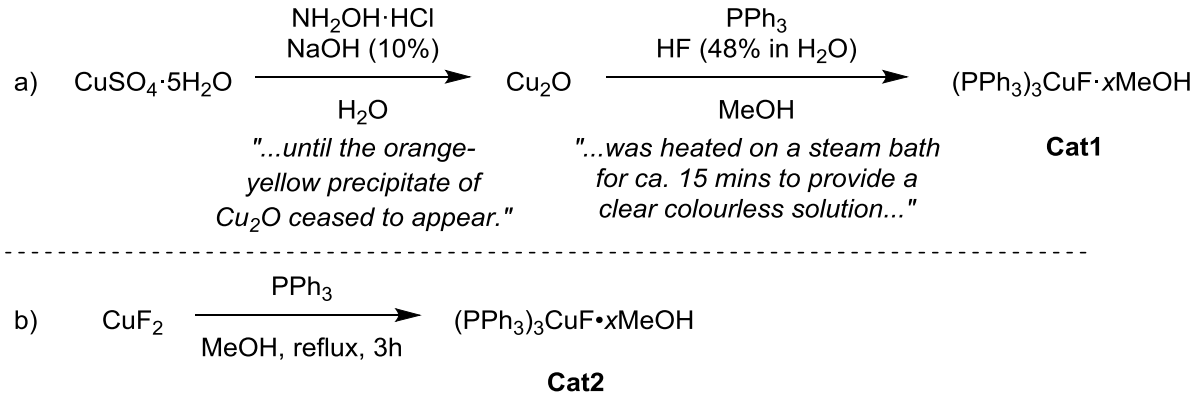

Scheme 3.43. Synthesis of the desired catalyst.

In theory, both of these methods afforded the desired catalyst as a complex with methanol, although we later found *via* ^1H NMR that the batch of catalyst that we had first used contained no methanol. We therefore decided to test the commercially available $(PPh_3)_3CuF$ (**CatCom**), which contained no methanol, and found that this catalyst was also inactive in the reaction conditions. Furthermore, in contrast to our home-made catalyst batches, no signal was detected in the ^{19}F NMR of the commercial catalyst; presumably due to different species in equilibrium or coupling with the neighbouring phosphorus atoms.[181]

These results led us to believe that the true catalytic species responsible for the *E* isomer was in fact not $(PPh_3)_3CuF$ as we first believed, but a different copper complex. Therefore, we tested the reaction with several other complexes, including both copper(I) and copper(II) metal species (CuI, CuCl, $Cu(OTf)_2$, and CuF_2), as well as mixtures of CuF_2 and triphenylphosphine, but to no avail. What's more, these tests all gave poor conversions and the same mixture of (*E*)- and (*Z*)-**3.126**, neither one in a significant majority.

[179] M. K. Chaudhuri, S. S. Dhar and N. Vijayashree, *Trans. Met. Chem.*, 2000, **25**, 559-561.
[180] J. M. Larsson, S. R. Pathipati and K. J. Szabó, *J. Org. Chem.*, 2013, **78**, 7330-7336.
[181] D. J. Gulliver, W. Levason and M. Webster, *Inorg. Chim. Acta*, 1981, **52**, 153-159.

Following this, we decided to investigate the batches of the synthesised catalyst as the fluoride donor in stoichiometric amounts, given that Zhu demonstrated that good results could also be obtained this way.[173, 174] To our surprise the reactions took place to completion, albeit resulting in varying amounts of the *E* and *Z* isomers (Table 3.6). Frustratingly, the commercial catalyst was also active in Zhu's stoichiometric conditions—erasing our doubts that fluorine was even present in the commercially bought batch—although it resulted in the opposite selectivity (entry 1, Table 3.6). In these tests we also found that toluene gave slightly higher *E*:*Z* selectivity.

With renewed hope, we once again attempted the synthesis of the catalyst using the original procedure (Method a, Scheme 3.43). This time, adding less triphenylphosphine to the mixture resulted in an active species (**Cat3**)—leading us to believe that a species such as $(PPh_3)_2CuF_2$ could be responsible for the reaction. We were unable to confirm this, however.

Table 3.6. New optimisation of the metal-catalysed *syn*-hydrofluorination of 3.125g.

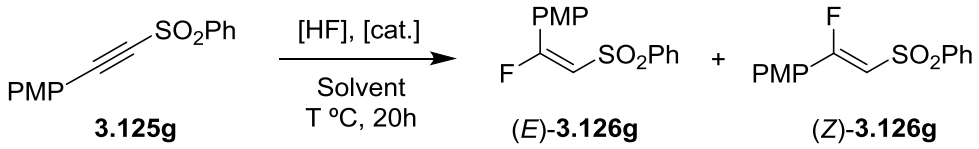

3.125g (*E*)-**3.126g** (*Z*)-**3.126g**

Entry	Catalyst	[cat.] (mol%)	[HF]	Solvent	T (°C)	Conv. (%)[a]	*E*:*Z*[b]
1	**Cat1**	100	-	THF	70	100	2:3
2	**Cat1**	10	$3HF{\cdot}Et_3N$	Dioxane	70	90	1:1
3	**Cat2**	100	-	THF	70	100	1:1
4	**CatCom**	100	-	THF	70	100	2:3
5	**Cat2**	100	-	Toluene	70	100	3:1
6	**Cat3**	10	$3HF{\cdot}Et_3N$	Dioxane	70	100	3:1
7	**Cat3**	10	$3HF{\cdot}Et_3N$	Toluene	70	100	4:1

[a] Determined via ^1H NMR. [b] Determined by ^1H and ^{19}F NMR (*vide infra*).

Nonetheless, after a short optimisation we found that toluene was the best solvent, possibly due to its non-coordinating nature (entry 7, Table 3.6).

We therefore took these conditions forward to study the scope of this reaction. We observed a clear trend with regards to the substrate nature and the selectivity of the reaction; substrates containing electron-donating groups with respect to the alkyne group resulted in the best *E*-selectivity, whereas more electron-poor alkynes resulted in poor selectivity, or even slight *Z*-selectivity. Despite this, the *E* and *Z* isomers were easily separable by flash column chromatography, and (*E*)-β-fluorovinyl sulfones were eventually obtained in synthetically useful yields (Table 3.7). The selectivity was easily determined

through ^{19}F NMR; the doublet corresponding to the *E* isomer appeared at roughly -70 ppm, whereas the related *Z* isomer would appear at around -90 ppm (Figure 3.4).

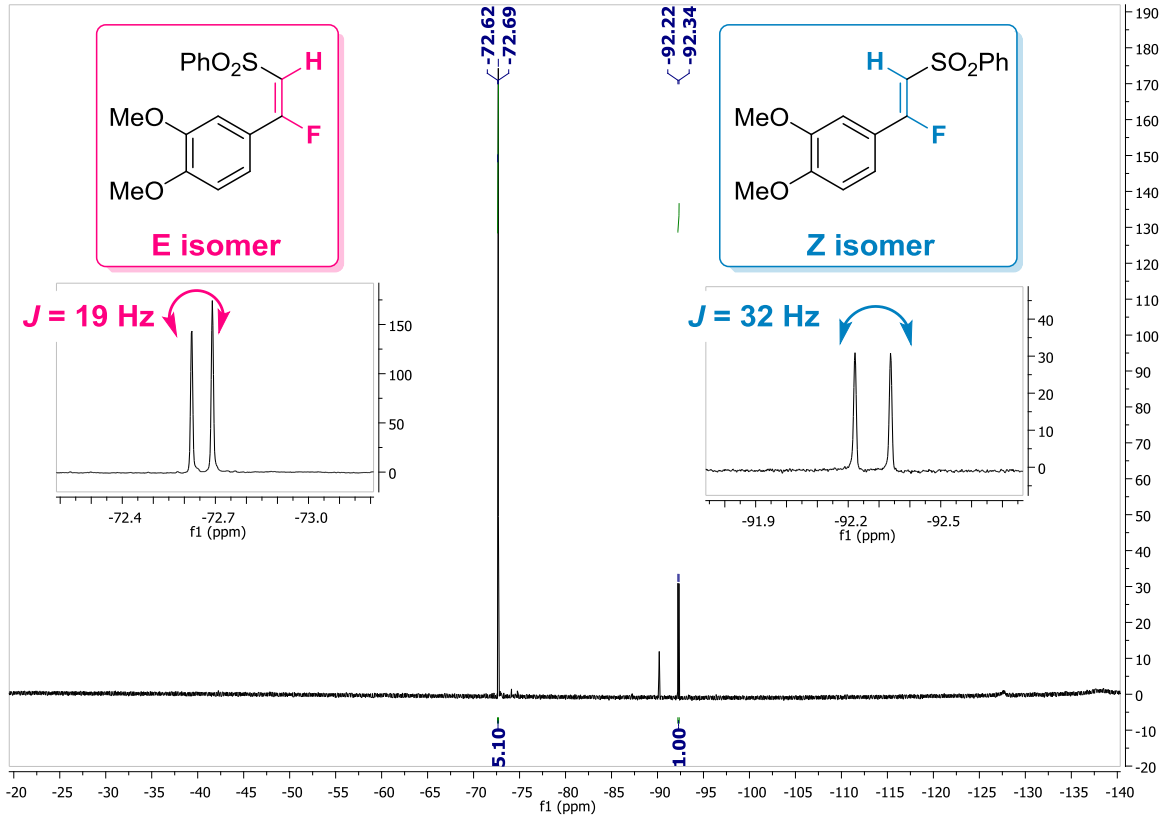

Figure 3.4. Determination of *E*/*Z* selectivity through ^{19}F NMR.

Table 3.7. Scope of the copper-catalysed *syn*-hydrofluorination of alkynyl sulfones.

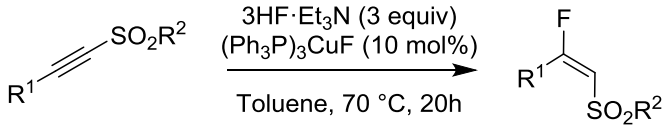

3.125 (*E*)-**3.126**
Yield%[a] (*E*:*Z*)[b]

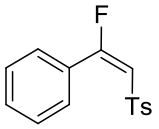

(*E*)-**3.126a**
35% (2:1)

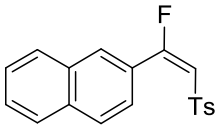

(*E*)-**3.126b**
38% (3:1)

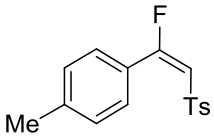

(*E*)-**3.126d**
43% (3:1)

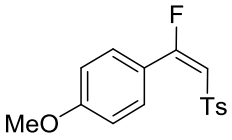

(*E*)-**3.126f**
51% (4:1)

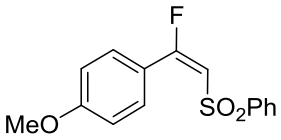

(*E*)-**3.126g**
56% (4:1)

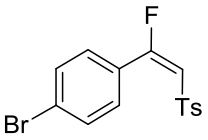

(*E*)-**3.126j**
27% (1:1)

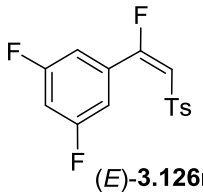

(*E*)-**3.126m**[c]
-% (2:3)

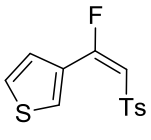

(*E*)-**3.126o**
63% (5:1)

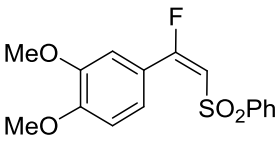

(*E*)-**3.126p**
60% (5:1)

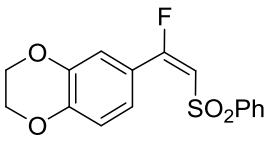

(*E*)-**3.126q**
53% (4:1)

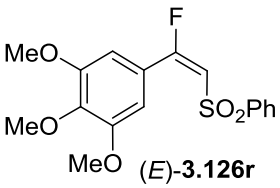

(*E*)-**3.126r**
58% (5:1)

[a] Isolated yield of (*E*)-**3.126**. [b] *E*:*Z* ratio determined by ^{19}F NMR of crude reaction mixture. [c] Product could not be isolated.

3.3.2. Reactivity of β-fluorovinyl sulfones

After carrying out the selective synthesis of both (*E*)- and (*Z*)-β-fluorovinyl sulfones, we began to explore their reactivity. Firstly, we tested some simple nucleophilic additions with a variety of nucleophiles. Unfortunately, as Berkowitz observed with his 2,2-difluorovinyl phenyl sulfone **3.121**, many nucleophiles reacted with our model substrate (*Z*)-**3.126a** *via* an addition-elimination mechanism, in which the fluorine was lost each time. Nucleophiles that reacted in this way included amines (pyrrolidine, piperidine and benzylamine) and *n*-butyllithium resulting in **3.139** and **3.140** respectively (Scheme 3.44). Others such as diethyl malonate, nitromethane, allyl trimethylsilane, trifluoromethyl trimethylsilane (Prakash's reagent), and trimethylsilyl acetylene failed to react at all.

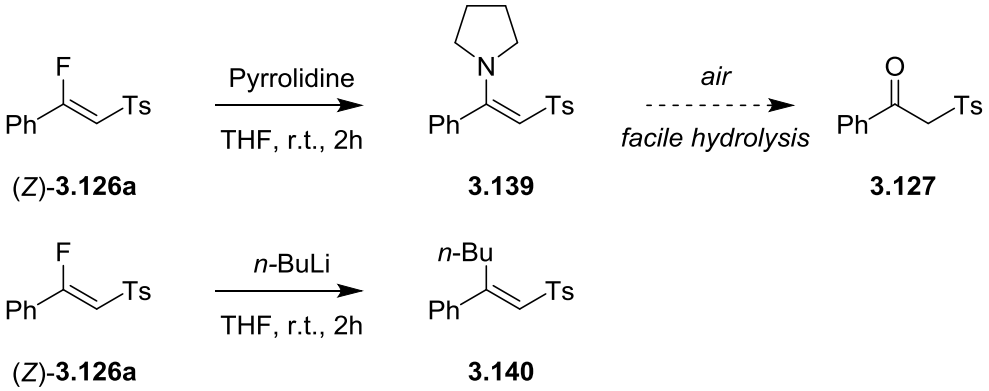

Scheme 3.44. Reaction of β-fluorovinyl sulfones with certain nucleophiles. Enamine 3.139 was highly susceptible to hydrolysis.

After seeing these results, we realised that a fluorine atom in the β position would always be susceptible to elimination in this class of simple 1,4-addition reactions. We also explored metal-catalysed addition reactions as demonstrated by Charette, Carretero and Nishimura.[132-139] However, these reactions gave slightly different results in our case. Firstly, we tried the rhodium-catalysed addition of arylboronic acids as described by Nishimura and co-workers.[138] In this reaction, we were able to detect addition-elimination product **3.141** (Scheme 3.45); this meant the substrate was indeed reactive in these reaction conditions. We first thought that the base, potassium phosphate, was too strong for the fluoride substituent, which resulted in effectively a double-benzylic position. We therefore attempted the reaction with different bases, and even in more acidic conditions using ammonium chloride, but to no avail. The result was always the same; around a 10% conversion and **3.141** as the only product. This led us to believe that the actual mechanism was slightly different, and

the rhodium was actually responsible for the loss of fluorine *via* β-fluoride elimination. Since we used a 5 mol% catalyst loading (therefore 10 mol% in terms of rhodium metal) and always saw around 10% conversion, we assumed that the reaction failed to proceed to completion due to the resulting rhodium-fluoride species being inactive as a catalyst in this reaction (Scheme 3.45).

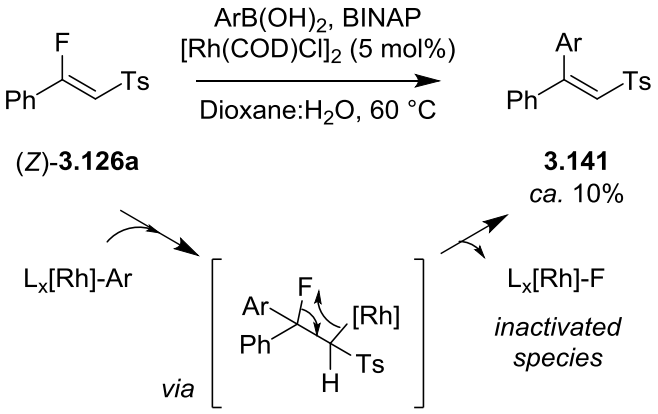

Scheme 3.45. Results of attempted rhodium-catalysed addition of arylboronic acids to (*Z*)-3.126a.

In this field, we also attempted some of the reactions disclosed by Charette[131] and Carretero,[165] namely the addition of diethyl zinc and reduction with phenylsilane respectively. Our substrate was unreactive in these cases, which didn't come as a total surprise given that the original reports detailed the dependency of the reactions on the 2-pyridyl sulfone moiety. With this is mind, we also attempted the synthesis of various alkynyl 2-pyridyl sulfones **3.142** in order to obtain the corresponding β-fluorovinyl 2-pyridyl sulfones and confirm the different reactivity observed by other authors.[127-133] However, all synthetic routes tested failed to yield the target **3.142** (Scheme 3.46).

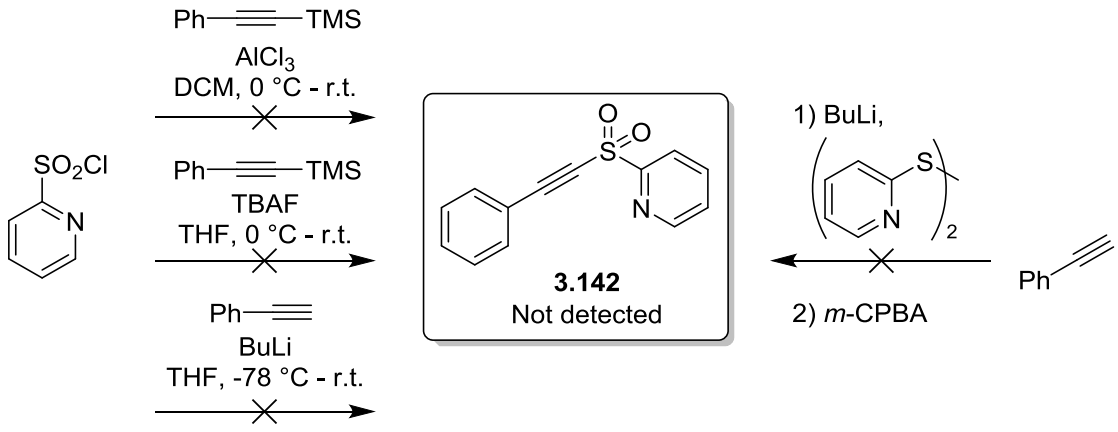

Scheme 3.46. Attempted syntheses of alkynyl 2-pyridyl sulfones 3.142.

After these failed reactions, we decided to move in a different direction with this study. Given the facile loss of fluorine in this type of addition reaction, we hypothesised that these substrates would benefit from more concerted processes, thereby avoiding the formation of negative charges during the reaction. To this end, we explored both Diels-Alder and cycloaddition reactions between various dipoles—such as nitrones, azides, and ylides[182]—and our fluorovinyl sulfones. Both the *E* and *Z* isomers were tested, and all reactions were followed by TLC and NMR analysis. Unfortunately, these reactions also failed to give any promising product, although in several cases *E*/*Z* isomerisation was observed when the starting fluorovinyl sulfones were subjected to high temperatures.

We then started to look at hydrogenation reactions. This would surely be a challenging prospect; vinyl halides are generally considered to be poor substrates for hydrogenation reactions, given the tendency of C—X bonds to cleave under such reaction conditions. Despite this, the hydrogenation of vinyl fluorides—though still a fairly understudied subject—is perhaps the most common owing to the relative strength of the C—F bond compared to its chloride and bromide counterparts.[183]

We began this study using standard hydrogenation conditions, and the reaction took place and proceeded to completion. However, the result was a mixture of the desired saturated β-fluoroalkyl sulfone **3.143a**, along with a relatively high proportion of defluorinated product **3.144a** (Scheme 3.47).

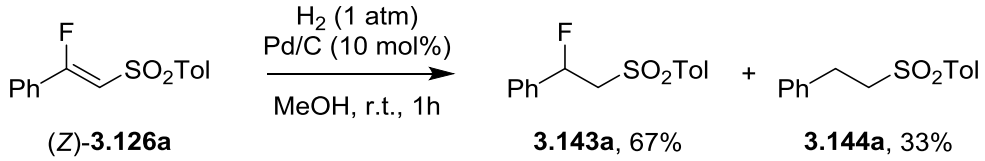

(*Z*)-**3.126a** **3.143a**, 67% **3.144a**, 33%

Scheme 3.47. First attempt at the hydrogenation of model fluorovinyl sulfone (*Z*)-3.126a.

We decided to try several other hydrogenation methodologies to obtain the resulting saturated β-fluoroalkyl sulfones **3.143** in higher selectivities, including the use of other metal catalysts and some transfer hydrogenation procedures with ammonium formate or diimine as the hydrogen source (entries 1-10, Table 3.8). Given the limited success of these tests, we decided to persist with the standard palladium over activated charcoal and attempt to improve the selectivity. Various studies have described the effect of solvents on hydrodehalogenation processes—the related hydrodechlorination has been more widely studied due to environmental issues—and usually conclude that the use of polar

[182] For an informative review on the types of cycloaddition reactions tested here, see: L. M. Stanley and M. K. Sibi, *Chem. Rev.*, 2008, **108**, 2887-2902.
[183] D. M. Sedgwick and G. B. Hammond, *J. Fluorine Chem.*, 2018, **207**, 45-58.

protic solvents is the most effective at removing the halide from the final product.[184] In this context, we ran a small optimisation of more common solvents in order to achieve a higher selectivity and less hydrodefluorination (entries 10-20, Table 3.8). In the end, we found that the reaction was more sluggish in the non-polar toluene, which proved useful in terms of controlling the selectivity. In this way, we managed to obtain full conversion of **3.126a** to **3.143a** with an acceptable selectivity of 12:1, by increasing the reaction time (entries 18-20, Table 3.8). Unfortunately, we were unable to purify the resulting crude mixture through standard column chromatography—all three species involved (fluorovinyl sulfone **3.126**, saturated fluoroalkyl sulfone **3.143** and the corresponding hydrodefluorination product **3.144**) had very similar R_F values and were not easily seen in UV light, nor with standard TLC stains—meaning it was preferable to reach full conversion despite a slightly higher degree of the non-fluorinated product. Nevertheless, separation *via* HPLC was possible.

[184] a) M. Hudlicky, *J. Fluorine Chem.*, 1979, **14**, 189-199. b) K. J. Stranger, R. J. Angelici, *J. Mol. Catal. A Chem.*, 2004, **207**, 59-68.

Table 3.8. Hydrogenation of fluorovinyl sulfones.

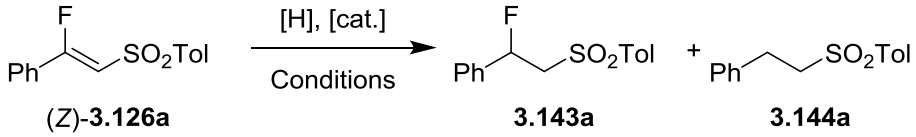

(*Z*)-**3.126a** **3.143a** **3.144a**

Entry	[H]	[cat.][c]	Solvent	T (˚C)	Time (h)	Conv. (%)[g]	**3.143**:**3.144**[g]
1	H_2 (1 atm)	Pd/C	MeOH	r.t.	1	100	2:1
2	$NH_4{\cdot}HCO_2$	-	MeOH	r.t.	24	-	-
3[a]	$NH_4{\cdot}HCO_2$	Pd/C	MeOH	r.t.	24	-	-
4	$NH_4{\cdot}HCO_2$	-	EtOH	110	8	N.D.[h]	-
5	N_2H_4/H_2O_2	$CuSO_4$	EtOH	r.t.	24	-	-
6[b]	$TsNHNH_2$	-	Toluene	150	8	N.D.[i]	N.D.
7[b]	$TsNHNH_2$	-	Toluene	160[f]	3	N.D.[j]	N.D.
8	$NaBH_4$	-	MeOH	r.t.	24	-	-
9	$PhSiH_3$	CuO*t*-Bu[d]	Toluene/H_2O	r.t.	24	-	-
10	H_2 (1 atm)	$Pd(OH)_2/C$	MeOH	r.t.	1	100	1:1
11	H_2 (1 atm)	PtO_2	MeOH	r.t.	24	-	-
12	H_2 (1 atm)	Pd/C	EtOAc	r.t.	1	100	3:1
13	H_2 (1 atm)	Pd/C	MTBE	r.t.	1	100	6:1
14	H_2 (1 atm)	Pd/C	Et_2O	r.t.	1	100	3:1
15	H_2 (1 atm)	Pd/C	AcOH	r.t.	1	100	1:10
16	H_2 (1 atm)	Pd/C	Dioxane	r.t.	1	100	7:1
17	H_2 (1 atm)	Pd/C	Cyclohexane	r.t.	1	100	7:1
18	H_2 (1 atm)	Pd/C	Toluene	r.t.	1	30	>25:1
19	H_2 (1 atm)	Pd/C[e]	Toluene	r.t.	1.5	80	>25:1
20	H_2 (1atm)	Pd/C[e]	Toluene	r.t.	2	100	12:1

[a] Reaction conditions taken from Ranu *et al.*[185] [b] 4 Å MS added to the reaction mixture. [c] Catalyst loading 10 mol% unless stated otherwise. [d] Catalyst formed *in situ* with CuCl and NaO*t*-Bu.[186] [e] Catalyst loading 15 mol%. [f] Reaction carried out in a microwave oven. [g] Determined by ^{1}H NMR unless stated otherwise. N.D. = Not determined. [h] Target compound not detected; evidence of addition-elimination by EtOH. [i] Traces of **3.143a** detected in a complex mixture. [j] Complex mixture, partial isomerisation of (*Z*)- to (*E*)-**3.126a**.

[185] B. C. Ranu, S. K. Guchhait and K. Ghosh, *J. Org. Chem.*, 1998, **63**, 5250-5251.

[186] D. H. Appella, Y. Moritani, R. Shintani, E. M. Ferreira and S. L. Buchwald, *J. Am. Chem. Soc.*, 1999, **121**, 9473-9474.

We also carried out some control experiments to determine the manner in which the hydrodefluorination reaction occurred. There are generally three speculated mechanisms for this: 1) hydrogenation of the C—C double bond to give the desired **3.143**, followed by the elimination of HF and hydrogenation of the resulting defluorinated vinyl sulfone **3.145**; 2) a concerted mechanism directly resulting in **3.144** as proposed by Hudlicky *via* a carbene intermediate;[184a] and 3) direct cleavage of the C—F bond in **3.143** promoted by the palladium catalyst. Vinyl sulfone **3.145** was not observed at any point and, in contrast to Andersson[187] and Hudlicky's work with α-fluorovinyl carbonyls, we observed that fluoroalkyl sulfone **3.143** reacted further in the same reaction conditions resulting in further loss of fluorine. These observations led us to believe that direct cleavage of the C(sp^3)—F bond was responsible for hydrodefluorination (Scheme 3.48).

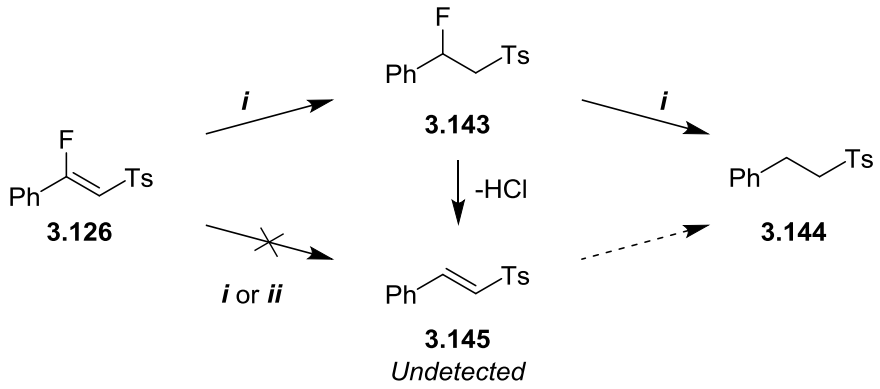

i. H_2 (1 atm), Pd/C (10 mol%), MeOH. ***ii.*** Pd/C (10 mol%), MeOH

Scheme 3.48. Control experiments to determine the mechanism of hydrodefluorination.

Having determined the best conditions for the hydrogenation of (*Z*)-β-fluorovinyl sulfones to β-fluoroalkyl sulfones, we evaluated the scope of the reaction. The conversions and selectivities were determined *via* ^{1}H NMR spectroscopy, given that the fluorinated **3.143** and non-fluorinated **3.144** could be easily distinguished (Figure 3.5). We found that β-fluorovinyl sulfones with electron-neutral aromatic rings (entries 1-5, Table 3.9), as well as those bearing electron-donating groups (entries 6-7, Table 3.9), all reacted well in similar time frames to give moderate to high selectivities. However, substrates bearing substituents positioned to withdraw electron density from the double bond reacted much more slowly (entries 8-11, Table 3.9). Interestingly, in the hydrogenation reaction the *m*-methoxy substituents in substrate **3.126i** exerted a deactivating effect, similar to the difluorinated aromatic group in **3.126m**. This is in accordance with the Hammett coefficient for methoxy groups in the *meta* position, in which their electron-withdrawing effect overrides their resonance effect (*this was also seen*

[187] M. Engman, J. S. Diesen, A. Paptchikhine and P. G. Andersson, *J. Am. Chem. Soc.*, 2007, **129**, 4536–4537.

in Chapter 2, refer to pages 103-104). The hydrogenation of thiophene-derived fluorovinyl sulfone **3.126o** failed to complete with 15 mol% catalyst loading, even after submitting the same mixture to the reaction conditions several times. We suspected that the catalyst was poisoned in some way by the thiophene product, which was confirmed when the reaction proceeded to completion in a normal time frame upon treating the substrate with a stoichiometric amount of palladium over charcoal under an atmosphere of hydrogen.

The related α-fluorovinyl sulfone **3.146**, β-fluoro acrylate **3.132**, and aliphatic fluorovinyl sulfone **3.126u** were also successfully hydrogenated in high selectivities and yields (entries 13, 15 and 16, Table 3.9). The higher selectivity resulting from the hydrogenation of α-fluorovinyl sulfone **3.146** suggests that the β-fluorine is more susceptible to hydrodefluorination, which is in accordance with Sauvetre and co-workers' results: with related α-fluoroalkenyl carbonyl compounds no loss of fluorine was observed, despite using methanol as the solvent.[188] Methyl sulfone derivative **3.126s** displayed less hydrodefluorination over a reaction time of three hours, once again suggesting that our problems had arisen from the more electron-withdrawing nature of the phenyl sulfone.

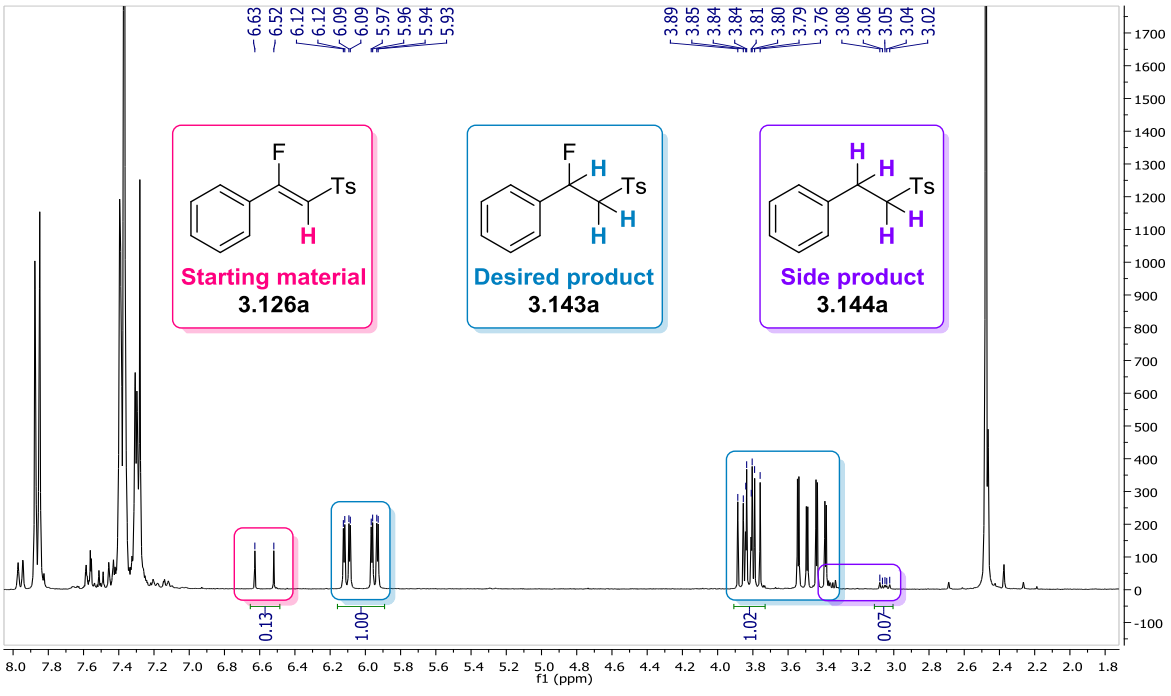

Figure 3.5. Determination of conversions and selectivities of hydrogenation reactions *via* ^{1}H NMR.

[188] R. Sauvetre, J.-F. Normant and P. Martinet, *J. Fluorine Chem.*, 1991, **52**, 419–432.

Table 3.9. Scope of the hydrogenation of fluorovinyl sulfones.

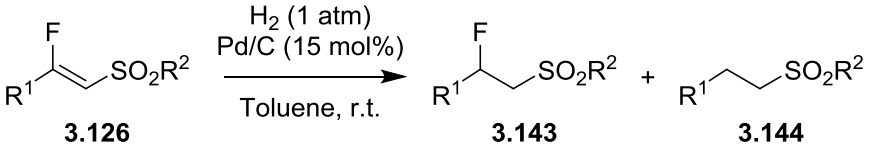

3.126 **3.143** **3.144**

Entry	Substrate	Product	Time (h)	Conv. (%)	Yield (%)[b]	**3.143:3.144**[e]
1	(*Z*)-**3.126a**	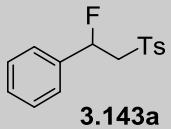 **3.143a**	2	100	96	12:1
2	(*Z*)-**3.126b**	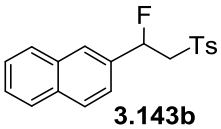 **3.143b**	2.5	100	97	7:1
3	(*Z*)-**3.126c**	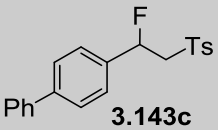 **3.143c**	3	100	94	8:1
4	(*Z*)-**3.126d**	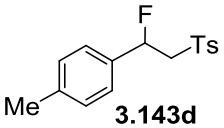 **3.143d**	2	100	92	32:1
5	(*Z*)-**3.126e**	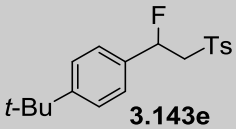 **3.143e**	3	95	96	24:1
6	(*Z*)-**3.126f**	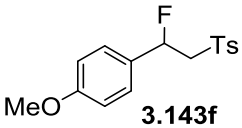 **3.143f**	3	100	96	13:1
7	(*Z*)-**3.126g**	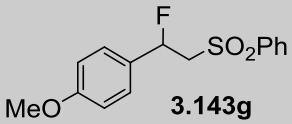 **3.143g**	2	100	95	24:1
8	(*Z*)-**3.126i**	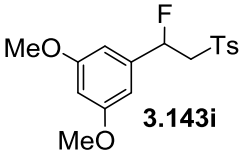 **3.143i**	60	100	95	19:1
9	(*Z*)-**3.126j**	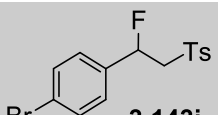 **3.143j**	16	40	0[c]	-

10	(*Z*)-**3.126m**	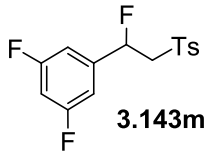 **3.143m**	60	100	94	12:1
11	(*Z*)-**3.126n**	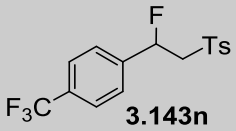 **3.143n**	120	80	90[d]	4:1
12[a]	(*Z*)-**3.126o**	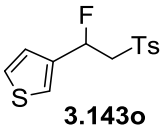 **3.143o**	2.5	100	85	13:1
13	(*Z*)-**3.126s**	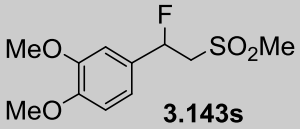 **3.143s**	3	80	96[d]	>99:1[f]
14	(*Z*)-**3.126u**	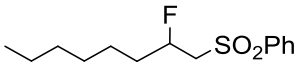 **3.143u**	1.5	100	94	13:1
15	(*Z*)-**3.146**	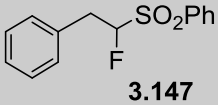 **3.147**	2	100	94	24:1
16	(*Z*)-**3.132**	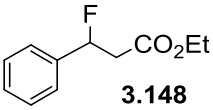 **3.148**	1.5	100	90	10:1

[a] Catalyst loading of 100 mol% used. [b] Yield refers to inseparable mixture of **3.143** and **3.144**.[c] The only product detected was **3.126a** resulting from the cleavage of the aromatic C—Br bond. [d] Yield refers to the inseparable mixture of unreacted **3.126**, **3.143**, and **3.144**. [e] Ratio measured *via* ^{1}H NMR spectrum of the crude mixture (refer to Figure 3.5). [f] No defluorinated product observed after three hours of reaction time.

We also studied the hydrogenation of the corresponding *E* isomer of our model substrate (*E*)-**3.126a**. In this case, the substrate was less reactive and required a much longer reaction time to achieve full conversion (Table 3.10). This is somewhat different to what one would expect from this type of reaction.

Generally speaking, the reaction rate of catalytic heterogeneous hydrogenation correlates directly to the stability of the olefin in question. Therefore, less stable alkenes generally react faster under hydrogenation conditions, and generally *cis* alkenes are less stable due to steric effects.[189] In our case, strictly speaking the *E* isomers are in the *trans* configuration, although sterically speaking this is not the case; sterically, our substrate (*E*)-**3.126a** is comparable to a more traditional *cis* alkene. Moreover, the

[189] L. C. Begley, K. J. Kakanskas, A. Monaghan and S. D. Jackson, *Catal. Sci. Technol.*, 2012, **2**, 1287–1291

isomerisation seen upon submitting the *E* isomers to high temperatures suggests that the *Z* isomers are more thermodynamically stable. Therefore, one would expect the reaction rate of the *E* isomers to be higher than for the corresponding *Z* isomers.

In this sense, we expect that the difference has more to do with electronic rather than steric effects.

Furthermore, the hydrogenation of the *E* isomer resulted in a higher degree of defluorinated product. This result reinforces our previous observations that the hydrodefluorination process takes place on the resulting β-fluoroalkyl sulfone product **3.143**, rather than taking place directly from the vinyl fluoride starting material with the double bond intact (refer to Scheme 3.47). The hydrogenation process of the *E* isomer is slower, while the resulting product is the same and therefore fluorine would be lost from the product at the same rate, resulting in a greater amount of defluorinated **3.144a**.

Table 3.10. Hydrogenation of the related *E* isomer, (*E*)-3.126a

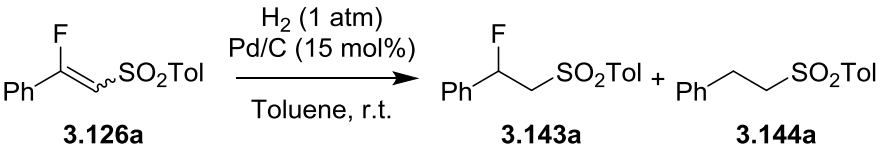

3.126a **3.143a** **3.144a**

Entry	Substrate	Time (h)	Conv. (%)	**3.143a**:**3.144a**
1	(*Z*)-**3.126a**	2	100	12:1
2	(*E*)-**3.126a**	2	0	-
3	(*E*)-**3.126a**	4	10	1:1
4	(*E*)-**3.126a**	20	95	2:3

3.3.3. Preliminary studies of the homogeneous hydrogenation of vinyl fluorides.

Hydrogenation is fundamental process in organic chemistry and has been used for over a century to add elemental hydrogen across unsaturated bonds.[150] Many advances have been made in the area of hydrogenation since early examples in the 19th century; perhaps the most important came in the mid-20th century when Wilkinson developed the first homogeneous rhodium complex to rival the reactivity of well-established heterogeneous catalysts, as mentioned earlier. Following this, Knowles and Noyori were able to further develop the homogeneous version of the reaction to allow enantioselective hydrogenation. They later shared the Nobel Prize in Chemistry in 2001 "for their work on chirally catalysed hydrogenation reactions", which has now been successfully applied to a wide range of substrates and industrial processes—the first example of asymmetric hydrogenation was swiftly applied to the industrial synthesis of L-DOPA (Scheme 3.49).[151, 190]

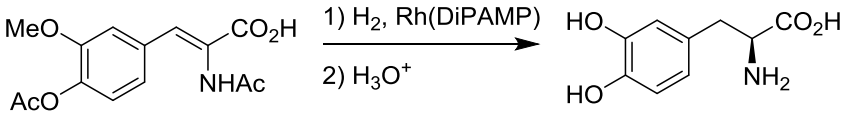

Industrial synthesis of L-DOPA developed by Knowles et al. at Monsanto

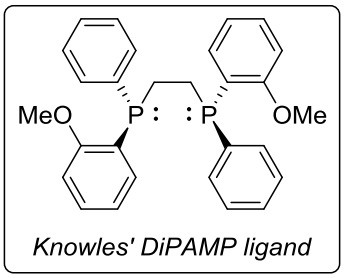

Knowles' DiPAMP ligand

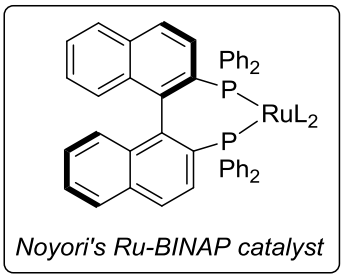

Noyori's Ru-BINAP catalyst

Scheme 3.49. Nobel prizes in 2001 for developments in asymmetric hydrogenation: Knowles' DiPAMP ligand and its immediate application in the industrial synthesis of L-DOPA; and Noyori's Ru-BINAP catalyst.

However, the field still faces many challenges, particularly in the asymmetric area; the earlier examples were almost exclusively carried out using specific substrates bearing functional groups in proximity to the alkene able to coordinate to the metal centre and help in directing the selectivity. Recently, more substrates have become amenable to the transformation following further advances in the development of chiral ligands and catalysts, although many classes of substrates remain

[190] R. Noyori, *Angew. Chem. Int. Ed*., 2002, **41**, 2008–2022.

underrepresented in the field: vinyl halides are one such class. As discussed previously, vinyl halides are generally considered poor substrates for hydrogenation reactions, since they present the additional challenge of dehalogenation. Examples of selectively reducing alkenyl halides to alkyl halides are extremely scarce, although a few do exist. Amongst these transformations, it is perhaps most common to start with vinyl fluorides given that the C—F bond is the strongest of the carbon-halide bonds, thus making them the most resistant to dehalogenation. In recent years, vinyl fluorides have seen an increased interest as substrates for hydrogenation, possibly due to the increasing demand for new methodologies of introducing fluorine into organic molecules.[183, 191]

Since the hydrogenation of fluorovinyl sulfones was unknown in the literature, after carrying out the work in the previous section we set our sights on something far more ambitious: the homogeneous, and therefore potentially asymmetric, hydrogenation of these substrates. The following work was carried out partly during a short stay (July-October 2017) in the University of Louisville, Kentucky (USA), in the research group of Prof. G. B. Hammond. The structures of some representative ligands and catalyst complexes used throughout this study are summarised in Figure 3.6.

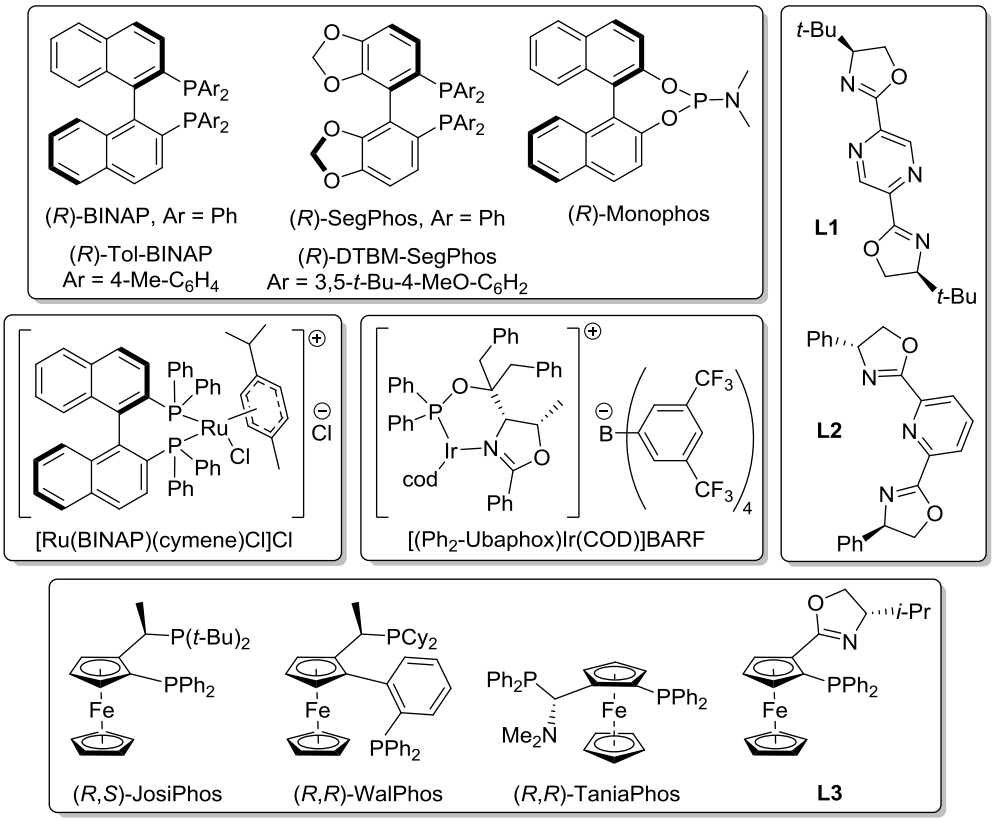

Figure 3.6. Selection of representative ligands and catalyst complexes used in this study.

[191] For some representative examples, see: a) M. Saburi, L. Shao, T. Sakurai and Y. Uchida, *Tetrahedron Lett*., 1992, **33**, 7877–7880. b) S. W. Krska, J. V. Mitten, P. G. Dormer, D. Mowrey, F. Machrouhi, Y. Sun and T. D. Nelson, *Tetrahedron*, 2009, **65**, 8987–8994. c) M. Engman, J. S. Diesen, A. Paptchikhine and P. G. Andersson, *J. Am. Chem. Soc*., 2007,**129**, 4536–4537.

Aromatic β-fluorovinyl sulfone **3.126a** and aliphatic derivative **3.126q** were first tested as the model substrates, and we found immediately that the aromatic group hindered the hydrogenation reaction, in accordance with Saburi's work dealing with acrylic acids.[192] Our initial screenings showed that hydrodefluorination also took place here, comparative to that seen with the heterogeneous hydrogenation described previously (Table 3.11). However, a recent report from Krska and co-workers at Merck suggested that the fluorine loss in homogeneous hydrogenation differed slightly from the heterogeneous scenario. The authors found that rather than the solvent, the ligand had a much more dramatic effect on the hydrodefluorination and used methanol for all the reactions, and claim that other solvents greatly improved neither the chemo- nor the enantioselectivity.[191b]

Table 3.11. Initial screenings with fluorovinyl sulfones.

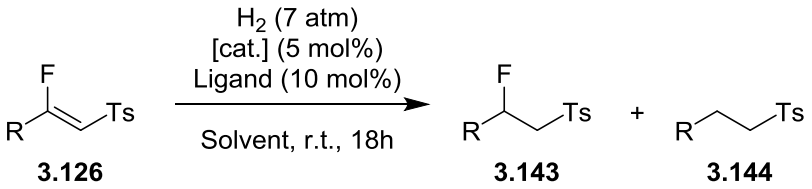

3.126 **3.143** **3.144**

Entry	R	[cat.]	Ligand	Solvent	Conv. (%)[a]	**3.143:3.144**[a]
1	*n*-Hex	$[Rh(COD)_2]BF_4$	BINAP	EtOAc	99%	7:1
2	*n*-Hex	$[Rh(COD)_2]BF_4$	Tol-BINAP	EtOAc	73%	3:1
3	*n*-Hex	[Ru(BINAP)(cymene)Cl]Cl	-	MeOH	0%	-
4	Ph	$[Rh(COD)_2]BF_4$	BINAP	EtOAc	0%	-
5	Ph	$[Rh(COD)_2]BF_4$	BINAP	DCM	30%	3:1
6	Ph	[Ru(BINAP)(cymene)Cl]Cl	-	MeOH	0%	-
7	PMP	$[Rh(COD)_2]BF_4$	BINAP	EtOAc	0%	-

[a] Determined by ^1H NMR.

With regards to the aromatic fluorovinyl sulfone **3.126a**, we found that the reaction was sensitive to a number of factors, including hydrogen pressure: when using 20 atmospheres of hydrogen, the reaction failed to proceed, even in methanol, and the starting fluorovinyl sulfone was recovered. At atmospheric pressure, however, with a combination of $[Rh(COD)_2]BF_4$ and Segphos in methanol produced the reaction to 60% conversion resulting in a low selectivity of 2:1. We reasoned this could be due to the poor coordinating ability of such an electron-deficient double bond, meaning at higher hydrogen

[192] a) M. Saburi, L. Shao, T. Sakurai and Y. Uchida, *Tetrahedron Lett.*, 1992, **33**, 7877–7880. b) M. Saburi, H. Takeuchi, M. Ogasawara, T. Tsukahara, Y. Ishii, T. Ikariya, T. Takahishi and T. Uchida, *J. Organomet. Chem.*, 1992, **428**, 155–167.

pressures the coordination of the double bond could not compete with hydrogen. Other reports have carried out similar hydrogenations at very high pressures (50-100 atm), although this is usually accompanied with heating the reaction mixture for good results;[191b-c, 193] unfortunately, we lacked the facilities to use such conditions.

We also attempted the asymmetric hydrogenation of an "unfunctionalised" vinyl fluoride **3.149**; an ambitious transformation given the small size of the fluorine atom as a substituent. Although the reaction was carried out successfully, initially there was a large degree of hydrodefluorination; especially when using methanol as the solvent. Protic solvents seemed to promote the reaction the most, and coordinating solvents such as dioxane and acetone showed some conversion and better chemoselectivity, whereas non-coordinating solvents were unsuccessful. The solvent that gave the best results in terms of conversion and chemoselectivity was a mixture of dioxane and isopropanol, inspired by Zhou *et al.*[193] Rhodium-based catalyst systems showed the most promise early on, however, all of the conditions tested gave rise to racemic products (Table 3.12).

Table 3.12. Solvent effects and initial screenings of other catalyst systems.

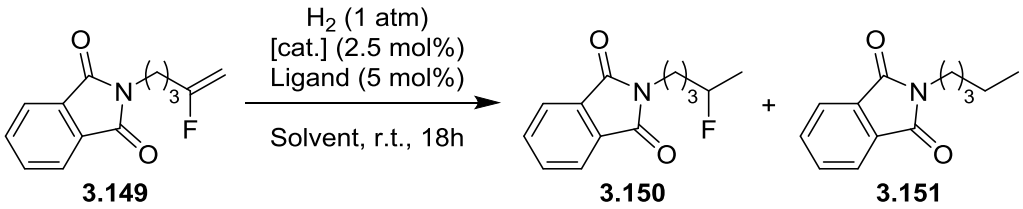

3.149 **3.150** **3.151**

Entry	[cat.]	Ligand	Solvent	Conv. (%)[b]	3.150:3.151[b]	ee[c]
1	$[Rh(COD)Cl]_2$	Walphos	*i*-PrOH	100%	3:1	<5%
2	$[Rh(COD)Cl]_2$	Walphos	MeOH	100%	1:1	<5%
3	$[Rh(COD)Cl]_2$	Walphos	Acetone	30%	>15:1	<5%
4	$[Rh(COD)Cl]_2$	Walphos	Dioxane	60%	>15:1	<5%
5	$[Rh(COD)Cl]_2$	Walphos	Toluene	0%	-	-
6	$[Rh(COD)Cl]_2$	Walphos	DCM	0%	-	-
7	$[Rh(COD)Cl]_2$	Walphos	D-IP[a]	100%	12:1	<5%
8	$[Ir(COD)Cl]_2$	Walphos	DCM	0%	-	-
9	[(Ph_2-Ubaphox)Ir(COD)]BARF	-	DCM	0%	-	-
10	[Ru(BINAP)(cymene)Cl]Cl	-	MeOH	0%	-	-

[a] D-IP = Dioxane:*i*-PrOH (3:1). [b] Determined by ^{1}H NMR. [c] Determined by HPLC in an IC Chiralpak column.

[193] R.-N. Guo, X.-F. Cai, L. Shi, Z.-S. Ye, M.-W. Chen and Y.-G. Zhou, *Chem. Commun.*, 2013, **49**, 8537-8539.

We also tried varying other conditions, since existing examples of enantioselective hydrogenation of vinyl halides have used higher temperatures and pressures. Furthermore, given the difficulty in enantioselectively hydrogenating **3.149**, we decided to try other fluorinated substrates with different functional groups proximal to the C=C double bond, such as fluoroacrylates or allylic alcohols (Table 3.13). TaniaPhos (refer to Figure 3.6 for the structure) was also tested due to the tertiary amine group present: we envisioned that an acidic additive could protonate this group, and potentially form a hydrogen bond with the fluorine atom of the substrates (Figure 3.7). Unfortunately, this mixture also failed to give any enantioselectivity, although the chemoselectivity was good.

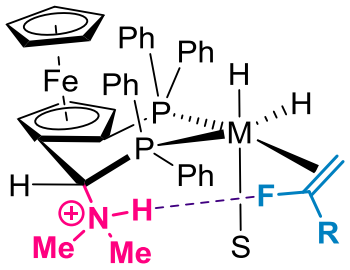

Figure 3.7. Transition state for the envisioned H-bond directed enantioselective reaction with Taniaphos.

Despite the lack of enantioselectivity observed in these reactions, this study shows that the homogenous hydrogenation of a variety of vinyl fluorides can be carried out in a selective manner. Some representative examples from this study are summarised in Table 3.13.

Entry	Substrate	Solvent[d]	[cat.][e]	Ligand[f]	Time (h)	H_2 (atm)	Conv.[h]	Selectivity[h]	ee[i]
1		D-IP	$[Rh(COD)Cl]_2$	Walphos	5	7	100%	12:1	<5%
2[a]		Toluene	$[Ir(COD)Cl]_2$	Taniaphos	16	1	90%	15:1	<5%
3[a]		MeCy	$[Ir(COD)Cl]_2$	Taniaphos	16	1	0%	-	-
4		DCM	$[Ir(COD)Cl]_2$	Josiphos	5	7	0%	-	-
5		Dioxane	$[Rh(COD)_2]BF_4$	Walphos	16	7	60%	5:1	[j]
6		D-IP	$[Rh(COD)_2]BF_4$	Walphos	16	7	100%	3:1	[j]
7		Dioxane	$[Rh(COD)_2]BF_4$	Monophos[g]	16	1	0%	-	-
8		D-IP	$[Rh(COD)Cl]_2$	Segphos	16	1	100%	10:1	<5%
9[a]		D-IP	$[Rh(COD)Cl]_2$	Taniaphos	16	1	100%	15:1	<5%
10		D-IP	$[Rh(COD)Cl]_2$	Josiphos	16	1	100%	12:1	<5%
11[a]		D-IP	$[Rh(COD_2]BF_4$	Taniaphos	16	1	0%	-	-
12[a]		D-IP	$[Rh(COD)Cl]_2$	Taniaphos	5	7	100%	18:1	<5%
13		D-IP	$[Rh(COD)_2]BF_4$	Josiphos	16	1	80%	12:1	<5%
14[b]		MeOH	[Ru(BINAP)(cymene)Cl]Cl	-	16	1	50%	-	<5%
15[c]		DCM	$[(Ph_2$-Ubaphox)Ir(COD)]BARF	-	72	7	60%	5:1	<5%

[a] Reaction contained BzOH (5 mol%) additive. [b] Reaction was carried out at 40°C. [c] 4Å MS added to the reaction mixture. [d] D-IP = Dioxane:*i*-PrOH (3:1). MeCy = Methylcyclohexane. [e] Catalyst loading was calculated for 5 mol% metal. [f] Ligands were used at 5 mol%. [g] 10 mol% ligand added for a ligand:metal ratio of 2:1. [h] Determined by ^1H and ^{19}F NMR. [i] Determined by HPLC. [j] We were unable to separate the enantiomers by HPLC.

Table 3.13. Representative reactions carried out into the search for enantioselectivity.

3.4. Conclusions.

We have successfully and selectively synthesised a family of (*E*)- and (*Z*)-β-fluorovinyl sulfones starting from the corresponding alkynyl sulfones for the first time. The *E* isomers were obtained *via* copper-catalysed addition of 3HF·Et_3N, whereas the *Z* isomers were achieved using a simple and practical metal-free addition of TBAF.

The reactivity of the resulting fluorovinyl sulfones was studied, and their selective hydrogenation to saturated fluoroalkyl sulfones was carried out; an unprecedented reaction in the chemical literature. This was done in both a heterogeneous and homogeneous manner. Although the homogeneous reaction was unfruitful in the search for an asymmetric version, this study proves that these challenging substrates can be hydrogenated with minimum fluorine loss.

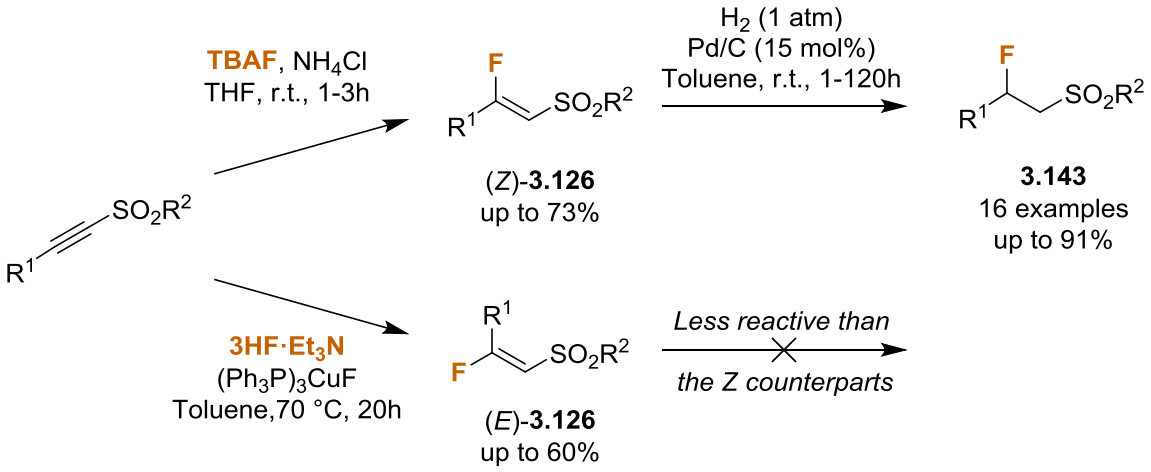

3.5. Experimental section.

Reactions were carried out under a nitrogen atmosphere unless otherwise indicated. Solvents were purified prior to use: THF was distilled from sodium and DCM from calcium hydride. Reagents were used as received from the suppliers without further purification, unless stated otherwise. The reactions were monitored by TLC on 0.25mm precoated silica-gel plates, which were revealed with UV light and aqueous ceric ammonium molybdate or potassium permanganate stains. Flash column chromatography was performed with the indicated solvents on silica gel 60 (particle size: 0.040−0.063 mm). ^{1}H, ^{13}C and ^{19}F NMR spectra were recorded by a 300 MHz spectrometer. Chemical shifts are given in ppm (δ), referenced to the residual proton resonances of the solvents. Coupling constants (*J*) are given in Hertz (Hz). The letters s, d, t, q and m stand for singlet, doublet, triplet, quartet and multiplet respectively. The letters br indicate that the signal is broad. A QTOF mass analysis system was used for the HRMS measurements.

*3.5.1. Synthesis of terminal alkynes **3.133a-c**.*

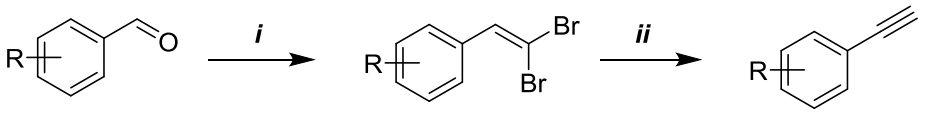

3.134p, R = 3,4-diMeO, 88%
3.134q, R = 3,4-O-$(CH_2)_2$-O-, 88%
3.134r, R = 3,4,5-triMeO, 91%

3.133p-r, quant.

i. Dibromomethylenation reaction. The corresponding aldehyde (1 equiv) and carbon tetrabromide (2 equiv) were dissolved in anhydrous DCM (0.3M), and triphenylphosphine (4 equiv) was added portion-wise over 20 minutes at 0 °C. The resulting brown solution was allowed to slowly warm to room temperature and was stirred until the reaction completed (analysed *via* TLC, approximately 2 hours). Water was then added to quench the reaction, and the mixture was extracted with DCM (2 x 20 ml). The combined organic layers were washed with brine, dried over anhydrous Na_2SO_4, and concentrated *in vacuo.* The resulting crude mixture was purified *via* flash column chromatography [*n*-hexane:ethyl acetate (15:1)].

ii. DBU-mediated elimination. DBU (4 equiv) was added to a solution of 1,1-dibromoalkene **3.134** at room temperature over a period of 30 minutes, and the reaction was stirred for a further 16

hours. Following this, HCl (6M in water, 50 equiv) was added over a period of 30 minutes at 0 °C, and the biphasic mixture was left for a further 30 minutes. The resulting was extracted with hexane:AcOEt (1:1) and the combined organic layers washed with brine, dried over K_2CO_3, and concentrated *in vacuo*. No further purification was necessary and all spectroscopic data coincided with those given in the literature.

Compounds **3.134p-q** and **3.133p-q** have been previously described by Pelter, Ward *et al.*,[194] whereas compounds **3.134r** and **3.133r** have been described by Doddi *et al.*[195]

*3.5.2. General procedure for alkynyl sulfone synthesis via method **A**.*

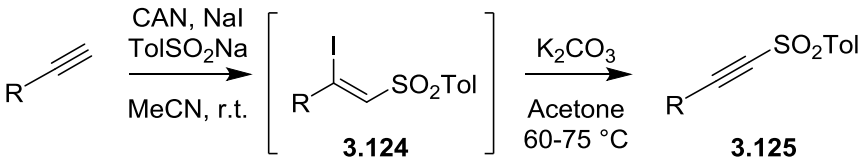

Ceric ammonium nitrate (2.5 equiv) was added portion-wise to a mixture of the corresponding acetylene (1 equiv), sodium *p*-toluenesulfinate (1.2 equiv) and NaI (1.2 equiv) in MeCN (0.08 M) under a nitrogen atmosphere. After the completion of the reaction (1-3h approx.), water was added and the reaction mixture was extracted with DCM. The organic layer was separated, washed with brine, dried over anhydrous Na_2SO_4, filtered and concentrated to dryness. The residue was then redissolved in anhydrous acetone (0.1 M) and heated at 60-75 °C with K_2CO_3 (3 equiv) for 16 h. After the completion of the reaction, water was added and the reaction mixture was extracted once again with DCM. The combined organic extracts were washed with brine and dried over anhydrous Na_2SO_4. The solvent was removed *in vacuo* using a rotary evaporator and the residue was purified by column chromatography to afford the desired product. Compounds **3.125d** and **3.125f** have been previously described by Nair *et al.*[171]; compounds **3.125a** and **3.125e** by Zhu, Jiang *et al.*[196]; compounds **3.125b**, **3.125i-j**, and **3.125n** by Kuhakarn *et al*.[197]; compound **3.125c** and **3.125o** by Wei, Wang *et al.*[198]; and compounds **3.125h**, **3.125l** and **3.125v** by Schwarz and König.[199]

[194] A. Pelter, R. S. Ward and G. M. Little, *J. Chem. Soc. Perkin Trans. 1*, 1990, 2775-2790.
[195] A. K. Morri, Y. Thummala and V. R. Doddi, *Org. Lett.*, 2015, **17**, 4640-4643.
[196] P. Chen, C. H. Zhu, R. Zhu, W. Wu and H. Jiang, *Chem. Asian. J.* 2017, **12**, 1875–1878.
[197] J. Meesin, P. Katrun, C. Pareseecharoen, M. Pohmakotre, V. Reutrakul, D. Soorukram and C. Kuhakarn, *J. Org. Chem.,* 2016, **81**, 2744-2752.
[198] L. Wang, W. Wei, D. Yang, H. Cui, H. Yue and H. Wang, *Tetrahedron Lett.*, 2017, **58**, 4799-4802.
[199] J. Schwarz and B. König, *ChemPhotoChem*, 2017, **1**, 237-242.

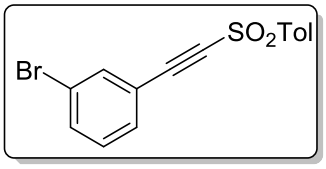

1-Bromo-3-(tosylethynyl)benzene, 3.125k

Flash chromatography of the crude reaction product [*n*-hexane-EtOAc (10:1)] afforded **3.125k** as a white solid (44%, 340 mg), with a melting point of 130–132 °C.

^{1}H NMR ($CDCl_3$, 300 MHz): δ 2.50 (s, 3H), 7.26 (dd, *J*= 9.9, 6.0 Hz, 1H), 7.42 (d, *J*= 9.0 Hz, 2H), 7.45–7.49 (m, 1H), 7.59–7.63 (m, 1H), 7.67 (dd, *J*= 3.0, 3.0 Hz, 1H), 7.97 (d, *J*= 9.0 Hz, 2H) ppm.

^{13}C NMR (CDCl3, 75.5 MHz): δ 21.8 (CH_3), 86.5 (C), 90.6 (C), 120.0 (C), 122.4 (C), 127.6 (CH), 130.0 (CH), 130.1 (CH), 131.2 (CH), 134.5 (CH), 135.2 (CH), 138.6 (C), 145.6 (C) ppm.

HRMS (EI) calcd. for $C_{15}H_{12}BrO_2S$ [M+H$^+$]: 334.9736, found: 334.9728.

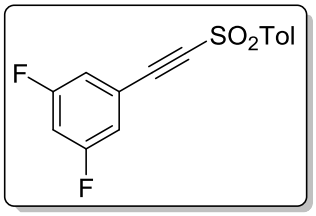

1,3-Difluoro-5-(tosylethynyl)benzene, 3.125m

Flash chromatography of the crude reaction product [*n*-hexane-EtOAc (10:1)] afforded **3.125m** as a white solid (67%, 150 mg), with a melting point of 105–107 °C.

^{1}H NMR ($CDCl_3$, 300 MHz): δ 2.50 (s, 3H), 6.93–6.99 (m, 1H), 7.04-7.08 (m, 2H), 7.43 (dd, *J*= 9.0, 0.6 Hz, 2H), 7.96 (d, *J*= 9.0 Hz, 2H) ppm.

^{13}C NMR ($CDCl_3$, 75.5 MHz): δ 21.8 (CH_3), 86.9 (C), 89.2 (C), 107.8 (dd, *J*= 25.0, 25.0 Hz, CH), 115.7 (dd, *J*= 28.0, 9.0 Hz, CH), 120.0 (dd, *J*= 120, 12.0 Hz, C), 127.7 (CH), 130.1 (CH), 138.3 (C), 145.9 (C), 162.1 (d, *J*= 252.2 Hz, CF), 163.7 (d, *J*= 252.2 Hz, CF) ppm.

^{19}F NMR ($CDCl_3$, 282.4 MHz): δ −107.3-(-107.4) (m, 2F) ppm.

HRMS (EI) calcd. for $C_{15}H_{11}F_2O_2S$ [M+H$^+$]: 293.0442, found: 293.0434.

3.5.3. General procedure for alkynyl sulfone synthesis via method **B**.

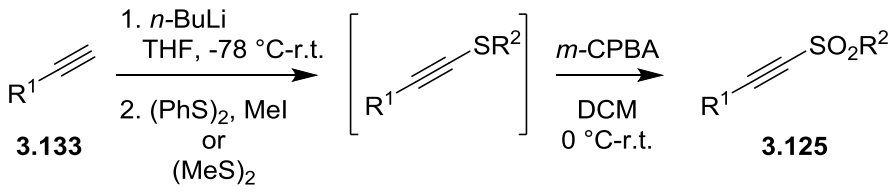

The terminal alkyne starting material (1 equiv) was dissolved in THF (0.1 M) and cooled to -78 °C, and *n*-BuLi (2.5 M in hexanes, 1.1 equiv) was added slowly. The resulting mixture was stirred at this temperature for an hour, and then removed from the acetone/dry ice bath and stirred for a further 30 minutes whilst slowly warming to room temperature. Phenyl or methyl disulfide (1.2 equiv) and iodomethane (1.2 equiv, unnecessary when using methyl disulphide) were then added, and the mixture was stirred for 6h at room temperature. After this time, a saturated aqueous NH_4Cl solution was added to quench the reaction, and the resulting biphasic mixture was extracted with diethyl ether. The combined organic layers were dried over anhydrous Na_2SO_4, concentrated *in vacuo*, and the resulting residue was submitted to high vacuum to remove the phenyl methyl sulphide side-product. The crude mixture was dissolved in DCM (0.1 M) and cooled to 0 °C. *m*-CPBA (3 equiv) was then added portion-wise, ensuring that the reaction mixture didn't heat up excessively—if this is uncontrolled and the *m*-CPBA is added at room temperature or higher a vigorous reaction can take place by which the reaction mixture can overflow. The resulting mixture was stirred at 0 °C for one hour and then a further 12h at room temperature. After this time, a saturated aqueous solution of sodium bisulphite was added, along with further water. The organic phase was washed successively with further sodium bisulphite solution, saturated aqueous sodium bicarbonate solution, and brine. The resulting organic layer was dried over anhydrous Na_2SO_4, concentrated *in vacuo* and purified by flash column chromatography. Compound **3.125g** has been previously described by Nair *et al.*,[171] compounds **3.125p** and **3.125q** have been described by Pelter, Ward *et al.*[194] and compound **3.125u** by Hammond, Bo *et al*.[105]

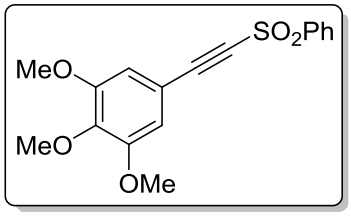

1,2,3-Trimethoxy-5-((phenylsulfonyl)ethynyl)benzene, 3.125r

Flash chromatography of the crude reaction product [*n*-hexane-EtOAc (5:1)] afforded **3.125r** as a white solid (61%, 566 mg), with a melting point of 114-116 °C.

^{1}H NMR ($CDCl_3$, 300 MHz): δ 3.85 (s, 6H), 3.88 (s, 3H), 6.78 (s, 2H), 7.57-7.65 (m, 2H), 7.69-7.74 (m, 1H), 8.06-8.17 (m, 2H) ppm.

^{13}C NMR ($CDCl_3$, 75.5 MHz): δ 56.3 (CH_3), 61.0 (CH_3), 84.5 (C), 94.0 (C), 110.1 (CH), 112.3 (C), 127.4 (CH), 129.4 (CH), 134.1 (CH), 141.7 (C), 141.8 (C), 153.2 (C) ppm.

HRMS (EI) calcd. for $C_{17}H_{20}NO_5S$ [M+NH_4^+]: 350.1057, found: 350.1057.

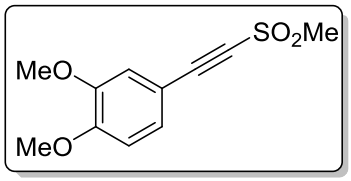

1,2-Dimethoxy-4-((methylsulfonyl)ethynyl)benzene, 3.125s

Flash chromatography of the crude reaction product [*n*-hexane-EtOAc (3:1)] afforded **3.125s** as a white solid (46%, 35 mg), with a melting point of 105–107 °C.

^{1}H NMR ($CDCl_3$, 300 MHz): δ 3.28 (s, 3H), 3.87 (s, 3H), 3.90 (s, 3H), 6.85 (d, *J*=8.4 Hz, 1H), 7.03 (d, *J*=1.9 Hz, 1H), 7.22 (dd, *J*=8.3, 1.9 Hz, 1H) ppm.

^{13}C NMR ($CDCl_3$, 75.5 MHz): δ 46.9 (CH_3), 56.1 ($2CH_3$), 83.5 (C), 92.7 (C), 109.1 (C), 111.2 (CH), 114.8 (CH), 127.3 (CH), 148.9 (C), 152.3 (C) ppm.

HRMS (EI) calcd. for $C_{11}H_{16}NO_4S$ [M+NH_4^+]: 258.0795, found: 258.0794.

3.5.4. Synthesis of terminal alkynyl sulfone **3.125t.**

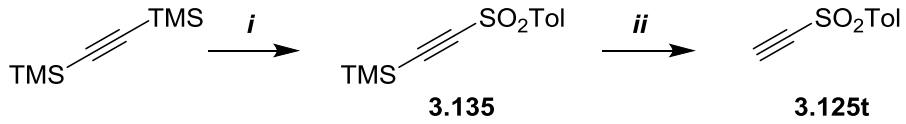

3.135 **3.125t**

i. Aluminium chloride-mediated tosylation. Tosyl chloride (2.52 g, 13.2 mmol) and aluminium chloride (1.77 g, 13.2 mmol) were dissolved in anhydrous DCM (50 ml) and stirred for 30 minutes at room temperature. The mixture was then cooled to 0 °C, and bis(trimethylsilyl)acetylene (1.88 g, 11.0 mmol) was added slowly as a solution in anhydrous DCM (50 ml), and the reaction was allowed to stir for 30 minutes at 0 °C, and then for a further 14h at room temperature. After this time, the reaction mixture was once again cooled to 0 °C, and HCl (3M in water) was added slowly to quench the reaction. If the addition is fast or at room temperature, a violent reaction can take place by which the reaction mixture can overflow. Following this, the mixture was transferred to a separatory funnel and the organic layer was washed successively with water (20 ml), aqueous sodium bicarbonate (20 ml), and brine (20 ml). The resulting organic layer was then dried over anhydrous Na_2SO_4, concentrated *in vacuo*, and recrystallised from hot hexanes to afford **3.135** (42%, 1.17 g). No further purification was necessary.

ii. Elimination of the TMS protecting group. Previously synthesised **3.135** (80 mg, 0.32 mmol) was dissolved in methanol (3 ml) and cooled to 0 °C. The resulting solution was stirred and maintained at 0 °C during the dropwise addition of an aqueous solution of sodium fluoride (0.1M) (4.8 ml, 0.48 mmol). The reaction mixture was stirred for 90 minutes at the same temperature and subsequently diluted with water. The mixture was extracted with Et_2O (3 x 15 ml), washed with water (2 x 15 ml), saturated $NaHCO_3$ (2 x 15 ml), and brine (2 x 15 ml), dried over anhydrous Na_2SO_4 and concentrated to dryness. The crude product was recrystallised from hot hexanes to afford the pure product as colourless crystals (82%, 47 mg). All spectroscopic data was concordant with that described in the literature.[177]

3.5.5. General procedure for the synthesis of (Z)-β-fluorovinyl sulfones.

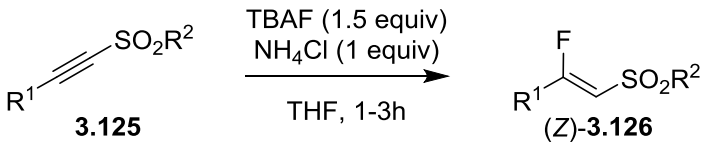

TBAF (1 M in THF) (1.5 equiv) was added to a solution of the corresponding alkynyl sulfone (1 equiv) and NH_4Cl (1 equiv) in THF (0.1 M) under a nitrogen atmosphere at room temperature. After completion of the reaction (TLC analysis, typically 1-3h), the reaction mixture was quenched with aqueous NH_4Cl (sat.) and extracted with ethyl acetate. The organic layer was separated and dried over anhydrous Na_2SO_4. The solvent was removed *in vacuo* and the residue was purified by flash chromatography using mixtures of hexane and ethyl acetate as the eluent. Compound **3.126a** has been previously described by Hammond, Bo *et al.*[105] Ethyl (Z)-3-fluoro-3-phenylacrylate (**3.132**) has been described previously by Qing *et al.*[200]

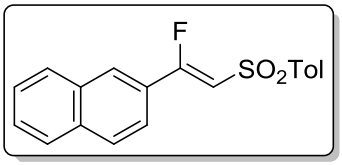

(*Z*)-**2-(1-Fluoro-2-tosylvinyl)naphthalene,** (*Z*)-**3.126b**

Flash chromatography of the crude reaction product [*n*-hexane-EtOAc (10:1)] afforded (*Z*)-**3.126b** as a white solid (69%, 28 mg), with a melting point of 130–132 °C.

^{1}H NMR ($CDCl_3$, 300 MHz): δ 2.46 (s, 3H), 6.69 (d, *J*= 33.0 Hz, 1H), 7.39 (d, *J*= 9.0 Hz, 2H), 7.52 (d, *J*= 9.0 Hz, 1H), 7.57–7.62 (m, 2H), 7.84–7.89 (m, 3H), 8.00 (d, *J*= 9.0 Hz, 2H), 8.12 (s, 1H) ppm.

^{13}C NMR ($CDCl_3$, 75.5 MHz): δ 21.7 (CH_3), 110.0 (d, *J*= 12.8 Hz, CH), 121.5 (d, *J*= 7.6 Hz, CH), 125.8 (d, *J*= 25.7 Hz, C), 127.1 (d, *J*= 7.6 Hz, CH), 127.3 (CH), 127.7 (CH), 127.8 (CH), 128.5 (CH), 129.0 (CH), 129.8 (CH), 132.5 (C), 134.8 (C), 139.3 (C), 144.6 (C), 164.0 (d, *J*= 273.3 Hz, CF) ppm.

^{19}F NMR ($CDCl_3$, 282.4 MHz): δ −93.9 (d, *J*= 31.0, 1F) ppm.

HRMS (EI) calcd. for $C_{19}H_{16}FO_2S$ [M+H$^+$]: 327.0850, found: 327.0852.

[200] S. Peng, F. -L. Qing, Y. -Q. Li and C. -M. Hu, *J. Org. Chem.*, 2000, **65**, 694–700.

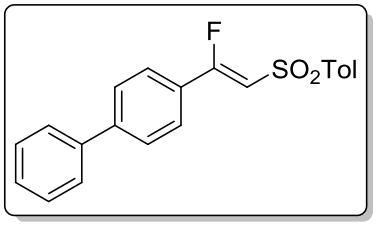

(*Z*)-**4-(1-Fluoro-2-tosylvinyl)-1,1'-biphenyl,** (*Z*)-**3.126c**

Flash chromatography of the crude reaction product [*n*-hexane-EtOAc (10:1)] afforded (*Z*)-**3.126c** as a white solid (72%, 27 mg), with a melting point of 196–198 °C.

^{1}H NMR ($CDCl_3$, 300 MHz) δ 2.47 (s, 3H), 6.60 (d, *J*= 33.0 Hz, 1H), 7.37–7.50 (m, 5H), 7.59-7.65 (m, 6H), 7.98 (d, *J*= 9.0 Hz, 2H) ppm.

^{13}C NMR ($CDCl_3$, 75.5 MHz) δ 21.7 (CH_3), 109.5 (d, *J*= 13.6 Hz, CH), 126.4 (d, *J*= 8.3, 2CH), 127.1 (CH), 127.2 (C), 127.7 (CH), 128.4 (CH), 129.0 (CH), 129.8 (CH), 139.3 (d, *J*= 8.3 Hz, C), 144.6 (C), 145.2 (C), 163.3 (d, *J*= 273.3 Hz, CF) ppm.

^{19}F NMR ($CDCl_3$, 282.4 MHz): δ −93.8 (d, *J*= 32.0 Hz, 1F) ppm.

HRMS (EI) calcd. for $C_{21}H_{18}FO_2S$ [M+H$^+$]: 353.1006, found: 353.1003.

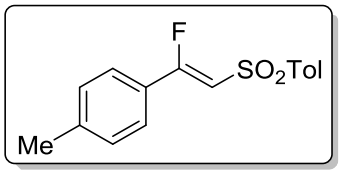

(*Z*)-**1-((2-Fluoro-2-(4-tolyl)vinyl)sulfonyl)-4-methylbenzene,** (*Z*)-**3.126d**

Flash chromatography of the crude reaction product [n-hexane-EtOAc (10:1)] afforded (*Z*)-**3.126d** as a white solid (67%, 28 mg), with a melting point of 100–102 °C.

^{1}H NMR ($CDCl_3$, 300 MHz): δ 2.39 (s, 3H), 2.46 (s, 3H), 6.52 (d, *J*= 33.0 Hz, 1H), 7.23 (d, *J*= 9.0 Hz, 2H), 7.37 (d, *J*= 9.0 Hz, 2H), 7.46 (d, *J*= 9.0 Hz, 2H), 7.95 (d, *J*= 9.0 Hz, 2H) ppm.

^{13}C NMR ($CDCl_3$, 75.5 MHz): δ 21.5 (CH_3), 21.6 (CH_3), 108.7 (d, *J*= 13.6 Hz, CH), 125.8 (CH), 125.9 (CH), 126.1 (C), 127.6 (CH), 129.7 (CH), 139.4 (C), 143.2 (C), 144.4 (C), 164.5 (d, *J*= 274.0 Hz, CF) ppm.

^{19}F NMR ($CDCl_3$, 282.4 MHz): δ −93.4 (d, *J*= 31.0 Hz, 1F) ppm.

HRMS (EI) calcd. for $C_{16}H_{16}FO_2S$ [M+H$^+$]: 291.0850, found: 291.0858.

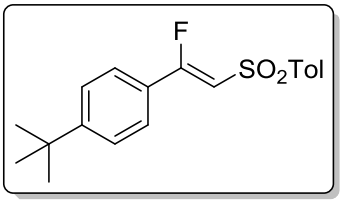

(*Z*)-**1-(*tert*-Butyl)-4-(1-fluoro-2-tosylvinyl)benzene,** (*Z*)-**3.126e**

Flash chromatography of the crude reaction product [*n*-hexane-EtOAc (15:1)] afforded (*Z*)-**3.126e** as a white solid (67%, 28 mg), with a melting point of 122-124 °C.

^{1}H NMR ($CDCl_3$, 300 MHz): δ 1.32 (s, 9H), 2.46 (s, 3H), 6.52 (d, *J*= 33 Hz, 1H), 7.37 (d, *J*= 9.0 Hz, 2H), 7.44 (d, *J*= 9.0 Hz, 2H), 7.51 (d, *J*= 9.0 Hz, 2H), 7.95 (d, *J*= 9.0 Hz, 2H) ppm.

^{13}C NMR ($CDCl_3$, 75.5 MHz): δ 21.6 (CH_3), 30.9 (CH_3), 35.1 (C), 108.8 (d, *J*= 13.6 Hz, CH), 125.8 (d, *J*= 7.5 Hz, CH), 126.0 (d *J*= 2.3 Hz, CH), 127.6 (CH), 129.7 (CH), 139.4 (C), 144.4 (C), 156.3 (C), 164.2 (d, *J*= 273.3 Hz, CF) ppm.

^{19}F NMR ($CDCl_3$, 282.4 MHz): δ -93.4 (d, *J*= 31.1 Hz, 1F) ppm.

HRMS (EI) calcd. for $C_{19}H_{22}FO_2S$ [M+H$^+$]: 333.1319, found: 333.1327.

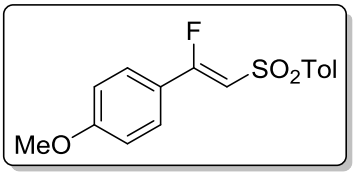

(*Z*)-**1-[(2-Fluoro-2-(4-methoxyphenyl)vinyl)sulfonyl)]-4-methylbenzene,** (*Z*)-**3.126f**

Flash chromatography of the crude reaction product [*n*-hexane-EtOAc (5:1)] afforded (*Z*)-**3.126f** as a white solid (71%, 45 mg), with a melting point of 74-75 °C.

^{1}H NMR ($CDCl_3$, 300 MHz):δ 2.45 (s, 3H), 3.84 (s, 3H), 6.43 (d, *J*= 32.8 Hz, 1H), 6.92 (d, *J*= 9.1 Hz, 1H), 7.36 (d, *J*= 9.0 Hz, 1H), 7.51 (d, *J*= 9.0 Hz, 1H), 7.94 (d, *J*= 9.0 Hz, 1H) ppm.

^{13}C NMR ($CDCl_3$, 75.5 MHz):δ 21.6 (CH_3), 55.2 (CH_3), 107.4 (d, *J*= 13.4 Hz, CH), 114.5 (CH), 120.9 (d, *J*= 25.6 Hz, C), 127.5 (CH), 127.8 (d, *J*= 8.2 Hz, CH), 129.7 (CH), 139.5 (C), 144.3 (C), 162.9 (C), 164.2 (d, *J*= 272.2 Hz, CF) ppm.

^{19}F NMR ($CDCl_3$, 282.4 MHz): δ -93.3 (d, *J*= 33.9 Hz, 1F) ppm.

HRMS (EI) calcd. for $C_{16}H_{16}O_3S$ [M+H$^+$]: 307.0799, found: 307.0800.

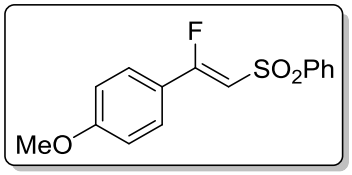

(*Z*)-**1-(1-Fluoro-2-(phenylsulfonyl)vinyl)-4-methoxybenzene,** (*Z*)-**3.126g**

Flash chromatography of the crude reaction product [*n*-hexane-EtOAc (10:1)] afforded (*Z*)-**3.126g** as a white solid (72%, 40 mg), with a melting point of 78-80 °C.

^{1}H NMR ($CDCl_3$, 300 MHz): δ 3.86 (s, 3H), 6.45 (d, *J*= 33.0 Hz, 1H), 6.93 (d, *J*= 9.0 Hz, 2H), 7.51-7.65 (m, 5H), 8.07 (d, *J*= 9.0 Hz, 2H) ppm.

^{13}C NMR ($CDCl_3$, 75.5 MHz): δ 55.5 (CH_3), 107.1 (d, *J*= 13.6 Hz, CH), 114.5 (CH), 120.8 (d, *J*= 25.6 Hz, C), 127.5 (CH), 127.9 (*J*= 8.3 Hz, 2CH), 129.1 (CH), 133.3 (CH), 142.4 (C), 163.0 (C), 164.5 (d, *J*= 273.0 Hz, C) ppm.

^{19}F NMR ($CDCl_3$, 282.4 MHz): δ -92.7 (d, *J*= 33.0 Hz, 1F) ppm.

HRMS (EI) calcd. for $C_{15}H_{13}FO_3S$ [M+H$^+$]: 293.0642, found: 293.0642.

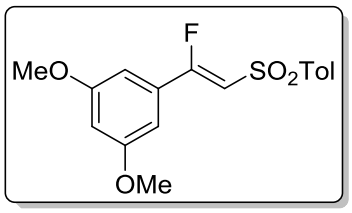

(*Z*)-**1-(1-Fluoro-2-tosylvinyl)-3,5-dimethoxybenzene,** (*Z*)-**3.126i**

Flash chromatography of the crude reaction product [*n*-hexane-EtOAc (10:1)] afforded (*Z*)-**3.126i** as a white solid (70%, 30 mg), with a melting point of 158-160 °C.

^{1}H NMR ($CDCl_3$, 300 MHz): δ 2.47 (s, 3H), 3.80 (s, 6H), 6.53 (d, *J*= 33.0 Hz, 1H), 6.57-6.59 (m, 1H), 6.67 (d, *J*= 3.0 Hz, 2H), 7.38 (d, *J*= 9.0 Hz, 2H), 7.94 (d, *J*= 9.0 Hz, 2H) ppm.

^{13}C NMR ($CDCl_3$, 75.5 MHz):δ 21.7 (CH_3), 55.6 (CH_3), 103.9 (CH), 104.3 (d, *J*= 52.1 Hz, CH), 110.2 (d, *J*= 13.6 Hz, CH), 127.7 (2CH), 129.8 (2CH), 130.5 (d, *J*= 26.4 Hz, C), 139.1 (C), 144.6 (C), 161.1 (C), 163.7 (d, *J*= 274.0 Hz, CF) ppm.

^{19}F NMR ($CDCl_3$, 282.4 MHz): δ -92.3 (d, *J*= 31.0 Hz, 1F) ppm.

HRMS (EI) calcd. for $C_{17}H_{18}FO_4S$ [M+H$^+$]: 337.0904, found: 337.0895.

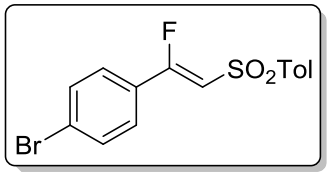

(*Z*)-**1-Bromo-4-(1-fluoro-2-tosylvinyl)benzene,** (*Z*)-**3.126j**

Flash chromatography of the crude reaction product [*n*-hexane-EtOAc (10:1)] afforded (*Z*)-**3.126j** as a white solid (63%, 22 mg), with a melting point of 145-147 °C.

^{1}H NMR ($CDCl_3$, 300 MHz): δ 2.47 (s, 3H), 6.56 (d, *J*= 33.0 Hz, 1H), 7.38 (d, *J*= 9.0 Hz, 2H), 7.42 (d, *J*= 9.0 Hz, 2H), 7.58 (d, *J*= 9.0 Hz, 2H), 7.95 (d, *J*= 9.0 Hz, 2H) ppm.

^{13}C NMR ($CDCl_3$, 75.5 MHz): δ 21.7 (CH_3), 110.3 (d, *J*= 13.6 Hz, CH), 127.2 (CH), 127.3 (CH), 127.6 (d, *J*= 26.7 Hz, C), 127.7 (CH), 129.9 (CH), 132.3 (C), 144.8 (C), 163.5 (d, *J*= 273.3 Hz, CF) ppm.

^{19}F NMR ($CDCl_3$, 282.4 MHz): δ -94.2 (d, *J*= 31.0 Hz, 1F) ppm.

HRMS (EI) calcd. for $C_{15}H_{13}BrFO_2S$ [M+H$^+$]: 354.9798, found: 354.9806.

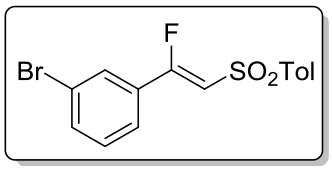

(*Z*)-**1-Bromo-3-(1-fluoro-2-tosylvinyl)benzene,** (*Z*)-**3.126k**

Flash chromatography of the crude reaction product [*n*-hexane-EtOAc (10:1)] afforded (*Z*)-**3.126k** as a white solid (60%, 20 mg), with a melting point of 81-83 °C.

^{1}H NMR ($CDCl_3$, 300 MHz): δ 2.47 (s, 3H), 6.57 (d, *J*= 30.0 Hz, 1H), 7.33 (d, *J*= 9.0 Hz, 1H), 7.38 (d, *J*= 6.0 Hz, 2H), 7.50 (d, *J*= 9.0 Hz, 1H), 7.61-7.64 (m, 1H), 7.69-7.70 (m, 1H), 7.95 (d, *J*= 9.0 Hz, 2H) ppm.

^{13}C NMR ($CDCl_3$, 75.5 MHz): δ 21.7 (CH_3), 111.2 (d, *J*= 13.6 Hz, CH), 123.1 (C), 124.4 (d, *J*= 7.5 Hz, CH), 127.7 (CH), 128.8 (d *J*= 8.3 Hz, CH), 129.9 (CH), 130.5 (CH), 135.2 (CH), 138.8 (C), 144.8 (C), 162.0 (d, *J*= 274.0 Hz, CF) ppm.

^{19}F NMR ($CDCl_3$, 282.4 MHz): δ -94.1 (d, *J*= 31.1 Hz, 1F) ppm.

HRMS (EI) calcd. for $C_{15}H_{13}BrFO_2S$ [M+H$^+$]: 354.9798, found: 354.9793.

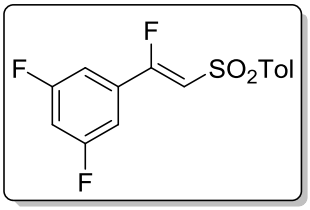

(*Z*)-**1,3-Difluoro-5-(1-fluoro-2-tosylvinyl)benzene,** (*Z*)-**3.126m**

Flash chromatography of the crude reaction product [*n*-hexane-EtOAc (10:1)] afforded (*Z*)-**3.126m** as a white solid (30%, 21 mg), with a melting point of 158-160 °C.

^{1}H NMR ($CDCl_3$, 300 MHz): δ 2.48 (s, 3H), 6.57 (d, *J*= 30.0 Hz, 1H), 6.92-7.00 (m, 1H), 7.08-7.11 (m, 2H), 7.40 (d, *J*= 9.0 Hz, 2H), 7.95 (d, *J*= 9.0 Hz, 2H) ppm.

^{13}C NMR ($CDCl_3$, 75.5 MHz): δ 21.7 (CH_3), 107.7 (dd, *J*= 24.8, 24.9 Hz, CH), 109.0 (dd, *J*= 27.1, 27.2 Hz, CH), 112.1 (d, *J*= 12.8 Hz, CH), 127.8 (CH), 129.9 (CH), 131.9 (d, *J*= 28.7 Hz, C), 138.5 (C), 145.1 (C), 161.1 (d, *J*= 274.0 Hz, CF), 163.0 (d, *J*= 251.4 Hz, CF), 163.2 (d, *J*= 251.5 Hz, CF) ppm.

^{19}F NMR ($CDCl_3$, 282.4 MHz): δ -106.7 (s, 2F), -94.2 (d, *J*= 31.0 Hz, 1F) ppm.

HRMS (EI) calcd. for $C_{15}H_{12}F_3O_2S$ [M+H^+]: 313.0505, found: 313.0506.

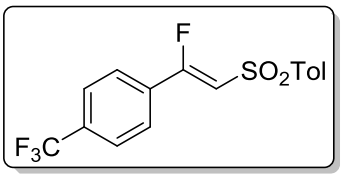

(*Z*)-**1-((2-Fluoro-2-(4-(trifluoromethyl)phenyl)vinyl)sulfonyl)-4-methylbenzene,** (*Z*)-**3.126n**

Flash chromatography of the crude reaction product [*n*-hexane-EtOAc (5:1)] afforded (*Z*)-**3.126n** as a white solid (28%, 20 mg), with a melting point of 129-131 °C.

^{1}H NMR ($CDCl_3$, 300 MHz): δ 2.45 (s, 3H), 6.64 (d, *J*= 32.0 Hz, 1H), 7.37 (dd, *J*= 8.6, 0.7 Hz, 1H), 7.68 (s, 2H), 7.94 (d, *J*= 8.0 Hz, 1H) ppm.

^{13}C NMR ($CDCl_3$, 75.5 MHz): δ 21.6 (CH_3), 111.9 (d, *J*= 13.1 Hz, C), 111.9 (d, *J*= 13.1 Hz, C), 125.9 (q, *J*= 2.4 Hz, CH), 126.2 (d, *J*= 7.6 Hz, CH), 127.8 (CH), 129.9 (CH), 132.2 (d, *J*= 27.4 Hz, C), 133.8 (d, *J*= 33.1 Hz, C), 138.6 (C), 144.9 (C), 162.1 (d, *J*= 274.0 Hz, C) ppm.

^{19}F NMR ($CDCl_3$, 282.4 MHz): δ -94.84 (d, *J* = 31.9 Hz, CF), -63.71 (s, CF_3) ppm.

HRMS (EI) calcd. for $C_{16}H_{16}F_4NO_2S$ [M+NH_4^+]: 362.0832, found: 362.0825.

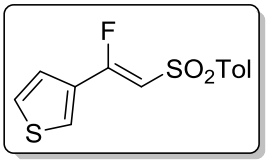

(*Z*)-**3-(1-Fluoro-2-tosylvinyl)thiophene,** (*Z*)-**3.126o**

Flash chromatography of the crude reaction product [*n*-hexane-EtOAc (5:1)] afforded (*Z*)-**3.126o** as a white solid (70%, 65 mg), with a melting point of 121-123 °C.

^{1}H NMR ($CDCl_3$, 300 MHz): δ 2.46 (s, 3H), 6.39 (d, *J*= 33.2 Hz, 1H), 7.15 (d, *J*= 6.0 Hz, 1H), 7.35-7.38 (m, 3H), 7.74 (d, *J*= 3.0 Hz, 1H), 7.94 (d, *J*= 9.0 Hz, 1H) ppm.

^{13}C NMR ($CDCl_3$, 75.5 MHz): δ 21.6 (CH_3), 109.0 (d, *J*= 12.5 Hz, CH), 124.4 (d, *J*= 7.5 Hz, CH), 127.6 (CH), 128.0 (CH), 128.2 (d, *J*= 6.0 Hz, CH), 129.8 (2CH), 131.0 (d, *J*= 27.9 Hz, C), 139.3 (C), 144.5 (C), 160.0 (d, *J*= 270.9 Hz, CF) ppm.

^{19}F NMR ($CDCl_3$, 282.4 MHz): δ -92.7 (d, *J*= 32.1 Hz, 1F) ppm.

HRMS (EI) calcd. for $C_{13}H_{12}FO_2S_2$ [M+H$^+$]: 283.0257, found: 283.0254.

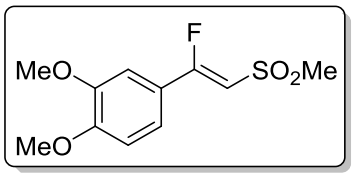

(*Z*)-**4-(1-Fluoro-2-(methylsulfonyl)vinyl)-1,2-dimethoxybenzene,** (*Z*)-**3.126s**

Flash chromatography of the crude reaction product [*n*-hexane-EtOAc (1:1)] afforded (*Z*)-**3.126s** as a white solid (86%, 21 mg), with a melting point of 110-112 °C.

^{1}H NMR ($CDCl_3$, 300 MHz): δ 3.19 (s, 3H), 3.92 (s, 3H), 3.94 (s, 3H), 6.35 (d, *J*= 33.6 Hz, 1H), 6.92 (d, *J*= 8.6 Hz, 1H), 7.04 (d, *J*= 1.8 Hz, 1H), 7.27 (dd, *J*= 8.5, 1.7 Hz, 1H) ppm.

^{13}C NMR ($CDCl_3$, 75.5 MHz): δ 44.7 (CH_3), 56.1 (CH_3), 56.2 (CH_3), 106.7 (d, *J*= 13.8 Hz, CH), 108.2 (d, *J*= 8.9 Hz, CH), 111.1 (CH), 120.1 (d, *J*= 10.4 Hz, CH), 120.6 (d, *J*= 27.8 Hz, C), 149.3 (C), 152.9 (C), 165.1 (d, *J*= 269.4 Hz, C) ppm.

^{19}F NMR ($CDCl_3$, 282.4 MHz): δ −92.8 (d, *J*= 33.8 Hz, 1F) ppm.

HRMS (EI) calcd. for $C_{11}H_{14}FO_4S$ [M+H$^+$]: 261.0591, found: 289.0589.

3.5.6. General procedure for the synthesis of (E)-β-fluorovinyl sulfones.

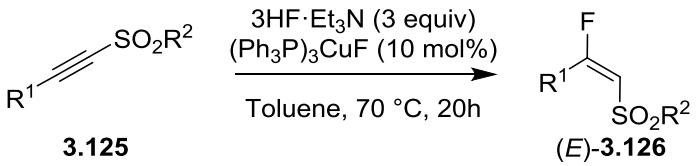

3.125 (*E*)-**3.126**

A screw-top eppendorf tube was charged with alkynyl sulfone (1 equiv) and $(Ph_3P)_3CuF$ (10 mol%), and purged with nitrogen. Toluene (0.05 M) was then added, followed by $3HF{\cdot}Et_3N$ (3 equiv), and the resulting mixture was heated at 70 °C for 20h in an oil bath. When the reaction was complete, the crude mixture was concentrated and purified by flash column chromatography using mixtures of hexane and ethyl acetate as the eluent (assuming the reaction was complete; if not, mixtures of hexane and DCM (1:1) had to be used in order to separate the product from the alkynyl sulfone starting material).

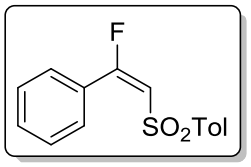

(*E*)-**1-((2-Fluoro-2-phenylvinyl)sulfonyl)-4-methylbenzene,** (*E*)-**3.126a**

Flash chromatography of the crude reaction product [*n*-hexane:EtOAc (4:1)] afforded (*E*)-**3.126a** as a colourless oil (35%, 65 mg).

^{1}H NMR ($CDCl_3$, 300 MHz): δ 2.32 (s, 3H), 6.38 (d, *J*= 18.4 Hz, 1H), 7.13-7.21 (m, 2H), 7.32-7.39 (m, 2H), 7.42-7.47 (m, 1H) ppm.

^{13}C NMR ($CDCl_3$, 75.5 MHz): 22.0 (CH_3), 114.9 (d, *J*= 31.8 Hz, C), 127.8 (CH), 128.2 (d, *J*= 16.3 Hz, C), 128.5 (CH), 130.0 (d, *J*= 5.0 Hz, CH), 130.1 (CH), 132.4 (d, *J*= 2.2 Hz, CH), 138.9 (d, *J*= 2.9 Hz, C), 144.9 (C), 168.0 (d, *J*= 276.4 Hz, C) ppm.

^{19}F NMR ($CDCl_3$, 282.4 MHz): δ -72.19 (d, *J*= 18.4 Hz, 1F) ppm.

HRMS (EI) calcd. for $C_{15}H_{14}FO_2S$ [$M+H^+$]: 277.0693, found: 277.0698.

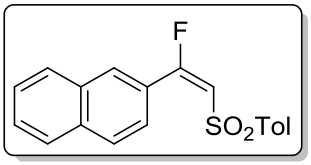

(*E*)-**2-(1-Fluoro-2-tosylvinyl)naphthalene,** (*E*)-**3.126b**

Flash chromatography of the crude reaction product [*n*-hexane:EtOAc (5:1)] afforded (*E*)-**3.126b** as a pale yellow solid (38%, 16 mg) with a melting point of 42-43 °C.

^{1}H NMR ($CDCl_3$, 300 MHz): δ 2.39 (s, 3H), 6.56 (d, *J*= 18.4 Hz, 1H), 7.21 (d, *J*= 8.0 Hz, 2H), 7.52-7.69 (m, 5H), 7.84–7.98 (m, 3H), 8.24 (s, 1H) ppm.

^{13}C NMR ($CDCl_3$, 75.5 MHz): δ 21.5, 114.7 (d, *J*= 32.0 Hz), 124.9 (d, *J*= 3.8 Hz), 125.6 (d, *J*= 25.7 Hz), 126.9, 127.3, 127.4, 127.8 (d, *J*= 8.2 Hz), 128.3, 128.7, 129.1, 129.6, 131.2 (d, *J*= 6.5 Hz), 132.0, 134.7, 138.5, 144.5, 167.7 (d, *J*= 276.6 Hz, CF) ppm.

^{19}F NMR ($CDCl_3$, 282.4 MHz): δ −71.9 (d, *J*= 18.4 Hz, 1F) ppm.

HRMS (EI) calcd. for $C_{19}H_{19}FNO_2S$ [M+NH_4^+]: 344.1115, found: 344.1120.

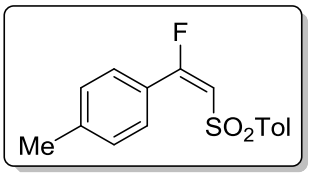

(*E*)-**1-((2-Fluoro-2-(4-tolyl)vinyl)sulfonyl)-4-methylbenzene,** (*E*)-**3.126d**

Flash chromatography of the crude reaction product [*n*-hexane:EtOAc (4:1)] afforded (*E*)-**3.126d** as a colourless oil (43%, 18 mg).

^{1}H NMR ($CDCl_3$, 300 MHz): δ 2.41 (s, 6H), 6.39 (d, *J*= 18.5 Hz, 1H), 7.22-7.29 (m, 4H), 7.57 (d, *J*= 8.0 Hz, 2H), 7.66 (d, *J*= 8.3 Hz, 2H) ppm.

^{13}C NMR ($CDCl_3$, 75.5 MHz): δ 21.6 (CH_3), 21.7 (CH_3), 113.7 (d, *J*= 32.6 Hz, CH), 125.6 (d, *J*= 26.0 Hz, C), 127.3 (CH), 127.9 (CH), 128.8 (CH), 129.1 (CH), 129.5 (CH), 129.6 (d, *J*= 5.6 Hz, CH), 129.7 (CH), 130.0 (CH), 138.7 (d, *J*= 2.7 Hz, C), 142.7 (C), 144.4 (C), 167.8 (d, *J*= 275.7 Hz, CF) ppm.

^{19}F NMR ($CDCl_3$, 282.4 MHz): δ −72.0 (d, *J*= 18.6 Hz, 1F) ppm.

HRMS (EI) calcd. for $C_{16}H_{19}FNO_2S$ [M+NH_4^+]: 308.1115, found: 308.1116.

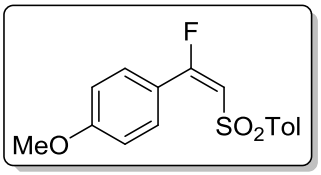

(*E*)-**1-((2-Fluoro-2-(4-methoxyphenyl)vinyl)sulfonyl)-4-methylbenzene,** (*E*)-**3.126f**

Flash chromatography of the crude reaction product [*n*-hexane:EtOAc (3:1)] afforded (*E*)-**3.126f** as a colourless oil (51%, 30 mg).

^{1}H NMR ($CDCl_3$, 300 MHz): δ 2.41 (s, 3H), 3.87 (s, 3H), 6.33 (d, *J*= 18.8 Hz, 1H), 6.94 (dd, *J*= 9.1, 0.9 Hz, 2H), 7.25 (t, *J*= 0.7 Hz, 1H), 7.27 (t, *J*= 0.7 Hz, 1H), 7.65 (s, 2H), 7.68 (s, 2H) ppm.

^{13}C NMR ($CDCl_3$, 75.5 MHz): δ 21.6 (CH_3), 55.4 (CH_3), 112.6 (d, *J*= 33.5 Hz, C), 113.5 (CH), 120.6 (d, *J*= 26.6 Hz, C), 127.3 (CH), 129.7 (CH), 131.5 (d, *J*= 5.6 Hz, CH), 138.8 (d, *J*= 3.1 Hz, C), 144.4 (C), 162.6 (C), 167.4 (d, *J*= 274.4 Hz, C) ppm.

^{19}F NMR ($CDCl_3$, 282.4 MHz): δ -73.15 (d, *J*= 19.8 Hz, 1F) ppm.

HRMS (EI) calcd. for $C_{16}H_{15}FO_3S$ [M+H^+]: 307.0799, found: 307.0803.

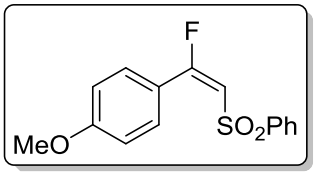

(*E*)-**1-(1-Fluoro-2-(phenylsulfonyl)vinyl)-4-methoxybenzene**, (*E*)-**3.126g**

Flash chromatography of the crude reaction product [*n*-hexane:EtOAc (3:1)] afforded (*E*)-**3.126g** as a colourless oil (56%, 40 mg).

^{1}H NMR ($CDCl_3$, 300 MHz): δ 3.86 (s, 3H), 6.35 (d, *J*= 18.6 Hz, 1H), 6.93 (d, *J*= 8.4 Hz, 2H), 7.38-7.50 (m, 2H), 7.51-7.61 (m, 1H), 7.66 (d, *J*= 8.6 Hz, 2H), 7.78 (dd, *J*= 5.3, 3.3 Hz, 2H) ppm.

^{13}C NMR ($CDCl_3$, 75.5 MHz): δ 55.5 (CH_3), 112.4 (d, *J*= 33.6 Hz, CH), 113.6 (CH), 120.5 (d, *J*= 26.6 Hz, C), 127.2 (CH), 129.1 (CH), 131.5 (d, *J*= 5.6 Hz, CH), 133.4 (CH), 141.7 (d, *J*= 2.5 Hz, C), 162.7 (C), 167.8 (d, *J*= 275.1 Hz, C) ppm.

^{19}F NMR ($CDCl_3$, 282.4 MHz): δ -71.8 (d, *J*= 18.6 Hz, 1F) ppm.

HRMS (EI) calcd. for $C_{15}H_{17}FNO_3S$ [M+NH_4^+]: 310.0908, found: 310.0911.

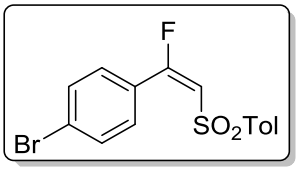

(*E*)-**1-Bromo-4-(1-fluoro-2-tosylvinyl)benzene**, (*E*)-**3.126i**

Flash chromatography of the crude reaction product [*n*-hexane:EtOAc (5:1)] afforded (*E*)-**3.126i** as a colourless oil (27%, 13mg).

^{1}H NMR ($CDCl_3$, 300 MHz): δ 2.42 (s, 3H), 6.45 (d, *J*= 18.5 Hz, 1H), 7.28 (dd, *J*= 8.5, 0.6 Hz, 2H), 7.52-7.66 (m, 6H) ppm.

^{13}C NMR ($CDCl_3$, 75.5 MHz): δ 21.6 (CH_3), 114.9 (d, *J*= 31.3 Hz, CH), 127.0 (C), 127.1 (C), 127.4 (CH), 129.8 (CH), 131.0 (d, *J*= 4.9 Hz, CH), 131.4 (CH), 138.3 (C), 144.8 (C), 166.27 (d, *J*= 275.7 Hz, C) ppm.

^{19}F NMR ($CDCl_3$, 282.4 MHz): δ -73.5 (d, *J*= 18.5 Hz, 1F) ppm.

HRMS (EI) calcd. for $C_{15}H_{16}BrFNO_2S$ [M+NH_4^+]: 372.0064, found: 372.0068.

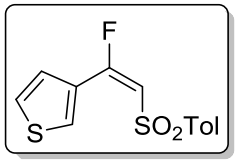

(*E*)-**3-(1-Fluoro-2-tosylvinyl)thiophene,** (*E*)-**3.126o**

Flash chromatography of the crude reaction product [*n*-hexane:EtOAc (4:1)] afforded (*E*)-**3.126o** as a colourless oil (63%, 23 mg).

^{1}H NMR ($CDCl_3$, 300 MHz): δ 2.41 (s, 3H), 6.36 (d, *J*= 20.4 Hz, 1H), 7.29–7,26 (m, 2H), 7.34 (ddd, *J*= 5.2, 3.0, 1.4 Hz, 1H), 7.51 (dd, *J*= 5.2, 1.3 Hz, 1H), 7.71 (d, *J*= 8.3 Hz, 2H), 8.19 (ddd, *J*= 3.0, 1.3, 0.7 Hz, 1H) ppm.

^{13}C NMR ($CDCl_3$, 75.5 MHz): δ 21.6 (CH_3), 112.7 (d, *J*= 33.1 Hz, C), 125.8 (CH), 127.1 (s, CH), 127.5 (d, *J*= 5.0 Hz, CH), 129.8 (CH), 132.3 (d, *J*= 8.3 Hz, C), 138.7 (d, *J*= 2.8 Hz, C), 144.6 (C), 162.4 (d, *J*= 269.0 Hz, C) ppm.

^{19}F NMR ($CDCl_3$, 282.4 MHz): δ -77.8 (dd, *J*= 20.5, 1.3 Hz, 1F) ppm.

HRMS (EI) calcd. for $C_{15}H_{13}FO_2S$ [M+H^+]: 283.0257, found: 283.0257.

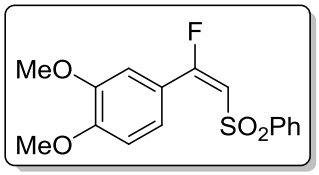

(*E*)-**4-(1-Fluoro-2-(phenylsulfonyl)vinyl)-1,2-dimethoxybenzene,** (*E*)-**3.126p**

Flash chromatography of the crude reaction product [*n*-hexane:EtOAc (2:1)] afforded (*E*)-**3.126p** as a white solid (60%, 24 mg) with a melting point of 51-53 °C.

^{1}H NMR ($CDCl_3$, 300 MHz): δ 3.89 (s, 3H), 3.93 (s, 3H), 6.37 (d, *J*= 18.8 Hz, 1H), 6.89 (d, *J*=8.4 Hz, 1H), 7.25 (d, *J*=2.1 Hz, 1H), 7.34 (ddd, *J*= 8.4, 2.0, 0.6 Hz, 1H), 7.41-7.50 (m, 2H), 7.53-7.61 (m, 1H), 7.75-7.81 (m, 2H) ppm.

^{13}C NMR ($CDCl_3$, 75.5 MHz): δ 56.0 ($2OCH_3$), 110.3 (CH), 112.2 (d, *J*= 5.4 Hz, CH), 112.7 (d, *J*= 33.7 Hz, CH), 120.5 (d, *J*= 26.8 Hz, C), 123.7 (d, *J*= 6.5 Hz, CH), 127.2 (CH), 129.1 (CH), 133.4 (CH), 141.6 (d, *J*= 2.5 Hz, C), 148.4 (C), 152.4 (C), 167.5 (d, *J*= 275.0 Hz, C) ppm.

^{19}F NMR ($CDCl_3$, 282.4 MHz): δ -72.7 (d, *J*= 18.9 Hz, 1F) ppm.

HRMS (EI) calcd. for $C_{16}H_{19}FNO_4S$ [$M+NH_4^+$]: 340.1013, found: 340.1019.

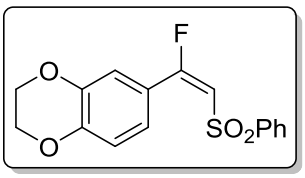

(*E*)-**6-(1-Fluoro-2-(phenylsulfonyl)vinyl)-2,3-dihydrobenzo[b][1,4]dioxine,** (*E*)-**3.126q**

Flash chromatography of the crude reaction product [*n*-hexane:EtOAc (2:1)] afforded (*E*)-**3.126q** as a colourless oil (53%, 19 mg).

^{1}H NMR ($CDCl_3$, 300 MHz): δ 4.31 (dqd, *J*= 7.0, 3.3, 1.5 Hz, 4H), 6.37 (d, *J*= 18.6 Hz, 1H), 6.91 (dd, *J*= 8.4, 0.8 Hz, 1H), 7.19-7.27 (m, 2H), 7.46-7.54 (m, 2H), 7.56-7.63 (m, 1H), 7.80-7.85 (m, 2H) ppm.

^{13}C NMR ($CDCl_3$, 75.5 MHz): δ 64.1 (CH_2), 64.6 (CH_2), 112.8 (d, *J*= 33.5 Hz, CH), 117.1 (CH), 118.8 (d, *J*= 5.5 Hz, CH), 121.2 (d, *J*= 26.6 Hz, C), 123.6 (d, *J*= 5.9 Hz, CH), 127.3 (CH), 129.0 (CH), 133.4 (CH), 141.6 (C), 143.0 (C), 147.1 (C), 167.3 (d, *J*= 275.8 Hz, CF) ppm.

^{19}F NMR ($CDCl_3$, 282.4 MHz): δ -71.8 (d, *J*= 18.6 Hz, 1F) ppm.

HRMS (EI) calcd. for $C_{16}H_{17}FNO_4S$ [$M+NH_4^+$]: 338.0857, found: 338.0866.

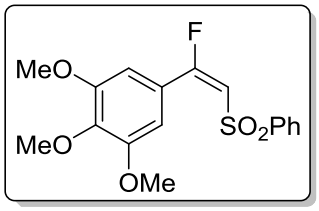

(*E*)-**5-(1-Fluoro-2-(phenylsulfonyl)vinyl)-1,2,3-trimethoxybenzene,** (*E*)-**3.126r**

Flash chromatography of the crude reaction product [*n*-hexane:EtOAc (2:1)] afforded (*E*)-**3.126r** as a colourless oil (58%, 23 mg).

^{1}H NMR ($CDCl_3$, 300 MHz): δ 3.86 (s, 6H), 3.91 (s, 3H), 6.44 (d, *J*= 18.6 Hz, 1H), 7.42-7.49 (m, 2H), 7.52-7.60 (m, 1H), 7.75-7.81 (m, 2H) ppm.

^{13}C NMR ($CDCl_3$, 75.5 MHz): δ 56.3 (CH_3), 61.0 (CH_3), 107.1 (d, *J*= 5.6 Hz, CH), 113.9 (d, *J*= 32.9 Hz, CH), 123.0 (d, *J*= 26.8 Hz, C), 127.2 (CH), 128.7 (d, *J*= 8.2 Hz, CH), 129.0 (CH), 129.9 (CH), 133.4 (CH), 133.8 (d, *J*= 13.9 Hz, CH), 141.4 (C), 152.7 (C), 167.4 (d, *J*= 276.5 Hz, C) ppm.

^{19}F NMR ($CDCl_3$, 282.4 MHz): δ -73.0 (d, *J*= 18.6 Hz, 1F) ppm.

HRMS (EI) calcd. for $C_{17}H_{21}FNO_5S$ [$M+NH_4^+$]: 370.1119, found: 370.1123.

3.5.7. General procedure for the hydrogenation of β-fluorovinyl sulfones.

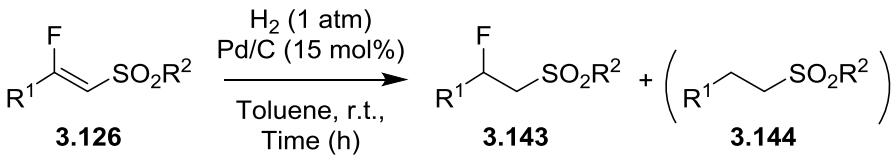

Palladium over activated charcoal (15 mol%) was added to a solution of the corresponding β-fluorovinyl sulfone (1 equiv) in toluene (0.033 M), and the reaction flask was charged with hydrogen gas by purging several times, without stirring. The reaction was then stirred under H_2 (atmospheric pressure) at room temperature for the required time. The mixture was then filtered to remove the catalyst, and the solvent was evaporated *in vacuo*. In most cases, compounds **3.143** contain small amounts of inseparable defluorinated sulfones **3.144**. Compound **3.143a** has been described by Liu *et al*.[201] Both α-fluorovinyl sulfone **3.146** and the hydrogenated **3.147** have been described by Prakash *et al.*[103]

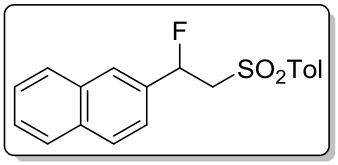

2-(1-Fluoro-2-tosylethyl)naphthalene, 3.143b

Crude reaction product **3.143b** (96%, 20 mg) was obtained as a viscous oil after 2.5h reaction time.

^{1}H NMR ($CDCl_3$, 300 MHz): δ 2.45 (s, 3H), 3.57 (ddd, *J*= 30.0, 15.0, 3.0 Hz, 1H), 3.86-3.98 (m, 1H), 6.18 (ddd, *J*= 45.0, 9.0, 3.0 Hz, 1H), 7.33-7.38 (m, 3H), 7.52-7.55 (m, 2H), 7.76-7.87 (m, 6H) ppm.

^{13}C NMR ($CDCl_3$, 75.5 MHz): δ 21.6 (CH_3), 62.6 (d, *J*= 26.4 Hz, CH_2), 88.8 (d, *J*= 177.4 Hz, CHF), 122.5 (d, *J*= 5.3 Hz, CH), 125.3 (d, *J*= 7.5 Hz, CH), 126.8 (CH), 126.9 (CH), 127.7 (CH), 128.1 (CH), 128.3 (2CH), 128.9 (CH), 129.8 (2CH), 132.9 (C), 133.5 (C), 134.1 (d, *J*= 20.4 Hz, C), 136.6 (C), 145.0 (C) ppm.

^{19}F NMR ($CDCl_3$, 282.4 MHz): δ -173.1 (ddd, *J*= 45.1, 28.2, 11.3 Hz, 1F) ppm.

HRMS (EI) calcd. for $C_{19}H_{21}FNO_2S$ [M+NH_4^+]: 346.1272, found: 346.1268.

[201] Z. Yuan, H.-Y. Wang, X. Mu, P. Chen, Y.-L. Guo and G. Liu, *J. Am. Chem. Soc.*, 2015, **137**, 2468−2471.

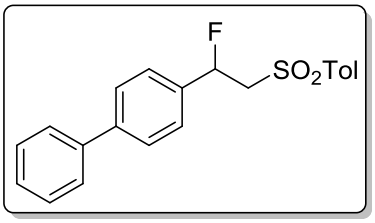

4-(1-Fluoro-2-tosylethyl)-1,1'-biphenyl, 3.143c

Crude reaction product **3.143c** (94%, 16 mg) was obtained as a viscous oil after 3h reaction time.

^{1}H NMR ($CDCl_3$, 300 MHz): δ 2.47 (s, 3H), 3.52 (ddd, *J*= 30.0, 15.0, 3.0 Hz, 1H), 3.81-3.93 (m, 1H), 6.08 (ddd, *J*= 45.0, 9.0, 3.0 Hz, 1H), 7.36-7.61 (m, 11H), 7.87 (d, *J*= 9.0 Hz, 2H) ppm.

^{13}C NMR ($CDCl_3$, 75.5 MHz): δ 21.7 (CH_3), 62.7 (d, *J*= 25.7 Hz, CH_2), 88.5 (d, *J*= 177.4 Hz, CHF), 126.0 (d, *J*= 6.8 Hz, 2CH), 127.1 (CH), 127.6 (CH), 127.7 (CH), 128.3 (CH), 128.8 (CH), 129.9 (CH), 135.7 (d, *J*= 19.6 Hz, C), 136.7 (C), 140.2 (C), 142.4 (C), 145.0 (C) ppm.

^{19}F NMR ($CDCl_3$, 282.4 MHz): δ -173.1 (ddd, *J*= 45.1, 31.1, 11.3 Hz, 1F) ppm.

HRMS (EI) calcd. for $C_{21}H_{23}FNO_2S$ [M+NH_4^+]: 372.1428, found: 372.1426.

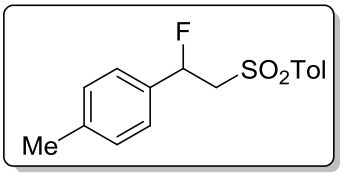

1-((2-Fluoro-2-(*p*-tolyl)ethyl)sulfonyl)-4-methylbenzene, 3.143d

Crude reaction product **3.143d** (92%, 23 mg) was obtained as a viscous oil after 2h reaction time.

^{1}H NMR ($CDCl_3$, 300 MHz): δ 2.36 (s, 3H), 2.48 (s, 3H), 3.45 (ddd, *J*= 30.0, 15.0, 3.0 Hz, 1H), 3.76-3.89 (m, 1H), 7.18 (s, 4H), 7.38 (d, *J*= 9.0 Hz, 2H), 7.86 (d, *J*= 9.0 Hz, 2H) ppm.

^{13}C NMR ($CDCl_3$, 75.5 MHz): δ 21.2 (CH_3), 21.7 (CH_3), 62.7 (d, *J*= 26.4 Hz, CH_2), 88.5 (d, *J*= 176.0 Hz, CHF), 125.6 (d, *J*= 6.0 Hz, CH), 128.3 (CH), 129.5 (CH), 129.8 (CH), 133.9 (d, *J*= 20.4 Hz, C), 136.7 (C), 139.4 (C), 144.9 (C) ppm.

^{19}F NMR ($CDCl_3$, 282.4 MHz): δ -171.7 (ddd, *J*= 48.0, 31.0, 14.0 Hz, 1F) ppm.

HRMS (EI) calcd. for $C_{16}H_{21}FNO_2S$ [M+NH_4^+]: 310.1272, found: 310.1269.

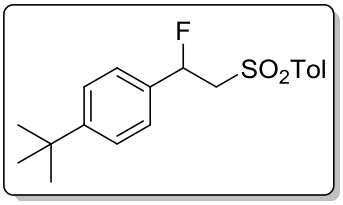

1-(*tert*-Butyl)-4-(1-fluoro-2-tosylethyl)benzene, 3.143e

Crude reaction product **3.143e** (96%, 16 mg) was obtained as a viscous oil after 3h reaction time.

^{1}H NMR ($CDCl_3$, 300 MHz): δ 1.32 (s, 9H), 2.47 (s, 3H), 3.43 (ddd, *J*= 33.0, 15.0, 3.0 Hz, 1H), 3.77-3.90 (m, 1H), 5.99 (ddd, *J*= 45.0, 9.0, 3.0 Hz, 1H), 7.22 (d, *J*= 9.0 Hz, 2H), 7.35-7.40 (m, 4H), 7.85 (d, *J*= 9.0 Hz, 2H) ppm.

^{13}C NMR ($CDCl_3$, 75.5 MHz): δ 21.7 (CH_3), 31.2 (CH_3), 34.7 (C), 62.7 (d, *J*= 26.4 Hz, CH_2), 88.5 (d, *J*= 176.7 Hz, CHF), 125.4 (d, *J*= 6.0 Hz, CH), 125.8 (CH), 128.3 (CH), 129.8 (CH), 133.8 (d, *J*= 13.6 Hz, C), 136.7 (C), 144.9 (C), 152.6 (C) ppm.

^{19}F NMR ($CDCl_3$, 282.4 MHz): δ -171.9 (ddd, *J*= 48.0, 31.1, 14.0 Hz, 1F) ppm.

HRMS (EI) calcd. for $C_{19}H_{27}FNO_2S$ [M+NH_4^+]: 352.1741, found: 352.1742.

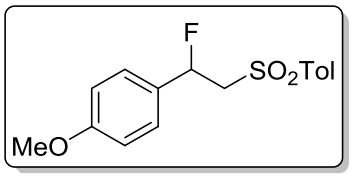

1-((2-Fluoro-2-(4-methoxyphenyl)ethyl)sulfonyl)-4-methylbenzene, 3.143f

Crude reaction product **3.143f** (96%, 21 mg) was obtained as a viscous oil after 3h reaction time.

^{1}H NMR ($CDCl_3$, 300 MHz): δ 2.47 (s, 3H), 3.45 (ddd, *J*= 30.0, 15.0 3.0 Hz, 1H), 3.81 (s, 3H), 3.78-3.90 (m, 1H), 5.95 (ddd, *J*= 48.0, 9.0, 3.0 Hz, 1H), 6.89 (d, *J*= 9.0 Hz, 2H), 7.22 (d, *J*= 9.0 Hz, 2H), 7.37 (d, *J*= 9.0 Hz, 2H), 7.84 (d, *J*= 9.0 Hz, 2H) ppm.

^{13}C NMR ($CDCl_3$, 75.5 MHz): δ 21.7 (CH_3), 55.3 (CH_3), 62.5 (d, *J*= 27.2 Hz, CH_2), 88.4 (d, *J*= 175.9 Hz, CHF), 114.2 (CH), 127.3 (d, *J*= 6.0 Hz, CH), 128.3 (CH), 128.9 (d, *J*= 20.4 Hz, C), 129.8 (CH), 136.7 (C), 144.9 (C), 160.4 (C) ppm.

^{19}F NMR ($CDCl_3$, 282.4 MHz): δ -168.0 (ddd, *J*= 45.2, 28.2, 11.3 Hz, 1F) ppm.

HRMS (EI) calcd. for $C_{16}H_{21}FNO_3S$ [M+NH_4^+]: 326.1221, found: 326.1215.

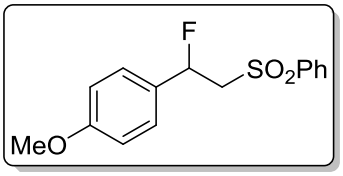

1-(1-Fluoro-2-(phenylsulfonyl)ethyl)-4-methoxybenzene, 3.143g

Crude reaction product **3.143g** (95%, 19 mg) was obtained as a viscous oil after 2h reaction time.

^{1}H NMR ($CDCl_3$, 300 MHz): δ 3.47 (ddd, *J*= 33.0, 15.0, 3.0 Hz, 1H), 3.81 (s, 3H), 3.78-3.93 (m, 1H), 5.97 (ddd, *J*= 48.0, 9.0, 3.0 Hz, 1H), 6.88 (d, *J*= 9.0 Hz, 2H), 7.22 (d, *J*= 9.0 Hz, 2H), 7.55-7.60 (m, 2H), 7.65-7.70 (m, 1H), 7.97 (d, *J*= 9.0 Hz, 2H) ppm.

^{13}C NMR ($CDCl_3$, 75.5 MHz): δ 55.3 (OCH_3), 62.5 (d, *J*= 27.2 Hz, CH_2), 88.3 (d, *J*= 175.2 Hz, CHF), 114.3 (2CH), 127.3 (d, *J*= 5.3 Hz, CH), 128.3 (CH), 128.7 (d, *J*= 20.4 Hz, C), 129.2 (CH), 133.9 (CH), 139.7 (C), 160.4 (C) ppm.

^{19}F NMR ($CDCl_3$, 282.4 MHz): δ -167.8 (ddd, *J*= 48.0, 31.1, 14.1 Hz, 1F) ppm.

HRMS (EI) calcd. for $C_{15}H_{19}FO_3S$ [M+NH_4^+]: 312.1064, found: 312.1056.

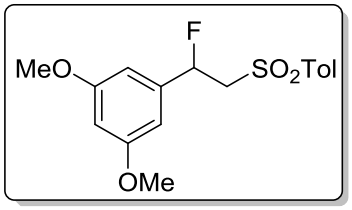

1-(1-Fluoro-2-tosylethyl)-3,5-dimethoxybenzene, 3.143i

Crude reaction product **3.143i** (95%, 12 mg) was obtained as a viscous oil after 60h reaction time.

^{1}H NMR ($CDCl_3$, 300 MHz): δ 2.48 (s, 3H), 3.45 (ddd, *J*= 33.5, 15.0, 3.1 Hz, 1H), 3.72-3.84 (m, 1H), 3.78 (s, 6H), 5.90 (ddd, *J*= 48.1, 9.0, 3.1 Hz, 1H), 6.41 (s, 3H), 7.39 (d, *J*= 9.0 Hz, 2H), 7.86 (d, *J*= 9.0 Hz, 2H) ppm.

^{13}C NMR ($CDCl_3$, 75.5 MHz): δ 21.7 (CH_3), 55.4 (CH_3), 62.4 (d, *J*= 25.7 Hz, CH2), 88.5 (d, *J*= 180.0 Hz, CHF), 101.0 (CH), 103.2 (d, *J*= 6.8 Hz, CH), 128.3 (CH), 129.9 (CH), 136.7 (C), 139.3 (d, *J*= 20.4 Hz, C), 145.0 (C), 161.2 (2C) ppm.

^{19}F NMR ($CDCl_3$, 282.4 MHz): δ -175.2 (ddd, *J*= 48.0, 33.5, 14.0 Hz, 1F) ppm.

HRMS (EI) calcd. for $C_{17}H_{20}FO_4S$ [M+H^+]: 339.1061, found: 339.1050.

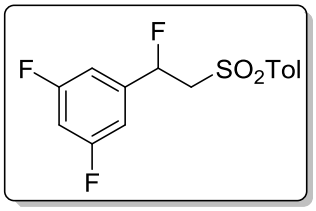

1,3-Difluoro-5-(1-fluoro-2-tosylethyl)benzene, 3.143m

Crude reaction product **3.143m** (94%, 18 mg) was obtained as a viscous oil after 60h reaction time.

^{1}H NMR ($CDCl_3$, 300 MHz): δ 2.48 (s, 3H), 3.44 (ddd, *J*= 30.0, 15.0, 3.0 Hz, 1H), 3.75 (ddd, *J*= 21.0, 15.0, 9.0 Hz, 1H), 6.00 (ddd, *J*= 45.0, 9.0, 3.0 Hz, 1H), 6.77-6.85 (m, 3H), 7.40 (d, *J*= 9.0 Hz, 2H), 7.85 (d, *J*= 9.0 Hz, 2H) ppm.

^{13}C NMR ($CDCl_3$, 75.5 MHz): δ 21.7 (CH_3), 62.4 (d, *J*= 25.7 Hz, CH_2), 87.4 (d, *J*= 180.4 Hz, CHF), 104.6 (dd, *J*= 25.7 Hz, CH), 108.5 (ddd, *J*= 25.6, 7.5 Hz, 2CH), 128.2 (CH), 129.9 (CH), 136.4 (C), 140.7 (C), 145.3 (C), 163.1 (d, *J*= 252.4 Hz, CF), 163.1 (d, *J*= 252.4 Hz, CF) ppm.

^{19}F NMR ($CDCl_3$, 282.4 MHz): δ -176.6 (ddd, *J*= 45.1, 28.2, 14.0 Hz, 1H), -107.5-(-107.4) (m, 2F) ppm.

HRMS (EI) calcd. for $C_{15}H_{17}F_3NO_2S$ [M+NH_4^+]: 332.0927, found: 332.0926.

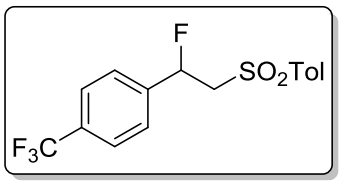

4-(1-Fluoro-2-tosylethyl)-1-trifluoromethylbenzene, 3.143n

Crude reaction product **3.143n** (90%, 9 mg) was obtained as a viscous oil. Data taken from the crude mixture. Only the most characteristic signals for **3.143n** are described in the following data, due to the difficulties in isolating this compound (see spectrum).

^{1}H NMR ($CDCl_3$, 300 MHz): δ 2.48 (s, 3H), 3.48 (ddd, *J*= 30.0, 15.0, 3.0 Hz, 1H), 3.80 (ddd, *J*= 24.0, 15.0, 9.0 Hz, 1H), 6.09 (ddd, *J*= 48.0, 9.0, 3.0 Hz, 1H) ppm.

^{13}C NMR ($CDCl_3$, 75.5 MHz): δ 21.6 (CH_3), 62.5 (d, *J*= 24.9 Hz, CH_2), 87.9 (d, *J*= 179.7 Hz, CHF) ppm.

^{19}F NMR ($CDCl_3$, 282.4 MHz): δ -177.0 (ddd, *J*= 46.0, 30.0, 14.2 Hz, 1F), -63.1 (s, 3F) ppm.

HRMS (EI) calcd. for $C_{16}H_{18}F_4NO_2S$ [M+NH_4^+]: 364.0989, found: 364.0993.

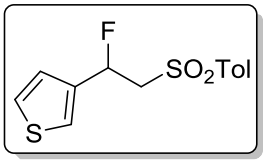

3-(1-Fluoro-2-tosylethyl)thiophene, 3.143o

Crude reaction product **3.143o** (85%, 10 mg) was obtained as a viscous oil after 2.5h reaction time. In this case, Pd/C (100 mol%) had to be used due to catalyst poisoning by the product.

^{1}H NMR ($CDCl_3$, 300 MHz): δ 2.47 (s, 3H), 3.52 (ddd, *J*= 30.0, 15.0, 3.0 Hz, 1H), 3.79-3.92 (m, 1H), 6.10 (ddd, *J*= 6.0 Hz, 1H), 7.30-7.34 (m, 2H), 7.38 (d, *J*= 9.0 Hz, 2H), 7.84 (d, *J*= 9.0 Hz, 2H) ppm.

^{13}C NMR ($CDCl_3$, 75.5 MHz): δ 21.7 (CH_3), 62.0 (d, *J*= 25.7 Hz, CH_2), 84.8 (d, *J*= 174.4 Hz, CHF), 123.6 (d, *J*= 7.5 Hz, CH), 124.8 (d, *J*= 3.0 Hz, CH), 127.3 (CH), 128.3 (CH), 129.9 (CH), 136.6 (C), 137.8 (d, *J*= 21.9 Hz, C), 145.1 (C) ppm.

^{19}F NMR ($CDCl_3$, 282.4 MHz): δ -167.5 (ddd, *J*= 45.2, 28.2, 11.3 Hz, 1F) ppm.

HRMS (EI) calcd. for $C_{13}H_{17}FNO_2S_2$ [M+NH_4^+]: 302.0679, found: 302.0682.

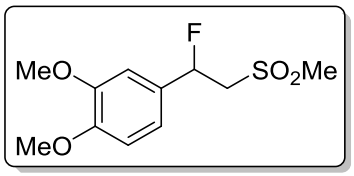

4-(1-Fluoro-2-(methylsulfonyl)ethyl)-1,2-dimethoxybenzene, 3.143s

Crude reaction product **3.143s** (96%, 11 mg) was obtained as a viscous oil after 3h reaction time. Only the most characteristic signals for **3.143s** are described in the following data, due to the difficulties in isolating this compound (see spectrum). An acceptable ^{13}C spectrum was unobtainable due to the small quantity of product obtained as an inseparable mixture with a small amount of starting material **3.126s**.

^{1}H NMR ($CDCl_3$, 300 MHz): δ 3.06 (t, *J*= 1.1 Hz, 3H), 3.13-3.40 (m, 1H), 3.78 (ddd, *J*= 15.4, 12.2, 10.1 Hz, 3H), 5.99 (ddd, *J*=47.3, 10.1, 2.0 Hz, 1H) ppm.

^{19}F NMR ($CDCl_3$, 282.4 MHz): δ −169.19 (ddd, *J*= 47.3, 34.9, 12.2 Hz, 1F) ppm.

HRMS (EI) calcd. for $C_{11}H_{17}FNO_4S$ [M+NH_4^+]: 278.0857, found: 278.0872.

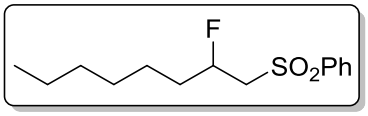

((2-Fluorooctyl)sulfonyl)benzene, 3.143u

Crude reaction product **3.143u** (94%, 14 mg) was obtained as a viscous oil after 1.5h reaction time.

^{1}H NMR ($CDCl_3$, 300 MHz): δ 0.89-1.72 (m, 13H), 3.28 (ddd, *J*= 30.0, 15.0, 3.0 Hz, 1H), 3.54-3.60 (m, 1H), 4.92-5.15 (m, 1H), 7.57-7.71 (m, 3H), 7.95-7.97 (m, 2H) ppm.

^{13}C NMR ($CDCl_3$, 75.5 MHz): δ 13.9 (CH_3), 22.4 (CH_2), 24.4 (d, *J*= 4.5 Hz, CH_2), 28.7 (CH_2), 31.5 (CH_2), 34.8 (d, *J*= 20.4 Hz, CH_2), 61.0 (d, *J*= 23.4 Hz, CH_2), 88.1 (d, *J*= 174.4 Hz, CHF), 128.2 (CH), 129.2 (CH), 133.9 (CH), 139.7 (C) ppm.

^{19}F NMR ($CDCl_3$, 282.4 MHz): δ -180.0 (m, 1F) ppm.

HRMS (EI) calcd. for $C_{14}H_{25}FNO_2S$ [$M+NH_4^+$]: 290.1585, found: 290.1578.

Chapter 4

Synthesis and biological evaluation of novel p-terphenyls as α-helix mimetics

4.0. A brief introduction to drug development.

The development of new pharmaceuticals implies a wide spectrum of procedures and research efforts, ranging from the discovery of new molecular entities (NMEs) that demonstrate certain favourable biological activities, all the way through to the optimisation of a lead compound and the large scale production and commercialisation of the resulting drug. In recent years, the process has become increasingly expensive, unstable and slow. Consequently, the cost invested in the discovery of new lead compounds has increased exponentially; a trend that has not been reflected in the number of new drugs reaching marketable status (Figure 4.1).

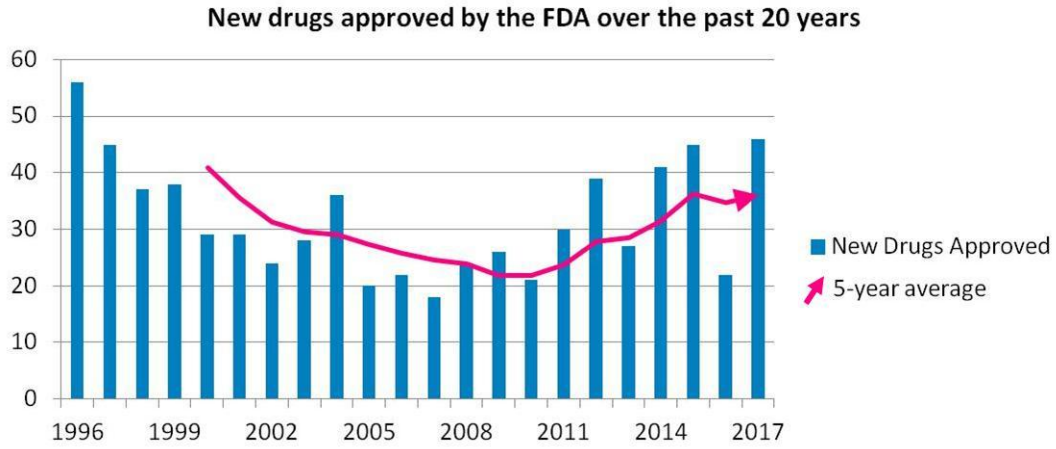

Figure 4.1. New drugs approved by the FDA between 1996 and 2017.[202, 203]

In fact, as little as one NME in every 5,000-10,000 makes it through the rigorous development process, reaching marketable status after an average investment of 10-15 years of intensive research and a total of 2.8-3 billion USD (according to current estimates).[204] Despite these somewhat foreboding data, the pharmaceutical industry continues to advance and offers hope to millions of people suffering from a wide variety of diseases around the globe. For example, in 2017 the American Food and Drugs Administration (FDA) approved 46 new drugs to treat a range of diseases, including but not limited to Parkinson's disease, Chagas disease, hepatitis, and various forms of cancer.[203]

[202] B. Hughes, *Nat. Rev. Drug Discov.*, 2009, **8**, 93-96.

[203] FDA, *2017 New Drug Therapy Approvals*, January 2018, www.fda.gov

[204] a) R. Mullin, Tufts Study Finds Big Rise In Cost Of Drug Development, *Chem. Eng. News* [Online]. Published online: Nov 20, 2014. https://cen.acs.org/articles/92/web/2014/11/Tufts-Study-Finds-Big-Rise.html (accessed Jun 30, 2018). b) J. A. DiMasi, H. J. Grabowski and R. W. Hansen, *J. Health Econ.*, 2016, **47**, 27-33.

Currently, there are several approaches towards drug discovery. Of these, perhaps the most widely used is high-throughput screening, a technique that relies on the rapid screening of thousands of compounds with set biological targets in the search of a favourable response. This is often the fastest way by which pharmaceutical companies are able to identify a small library of hits to take forward for further tests. Research into practices such as diversity oriented synthesis is crucial for this approach to drug discovery, allowing the rapid synthesis of large libraries of compounds with varied 3D structures.

Another method involves the rational design of a lead compound, combining the ideas and hypotheses of scientists with computational data in order to study 3D models of biological targets; a fact that represents both the main advantage and main limitation of this approach. Since this approach relies heavily on data and modes of action of biological targets that are already public knowledge, it is easier to later make changes to the structure and modify the compound's activity if need be. Therefore, this approach can only provide a solution to problems that are *already understood*.[205] In contrast, high-throughput screening can provide answers without first knowing how or why a compound exerts a favourable biological response.

In any case, once a hit is identified through high throughput screening, the mode of action must be elucidated and from there the modification and optimisation of the compound will include many computational models to understand the interactions formed between molecule and target.

This chapter continues a long-term project within our research group, involving the rational design and lead optimisation of new small molecule peptidomimetics that show favourable therapeutic potential against some of the most dangerous diseases of our time.

[205] A. Whitty, *Future Med. Chem.*, 2011, **7**, 797-801.

4.1. Objectives.

This chapter forms part of an ongoing study within our research group, in collaboration with the groups of J. Gallego (Universidad Católica de Valencia) and J. Alcamí (Instituto de Salud Carlos III), dealing with the synthesis and biological activity of novel *p*-terphenyls as Rev protein mimics capable of inhibiting HIV replication.

In this context, the main objectives of this work were the synthesis and biological evaluation of a new series of terphenyl structures. The present chapter should be considered together with the work presented in 2017 by L. Herrera in her doctoral thesis.[206] Much of the work contained in Herrera's doctoral thesis was carried out simultaneously to this work, and dealt with the synthesis and biological evaluation of *p*-terphenyls with a new substitution pattern, specifically with the side-chains in 1,4 relative positions. This will also be discussed in the following sections, as applicable.

Therefore, this project will include monolaterally-substituted derivatives, varying side-chain patterns, and other more complex structures specifically designed to further study the structure-activity relationship of our *p*-terphenyls—generally with side-chains in 1,3 relative positions—and their interaction with the RRE (Rev Response Element) of HIV-1.

We will also begin to explore other interactions which could be targeted by our terphenyl peptidomimetics. One such example is the MTIP-MyoA interaction involved in the malaria infection, which will be discussed in turn.

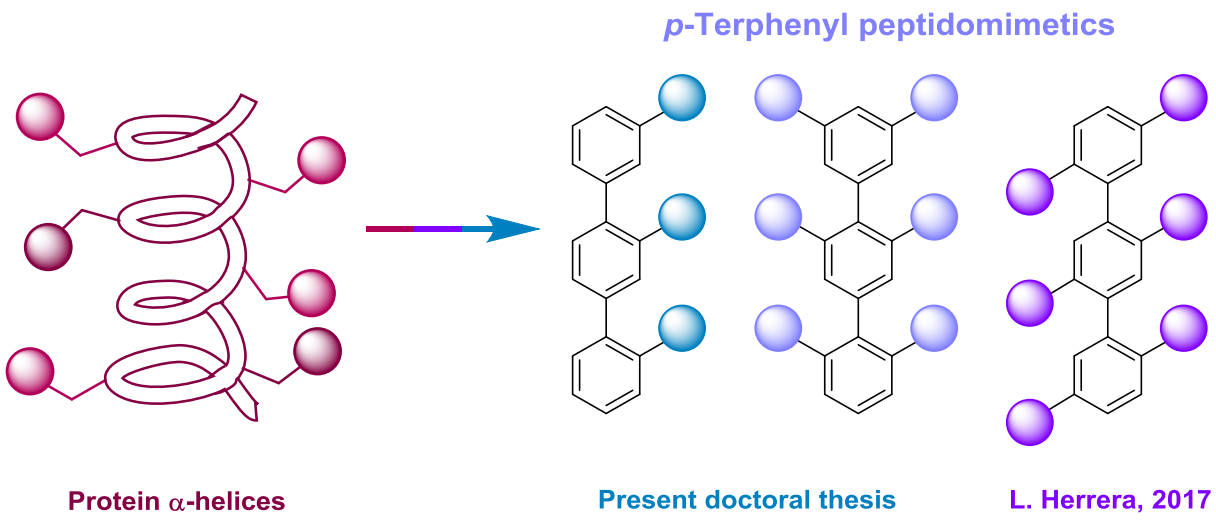

[206] L. Herrera, PhD Thesis, Universitat de València, 2017.

4.2. Acquired immunodeficiency syndrome.

4.2.1. Introduction.

Acquired immune deficiency syndrome, or AIDS, has become one of the most dangerous pandemics of our time, with up to 37 million people living with HIV infection in 2016.[207] Of these, around 25 million reside in sub-Saharan Africa—this is due to numerous factors, but perhaps mainly because the epidemic originated in this part of the world. Since the beginning of the epidemic in the early 1980s, more than 80 million people are thought to have been infected with the virus, with approximately half that figure succumbing to an AIDS-related death.

AIDS is the final result of HIV (Human Immunodeficiency Virus) infection and was first recognised as a disease in the 1980s. HIV infection does not kill directly, instead acting by compromising the patient's immune system and rendering them susceptible to other opportunistic infections. HIV is not just one virus, but a set of viral strains. The main two types are HIV-1, which is responsible for the vast majority of global infections, and HIV-2, which is confined to western Africa.

HIVs are generally accepted to have originated from Simian Immunodeficiency Viruses (SIVs) and evolved into strains capable of infecting humans (HIVs) through various interspecies contamination events. HIV-1, the much more infectious type, has been shown to have evolved from SIVs originating in chimpanzees, specifically SIVcpz*Ptt* and SIVcpz*Pts* from Central chimpanzees (*Pan troglodytes troglodytes*) and Eastern chimpanzees (*Pan troglodytes schweinfurthii*) respectively.[208] Given the genetic similarities between humans and chimpanzees it's clear to see why HIV-1 is the most infectious to humans; in fact, a single strain from this type is mostly responsible for the global pandemic. On the other hand, HIV-2 is thought to have originated in sooty mangabeys (*Cercocebus atys*), a different species of ape that carries another strain of simian immunodeficiency virus known as SIVsmm. These apes are rather less similar genetically to humans and as such their virus is less infectious to us; people infected with HIV-2 rarely even develop AIDS. Due to this, HIV-2 infection has remained largely confined to the West African countries—where the sooty mangabey's habitat lies—and has not spread to other parts of the globe.

The most plausible explanation for the cross-species contamination event is thought to be due to the tendency of communities in these areas to keep such species as pets, or to use them for so-called

[207] UNAIDS, *UNAIDS Data 2017*, July 2017, www.unaids.org
[208] P. M. Sharp and B. H. Hahn, *Cold Spring Harb. Perspect. Med.*, 2011, **1**, a006841.

"bush-meat" as a food source; an open cut or wound could easily come into contact with the blood of an infected primate whilst preparing a meal.[209]

Despite the large number of people still living with HIV infection, the number of AIDS-related deaths has dropped significantly over the past decade. Peaking at 1.9 million deaths in 2005, the figure has dropped around 48% and in 2016 this figure stood at 1 million. Nevertheless, AIDS-related illnesses remain the leading cause of deaths among women of reproductive age globally. Similarly, new HIV infections have dropped by 16% since 2010, although over the past few years there has been an alarming rise in new infections in Eastern Europe and central Asia.

These drops are due to massive global efforts to develop more effective treatments and to increase the coverage of people receiving the correct treatment—there is a clear inverse relationship between the number of people receiving treatment and the number of new infections. However, global coverage of patients receiving treatment remains one of the biggest challenges; excluding Western Europe and North America, in most areas less than 50% of the patients are receiving the proper treatment.

It's worth noting that, despite these advances, there is still no way to cure HIV infection—and we are still far from achieving such a feat. However, current therapies are capable of efficiently paralysing the replication and proliferation of the virus, both protecting the patient from AIDS-related illnesses and suppressing transmission to others. These advances have effectively ended the AIDS epidemic in certain parts of the world: people are instead living with chronic HIV infection.[210]

[209] P. M. Sharp, E. Bailes, R. R. Chaudhuri, C. M. Rodenburg, M. O. Santiago and B. H. Hahn, *Philos. Trans. R. Soc. Lond. B.*, 2001, **356**, 867–876.
[210] S. G. Deeks, S. R. Lewin and D. V. Havlir, *Lancet*, 2013, **382**, 1525-1533

4.2.2. HIV infection.

HIV is a species of *Lentivirus*, a genus of retrovirus characterised by long incubation periods—as the name suggests. HIV infection occurs in various stages, starting with an incubation period followed by acute infection (sometimes referred to as primary infection), then a latency period which can last for anywhere between months and many years before finally resulting in AIDS (Figure 4.2).

Upon transmission of the virus, it begins replicating in the mucosal and submucosal endothelial tissues around the area of transmission. At first the virus is not present in the plasma and as such is undetectable, until around 7-21 days have passed and the virus finally starts entering the plasma, at which point the virus is detectable at around 1-5 virions per millilitre of plasma *via* sensitive qualitative methods of nucleic acid amplification, although usually the infection is detected much later than this. This initial period is characterised by the appearance of various viral markers and antibodies in the blood, including inflammatory cytokines and the viral RNA.[211]

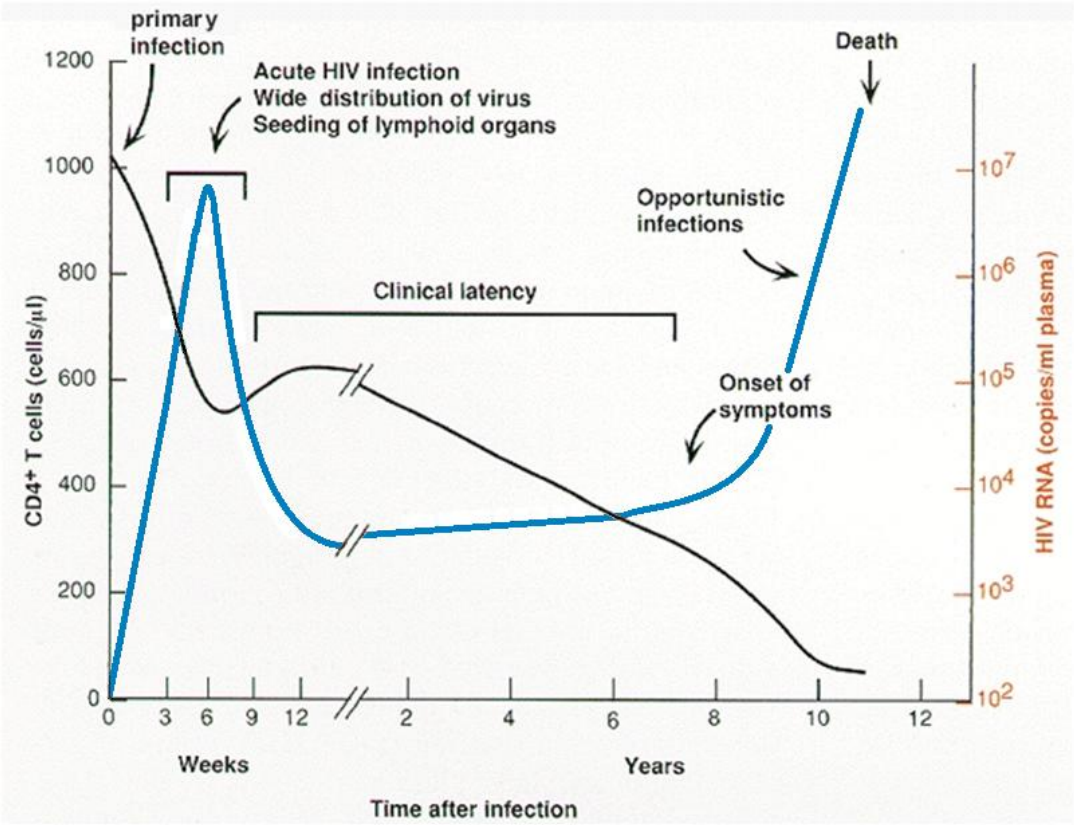

Figure 4.2. Development of HIV infection over time.

[211] M. S. Cohen, G. M. Shaw, A. J. McMichael and B. F. Haynes, *N. Engl. J. Med.*, 2011, **364**, 1943-1954.

Symptoms can start to appear after this initial incubation period during the acute infection, and can take any number of forms since they aren't directly caused by the virus. On the contrary, all symptoms associated to HIV/AIDS are indirect, and are due to the reduced capability of the host's immune system to deal with foreign threats due to the decline in $CD4^+$ T-cells (messengers that recognise pathogens in the system and trigger signalling pathways to recruit lymphocytes, often CD8 cells, to eliminate the pathogen).[212] The acute infection corresponds with a primary dip in the $CD4^+$ T-cell levels and a temporary maximum in the HIV RNA levels (Figure 4.2). In these first few weeks, the host is susceptible to the first onset of detectable symptoms which can vary from person to person but can take the form of joint aches and pains, nausea, diarrhoea, headaches, swollen lymph glands or fevers; all common symptoms for other milder illnesses such as influenza, leading to a possible HIV infection being overlooked.[213]

The latency period on average lasts between 8-12 years, but this is increasing slowly over the years as more people are being treated with antiretroviral drugs, and as treatments become more effective. This treatment is capable of diminishing HIV presence to almost undetectable levels, but once the patient stops taking the treatment the virus bounces back to elevated levels in the plasma, and as such the patient regresses to a more infectious state (the risk of transmission is higher when the viral load is higher). Eventually at the end of this latency period, the $CD4^+$ T-cell levels drop severely and AIDS develops, bringing with it a new onset of symptoms and opportunistic illnesses, which can lead to the death of the patient.

[212] T. Pan, S. Wu, X. He, H. Luo, Y. Zhang, M. Fan, G. Geng, V. C. Ruiz, J. Zhang, L. Mills, C. Bai and H. Zhang, *PLoS One*, 2014, **9**, e93944.

[213] a) J. M. Coffin, S. H. Hughes and H. E. Varmus, *Retroviruses*, Cold Spring Harbor Laboratory Press, Cold Spring Harbor (NY), 1997. b) N. L. Wilson, D. E. Vance, L. D. Moneyham, J. L. Raper, M. J. Mugavero and S. L. Heath, *J. Assoc. Nurses AIDS Care*, 2014, **25**, 483–495.

4.2.3. HIV pathogenesis and biological cycle.

The mechanism of infection of HIV is similar to that of other viruses belonging to the family *Retroviridae.* The viruses of this family contain single-stranded positive-sense RNA, using their own reverse transcriptase to produce DNA once inside a host cell; this is the reverse of the usual DNA to RNA pattern, hence the name *retrovirus* (*retro* meaning backwards). Although the different virions belonging to this family of virus lead to very different infections, their structure and components are similar.

The HIV virion measures roughly 120 nm in diameter and has an approximately spherical shape. The casing of each virion is made up of a lipid bilayer, originating from the host cell, adorned with glycoproteins gp120 which are anchored to the surface by transmembrane proteins gp41. This casing protects the important genetic information contained in the interior of each virion: two copies of viral RNA, bound to proteins p6 and p7, encapsulated in a truncate-conical capsid formed of p24 proteins. The capsid also contains viral enzymes—an inverse transcriptase, an integrase and a protease—vital in the replication and proliferation of the virus (Figure 4.3).[214]

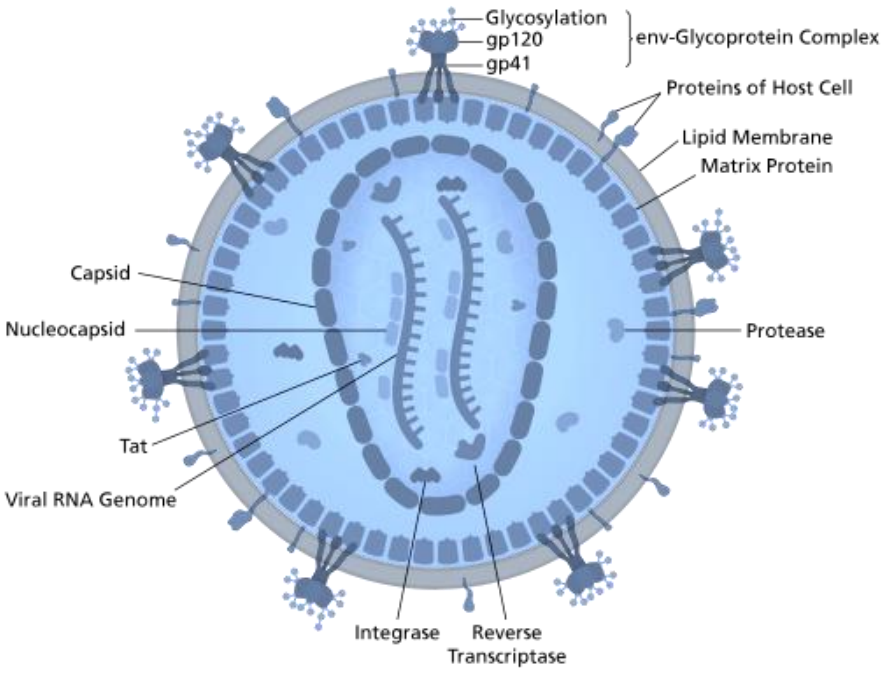

Figure 4.3. Structure of the HIV-1 virus.

[214] a) J. M. Costin, *Virol. J.*, 2007, **4**:100. b) W. K. Wang, M. Y. Chen, C. Y. Chuang, K. T. Jeang and L. M. Huang, *J. Microbiol. Immunol. Infect*., 2000, **33**, 131-140. c) S. A. Schwartz and M. P. N. Nair, *Clin. Diagn. Lab. Immunol.*, 1999, **6**, 295-305.

The mechanism of infection can be divided into two distinct phases: 1) early stage, which constitutes everything from the binding of the virus to the formation of the provirus; and 2) late stage, which constitutes everything from the expression of viral genetic material to the liberation of new virions from the host cell.

The virus first binds to the lipid membrane of the host cell, mediated by the glycoproteins gp120 on the surface of the virion—they are highly specific for the recognition of the CD4 receptors and either CCR5 or CXCR4 chemokine receptors which are present on the membranes of macrophages and $CD4^+$ T-cells.[215] This is the reason for the specific targeting of the immune system associated with HIV infection: the virus selectively enters and infects this type of cell, although in some cases the virus can enter other cells such as astrocytes or renal epithelial cells, causing HIV-associated neurocognitive disorder and nephropathy respectively (Figure 4.4).[213a, 216]

Once the virus is bound to the host cell, a sequence of conformational changes takes place, leading to an interaction with a cellular co-receptor and the fusion of the viral lipid bilayer with the lipid membrane of the host cell, depositing the contents of the virus into the interior of the host cell. The viral protein capsid containing the viral RNA then breaks down, leaving it free and unprotected in the cytoplasm of the host cell. From there, the viral RNA is reverse-transcribed using the virus' own reverse transcriptase, thereby producing a double-stranded section of complementary DNA—denominated the provirus—which is then transferred to the nucleus and inserted into the host's own DNA through the action of the viral integrase enzyme. In this state, the provirus can remain latent for long periods of time (Figure 4.4).

The HIV-1 provirus contains 9,800 nucleotide pairs and contains nine separate genes. The genes code for proteins very similar to other virus in the family *Retroviridae*: three genes that code for structural or functional proteins (in this case the glycoprotein *gp120*, polyproteins *gag* and *pol*); two that code for regulatory proteins (*tat* and *rev*); and four that code for accessory proteins (*vpu*, *vpr*, *vif* and *nef*).[217]

[215] M. Spear, J. Guo, and Y. Wu, *Immunol. Rev.*, 2013, **256**, 300–312.
[216] G. Maartens, C. Celum, and S. R. Lewin, *Lancet*, 2014, **384**, 258–271.
[217] a) R. A. Subbramanian and E. A. Cohen, *J. Virol*., 1994, **68**, 6831-6835. b) S. M. Kingsman and A. J. Kingsman, *Eur. J. Biochem.*, 1996, **240**, 491-507.

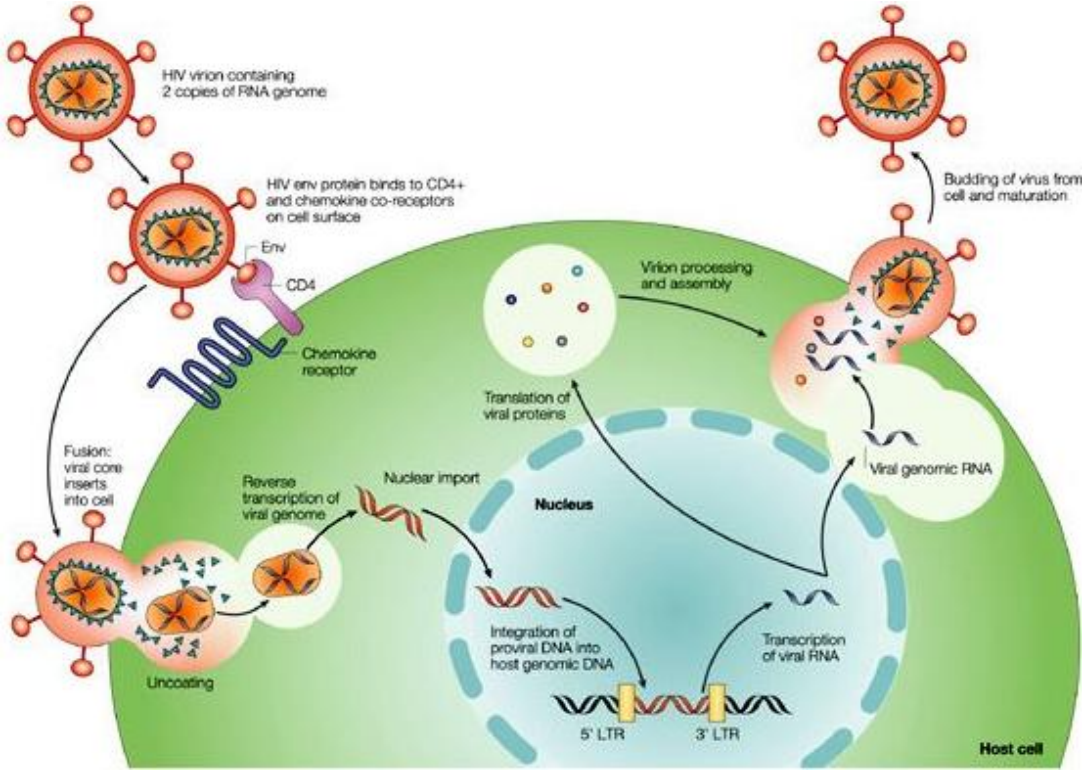

Figure 4.4. HIV life cycle.[218]

The late stage of the infection begins with transcription of the provirus, for which it relies on the host's own transcription mechanism. This results in messenger RNA (mRNA), which can then be shuttled out of the cell nucleus and into the cytoplasm through the action of the regulatory protein Rev. Once in the cytoplasm, the mRNA provides all the genetic information necessary for the translation, or synthesis, of viral proteins. The result of the translation process, however, is a long chain of polyproteins which often must then be cleaved into functional fragments; the virus contains its own specific protease enzyme for this purpose. These proteins, along with two strands of viral RNA, then assemble the internal components of a new virus particle. Subsequently, the exposed viral components approach the cell membrane and, through a process known as budding, the cell membrane forms a lipid bilayer around the viral components, and allows the new virion to pass through into the extracellular medium. The virus subsequently undergoes a maturation process during which it gains its capacity to infect new host cells (Figure 4.4).[219]

Strictly speaking, acquired immunodeficiency syndrome is not caused directly by HIV infection; the virus causes a sequence of harmful events that leads to what we know as AIDS. This simply refers to the dangerously low levels of $CD4^+$ T-cells per millilitre of plasma observed in HIV-infected patients. This

[218] A. Rambaut, D. Posada, K. A. Crandall and E. C. Holmes, *Nat. Rev. Genet.*, 2004, **5**, 52-61.
[219] a) D. C. Chan and P. S. Kim, *Cell*, 1998, **93**, 681-684. b) J. Sodroski, *Science*, 1998, **280**, 1884-1888.

syndrome usually develops in the late stage of infection after the latent period associated to *lentivirus.* This period can last anywhere from months to years, but with current treatments it's not uncommon for this period to take 8-12 years, although it can vary greatly between patients.[220] The pathway causing the death of the infected $CD4^+$ T-cells, along with their abrupt depletion during the primary infection, is still poorly understood. This was highlighted by Thomas in 2009, and is thought to be one of the biggest mysteries of the disease—we still don't know the mechanisms by which HIV infection causes AIDS.[221] However, in 2014 a series of reports surfaced describing several mechanisms to explain this phenomenon, and all coincided that the main mechanism is a form of apoptosis (programmed cell death).[212, 222] For example, Greene *et al.* detailed how HIV causes the death of host quiescent T-cells through pyroptosis, a chronic inflammatory form of apoptosis designed to recruit new immune cells to the site in order to continue fighting the infection based on the activation of caspase-1 (Figure 4.5).[222a]

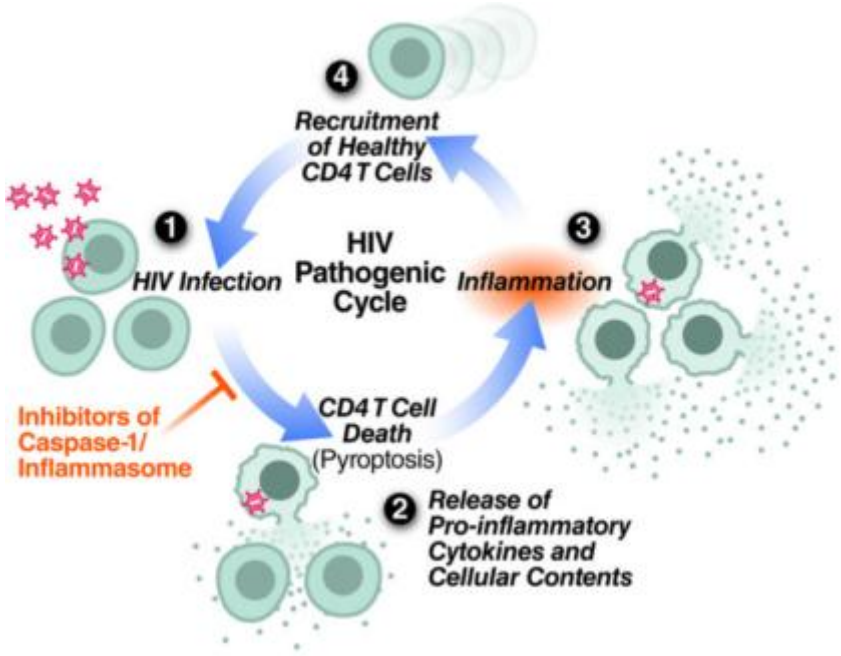

Figure 4.5. Cycle detailed by Greene *et al.* describing how HIV could cause the rapid depletion of $CD4^+$ T-cells by pyroptosis, leading to AIDS.

[220] N. L. Wilson, D. E. Vance, L. D. Moneyham, J. L Raper, M. J. Mugavero and S. L. Heath, *J. Assoc. Nurses AIDS Care*, 2014, **25**, 483-495.
[221] C. Thomas, *Nat. Med.*, 2009, **15**, 855-859.
[222] a) G. Doitsh, N. L. K. Galloway, X. Geng, Z. Yang, K. M. Monroe, O. Zepeda, P. W. Hunt, H. Hatano, S. Sowinski, I. Muñoz-Arias and W. C. Greene, *Nature*, 2014, **505**, 509-514. b) H. Ipp, A. E. Zemlin, R. T. Erasmus and R. H. Glashoff, *Crit. Rev. Clin. Lab. Sci.*, 2014, **51**, 98-111.

4.2.4. Regulatory protein Rev.

The regulatory HIV-1 Rev protein plays a fundamental role in the replication cycle of the virus, given that it is responsible for the transport of the viral RNA from the host cell nucleus to the cytoplasm, where the packaging and encapsulation of new virions takes place—hence the name Rev, an abbreviation of *regulator of expression of virion proteins.*[223] This protein recognises a specific part of the mRNA, known as the RRE (an acronym of *Rev Response Element*), through an α-helix rich in arginine residues (Figure 4.6, a-b).[224]

The RRE is a highly structured section of RNA, made up of several hairpin-type motifs around a central hub, characterised for containing certain anomalous base pairs. The most important of these is found in the IIB stem, which presents consecutive G-G and G-A mismatches,[225] resulting in an internal loop approximately 5 Å wider than the rest of the stem.[226] This internal loop is a perfect fit for the arginine-rich α-helix of Rev (also known as Rev_{34-50} to refer to the residues forming the α-helix), allowing for the selective formation of a Rev-RRE ribonucleoprotein complex; the first step in the process of nuclear export (Figure 4.6, c-d).[227]

It is worth noting that nuclear RNA export is a highly regulated process. There are many membrane-bound receptors that aid the crossing of large molecules, such as nucleic acids or proteins, since alone they are usually unable to pass the lipid membrane. These receptors facilitate the exchange of proteins from one side of the cell membrane to the other, although the situation is more difficult for nucleic acids. In past years, it was believed that RNAs were able to cross the membrane using these receptors as a free strand, although this has since been proven inaccurate—for the transport of this class of biological molecules, it's necessary to first construct a protein-RNA complex.

[223] a) M. Emerman, R. Vazeux and K. Peden, *Cell*, 1989, **57**, 1155-1165. b) M. H. Malim, J. Hauber, S. Y. Le, J. V. Maizel and B. R. Cullen, *Nature,* 1989, **338**, 254-257. c) V. W. Pollard and M. H. Malim, *Annu. Rev. Microbiol.*, 1998, **52**, 491-532.
[224] J. Kjems, B. J. Calnan, A. D. Frankel and A. P. Sharp, *EMBOJ*, 1992, **11**, 1119-1129.
[225] K. Nakatani, S. Horie, Y. Goto, A. Kobori and S. Hagihara, *Bioorg. Med. Chem.*, 2006, **14**, 5384-5388.
[226] D. P. Bartel, M. L. Zapp, M. R. Greene and J. W. Szostak, *Cell*, 1991, **67**, 529-536.
[227] B. R. Cullen, *Nature*, 2005, **433**, 26-27.

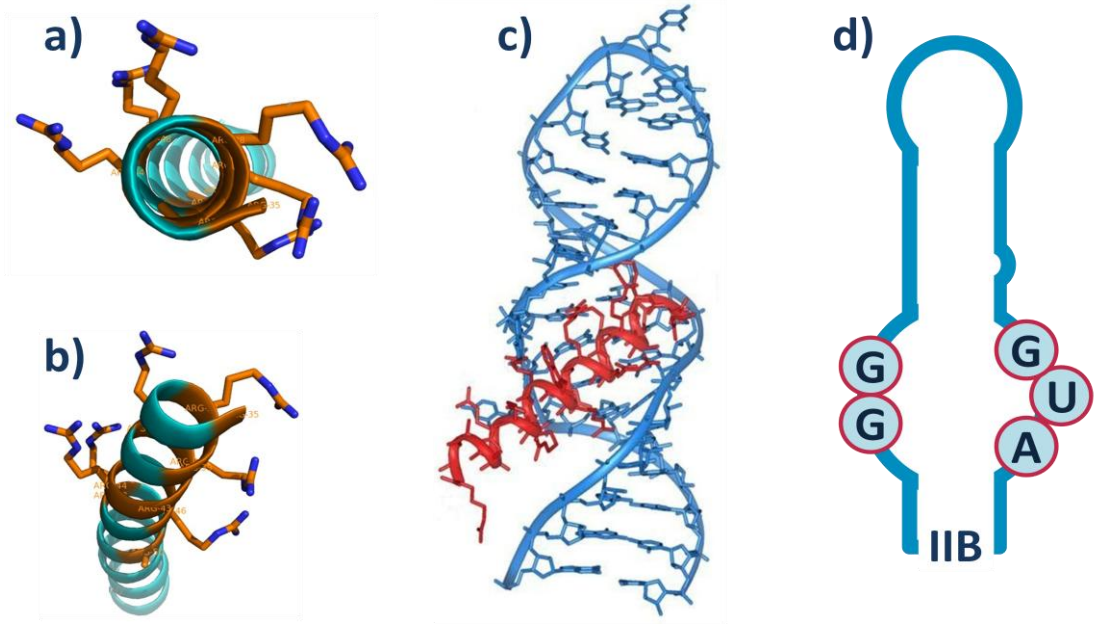

Figure 4.6. a) and b) The arginine-rich α-helix of Rev responsible for binding to the RRE viewed from different angles (Arg residues highlighted in orange). c) The Rev_{34-50}-IIB loop complex. d) A schematic showing the mismatching base-pairs in the IIB hairpin in the RRE, forming the Rev binding site.

In the early stage of HIV infection, the proviral DNA is integrated into the host DNA, and transcribed to form viral mRNA. Inside the nucleus, the mRNA is split into smaller fragments that code for each gene. The smaller fragments are able to cross the nuclear membrane, while the whole mRNA strands remain in the nucleus. Therefore, in this phase, the virus is unable to replicate since the strand of RNA never reaches the cytoplasm, where the encapsulation process of new virions takes place.

However, the fragment containing the *rev* gene is indeed able to reach the cytoplasm, where it is translated into the Rev protein.[223c] This protein is capable of crossing the nuclear membrane and, once back inside the nucleus, the Rev protein binds to the RRE of the full mRNA strand to form the Rev-RRE complex as described earlier. After the formation of this primary complex between the α-helix of Rev and the high-affinity bulge in the RRE, it is thought that the other loops present in the RRE show an increased affinity to Rev. In 2010, Frankel *et al.* proposed that this leads to up to six molecules of Rev binding to the same RNA strand, and that Rev actually oligomerises—through hydrophobic interactions built around a core of Leu22 and Ile59—upon binding, resulting in a "jellyfish-type" structure (Figure 4.7).[228] The Rev protein also contains a short leucine-rich nuclear export signal that directly interacts with a nuclear Ran-GTP bound karyopherin (proteins involved in transporting molecules across the nuclear membrane of eukaryotic cells) RNA export factor called Crm1, which is essential to the actual

[228] M. D. Daugherty, B. Liu and A. D. Frankel, *Nat. Struct. Mol. Biol*., 2010, **17**, 1337-1343.

transport of the RNA complex across the nuclear membrane. In this way, the Crm1-bound ribonucleoprotein Rev-RRE "jellyfish-type" complex is able to pass the nuclear membrane, allowing for the replication cycle of the virus to continue.[229]

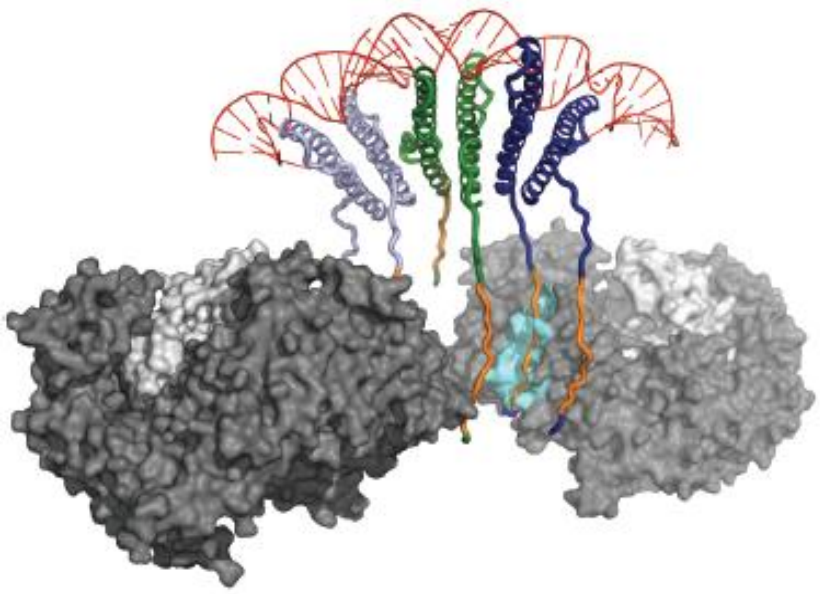

Figure 4.7. "Jellyfish-type" structure proposed by Frankel *et al.*[228]

[229] B. R. Cullen, *J. Cell. Sci.*, 2003, **116**, 587-597.

4.2.5. Current treatments against HIV infection.

Although there is still no cure to HIV infection, we are now able to prevent the replication and proliferation of the virus, making it less infectious and protecting the patient's immune system to a certain degree. Various biological processes represent viable targets throughout the virus replication cycle, but the most common targets for current treatments are the following: 1) viral recognition and binding to the $CD4^+$ T-cell to prevent the virus ever entering the cell (entry inhibitors); 2) transcription of viral RNA to form proviral DNA (reverse transcriptase inhibitors); 3) integration of viral DNA into the host DNA (integrase inhibitors); and 4) production of vital viral proteins (protease inhibitors). HIV infection is typically treated with a mixture of drugs from several of these classes in order to halt the spread of the virus as much as possible—this type of treatment is commonly referred to as highly active antiretroviral therapy (abbreviated to HAART). These mixtures generally consist of two different nucleoside reverse transcriptase inhibitors and one non-nucleoside reverse transcriptase inhibitor, protease inhibitor or integrase inhibitor which will all be discussed in turn.

It's worth noting that, at present, there are no antiretroviral drugs on the market that exploit the Rev-RRE interaction, making this an attractive target to overcome any resistance phenomena arising to current treatments.

4.2.5.1. Entry inhibitors.

The entry of HIV-1 to the host CD4-expressing cells (T-cells or macrophages) involves a complex cascade of events and interactions between the viral envelope protein (Env) and the surface proteins of the host cell (Figure 4.8).[230] Env is the name given to the homotrimeric structure made up of three surface glycoproteins gp120 non-covalently bound to three membrane-bound glycoproteins gp41. Firstly, as mentioned previously, the virus glycoproteins gp120 bind to the CD4 receptors on the surface of the host cell. However, this interaction alone is not enough for the virus to enter the host cell; for that, another membrane-bound co-receptor is necessary. This can be either CCR5 or CXCR4, depending on the virus tropism—the tropism refers to exactly which type of cell the virus infects, and can be either R5 or X4 for those that infect cells using the CCR5 or CXCR4 co-receptors respectively. The primary union of gp120 and CD4 therefore causes a conformational change in Env which opens up an otherwise buried pocket of gp120, and interaction of this region with the corresponding co-receptor produces further structural rearrangements. In this way, a helical region of the three gp41 proteins (denominated the HR1 trimer) are pushed forwards into the host cell membrane, causing a further change by which a second helical region of gp41 (denominated HR2) moves to bind with the first HR1 trimer. This change essentially contracts the gp41 glycoprotein and pulls the virus into close proximity to the host cell membrane. A second Env-CD4 complex reinforces the interaction and allows the two membranes to fuse, leading to the liberation of the virus contents in the interior of the host cell.

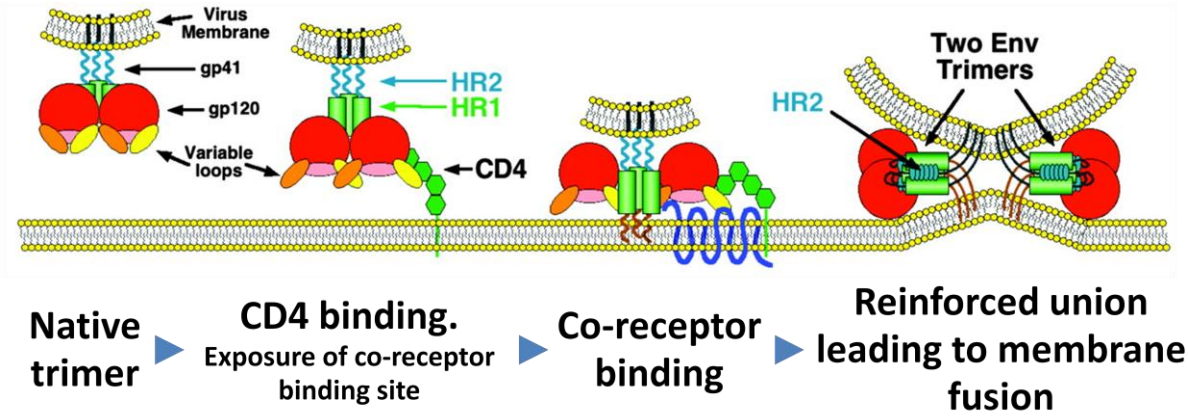

Figure 4.8. Cascade of conformational changes and interactions leading to viral entry into the host cell.[230a]

[230] a) J. P. Moore and R. W. Doms, *PNAS*, 2003, **100**, 10598-10602. b) J. B. Munro, J. Gorman, X. Ma, Z. Zhou, J. Arthos, D. R. Burton, W. C. Koff, J. R. Courter, A. B. Smith III, P. D. Kwong, S. C. Blanchard and W. Mothes, *Science,* 2014, **346**, 759-763.

Entry inhibitors represent a relatively new class of antiretroviral drugs against HIV; there are only a few entry inhibitors currently on the market for use in HAART, all approved within the last 15 years. The first of these was Enfuvirtide—a peptide marketed by Roche under the trade name Fuzeon—which was approved by the FDA in 2003.[231] This drug is commonly referred to a fusion inhibitor, referring to its specific role in inhibiting the final membrane fusion step in the entry cascade. In terms of structure, Enfuvirtide is homologous to a 36 amino acid segment of the HR2 region of gp41, thereby binding to HR1 and preventing the contraction of gp41 which approximates the virus to the host cell membrane.[232]

Maraviroc was the second entry inhibitor to be approved by the FDA in 2007, marketed by Pfizer under the trade names Selzentry or Celsentri.[233] This entry inhibitor acts by binding to the CCR5 co-receptor, thus blocking its interaction with gp120 and preventing viral entry. The compound was discovered using a high-throughput screening method which identified imidazopyridine-based structure UK-107,543 as the most potent ligand for the CCR5 receptor. Subsequent optimisation in terms of potency, pharmacokinetics, absorption and interactions with other important targets resulted in Maraviroc (Scheme 4.1).[234] The downside of this mode of action is that although Maraviroc is effective for viruses that use CCR5 to enter the cell (the R5 strains), those that use CXCR4 to enter are unaffected. This means the drug is useless for patients expressing CRCX40-tropic viruses, and that over time it is likely that the virus will switch to the other strain due to natural selection—only X4 viruses will continue to infect new cells and replicate.

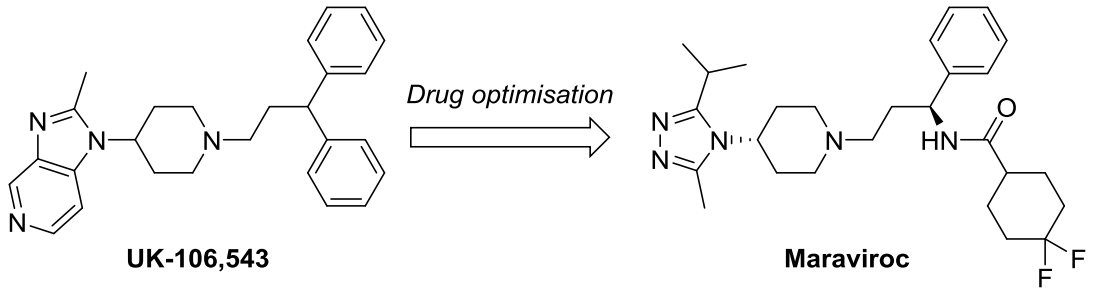

Scheme 4.1. Structures of lead compound UK-106,543 and optimised marketable drug Maraviroc.

[231] https://web.archive.org/web/20090825164901/http://www.fda.gov/ForConsumers/ByAudience/ForPatientAdvocates/HIVandAIDSActivities/ucm125088.htm (Accessed 10th July 2018)

[232] M. L. Greenberg and N. Cammack, *J. Antimicrob. Chemother.*, 2004, **54**, 333-340.

[233] a) S. S. Lieberman-Blum, H. B. Fung and J. C. Bandres, *Clin. Ther.*, 2008, **30**, 1228-1250. b) G. Fätkenheuer, A. L. Pozniak, M. A. Johnson, A. Plettenberg, S. Staszewski, A. I. M. Hoepelman, M. S. Saag, F. D. Goebel, J. K. Rockstroh, B. J. Dezube, T. M. Jenkins, C. Medhurst, J. F. Sullivan, C. Ridgeway, S. Abel, I. T. James, M. Youle and E. van der Ryst, *Nat. Med.*, 2005, **11**, 1170-1172.

[234] P. Dorr, M. Westby, S. Dobbs, P. Griffin, B. Irvine, M. Macartney, J. Mori, G. Rickett, C. Smith-Burchnell, C. Napier, R. Webster, D. Armour, D. Price, B. Stammen, A. Wood and M. Perros, *Antimicrob. Agents Chemother.*, 2005, **49**, 4721-4732.

A third example, this time a monoclonal antibody by the name of Ibalizumab (trade name Trogarzo), was developed by TaiMed Biologics and gained FDA approval earlier this year in March 2018.[235] The mechanism of action is different to those previously described, this time binding directly to a region of CD4 present on the host cell surface. In this way, the drug avoids any differences in virus tropism; all HIV-1 viral strains must first bind to CD4 receptors to enter the host cell.[236]

Besides these scarce examples of entry inhibitors actually on the market, there are several others in various stages of development. One such example is the small molecule Fostemsavir (BMS-663068), an investigational drug currently being studied in phase III clinical trials by Bristol-Myers Squibb.[237] Furthermore, another monoclonal antibody by the name of PRO 140 is currently under development by Cytodyn Inc., and has recently completed a primary endpoint of phase II/III clinical trials in February 2018.[238]

Entry inhibitors represent an upcoming and promising class of antiretroviral therapy, given their extracellular site of action avoiding contact with many potential problematic secondary interactions inside the host cell.[230a]

[235] https://www.accessdata.fda.gov/scripts/opdlisting/oopd/detailedIndex.cfm?cfgridkey=321910 (Accessed 5th July 2018)

[236] J. M. Jacobson, D. R. Kuritzkes, E. Godofsky, E. DeJesus, J. A. Larson, S. P. Weinheimer and S. T. Lewis, *Antimicrob. Agents Chemother.*, 2009, **53**, 450-457.

[237] a) https://aidsinfo.nih.gov/drugs/508/fostemsavir/0/patient (Accessed 5th July 2018). b) Z. Li, N. Zhou, Y. Sun, N. Ray, M. Lataillade, G. J. Hanna and M. Krystal, *Antimicrob. Agents Chemother.*, 2013, **57**, 4172-4180.

[238] a) https://www.cytodyn.com/media/press-releases/detail/271/cytodyn-reports-primary-endpoint-achieved-in-pro-140 (Accessed 5th July 2018). b) *AIDS Patient Care ST.*, 2008, **22**, 159-160.

4.2.5.2. Reverse transcriptase inhibitors.

This class of antiretroviral drugs is the most widely used at present, most likely because they were the first to be researched and commercialised. 3'-Azido-2',3'-dideoxythymidine (AZT or Zidovudine), a thymidine analogue, was the first drug of its kind to reach commercial status in 1987 and was also one of the fastest drugs to make it through the pipeline in recent years; AZT was first proven to be active against HIV in the laboratory in 1985 and was approved by the FDA just 25 months later.[239] The nucleoside structure must first be phosphorylated by various kinases *in vivo* to be active, after which it bears a strong resemblance to thymidine triphosphate which is the natural substrate for the viral reverse transcriptase—the only difference is the replacement of the 3'-hydroxyl group in the endogenous substrate with an azide group (Figure 4.9).[240] Hence, in the phosphorylated form, the drug acts as a competitive inhibitor for viral reverse transcriptase, with AZT being incorporated into the proviral DNA strand. The next nucleotide is then rendered unable to form a bond between the 3' group and the phosphate group in 5' of the next nucleotide in the sequence, ultimately hindering viral DNA production and consequently viral replication.

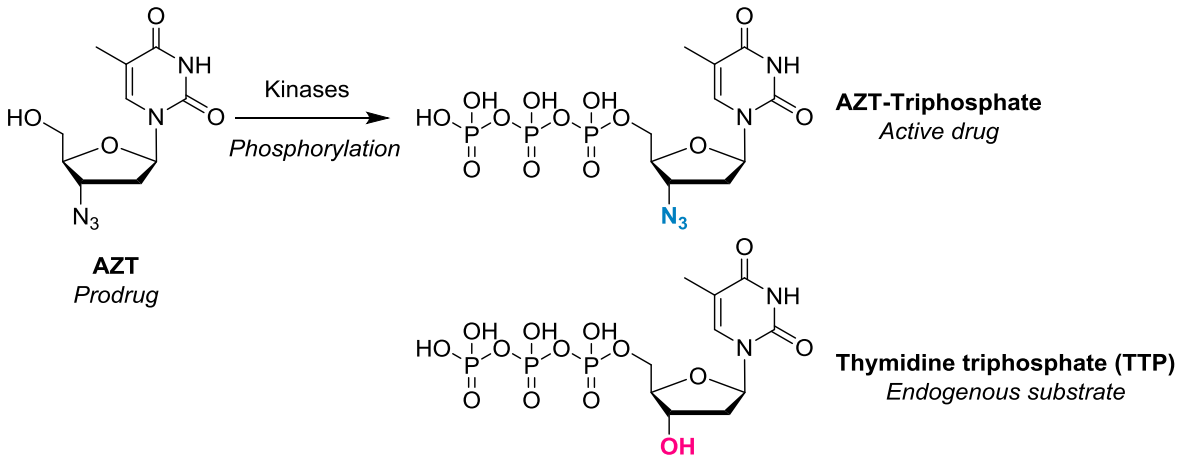

Figure 4.9. Structural similarities between AZT-triphosphate and TTP.

In the years following the introduction of AZT there were many developments in the area of reverse transcriptase inhibitors, and currently there are three different classes of these inhibitors on the market. These are nucleoside reverse transcriptase inhibitors (NRTIs), nucleotide reverse transcriptase inhibitors (NtRTIs) and non-nucleoside reverse transcriptase inhibitors (NNRTIs). Both NRTIs and NtRTIs

[239] H. Mitsuya, R. Yarchoan and S. Broder, *Science*, 1990, **249**, 1533-1544.
[240] A. R. Van Rompey, M. Johansson and A. Karlsson, *Pharmacol. Ther.*, 2000, **87**, 189-198.

have the same mode of action—as their name suggests, they are based on endogenous DNA bases and competitively inhibit the reverse transcriptase enzyme to hinder viral DNA production—but NNRTIs are more chemically diverse and act *via* a slightly different mechanism, since they are not based on the nucleotide substrate.

NNRTIs are generally more well suited to the task in hand, achieving better selectivities and binding affinities than N(t)RTIs, as well as having other pharmacokinetic and pharmacodynamic differences. For example, N(t)RTIs need metabolising *in vivo* to the active triphosphate form whereas NNRTIs can interact directly with the target and do not necessarily require prior activation. NNRTIs act by binding to an allosteric site on the reverse transcriptase enzyme roughly 10 Å away from the substrate binding site that is both structurally and functionally associated with the substrate binding site.[241] This binding pocket lies between the three-stranded β-sheet containing catalytic aspartic acid residues D110, D185 and D186, which changes conformation once bound to the NNRTI. Therefore, it is believed that the inhibitory effect is due to an inactive conformation at the substrate binding site when this allosteric pocket is occupied (Figure 4.10).

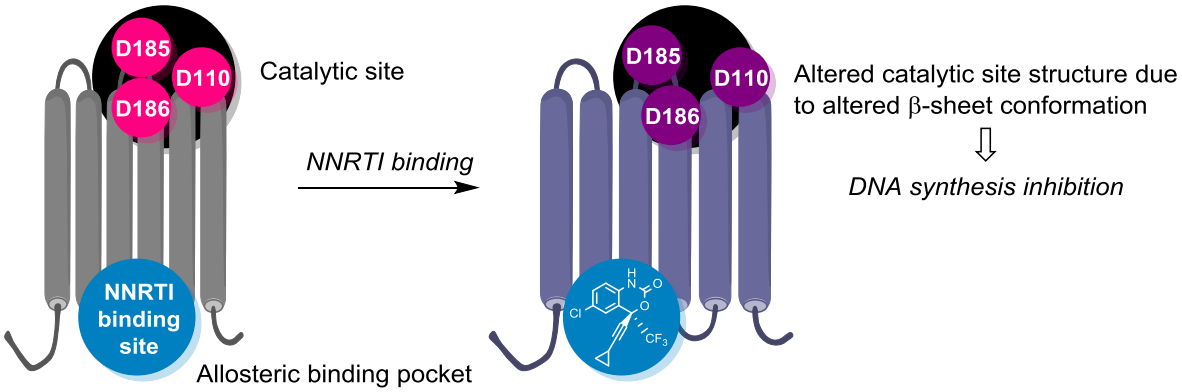

Figure 4.10. Mechanisms leading to reverse transcriptase inhibition by NNRTIs.

Although NNRTIs usually exert their inhibitory activity through binding to the same allosteric pocket, not all of these exploit the same interactions to induce the conformational changes leading to inhibition of DNA synthesis. This is somewhat due to the emergence of NNRTI-resistant strains of HIV; the rapid replication of the HIV-1 virus often results in a mutation around the NNRTI binding pocket, and therefore removes certain possible interactions. Since a mutation in the allosteric binding pocket does

[241] E. De Clerq, *Antiviral Res.*, 1998, **38**, 153-179.

not necessarily influence the catalytic ability and function of the enzyme, virus viability does not suffer from these mutations, resulting in various NNRTI-resistant strains.

The exact reasons for these mutations and the mechanisms of resistance are still poorly understood. Having said that, it has been shown that the Y181C and Y188L mutations confer resistance due to the elimination of favourable interactions formed between the drug and the enzyme, whereas the K103N mutation is thought to reduce the rate of NNRTI binding due to slightly altered structure of the binding pocket.[242]

For this reason, we must continue to develop structurally diverse drugs of this kind; there are currently over 30 different structural subgroups within this class of inhibitors (Figure 4.11). The first NNRTI, Nevirapine (marketed under the trade name Viramune and developed by Boehringer Ingelheim), was approved by the FDA in 1996. Nevirapine contains a tricyclic dipyridodiazepinone core, and interacts with residues Tyr-181 and Tyr-188.[243] This makes it susceptible to the K103N mutation, similar to the structurally different NNRTI Efavirenz.[244] This second drug was approved in 1998 by the FDA, and is one of the most important antiretroviral drugs on the market; it is included in the World Health Organisation's List of Essential Medicines, the safest and most effective drugs necessary for a functioning health system.[245]

Lersivirine was an investigational drug in development by ViiV Healthcare, but was recently discontinued since phase III results demonstrated that this drug was not as effective at inhibiting viral replication as other drugs currently on the market such as Efavirenz. Interestingly, this compound showed a different binding mode to other NNRTIs—forming interactions with Trp-229 with the 3,5-dicyanophenoxy ring—making its resistance profile somewhat different also. In this way, Lersivirine could have proved useful for patients presenting K103N or Y181C viral mutants.[246] A second drug, Fosderivine, was also in development by ViiV Healthcare, but was discontinued when a phase II study resulted in 5 of 35 patients suffering seizures.[247] Nevertheless, these studies could provide useful insights for the development of a new generation of NNRTIs.[248]

---

[242] V. Miller, M.-P. de Béthune, A. Kober, M. Stürmer, K. Hertogs, R. Pauwels, P. Stoffels and S. Staszewski, *Antimicrob. Agents Chemother.*, 1998, **42**, 3123-3129.

[243] D. Richman, C.-K. Shih, I. Lowy, J. Rose, P. Prodanovich, S. Goff and J. Griffin, *PNAS*, 1991, **88**, 11241-11245.

[244] G. L. Melikian, S.-Y. Rhee, V. Varghese, D. Porter, K. White, J. Taylor, W. Towner, P. Troia, J. Burack, E. DeJesus, G. K. Robbins, K. Razzeca, R. Kagan, T. F. Liu, W. J. Fessel, D. Israelski and R. W. Shafer, *J. Antimicrob. Chemother.*, 2014, **69**, 12-20.

[245] http://www.who.int/medicines/publications/essentialmedicines/en/ (Accessed 7th July 2018).

[246] M. Platten and G. Fätkenheuer, *Expert Opin. Investig. Drugs*, 2013, **22**, 1687-1694.

[247] D. A. Margolis, J. J. Eron, E. DeJesus, S. White, P. Wannamaker, B. Stancil and M. Johnson, *Antivir. Ther.*, 2014, **19**, 69-78.

[248] M.-P. de Béthune, *Antivir. Res.*, 2010, **85**, 75-90.

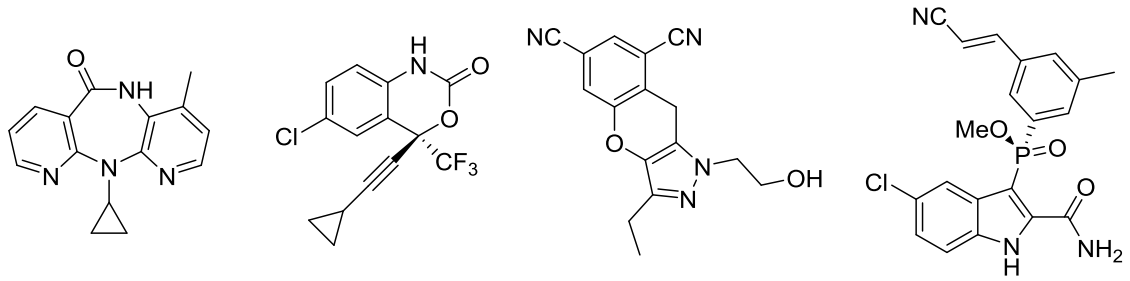

Nevirapine
FDA approved 1996

Efavirenz
FDA approved 1998

Lersivirine
Discontinued

Fosdevirine
Discontinued

Figure 4.11. Varying structures of approved and discontinued NNRTIs.

4.2.5.3. Integrase Inhibitors.

Integrase is the enzyme responsible for the integration of the proviral DNA into the host DNA, hence the name *integrase*. The functional enzyme is produced *via* proteolytic cleavage of the Gag-Pol polypeptide coded by the *pol* gene.[249] Despite its vital importance in the replication cycle of HIV-1, compounds targeting the integrase enzyme represent a relatively new class of antiretroviral drugs. This has been attributed to the complexity of the integration process—although once we understood the reaction and *in vitro* models were available, the first integrase inhibitors were developed fairly rapidly. Raltegravir (marketed by Merck as its potassium salt under the trade name Isentress), the first small-molecule integrase inhibitor, was approved for use in 2007 (Figure 4.12).[250] Originally it was only approved for use in patients in which other first-line treatments had no effect, but in 2009 it was approved for use as a first-line treatment in all patients and is now included in the World Health Organisation's List of Essential Medicines, just like Efavirenz.[244, 245] Since then, several more examples of integrase inhibitors have been approved, such as Elvitegravir (trade name Stribild, developed by Gilead Sciences) and Dolutegravir (trade name Tivicay, developed by ViiV Healthcare), as well as many more in the pipeline.

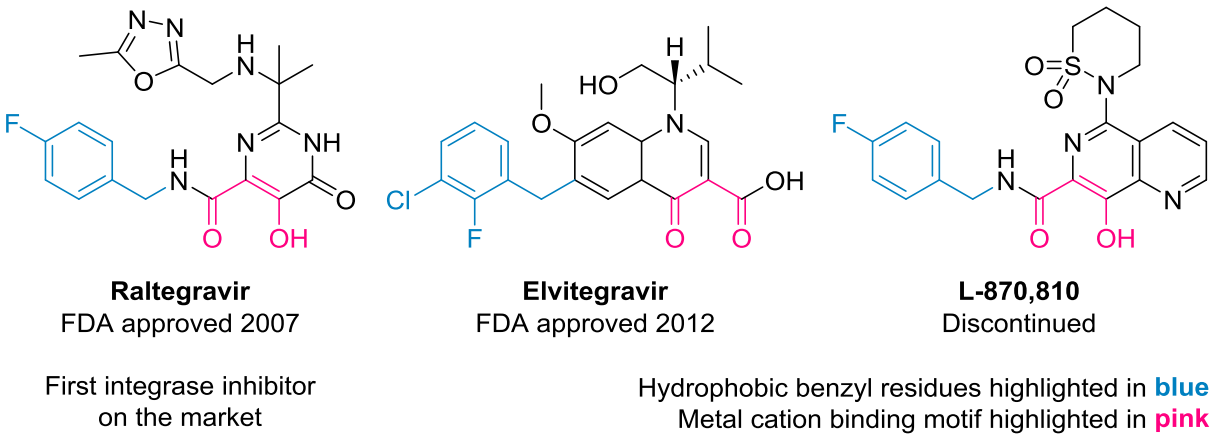

Figure 4.12. Chemical structure of some integrase inhibitors showing common features.

Integrase is made up of three separate sections, and all three are necessary for its catalytic activity: the N-terminal domain; the catalytic core domain; and the C-terminal domain. The N-terminal domain contains an essential His-His-Cys-Cys sequence (specifically His-12, His-16, Cys-40 and Cys-43), which

[249] D. J. McColl and X. Chen, *Antivir. Res.*, 2010, **85**, 101-118.
[250] S. Sayana and H. Khanlou, *Expert Rev. Infect. Ther.*, 2008, **6**, 419-428.

together chelate a zinc ion (Zn^{2+}) to form a zinc-finger motif. The core catalytic domain contains three completely conserved residues responsible for the activity, which are Asp64, Asp116 and Glu152—also known as the DDE triad. Between them these residues chelate two positive ions, Mg^{2+} or Mn^{2+}, which act as a guide for the viral DNA. The final C-terminal domain contains non specific DNA binding sites, and is responsible for binding the viral DNA which is then pulled through to the core catalytic domain in order for strand transfer to occur.[251] Current integrase inhibitors block this process, and therefore they are termed INSTIs (**IN**tegrase **S**trand **T**rans**f**er **I**nhibitors).

The INSTI mechanism of action has been studied in detail; for example, in 2008 Chen *et al.*[252] used computational modelling to show how this class of molecules binds to the enzyme and therefore blocks integrase activity, using an investigational drug denominated L-870,810 that was discontinued after liver and kidney toxicity was discovered in dog models.[253] This compound is structurally similar to both Raltegravir and Elvitegravir, and contains similar motifs that allow it to exert an inhibitory effect on the HIV-1 integrase enzyme (Figure 4.12). The mode of action of these INSTIs is based on the competitive chelation of the divalent metal ions in the catalytic core domain used to guide the viral DNA into the host DNA, preventing the continuation of the integration process (Figure 4.13). This is augmented by the benzyl residue favourably interacting with a hydrophobic pocket which opens up only at certain points of the integration process—when the inhibitor binds to this site and chelates the metal ion, the integrase structure is rendered more rigid and the integration reaction is inhibited.

Despite these advances, we now know that integrase is important for more than this pivotal role in the replication cycle of HIV-1, such that future integrase inhibitors may not inhibit the actual integration process itself, but other important processes that may be mediated by integrase.[254]

[251] M. Thomas and L. Brady, *Trends Biotechnol.*, 1997, **15**, 167-172.
[252] X. Chen, M. Tsiang, F. Yu, M. Hung, G. S. Jones, A. Zeynalzadegan, X. Qi, H. Jin, C. U. Kim, S. Swaminathan and J. M. Chen, *J. Mol. Biol.*, 2008, **380**, 504-519.
[253] F. W. N. M. Wit, J. M. A. Lange and P. A. Volberding, in *Global HIV/AIDS Medicine*, ed. P. A. Volberding, M. A. Sande, W. C. Greene, J. M. A. Lange and J. E. Gallant, Elsevier, Amsterdam, 1st edn., 2008, ch. 12, pp. 123-135.
[254] T. Masuda, *Front. Microbiol.*, 2011, **2**, 1-5.

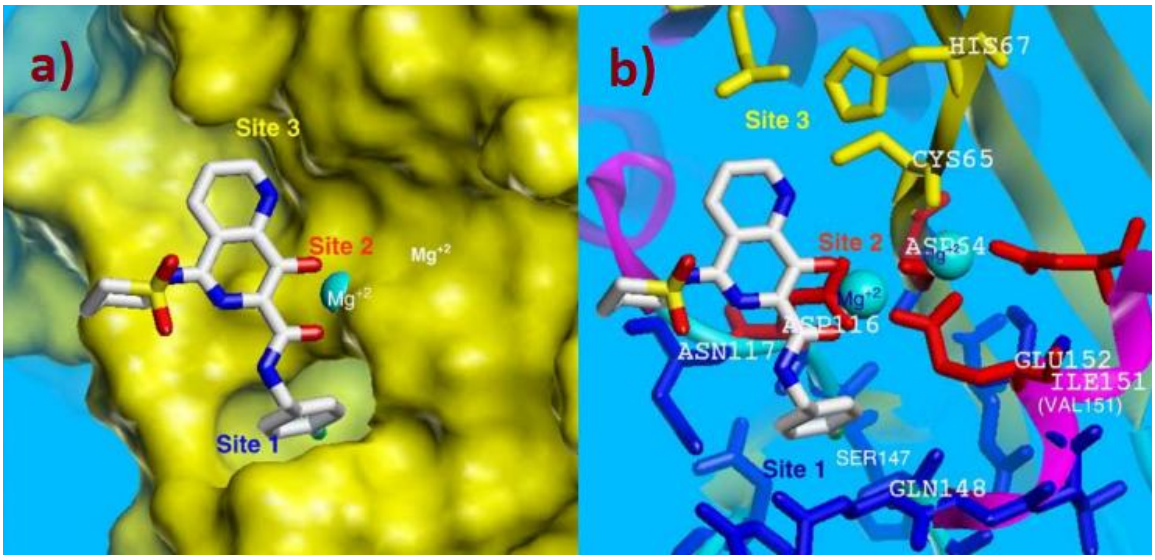

Figure 4.13. a) Coordination of L-870,810 (white stick model) to the catalytic core domain of HIV-1 integrase (yellow surface) showing the 3D structure of the hydrophobic pocket (Site 1). b) Model with key residues highlighted; the hydrophobic pocket in blue and the DDE triad chelating the Mg^{2+} ions in red (Site 2). Taken from Chen *et al.*[252]

4.2.5.4. Protease inhibitors.

This class of drugs inhibits the action of viral protease, and represents the second class of antiretroviral therapy to be approved for use. Protease is responsible for the cleavage of polypeptides resulting from the translation of viral mRNA, thereby producing important viral proteins necessary for the formation of new virions. Saquinavir, the first example of a protease inhibitor, was developed by Hoffman-La Roche and approved for use in 1995 after another incredibly short application process lasting just 97 days. The rapid clinical phases seen in some antoretroviral therapies, such as AZT and Saquinavir, is a testament to the desperation of the AIDS epidemic in early years; between 1980 and 1987 when AZT was first approved there was absolutely no way of treating HIV infection, and a positive diagnosis was essentially a death sentence.

Protease inhibitors are now widely used in HAART, along with reverse transcriptase and integrase inhibitors, and generally present a peptidomimetic structure mimicking the native substrate. For example, Saquinavir contains a hydroxyethylamine moiety in place of a peptide bond, granting it a 3D structure similar to an intermediate transition-state stabilised by the enzyme during peptide cleavage (Figure 4.14). However, a common problem with drugs with peptide-based structures of this type is that the oral availability is hampered due to affinity for efflux pumps, decreasing its oral availability—something that could have been detected earlier, had more detailed clinical trails been carried out.[255] Problems with peptide-based structures as drugs will be discussed in more detail in the following section.

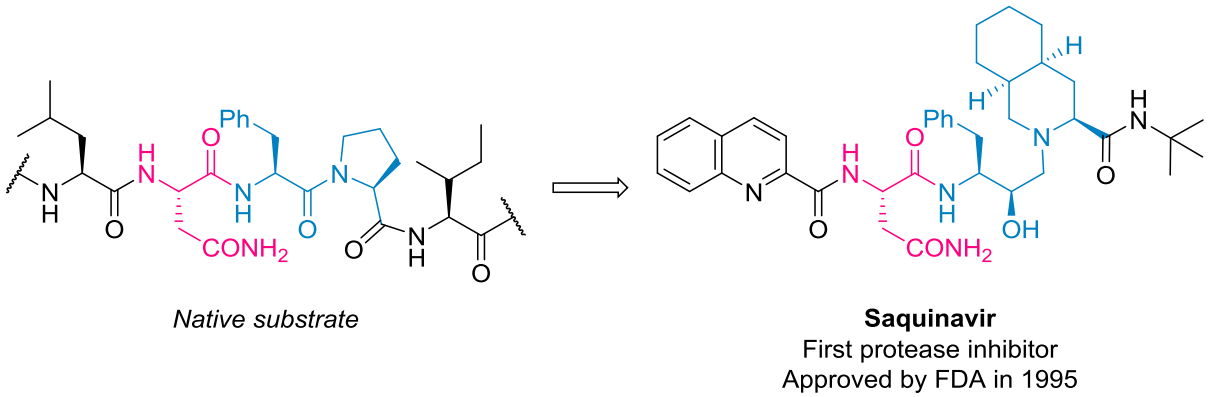

Figure 4.14. Structural basis of the first protease inhibitor Saquinavir.

[255] A. Sosnik, D. A. Chiappetta and A. M. Carcaboso, *J. Control. Release*¸ 2009, **138**, 2-15.

Since then, there has been a trend in new protease inhibitors to contain fewer peptide bonds, in an attempt to avoid the interaction with efflux pumps, whilst maintaining affinity for the protease active site.[256]

[256] C.-H. Shen, Y.-F. Wang, A. Y. Kovalevsky, R. W. Harrisson and I. T. Weber, *FEBS J.*, 2010, **277**, 3699-3714.

4.3. Peptidomimetics.

4.3.1. Introduction.

The identification of small-molecule peptidomimetics is key in the development of new molecular entities that are able to interfere with biological processes mediated by peptides or proteins. The idea behind peptidomimetics, as the name suggests, is to mimic the 3D structure of a peptide; a premise that has gained increasing interest recently as the scientific community unravels the mysteries of cellular processes, due to emerging areas such as proteomics.[257] Protein-protein interactions are ubiquitous in biological systems, regulating a plethora of processes from recognition and signal transmission to apoptosis, and therefore interfering with this type of interactions could give rise to pharmaceuticals with unprecedented activities and novel modes of action. However, traditional methods of interfering with these interactions—logically, through the use of peptide drugs—present certain problems. Nevertheless, there are still several examples of peptide drugs such as insulin or oxytocin, although they represent just 2% of the global market.

Peptide drugs face many challenges with absorption, distribution, metabolism and excretion (ADME).[258] Firstly, the low lipophilia of the peptide bond and ability to form many hydrogen bonds render most peptides incapable of passing lipid membranes, and therefore they generally demonstrate very low bioavailability (<1%), although there are some exceptions such as cyclosporine A (a cyclic peptide used as an orally active immunosuppressive drug).[259] Secondly, peptides are susceptible to cleavage and elimination by endogenous proteases. Due to the fundamental role that proteins and peptides play in biological systems, there are also many ways of removing them from the body quickly and efficiently, in order to effectively control the levels of hormones and other peptides. Consequently, the amount of peptide drugs that are finally approved for use is very low: a recent study of 484 peptide drug candidates found that eventually 54% were discontinued, and only 12% were approved.[260]

For these reasons, Lipinski famously described a series of drug-like qualities—generally known as *Lipinski's rule of 5*—that new drug candidates should present to have the best chance of success during

[257] M. K. P. Jayatunga, S. Thompson and A. D. Hamilton, *Bioorganic Med. Chem. Lett.*, 2014, **24**, 717-724.
[258] L. Di, *AAAPS J.*, 2015, **17**, 134-143.
[259] T. Rezai, J. E. Bock, M. V. Zhou, C. Kalyanaraman, R. S. Lokey and M. P. Jacobson, *J. Am. Chem. Soc.*, 2006, **128**, 14073-14080.
[260] J. L. Lau and M. K. Dunn, *Bioorganic Med. Chem.*, 2018, **26**, 2700-2707.

clinical trials.[261] These guidelines state that an orally administered drug should violate no more than one of the following rules:

- No more than five hydrogen-bond donors (N—H or O—H bonds)
- No more than ten hydrogen bond acceptors (N or O atoms)
- A molecular mass less than 500 $gmol^{-1}$
- A log*P* value not greater than 5

The great majority of drugs follow these rules, although as with any general rule, there are plenty of exceptions. Oral administration of drugs is far preferred to any other method as it is non-intrusive, most convenient for both medical professionals and the patient, and presents the best patient compliance. However, the oral administration of drugs presents certain challenges. For a drug to be well absorbed *via* oral administration, it must have high membrane permeability in order to pass through the walls of the intestine into the blood stream. Furthermore, it must first survive in the acidic conditions and metabolism of the stomach and to a certain extent that of the liver, to remain in the plasma for the time necessary to exert the desired effect. Peptides therefore must be injected directly into the patient's blood stream in order to avoid metabolism in the stomach and to bypass membrane permeability issues; although this means patients must either inject themselves or visit the doctor for each injection, neither of which is an ideal situation.

The use of peptidomimetics provides a solution to this problem. By using small molecules that mimic just the active fragment of the peptide—often referred to as the pharmacophore—the compound is much more likely to fall within Lipinski's guidelines, and ultimately more likely to reach marketable status. Peptidomimetics can be classified into several distinct groups, as seen in the following sections.

[261] C. A. Lipinski, *Drug Discov. Today Technol.*, 2004, **1**, 337-341.

4.3.2. Classification of peptidomimetics.

Historically, peptidomimetics have been classified into type-I, type-II and type-III mimics. This classification can often be fairly blurred at the edges, especially between type-I and type-II peptidomimetics.[262] The first class is generally referred to as containing peptidomimetics directly based on the peptide backbone, often matching atom-for-atom the backbone of the native peptide agonist. Consequently, these compounds rely heavily on mimicking the same interactions that the native peptide would make with the receptor. On the other hand, type-II mimetics originally emerged as *functional* mimetics—compounds found to interact with a certain peptide receptor. Initially, these compounds were therefore presumed to contain a structure similar to the native peptide, although this was later proved incorrect. Type-II peptidomimetics do not necessarily bind to exactly the same site as the native peptide. On the contrary, they often act as allosteric inhibitors. The classification of type-III peptidomimetics, however, is much more straightforward; type-III peptidomimetics are non-peptide small molecules that contain structural motifs capable of projecting certain functional groups into the correct 3D space in order to interact favourably with the receptor.

Recently, Grossmann *et al.* described a similar classification system based on the actual structure of the peptidomimetic, removing the element of doubt between certain classes.[263]

- Class A. Small peptide-based structures with a peptide backbone and slight modifications to side chain structure.
- Class B. Small peptide-based structures with a modified peptide backbone, and perhaps more modifications to side chain structure.
- Class C. Non-peptide small molecules that are capable of projecting substituents into a configuration analogous to the peptide.
- Class D. Non-peptide small molecules that have an unrelated structure but mimic the mode of action.

Of these, class C structures will be the most important to this project, representing the “ideal” within the concept of peptidomimetics.

[262] A. S. Ripka and D. H. Rich, *Curr. Opin. Chem. Biol.*, 1998, **2**, 441-452.
[263] M. Pelay-Gimeno, A. Glas, O. Koch and T. N. Grossmann, *Angew. Chem. Int. Ed.*, 2015, **54**, 8896-8927.

4.3.3. Strategies in peptidomimetic design.

Many strategies exist for the design of peptidomimetics. Traditionally, these were generally peptide-based modifications to side chains in order to lock certain conformations; the shift from a full-length peptide chain to just the pharmacophore can remove important structural features.[264] Some common class A and B modifications can be seen in Figure 4.15 using an example peptide.

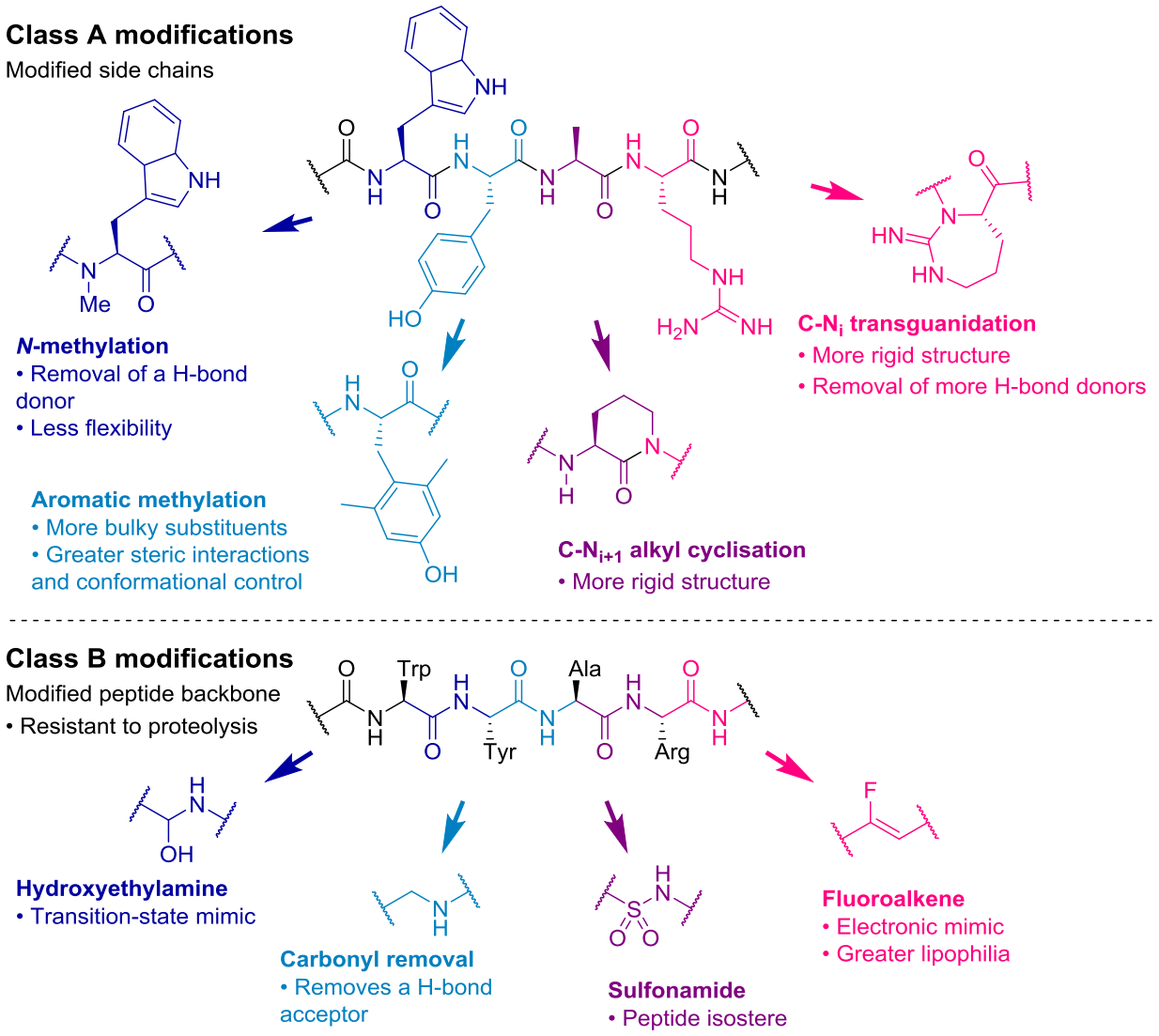

Figure 4.15. Class A and B modifications using an example Trp-Tyr-Ala-Arg sequence.

[264] a) V. J. Hruby and P. M. Balse, *Curr. Med. Chem.*, 2000, **7**, 945-970. b) M. Szelke, B. Leckie, A. Hallett, D. M. Jones, J. Sueiras, B. Atrash and A. F. Lever, *Nature*, 1982, **299**, 555-557.

In modern times, with more knowledge of structural biology and chemistry we have shifted more towards the use of class C peptidomimetics. In this sense, certain privileged structures present the necessary conformations to properly mimic various peptide structural motifs.

Class C mimics are somewhat more complex since they generally focus on the secondary structures of proteins and are not based on peptide backbones, although they can generally be grouped into three distinct types depending on the motif they mimic: turns, β-sheets, or α-helices (Figure 4.16).

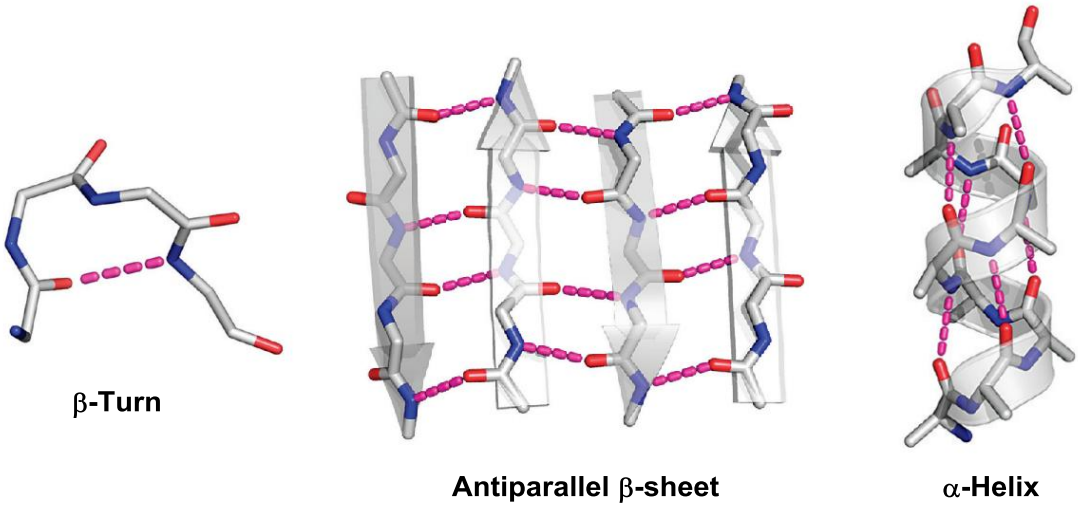

Figure 4.16. Important protein secondary structures and common motifs in peptidomimetic design.[265]

[265] O. Koch, J. Cole, P. Block and G. Klebe, *J. Chem. Inf. Model*, 2009, **49**, 2388-2402.

4.3.3.1. Turn mimics.

Turn structures are extremely common in nature; without this class of structural motif proteins would not be able to adopt the folded and globular forms we so often encounter in protein structure. Although there are many forms of turn structure, depending on the number of amino acid residues between the key C=O---HN hydrogen bond, the most common are β-turns (also denominated β-hairpins or reverse turns) and γ-turns (Figure 4.17).[266] Given that γ-turns are fairly similar to the open chain conformation, in this section we will focus on the related β-turns.

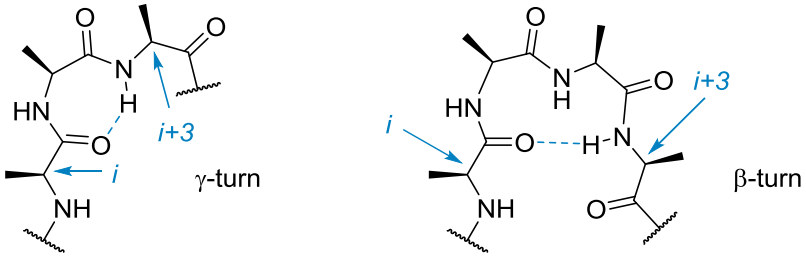

Figure 4.17. γ- and β-turns.

Among the first small-molecule β-turn mimics was thiazolidinone **4.1**, found to mimic the structure of the D-Ala-L-Pro turn.[267] It's worth mentioning that proline plays a unique role in these situations; being the only natural amino acid containing a cyclic structure, it lacks an N—H hydrogen bond donor and provides rigidity and conformational bias towards a turn-like structure (Figure 4.18).[263] Although **4.1** is a peptide-based structure, this discovery paved the way to other class C small molecules that successfully mimic the structure of a β-turn without the need for peptide bonds. Of these, perhaps the most common is the benzodiazepine structure **4.2**, which was first demonstrated to mimic a Pro-Ala junction by Ripka and De Lucca in 1993, just like the thiazolidinone structure described previously.[268] In addition, carbohydrate-based structures **4.3** have been found to mimic the β-turn conformation found in Somatostatin (based on existing cyclic class A peptidomimetic **4.4**).[269] More recently, in 2011 Boger *et*

[266] C. Toniolo and E. Beneditti, *Crit. Rev. Biochem.*, 1980, **9**, 1-44.
[267] U. Nagai and K. Sato, *Tetrahedron Lett.*, 1985, **26**, 647-650.
[268] W. C. Ripka, G. V. De Lucca, A.C. Bach II, R. S. Pottorf and J. M. Blaney, *Tetrahedron*, 1993, **49**, 3593-3608.
[269] R. Hirschmann, K. C. Nicolaou, S. Pietranico, J. Salvino, E. M. Leahy, P. A. Sprengeler, G. Furst and A. B. Smith III, *J. Am. Chem. Soc.*, 1992, **114**, 9218-9220.

al. designed a library of *trans*-pyrrolidine-3,4-carboxamides **4.5** that were proven to be efficient inhibitors of various opioid receptors that recognise a β-turn motif in their endogenous ligands.[270]

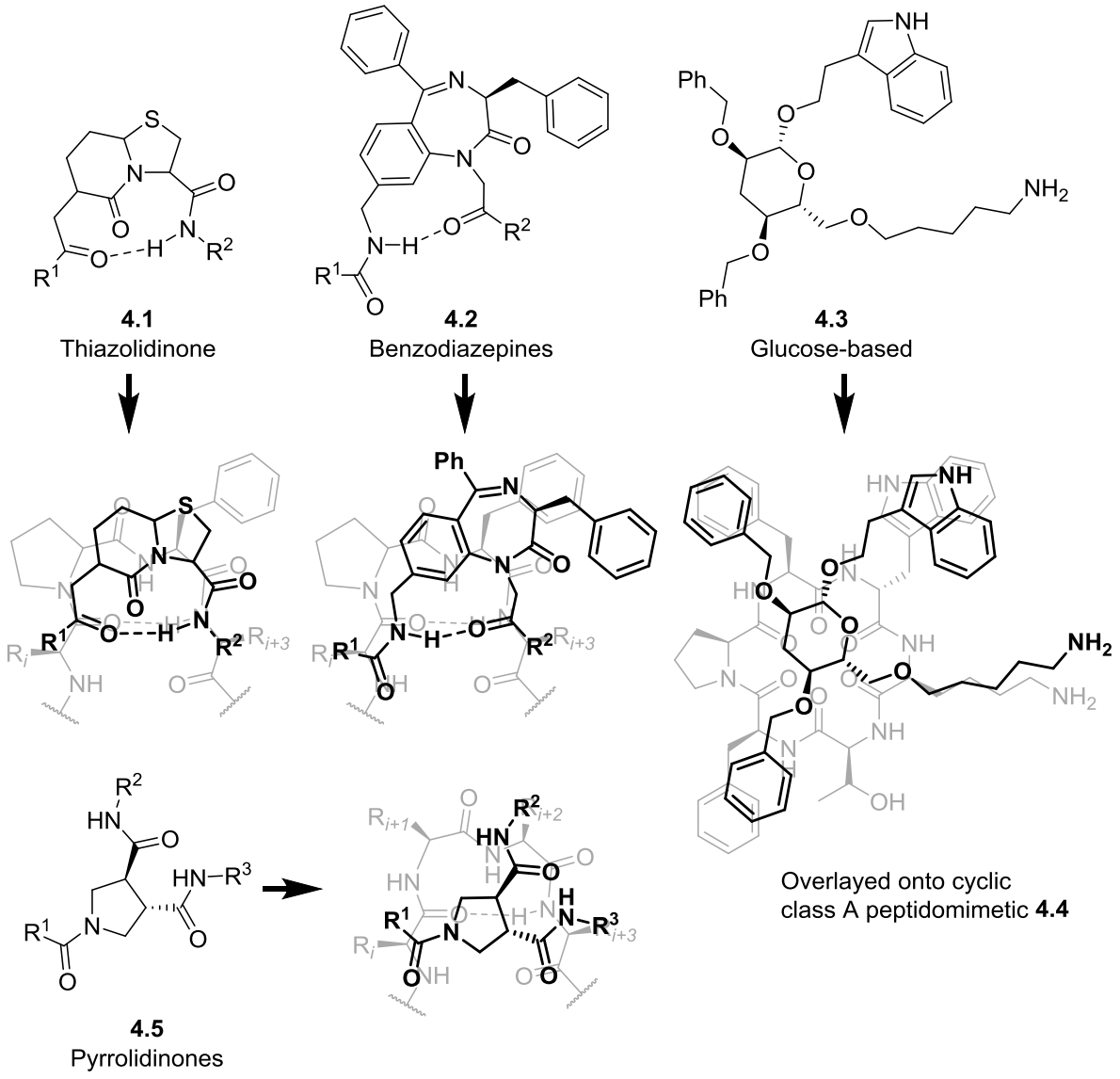

Figure 4.18. Selected β-turn structural mimics.

[270] L. R. Whitby, Y. Ando, V. Setola, P. K. Vogt, B. L. Roth and D. L. Boger, *J. Am. Chem. Soc.*, 2011, **133**, 10184-10194.

4.3.3.2. β-Sheet mimics.

This type of structure is in some ways an extension of the previously mentioned β-turns, in that the turn allows the peptide to fold over onto itself in such a way that the two chains are aligned in parallel, held together by hydrogen bonds between them. This conformation forces the side chain residues to adopt an alternating up-down configuration, and prevents same-chain hydrogen bonding.[271] Therefore, structural mimics of β-sheets and β-hairpins began with the corresponding β-turn mimics discussed previously, with early studies focusing on the same Pro-Ala turn formation and ways to stabilise small β-hairpin type formations.[272] This was achieved using several specifically designed structures—including epindolidiones,[273] 5-amino-2-methoxybenzamide derivatives,[274] 1,2-dihydro-3(6*H*)-pyridinone units,[275] and diphenylacetylenes,[276] among others—to force a small peptide to adopt the desired conformation (Figure 4.19).

Due to the complexity of β-sheet conformations—they rely heavily on hydrogen-bond stabilisation and contain large spaces between each set—there are relatively few class C examples of this type (Figure 4.20).[263] One of the first examples of a structural mimetic was the 1,3-disubstituted triazole backbone, which adopts a zig-zag conformation reminiscent of the β-sheet structure in solution.[277] An elegant example came from Hamilton and Wyrembak in 2009 with the disclosure of 2,2-disubstituted indolin-3-ones as β-sheet mimetics.[278] This class of compound was found to be the same length as five peptide residues, with the substituents in the 2 positions of each subsequent indolinone lining up almost exactly with the residues in the *i*, *i* + 2, and *i* + 4 positions respectively. More recently, Burgess *et al.* demonstrated how subtle changes in the building blocks of a sequence can dramatically change the 3D structure of the whole compound.[279] These authors used either piperidine-piperidinone or pyrrolidine-pyrrolidinone to produce peptidomimetics, and found that the pentamer based on 6-membered rings mimicked a β-sheet structure, whereas the related compound constructed of 5-membered rings mimicked an α-helix.

[271] B. L. Sibanda and J. M. Thornton, *Nature*, 1985, **316**, 170-174.
[272] T. S. Haque, J. C. Little and S. H. Gellman, *J. Am. Chem. Soc.*, 1996, **118**, 6975-6985.
[273] D. S. Kemp, B. R. Bowen and C. C. Muendel, *J. Org. Chem.*, 1990, **55**, 4650-4657.
[274] J. S. Nowick, D. L. Holmes, G. Mackin, G. Noronha, A. J. Shaka and E. M. Smith, *J. Am. Chem. Soc.*, 1996, **118**, 2764-1765.
[275] S. T. Phillips, M. Rezac, U. Abel, M. Kossenjans and P. A. Bartlett, *J. Am. Chem. Soc.*, 2002, **124**, 58-66.
[276] H. Lingard, J. T. Han, A. L. Thompson, I. K. H. Leung, R. T. W. Scott, S. Thompson and A. D. Hamilton, *Angew. Chem.,* 2014, **126**, 3724-3727.
[277] N.G. Angelo and P.S. Arora, *J. Am. Chem. Soc.*, 2005, **127**, 17134-17135.
[278] P.N. Wyrembak and A.D. Hamilton, *J. Am. Chem. Soc.*, 2009, **131**, 4566-4567.
[279] D. Xin, L.M. Perez, T.R. Ioerger and K. Burgess, *Angew. Chem. Int. Ed.*, 2014, **53**, 3594-3598.

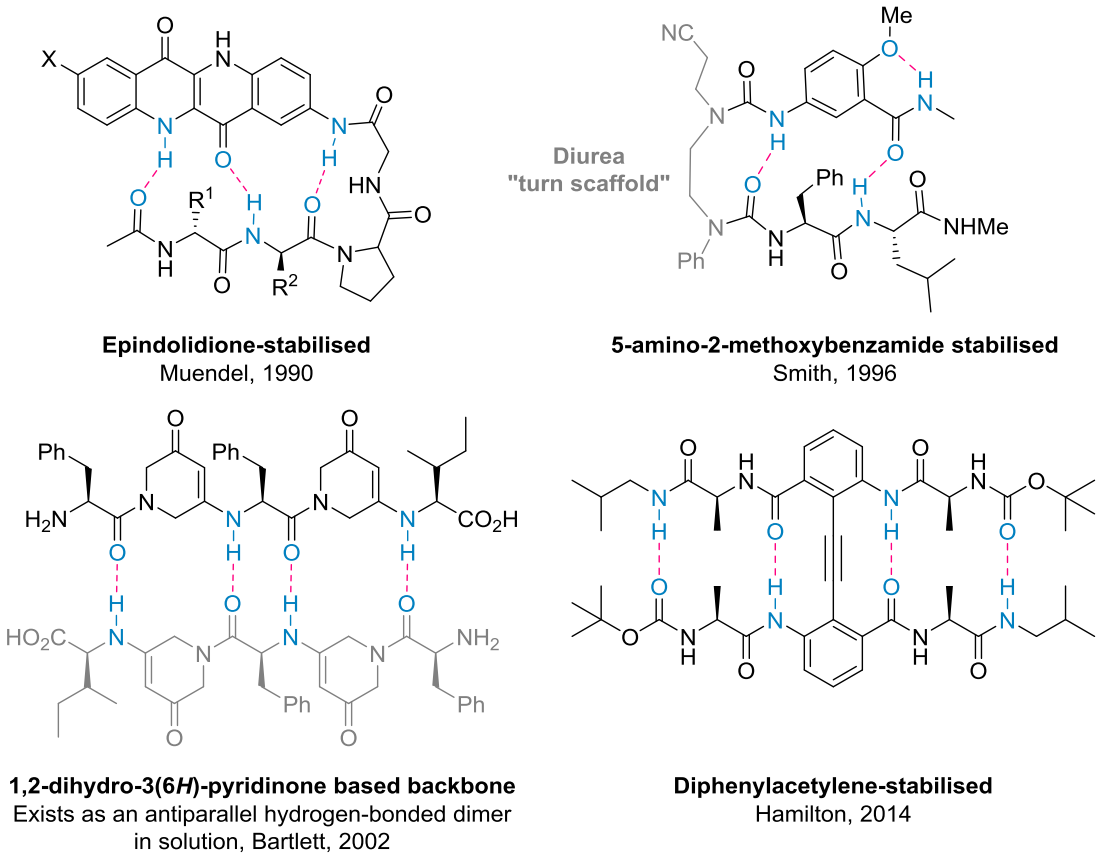

Figure 4.19. Selected β-sheet mimetics based on stabilisation and conformation locking of peptides.

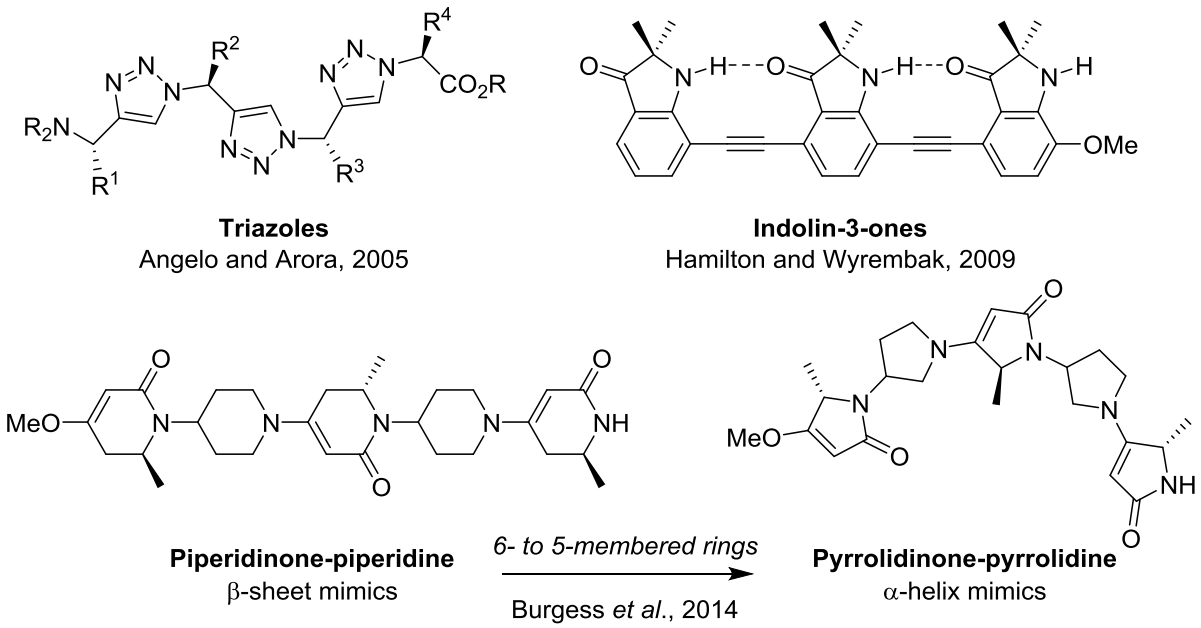

Figure 4.20. Selected structural class C mimics of β-sheets.

4.3.3.3. α-Helix mimics.

α-Helices are abundant in nature, regulating uncountable biological processes through protein-protein, protein-RNA or protein-DNA interactions, among others. The previously discussed HIV-1 Rev protein (*see Section 4.2.4. Regulatory protein Rev*) is just one example of a protein presenting this structure, but there are many more—in fact, it is estimated that helices make up 30-40% of structured protein domains.[263] Much like the related β-hairpin mimics, early examples focused on the stabilisation of short peptide chains into helical conformations *via* one of two ways. The first of these is through covalent bonds between adjacent side chains: the formation of disulfides,[280] lactams,[281] and the ring-closing metathesis of olefins[282] have all been used to this end. The second is through non-covalent interactions between side chains, such as hydrophobic interactions,[283] ion pairs[284] or cation-π interactions (Figure 4.21).[285]

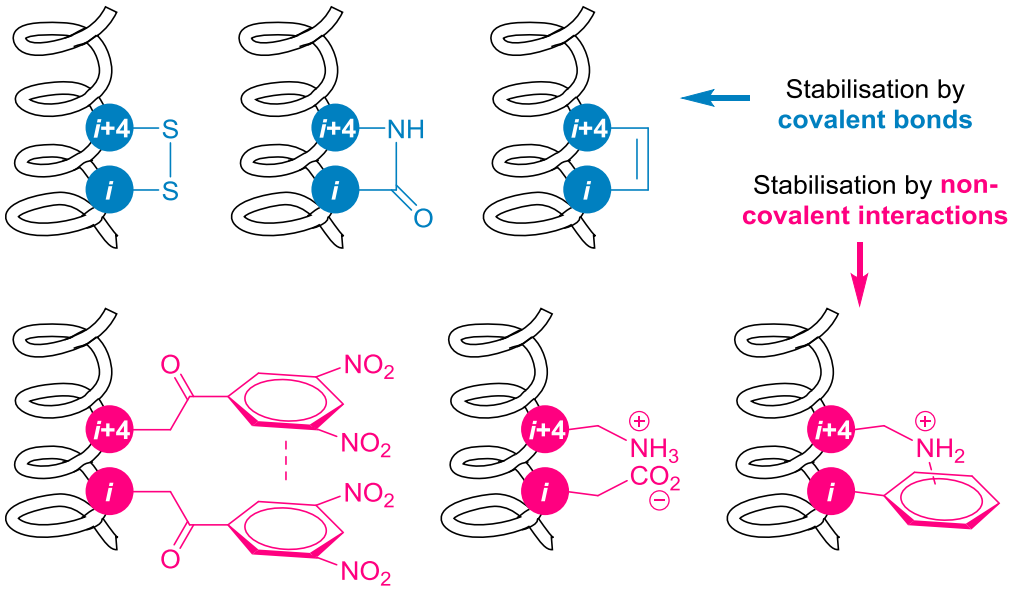

Figure 4.21. Schematic depiction of the different methods employed to stabilise α-helices.

Many advances have been made over the past decade towards improved class C mimics of the α-helix structure, starting with the pioneering work by Howson *et al*. involving 1,6-disubstituted indanes which

[280] D. Y. Jackson, D. S. King, J. Chmielewski, S. Singh and P. G. Schultz, *J. Am. Chem. Soc.*, 1991, **113**, 9391-9392.
[281] C. Yu and J. W. Taylor, *Bioorg. Med. Chem.*, 1999, **7**, 161-175.
[282] H. E. Blackwell and R. H. Grubbs, *Angew. Chem. Int. Ed.*, 1998, **37**, 3281-3284.
[283] J. S. Albert and A. D. Hamilton, *Biochemistry*, 1995, **34**, 984-990.
[284] J. M. Scholtz, H. Qian, V. H. Robbins and R. L. Baldwin, *Biochemistry*, 1991, **32**, 9668-9676.
[285] L. K. Tsou, C. D. Tatko and M. L. Waters, *J. Am. Chem. Soc.*, 2002, **124**, 14917-14921.

mimicked the positions *i* and *i* + 1 of an α-helical dipeptide fragment.[286a] Although this work cannot fully be considered an α-helix mimetic—given that at least 5 residues are required to form an α-helix—it paved the way to more structurally diverse and complex studies. The same group also extended this to the 1,1,6-trisubstituted indanes—mimics of the *i* - 1, *i*, and *i* + 1 residues—that were shown to have affinity for tachykinin receptors, which have important implications in apoptosis processes (Figure 4.22).[286b]

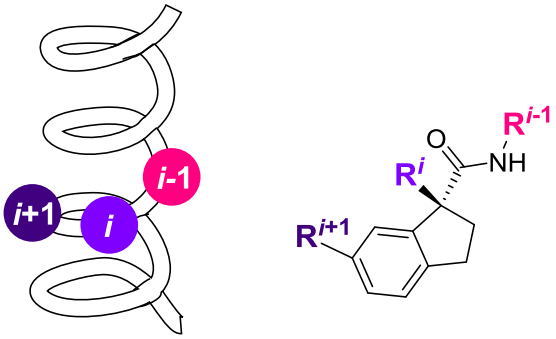

Figure 4.22. Pioneering work by Howson *et al.* into the use of indanes as α-helix mimics.

Following this, in the year 2001 Hamilton and co-workers described a backbone that would revolutionise the area of α-helix mimics; the *p*-terphenyl.[287] This was the first report to tackle the mimicry of a large area of an α-helix, over more than two turns. In their seminal report, the authors described how the three substituents on each ring of the *p*-terphenyl mimicked almost perfectly the residues *i*, *i* + 3 (or *i* + 4) and *i* + 7 of an α-helix (Figure 4.23). This is due to the staggered conformation of the terphenyl rings, produced by the steric repulsion between the substituent in *ortho* with the hydrogen of the adjoining ring. This strategy was then used to design inhibitors for the interaction between calmodulin (a protein that serves as the primary receptor for intracellular Ca^{2+} and contains an α-helix crucial for target binding) with smooth muscle myosin light chain kinase (a calmodulin receptor),[288] resulting in several terphenyl derivatives with potent inhibitory activity (Figure 4.23). This was taken further and the same compounds were used to inhibit the interaction between calmodulin and 3'-5'-cyclic nucleotide phosphodiesterase, an enzyme whose function it is to degrade the

[286] a) D. C. Horwell, W. Howson, W. P. Nolan, G. S. Ratcliffe, D. C. Rees and H. M. G. Willems, *Tetrahedron*, 1995, **51**, 203-216. b) D. C. Horwell, W. Howson, G. S. Ratcliffe and H. M. G. Willems, *Bioorg. Med. Chem.*, 1996, **4**, 33-42.
[287] B. P.Orner, J. T. Ernst and A. D. Hamilton, *J. Am. Chem. Soc.*, 2001, **123**, 5382-5383.
[288] W. E. Meador, A. R. Means and F. A. Quiocho, *Science*, 1992, **257**, 1251-1255.

phosphodiester bond in cyclic adenosine monophosphate (cAMP),[289] with IC_{50} values in the nanomolar range. The same authors went on to develop terphenyl inhibitors for a number of biological processes, such as the Bak/Bcl-X_L anti-apoptotic protein-protein interaction (which has previously been inhibited through the use of covalently stabilised short peptide chains)[290] and even HIV-1 cell entry (Figure 4.23).[291] The latter is based on the disruption of the gp41 core complex within the Env core (refer to Figure 4.8), preventing the virus fusion process. This is achieved by interfering with the folding of the gp41 proteins into the six-helix bundle to approximate the virus to the cell membrane; the hydrophobic terphenyl successfully mimics a region of the C- or N-terminal rich in Leu and Ile residues. Furthermore, in 2006 the authors elucidated how the substitution of the central phenyl ring for an indane could mimic both the *i* + 3 and *i* + 4 residues, along with the standard *i* and *i* + 7.[292]

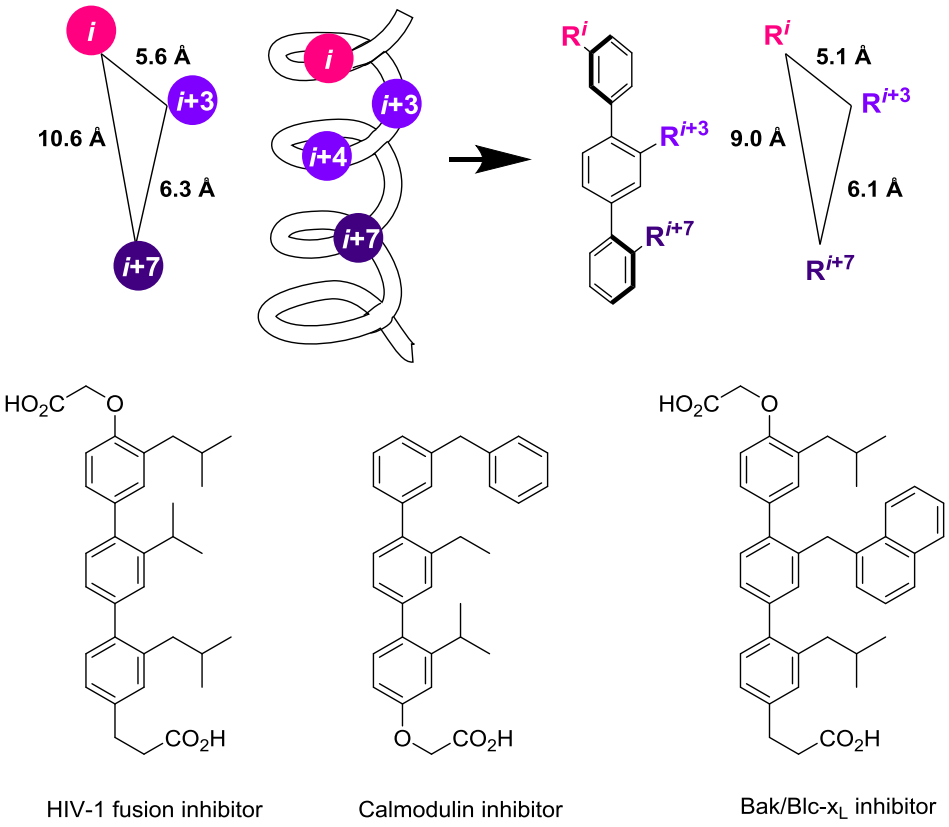

Figure 4.23. *p*-Terphenyls as α-helix mimics; note the similar distances between the three residues.

[289] T. Yuan, M. P. Walsh, C. Sutherland, H. Fabian and H. J. Vogel, *Biochemistry*, 1999, **38**, 1446-1455.

[290] a) O. Kutzki, H. Soon Park, J. T. Ernst, B. P. Orner, H. Yin and A. D. Hamilton, *J. Am. Chem. Soc.*, 2002, **124**, 11838-11839. b) H. Yin, G.-I. Lee, K. A. Sedey, O. Kutzki, H. S. Park, B. P. Orner, J. T. Ernst, H.-G. Wang, S. M. Sebti and A. D. Hamilton, *J. Am. Chem. Soc.*, 2005, **127**, 10191-10196. For information on other short peptide inhibitors see: c) L. D. Walensky, A. L. Kung, I. Escher, T. J. Malia, S. Barbuto, R. D. Wright, G. Wagner, G. L. Verdine and S. J. Korsmeyer, *Science*, 2004, **305**, 1466-1470. d) J. W. Chin and A. Schepartz, *Angew. Chem. Int. Ed.*, 2001, **40**, 3806-3809.

[291] J. T. Ernst, O. Kutzki, A. K. Debnath, S. Jiang, H. Lu and A. D. Hamilton, *Angew. Chem. Int. Ed.*, 2002, **41**, 278-281.

[292] I. Chul Kim and A. D. Hamilton, *Org. Lett.*, 2006, **8**, 1751-1754.

Since then, various new scaffolds have been designed based on the original terphenyl design disclosed by Hamilton, often accompanying the introduction of heteroatoms in the backbone in order to augment aqueous solubility, such as *p*-terpyridine **4.7** (Figure 4.24).[257, 293] Moreover, these new additions to the class C α-helix mimetics have focused on mimicking a growing number of side chains on more than one face of the helix. The major drawback with Hamilton's design was that his terphenyls were only able to mimic one face of the helix (for example those seen in Figure 4.23, or *p*-terpyridine **4.7**), meaning that only superficial interactions could be mimicked effectively. This has since been addressed in a number of ways. Firstly, with the development of next generation peptidomimetics such as those based on benzamide structures able to mimic many more side chains than the standard *p*-terphenyl (**4.6a-d**, Figure 4.24). On the other hand, in 2012 Zhang *et al.* demonstrated how an anthracene-based could mimic two opposite sides of the BH3 α-helix to inhibit its interaction with Blc-1 and Mlc-1, which are also involved in the regulation of apoptosis (**4.8**, Figure 4.24).[294]

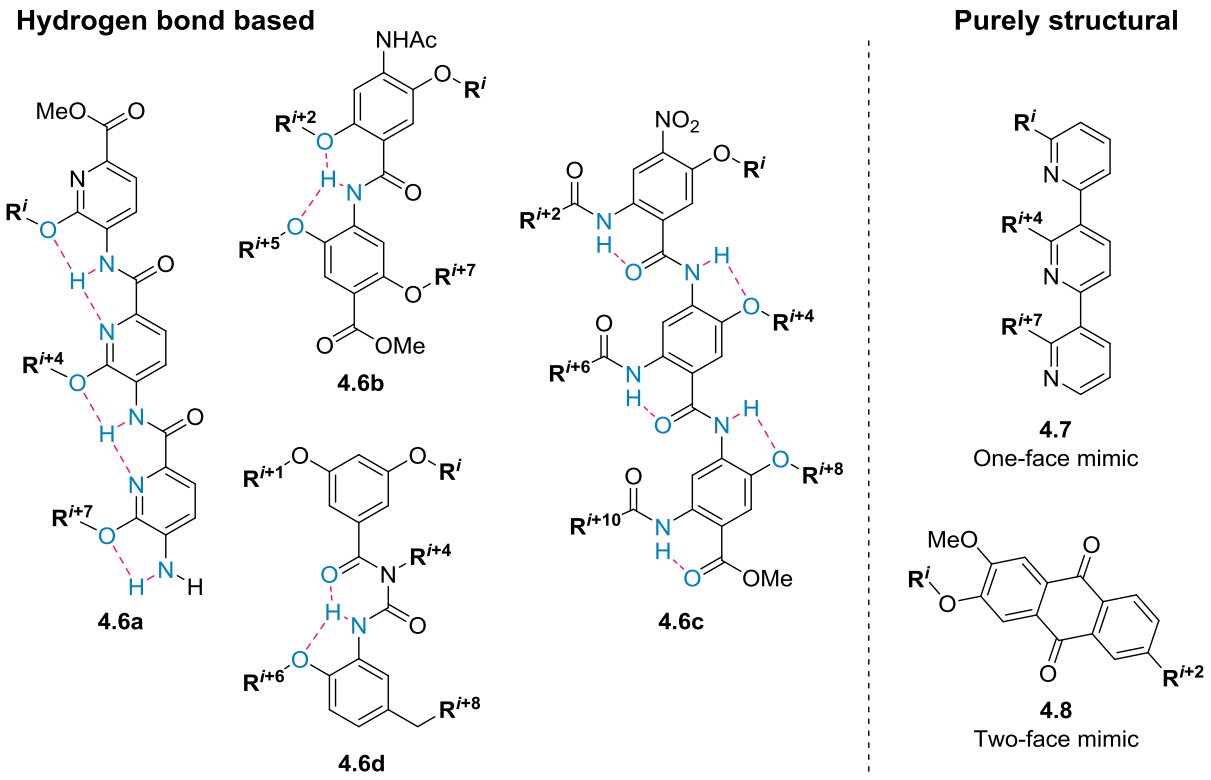

Figure 4.24. Further terphenyl-derived bifacial α-helix mimics.

[293] J. M. Davis, A. Truong and A. D. Hamilton, *Org. Lett.*, **2005**, *7*, 5405-5408.
[294] Z. Zhang, X. Li, T. Song, Y. Zhao and Y. Feng, *J. Med. Chem.*, 2012, **55**, 10735-10741.

Curiously, β-hairpins have also been used to mimic the projection of side chains in an α-helical arrangement (Figure 4.25, a). Robinson and co-workers first proved this in 2004, when they used a β-hairpin based on a D-Pro-L-Pro turn to mimic the structure of the p53 tumour suppressor α-helix,[295] and by doing so inhibited the interaction of this protein with HDM2—an attractive biological target in emerging cancer therapies.[296] The same authors also applied this to the inhibition of the formation of the Rev-RRE complex.[297] By mimicking the arginine residues present in Rev they achieved a high affinity for the RRE (K_d = 2 nM), although their Rev mimic had a low specificity towards other similar RNA targets. These results proved that it is possible to achieve very potent inhibition of the Rev-RRE interaction by using synthetic and non-endogenous ligands (Figure 4.25, b).

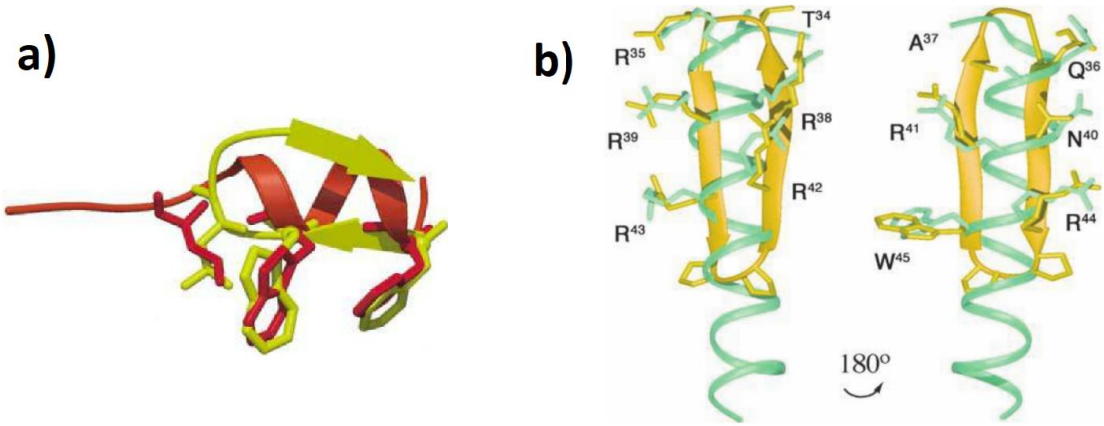

Figure 4.25. a) Superposition of synthetic β-hairpin (yellow) and the p53 α-helix (red). b) Superposition of synthetic β-hairpin (yellow) and the Rev α-helix (green).

[295] R. Fasan, R. L. A. Dias, K. Moehle, O. Zerbe, J. W. Vrijbloed, D. Obrecht and J. A. Robinson, *Angew. Chem. Int. Ed.*, 2004, **43**, 2109-2112.
[296] P. Chène, *Nature*, 2003, **3**, 102-109.
[297] K. Moehle, Z. Athanassiou, K. Patora, A. Davidson, G. Varani and J. A. Robinson, *Angew. Chem. Int. Ed.*, 2007, **46**, 9101-9104.

4.4. The Suzuki-Miyaura cross-coupling reaction.

Palladium is known to most people as a component in the catalytic converters of automobiles, or even as a precious metal used in jewellery, but most remain unaware of the essential role of palladium in modern organic synthesis.[298] As a testament to its wide utility, in 2010 the Nobel Prize in Chemistry was awarded to Richard Heck, Ei-ichi Negishi and Akira Suzuki for "the development of palladium-catalysed cross couplings in organic synthesis."[299]

Although the area of metal-catalysed cross couplings emerged during the 1970s, it wasn't until the 1990s that the area started to gain interest and, by the 2000s, a great variety of cross-coupling reactions had been developed—including carbon(sp^2)-heteroatom, carbon(sp^2)-carbon(sp^2), and carbon(sp^2)-carbon(sp) among others. Over the past decade, the number of patents and publications involving such cross-coupling reactions has grown exponentially, by far the most popular of these being the Suzuki coupling, followed by the related Heck and Sonogashira couplings.[300] This trend has also been seen in industrial processes, and nowadays many pharmaceuticals and agrochemicals contain a cross-coupling reaction in their synthesis.

In general terms, the Suzuki-Miyaura reaction can be defined as the cross coupling between an organoborane compound and an organic halide (or pseudo-halide), catalysed by a palladium metal complex in basic media (Scheme 4.2). The Suzuki reaction has several advantages over other related cross couplings: 1) the organoboronate coupling partners are bench-stable and non-toxic; 2) the superior functional group tolerance; and 3) the mild reaction conditions required to activate the organoboronates.

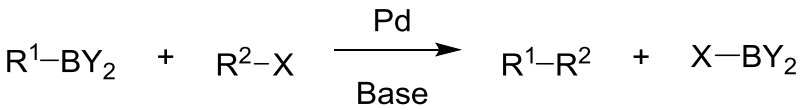

Scheme 4.2. The Suzuki-Miyaura cross coupling reaction.

[298] X.-F. Wu, P. Anbarasan, H. Neumann and M. Beller, *Angew. Chem. Int. Ed.*, 2010, **49**, 9047-9050.
[299] a) A. Suzuki, *Angew. Chem. Int. Ed.*, 2011, **50**, 6723-6737. b) E. Negishi, *Angew. Chem. Int. Ed.*, 2011, **50**, 6738-6764.
[300] T. J. Colacot, *Platinum Met. Rev.*, 2011, **55**, 84-90.

The mechanism of the reaction follows an analogous catalytic cycle to other metal-catalysed cross couplings (Scheme 4.3).[301] These reactions take place in three key steps: oxidative addition, transmetallation, and reductive elimination.

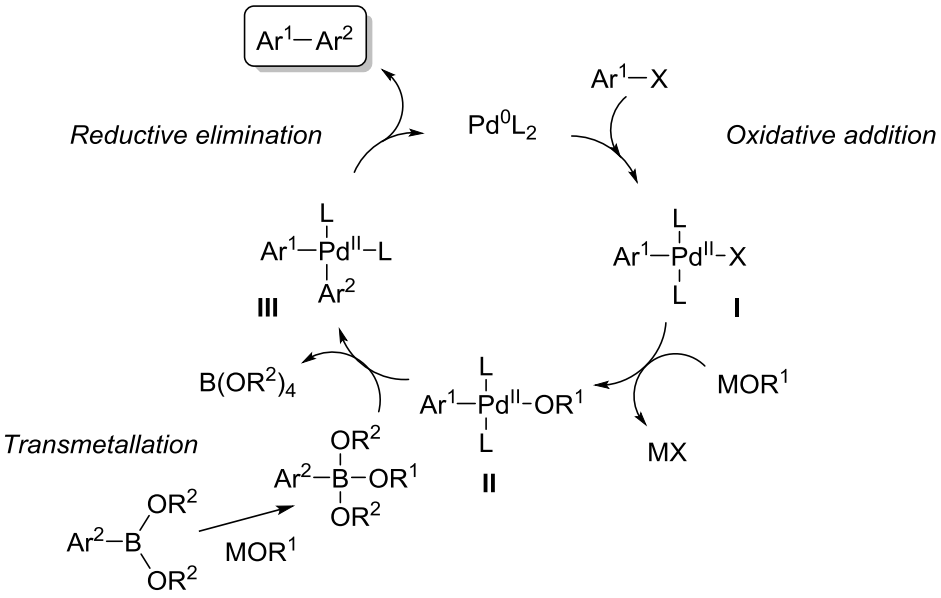

Scheme 4.3. Catalytic cycle for cross-coupling reactions.

Oxidative addition of aryl, benzyl, alkenyl, alkynyl and allyl halides or pseudo-halides to palladium(0) complexes results in stable *trans*-σ-palladium(II) species **I**. This step usually represents the rate-determining step in the reaction; the weaker the C—X bond the faster the reaction, usually in the order I > Br > OTf >> Cl. On the other hand, aryl or alkenyl halides bearing electron-withdrawing groups activate the C—X bond and the reaction takes place faster. From there, complex **I** undergoes a ligand exchange with the base, forming complex **II**.[302]

The transmetallation step involves reaction of this intermediate with the organoboronate coupling partner—which requires prior base-mediated activation—and subsequent isomerisation from the trans complex to *cis*-σ-palladium(II) species **III**. Of the three key steps, the transmetallation is the least

[301] a) J. K. Kochi, *Organometallic Mechanisms and Catalysis*, Academic, New York, 1978. b) R. F. Heck, *Palladium Reagents in Organic Syntheses,* Academic, New York, 1985. c) F. R. Hartley and S. Patai, *The Chemistry of Metal-Carbon Bond*, Wiley, New York, 1985, Vol. 3. d) F. J. McQuillin, D. G. Parker and G. R. Stephenson, *Transition Metal Organometallics for Organic Synthesis*, Cambridge University Press, Cambridge, 1991.

[302] a) C. Amatore, A. Jutand and A. Suarez, *J. Am. Chem. Soc.*, 1993, **115**, 9531-9541. b) C. Amatore, A. Jutand and M. A. M'Barki, *Organometallics*, 1992, **11**, 3009-3013.

understood; there are many factors to consider, as it relies heavily on the organometallic species in question and the specific reaction conditions.[303]

Finally, the cross-coupling product is liberated from intermediate **III**, re-establishing the catalytic palladium(0) species. For this to occur, intermediate **III** must be in the *cis* conformation for the two aryl groups to interact and form the new C—C bond.[304]

It's worth noting that the Suzuki cross coupling is generally accepted as the most important method for the synthesis of biaryls.[298] This can be seen in the synthesis of several pharmaceutically relevant biaryls, such as the alternative synthesis of Losartan (a potent nonpeptide angiotensin II receptor antagonist) by Merck in 1994,[305] or the industrial scale-up of biaryl **4.9** (a key intermediate in the synthesis of ONU-6162, a potential CNS agent) developed by Pharmacia Corporation (Scheme 4.4).[306]

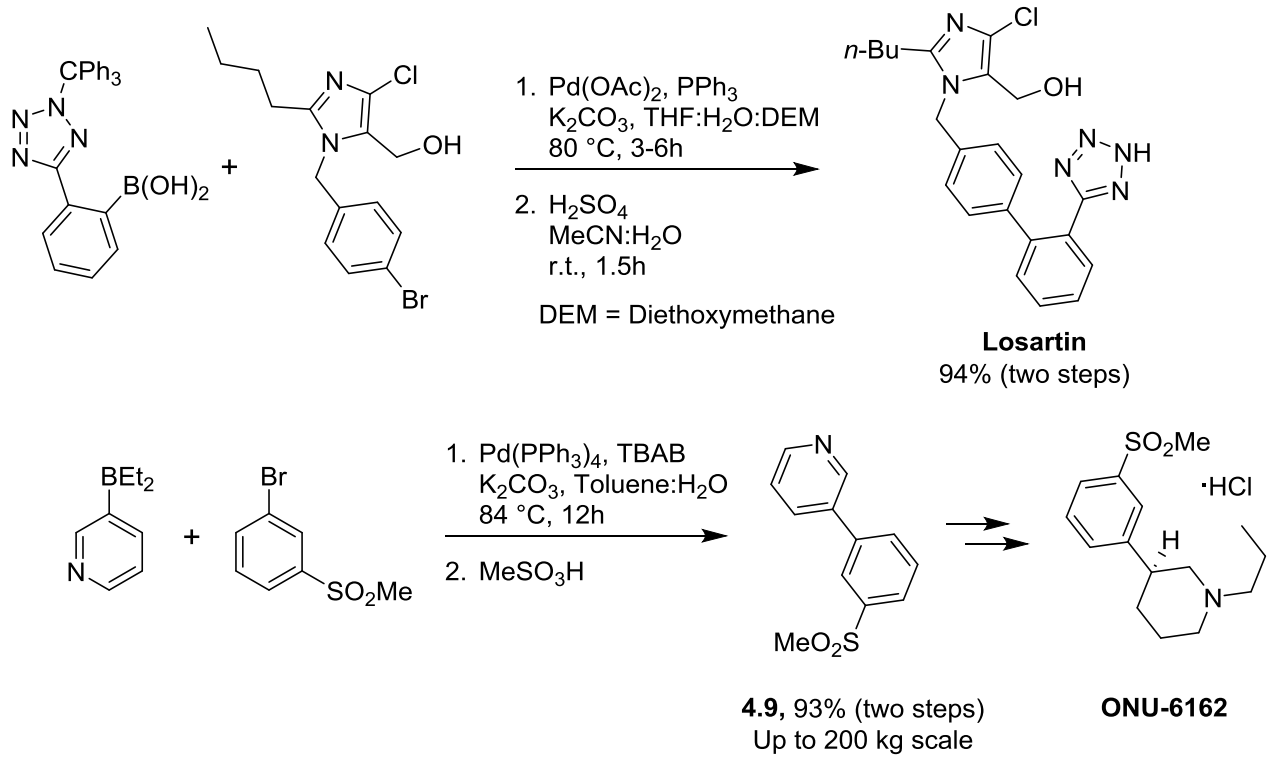

Scheme 4.4. Representative examples of the Suzuki-Miyaura coupling in industrial processes.

[303] a) A. A. C. Braga, N. H. Morgon, G. Ujaque, A. Lledós and F. Maseras, *J. Organomet. Chem.*, 2006, **691**, 4459-4466. b) N. Miyaura, *J. Organomet. Chem.*, 2002, **653**, 54-57.

[304] F. Ozawa, T. Hidaka, T. Yamamoto and A. Yamamoto, *J. Organomet. Chem.*, 1987, **330**, 253-263.

[305] R. D. Larsen, A. O. King, C. Y. Chen, E. G. Corley, B. S. Foster, F. E. Roberts, C. Yang, D. R. Liebermann, R. A. Reamer, D. M. Tschaen, T. R. Verhoeven, P. J. Reider, Y. S. Lo, L. T. Rossano, A. S. Brookes, D. Meloni, J. R. Moore, J. F. Arnett, *J. Org. Chem.*, 1994, **59**, 6391-6394.

[306] M. F. Lipton, M. A. Mauragis, M. T. Maloney, M. F. Veley, D. W. VanderBor, J. J. Newby, R. B. Appell and E. D. Daugs, *Org. Proc. Res. Dev.*, 2003, **7**, 385-392.

Advances in ligand functionality have also contributed to the superiority of the Suzuki coupling over related cross-coupling reactions in the synthesis of biaryls **4.10**; essentially any biaryl can be achieved through the use of the Suzuki cross-coupling reaction. The work by Buchwald and co-workers over the years highlight the use of biphenyl-based phosphines in order to obtain highly sterically hindered biaryls, and making possible the use of the less reactive aryl chlorides as starting materials (Scheme 4.5).[307]

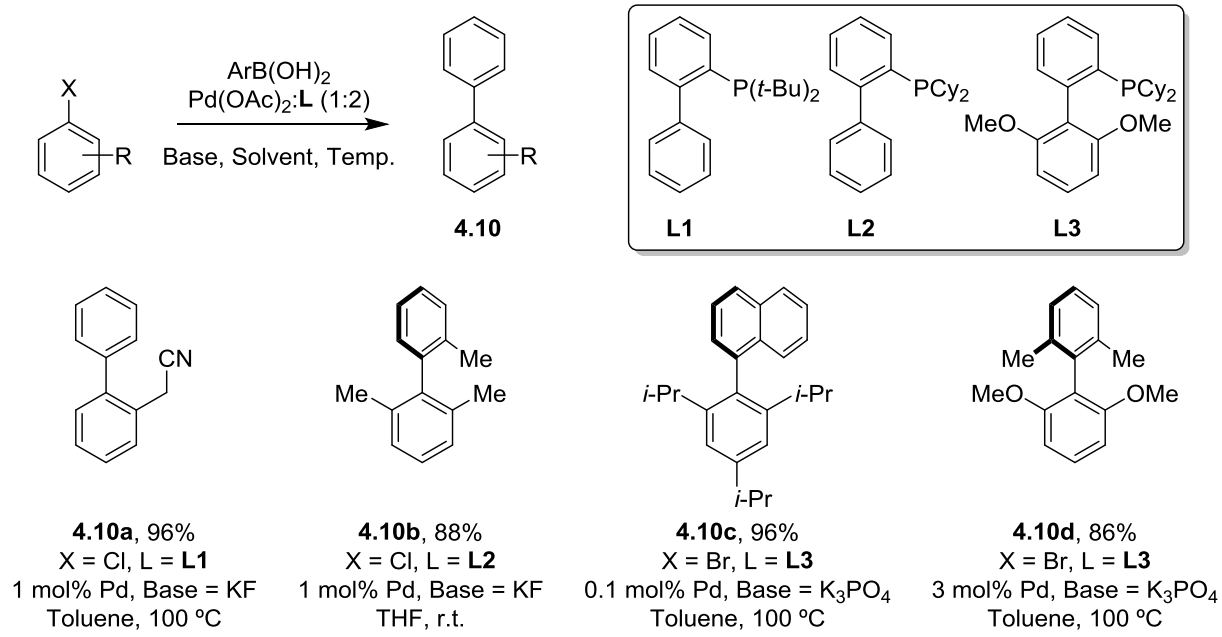

Scheme 4.5. Examples of biaryl synthesis using highly active palladium-biphenylphosphine complexes.

[307] R. Martin and S. L. Buchwald, *Acc. Chem. Res.*, 2008, **41**, 1461-1473.

4.5. Background.

In 2013, our research group first described how the *p*-terphenyl scaffold could be used in the rational design of mimics of the HIV-1 Rev_{34-50} α-helix, together with the groups of J. Gallego (Universidad Católica de Valencia) and J. Alcamí (Instituto de Salud Carlos III).[308] The early terphenyl structures described by Hamilton and co-workers (*see Section 4.3.3.3. α-Helix mimics*)[283, 290-292] bearing a monolateral substitution pattern were limited to mimicking just one face of a peptide structure, or an angle of 180°, and were consequentially limited to mimicking superficial interactions. The authors therefore reasoned that the use of *hexasubstituted* terphenyls instead of the aforementioned *trisubstituted* terphenyls could open up more possibilities for this class of peptidomimetics, given that more residues could be mimicked in this way.

This way, the authors hypothesised that the resulting bilateral terphenyls would be able to mimic residues in the *i*, *i* + 1, *i* + 4, *i* + 5, *i* + 7, and *i* + 8 positions (Figure 4.26). With the possibility of mimicking a larger 360° angle, we thought that this new terphenyl structure would have a greater potential to inhibit interactions in which the α-helix is deeply embedded in the corresponding receptor, such as Rev-RRE binding.

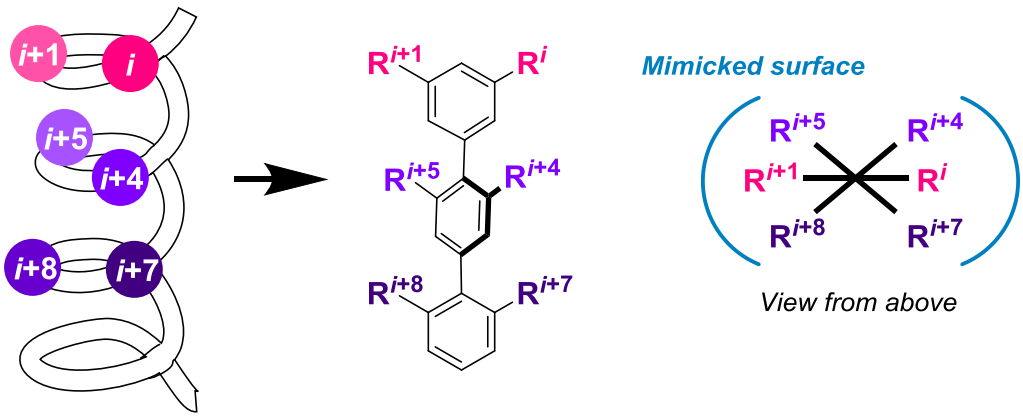

Figure 4.26. Design of novel bilaterally substituted terphenyls.

The terphenyl structures tested contained two ethylamine chains on both terminal phenyl rings, along with various substitutions on the central rings. This was due to the structure of the native Rev protein;

[308] a) L. González-Bulnes, I. Ibáñez, L. M. Bedoya, M. Beltrán, S. Catalán, J. Alcamí, S. Fustero and J. Gallego, *Angew. Chem. Int. Ed.*, 2013, **52**, 13405-13409. b) L. González-Bulnes, I. Ibáñez, S. Catalán, P. Barrio, S. Prado, A. Cantero, J. Alcamí, S. Fustero and J. Gallego. Int. Pat., 2014128198A1 20140828, 2014.

as previously discussed, the Rev α-helix that binds to the RRE is rich in arginine residues, a basic residue capable of establishing ionic interactions, as well as being both a donor and acceptor of hydrogen bonds. However, the introduction of guanidine groups into a bilaterally substituted terphenyl would be difficult due to their high polarity and challenging purification (the Rev helix contains various, and a terphenyl structure containing several guanidine groups would presumably be difficult to isolate in the required purity for biological assays). Therefore, the authors opted for primary amine side chains given their similar basicity and hydrogen bonding capabilities.

A sequential Suzuki-Miyaura cross-coupling strategy was employed for the synthesis of the terphenyl scaffolds, using previously functionalised synthons (Scheme 4.6).

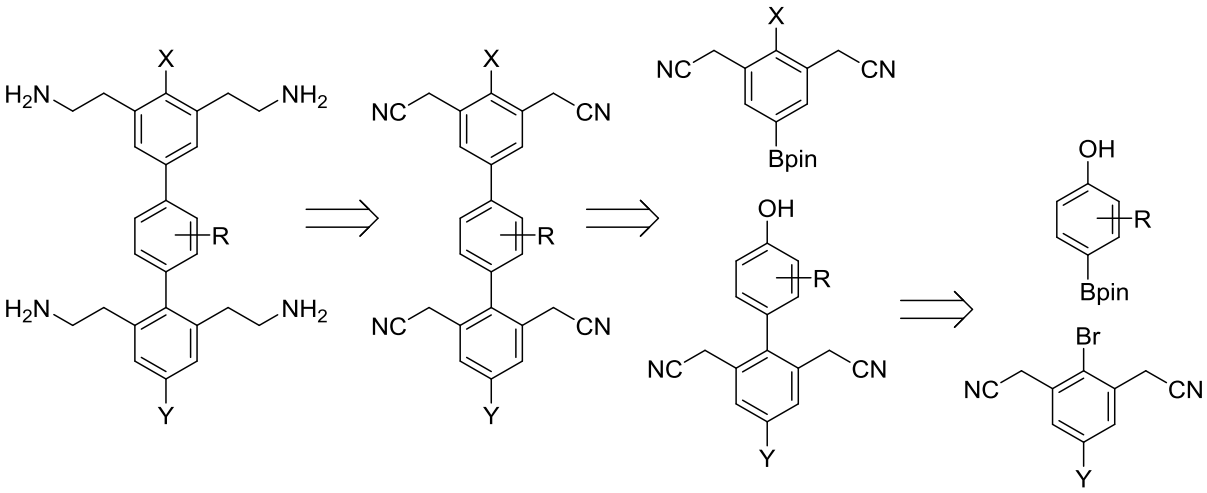

Scheme 4.6. Retrosynthesis of bilateral terphenyl structures tested by Fustero, Gallego and Alcamí *et al.*

In this way, the synthesis of the desired terphenyls passed through intermediate biphenyl structures, some of which were also tested for affinity for the HIV-1 RRE. However, these compounds showed a much weaker union to the RRE than the corresponding terphenyls. These results showed that the staggered conformation of the terphenyl scaffold, as well as the extra interactions established with a third phenyl ring, were important for the binding to the receptor. The best of the terphenyls tested was **Ter.0**, which presents hydroxy and methoxy groups in the terminal positions, and two methyl groups in the central phenyl ring (Figure 4.27, a).

The binding site of the terphenyls was confirmed *via* NMR TOCSY experiments. The ppm shifts in the signals corresponding to the nucleotides within the RRE when exposed to 0, 1, or 2 equivalents of the terphenyl ligand can give information about exactly where the terphenyl binds—and the greatest shifts

were observed in the signals arising from the nucleotides inside the widened loop of the RRE, which is the binding site of the endogenous Rev protein (Figure 4.27, b-c).

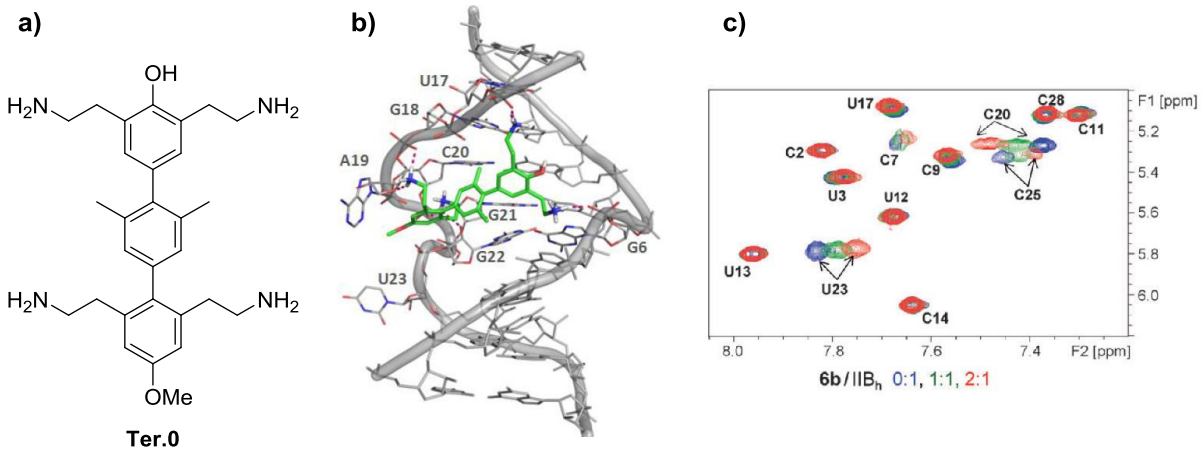

Figure 4.27. a) Structure of lead compound Ter.0. b) Modelling of Ter.0 inside the RRE, showing the nucleotides with which interactions are established. c) NMR TOCSY experiments showing the ppm shifts in affected nucleotide signals.[308]

Furthermore, the bilaterally-substituted terphenyl **Ter.0** inhibited the formation of the Rev-RRE complex (IC_{50} = 7.0 µM) and displayed moderate selectivity for the RRE over other similar RNA strands. In addition, the compound showed high *in vivo* activity (EC_{50} = 3.4 µM) and, most importantly, showed very little cyctotoxicity even at the maximum concentration tested (CC_{50} = >100 µM).

More recently, within the same collaboration between our research group, J. Gallego (UCV) and J. Alcamí (ISCIII), a second generation of *p*-terphenyls was developed and tested for inhibition of the Rev-RRE complex formation. These results featured in the doctoral thesis of Dr. L. Herrera in 2017[206] and, at the time of writing, the corresponding manuscript is in preparation.[309] Despite building on the idea that a bilateral substitution pattern should be beneficial for their inhibitory activity, this new series of terphenyl scaffolds contained a major structural difference: the alkylamine chains were positioned in a relative 1,4-substitution pattern. In this way, the residues expected to be mimicked were those in the *i*, *i* + 2, *i* + 4, *i* + 6, *i* + 7, and *i* + 9 positions of Rev_{34-50} (Figure 4.28).

[309] D. M. Sedgwick/C. Medina, L. Herrera, L. Beltrán, A. Moreno, P. Barrio, L. M. Bedoya, J. Alcamí, S. Fustero and J. Gallego, *Manuscript in preparation.*

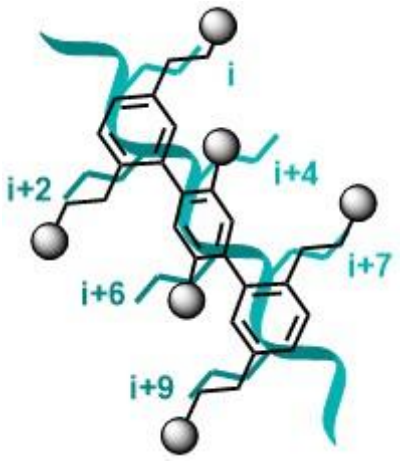

Figure 4.28. New terphenyl derivatives bearing a relative 1,4-substitution pattern overlaying an α-helix.

Several of these derivatives were also found to successfully inhibit the Rev-RRE interaction in the micromolar range in fluorescence polarisation anisotropy assays[310] (e.g. compound **4.12** demonstrated an IC_{50} value of 27.0 μM). The *in vivo* experiments were similarly successful, with compound **4.12** showing an EC_{50} value of just 10.4 μM. Again, these compounds generally showed very little cytotoxicity (Figure 4.29). Some representative examples from the two studies can be seen below, including **Ter.0** (the best performing terphenyl of the 1,3 relatively substituted series) and **4.12** (the best performing terphenyl of the 1,4 relatively substituted series).

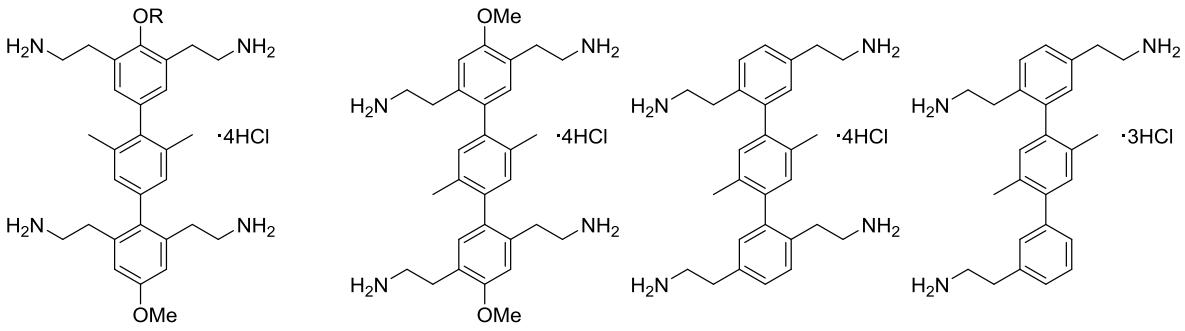

Ter.0, R = H
IC_{50} = 6.8 μM
EC_{50} = 3.4 μM
CC_{50} = >100 μM

4.11, R = Bn
IC_{50} = 32.0 μM
EC_{50} = 24.8 μM
CC_{50} = >100 μM

4.12
IC_{50} = 27.0 μM
EC_{50} = 10.4 μM
CC_{50} = >100 μM

4.13
IC_{50} = 55.9 μM
EC_{50} = 83.3 μM
CC_{50} = >100 μM

4.14
IC_{50} = >50<100 μM
EC_{50} = 14.1 μM
CC_{50} = >100 μM

Figure 4.29. Selected examples of the most active terphenyl derivatives from past studies in the group.

[310] N. W. Luedtke and Y. Tor, *Biopolymers*, 2003, **70**, 103-119.

In addition, an electrophoretic mobility shift assay was carried out in this study. The purpose of this test was to determine whether the compounds inhibited the formation of full length Rev-RRE ribonucleoprotein complexes; since the association of Rev to the RRE is not one-to-one (refer to Figure 4.7), the binding of more Rev units to a single strand of free RRE can be observed *via* electrophoresis, a technique used to separate macromolecules based on their size (Figure 4.30).

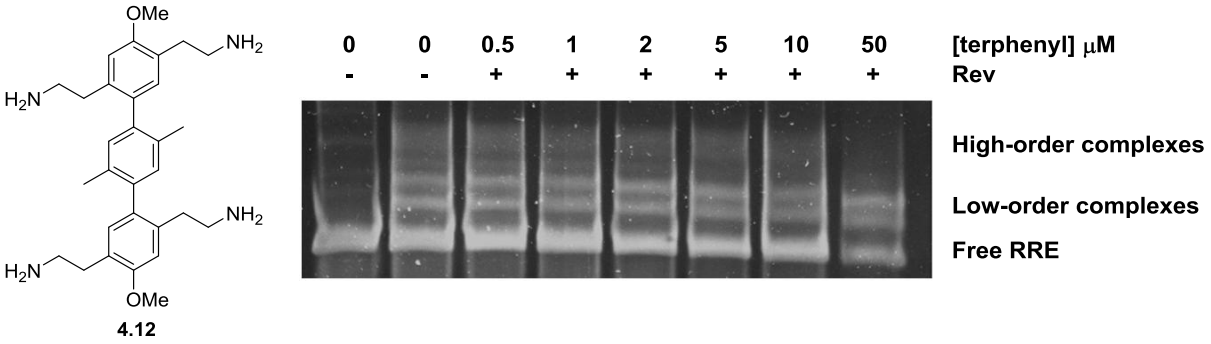

Figure 4.30. The structure of the most active terphenyl of the second series, 4.12, along with the electrophoretic mobility shift assay showing the inhibition of high-order Rev-RRE complex formation.[309]

The same NMR TOCSY studies were also carried out on **4.12**, with somewhat similar results to those of the lead compound **Ter.0** (Figure 4.31).

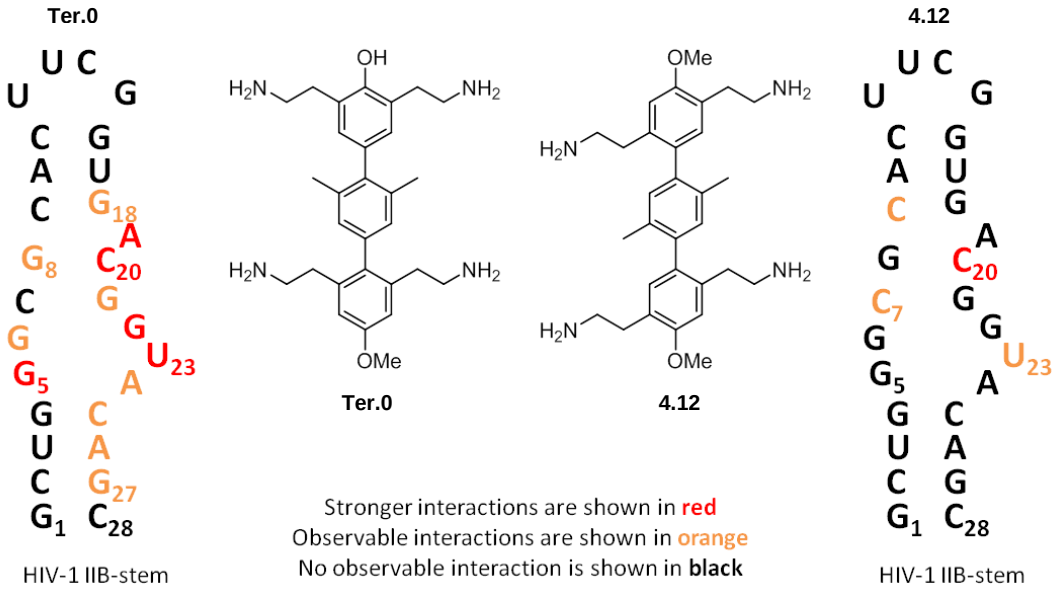

Figure 4.31. NMR studies into the binding site of lead compound Ter.0 and the most active of the new series.

These results proved that other terphenyl structures are also capable of mimicking the Rev_{34-50} α-helix, although the inhibitory activity of this series was very dependent on the structure of the side chains.

4.6. Results and discussion.

4.6.1. Monolateral p*-terphenyls.*

According to our hypothesis, bilaterally-substituted terphenyls should better mimic a biological interaction given the 360° projection of the substituents. However, the terphenyl structures disclosed by Hamilton in his seminal report regarding terphenyls as peptidomimetics had just one substitution on each aromatic ring. Therefore, we decided to synthesise a small library of monolaterally-substituted terphenyls in order to prove that the bilateral substitution was key to the observed activity of the previously discussed terphenyls. Furthermore, if we were incorrect and the following monolateral derivatives proved just as effective as the aforementioned bilateral terphenyls, we reasoned that the synthesis would be much simpler, faster, and less expensive, given that less complex starting materials would be required for less complex target structures.

Therefore, in collaboration with J. Gallego, we designed three monolaterally-substituted *p*-terphenyls in order to test this hypothesis (Figure 4.32). **Ter.1** and **Ter.2** are direct monolateral analogues of **Ter.0**, the lead compound from previous studies in our group, whereas **Ter.3**-**5** are simplifications designed to explore the necessity of the oxygen-based substituents in positions 1 and 4''.

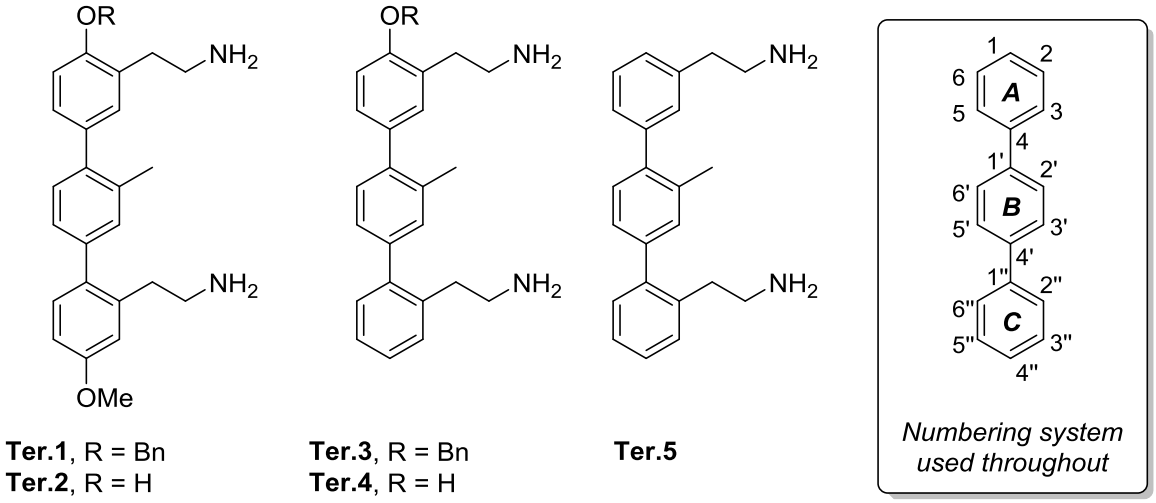

Ter.1, R = Bn
Ter.2, R = H

Ter.3, R = Bn
Ter.4, R = H

Ter.5

Figure 4.32. Target unilaterally-substituted terphenyl structures.

The synthesis of these compounds would follow the example previously established in the group; the terphenyls would be constructed *via* a series of Suzuki-Miyaura coupling reactions between specially

designed synthons, identified by retrosynthetic analysis of the target compounds (Scheme 4.7). In turn, the necessary alkylamine chains would be accessed *via* reduction of the corresponding nitrile incorporated into each synthon before coupling. **Ter.2** and **Ter.4** would be obtained through the hydrogenolysis of the benzyl ethers present in **Ter.1** and **Ter.3** respectively.

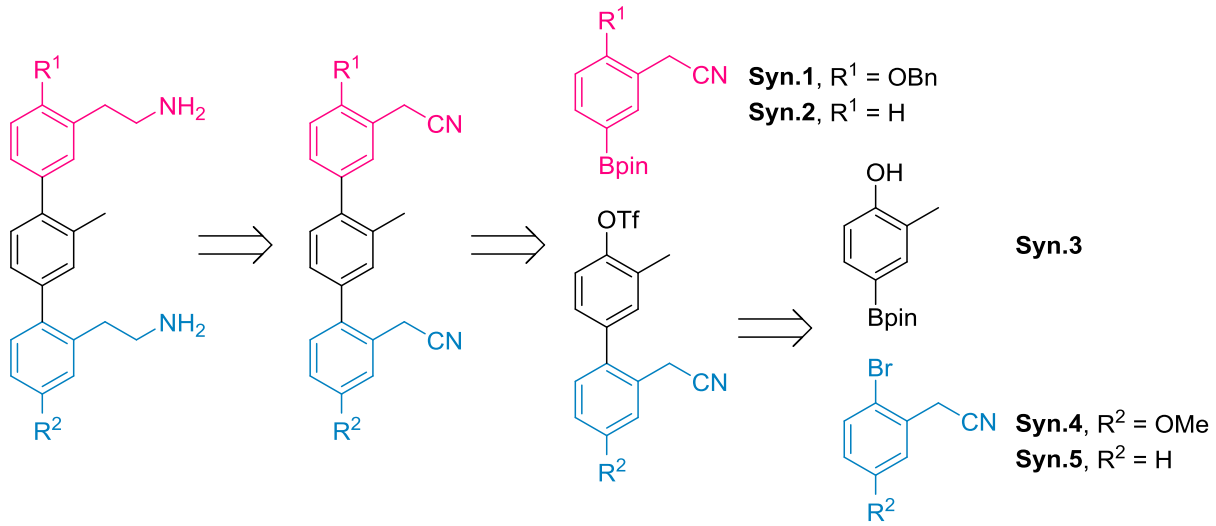

Scheme 4.7. Retrosynthetic analysis and identification of the necessary synthons.

4.6.1.1. Synthesis of monolateral terphenyl derivatives.

Synthesis of monolateral synthons Syn.1-5.

We first reasoned that the synthesis of these synthons would be more straightforward than those described previously in the group, given that these derivatives only presented one side chain rather than two. Therefore, we first thought that a radical bromination of **4.15** would provide quick and easy access to the bromomethyl intermediate **4.16** (Scheme 4.8). A simple S_N2 reaction with a cyanide source and subsequent borylation would afford desired synthons **Syn.1** and **Syn.2** in just three steps.

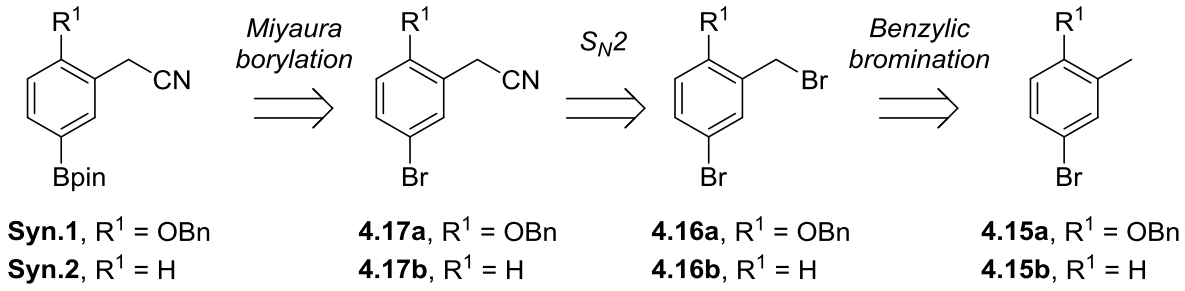

Syn.1, R^1 = OBn
Syn.2, R^1 = H

4.17a, R^1 = OBn
4.17b, R^1 = H

4.16a, R^1 = OBn
4.16b, R^1 = H

4.15a, R^1 = OBn
4.15b, R^1 = H

Scheme 4.8. Retrosynthetic analysis of Syn.1-2.

However, benzylic bromination of **4.15a** with NBS failed to produce **4.16a** as we first planned; most likely due to the competing benzylic position on the benzyl ether, something we had initially overlooked. Unfortunately, this meant we had to resort to changing the protecting group—adding several extra steps to the sequence, since we specifically wanted the benzyl ether substituent to be present in **Ter.1** and **Ter.3**, given the favourable activity demonstrated in previous studies in our group. We therefore attempted the reaction both with the methyl- and TBS-protected substrates **4.15c** and **4.15d**, respectively. Only methyl-protected **4.15c** gave rise to the desired product, but we were unable to remove the methyl substituent afterwards. The demethylation of methoxy groups is somewhat difficult and generally requires strongly acidic conditions. In this context, the treatment of both **4.16c** and **4.17c**—obtained *via* subsequent treatment of bromomethyl derivative **4.15c** with sodium cyanide—with HBr and BBr_3 proved unsuccessful (Scheme 4.9).

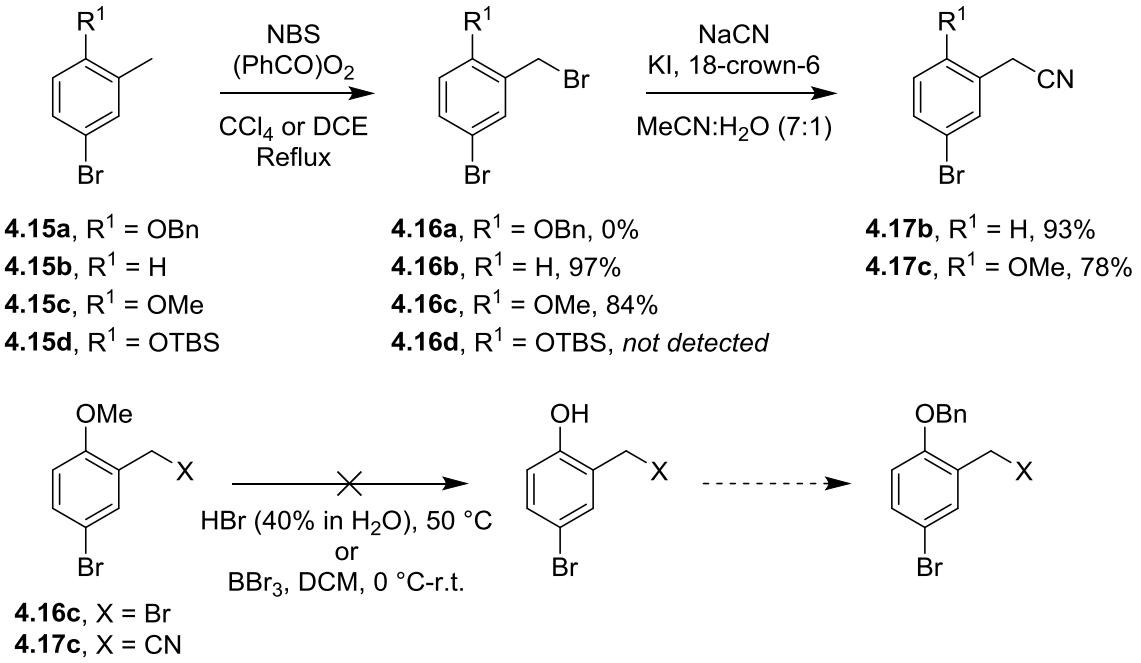

Scheme 4.9. Attempted synthetic routes towards benzylated synthon Syn.1 and synthesis of 4.17b, the precursor of Syn.2.

Following this, with regards of the synthesis of **Syn.1** we resorted to a route analogous to that described previously in our group, starting from the corresponding aldehyde (Scheme 4.10). Commercial substrate 5-bromosalicylaldehyde **4.18** was benzylated with benzyl bromide and potassium triphosphate, and the resulting aldehyde was then reduced with sodium borohydride. Intermediate alcohol **4.19** was then converted into the desired benzyl bromide derivative **4.16a** through the use of phosphorus tribromide, and subsequently treated with sodium cyanide in the presence of potassium iodide and 18-crown-6 to afford **4.17a** in excellent overall yield (Scheme 4.10). It's worth noting that all of these reactions were fairly clean and the crude mixture was used in each step; only **4.17a** was isolated by column chromatography.

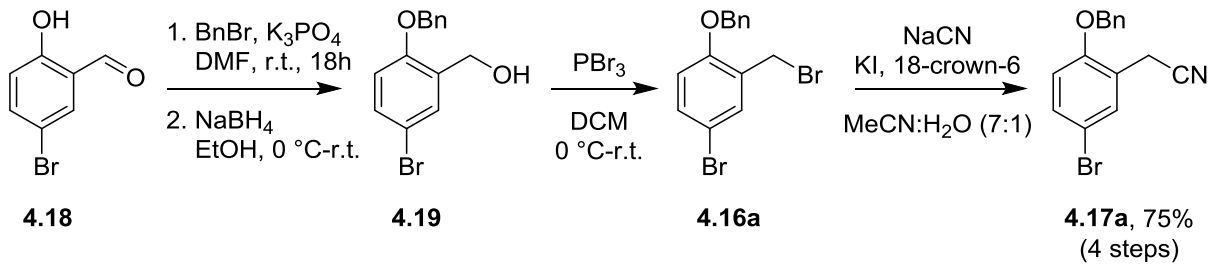

Scheme 4.10. Final synthesis of key intermediate 4.17a on the route to Syn.1.

Once the final nitrile-bearing aryl bromides **4.17a** and **4.17b** were synthesised, both were subjected to Miyaura borylation in order to introduce the boronic ester groups in **Syn.1** and **Syn.2** respectively, required for the final Suzuki coupling. **Syn.3** was also synthesised *via* Miyaura borylation of commercially available substrate 2-methyl-4-bromophenol **4.20** (Scheme 4.11).

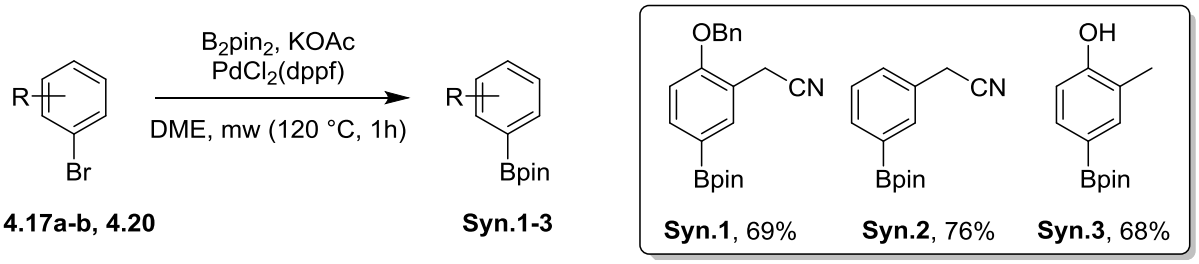

Scheme 4.11. Miyaura borylations to form the final synthons Syn.1-3.

We then turned our attention to synthons **Syn.4** and **Syn.5**. The synthesis of these compounds was relatively straightforward: **Syn.4** was synthesised *via* an analogous route to that utilised for **Syn.2**, consisting of benzylic bromination and S_N2 introduction of the nitrile; and **Syn.5** was commercially available (Scheme 4.12).

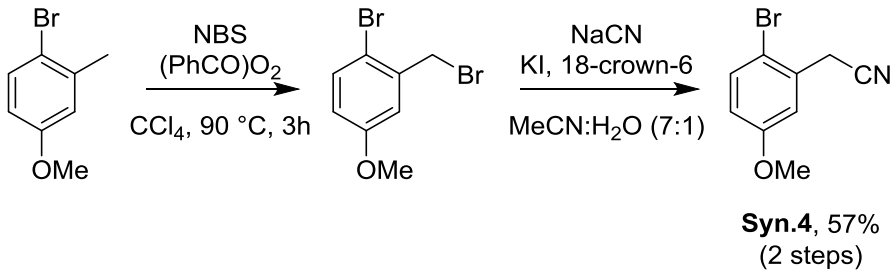

Scheme 4.12. Synthesis of Syn.4.

Construction of terphenyl structures Ter.1-5.

With the synthesis of all the necessary synthons complete, we turned our attention to constructing the terphenyl structures. This was carried out in a sequence already established in our research group, *via* sequential Suzuki couplings. Firstly, **Syn.4** and **Syn.5** were coupled with **Syn.3** to give 1'-hydroxybiphenyls **4.21**. Subsequent formation of the corresponding triflates prepared these biphenyl

structures for the following coupling reaction necessary to achieve the terphenyl scaffold (Scheme 4.13).

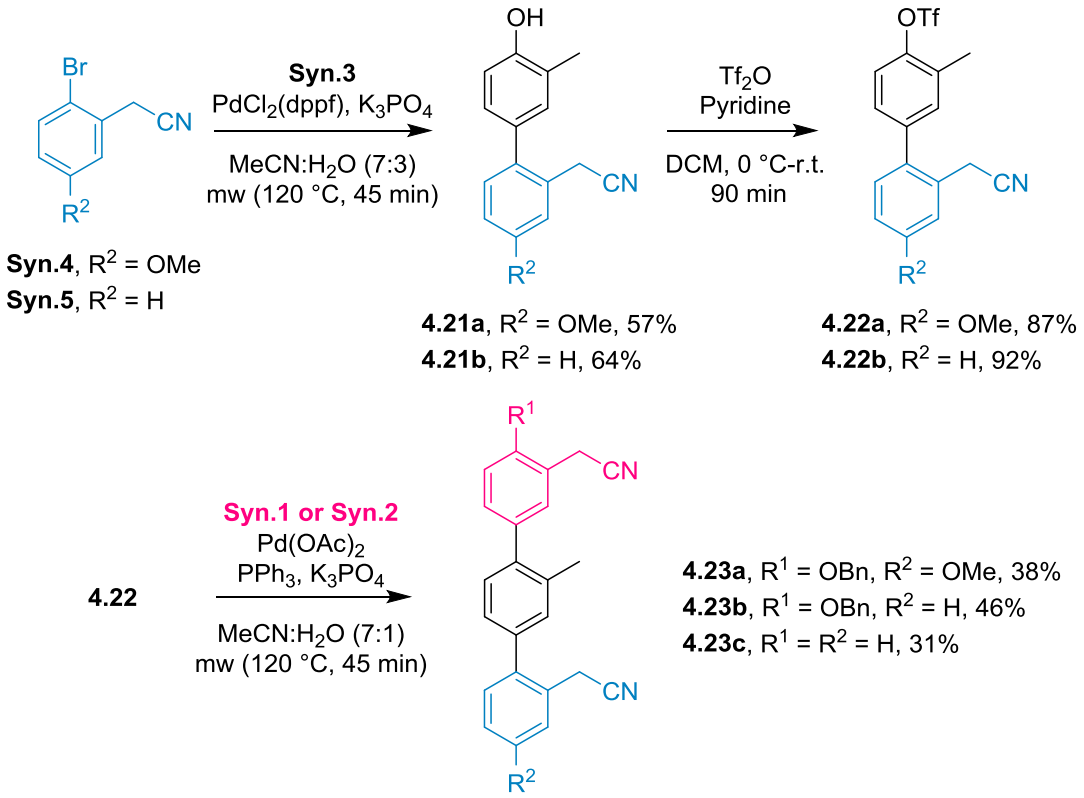

Scheme 4.13. Construction of the terphenyl scaffolds.

Only moderate yields were observed in the cross-coupling reactions, though we suspect each coupling could be optimised to give a higher yield. However, these reactions were carried out using conditions previously used in the group without further optimisation, given that this project was based on achieving specific structures for preliminary *in vitro* and *in vivo* tests, which required only several milligrams each.

From the terphenyl structures **4.23**, the nitrile groups were reduced using borane in THF to give final terphenyls **Ter.1**, **Ter.3** and **Ter.5**. A small amount of **Ter.1** and **Ter.3** was then subjected to hydrogenation conditions to remove the benzyl ether protecting group, affording **Ter.2** and **Ter.4** respectively (Scheme 4.14).

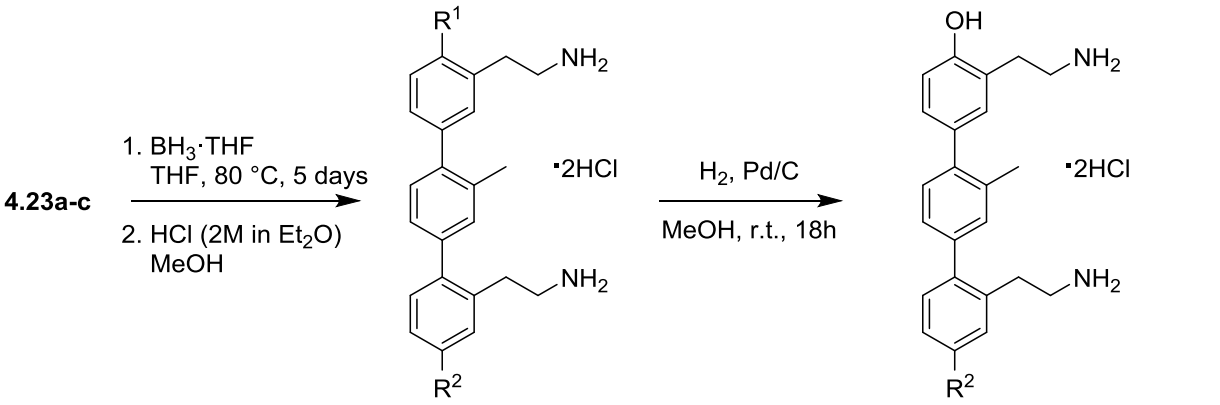

Ter.1, R^1 = OBn, R^2 = OMe, 48%
Ter.3, R^1 = OBn, R^2 = H, 41%
Ter.5, R^1 = R^2 = H, 54%

Ter.2, R^2 = OMe, 89% from **Ter.1**
Ter.4, R^2 = H, 96% from **Ter.3**

Scheme 4.14. Final steps towards Ter.1-5. Nitrile reduction affording the desired amine residues and hydrogenolysis of the benzyl ethers to form Ter.2 and Ter.4 respectively.

4.6.1.2. Biological evaluation of monolateral terphenyls ***Ter.1-5****.*

With the aim of evaluating this small series of monolaterally-substituted *p*-terphenyls, analogous to those described by Hamilton, we carried out various biological assays both *in vitro* and *in vivo*.

Throughout this project, the *in vitro* assays—more specifically, the fluorescence anisotropy assays, gel electrophoresis assays, and NMR experiments—were carried out by the group of José Gallego in the Universidad Católica de Valencia (UCV), whereas the *in vivo* studies were developed by the group of José Alcamí in the Instituto de Salud Carlos III (ISCIII) in Madrid.

Fluorescence polarisation anisotropy studies

The first studies of these compounds was always an *in vitro* technique, specifically fluorescence polarisation anisotropy.[310] This experimental technique is based on the interaction between polarised light and a fluorophore-labelled analyte. When the fluorophore is excited with polarised light, the emission is also at least partially polarised; this is because the transition moments of absorption and emission lie among specific directions within the fluorophore structure.[311] This depends both on the size of the molecule and the viscosity of the media; smaller molecules tumble faster than larger ones, and this occurs faster in less viscous media. Therefore, by exploiting this difference it's possible to determine the degree of binding between a fluorophore-labelled ligand and its receptor using the variation of fluorescence anisotropy between the free ligand—which is considered to be free to rotate in solution, therefore negating any polarisation of emitted fluorescence—and the ligand-receptor complex (Figure 4.33). This type of assay has been used effectively in experiments to determine the inhibition constants of various aminoglycosides such as neomycin, which has a high affinity for the IIB loop in HIV-1 RRE.[312]

To this end, we used a peptide chain with a structure analogous to $Rev_{34\text{-}50}$ labelled with fluorescein isothiocyanate (FITC, the complex will from now on be referred to as *RevpFITC*). In this way it was possible to determine the dissociation constant of this ligand, as well as its displacement from the receptor upon the addition of an external inhibitor—in this case our terphenyl compounds.

To validate any results observed with this method we also measured the K_i of neomycin, obtaining a value of 6.4 µM which is concordant with the relevant literature.[313]

[311] J. R. Lakowicz, *Principles of Fluorescence Spectroscopy*, Springer, 2006.
[312] Y. Wang, K. Hamasaki, R. R. Rando, *Biochemistry*, 1997, **36**, 768-779.
[313] K. A. Lacourciere, J. T. Stivers and J. P Marino, *Biochemistry*, 2000, **39**, 5630-5641.

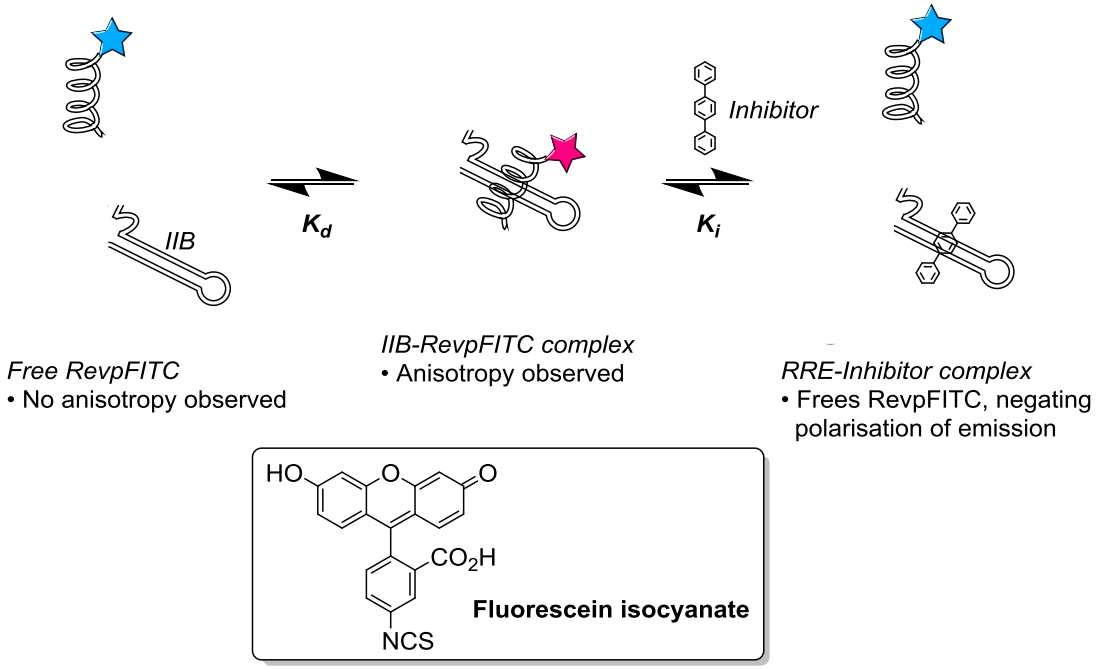

Figure 4.33. Schematic representation of the fluorescence polarisation anisotropy assay.

None of the monolaterally substituted terphenyls proved to have a high affinity for the RRE in this assay, although **Ter.1** demonstrated an IC_{50} of 76.0 μM (Figure 4.34). Notably **Ter.2**, the monolaterally substituted analogue of **Ter.0**, also proved inactive here. We had expected results such as these; this meant that the bilateral substitution was in fact important for inhibiting the Rev-RRE interaction as we had first hypothesised. Since the union with Rev is deeply embedded in the RRE, we expected that mimicking all three faces of the α-helix would be important for the inhibitory activity, and these results show that this is the case.

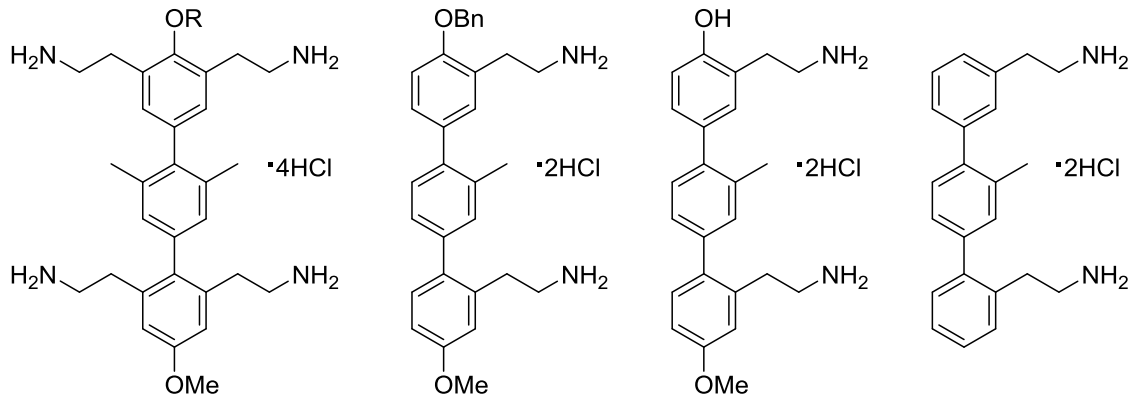

Ter.0, R = H IC_{50} = 6.8 μM
4.11, R = Bn IC_{50} = 32.0 μM
Ter.1 IC_{50} = 76.0 μM
Ter.2 IC_{50} = >100 μM
Ter.5 IC_{50} = >100 μM

Figure 4.34. Fluorescence polarisation anisotropy inhibition data.

Cellular assays.

Our terphenyl compounds were also tested against HIV-1 replication *in vivo*, in the group of J. Alcamí (Instituto de Salud Carlos III). For these assays, we employed MT-2 cells—a cell line containing the HIV-1 genome.

Interestingly, we found these compounds to be active in this assay—something we did not expect after the poor fluorescence polarisation anisotropy results. What's more, they proved to be just as active as the previous lead compound, **Ter.0**. This indicated that these monolaterally substituted terphenyls were interacting with the cells in a different way, maintaining the anti-HIV activity. However, in contrast to **Ter.0**, the monolateral derivatives were also shown to be highly cytotoxic (Figure 4.35).

A potential explanation for this could be *non-specific binding to DNA rather than RNA*; we observed that these monolaterally substituted terphenyls have a 3D structure fairly similar to the pyrrole-imidazole based polyamides developed by Dervan *et al.*, which bind to the minor groove of DNA.[314]

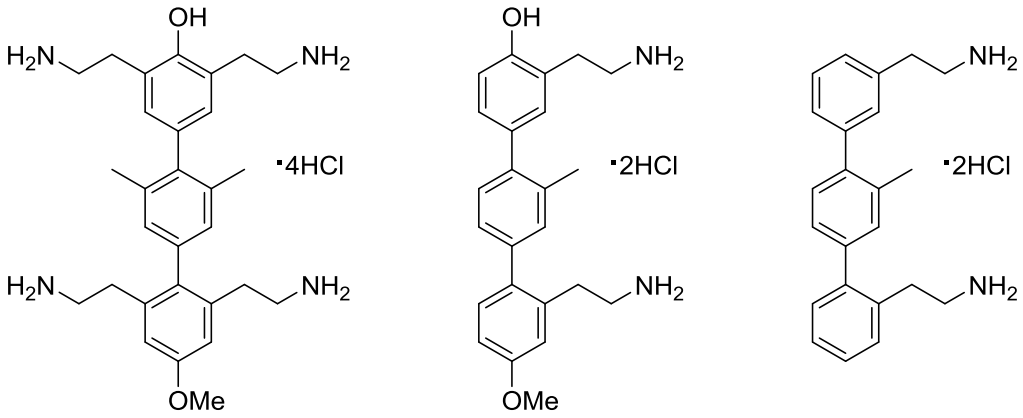

Figure 4.35. *In vivo* activities of monolateral terphenyls in comparison to the related Ter.0.

[314] a) P. B. Dervan and B. S. Edelson, *Curr. Opin. Struct. Biol.*, 2003, **13**, 284-299. b) N. G. Nickols and P. B. Dervan, *PNAS*, 2007, **104**, 10418-10423.

NMR experiments.

In light of these unexpected results, we speculated that the *in vivo* activity could arise from binding to DNA. Specifically, the lower observed EC_{50}, together with the higher cytotoxicity, could potentially be explained by binding to the long terminal repeat of the viral DNA genome, which acts as a promoter for viral RNA transcription. Therefore, we decided to evaluate the interaction between DNA and the monolaterally substituted terphenyl derivatives *via* 2D NMR TOCSY (Total Correlation Spectroscopy) experiments, carried out by J. Beltrán and J. Gallego.[315]

To this end, we used an autocomplementary DNA sequence to explore if these terphenyls showed any affinity for DNA (Figure 4.36).

$$\begin{array}{cccccccc|cccccccc} C_1 & G_2 & C_3 & T_4 & T_5 & G_6 & G_7 & A_8 & T & C & C & A & A & G & C & G \\ G_{16} & C_{15} & G_{14} & A_{13} & A_{12} & C_{11} & C_{10} & T_9 & A & G & G & T & T & C & G & C \end{array}$$

Figure 4.36. Autocomplementary DNA_d sequence used to evaluate terphenyl DNA affinity.

We found that both **Ter.2** and **Ter.5** bound to DNA, and that **Ter.2** induces a stronger perturbation in the DNA chemical shifts than **Ter.5**. This could be seen clearly in the TOCSY plot, with both terphenyls causing a displacement in the chemical shift of the C_{10} and C_{11} nucleotides (Figure 4.37, a and b). This was in contrast to **Ter.0**, that showed a weaker shift in just C_{10} (Figure 4.37, c).[308]

In conclusion, monolaterally-substituted terphenyls do not effectively bind to the IIB stem of the RRE, and therefore do not effectively mimic the $Rev_{34\text{-}50}$ α-helix. Although they show activity *in vivo,* the mechanism of action is suspected to be somewhat different given the high toxicity and failure to produce a significant response in *in vitro* experiments, as well as showing a certain affinity for DNA. This is in stark contrast to the bilateral derivatives studied previously, which show a clear affinity for the RRE *in vitro* and are active *in vivo* without showing significant cytotoxicity.

[315] J. Beltrán, BSc Thesis, Universidad Católica de Valencia, 2016

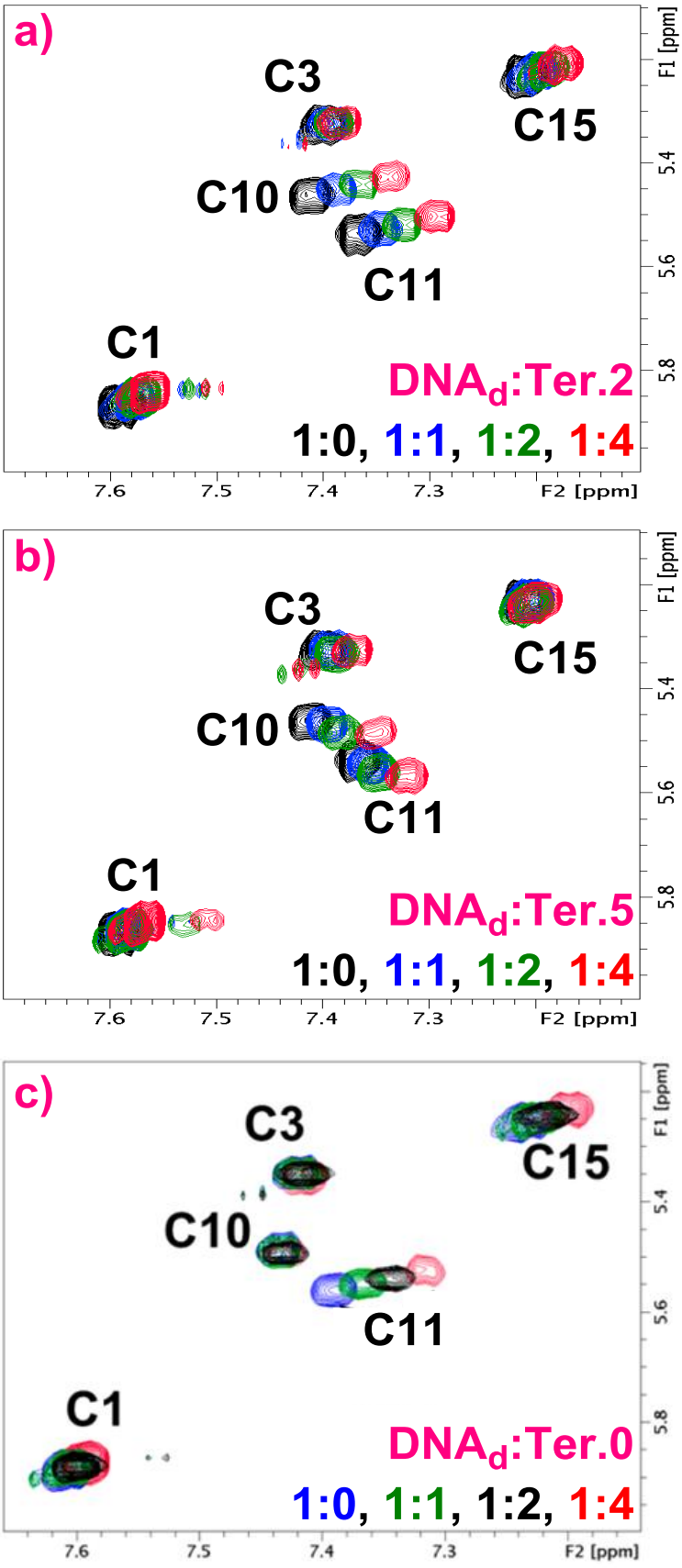

Figure 4.37. TOCSY plots to determine DNA binding.

4.6.2. Bilateral p*-terphenyls: effect of substituents in positions 1 and 4''.*

In addition to exploring the possibility of going forward with simplified monolaterally-substituted terphenyls, we aimed to further explore the structure-activity relationship of the related bilateral derivatives, such as those previously described in our group. Taking the lead **Ter.0** as a starting point, we first looked at the oxygen-based substituents in the 1 and 4'' positions.

During the *in silico* analysis of these compounds carried out in the group of J. Gallego (Universidad Católica de Valencia), no major interactions were identified between these groups and the biological target. Therefore, it should be possible to remove these groups and maintain the activity. Doing so would potentially simplify the synthesis of new terphenyl derivatives, allowing a much faster turnover for new compounds for biological testing.

In this context, we first designed a series of terphenyls bearing different combinations of 1 and 4'' substitutions, **Ter.6-9**, to gain an insight into the effects of such substitutions on the biological activity (Scheme 4.15). The synthesis of these terphenyls would again require the prior synthesis of several synthons, identified *via* retrosynthetic analysis of each terphenyl as seen previously, taking into account the same synthetic steps to construct the terphenyl scaffold: that is, a series of Suzuki couplings between specially designed synthons to construct the terphenyl structure; nitrile reduction to access the alkylamine chains; and possible removal of benzyl ether protecting groups by hydrogenolysis.

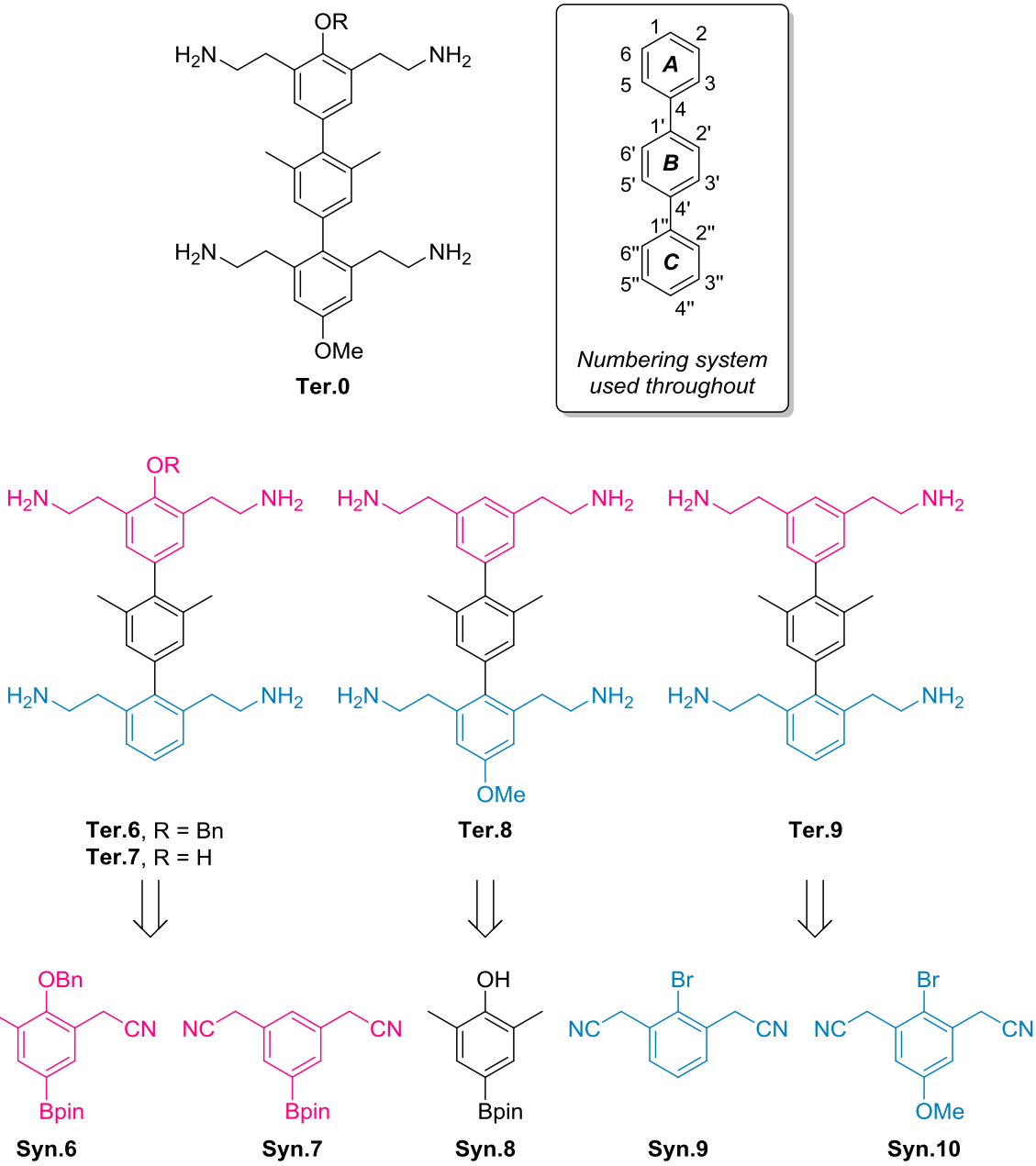

Scheme 4.15. New terphenyls to study the SAR of substitutions in positions 1 and 4'', and their retrosynthetic analysis.

4.6.2.1. Synthesis of bilateral terphenyls **Ter.6-9**.

Synthesis of synthons Syn.6-10.

Fortunately, **Syn.8** was commercially available, and was used as received from the commercial source.

Both **Syn.6** and **Syn.10** had been synthesised previously in the group, during the synthesis of **Ter.0**.[308] Therefore, we followed the same synthetic route towards these synthons as previously described. In this context, **Syn.6** was synthesised starting with the Duff formylation of 4-bromophenol (Scheme 4.16). The phenol group of dialdehyde intermediate **4.24** was then protected as a benzyl ether for the remainder of the synthesis, and the aldehyde groups were reduced with sodium borohydride. The resulting diol was then subject to a modified Appel reaction with triphenylphosphine and *N*-bromosuccinimide to introduce the bromine atoms in **4.27**, which were then replaced with nitrile groups through S_N2 reaction with sodium cyanide. Finally, Miyaura borylation of the resulting dinitrile compound **4.28** completed the synthesis of **Syn.6**.

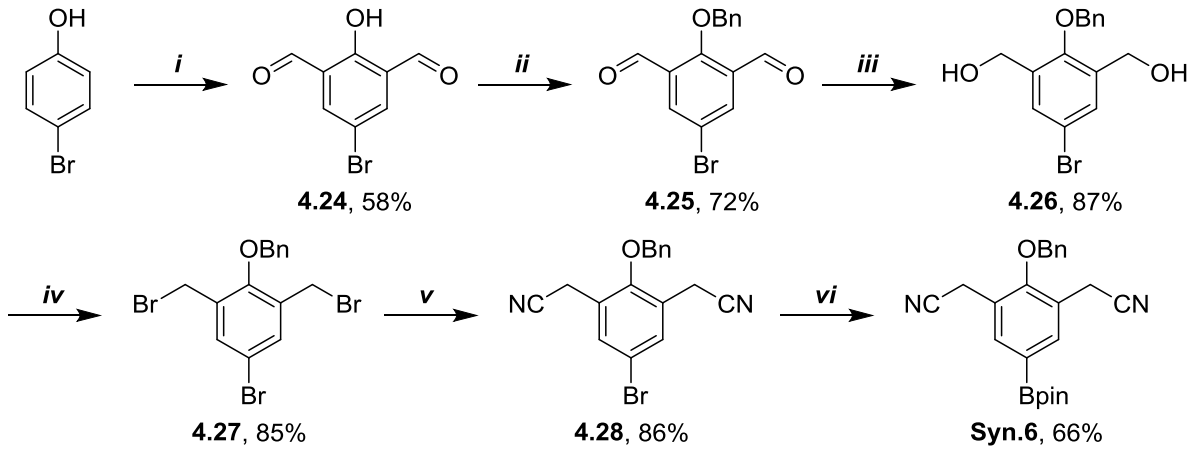

Reactants and conditions:
i. Hexamethylenetetramine (HMTA), TFA, mw (120 °C, 1.5h), then H_2SO_4, H_2O, r.t. 2h. ***ii.*** BnBr, K_3PO_4, DMF, r.t., 18h. ***iii.*** $NaBH_4$, EtOH, 0 °C-r.t., 3h. ***iv***. NBS, PPh_3, DCM, 0 °C-r.t., 18h. ***v.*** NaCN, KI, 18-crown-6, MeCN:H_2O (7:1), r.t., 24h. ***vi***. B_2pin_2, KOAc, $PdCl_2$(dppf), DME, mw (120 °C, 1h).

Scheme 4.16. Synthesis of Syn.6.

On the other hand, **Syn.10** was synthesised starting with the methylation of commercially available 3,5-dimethyl-4-bromophenol (Scheme 4.17). Following this, the two benzylic methyl groups were oxidised through reaction with potassium permanganate, and the resulting carboxylic acids in **4.30** were converted into the corresponding methyl esters *via* Fischer esterification with methanol and sulphuric

acid. A simple reduction of the ester groups in **4.31** and subsequent Appel reaction furnished the dibromo intermediate **4.33**, which was then treated with sodium cyanide to afford the final **Syn.10**.

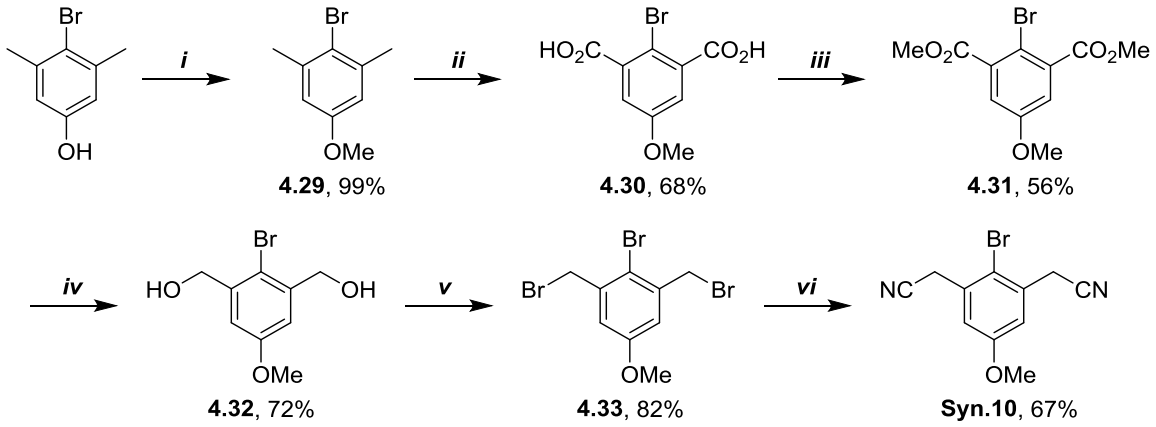

Reactants and conditions:
i. MeI, K_3PO_4, Acetone, 60 °C, 18h. ***ii.*** $KMnO_4$, *t*-BuOH:H_2O (1:1), 110 °C, 18h. ***iii.***H_2SO_4, MeOH, 60 °C, 18h. ***iv.*** $LiBH_4$, THF, 0 °C-r.t., 18h. ***v.*** NBS, PPh_3, DCM, 0 °C-r.t., 18h. ***vi.*** NaCN, KI, 18-crown-6, MeCN:H_2O (7:1), r.t., 24h.

Scheme 4.17. Synthesis of Syn.10.

With regards to **Syn.7**, we chose 5-bromo-*m*-xylene as a starting point, with the idea of introducing the bromine atoms directly through benzylic bromination, as seen previously in the synthesis of **Syn.2**. However, when using the conditions used in the synthesis of **Syn.2**, the desired 3,5-bis (bromomethyl)bromobenzene **4.34** was not obtained. Instead, the major product was **4.35**, resulting from dibromination of a single methyl substituent. The addition of fewer equivalents of NBS did not significantly improve the results, nor did the use of lower temperatures or concentrations. Eventually, a literature search revealed that by using a different activator for the reaction, AIBN, and adding the NBS portion-wise over three days, we would be able to achieve the desired compound in a moderate yield of 68% (Scheme 4.18).[316]

From there, the remaining steps (nucleophilic substitution of bromine atoms with sodium cyanide and borylation) took place uneventfully and in moderate to high yields.

[316] O. H. Omar, F. Babudri, G. M. Farinola, F. Naso and A. Operamolla, *Eur. J. Org. Chem.*, 2011, 529-537.

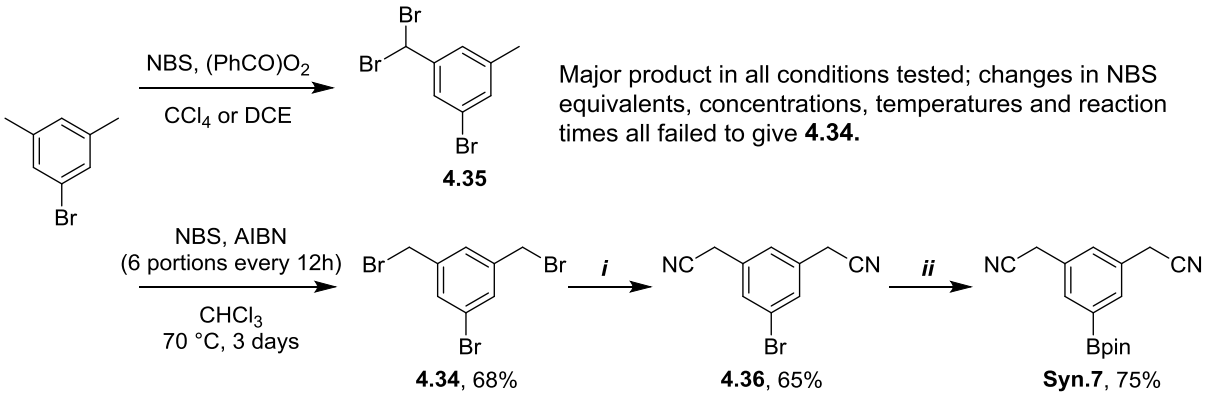

Scheme 4.18. Benzylic bromination of 5-bromo-*m*-xylene and synthesis of Syn.7.

We then focused on obtaining **Syn.9**, and identified commercially available 2,6-bis(bromomethyl)bromobenzene as an ideal starting point; the desired synthon would be accessible in just one step. Therefore, we submitted this starting material to our standard S_N2 conditions with sodium cyanide in the presence of potassium iodide and 18-crown-6, and obtained **Syn.9** in excellent yield (Scheme 4.19).

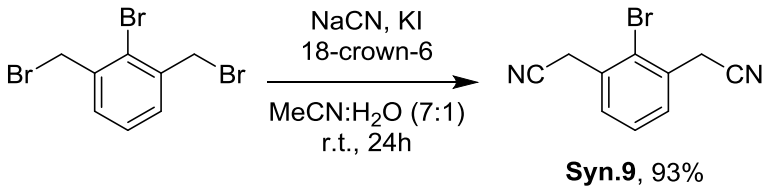

Scheme 4.19. Synthesis of Syn.9 in just one step from commercial 2,6-bis(bromomethyl)bromobenzene.

The real differences in the synthesis of these terphenyls derivatives lie in the synthesis of the required synthons. In this case, when comparing **Ter.9** (which requires the synthesis of **Syn.7** and **Syn.9**) to the original lead compound **Ter.0** (which requires the synthesis of **Syn.6** and **Syn.10**), there are 8 steps difference in the synthesis of the synthons, which translates to over a week's work in the laboratory (Scheme 4.20). This means that the synthesis of new derivatives lacking the extra groups in positions 1 and 4'' could be much faster, allowing for much faster testing and turnover in the search for improved activity. Also, fewer steps meant that we were able to stockpile each intermediate to a certain degree in order to repeat the synthesis of certain terphenyls for further biological assays.

Furthermore, the shorter synthetic route for the synthons means much fewer reagents wasted, as well as saving the waste of over 10 chromatographic columns: all of this meaning that the shorter synthetic route works out much cheaper and more efficient in the long run. Of course, this would ultimately all depend on the biological results of these terphenyl derivatives—if they had no effect on the RRE-Rev interaction, we would have no option but to include the substituents in the 1 and 4'' positions, despite the longer synthesis.

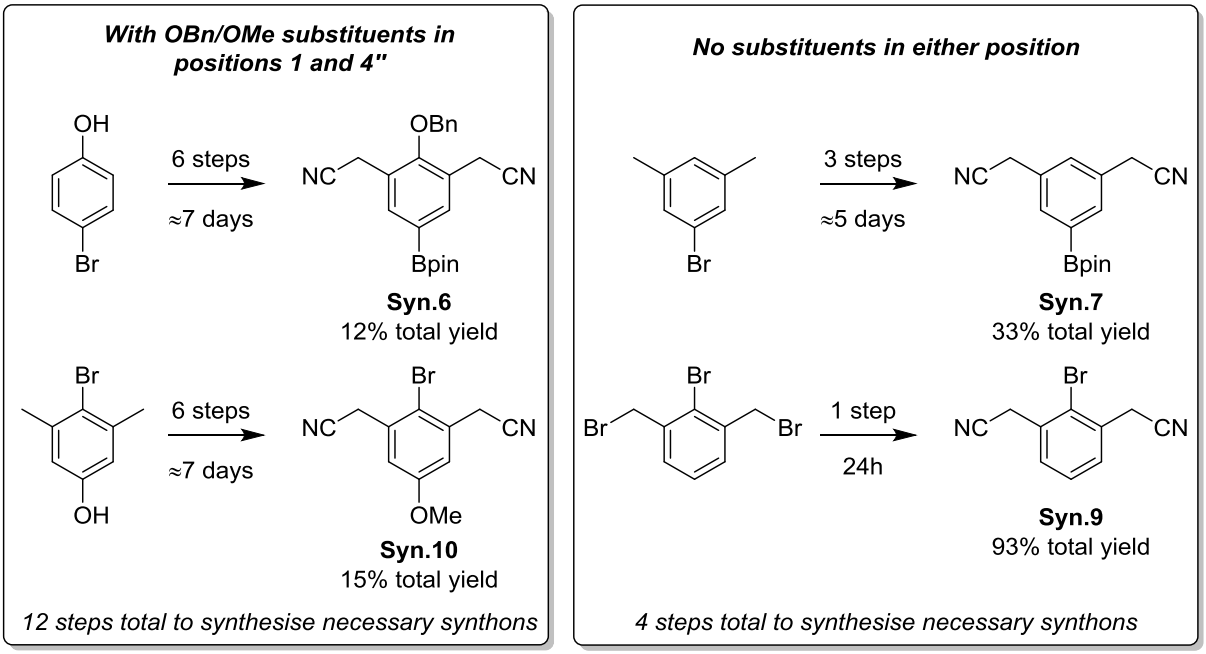

Scheme 4.20. Comparison of total yields and time required for synthetic routes with and without substituents in positions 1 and 4''.

Construction of terphenyl structures Ter.6-9

Once again, after the synthesis of the necessary synthons, we addressed the synthesis of the terphenyl structures, *via* the same method previously discussed; Suzuki coupling to obtain the hydroxybiphenyl, followed by the formation of the corresponding triflate and a second Suzuki coupling to obtain the final terphenyl scaffold. The nitrile groups were then reduced with borane in THF and the benzyl ether protecting group removed where necessary (Scheme 4.21).

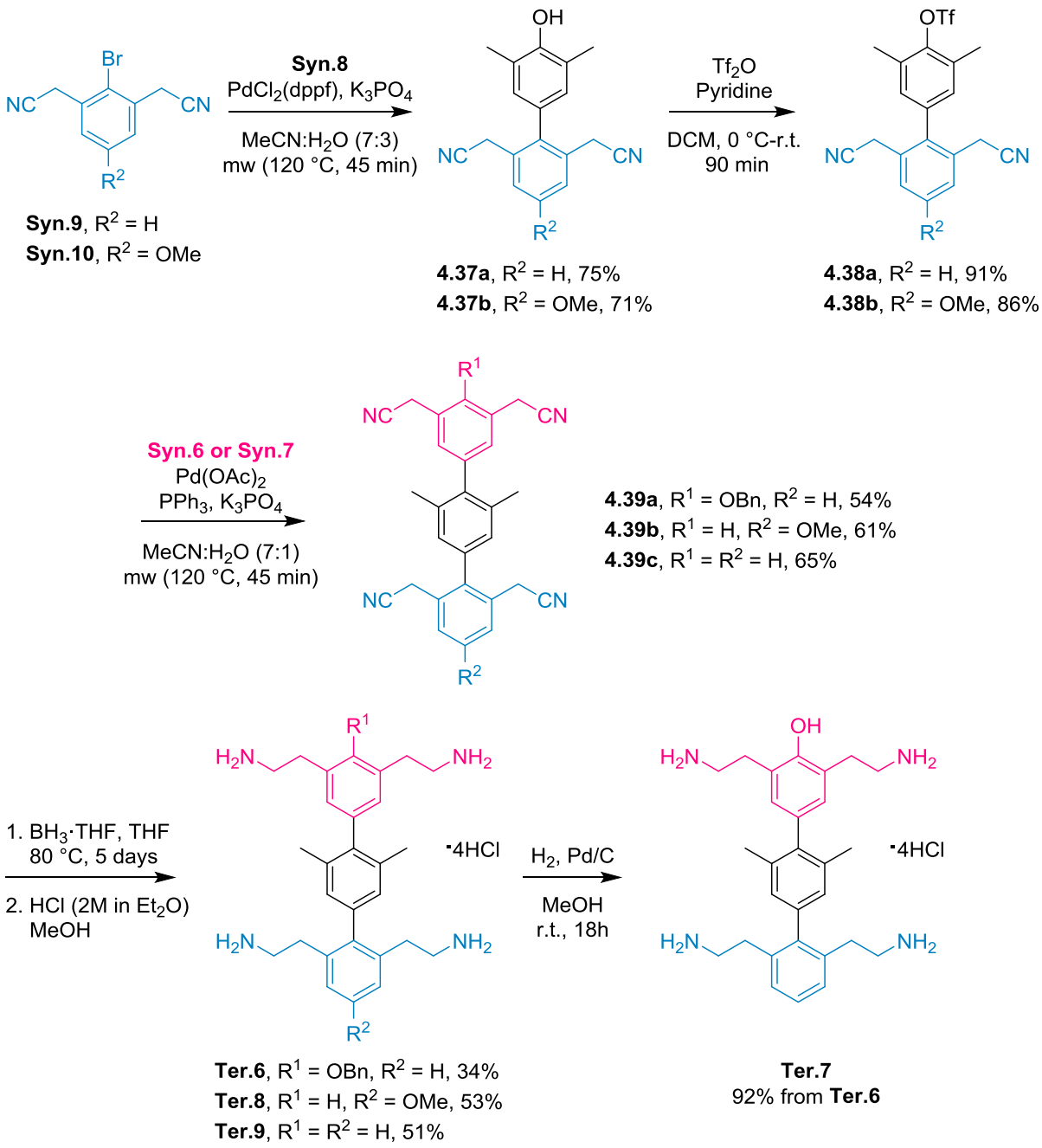

Scheme 4.21. Final steps towards the synthesis of Ter.6-9; Suzuki couplings and reduction of the nitrile groups.

*4.6.2.2. Biological evaluation of bilateral terphenyls **Ter.6-9**.*

With regards to the biological evaluation of this terphenyl series, we carried out both *in vitro* and *in vivo* experiments, analogous to the experiments described previously for the evaluation of the corresponding monolateral derivatives (*refer to section 4.6.1.2. Biological evaluation of monolateral terphenyls **Ter.1-5***).

In this case, comparing the biological results for **Ter.6-9** to the previously studied **Ter.0**, we can deduce that neither the hydroxy nor methoxy groups have a significant effect on the interaction of the terphenyl compounds with the IIB stem of the RRE. Although **Ter.0** remains the most active, **Ter.9** shows only slightly less affinity for the IIB stem in the fluorescence polarisation anisotropy experiments (Figure 4.38). Several interesting details arose from this series.

- In terms of the *in vitro* assays, the order of inhibition capacity of the RRE IIB-Rev_{34-50} complex formation was **Ter.0 ≈ Ter.9 > Ter.8 ≈ Ter.7**. This indicated that the best interaction with the RRE was achieved with either both groups or neither, whereas the presence of just one group hindered this interaction.
- **Ter.6** resulted more active in all assays than **Ter.7**, whereas this trend was reversed in the original **Ter.0**. The improved *in vivo* activity of **Ter.6** compared to **Ter.7** could be related to the improved lipophilicity of the benzyl ether compared to the free phenol, although presumably the significant difference of the IC_{50} values is also important.

This had major implications in the design and synthesis of new terphenyl derivatives, as it allowed us to remove the two substituents in the 1 and 4'' positions, thereby significantly shortening the synthetic route towards new compounds (refer to Scheme 4.20). Therefore, from this point on, new terphenyl derivatives did not generally contain these two groups.

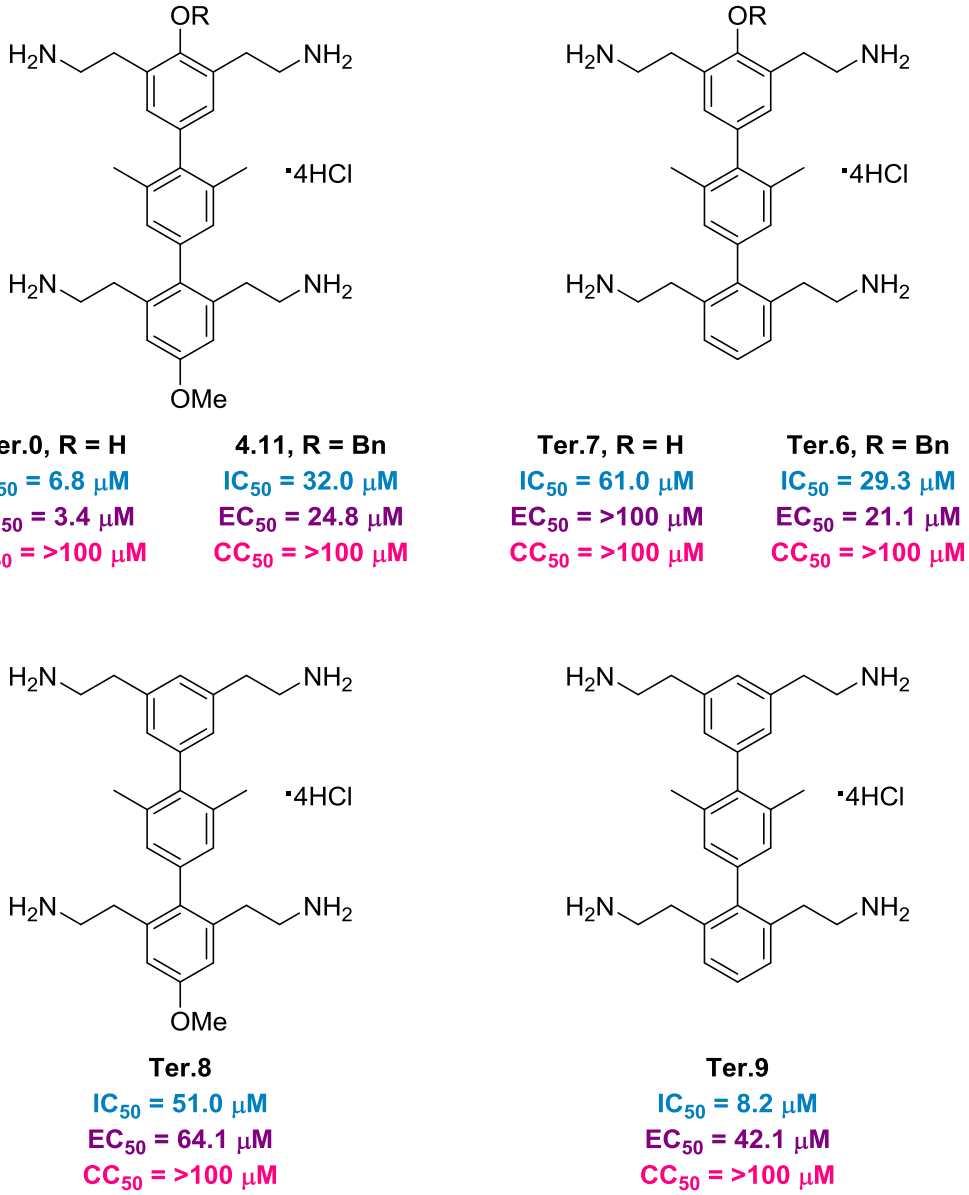

Figure 4.38. Biological results obtained for Ter.6-9.

Given the favourable results obtained for the benzyl ether **Ter.6** compared to the corresponding free phenol, which we reasoned could be due to the increased lipophilia, we also tested the pharmacokinetics of this compound in mice. These studies were performed in GVK Bio, a Contract and Research Development Organisation based in Hyderabad (India). This was carried out using cassette dosing—meaning that all four compounds were injected simultaneously—and initially the mice perished at a dose of 1 mg/kg. The dose was therefore lowered to 0.5 mg/kg, and in this way the study could be concluded with the mice in a healthy state.

In this context, **Ter.6** was tested alongside several other analogues from the series with relative 1,4 substitution, specifically **4.14** and **4.12**. A further compound, **114g5**, was used as a reference in this assay. This compound belongs to the MyriaScreen Diversity Library, a commercially available collection of compounds specifically designed for high-throughput screening and which follow Lipinski's rule of 5, therefore featuring desirable pharmacokinetic characteristics.

The three terphenyl compounds gave favourable results in this assay: 1) elevated values observed for the $AUC_{0-\infty}$ (the area under curve, a parameter used in pharmacokinetic studies to represent the *total drug exposure* extrapolated to time = infinity, with the extrapolated amount shown by the AUC_{Extra}); 2) long half times $t_{1/2}$; and 3) a much lower clearance CL_{obs} compared to reference **114g5**, presumably due to higher bioavailability and higher metabolic stability (Table 4.1).

Table 4.1. Pharmacokinetic studies on Ter.6 and other terphenyls with relative 1,4 substitution.

	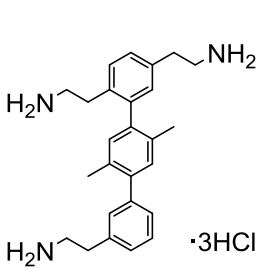 **4.14**	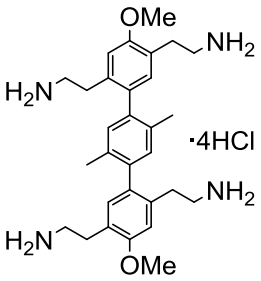 **4.12**	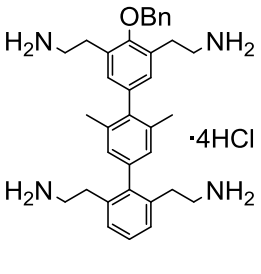 **Ter.6**	**114g5**
Dose (mg/kg)	0.63	0.50	0.50	0.50
C_0 (ng/ml)	1553.35	878.20	871.04	101.34
$t_{1/2}$ (h)	9.94	2.69	11.96	0.66
AUC_{0-inf} (ng·h/ml)	1636.24	573.88	681.92	65.98
AUC_{Extra} (%)	34.97	12.86	18.31	2.28
V_{obs} (ml/kg)	5.50	3.38	12.65	7.18
CL_{obs} (ml/h/kg)	6.39	14.52	12.22	126.30
MRT_{0-last} (h)	9.42	1.84	4.37	0.72

4.6.3. Bilateral p-terphenyls: effects of varying inter-amine distance.

Another possibility in the search for a better terphenyl-RRE interaction was the elongation of the alkylamine chains in positions 2 and 6, since the docking studies had shown that a terphenyl with a greater inter-amine distance in these positions could fit the target better. More specifically, *in silico* studies revealed that a longer chain could improve the contacts between the ligand and the opposite strands in the RNA binding site. This was also the premise of the study into terphenyls with the alkylamine chains in a relative 1,4 substitution pattern (with substitutions in 2, 5, 2', 5', 2'', and 5''), covered in a previous section.[206, 309] Although no significant advantages were observed in that work, these tests were carried out simultaneously. Furthermore, this would render the compounds slightly less symmetrical; the target could therefore better differentiate the alkylamine chains in 2 and 6, and those in 2'' and 6''.

In this sense, several of the new terphenyl structures in this section therefore present an extra CH_2 in the alkylamine chains on aromatic ring **A**. In this small series, the biphenyls containing rings **B** and **C** were the same as previously described during the synthesis of terphenyls **Ter.6**, **Ter.7** and **Ter.9**, and so the only new synthons that were required were generally those corresponding to upper phenyl ring **A** (Scheme 4.22).

Similarly, we decided to vary the substitution pattern of the terphenyl structures as a way of modifying the number of amino groups and the distance between them. Therefore, some structures in this section contain just one alkylamine chain in the *meta* position of phenyl **C**, after the observation that related triaminoterphenyls in the 1,4 series gave favourable results in both *in vitro* and *in vivo* assays (*refer to Figure 4.29, section 4.5. Background.*).[309] This could also be linked to the diminished positive charge on such compounds, since they only contain three amine groups rather than four; previously we had observed that in some *in vivo* assays, the benzyl protected terphenyls gave higher activities than their corresponding phenols, potentially due to the higher lipophilicity. A similar effect could be observed when dealing with less amine groups, despite the poor interaction observed with the monolaterally-substituted terphenyls in Section 4.6.1.2.

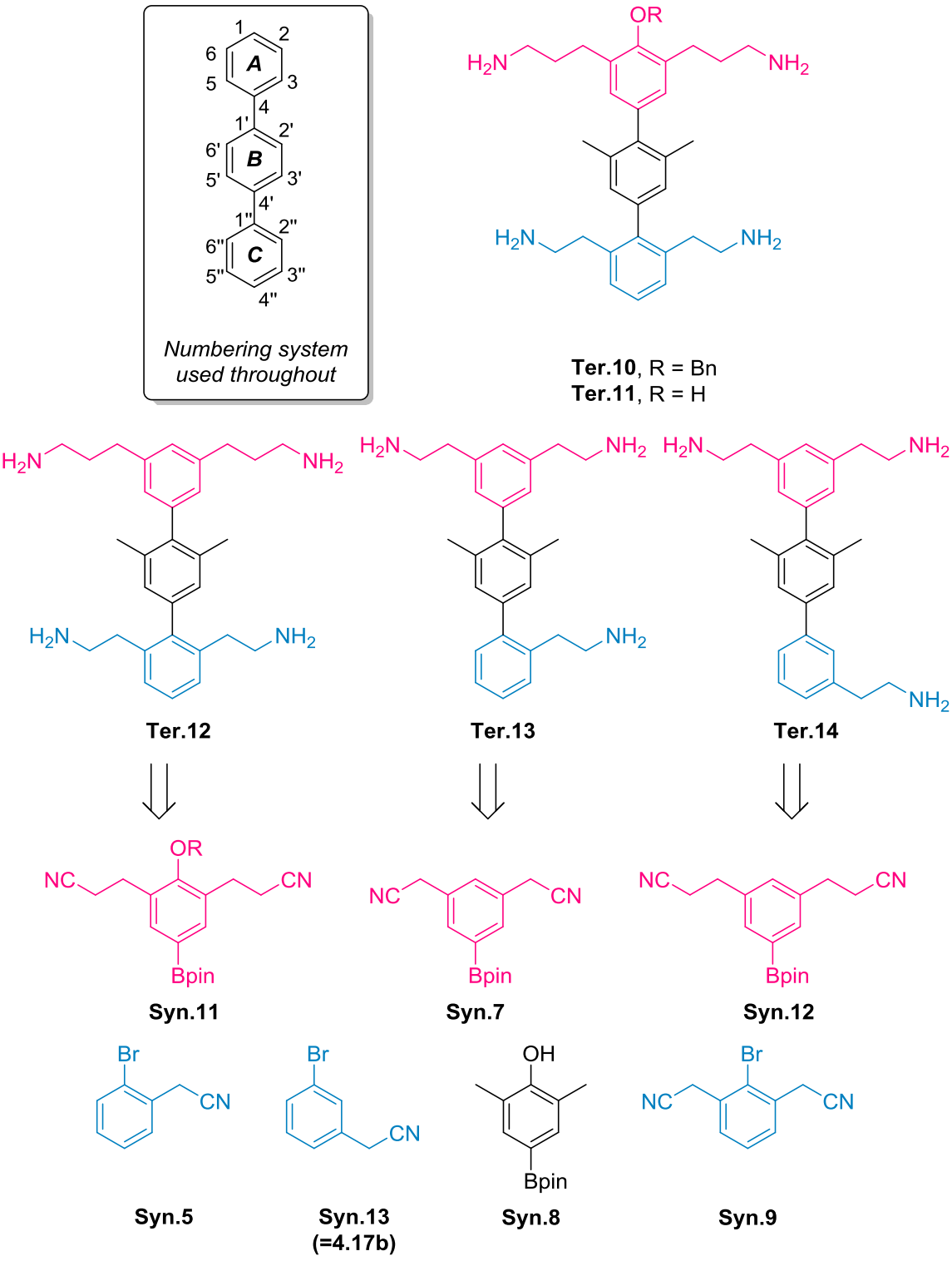

Scheme 4.22. New terphenyls to study the SAR of substitutions in positions 2 and 6, and their retrosynthetic analysis.

4.6.3.1. Synthesis of bilateral terphenyls **Ter.10-14**.

Synthesis of synthons Syn.11-13.

Synthons **Syn.5** and **Syn.7-9** had all been used previously; therefore, we focused our attention on the synthesis of the remaining synthons corresponding to phenyl ring **A** of the terphenyls in this series, in order to elongate the two alkylamine chains present. **Syn.13**, which now represents a synthon towards **Ter.14**, was used as intermediate **4.17b** during the synthesis of **Ter.5** (refer to Scheme 4.9).

Taking advantage of the previously synthesised dialdehyde **4.25**, we prepared **Syn.11** starting with a Wittig reaction using commercially available stabilised phosphine ylide to afford intermediate **4.40**, which was then reduced with sodium borohydride to form **4.41** with the desired saturated propanenitrile chains in positions 2 and 6 (Scheme 4.23). The Wittig reaction to form **4.40** was very clean and no purification was necessary before the subsequent reduction reaction, just a simple aqueous work up and change of solvent.

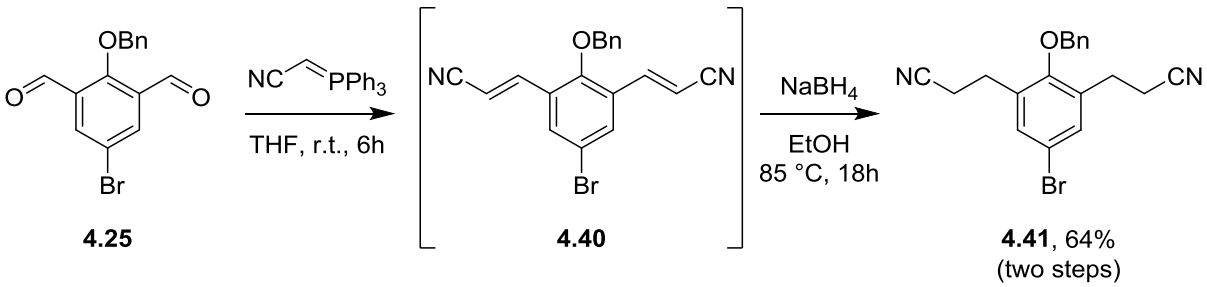

Scheme 4.23. Synthesis of dipropanenitrile derivative 4.41 towards the synthesis of Syn.11.

On the other hand, we found that 5-bromoisophthalaldehyde **4.43** was relatively expensive to use as a starting material, so we opted instead for the much cheaper dicarboxylic acid **4.42** as a starting point in the synthesis of **Syn.12**. To achieve the dialdehyde from the dicarboxylic acid, we identified three potential pathways: 1) formation of the corresponding Weinreb amide and subsequent reduction to the dialdehyde; 2) direct reduction to the corresponding diol and oxidation to dialdehyde **4.43**; or 3) formation of the diester, reduction and subsequent oxidation to the dialdehyde (Scheme 4.24).

The formation of the Weinreb amide before reduction gave rise to complex mixtures, and failed to give significant yields of the desired product. The other two routes, however, resulted in the dialdehyde in similar yields. Several conditions were tested for the oxidation step, such as Jones' reagent and manganese dioxide, but the best yield was obtained using pyridinium chlorochromate (PCC).

Dialdehyde **4.43** was then subjected to the same synthetic sequence as **4.25**—Wittig reaction and subsequent reduction with $NaBH_4$—to afford dinitrile compound **4.44**.

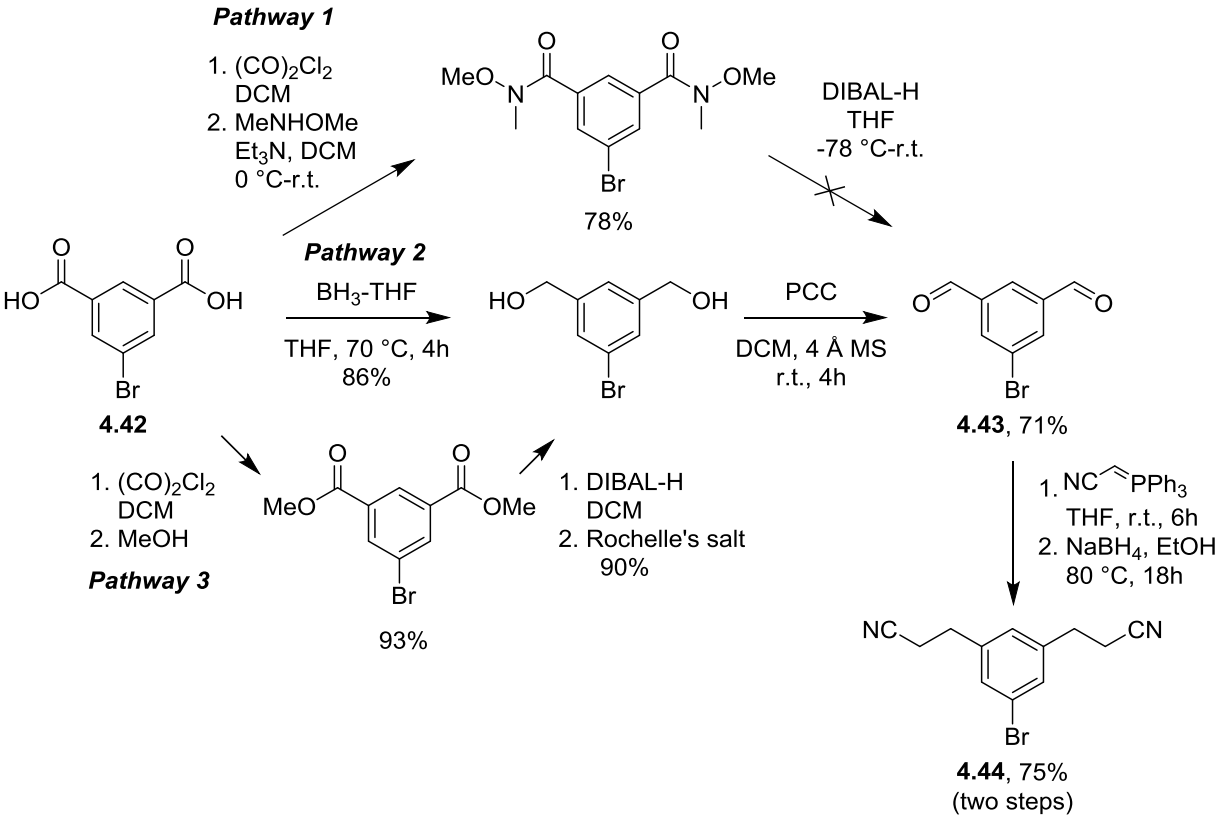

Scheme 4.24. Synthetic route towards dialdehyde 4.43 and subsequent Wittig reaction to form 4.44.

From there, dinitrile compounds **4.41** and **4.44** were subject to the previously established borylation conditions, although this was unsuccessful. This was attributed to the longer alkanenitrile chain being able to position itself in such a way as to coordinate with either the palladium or the boronate species. After several attempts at changing the reaction conditions, such as the temperature or the reaction time, we found that the addition of 1% DMSO to the reaction mixture and conventional heating steered the reaction to the desired synthons **Syn.11** and **Syn.12** (Scheme 4.25).[317]

[317] S. C. Goodacre, L. J. Street, D. J. Hallett, J. M. Crawforth, S. Kelly, A. P. Owens, W. P. Blackaby, R. T. Lewis, J. Stanley, A. J. Smith, P. Ferris, B. Sohal, S. M. Cook, A. Pike, N. Brown, K. A. Wafford, G. Marshall, J. L. Castro and J. R. Atack, *J. Med. Chem.*, 2006, **49**, 35-38.

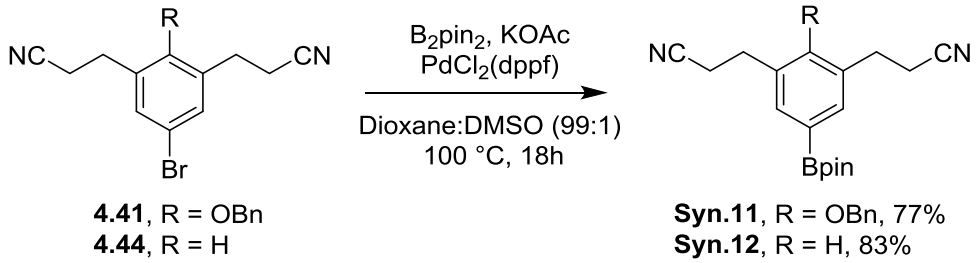

Scheme 4.25. Synthesis of Syn.11 and Syn.12 *via* borylation of dinitrile aryl bromides 4.41 and 4.44 respectively.

Construction of terphenyl structures Ter.10-12

The terphenyl structures were then constructed *via* the same Suzuki cross-coupling sequence. Since **Ter.10-12** share phenyl rings **B** and **C** with previously synthesised terphenyls **Ter.6**, **Ter.7** and **Ter.9**, the beginning of the synthetic sequences coincide until biphenyl triflate **4.38a**, though terphenyls **Ter.13** and **Ter.14** required newly synthesised triflates in order to construct the final terphenyl structure (Scheme 4.26).

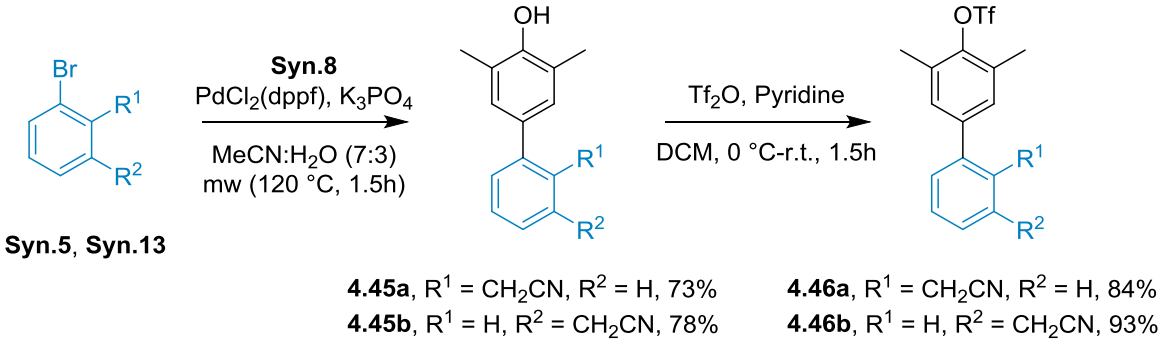

Scheme 4.26. Preparation of new triflates in the synthetic route towards terphenyls Ter.13 and Ter.14.

From there, the path towards the construction of the majority of the terphenyl structures was equivalent to that already seen. Once the terphenyl structures had been prepared (Scheme 4.27), the nitrile groups were reduced to the corresponding primary amines to afford the final terphenyl targets, and the benzyl ether protecting group removed *via* hydrogenolysis in the case of **Ter.11** (Scheme 4.28).

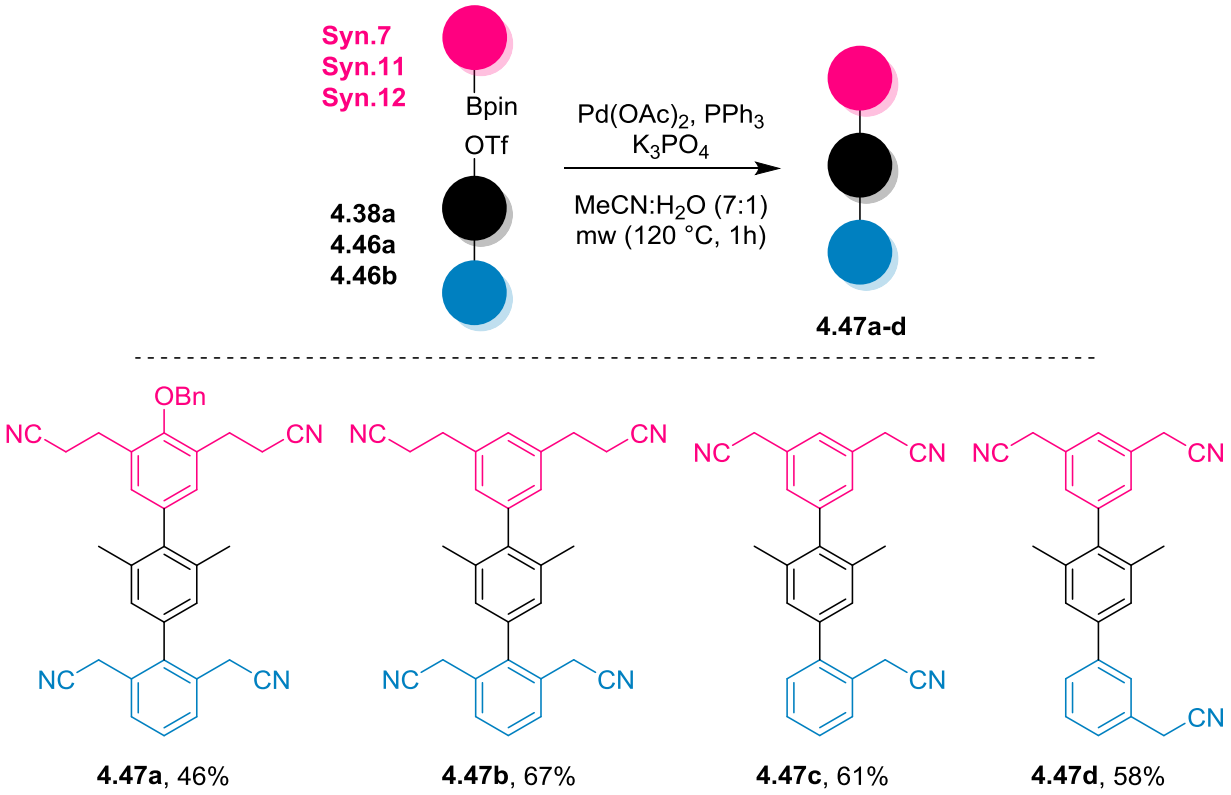

Scheme 4.27. Construction of terphenyl structures 4.47, precursors of Ter.10-14 respectively.

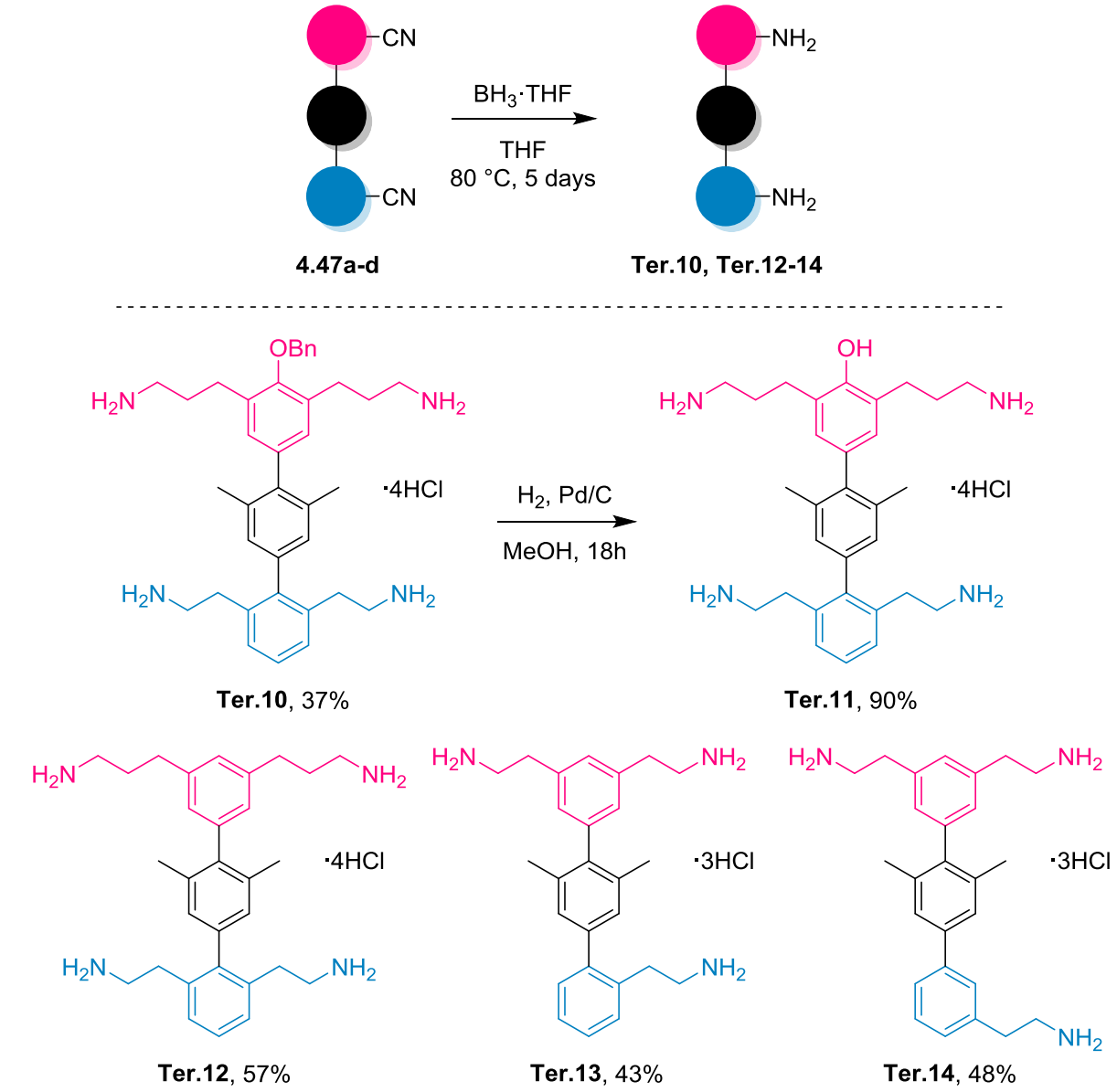

Scheme 4.28. Reduction of nitrile groups and final steps in the synthesis of Ter.10-14.

4.6.3.2. Biological evaluation of bilateral terphenyls *Ter.10-14*.

With regards to the biological evaluation of this terphenyl series, we again carried out both *in vitro* and *in vivo* experiments, analogous to those experiments described previously for the evaluation of the corresponding monolateral derivatives (*refer to section 4.6.1.2. Biological evaluation of monolateral terphenyls* ***Ter.1-5***).

In this series, we found that the elongation of the alkylamine chains of phenyl ring **A** did not drastically affect the biological activity of this class of compounds, as we had envisioned from the *in silico* analysis previously discussed. However, with regard to the differences between benzyl ethers and free phenols, the results here mirrored the results of the original report in which **Ter.0** was studied (Figure 4.39).

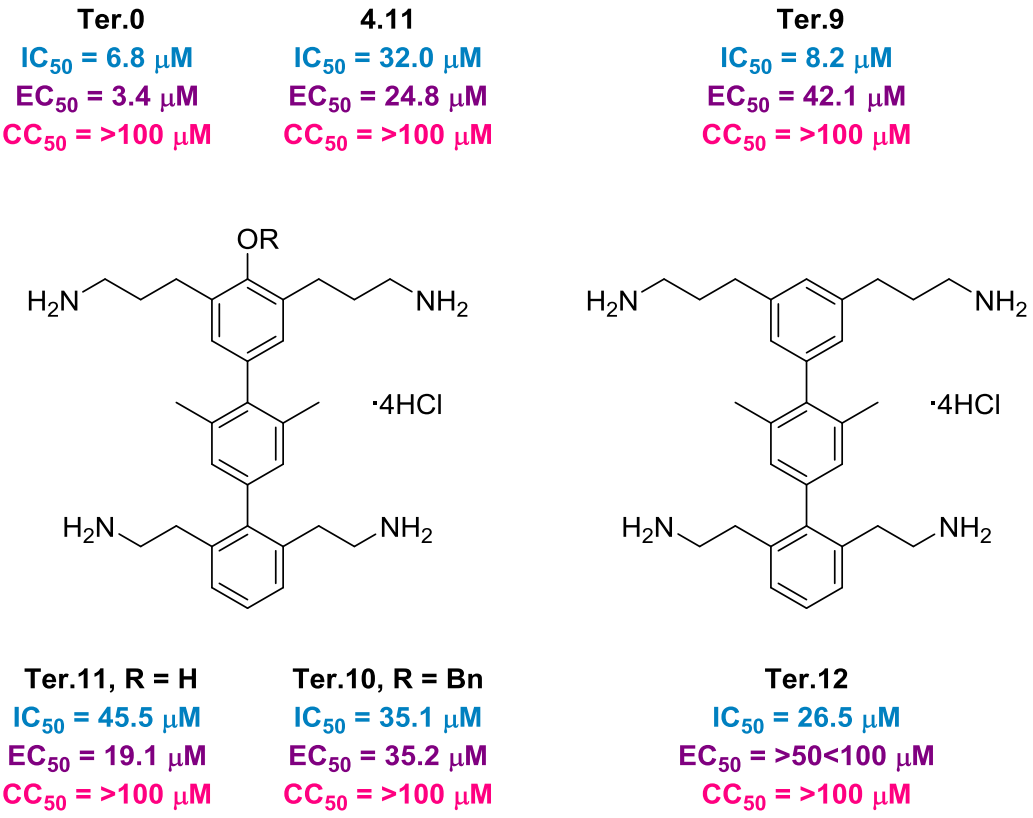

Figure 4.39. Biological results obtained for Ter.10-12, with past results for comparison.

Secondly, the differences in the varied substitution patterns seen in this series were striking. **Ter.13**, bearing a single ethylamine chain in the 2'' position, was inactive (much like **4.48**, see Figure 4.40).[309] When the single ethylamine chain was shifted to the 3'' position in **Ter.14**, however, the biological activity was dramatically enhanced, demonstrating a moderate IC_{50} and a potent EC_{50}. These results

followed the same trend seen in other terphenyls that had been previously synthesised in our research group, within the study into the terphenyls with the relative 1,4 substitution pattern (Figure 4.40).[206, 309] More importantly, **Ter.14** was found to be more cytotoxic than other active bilateral derivatives. This reinforces previous observations that the bilateral substitution pattern is important for the safety of these compounds; since the monolaterally substituted compounds containing two alkylamine chains displayed higher affinity for DNA than the target RNA and exerted their antiviral and cytotoxic activities *via* this mechanism, perhaps these mixed derivatives containing three alkylamine chains have a certain affinity for both.

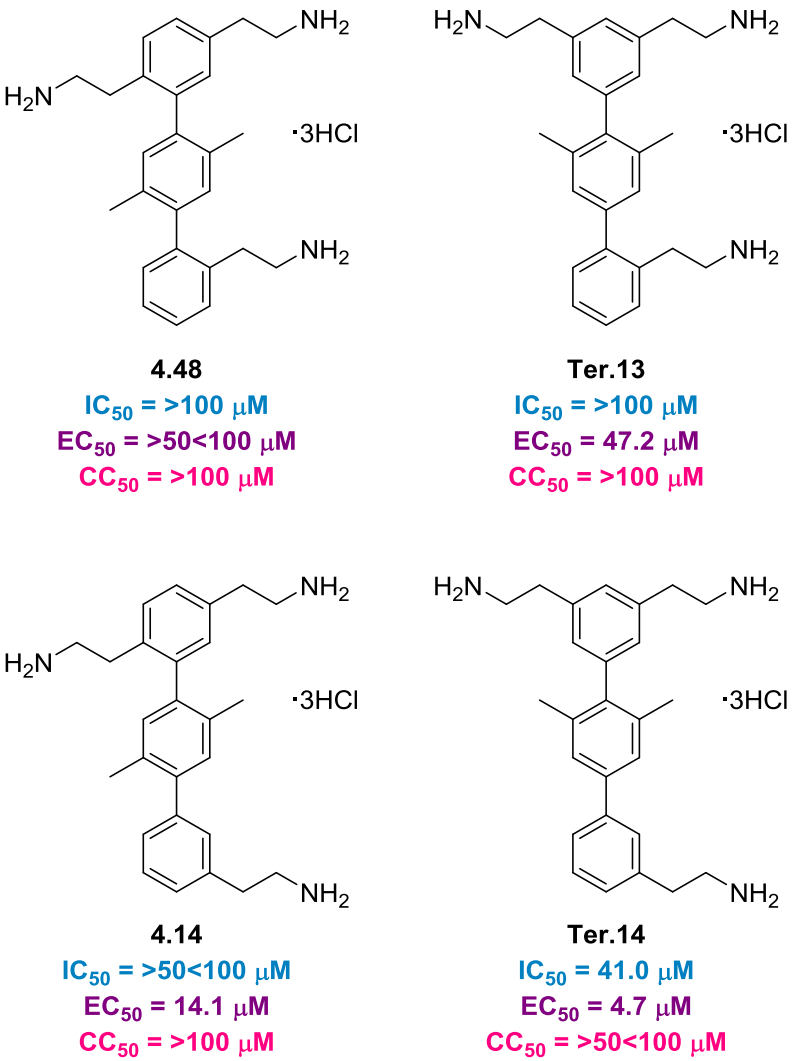

Figure 4.40. Biological results obtained for the Ter.13 and Ter.14.

We also tested the role of the counteranion in several of these compounds, since we assumed we would be able to better control the stoichiometry of the salt formation; using HCl an excess was always added, under the assumption that the remaining HCl would be removed from the mixture *in vacuo*, leaving the hydrochloride salt in perfect balance with the number of amine groups present. However, the hydrochloride salt was invisible to both NMR analysis and mass spectrometry, and so we had no way to test this. We therefore formed the mesylate and tosylate salts of **Ter.9**, **Ter.13** and **Ter.14** since these salts could be observed easily through ^{1}H NMR analysis, and are used widely in other pharmaceutical formulations.[318]

However, this was discontinued given that no significant difference was observed in any of the assays observed for these derivatives.

[318] D. P. Elder, E. Delaney, A. Teasdale, S. Eyley, V. D. Reif, K. Jacq, K. L. Facchine, R. S. Oestrich, P. Sandra and F. David, *J. Pharm. Sci.*, 2010, **99**, 2948-2961.

4.6.4. Bilateral p-terphenyls: effects of varying functional group.

In light of the unpromising results obtained in the biological assays for the previous terphenyls, we decided to synthesise a small series of compounds with more drastic changes in the structure (Scheme 4.29).

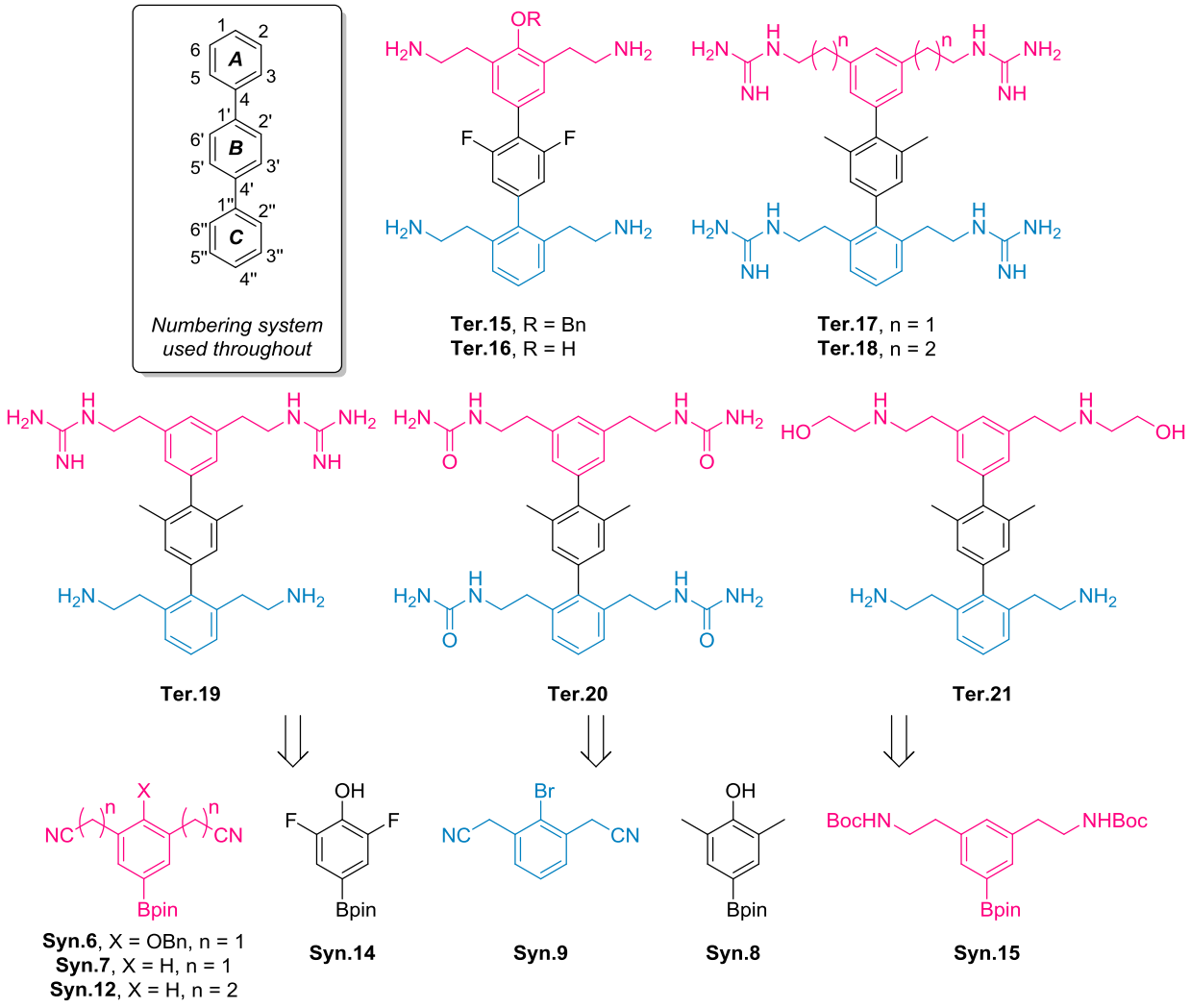

Scheme 4.29. New terphenyls to study the introduction of new functional groups, and the synthons required for their synthesis.

In this context, we first envisioned a fluorinated analogue of **Ter.6-7**, in an attempt to increase the lipophilicity. However, we decided that a direct exchange of the methyl groups in ring **B** for trifluoromethyl groups would be synthetically challenging, and the identification of commercial

compound **4.49** led us to modify this target to **Ter.15-16**, with simple fluorine substituents in positions 2' and 6' (Scheme 4.30).

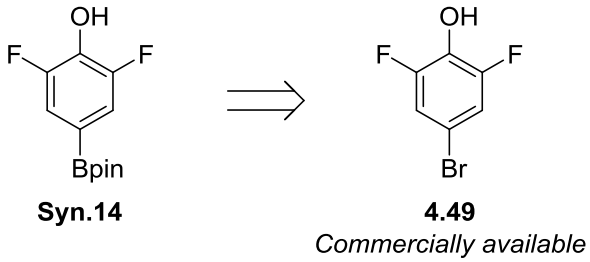

Scheme 4.30. Identification of 4.49 as the precursor for Syn.14 towards fluorinated derivatives Ter.15-16.

Ter.17-19 were steps towards the real challenge in this project; mimicking the active α-helix of the HIV-1 Rev protein using the 360° projection of substituents attached to a terphenyl scaffold. Hence, given the arginine-rich structure of the endogenous Rev protein, we wanted to test some guanidine-containing terphenyls. We knew that the alkylamine chains were capable of mimicking the interaction somewhat, but using the same guanidine functional group as the native Rev protein could potentially forge more interactions with the target RRE, thereby increasing the inhibitory activity. **Ter.20** would contain ureas, similar functional groups with the possibility of forming more interactions with the biological target than the simple amines that we had been working with thus far. **Ter.21** was a somewhat capricious option due to the common use of the aminoalcohol moiety in RNA-binding compounds.

In terms of their synthesis, both **Ter.19** and **Ter.21** would require a new synthon in order to selectively functionalise the amine chains in positions 2 and 6. Therefore, we decided that we would be able to selectively carry out downstream chemistry on terphenyls derived from **Syn.15**, containing *N*-Boc alkylamine chains.

4.6.4.1. Synthesis of bilateral terphenyls **Ter.15-21.**

Synthesis of terphenyls Ter.15-16.

In theory, the only new synthon necessary for this terphenyl was **Syn.14**, which was synthesised *via* Miyaura borylation using the same conditions as had been used throughout this project (Scheme 4.31).

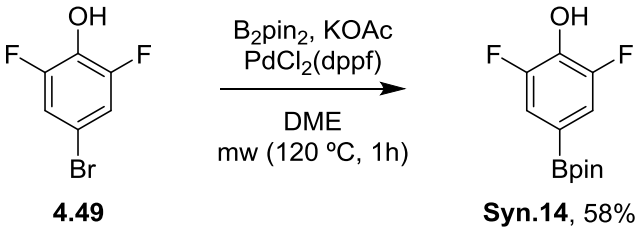

4.49 **Syn.14**, 58%

Scheme 4.31. Synthesis of Syn.14 from commercially available 4.49.

From there, the terphenyl was constructed as seen in the rest of the cases (Scheme 4.32). However, the final reduction of the nitrile groups was unsuccessful. The resulting crude product was difficult to purify and all identified fractions lacked fluorine; most likely due to the increased ability of aromatic fluoride substituents to undergo nucleophilic substitution, thereby being replaced by hydrogen during the prolonged treatment with borane.

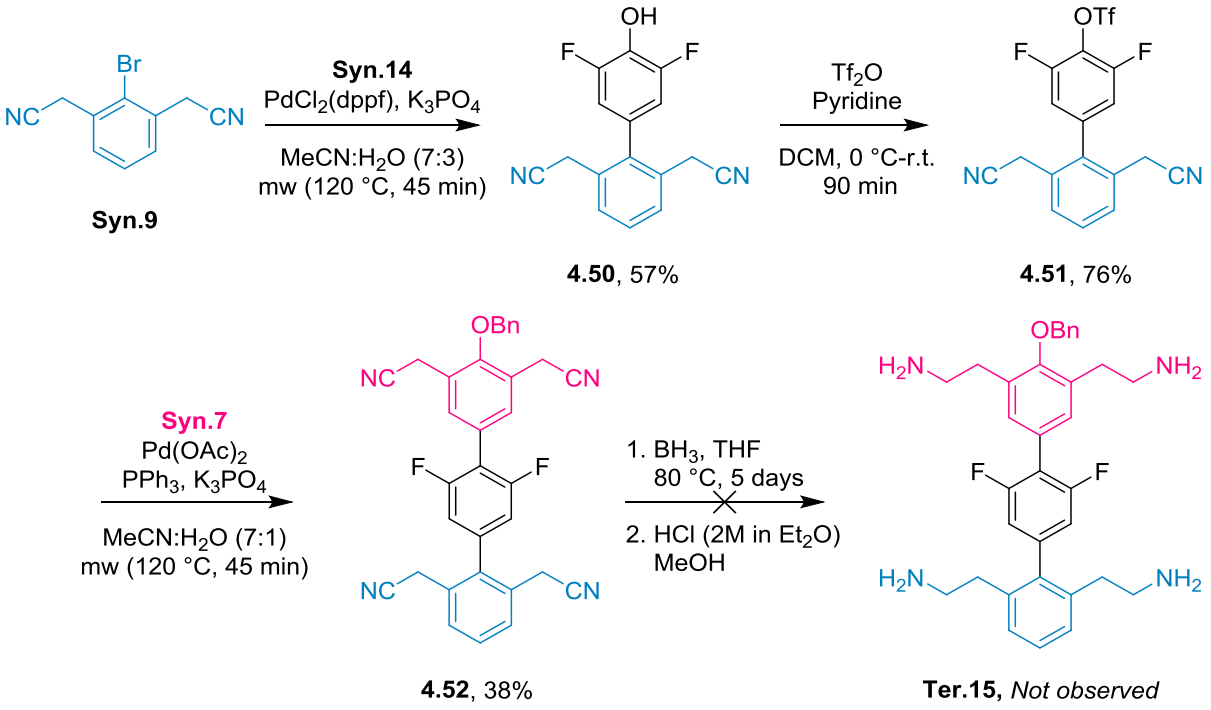

Scheme 4.32. So close yet so far.

Therefore, we resorted to an alternative route relying on the prior reduction of the nitrile groups, thus proceeding with protected amines. We identified different synthons for this cause, making use of the *N*-Boc protecting group due to its facile introduction (Scheme 4.33). We also removed the benzyl ether group in the 1 position for simplicity, since we had to synthesise the synthons from scratch, hence designing a new terphenyl which lacked this substituent, **Ter.22**.

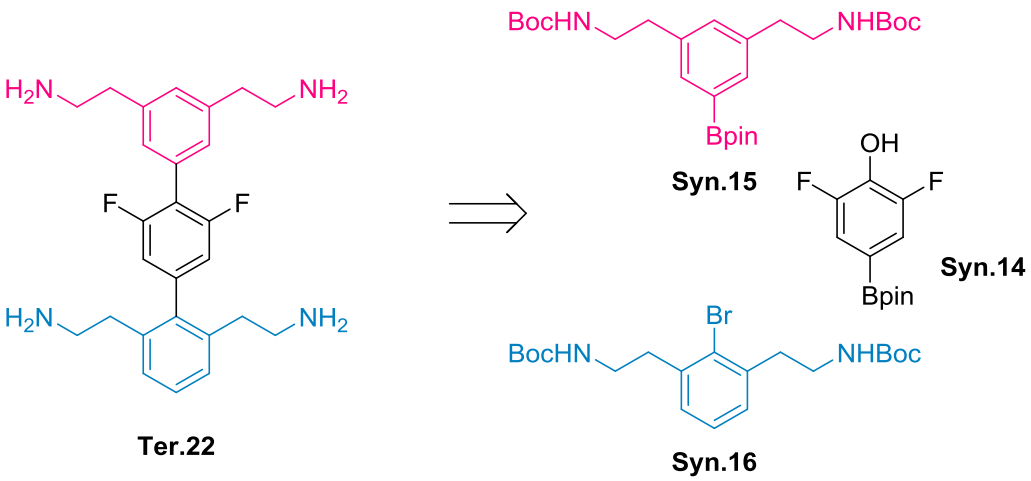

Scheme 4.33. Use of previously reduced synthons avoiding the exposure of aromatic fluorides to borane reduction towards a new target, Ter.22.

These synthons were synthesised easily from the corresponding nitriles **4.36** and **Syn.9** *via* borane reduction and subsequent Boc-protection and, in the case of **Syn.15**, a final borylation reaction. The conditions used here were somewhat different for this synthon, since a short bibliographic search revealed that substrates bearing similar aminoethyl chains reacted well under microwave irradiation in acetonitrile at high temperatures. This methodology resulted in high yields after just 15 minutes of reaction time, as opposed to the hour-long standard procedure used throughout this project (Scheme 4.34).[319]

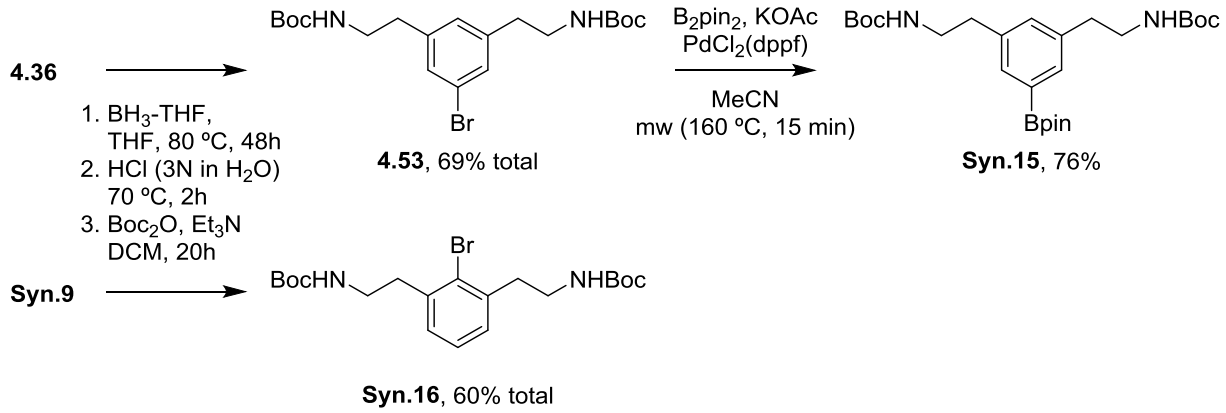

Scheme 4.34. Synthesis of synthons Syn.15-16.

Upon the successful synthesis of these new synthons, the route towards fluorinated terphenyl **Ter.22** was attempted once again, with the Suzuki couplings taking place in decent yields just as with the nitrile derivatives (Scheme 4.35).

This time, the deprotection of the Boc protecting groups proved problematic, most likely due to the purification of the product. We first utilised a standard deprotection procedure, an excess of trifluoroacetic acid (TFA) in dichloromethane, but we were unable to isolate the desired **Ter.22**. In terms of the reaction mechanism, after deprotection of the Boc groups, more trifluoroacetic acid would remain in the reaction media. Given that the resulting product contains four primary amines, the final result would be the trifluoroacetate salt. Therefore in the typical reaction work-up involving liquid-liquid extraction, the desired product would presumably remain in the aqueous phase. Even after basification of the aqueous phase, we were unable to detect the product in the organic phase; the final terphenyl structures are generally water-soluble. Hence, we were unable to separate the desired product from trifluoroacetate salts, and therefore were unable to acceptably purify the final terphenyl.

[319] C. Leblanc, R. A. Pulz and N. J. Stiefl, Int. Pat., 2009087225, 2009.

The synthesis of **Ter.22** was unfortunately never finalised and was abandoned after these two failed synthetic sequences.

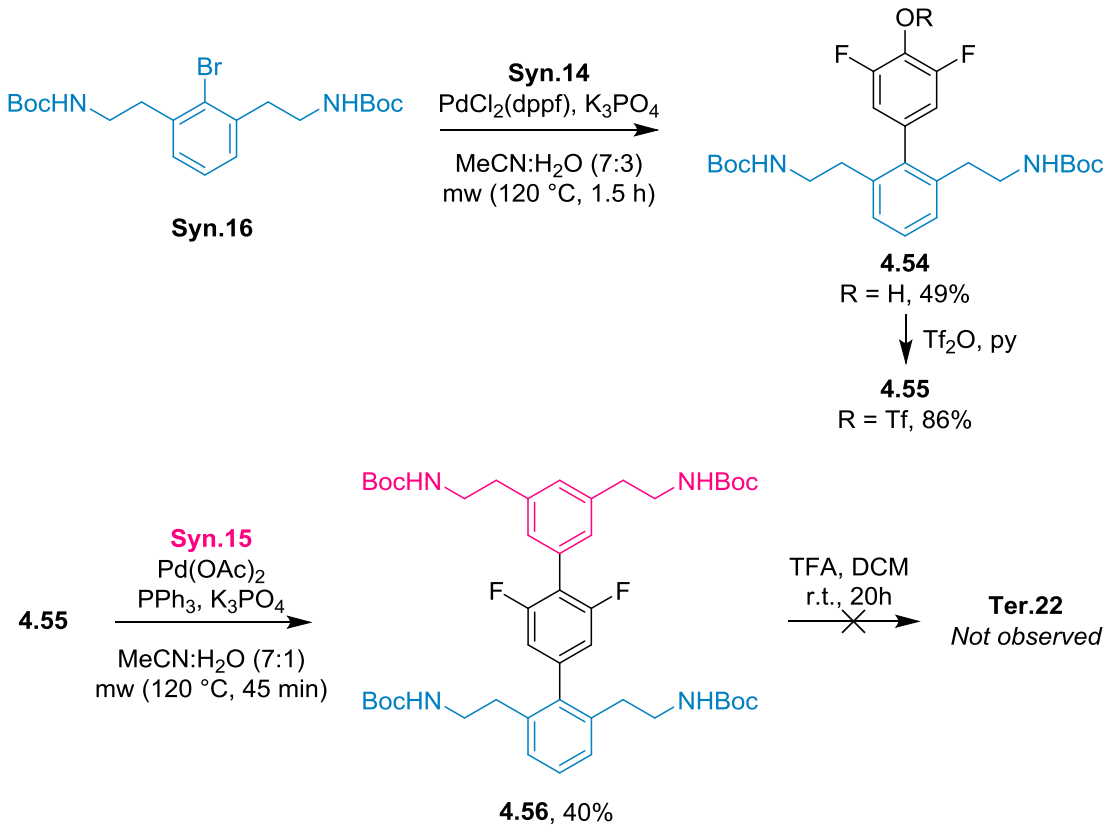

Scheme 4.35. Synthesis of second Ter.22 precursor 4.56, and failed attempt at *N*-Boc deprotection.

Synthesis of terphenyls Ter.17-19.

Turning to the more promising guanidine-bearing terphenyls **Ter.17-19**, we identified Goodman's reagent as a suitable choice for the introduction of the guanidine groups, which can be used to guanidinylate both primary and secondary amines in high yields under mild conditions (Scheme 4.36).[320] The original report even details the use of this reagent to introduce multiple guanidine groups into polypeptide-based amine substrates, showcasing the efficiency of this procedure.

[320] K. Feichtinger, H. L. Sings, T. J. Baker, K. Matthews and M. Goodman, *J. Org. Chem.,* 1998, **63**, 8432-8439.

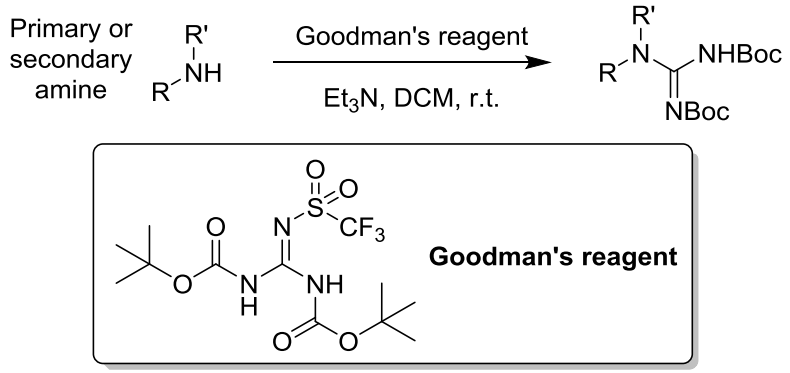

Scheme 4.36. Goodman's guanidinylation reagent.

Firstly, the terphenyl scaffold for **Ter.19** was synthesised, starting from biphenyl triflate **4.38a**. Subsequent Boc deprotection rendered the free amines which would then be suitable substrates for the guanidinylation reaction (Scheme 4.37). It's worth noting that in this case, with just two amines and two nitriles, the deprotection reaction proceeded smoothly in the mixture of trifluoroacetic acid/DCM, as well as the isolation.

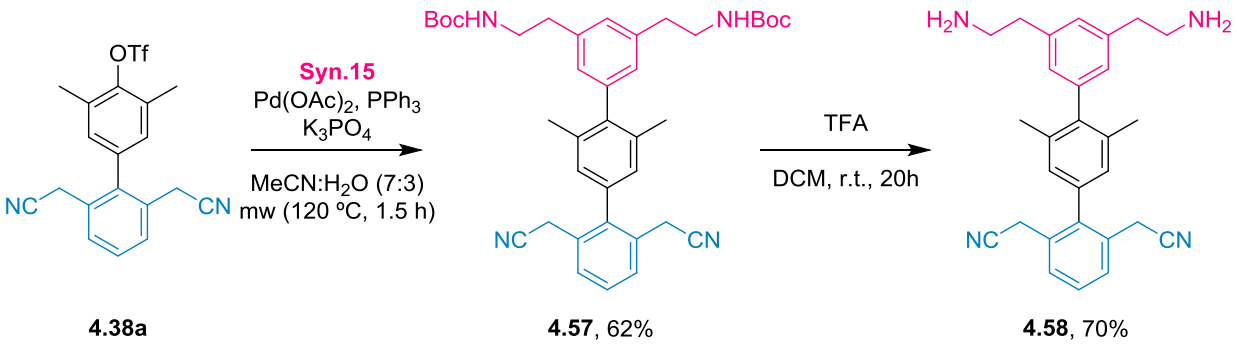

Scheme 4.37. Synthesis of terphenyl 4.58, precursor to the guanidinylation reaction towards Ter.19.

On the other hand, **Ter.17** and **Ter.18** were synthesised starting from **Ter.9** and **Ter.12** respectively. We first attempted to introduce the guanidine group following Goodman's reaction conditions, which involved adding the amine to a solution of the guanidinylation reagent and triethylamine in dichloromethane. This was successful in the case of **4.58**, however, for the other tetramine substrates the reaction failed to take place. This was most likely due to solubility issues; neither **Ter.9** nor **Ter.12** was soluble in dichloromethane. Similarly disappointing results were obtained when using a mixture of THF:DCM, although we found that adding a minimum of methanol to the reaction mixture—just

enough to dissolve all the reactants—gave much better results. In this way, guanidine-bearing terphenyls **4.59a-c** were obtained (Scheme 4.38).

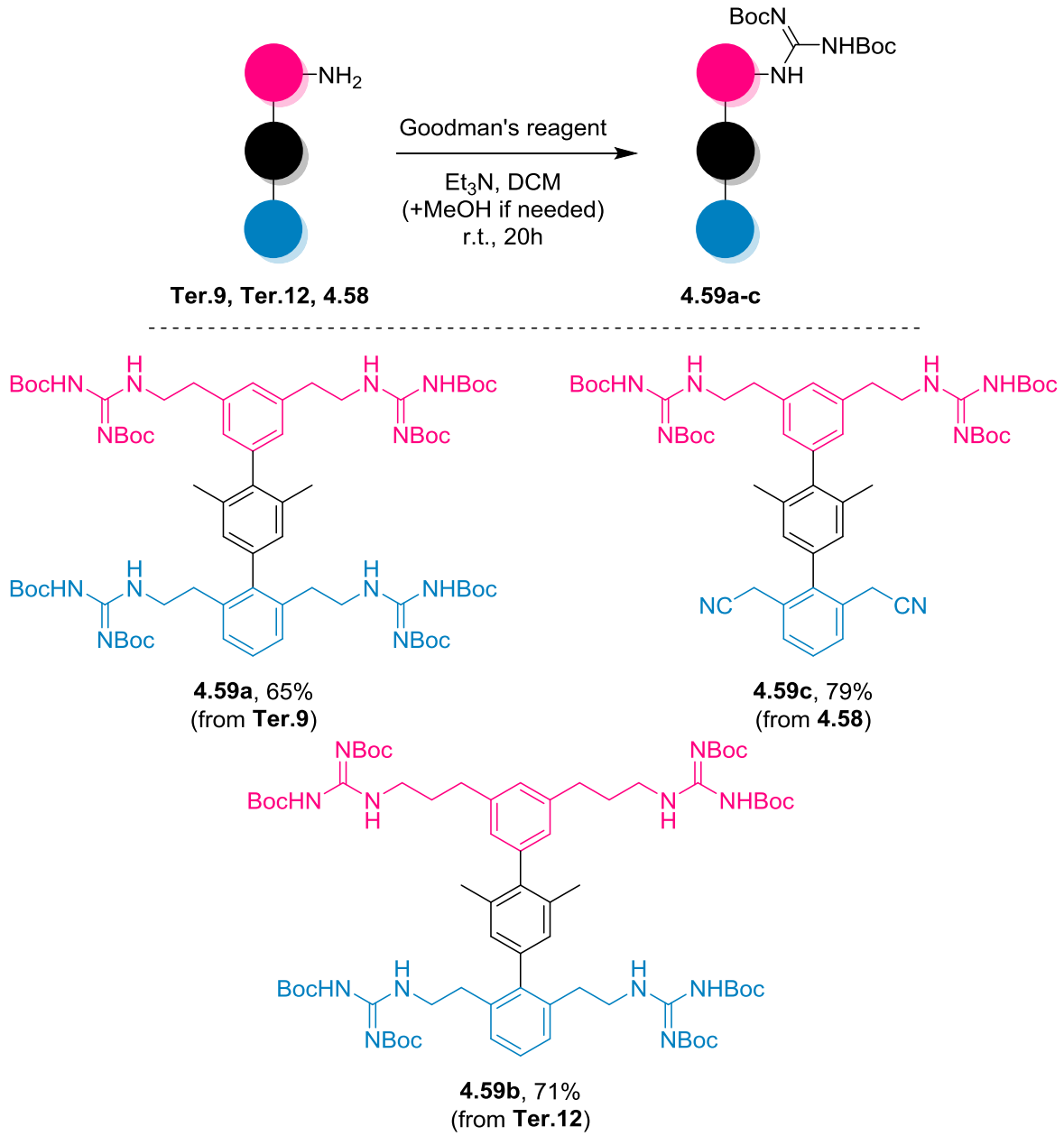

Scheme 4.38. Synthesis of guanidine-bearing terphenyls.

Once these terphenyls had been obtained, we proceeded to carry out the final steps. In the case of **Ter.17** and **Ter.18**, the only remaining step was the deprotection of the guanidines, whereas **Ter.19** required both a reduction of the nitrile groups and subsequent deprotection. Deprotection of the four guanidine groups in **4.59b** using TFA/DCM gave results similar to those in the previous section in the

attempt to synthesise fluorinated **Ter.22**—we were unable to purify **Ter.18** in this way. However, we found that treatment with a 1:1 mixture of HCl (4N in dioxane) and HCl (4N in water) successfully removed the Boc protecting groups when heated at 40 °C for 20h. Furthermore, these conditions required neither extraction nor further purification: all Boc groups were successfully removed, and simple concentration of the reaction mixture afforded **Ter.18·4HCl** in good yield (Boc removal leaves no residue, as all side-products are volatile). **Ter.17·4HCl** was obtained *via* the same method (Scheme 4.39).

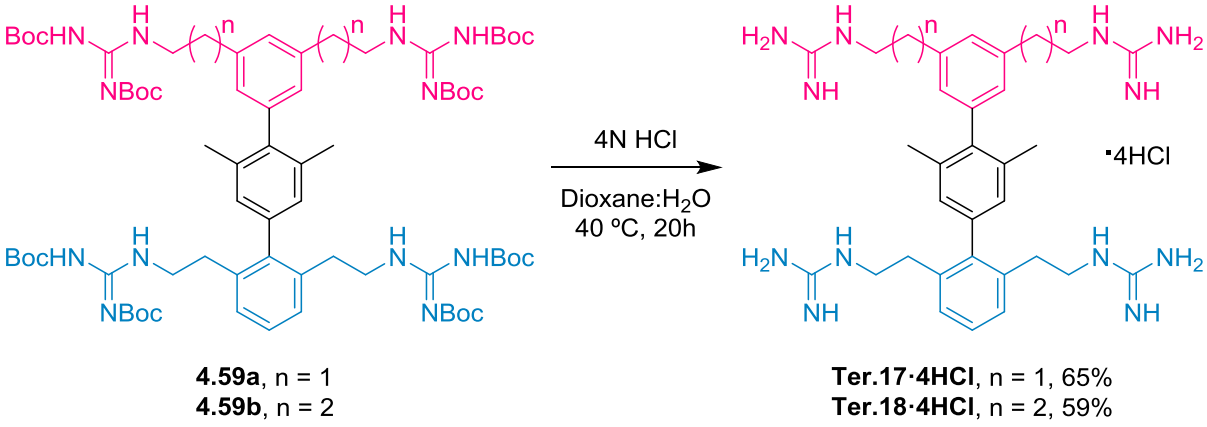

Scheme 4.39. Boc deprotection to afford Ter.17 and Ter.18.

Finally, the synthesis of **Ter.19** proved to be more troublesome than we had first expected, due to a problem we had initially overlooked. The borane reduction of the nitrile groups requires subsequent hydrolysis of the boron adducts that form during the reduction process, which we had usually carried out with aqueous hydrochloric acid. However, the Boc group is unstable in acidic conditions, and even using equimolar amounts of HCl and BH_3, the reaction was unsuccessful. The borane reduction of nitriles throughout this project had never been a "clean" reaction, and had always required purification by flash column chromatography afterwards. This also meant that we couldn't carry out the transformations in a one-pot manner, using HCl both to quench the borane in the reduction step and simultaneously carry out the Boc removal, since we would be unable to purify the resulting mixture. Due to this, **Ter.19** was also abandoned and the synthesis was not finalised.

Synthesis of terphenyl Ter.20

The synthesis of this urea-bearing terphenyl also used **Ter.9** as a starting point. Here, we envisioned using benzyl isocyanate to introduce the urea. This had the advantage of containing more hydrophobic

phenyl rings in an attempt to increase the solubility of the resulting tetraurea; ureas tend to be fairly insoluble in many organic solvents. Furthermore, this way we would be able to purify the benzylated intermediate before subjecting it to hydrogenolysis of the benzyl groups.

We therefore treated **Ter.9** with benzyl isocyanate in dichloromethane, and despite expected solubility issues we obtained the corresponding product in good yield and high purity (Scheme 4.40). However, **4.60** proved to be insoluble in almost every solvent tested, including water, although it was partly soluble in DMSO (just enough to obtain an acceptable ^{1}H NMR spectrum). These solubility problems hindered any advances and the subsequent hydrogenation reaction failed to proceed in all solvents tested. We therefore also abandoned the synthesis of this terphenyl derivative.

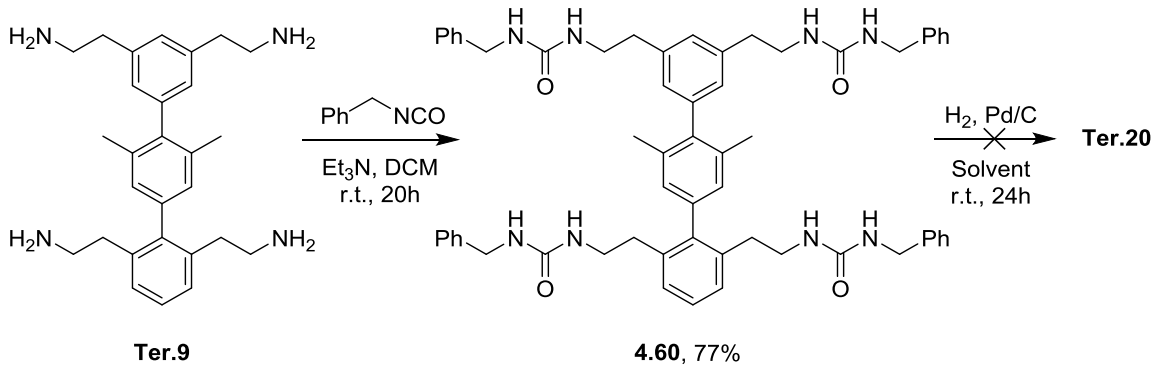

Scheme 4.40. Attempted synthesis of Ter.20.

Synthesis of terphenyl Ter.21.

The synthesis of this terphenyl was similar to that of **Ter.19**, in that ring **A** contained functionalised amines whereas ring **C** did not; an orthogonal protection strategy was also necessary in this case. In order to add the hydroxyethyl group onto the aminoethyl chains in positions 2 and 6, we identified 2-iodoethanol as a suitable substrate. We first tested the reaction with benzylamine, and obtained the desired product in almost quantitative yield (Scheme 4.41). What's more, liberation of the acid HI during the reaction meant that product **4.61** precipitated as the corresponding HI salt.

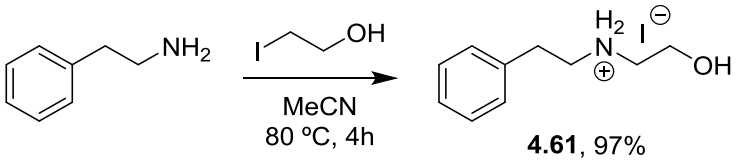

Scheme 4.41. Initial tests towards the introduction of the hydroxyethyl group.

With this in mind, terphenyl intermediate **4.58** was treated with 2-iodoethanol in acetonitrile as the solvent, giving rise to the corresponding product **4.62** in moderate yield. From there, we reduced the nitrile groups using borane-THF complex as we had done throughout this project—although we employed a greater excess of borane in this reaction due to the presence of the aminoalcohol substituents on ring **A** (Scheme 4.42).

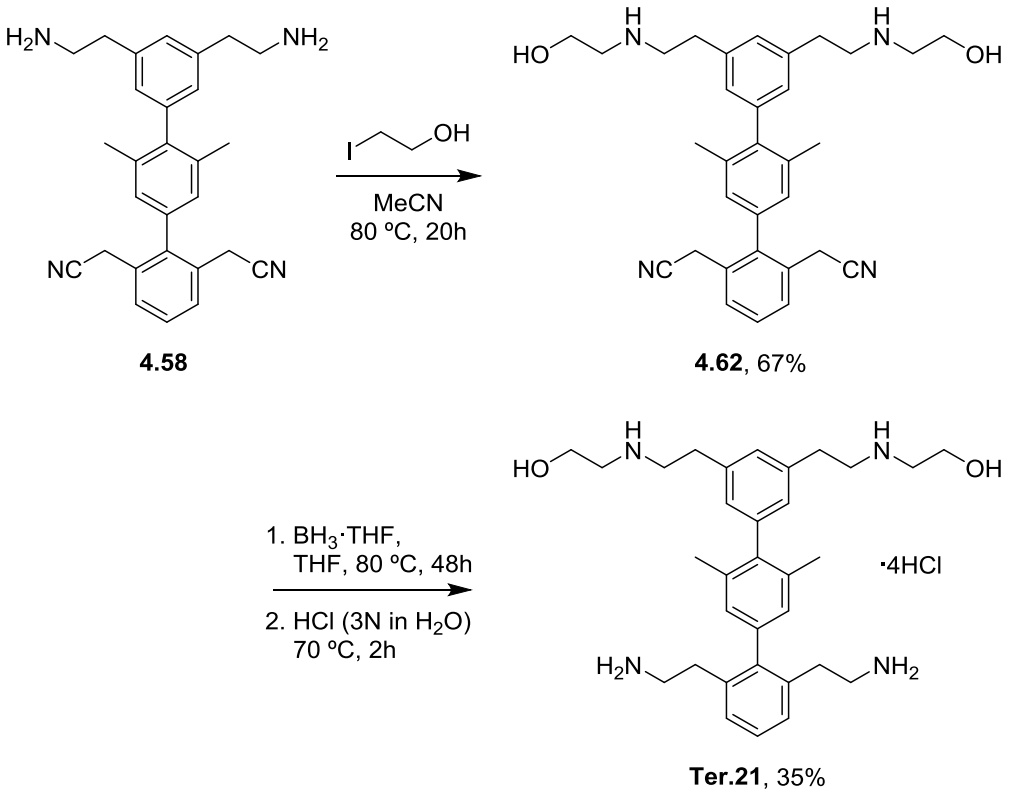

Scheme 4.42. Synthesis of Ter.21.

4.6.4.2. Biological evaluation.

Unfortunately, we only have preliminary results for *in vitro* studies relating to **Ter.17** and **Ter.18**. However, the results are promising. **Ter.17** and **Ter.18** are active in both the fluorescence anisotropy and electrophoresis assays, approximately at the same level as **4.12** (Figure 4.41). However, these experiments need to be replicated and the results confirmed. At the time of writing we do not have *in vivo* values (EC_{50} and CC_{50}) for these derivatives.

On the other hand, **Ter.21** was inactive at the maximum concentration employed in all assays (100 μM).

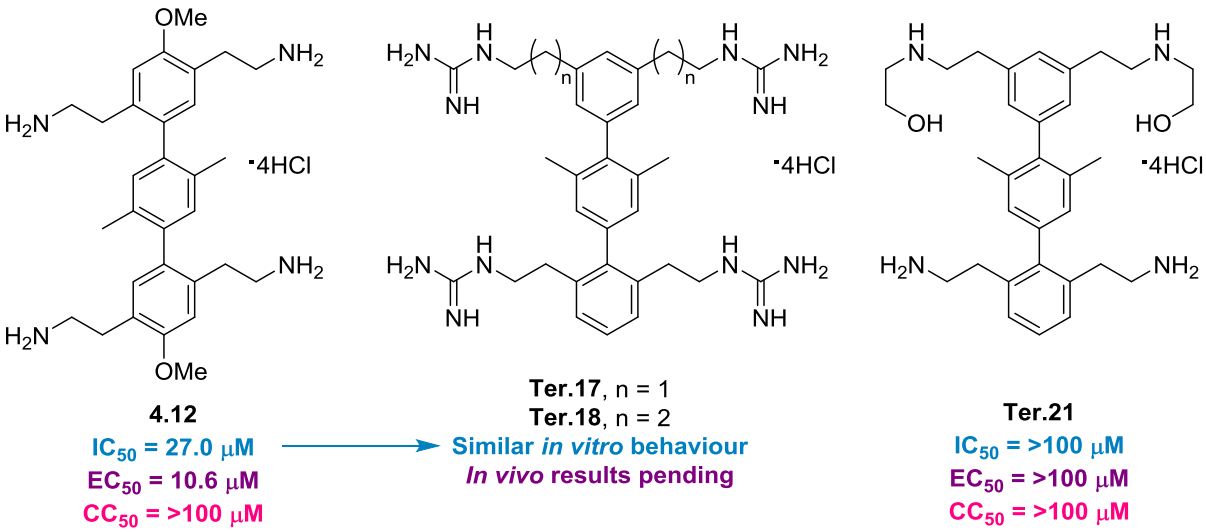

Figure 4.41. Biological results obtained for derivatives containing different functional groups.

4.7. Malaria

4.7.1. Introduction.

Malaria is the most widespread parasitic infection that affects humans. According to the WHO, in 2016 a total of 216 million new cases of malaria and 445,000 deaths were reported by 91 countries worldwide.[321] However, others argue that since the WHO relies on countries to report these infections, and since up to 90% of global infections are in Africa and other such underdeveloped areas, the real figures could be up to double this amount, with most estimates placing annual deaths around the 1 million mark.[322] A large percentage of malaria-related deaths correspond to Sub-Saharan African children under the age of 15. Although there are antimalarial treatments available, parasitic resistance and the high cost of dealing with the sheer number of infections in poor communities means that there is an urgent need for the development of cheaper medicines that are less susceptible to resistance phenomena.

Malaria is caused by protozoan parasites belonging to the *Plasmodium* genus. Four species of parasite account for nearly all global infections: *P. falciparum, P.vivax, P. malariae* and *P. ovale*. Of these, *P. falciparum* produces the most severe disease and is the cause of the majority of malaria-related deaths. The areas that suffer most from malaria correlate fairly well with those that also have the highest rates of HIV infection, and the two are thought to interact in several ways: 1) malaria could increase HIV viral load in infected people; 2) the compromised immune system of HIV patients worsens the fevers associated to malaria; and 3) the HIV virus interacts adversely with malaria during pregnancy.[323]

The parasitic life cycle begins with a bite from the vector—usually female mosquitoes from the *Anopheles* genus—during which sporozoites are injected into the host (Figure 4.42). Sporozoites are motile and once inside the body they migrate to the liver, where they infect liver hepatocytes and produce merozoites. These cells then burst free from the liver cells and infect red blood cells; this is the most severe stage of the infection, and can result in anaemia, fevers and vomiting. The cells continue to develop in the red blood cells and eventually produce gametocytes, the sexual stage of the parasite. The life cycle is complete when another vector bites the patient and consumes the gametocytes in the red blood cells.[324]

[321] World Health Organization, *World Malaria Report 2017*, Geneva: 2017. Licence: CC BY-NC-SA 3.0 IGO.
[322] R. W. Snow, C. A. Guerra, A. M. Noor, H. Y. Myint and S. I. Hay, *Nature*, 2005, **434**, 214-217.
[323] B. M. Greenwood, K. Bojang, C. J. M Whitty and G. A. T. Targett, *Lancet*, 2005, **365**, 1487-1498.
[324] R. Batista, A. de Jesus Silva Junior and A. Braga de Oliveira, *Molecules*, 2009, **14**, 3037-3072.

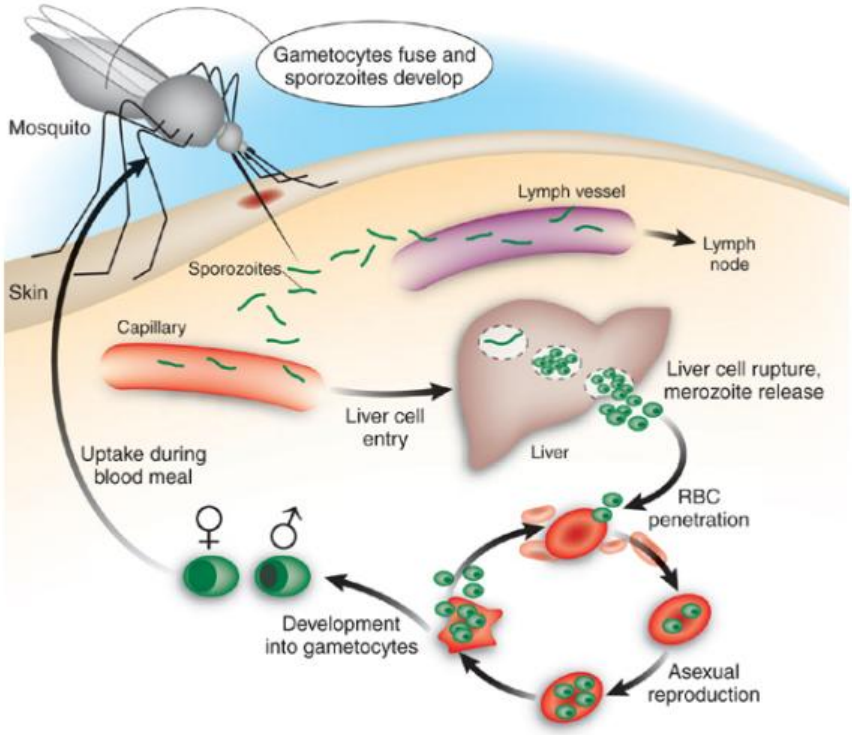

Figure 4.42. Life cycle of *Plasmodium* spp. parasites in humans, the cause of malaria.[324, 325]

[325] M. K. Jones and M. F. Good, *Nat. Med.*, 2006, **12**, 170-171.

4.7.2. Specific target and mimic design.

A key part of this cycle is the infection of red blood cells by the merozoite life-stage, during which the parasite attaches itself to the red blood cell surface *via* the apical complex—a defining feature of apicomplexan parasites that mediates host penetration and invasion.[326] Once attached, it passes through the erythrocyte (red blood cell) membrane and occupies a parasitophorous vacuole in which it replicates, effectively "hidden" from the host's immune system. Invasion takes just 30-60 seconds and is driven by a multi-protein motor complex located between the inner-membrane complex and the merozoite cell membrane (Figure 4.43).[327]

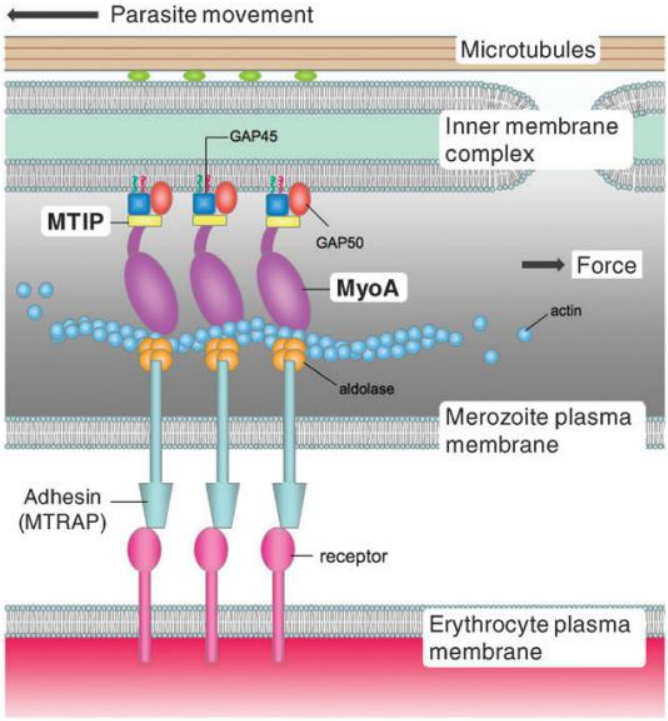

Figure 4.43. *Plasmodium* spp. motor complex structure.

This motor complex is highly conserved throughout the *Plasmodium* genus, both in sporozoites and merozoites, and features a myosin A (MyoA) protein that is anchored to the inner membrane *via* binding of an α-helical tail domain to the membrane-bound myosin-tail domain interacting protein (MTIP). This interaction is key in coupling MyoA ATP hydrolysis to the production of motive force, which

[326] N. Okamoto and P. J. Keeling, *PLoS One*, 2014, **9**, e84653. (doi:10.1371/journal.pone.0084653)
[327] J. C. Thomas, J. L. Green, R. I. Howson, P. Simpson, D. K. Moss, S. R. Martin, A. A. Holder, E. Cota and E. W. Tate, *Mol. BioSyst.*, 2010, **6**, 494-498.

is necessary for invasion of host red blood cells. This interaction currently remains an unexploited target in current antimalarial drugs, but represents an important possibility given the highly conserved nature of the structures of both MyoA and MTIP across similar parasitic species, which means that the inhibition of this interaction should be less susceptible to resistance phenomena.[328] Furthermore, antimalarial treatment based on the inhibition of this interaction would avoid all invasion processes, essentially *preventing* the disease rather than *curing* it.

Interestingly, the X-ray crystal structure of the MTIP-MyoA complex, available in the protein database (PDB), reveals that the α-helix of MyoA is deeply embedded in the MTIP protein, making it a suitable target to be mimicked by a bilaterally substituted terphenyl.[329] Using database searches,[330] the group of J. Gallego identified this protein-protein contact as a suitable target and was able to model some initial terphenyl designs, mimicking residues *i*, *i* + 1, *i* + 4, *i* + 5, *i* + 7, and *i* + 8 just like in the previously discussed bilaterally substituted terphenyls used in studies to inhibit the Rev-RRE interaction (Figure 4.44, a). Most importantly, several of the MyoA α-helix residues amenable to be mimicked by the terphenyl side chains, specifically R806 (*i* + 1), R812 (*i* + 7) and K813 (*i* + 8), had been identified as hotspots for this interaction,[330] and a good overlap was detected by molecular modelling between the butylamine side chains of terphenyl compounds designed to inhibit the MTIP-MyoA interaction and the charged hotspots of the protein. In terms of the new target, the residues within the MyoA α-helix to be mimicked would be the following: M805(*i*)R(*i* + 1)VQA(*i* + 4)H(*i* + 5)IR(*i* + 7)K813(*i* + 8) (Figure 4.44, b).

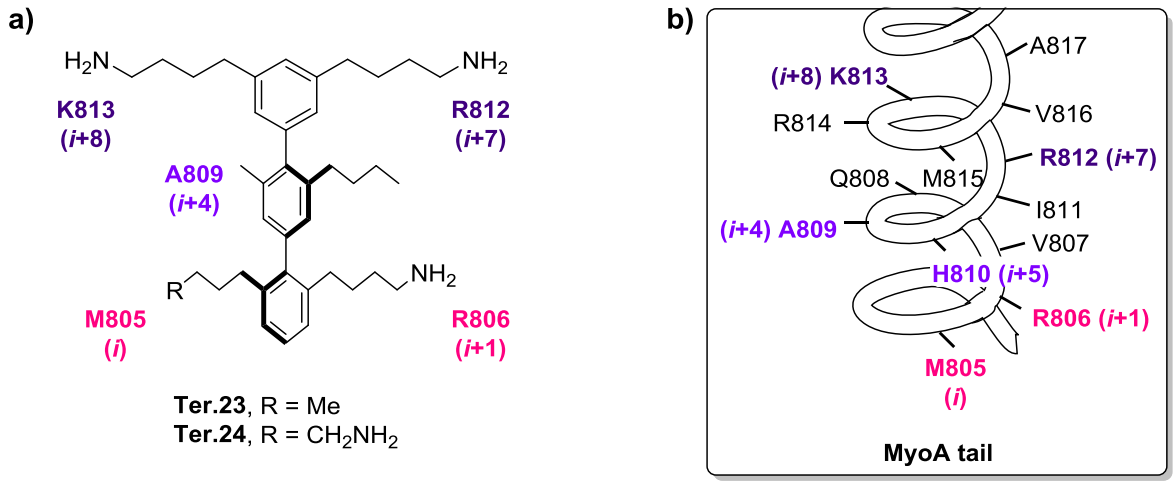

Figure 4.44. a) Structures of initial terphenyl designs. b) MyoA α-helix tail structure and the residues to mimic.

[328] a) S. Kortagere, W. J. Welsh, J. M. Morrisey, T. Daly, I. Ejigiri, P. Sinnis, A. B. Vaidya and L. W. Bergman, *J. Chem. Inf. Model*, 2010, **50**, 840-859. b) C. H. Douse, N. Vrielink, Z. Wenlin, E. Cota and E. W. Tate, *ChemMedChem*, 2015, **10**, 134-143.

[329] J. Bosch, S. Turley, C. M. Roach, T. M. Daly, L. W. Bergman and W. G. J. Hol, *J. Mol Biol.*, 2007, **372**, 77-88.

[330] C. M. Bergey, A. M. Watkins and P. S. Arora, *Bioinformatics*, 2013, **29**, 2806-2807.

The presence of positively-charged residues, i.e. Arg-812 and Lys-813, was important to our decision; given our previous experience working with Rev mimetics, we knew that alkylamine chains were capable of mimicking arginine residues resulting in active terphenyl compounds. **Ter.23** would contain an *n*-butyl chain in the 6'' position in an attempt to more efficiently mimic the methionine residue in the native helix. However, since we had less experience in the synthesis of asymmetrical terphenyls of this type containing aliphatic hydrocarbon chains, **Ter.24** was also explored—which contained a fourth butylamine chain in place of the *n*-butyl in the 6'' position (Figure 4.44). This terphenyl was found to have a strong overlap with the residues of the native MyoA within the MTIP binding site during *in silico* analysis (Figure 4.45).

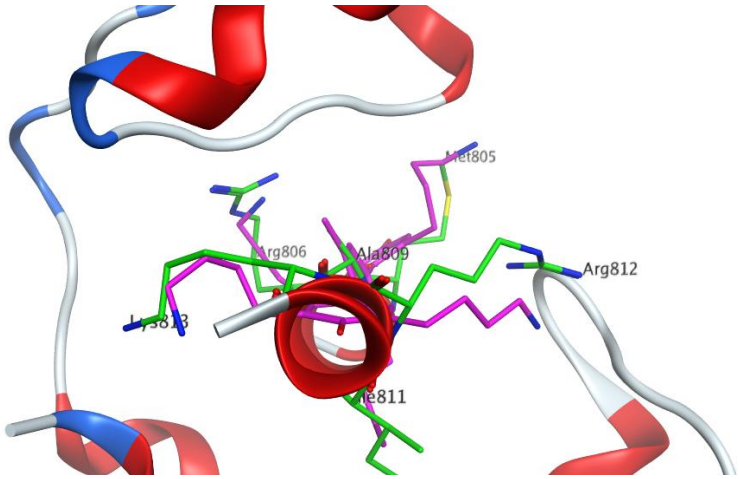

Figure 4.45. Overlap of Ter.24 (magenta) with MyoA (green side chains) within the MTIP (white) binding site.

Nevertheless, despite the synthetic challenge that it would likely present, we decided that **Ter.23** would be a better option. This study was based on protein-protein interactions, rather than protein-RNA interactions involved in the binding of Rev to the RRE region, and so we reasoned that excessive positive charge would be less beneficial in this case. Therefore **Ter.23**, which contains only positive charges in the same locations as the native MyoA protein should, in theory, provide a better imitation of the endogenous protein. Furthermore, methionine residue M805 is more similar to the *n*-butyl chain present in the 5'' position of **Ter.23** rather than the butylamine chain in **Ter.24**.

4.7.3. Retrosynthetic analysis of **Ter.23.**

This structure, in contrast with the previously seen examples, was somewhat less symmetrical and only contained three alkylamine substituents, the fourth being replaced by a simple alkyl chain (Figure 4.46).

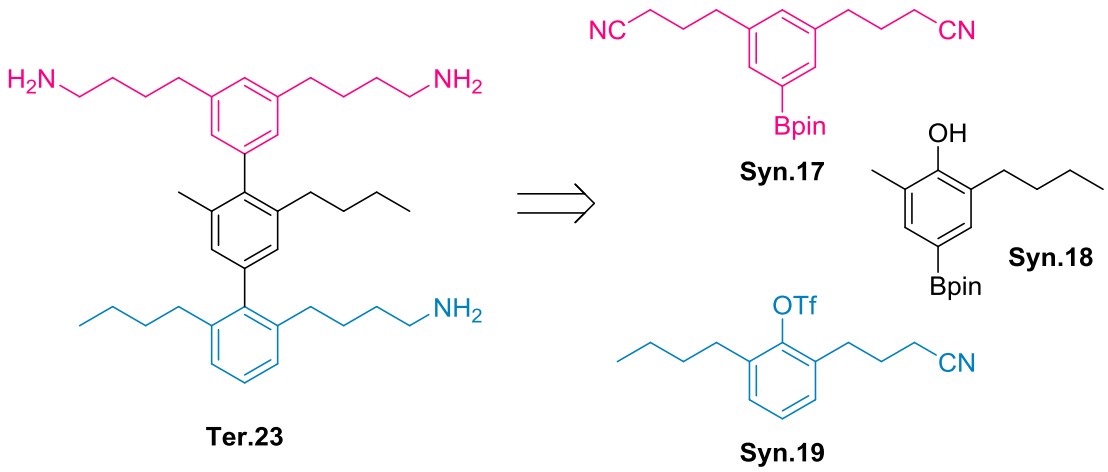

Figure 4.46. Structure and retrosynthesis of Ter.23.

When designing the synthetic route to **Ter.23**, we came across some problems. With regards to **Syn.17**, we imagined that perhaps the simplest way to carry this reaction out would be the synthesis of 3,5-diallylbromobenzene—which was described in the literature[331]—followed by a double cross metathesis with acrylonitrile and subsequent hydrogenation to obtain the aryl bromide precursor. However, this reaction was unsuccessful, and we decided that we could substitute the butylamine side chains on phenyl ring **A** with propylamine chains instead, given that we had seen previously that both ethyl- and propylamine chains were able to mimic arginine residues. This would simplify the synthesis greatly, since we could use previously synthesised **Syn.12** to access the required ring **A**. We would therefore focus on a terphenyl with a slightly different structure (*vide infra*).

Syn.18 would also be somewhat of a challenge due to the unsymmetrical substitutions on either side of the central terphenyl axis. Therefore, we decided that a Wittig reaction would be the easiest method to introduce the butyl substituent, starting from the corresponding aldehyde, which in turn could be installed using the Duff formylation used previously in the synthesis of **4.24** (Scheme 4.43).

[331] Y. Maegawa, M. Waki, A. Umemoto, T. Shimada and S. Inagaki, *Tetrahedron*, **69**, 5312-5318.

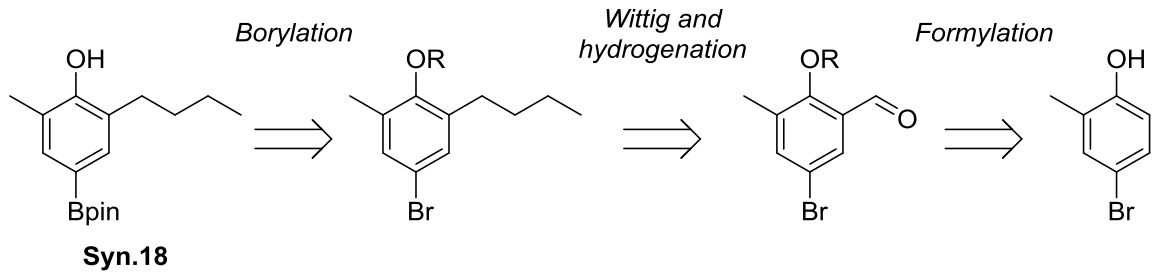

Scheme 4.43. Retrosynthesis of Syn.18.

With regards to **Syn.19**, we originally envisioned a cross-metathesis reaction between propene and 2-allylphenol—a cheap and commercially available reagent—to construct the butyl chain. However, we reasoned that as an initial structure to test the hypothesis, we could use a shorter propyl chain and save the cross-metathesis step (as well as possible protection/deprotection) (Scheme 4.44, a). Therefore, we set out to synthesise an analogous structure with a propyl chain on the lower synthon (Scheme 4.44, b).

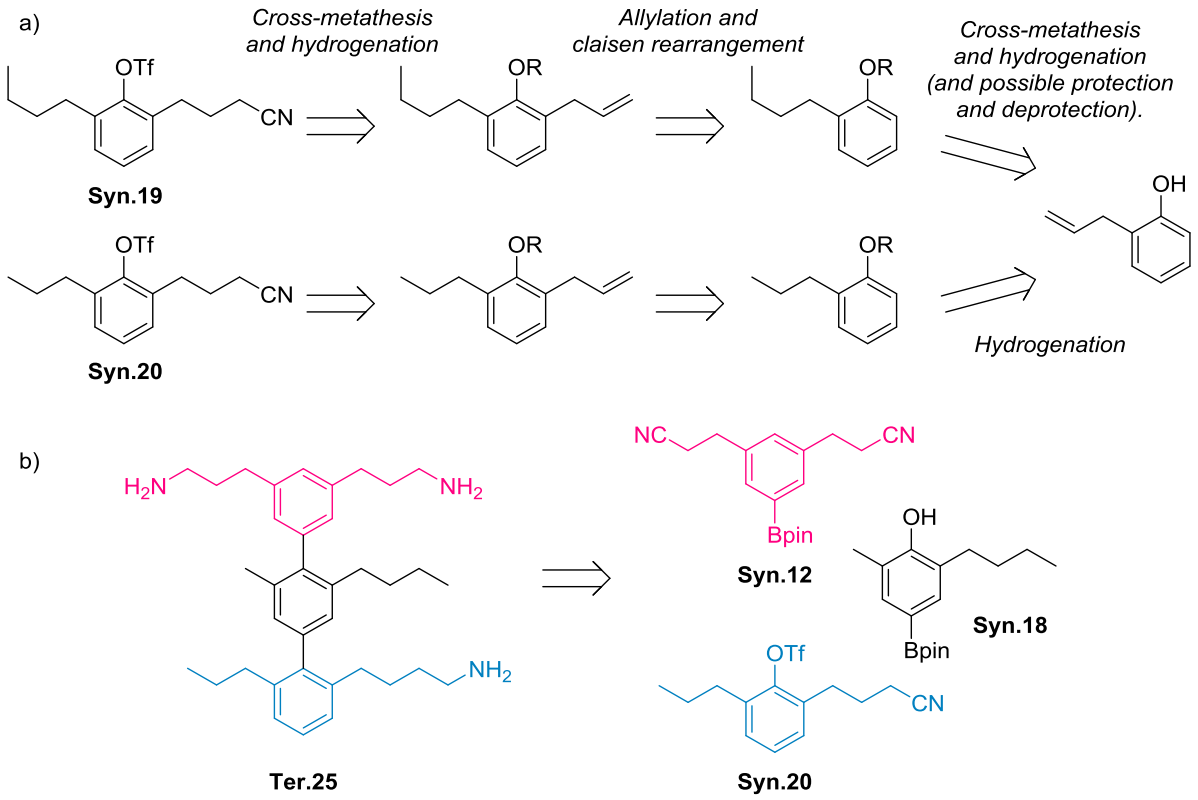

Scheme 4.44. a) Retrosynthetic analysis of Syn.19 and Syn.20; comparison of the butyl- vs. propyl-containing aromatic ring. b) New target structure after retrosynthetic analysis, Ter.25, and the required synthons.

4.7.4. Synthesis of terphenyl **Ter.25.**

Given that **Syn.12** had already been prepared (refer to Scheme 4.25), we first turned our attention to **Syn.18**. Starting from 2-methyl-4-bromophenol **4.20**, a Duff formylation gave rise to the desired aldehyde **4.63**, as planned (Scheme 4.45).

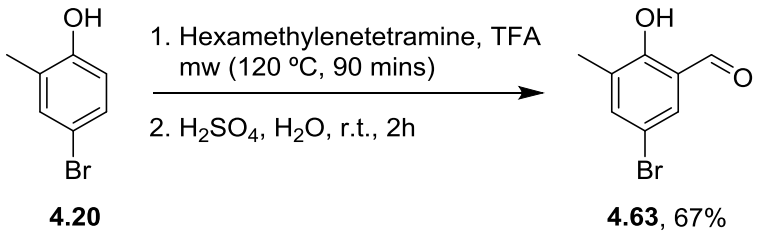

4.20 **4.63**, 67%

Scheme 4.45. Synthesis of 4.63 by Duff formylation.

The subsequent Wittig reaction with triphenylpropylphosphonium bromide gave certain problems; some bases were unsuccessful in promoting the reaction, and when the free phenol was used the reaction did not proceed (Table 4.2). Therefore, phenol **4.63** had to be protected—we chose to use a benzyl protecting group since this could be removed simultaneously to the hydrogenation of the double bond resulting from the Wittig reaction. Once the phenol was protected, reaction with triphenylpropylphosphonium bromide and sodium hexamethyldisilazane (NaHMDS) successfully formed the desired product, but the reaction failed to complete. No reaction was observed when using other bases such as sodium hydride and potassium *tert*-butoxide, given that the phosphonium ylide did not form (this particular ylide has a deep orange colour, which was absent when using these bases). Finally, the use of *n*-BuLi gave much better results, pushing the reaction to completion and drastically improving the yield. The result was an inseparable 2:1 mixture of the *cis* and *trans* isomers, although this would be homogenised during the hydrogenation reaction to remove the double bond downstream.

Table 4.2. Optimisation of the Wittig reaction to form intermediate 4.65.

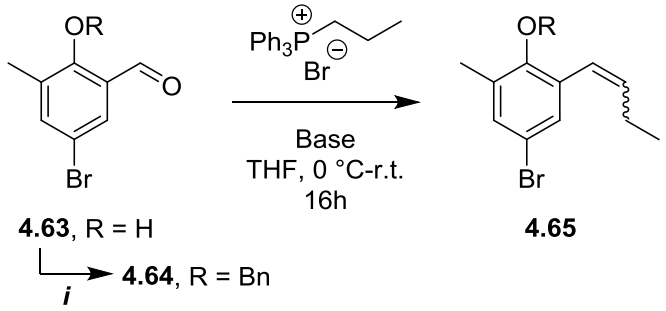

Entry	R	Base	Yield **4.65** (%)[b]
1	H	NaHMDS	0
2	Bn	NaHMDS	36
3	Bn	NaHMDS[a]	24
4	Bn	*t*-BuOK	0
5	Bn	NaH	0
6	Bn	*n*-BuLi	78

[a] More base was added (2 equivalents with respect to the phosphonium salt). [b] Yield refers to isolated yield of inseparable *cis*/*trans* mixture.

It was assumed that the boronic ester would be more stable in the hydrogenation step when compared to the aryl bromide given our previous experience in hydrogenation reactions. Therefore the borylation reaction was carried out using the *cis*/*trans* mixture of **4.65** obtained from the Wittig reaction, in order to prevent loss of the aromatic bromine substituent during the hydrogenation step, resulting in **4.66** in a high yield. Subsequent hydrogenation simultaneously removed the benzyl protecting group and reduced the double bond (Scheme 4.46).

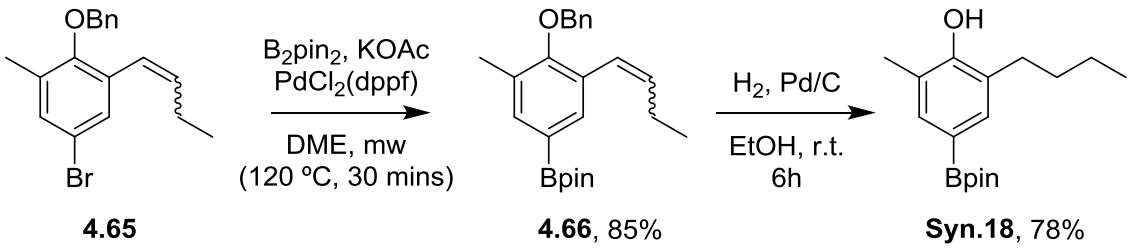

Scheme 4.46. Borylation and hydrogenation steps resulting in the final Syn.18.

With **Syn.18** in hand, we began working towards the synthesis of **Syn.20**. As stated in the previous section, we decided to prepare this synthon with a propyl chain rather than the initially designed butyl, in order to save a step in the synthetic route. The hydrogenation of starting 2-allylphenol took place

without complications, resulting in 2-propylphenol in a high yield. The allylation of this intermediate also took place in high yield to form the Claisen rearrangement precursor, **4.67** (Scheme 4.47).

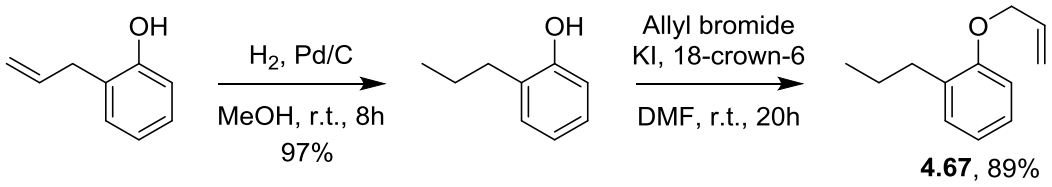

Scheme 4.47. Preparation of Claisen rearrangement precursor 4.67.

The following reaction was somewhat problematic, requiring high temperatures and resulting in moderate yields, with fairly complex crude mixtures that were sometimes difficult to separate by flash column chromatography. A basic literature search for reaction conditions revealed that the best conditions were often using basic solvents such as various aniline derivatives, pyridine or other amines. Therefore, we first attempted the reaction in these solvents at high temperatures, both in the microwave reactor and using conventional heating (Table 4.3). In the end, we found that the best results were obtained using DMF as a solvent in the microwave at 200 °C (entry 6, Table 4.3), although these conditions still only afforded a moderate 57% yield of **4.68**.

Table 4.3. Optimisation of the Claisen rearrangement.

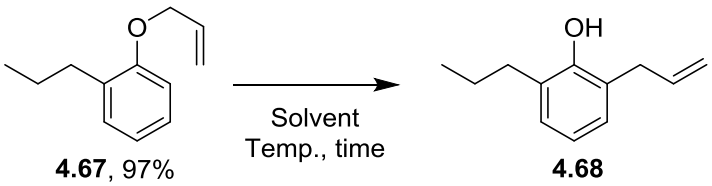

Entry	Solvent	Temp. (°C)	Time (h)	Yield **4.68** (%)[a]
1	Aniline	165	20	41
2	DMF	165	20	30
3	DMF:Pyridine (5:1)	165	20	32
4	Aniline	185	20	49
5	Aniline	185	40	52
6	DMF	200	20	57

[a] Isolated yield.

From there, we attempted a cross-metathesis reaction with acrylonitrile in order to lengthen the carbon chain and introduce the nitrile group. However, when we attempted the reaction with **4.68**, the desired product was not detected in any of the conditions tested (Table 4.4). Once again, the reaction was much more successful after protecting the free phenol as benzyl ether **4.69**. We found that we had to force the reaction with high temperatures, and the reaction worked best when carried out in the microwave. In addition, in order to achieve the best results we found it necessary to add several portions of catalyst, possibly due to catalyst inactivation or degradation.

Table 4.4. Optimisation of the cross-metathesis reaction with acrylonitrile.

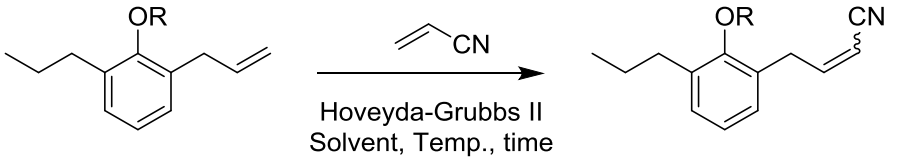

4.68, R = H

4.70

i → **4.69**, R = Bn

Conditions for *O*-benzylation: ***i***. BnBr, K_3PO_4, DMF, r.t., 92%

Entry	Solvent	Cat. load	Temp. (°C)	Time	Yield **4.70** (%)[a]
1	DCM	5 mol%	r.t.	24h	0
2	Toluene	5 mol%	r.t.	24h	0
3	Toluene	5 mol%	100 (mw)	1h	30
4	Toluene	2 x 5 mol%	100 (mw)	2 x 1h	57
5	Toluene	2 x 5 mol%	120	8h then 16h	55
6	Toluene	3 x 5 mol%	120 (mw)	3 x 1h	62

[a] Yield refers to the isolated yield of the inseparable mixture of *cis*/*trans* isomers.

Again, **4.70** was taken forward as a *cis*/*trans* mixture given its irrelevance in the following hydrogenation step. Both the hydrogenation and the formation of the final triflate **Syn.20** were straightforward and resulted in a high yields (Scheme 4.48).

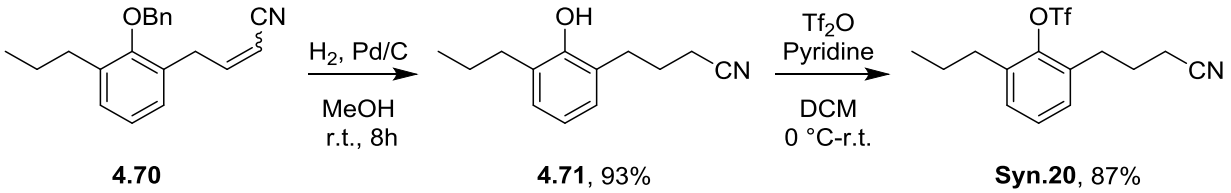

4.70 **4.71**, 93% **Syn.20**, 87%

Scheme 4.48. Hydrogenation and trifluoromethylsulfonylation to finalise the synthesis of Syn.20.

Following this, the construction of terphenyl **4.74** took place uneventfully using the same conditions as throughout this study: **Syn.18** and **Syn.20** were coupled in a Suzuki-Miyaura coupling, the resulting biphenyl converted into triflate, and coupled with **Syn.12** *via* further Suzuki-Miyaura coupling. The resulting terphenyl was again reduced with borane over 5 days, giving the final terphenyl **Ter.25** (Scheme 4.49).

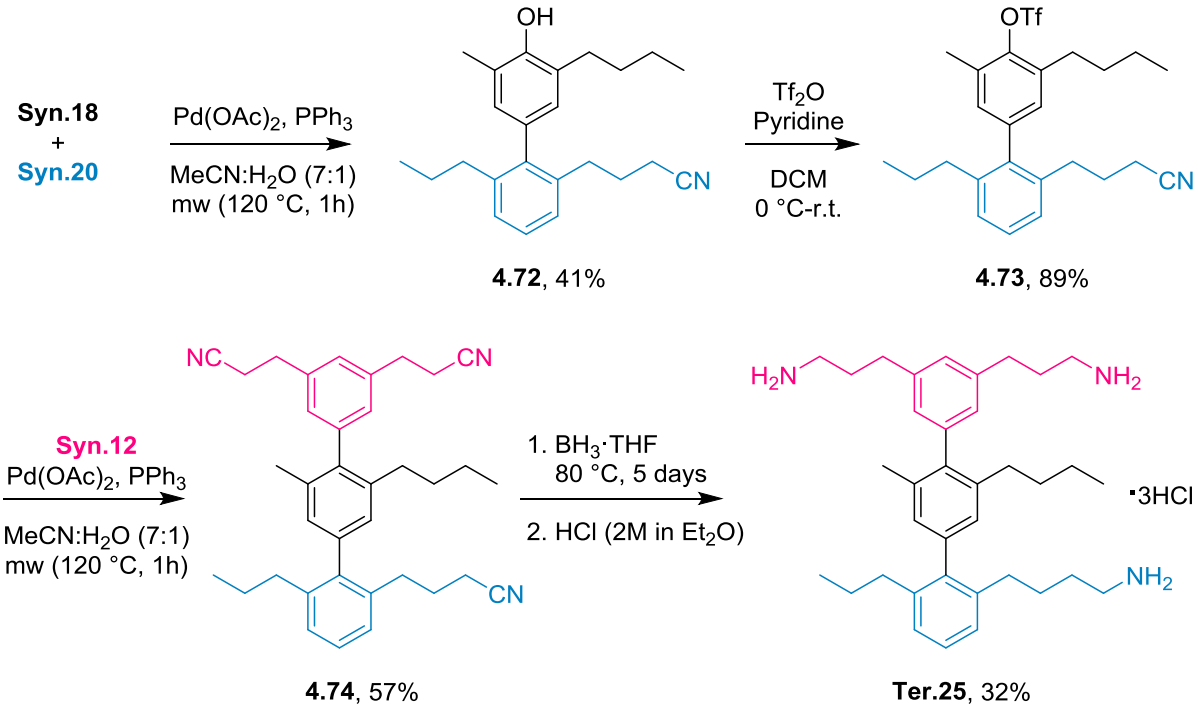

Scheme 4.49. Synthesis of final terphenyl Ter.25.

4.7.5. Biological evaluation.

The preliminary biological results of **Ter.25** are very promising. The group of J. Gallego (Universidad Católica de Valencia) have determined that **Ter.25** inhibits the formation of the MTIP-MyoA complex of *Plasmodium knowlesi* with an IC_{50} of 4 µM (Figure 4.47). For comparison, control experiments with **Ter.5** were carried out; this derivative displayed no affinity for the target, even at the highest concentration tested (100 µM). At the time of writing, no *in vivo* data was available.

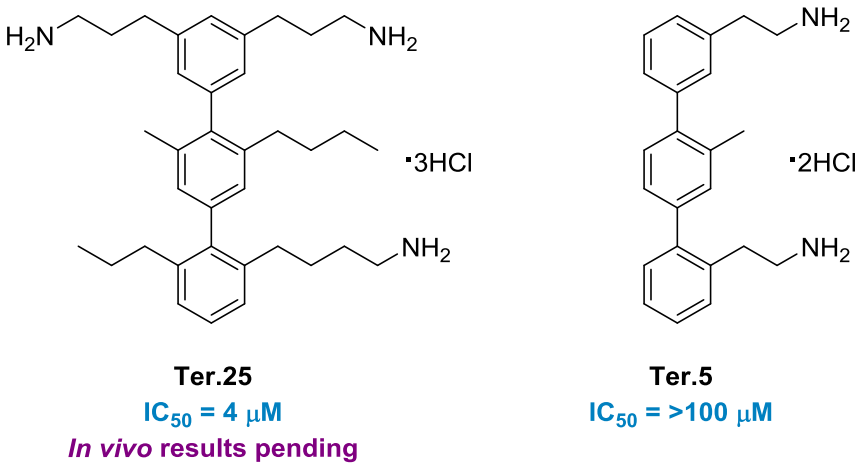

Ter.25
IC_{50} = 4 µM
In vivo results pending

Ter.5
IC_{50} = >100 µM

Figure 4.47. Promising *in vitro* results of Ter.25 in the inhibition of MTIP-MyoA complex formation.

4.8. Conclusions.

We have designed and synthesised a library of *p*-terphenyls capable of mimicking the 3D structure of the native HIV-1 Rev protein. Unfortunately, both the *in vitro* affinity for the target RNA region (the RRE) and the *in vivo* antiviral activities of the new series of compounds has failed to improve on previously reported values.

However, we have observed that the oxygen-based substituents in the 1 and 4'' positions make little difference with regards to the Rev-mimicking potential of this type of scaffold. This has allowed us to significantly shorten the synthetic sequence, decreasing the turnover time for the synthesis and biological testing of new derivatives.

Furthermore, we have successfully produced guanidine-bearing terphenyl derivatives which should be able to more accurately mimic the structure of the native Rev protein, which presents an α-helix rich in arginine residues. Preliminary *in vitro* experiments indicate that this is the case.

On the other hand, we have successfully described the first *p*-terphenyl capable of mimicking the protein-protein interaction MyoA-MTIP, present in *P. falciparum*, the parasite responsible for malaria. Fluorescence anisotropy experiments indicate a significant inhibitory capacity in the low micromolar range.

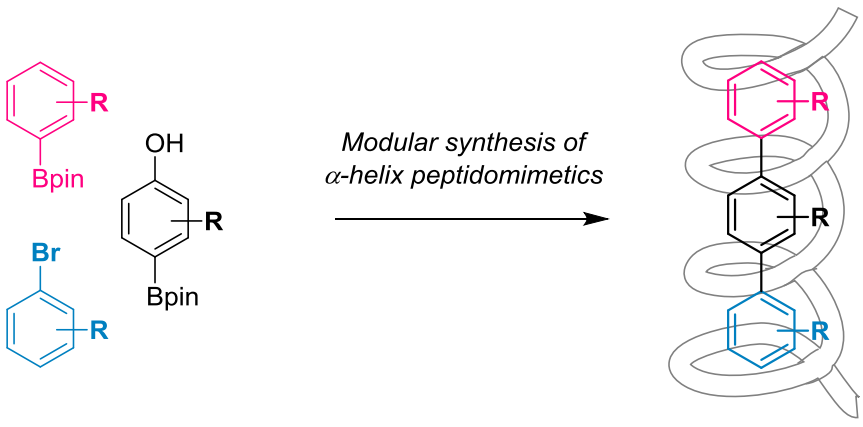

18 final terphenyls synthesised and tested for biological activity

4.9. Experimental section.

Reactions were carried out under a nitrogen atmosphere unless otherwise indicated. Solvents were purified prior to use: THF was distilled from sodium and DCM from calcium hydride. Reagents were used as received from the suppliers without further purification, unless stated otherwise. The reactions were monitored by TLC on 0.25mm precoated silica-gel plates, which were revealed with UV light and aqueous ceric ammonium molybdate or potassium permanganate stains. Flash column chromatography was performed with the indicated solvents on silica gel 60 (particle size: 0.040−0.063 mm). ^{1}H, ^{13}C and ^{19}F NMR spectra were recorded by a 300 MHz spectrometer. Chemical shifts are given in ppm (δ), referenced to the residual proton resonances of the solvents. Coupling constants (*J*) are given in Hertz (Hz). The letters s, d, t, q and m stand for singlet, doublet, triplet, quartet and multiplet respectively. The letters br indicate that the signal is broad. A QTOF mass analysis system was used for the HRMS measurements.

4.9.1. Synthesis of the required synthons.

4.9.1.1. Synthesis of **Syn.1**

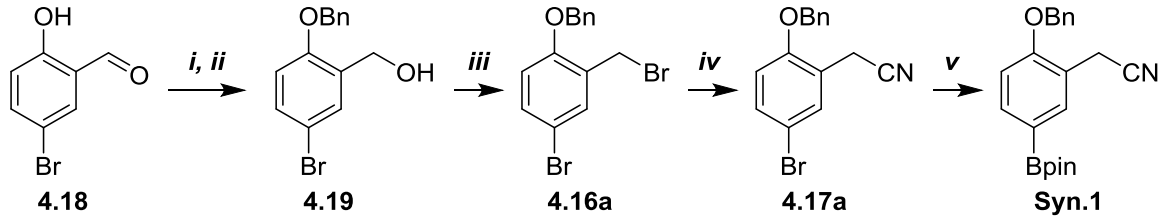

i. O-Benzylation. Commercially available 5-bromosalicylaldehyde **4.18** (1.00 g, 4.97 mmol) and potassium phosphate tribasic (2.11 g, 9.94 mmol) were dissolved in DMF (10 ml), and the resulting solution was stirred for 15 minutes at room temperature. After this time, benzyl bromide (1.8 ml, 14.91 mmol) was added and the mixture was left to stir at room temperature for a further 18 hours. Subsequently, the mixture was diluted with water (20 ml) and extracted with ethyl acetate (15 ml). The organic layer was washed with water (3 x 20 ml), saturated sodium bicarbonate solution (20 ml) and brine (20 ml). The organic layer was then dried over anhydrous sodium sulphate, filtered and concentrated to dryness. The crude mixture was purified by flash column chromatography using *n*-

hexane:EtOAc (10:1) as the eluent, to afford the corresponding benzyl ether as a white solid (1.32 g, 91%). The spectroscopic data were concordant with those reported in the literature.[332]

ii. Aldehyde reduction. The product of the previous step, 2-(benzyloxy)-5-bromobenzaldehyde (1.32 g, 4.53 mmol), was suspended in ethanol (45 ml) and the resulting mixture was cooled in an ice bath. Sodium borohydride (343 mg, 9.07 mmol) was then added portion-wise, and the reaction was left to stir for 2 hours at the same temperature. After this time, the reaction was carefully quenched with aqueous HCl (1M, 10 ml) and left for a further 10 minutes. The resulting mixture was then concentrated to remove the ethanol, and the concentrated mixture was extracted with ethyl acetate (3 x 20 ml). The combined organic layers were dried over anhydrous sodium sulphate, filtered and concentrated to dryness. The resulting crude **4.19** was used in the next step without need for further purification.

iii. Phosphorus tribromide-mediated bromination. The crude **4.19** (1.31 g, 4.53 mmol) was dissolved in anhydrous DCM (20 ml) and cooled in an ice bath. Once cooled, phosphorus tribromide (1M in DCM) (5.4 ml, 5.4 mmol) was added slowly and the reaction was stirred until no starting material remained (TLC analysis, typically 4h). After the reaction had finished, the brown solution was added to an extraction funnel and the organic layer washed with water (2 x 15 ml) and brine (15 ml). The organic layer was then dried over anhydrous sodium sulphate, filtered and concentrated to dryness. The resulting crude **4.16a** was used in the next step without need for further purification.

iv. Introduction of nitrile groups. The crude **4.16a** (1.47 g, 4.13 mmol), potassium iodide (34 mg, 0.21 mmol), 18-crown-6 (272 mg, 1.03 mmol) and sodium cyanide (303 mg, 6.19 mmol) were dissolved in MeCN:H_2O (8:1) (40 ml) and left to stir at room temperature for 24h. After this time, the mixture was diluted with water and extracted with ethyl acetate (3 x 20 ml). The combined organic layers were washed with brine (20 ml), dried with anhydrous sodium sulphate, filtered, and concentrated to dryness.

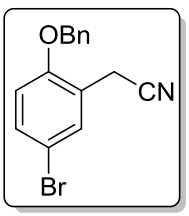

2-(2-(Benzyloxy)-5-bromophenyl)acetonitrile, 4.17a

[332] S.A.A. El Bialy, K.F. Abd El Kader and D.W. Boykin, *Heterocycl. Commun.*, 2011, **17**, 11-16.

Flash column chromatography using *n*-hexane:EtOAc (4:1) as the eluent afforded **4.17a** as a yellow solid (1.14 g, 82% from **4.18** benzyl ether) with a melting point of 54-55 °C.

^{1}H NMR ($CDCl_3$, 300 MHz): δ 3.71 (s, 2H), 5.12 (s, 2H), 6.86 (d, *J*= 8.8 Hz, 1H), 7.34-7.47 (m, 6H), 7.53 (d, *J*= 2.4 Hz, 1H) ppm.

^{13}C NMR ($CDCl_3$, 75.5 MHz): δ 18.7 (CH_2), 70.6 (CH_2), 113.2 (C), 113.5 (CH), 117.3 (C), 121.2 (C), 127.4 (CH), 128.4 (CH), 128.8 (CH), 132.1 (CH), 132.3 (CH), 135.9 (C), 155.0 (C) ppm.

HRMS (EI) calcd. for $C_{15}H_{16}BrN_2O$ [M+NH_4^+]: 319.0441, found: 319.0427.

v. Miyaura borylation (Version 1). A microwave vial was charged with 2-(2-(benzyloxy)-5-bromophenyl)acetonitrile **4.17a** (230 mg, 0.76 mmol), bis(pinacolato)diboron (231 mg, 0.91 mmol), and potassium acetate (223 mg, 2.28 mmol), and anhydrous dimethoxyethane was added (5 ml). Nitrogen gas was then bubbled through the solution for 5 minutes before adding $PdCl_2$(dppf) (56 mg, 0.076 mmol). The resulting mixture was heated in a microwave oven for 90 minutes at 120 °C. After this time, the reaction mixture was cooled and filtered through a pad of Celite, washing with DCM, and the filtrate concentrated to dryness.

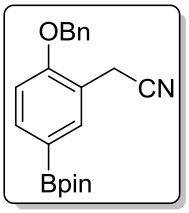

2-(2-(Benzyloxy)-5-(4,4,5,5-tetramethyl-1,3,2-dioxaborolan-2-yl)phenyl)acetonitrile, Syn.1

Flash column chromatography using *n*-hexane:EtOAc (4:1) as the eluent afforded **Syn.1** as a pale yellow oil (1.14 g, 82%).

^{1}H NMR ($CDCl_3$, 300 MHz): δ 1.34 (s, 12H), 3.71 (s, 2H), 5.16 (s, 2H), 6.96 (d, *J*= 8.2 Hz, 1H), 7.30-7.48 (m, 5H), 7.76 (dd, *J*= 8.2, 1.6 Hz, 1H), 7.79 (s, 1H) ppm.

^{13}C NMR ($CDCl_3$, 75.5 MHz): δ 19.2 (CH_2), 20.3 (CH_3), 70.6 (CH_2), 84.3 (C), 111.5 (C), 118.4 (C), 118.9 (C), 127.8 (CH), 128.1 (CH), 128.6 (CH), 129.1 (CH), 135.1 (CH), 136.6 (C), 137.2 (CH), 158.9 (C) ppm.

HRMS (EI) calcd. for $C_{21}H_{25}NO_3B$ [M+H^+]: 350.1922, found: 350.1916.

4.9.1.2. Synthesis of **Syn.2**.

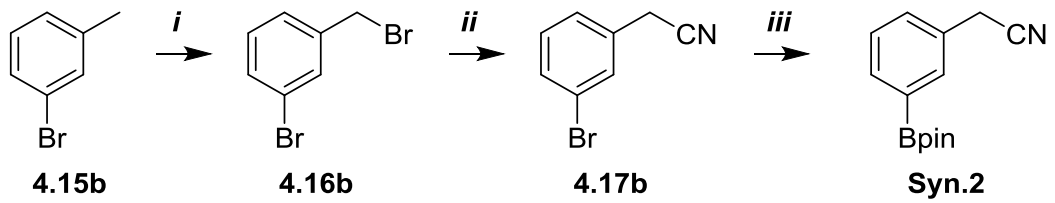

i. Benzylic bromination. Commercially available 3-bromotoluene **4.15b** (1 ml, 8.19 mmol) was dissolved in carbon tetrachloride, along with *N*-bromosuccinimide (1.60g, 9.01 mmol) and benzoyl peroxide (198 mg, 0.82 mmol). The mixture was heated at reflux for 3h and then cooled to room temperature. The resulting suspension was then filtered to remove the succinimide precipitate, and the filtrate was concentrated to dryness. The crude mixture was purified by flash column chromatography using *n*-hexane:EtOAc (20:1) as the eluent, to afford pure **4.16b** as a colourless oil (1.99 g, 97%). The spectroscopic data were concordant with those reported in the literature.[333]

ii. Introduction of nitrile groups. The product of the previous step was subject to the same conditions described previously (*see iv. Introduction of nitrile groups, Section 4.9.1.1*). The crude mixture was purified by flash column chromatography using *n*-hexane:EtOAc (5:1) as the eluent, to afford pure **4.17b** as a colourless oil (1.45 g, 93%). The spectroscopic data were concordant with those reported in the literature.[334]

iii. Miyaura borylation (Version 1). The product of the previous step was subject to the same conditions described previously (*see v. Miyaura borylation (Version 1), Section 4.9.1.1*). The crude mixture was purified by flash column chromatography using *n*-hexane:EtOAc (10:1) as the eluent, to afford **Syn.2** as a colourless oil (283 mg, 76%). The spectroscopic data were concordant with those reported in the literature.[335]

[333] Z. Ren, J. E. Schulz and G. Dong, *Org. Lett.*, 2015, **17**, 2696-2699.
[334] G. Wu, Y. Deng, C. Wu, Y. Zhang and J. Wang, *Angew. Chem. Int. Ed.*, 2014, **53**, 10510-10514.
[335] S. Yonezawa, T. Yamamoto, H. Yamakawa, C. Muto, M. Hosono, K. Hattori, K. Higashino, T. Yutsudo, H. Iwamoto, Y. Kondo, M. Sakagami, H. Togame, Y. Tanaka, T. Nakano, H. Takemoto, M. Arisawa and S. Shuto, *J. Med. Chem.*, 2012, **55**, 8838-8858.

4.9.1.3. Synthesis of **Syn.3**.

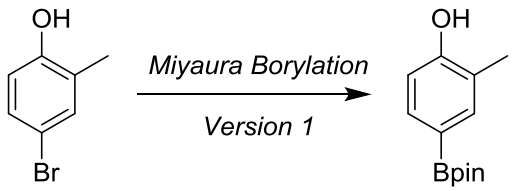

4.20 **Syn.3**

Commercially available 4-bromo-2-methylphenol **4.20** was subject to the same conditions described previously (*see v. Miyaura borylation (Version 1), Section 4.9.1.1*). The crude mixture was purified by flash column chromatography using *n*-hexane:EtOAc (10:1) as the eluent, to afford **Syn.3** as a pale yellow solid (413 mg, 68%). The spectroscopic data were concordant with those reported in the literature.[336]

4.9.1.4. Synthesis of **Syn.4**.

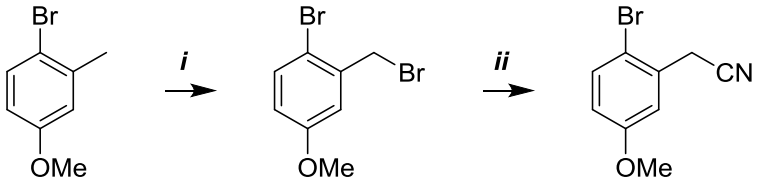

Syn.4

i. Benzylic bromination. Commercially available 4-bromo-2-methylanisole was subject to the same conditions described previously (*see i. Benzylic bromination, section 4.9.1.2*). The crude mixture was purified by flash column chromatography using *n*-hexane:EtOAc (15:1) as the eluent, to afford bromomethyl intermediate as a pale yellow solid (490 mg, 81%). The spectroscopic data were concordant with those reported in the literature.[337]

ii. Introduction of nitrile groups. The product of the previous step was subjected to the same conditions described previously (*see iv. Introduction of nitrile groups, Section 4.9.1.1*). The crude mixture was purified by flash column chromatography using *n*-hexane:EtOAc (5:1) as the eluent, to

[336] A. B. Williams and R. N. Hanson, *Tetrahedron*, 2012, **68**, 5406-5414.
[337] R. Breslow, S. Garratt, L. Kaplan and D. LaFollette, *J. Am. Chem. Soc.*, 1968, **90**, 4051-4055.

afford **Syn.4** as a yellow solid (277 mg, 70%). The spectroscopic data were concordant with those reported in the literature.[338]

4.9.1.5. Synthesis of *Syn.6*.

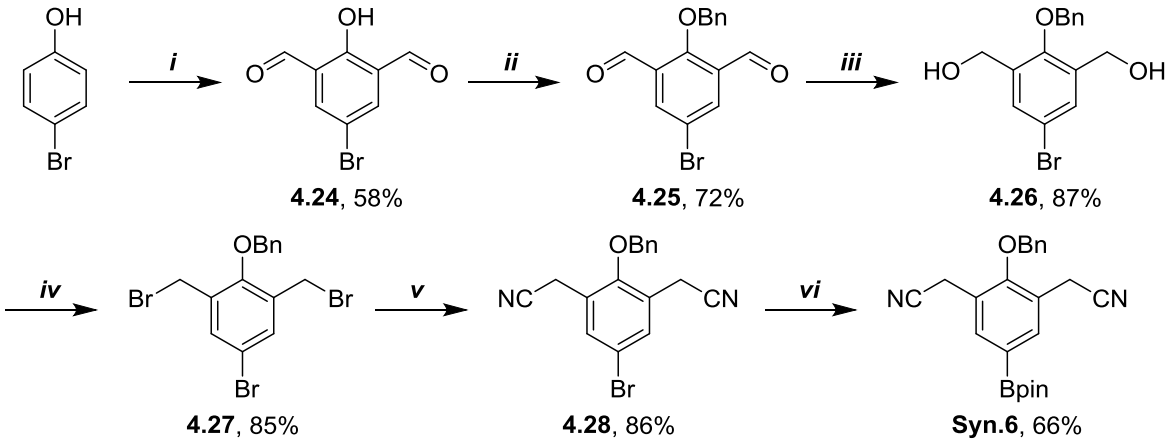

Reactants and conditions:
i. Hexamethylenetetramine (HMTA), TFA, mw (120 °C, 1.5h), then H_2SO_4, H_2O, r.t. 2h. ***ii.*** BnBr, K_3PO_4, DMF, r.t., 18h. ***iii.*** $NaBH_4$, EtOH, 0 °C-r.t., 3h. ***iv***. NBS, PPh_3, DCM, 0 °C-r.t., 18h. ***v.*** NaCN, KI, 18-crown-6, MeCN:H_2O (7:1), r.t., 24h. ***vi***. B_2pin_2, KOAc, $PdCl_2$(dppf), DME, mw (120 °C, 1h).

This very compound had been previously synthesised in our research group, hence we followed the same synthetic procedure as we reported in 2013.[308]

4.9.1.6. Synthesis of *Syn.7*.

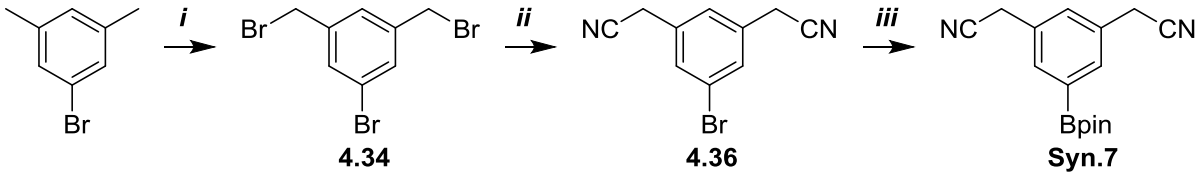

i. Double benzylic bromination. Commercially available 5-bromo-*m*-xylene (1 ml, 7.36 mmol) was dissolved in anhydrous chloroform, and *N*-bromosuccinimide (2.88 g, 16.19 mmol) was added in 6 portions over 3 days (1 portion every 12 hours). Whenever *N*-bromosuccinimide was added, azobisisobutyronitrile (AIBN) (5 mg) was added straight after. After the first addition, the mixture was

[338] H. Muratake and M. Natsume, *Tetrahedron*, 2006, **62**, 7056-7070.

heated to reflux and maintained at that temperature during the 3 days of reaction time, although the reaction was cooled before adding each portion of *N*-bromosuccinimide and AIBN. The resulting mixture was then cooled to room temperature and concentrated to dryness. The crude mixture was purified by flash column chromatography using *n*-hexane:EtOAc (20:1) as the eluent, to afford pure **4.34** as a white solid (1.72 g, 68%). The spectroscopic data were concordant with those reported in the literature.[339]

ii. Introduction of nitrile groups. Previously synthesised **4.34** (1.72 g, 5.00 mmol), potassium iodide (41 mg, 0.25 mmol), 18-crown-6 (330 mg, 1.25 mmol) and sodium cyanide (735 mg, 15 mmol) were dissolved in MeCN:H_2O (8:1) (50 ml) and left to stir at room temperature for 24h. After this time, the mixture was diluted with water and extracted with ethyl acetate (3 x 20 ml). The combined organic layers were washed with brine (20 ml), dried with anhydrous sodium sulphate, filtered, and concentrated to dryness. The crude mixture was purified by flash column chromatography using *n*-hexane:EtOAc (5:1) as the eluent, to afford pure **4.36** as a pale yellow solid (764 mg, 65%). The spectroscopic data were concordant with those reported in the literature.[336]

iii. Miyaura borylation (Version 1). The product of the previous step was subject to the same conditions described previously (*see v. Miyaura borylation (Version 1), Section 4.9.1.1*).

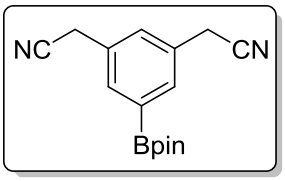

2,2'-(5-(4,4,5,5-Tetramethyl-1,3,2-dioxaborolan-2-yl)-1,3-phenylene)diacetonitrile, Syn.7

Flash column chromatography using *n*-hexane:EtOAc (5:1) as the eluent afforded **Syn.7** as a white solid (1.14 g, 75%) with a melting point of 96-97 °C.

^{1}H NMR ($CDCl_3$, 300 MHz): δ 1.37 (s, 12H), 3.78 (s, 4H), 7.43 (s, 1H), 7.73 (s, 2H) ppm.

^{13}C NMR ($CDCl_3$, 75.5 MHz): δ 23.4, 24.9, 84.4, 117.4, 130.1, 130.5, 134.0 ppm.

HRMS (EI) calcd. for $C_{16}H_{23}N_3O_2B$ [M+NH_4^+]: 300.1878, found: 300.1883.

[339] F. Yokokawa, S. Nilar, C. G. Noble, S. P. Lim, R. Rao, S. Tania, G. Wang, G. Lee, J. Hunziker, R. Karuna, U. Manjunatha, P.-Y. Shi and P. W. Smith, *J. Med. Chem.*, 2016, **59**, 3935-3952.

4.9.1.7. Synthesis of **Syn.9**.

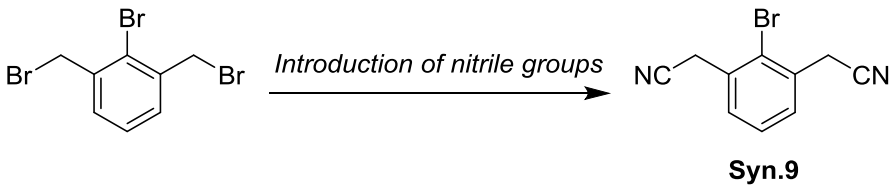

Syn.9

Commercially available 2,6-bis(bromomethyl)bromobenzene was subject to the same conditions described previously (*see ii. Introduction of nitrile groups, Section 4.9.1.6*). The crude mixture was purified by flash column chromatography using *n*-hexane:EtOAc (3:1) as the eluent, to afford **Syn.9** as a pale yellow solid (1.42 g, 93%). The spectroscopic data were concordant with those reported in the literature.[340]

4.9.1.8. Synthesis of **Syn.10**.

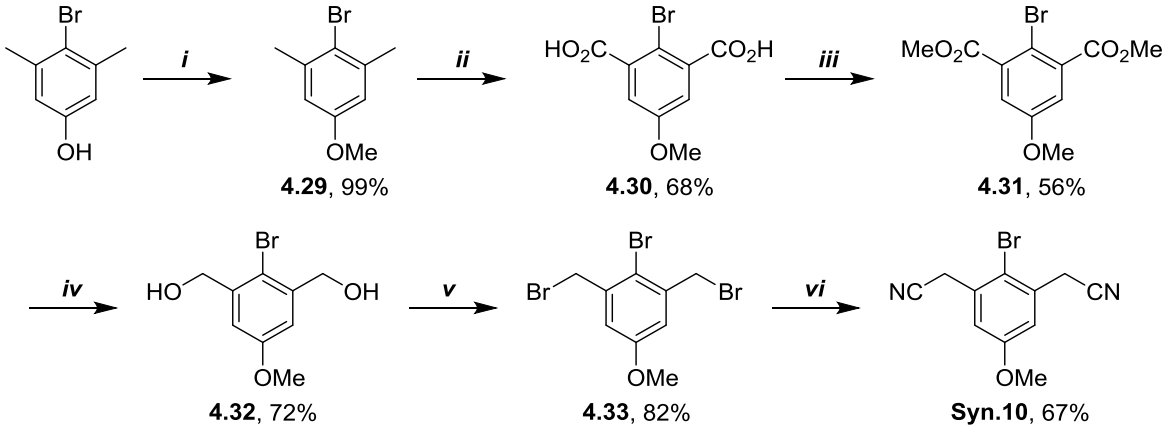

4.29, 99% **4.30**, 68% **4.31**, 56%

4.32, 72% **4.33**, 82% **Syn.10**, 67%

Reactants and conditions:
i. MeI, K_3PO_4, Acetone, 60 °C, 18h. ***ii.*** $KMnO_4$, *t*-BuOH:H_2O (1:1), 110 °C, 18h. ***iii***.H_2SO_4, MeOH, 60°C, 18h. ***iv***. $LiBH_4$, THF, 0 °C-r.t., 18h. ***v***. NBS, PPh_3, DCM, 0 °C-r.t., 18h. ***vi.*** NaCN, KI, 18-crown-6, MeCN:H_2O (7:1), r.t., 24h.

This very compound had been previously synthesised in our research group, hence we followed the same synthetic procedure as we reported in 2013.[308]

[340] K. Toyota, A. Nakamura and M. Yoshifuji, *Chem. Commun*, 2002, 3012-3013.

4.9.1.9. Synthesis of **Syn.11**.

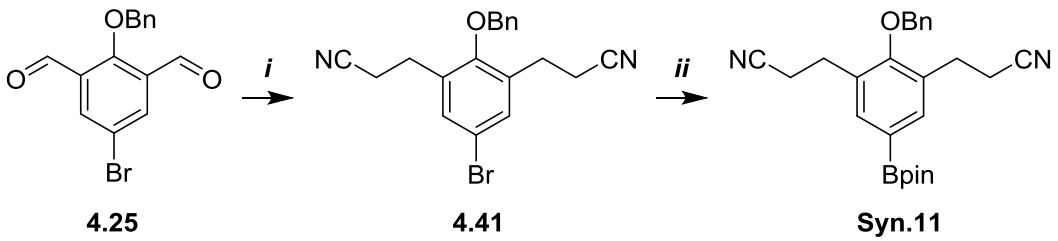

4.25 **4.41** **Syn.11**

i. Wittig reaction and conjugate reduction. Previously synthesised **4.25** (1.00 g, 3.13 mmol) was dissolved in anhydrous THF (15 ml), and (triphenylphosphoranylidene)acetonitrile (2.36 g, 7.83 mmol) was added. The mixture was allowed to stir until the starting material had been consumed (TLC analysis, typically 5h), and after this time water was added and the products were extracted with ethyl acetate (3 x 20 ml). The combined organic layers were washed with brine (20 ml), dried over anhydrous sodium sulphate, filtered and concentrated to dryness. The residue was then dissolved in anhydrous ethanol (30 ml), and sodium borohydride (473 mg, 12.52 mmol) was added portion-wise. The reaction was stirred under reflux for 16h. After this time, the resulting mixture was cooled to room temperature and quenched with water. The solution was concentrated to remove the ethanol and the product was extracted from the resulting aqueous slurry with ethyl acetate (3 x 20 ml). The combined organic layers were washed with brine (20 ml), dried over anhydrous sodium sulphate, filtered and concentrated to dryness.

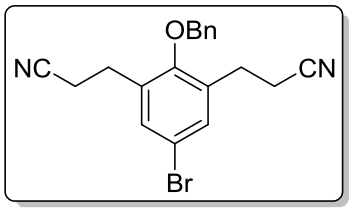

3,3'-(2-(Benzyloxy)-5-bromo-1,3-phenylene)dipropanenitrile, 4.41

Flash column chromatography using *n*-hexane:EtOAc (4:1) as the eluent afforded **4.41** as a pale yellow solid (740 mg, 64%) with a melting point of 49-50 °C.

^{1}H NMR ($CDCl_3$, 300 MHz): δ 2.62 (t, *J*= 7.5 Hz, 4H), 2.93 (t, *J*= 7.5 Hz, 4H), 4.88 (s, 2H), 7.33 (s, 2H), 7.36-7.51 (m, 5H) ppm.

^{13}C NMR ($CDCl_3$, 75.5 MHz): δ 17.8 (CH_2), 26.4 (CH_2), 76.5 (CH_2), 117.9 (C), 118.7 (C), 127.6 (CH), 128.8 (CH), 129.0 (CH), 132.2 (CH), 134.3 (C), 136.1 (C), 154.6 (C) ppm.

HRMS (EI) calcd. for $C_{19}H_{21}N_3OBr$ [M+NH_4^+]: 386.0863, found: 386.0875.

ii. Miyaura borylation (Version 2). Previously synthesised **4.41** (500 mg, 1.35 mmol), bis(pinacolato)diboron (536 mg, 2.03 mmol), and potassium acetate (397 mg, 4.05 mmol) were dissolved in 1,4-dioxane:DMSO (100:1) (5 ml) in a sealable reaction vessel. Nitrogen gas was then bubbled through the solution for 5 minutes before adding $PdCl_2$(dppf) (102.4 mg, 0.14 mmol). The reaction vessel was subsequently sealed and heated to 100 °C for 20h. After this time, the mixture was cooled to room temperature and concentrated *in vacuo*.

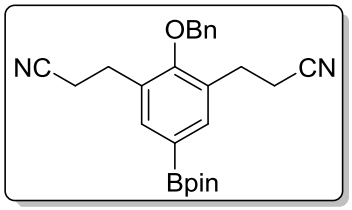

3,3'-(2-(Benzyloxy)-5-(4,4,5,5-tetramethyl-1,3,2-dioxaborolan-2-yl)-1,3-phenylene)dipropanenitrile, Syn.11

Flash column chromatography using *n*-hexane:EtOAc (3:1) as the eluent afforded **Syn.11** as a pale yellow solid (433 mg, 77%) with a melting point of 97-99 °C.

^{1}H NMR ($CDCl_3$, 300 MHz): δ 1.36 (s, 12H), 2.62 (t, *J*= 7.7 Hz, 4H), 2.97 (t, *J*= 7.7 Hz, 4H), 4.89 (s, 2H), 7.36-7.48 (m, 5H), 7.62 (s, 2H) ppm.

^{13}C NMR ($CDCl_3$, 75.5 MHz): δ 17.9 (CH_2), 24.9 (CH_3), 26.6 (CH_2), 76.3 (CH_2), 84.1 (C), 119.2 (C), 126.0 (br, C), 127.7 (CH), 127.6 (CH), 128.6 (CH), 128.9 (CH), 131.5 (C), 136.0 (CH), 136.4 (C), 158.1 (C) ppm.

HRMS (EI) calcd. for $C_{25}H_{33}N_3O_3B$ [M+NH_4^+]: 434.2609, found: 434.2626.

4.9.1.10. Synthesis of **Syn.12**.

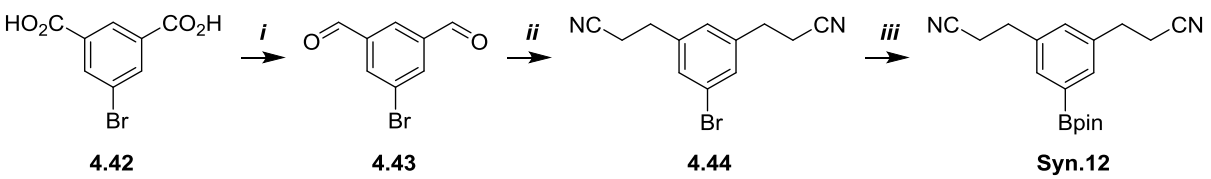

i. Carboxylic acid reduction and reoxidation to aldehyde level. Commercially available 5-bromoisophthalic acid **4.42** (1.00 g, 4.08 mmol) was dissolved in anhydrous THF (20 ml), and BH_3-THF (1M in THF) (20.4 ml, 20.4 mmol) was added slowly whilst stirring. Following this, the reaction mixture was refluxed for 4h. After this time, the reaction mixture was cooled in an ice bath, carefully quenched with aqueous HCl (3N) (10 ml), and stirred for 30 minutes in the ice bath and a further 30 minutes at room temperature. The mixture was then concentrated to remove the THF, and the resulting aqueous slurry extracted with ethyl acetate (5 x 20 ml). The combined organic layers were washed with brine (20 ml), dried over sodium sulphate, filtered and concentrated to dryness. The residue was then dissolved in anhydrous DCM (20 ml), and both 4 Å molecular sieves (500 mg) and pyridinium chlorochromate (2.20g, 10.2 mmol) were added. The resulting orange-brown mixture was stirred for 4h at room temperature, after which time the mixture was filtered through a pad of Celite, washing with DCM. The filtrate was then concentrated and purified through flash column chromatography using *n*-hexane:EtOAc (10:1) as the eluent, affording pure **4.43** as a white solid (530 mg, 61% from **4.42**). The spectroscopic data were concordant with those reported in the literature.[341]

ii. Wittig reaction and conjugate reduction. The dialdehyde product of the previous step was subject to the same conditions described previously (*see i. Wittig reaction and conjugate reduction, Section 4.9.1.9*). The resulting **4.44** was used in the next step without further purification.

ii. Miyaura borylation (Version 2). The product of the previous step was subject to the same conditions described previously (*see ii. Miyaura borylation (Version 2), Section 4.9.1.9*).

[341] K. Matsuda, N. Nakamura, K. Takahashi, K. Inoue, N. Koga and H. Iwamura, *J. Am. Chem. Soc.*, 1995, **117**, 5550-5560.

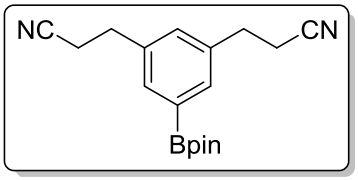

3,3'-(5-(4,4,5,5-Tetramethyl-1,3,2-dioxaborolan-2-yl)-1,3-phenylene)dipropanenitrile, Syn.12

Flash column chromatography using *n*-hexane:EtOAc (2:1) as the eluent afforded **Syn.12** as a pale yellow solid (567 mg, 83%) with a melting point of 41-42 °C.

^{1}H NMR ($CDCl_3$, 300 MHz): δ 1.32 (s, 12H), 2.61 (t, *J*= 7.4 Hz, 4H), 2.93 (t, *J*= 7.4 Hz, 4H), 7.20 (s, 1H), 7.54 (s, 2H) ppm.

^{13}C NMR ($CDCl_3$, 75.5 MHz): δ 19.2 (CH_2), 24.8 (CH_3), 31.3 (CH_2), 84.1 (C), 130.1 (br, C), 131.3 (CH), 133.4 (CH), 138.0 (C) ppm.

HRMS (EI) calcd. for $C_{18}H_{27}N_3O_2B$ [M+NH_4^+]: 328.2191, found: 328.2187.

4.9.1.11. Synthesis of ***Syn.14****.*

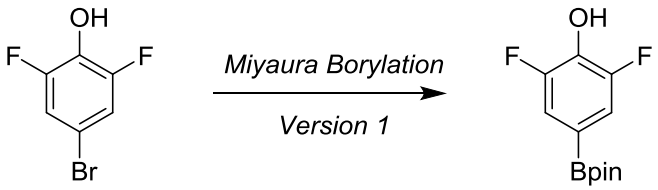

4.49 **Syn.14**

Commercially available 4-bromo-2,6-difluorophenol **4.49** was subject to the same conditions described previously (*see v. Miyaura borylation (Version 1), Section 4.9.1.1*).

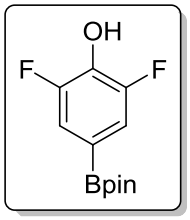

2,6-Difluoro-4-(4,4,5,5-tetramethyl-1,3,2-dioxaborolan-2-yl)phenol, Syn.14

Flash column chromatography using *n*-hexane:EtOAc (10:1) as the eluent afforded **Syn.14** as a colourless solid (264 mg, 58%) with a melting point of 106-108 °C.

^{1}H NMR ($CDCl_3$, 300 MHz): δ 1.35 (s, 12H), 5.82 (br s, 1H), 7.28-7.36 (m, 2H) ppm.

^{13}C NMR ($CDCl_3$, 75.5 MHz): δ 24.8 (CH_3), 84.3 (C), 117.5 (dd, *J*= 12.8, 6.7 Hz, CH), 120.3 (br, C), 135.5 (t, *J*= 16.0 Hz, CH), 151.4 (dd, *J*= 243.8, 4.3 Hz, CF) ppm.

^{19}F NMR ($CDCl_3$, 282.4 MHz): δ -136.43 (s, 2F) ppm.

HRMS (EI) calcd. for $C_{12}H_{19}NO_3BF_2$ [M+NH_4^+]: 274.1421, found: 274.1415.

4.9.1.12. Synthesis of ***Syn.15****.*

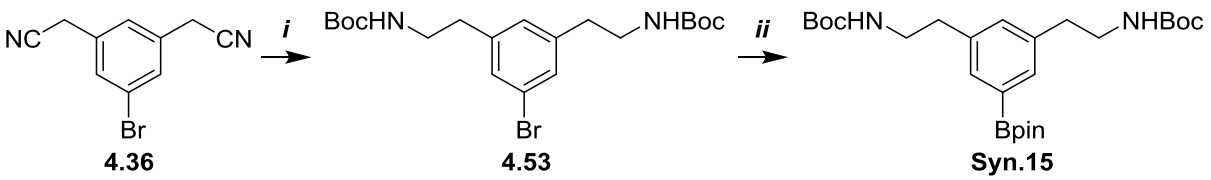

i. Nitrile reduction and amine protection. Previously synthesised **4.36** (500 mg, 2.13 mmol) was dissolved in anhydrous THF (8 ml) in a sealable reaction vessel and BH_3·THF (1M in THF) (22 ml, 22.0 mmol). The vessel was then sealed and the mixture was stirred at 70 °C for two days, after which time the reaction was cooled to room temperature, quenched with aqueous HCl (3N, 10 ml) and stirred for a further 2 hours open to air. The reaction was then concentrated to dryness and redissolved in anhydrous DCM (20 ml). Triethylamine (1.46 ml, 10.6 mmol) was added, followed by di-*tert*-butyl dicarbonate (2.31g, 10.6 mmol), and the mixture was stirred at room temperature for 18h. Following this, the reaction was quenched with saturated ammonium chloride solution (10 ml) and the organic layer was washed subsequently with saturated ammonium chloride solution (10 ml), saturated sodium bicarbonate solution (10 ml), water (2 x 10 ml), and brine (10 ml). The organic layer was dried over anhydrous sodium sulphate, filtered, and concentrated to dryness to afford a white solid **4.53** (652 mg, 69% from **4.36**), which was used in the next step without further purification.

ii. Miyaura borylation (Version 3). The crude product from the previous step (652 mg, 1.47 mmol) was added to a microwaveable reaction vial and dissolved in anhydrous acetonitrile (7.5 ml), along with bis(pinacolato)diboron (575 mg, 2.21 mmol) and potassium acetate (432 mg, 4.41 mmol). Nitrogen gas was then bubbled through the solution for 5 minutes before adding $PdCl_2$(dppf) (110 mg,

0.15 mmol). The reaction vessel was subsequently sealed and heated under microwave irradiation at 160 °C for 15 minutes. After this time, the mixture was cooled to room temperature and passed through a pad of Celite and the filtrate was concentrated *in vacuo*.

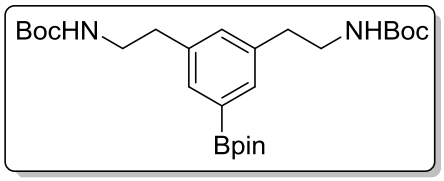

Di-*tert*-butyl ((5-(4,4,5,5-tetramethyl-1,3,2-dioxaborolan-2-yl)-1,3-phenylene)bis(ethane-2,1-diyl))dicarbamate, Syn.15

Flash column chromatography using *n*-hexane:EtOAc (5:1) as the eluent afforded **Syn.15** as a dense yellow oil (548 mg, 76%).

^{1}H NMR ($CDCl_3$, 300 MHz): δ 1.36 (s, 12H), 1.45 (s, 18H), 2.80 (t, *J*= 7.0 Hz, 4H), 3.39 (dd, *J*= 13.1, 6.7 Hz, 4H), 4.58 (br s, 2H), 7.28 (s, 1H), 7.52 (d, *J*= 1.7 Hz, 2H) ppm.

^{13}C NMR ($CDCl_3$, 75.5 MHz): δ 24.9, 28.4, 36.1, 79.2, 83.8, 113.9, 132.3, 133.3, 138.6, 155.9 ppm.

HRMS (EI) calcd. for $C_{26}H_{45}BN_2O_6$ [M+H$^+$]: 491.3287, found: 491.3271.

4.9.1.13. Synthesis of ***Syn.16****.*

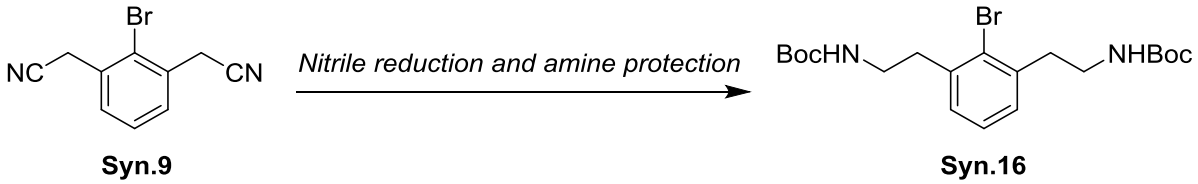

Syn.9 **Syn.16**

Previously synthesised 2,6-bis(acetonitrile)bromobenzene **Syn.9** was subject to the same conditions described previously (*see i. Nitrile reduction and amine protection, section 4.9.1.12*).

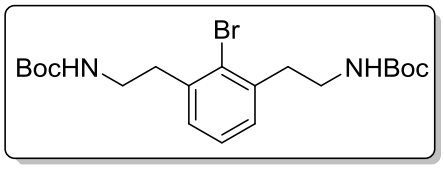

Di-*tert*-butyl ((2-bromo-1,3-phenylene)bis(ethane-2,1-diyl))dicarbamate, Syn.16

The crude mixture was purified by flash column chromatography using *n*-hexane:EtOAc (3:1) as the eluent, to afford **Syn.16** as a white solid (674 g, 60%) with a melting point of 96-98 °C.

^{1}H NMR ($CDCl_3$, 300 MHz): δ 1.44 (s, 18H), 2.99 (t, *J*=7.0 Hz, 4H), 3.4 (br s, 4H), 4.63 (br s, 2H), 7.07-7.13 (m, 2H), 7.19 (dd, *J*= 8.1, 6.6 Hz, 1H) ppm.

^{13}C NMR ($CDCl_3$, 75.5 MHz): δ 28.4 (CH_3), 37.3 (CH_2), 40.2 (CH_2), 79.2 (C), 126.9 (C), 127.2 (CH), 129.3 (CH), 139.2 (C), 155.9 (C) ppm.

HRMS (EI) calcd. for $C_{20}H_{32}BrN_2O_4$ [M+H$^+$]: 443.1540, found: 443.1537.

*4.9.1.14. Synthesis of **Syn.18**.*

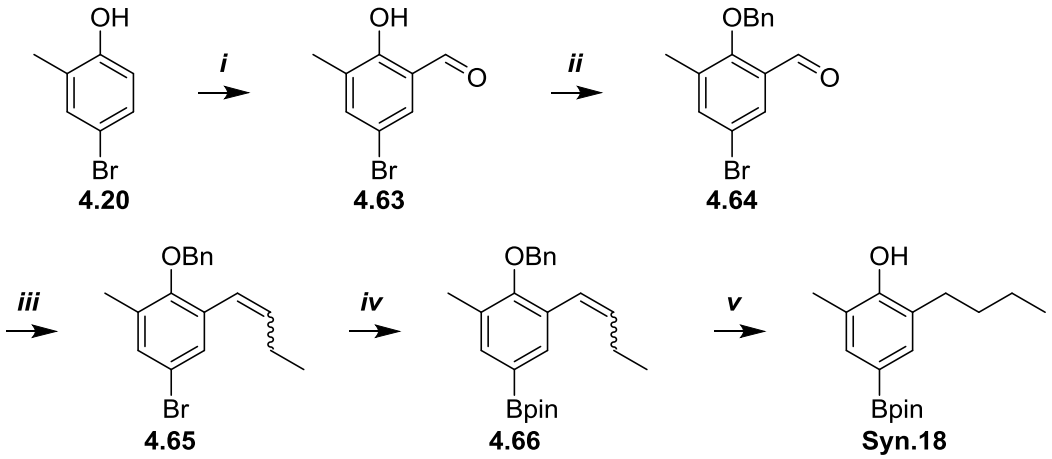

i. Duff formylation. Commercially available **4.20** (1.0 g, 5.35 mmol) was added to a microwaveable reaction vial, along with hexamethylenetetramine (HMTA) (1.12 g, 8.02 mmol) and trifluoroacetic acid (TFA) (10 ml). Care should be taken upon addition of the TFA since the mixture heats up considerably. Following this, the vessel was sealed and the reaction heated by microwave irradiation at 120 °C for 90 minutes. Subsequently, the mixture was transferred to a round-bottomed flask and concentrated H_2SO_4 (6 ml) and water (10 ml) was added and the mixture was stirred for a further 2

hours. Following this, the mixture was diluted with water and extracted with ethyl acetate (3 x 20 ml). The combined organic layers were washed with saturated aqueous sodium bicarbonate solution (3 x 20 ml) and brine (20 ml), dried over anhydrous sodium sulphate, filtered and concentrated to dryness. Flash chromatography using *n*-hexane:EtOAc (10:1) afforded the desired **4.63** as a yellow solid (771 mg, 67%). The spectroscopic data were concordant with those reported in the literature.[342]

ii. O-Benzylation. The product of the previous step was subject to the same conditions described previously (*see i. O-Benzylation, Section 4.9.1.1*). The crude mixture was used in the next step without further purification.

iii. Wittig reaction. A round-bottomed flask was charged with propyltriphenylphosphonium bromide (1.43 g, 3.70 mmol), purged with nitrogen, and THF was added (20 ml). The mixture was cooled in an ice bath, and *n*-butyllithium (2.5M in hexanes) (1.52 ml, 3.80 mmol) was added dropwise. The solution turned a dark orange colour that was crucial to the success of the reaction. This mixture was stirred at the same temperature for 15 minutes, and crude **4.64** (940 mg, 3.08 mmol) was then added and the reaction was stirred for 16 hours. After this time, saturated aqueous ammonium chloride solution (10 ml) was added carefully to quench the reaction, and the mixture was extracted with ethyl acetate (3 x 20 ml). The combined organic layers were then washed subsequently with water (2 x 10 ml) and brine (10 ml), dried over anhydrous sodium sulphate, filtered and concentrated.

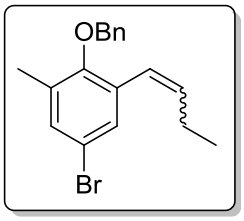

2-(Benzyloxy)-5-bromo-1-(but-1-en-1-yl)-3-methylbenzene, 4.65

The crude mixture was purified by flash column chromatography using *n*-hexane:EtOAc (15:1) as the eluent, to afford a 3:2 mixture of (*Z*)- and (*E*)-**4.65** as a white solid (796 g, 78%). **4.65** was characterised as a mixture, given the irrelevance of this isomerism to the synthetic sequence (the double bond will be later hydrogenated and the two isomers will converge into one saturated product).

^{1}H NMR ($CDCl_3$, 300 MHz): δ 1.00-1.15 (m, 2 x 3H), 2.17-2.39 (m, 2 x (3H + 2H)), 4.81 (s, 2 x 2H), 5.79 (dt, *J*= 11.5, 7.3 Hz, 1H, *Z* (major)), 6.30 (dt, *J*= 15.9, 6.4 Hz, 1H, *E* (minor)), 6.52 (d, *J*= 11.6, 1H, *Z* (major)), 6.63 (dt, *J*= 15.9, 1.5 Hz, 1H, *E* (minor)), 7.24-7.54 (m, 2 x 7H) ppm.

[342] C. Baleizão, B. Gigante, H. Garcia and A. Corma, *J. Catal.*, 2004, **221**, 77-84.

^{13}C NMR ($CDCl_3$, 75.5 MHz): δ 13.5, 14.2, 16.2, 22.1, 26.3, 74.7, 75.0, 116.1, 117.1, 122.7, 123.2, 126.9, 128.0, 128.1, 128.2, 128.5, 128.6, 130.7, 132.0, 132.3, 133.1, 133.5, 133.6, 133.8, 133.9, 135.2, 136.3, 137.1, 137.2, 153.4, 154.3 ppm.

iv. Miyaura borylation (Version 1). The product of the previous step was subject to the same conditions described previously (*see v. Miyaura borylation (Version 1), Section 4.9.1.1*).

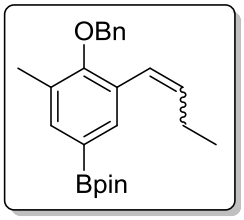

2-(4-(Benzyloxy)-3-(but-1-en-1-yl)-5-methylphenyl)-4,4,5,5-tetramethyl-1,3,2-dioxaborolane, 4.66

The crude mixture was purified by flash column chromatography using *n*-hexane:EtOAc (15:1) as the eluent, to afford a 2:1 mixture of (*Z*)- and (*E*)-**4.66** as a colourless oil (773 mg, 85%). **4.66** was characterised as a mixture, given the irrelevance of this isomerism to the synthetic sequence (the double bond will be later hydrogenated and the two isomers will converge into one saturated product).

^{1}H NMR ($CDCl_3$, 300 MHz): δ 1.02-1.15 (m, 2 x 3H), 1.38 (s, 2 x 18H), 2.21-2.38 (m, 2 x (2H + 3H)), 4.84 (s, 2 x 2H), 5.75 (dt, *J*= 11.5, 7.3 Hz, 1H, *Z* (major)), 6.40 (dt, *J*= 15.9, 6.4 Hz, 1H, *E* (minor)), 6.57 (d, *J*= 11.5, 1H, *Z* (major)), 6.70 (dt, *J*= 16.0, 1.4 Hz, 1H, *E* (minor)), 7.29-7.88 (m, 2 x 7H) ppm.

^{13}C NMR ($CDCl_3$, 75.5 MHz): δ 13.7, 14.3, 16.2, 22.1, 24.9, 26.4, 74.4, 74.8, 83.6, 83.7, 123.5, 124.3, 127.3, 128.1, 128.4, 128.5, 130.6, 130.7, 131.2, 134.1, 134.7, 135.1, 135.3, 136.2, 136.5, 137.5, 137.6, 157.2, 157.9 ppm.

HRMS (EI) calcd. for $C_{24}H_{34}BNO_3$ [M+NH_4^+]: 396.2705, found: 396.2706.

v. Hydrogenation and phenol deprotection. The 2:1 isomeric mixture (500 mg, 1.32 mmol) from the previous step was added to a round-bottomed flask, along with palladium over charcoal (10-20% w/w) (140 mg, 0.13 mmol), and the mixture was dissolved in anhydrous ethanol (10 ml). The flask was purged 5 times with hydrogen gas using a gas bag, and the reaction mixture was stirred vigorously for 8 hours. After this time, the mixture was filtered through a pad of Celite, washing with DCM, and the

filtrate was concentrated to dryness. No further purification was needed, and **Syn.18** was obtained as a pale yellow oil (299 mg, 78%).

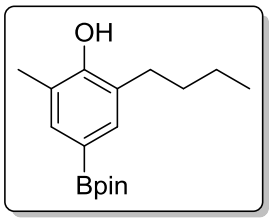

2-Butyl-6-methyl-4-(4,4,5,5-tetramethyl-1,3,2-dioxaborolan-2-yl)phenol, Syn.18

^{1}H NMR ($CDCl_3$, 300 MHz): δ 0.94 (t, *J*= 7.3 Hz, 3H), 1.27-1.45 (m, 14H), 1.53-1.68 (m, 2H), 2.25 (s, 3H), 2.55-2.65 (m, 2H), 4.89 (br s, 1H), 7.45 (d, *J*= 2.6 Hz, 2H) ppm.

^{13}C NMR ($CDCl_3$, 75.5 MHz): δ 13.98, 15.62, 22.8, 24.8, 29.8, 32.1, 83.5, 120.4 (br, C), 122.4, 127.3, 134.8, 135.5, 154.8 ppm.

HRMS (EI) calcd. for $C_{17}H_{28}BO_3$ [M+H$^+$]: 291.2126, found: 291.2132.

4.9.1.15. Synthesis of ***Syn.20***.

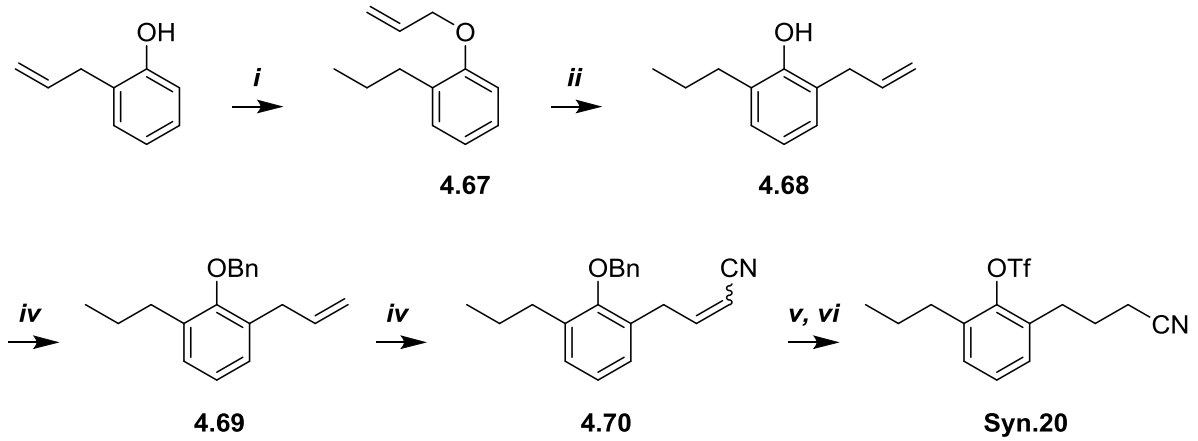

i. Hydrogenation and O-allylation. Commercially available 2-allylphenol (2.0 g, 14.9 mmol) and palladium over charcoal (10-20% w/w) (316 mg, 0.298 mmol) were placed in a round-bottomed flask and suspended in anhydrous methanol (30 ml). The flask was purged with hydrogen gas 5 times using a gas bag, and the mixture was stirred vigorously for 16h. After this time, the mixture was filtered

through Celite, washing with DCM, and the filtrate was concentrated to dryness. No further purification was needed and the residue was dissolved in anhydrous DMF (30ml). To this mixture, potassium iodide (123 mg, 0.75 mmol), 18-crown-6 (396 mg, 1.5 mmol), and allyl bromide (3.9 ml, 44.7 mmol) were added and the reaction was stirred at room temperature for 20h. After this time the mixture was diluted with water (20 ml) and extracted with diethyl ether (3 x 20 ml). The combined organic layers were then washed with water (5 x 20 ml), saturated aqueous sodium bicarbonate solution (2 x 20 ml) and brine (20 ml). The final ethereal phase was dried over anhydrous sodium sulphate, filtered and concentrated to dryness to afford **4.67** as a colourless oil (2.26 g, 86% from 2-allylphenol). No further purification was necessary, and spectroscopic data were concordant with those reported in the literature.[343]

ii. Claisen Rearrangement. *O*-allyl-2-propylphenol **4.67** (500 mg, 2.84 mmol) was dissolved in DMF (3 ml) in a sealable reaction vessel. The mixture was then sealed and heated at 200 °C for 20h, after which time the mixture was diluted with water and extracted with diethyl ether (2 x 10 ml). The combined ethereal layers were washed with water (3 x 15 ml), dried over anhydrous sodium sulphate, filtered and concentrated to dryness. The crude mixture was purified by flash column chromatography using *n*-hexane:EtOAc (30:1) as the eluent to afford pure **4.68** as a colourless oil (285 mg, 57%). The spectroscopic data of **4.68** were concordant with those reported in the literature.[343]

iii. O-Benzylation. The product of the previous step was subject to the same conditions described previously (*see i. O-Benzylation, Section 4.9.1.1*). The crude mixture was used in the next step without further purification.

iv. Cross metathesis. Crude **4.69** (200 mg, 0.75 mmol) was introduced into a microwaveable reaction vial and dissolved in anhydrous toluene (5 ml). Acrylonitrile (0.25 ml, 0.38 mmol) was added, followed by Hoveyda-Grubbs 2nd generation catalyst (23 mg, 0.038 mmol). The flask was sealed and heated to 120 °C under microwave irradiation for 1 hour. After this time, the reaction was cooled and a second portion of the catalyst (23 mg, 0.038 mmol) was added, and the reaction was once again heated to 120 °C under microwave irradiation for 1 hour. This was repeated once more, and then the reaction cooled to room temperature and concentrated to dryness.

[343] B. Roth, M. Y. Tidwell, R. Ferone, D. P. Baccanari, C. W. Sigel, D. DeAngelis and L. P. Elwell, *J. Med. Chem.*, 1989, **132**, 1949-1958.

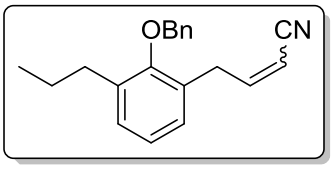

4-(2-(Benzyloxy)-3-propylphenyl)but-2-enenitrile, 4.69

The crude mixture was purified *via* flash column chromatography using *n*-hexane:EtOAc (8:1) as the eluent, affording the pure product as a 4:1 mixture of (*Z*)- and (*E*)-**4.69** as a pale yellow oil (136 mg, 62%). **4.69** was characterised as a mixture, given the irrelevance of this isomerism to the synthetic sequence (the double bond will be later hydrogenated and the two isomers will converge into one saturated product).

^{1}H NMR ($CDCl_3$, 300 MHz): δ 0.97 (t, *J*= 7.3 Hz, 2 x 3H), 1.59-1.79 (m, 2 x 2H), 2.61-2.72 (m, 2 x 2H), 3.52 (dd, *J*= 6.4, 1.8 Hz, 2H, *E* (minor)), 3.77 (dd, *J*= 7.5, 1.4 Hz, 2H, *Z* (major)), 4.81 (s, 2H, *E* (minor)), 4.85 (s, 2H, *Z* (major)), 5.21 (dt, *J*= 16.3, 1.8 Hz, 1H, *E* (minor)), 5.36 (dt, *J*= 10.8, 1.5 Hz, 1H, *Z* (major)), 6.59 (dt, *J*= 10.8, 7.5 Hz, 1H, *Z* (major)), 6.82 (dt, *J*= 16.3, 6.4 Hz, 1H, *E* (minor)), 7.01-7.51 (m, 2 x 8H) ppm.

^{13}C NMR ($CDCl_3$, 75.5 MHz): δ 14.2, 23.8, 32.1, 32.8, 34.0, 75.6, 99.7, 100.6, 116.0, 124.7, 127.4, 127.7, 127.8, 128.1, 128.2, 128.6, 129.4, 129.6, 130.4, 136.3, 137.1, 153.1, 154.1, 155.1 ppm.

HRMS (EI) calcd. for $C_{20}H_{25}N_2O$ [M+NH_4^+]: 309.1961, found: 309.1966.

v. Hydrogenation and phenol deprotection. The product of the previous step was subject to the same conditions described previously (*see v. Hydrogenation and phenol deprotection, Section 4.9.1.14*). No further purification was required, and **4.71** was obtained as a waxy pale yellow solid (247 mg, 93%).

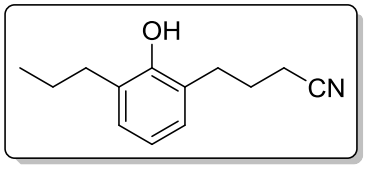

4-(2-Hydroxy-3-propylphenyl)butanenitrile, 4.71

^{1}H NMR ($CDCl_3$, 300 MHz): δ 1.02 (t, *J*= 7.3 Hz, 3H), 1.67 (dq, *J*= 14.8, 7.4 Hz, 2H), 1.94-2.12 (m, 2H), 2.36 (t, *J*=7.2 Hz, 2H), 2.51-2.63 (m, 2H), 2.81 (t, *J*= 7.3 Hz, 2H), 4.78 (br s, 1H), 6.84 (t, *J*= 7.5 Hz, 1H), 6.94-7.09 (m, 2H) ppm.

^{13}C NMR ($CDCl_3$, 75.5 MHz): δ 14.0, 16.6, 22.8, 25.5, 29.3, 32.0, 119.9, 120.5, 126.0, 127.4, 128.2, 128.4, 151.6 ppm.

HRMS (EI) calcd. for $C_{13}H_{21}N_2O$ [M+NH_4^+]: 221.1648, found: 221.1648.

vi. Triflate formation. Previously synthesised **4.71** (200 mg, 0.98 mmol) was dissolved in anhydrous DCM (10 ml) and the solution was cooled in an ice bath. Pyridine (0.2 ml, 2.46 mmol) was added and the reaction was stirred for 15 minutes in the ice bath, after which trifluoromethanesulfonic anhydride (1M in DCM) (1.5 ml, 1.5 mmol) was added slowly. The reaction was stirred for 20 minutes and a further 90 minutes at room temperature. Following this, the reaction was diluted with diethyl ether (10 ml) and quenched with aqueous HCl (1M, 5 ml). The mixture was extracted with diethyl ether (2 x 10 ml), and the combined ethereal phase was washed with water (2 x 15 ml) and brine (15 ml). The organic phase was dried over anhydrous sodium sulphate, filtered and concentrated to dryness.

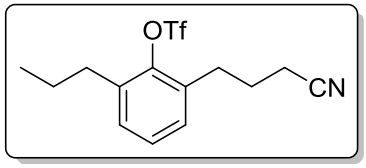

2-(3-Cyanopropyl)-6-propylphenyl trifluoromethanesulfonate, Syn.20

The crude mixture was purified *via* flash column chromatography using *n*-hexane:EtOAc (6:1) as the eluent, affording pure **Syn.20** as a colourless oil (286 mg, 87%).

^{1}H NMR ($CDCl_3$, 300 MHz): δ 0.98 (t, *J*= 7.3 Hz, 3H), 1.58-1.73 (m, 2H), 1.96-2.07 (m, 2H), 2.38 (t, *J*= 7.2 Hz, 2H), 2.67-2.77 (m, 2H), 2.87-2.96 (m, 2H), 7.11-7.34 (m, 3H) ppm.

^{13}C NMR ($CDCl_3$, 75.5 MHz): δ 13.8 (CH_3), 16.7 (CH_2), 23.2 (CH_2), 25.7 (CH_2), 29.6 (CH_2), 32.4 (CH_2), 118.6 (q, *J*= 320.5 Hz, CF_3), 119.1 (C), 128.6 (CH), 128.9 (CH), 129.9 (CH), 133.5 (C), 136.7 (C), 145.6 (C) ppm.

^{19}F NMR ($CDCl_3$, 282.4 MHz): δ -73.49 (s, 3F) ppm.

HRMS (EI) calcd. for $C_{14}H_{20}F_3N_2O_3S$ [M+NH_4^+]: 353.1141, found: 353.1143.

4.9.2. Synthesis of biphenyls.

4.9.2.1. Suzuki cross coupling (Biphenyl).

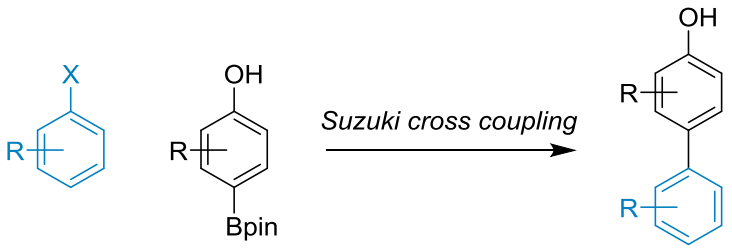

The required aryl bromide (or triflate) (1 equiv) was placed in a microwaveable vial along with the corresponding phenylboronic acid pinacol ester (1.1 equiv), and the mixture was dissolved in acetonitrile (0.3 M). Nitrogen gas was then bubbled through the solution for 5 minutes. Meanwhile, a solution of potassium phosphate tribasic (3 equiv) in degassed water (35% v/v of the required acetonitrile) was prepared. The aqueous solution was then added to the acetonitrile solution, followed by the addition of $PdCl_2$(dppf) (10 mol%), and the reaction vessel was sealed. The reaction was heated to 120 °C under microwave irradiation for 90 minutes, after which time the mixture was cooled to room temperature and extracted with ethyl acetate. The combined organic layers were dried over anhydrous sodium sulphate, filtered and concentrated. The crude mixture was purified *via* flash column chromatography using mixtures of *n*-hexane and ethyl acetate as the eluent.

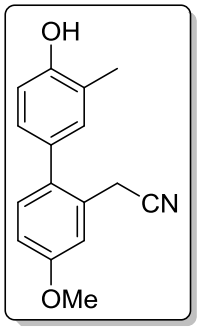

2-(4'-Hydroxy-4-methoxy-3'-methyl-[1,1'-biphenyl]-2-yl)acetonitrile, 4.21a

The crude mixture was purified *via* flash column chromatography using *n*-hexane:EtOAc (4:1) as the eluent, affording pure **4.21a** as a white solid (213 mg, 57%) with a melting point of 108-110 °C.

^{1}H NMR ($CDCl_3$, 300 MHz): δ 2.29 (s, 3H), 3.61 (s, 2H), 3.86 (s, 3H), 4.75 (br s, 1H), 6.82 (d, *J*= 8.1 Hz, 1H), 6.90 (dd, *J*= 8.5, 2.6 Hz, 1H), 6.97 (dd, *J*= 8.1, 2.3 Hz, 1H), 7.02 (d, *J*= 2.1 Hz, 1H), 7.05 (d, *J*= 2.6 Hz, 1H), 7.18 (d, *J*= 8.5 Hz, 1H) ppm.

^{13}C NMR ($CDCl_3$, 75.5 MHz): δ 16.3, 22.7, 55.9, 114.2, 114.6, 115.4, 118.8, 124.6, 128.2, 129.3, 132.1, 132.2, 132.3, 134.6, 153.9, 159.5 ppm.

HRMS (EI) calcd. for $C_{16}H_{16}NO_2$ [M+H$^+$]: 254.1176, found: 254.1174.

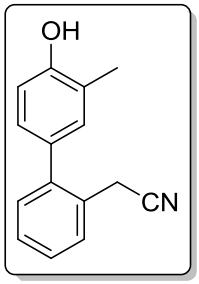

2-(4'-Hydroxy-3'-methyl-[1,1'-biphenyl]-2-yl)acetonitrile, 4.21b

The crude mixture was purified *via* flash column chromatography using *n*-hexane:EtOAc (4:1) as the eluent, affording pure **4.21b** as a pale brown oil (169 mg, 62%).

^{1}H NMR ($CDCl_3$, 300 MHz): δ 2.22 (s, 3H), 3.57 (s, 2H), 4.96 (br s, 1H), 6.77 (d, *J*=6.5 Hz, 1H), 6.92 (dd, *J*= 6.5, 1.8 Hz, 1H), 6.98 (d, *J*=1.8 Hz, 1H), 7.14-7.22 (m, 1H), 7.24-7.34 (m, 2H), 7.42-7.47 (m, 1H) ppm.

^{13}C NMR ($CDCl_3$, 75.5 MHz): δ 16.3, 22.5, 115.4, 118.9, 124.7, 128.0, 128.2, 128.3, 128.6, 129.3, 131.0, 132.0, 132.6, 142.2, 154.2 ppm.

HRMS (EI) calcd. for $C_{15}H_{14}NO$ [M+H$^+$]: 224.1070, found: 224.1066.

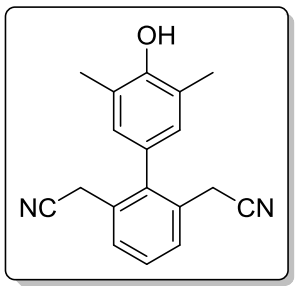

2,2'-(4'-Hydroxy-3',5'-dimethyl-[1,1'-biphenyl]-2,6-diyl)diacetonitrile, 4.37a

The crude mixture was purified *via* flash column chromatography using *n*-hexane:EtOAc (3:1) as the eluent, affording pure **4.37a** as a white to pink solid (312 mg, 75%) with a melting point of 129-131 °C.

^{1}H NMR ($CDCl_3$, 300 MHz): δ 2.31 (s, 6H), 3.46 (s, 4H), 4.80 (s, 1H), 6.79 (s, 2H), 7.45 (dd, *J*= 8.7, 6.6 Hz, 1H), 7.55 (d, *J*= 7.2 Hz, 2H) ppm.

^{13}C NMR ($CDCl_3$, 75.5 MHz): δ 16.5, 22.9, 118.4, 124.9, 128.5, 128.7, 129.0, 129.1, 130.4, 141.7, 153.0 ppm.

HRMS (EI) calcd. for $C_{18}H_{20}N_3O$ [M+NH_4^+]: 294.1601, found: 294.1601.

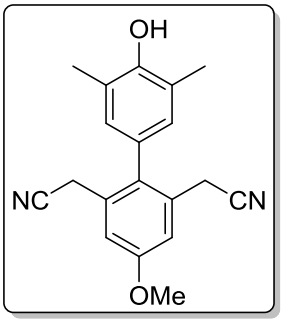

2,2'-(4'-Hydroxy-4-methoxy-3',5'-dimethyl-[1,1'-biphenyl]-2,6-diyl)diacetonitrile, 4.37b

The crude mixture was purified *via* flash column chromatography using *n*-hexane:EtOAc (3:1) as the eluent, affording pure **4.37b** as a white solid (114 mg, 71%). The spectroscopic data were concordant with those reported in the literature.[308]

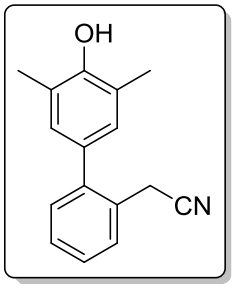

2-(4'-Hydroxy-3',5'-dimethyl-[1,1'-biphenyl]-2-yl)acetonitrile, 4.45a

The crude mixture was purified *via* flash column chromatography using *n*-hexane:EtOAc (4:1) as the eluent, affording pure **4.45a** as a pale brown solid (254 mg, 73%) with a melting point of 114-115 °C.

^{1}H NMR ($CDCl_3$, 300 MHz): δ 2.30 (t, *J*= 0.6 Hz, 6H), 3.66 (s, 2H), 4.78 (s, 1H), 6.89-6.92 (m, 2H), 7.24-7.28 (m, 1H), 7.34-7.39 (m, 2H), 7.50-7.54 (m, 1H) ppm.

^{13}C NMR ($CDCl_3$, 75.5 MHz): δ 16.4 (CH_3), 22.5 (CH_2), 118.9 (C), 123.7 (C), 128.2 (CH), 128.3 (C), 128.5 (CH), 129.2 (CH), 129.5 (CH), 131.0 (CH), 132.3 (C), 142.3 (C), 152.3 (C) ppm.

HRMS (EI) calcd. for $C_{16}H_{19}N_2O$ [M+NH_4^+]: 255.1492, found: 255.1490.

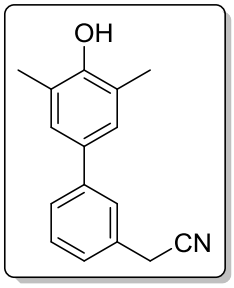

2-(4'-Hydroxy-3',5'-dimethyl-[1,1'-biphenyl]-3-yl)acetonitrile, 4.45b

The crude mixture was purified *via* flash column chromatography using *n*-hexane:EtOAc (4:1) as the eluent, affording pure **4.45b** as a white solid (263 mg, 78%) with a melting point of 97-99 °C.

^{1}H NMR ($CDCl_3$, 300 MHz): δ 2.32 (s, 6H), 3.80 (s, 2H), 4.76 (s, 1H), 7.21 (s, 2H), 7.22-7.25 (m, 1H), 7.37-7.44 (m, 1H), 7.47-7.52 (m, 2H) ppm.

^{13}C NMR ($CDCl_3$, 75.5 MHz): δ 16.5 (CH_3), 24.1 (CH_2), 118.4 (C), 123.9 (C), 126.3 (CH), 126.7 (CH), 126.9 (CH), 127.4 (C), 127.8 (CH), 129.8 (CH), 130.6 (C), 132.7 (C), 142.6 (C), 152.7 (C) ppm.

HRMS (EI) calcd. for $C_{16}H_{19}N_2O$ [M+NH_4^+]: 255.1492, found: 255.1489.

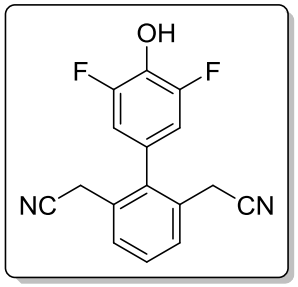

2,2'-(3',5'-Difluoro-4'-hydroxy-[1,1'-biphenyl]-2,6-diyl)diacetonitrile, 4.50

The crude mixture was purified *via* flash column chromatography using *n*-hexane:EtOAc (5:1) as the eluent, affording pure **4.50** as a white solid (142 mg, 57%) with a melting point of 142-143 °C.

^{1}H NMR ($CDCl_3$, 300 MHz): δ 3.38 (s, 4H), 6.70 (dd, *J*= 6.6, 1.6 Hz, 2H), 7.36-7.51 (m, 3H) ppm.

^{13}C NMR ($CDCl_3$, 75.5 MHz): δ 22.8 (CH_2), 113.0 (dd, *J*= 14.0, 8.2 Hz, CH), 117.6 (C), 127.9 (t, *J*= 8.0 Hz, C), 129.3 (CH), 130.1 (CH), 130.3 (C), 134.0 (t, *J*= 15.6 Hz, C), 139.1 (C), 152.7 (dd, *J*= 247.2, 6.4, CF) ppm.

^{19}F NMR ($CDCl_3$, 282.4 MHz): -131.79 (s, 2F) ppm.

HRMS (EI) calcd. for $C_{16}H_{16}FN_3O$ [M-F+H_2+NH_4^+]: 303.1616, found: 303.1618.

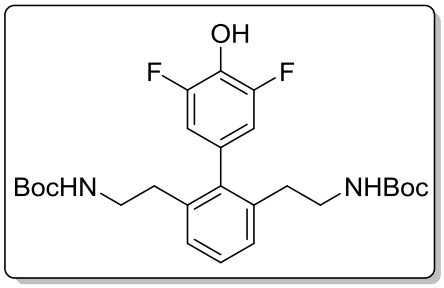

Di-*tert*-butyl ((3',5'-difluoro-4'-hydroxy-[1,1'-biphenyl]-2,6-diyl)bis(ethane-2,1-diyl))dicarbamate, 4.54

The crude mixture was purified *via* flash column chromatography using *n*-hexane:EtOAc (5:1) as the eluent, affording pure **4.54** as a dense orange oil (131 mg, 49%).

^{1}H NMR ($CDCl_3$, 300 MHz): δ 1.37 (s, 18H), 2.51 (t, *J*= 7.0 Hz, 4H), 3.15 (d, *J*= 5.7 Hz, 4H), 4.59 (t, *J*= 5.7 Hz, 2H), 6.68 (d, *J*= 8.2 Hz, 2H), 7.13 (d, *J*= 7.5 Hz, 2H), 7.20-7.29 (m, 1H) ppm.

^{13}C NMR ($CDCl_3$, 75.5 MHz): δ 28.3, 33.8, 41.2, 79.4, 112.8 (dd, *J*= 13.6, 7.9), 127.4, 128.0, 130.2 (t, *J*= 7.8 Hz), 132.8 (t, *J*= 15.7 Hz), 137.5, 139.9, 152.1 (dd, *J*= 224.8, 6.7 Hz), 155.9 ppm.

^{19}F NMR ($CDCl_3$, 282.4 MHz): -133.15 ppm.

HRMS (EI) calcd. for $C_{26}H_{35}F_2N_2O_5$ [M+H^+]: 493.2509, found: 493.2508.

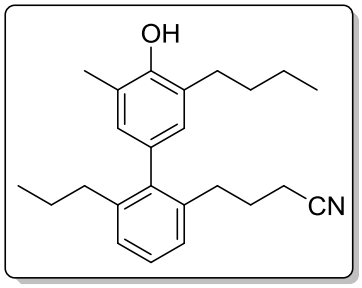

4-(3'-Butyl-4'-hydroxy-5'-methyl-6-propyl-[1,1'-biphenyl]-2-yl)butanenitrile, 4.72

The crude mixture was purified *via* flash column chromatography using *n*-hexane:EtOAc (5:1) as the eluent, affording pure **4.72** as a dense brown oil (98 mg, 41%).

^{1}H NMR ($CDCl_3$, 300 MHz): δ 0.78 (t, *J*= 7.3 Hz, 3H), 0.94 (t, *J*= 7.3 Hz, 3H), 1.32-1.49 (m, 4H), 1.52-1.65 (m, 2H), 1.66-1.79 (m, 2H), 2.15 (t, *J*= 7.5 Hz, 2H), 2.25-2.34 (m, 5H), 2.46-2.54 (m, 2H), 2.63 (td, *J*= 7.2, 1.6 Hz, 2H), 4.66 (br s, 1H), 6.72 (s, 2H), 7.07 (dd, *J*= 7.4, 1.4 Hz, 1H), 7.14 (dd, *J*= 7.6, 1.4 Hz, 1H), 7.21 (d, *J*= 7.5 Hz, 1H) ppm.

^{13}C NMR ($CDCl_3$, 75.5 MHz): δ 14.0 (CH_3), 14.1 (CH_3), 16.1 (CH_3), 16.6 (CH_2), 22.4 (CH_2), 24.5 (CH_2), 26.7 (CH_2), 29.7 (CH_2), 31.8 (CH_2), 32.7 (CH_2), 35.8 (CH_2), 119.6 (C), 122.8 (C), 126.3 (CH), 127.0 (CH), 127.1 (CH), 127.4 (C), 128.9 (CH), 129.3 (CH), 131.4 (C), 138.3 (C), 141.4 (C), 141.7 (C), 150.6 (C) ppm.

HRMS (EI) calcd. for $C_{24}H_{35}N_2O$ [$M+NH_4^+$]: 367.2744, found: 367.2747.

4.9.2.2. Formation of biphenyl triflates.

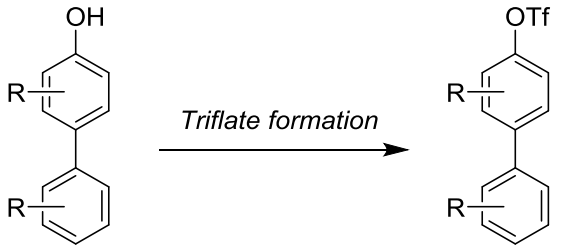

The activation of the previously synthesised biphenyls was carried out by the formation of the corresponding triflates, using the general procedure as described in the previous section (*see vi. Triflate formation, Section 4.9.1.15*).

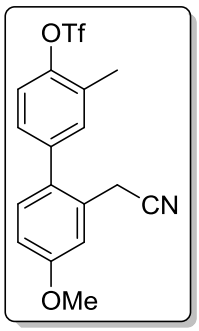

2'-(Cyanomethyl)-4'-methoxy-3-methyl-[1,1'-biphenyl]-4-yl trifluoromethanesulfonate, 4.22a

The crude mixture was purified *via* flash column chromatography using *n*-hexane:EtOAc (6:1) as the eluent, affording pure **4.22a** as a pale green oil (281 mg, 87%).

^{1}H NMR ($CDCl_3$, 300 MHz): δ 2.43 (s, 3H), 3.58 (s, 2H), 3.87 (s, 3H), 6.93 (dd, *J*= 8.5, 2.6 Hz, 1H), 7.07 (d, *J*= 2.6 Hz, 1H), 7.14-7.24 (m, 3H), 7.31 (d, *J*= 8.4 Hz, 1H) ppm.

^{13}C NMR ($CDCl_3$, 75.5 MHz): δ 16.9 (CH_3), 22.7 (CH_2), 55.9 (CH_3), 114.4 (CH), 115.0 (CH), 118.3 (C), 119.0 (q, *J*= 321.2 Hz, CF_3), 121.9 (CH), 128.8 (CH), 129.3 (C), 131.7 (C), 131.9 (CH), 132.8 (C), 133.4 (CH), 140.4 (C), 148.2 (C), 160.2 (C) ppm.

^{19}F NMR ($CDCl_3$, 282.4 MHz): δ -74.21 (s, 3F) ppm.

HRMS (EI) calcd. for $C_{17}H_{18}F_3N_2O_4S$ [$M+NH_4^+$]: 403.0934, found: 403.0924.

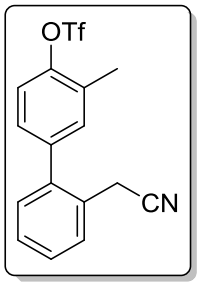

2'-(Cyanomethyl)-3-methyl-[1,1'-biphenyl]-4-yl trifluoromethanesulfonate, 4.22b

The crude mixture was purified *via* flash column chromatography using *n*-hexane:EtOAc (7:1) as the eluent, affording pure **4.22b** as a pale yellow oil (220 mg, 92%).

^{1}H NMR ($CDCl_3$, 300 MHz): δ 2.44 (s, 3H), 3.60 (s, 2H), 7.20 (ddd, *J*= 8.4, 2.3, 0.4 Hz, 1H), 7.26-7.29 (m, 2H), 7.34 (d, *J*= 8.4 Hz, 1H), 7.38-7.48 (m, 2H), 7.53-7.58 (m, 1H) ppm.

^{13}C NMR ($CDCl_3$, 75.5 MHz): δ 16.9 (CH_3), 22.5 (CH_2), 118.4 (C), 119.0 (q, *J*= 318.1 Hz, CF_3), 122.0 (CH), 128.1 (C), 128.6 (CH), 128.9 (CH), 129.3 (C), 129.6 (CH), 130.8 (CH), 131.9 (C), 133.2 (CH), 140.4 (C), 140.5 (C), 148.4 (C) ppm.

^{19}F NMR ($CDCl_3$, 282.4 MHz): δ -74.20 (s, 3F) ppm.

HRMS (EI) calcd. for $C_{16}H_{16}F_3N_2O_3S$ [M+NH_4^+]: 373.0828, found: 373.0822.

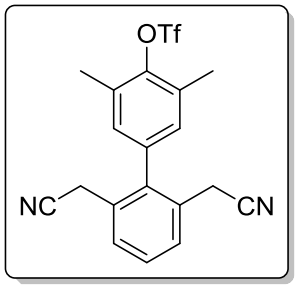

2',6'-Bis(cyanomethyl)-3,5-dimethyl-[1,1'-biphenyl]-4-yl trifluoromethanesulfonate, 4.38a

The crude mixture was purified *via* flash column chromatography using *n*-hexane:EtOAc (6:1) as the eluent, affording pure **4.38a** as a colourless solid (405 mg, 91%) with a melting point of 110-112 °C.

^{1}H NMR ($CDCl_3$, 300 MHz): δ 2.38 (s, 6H), 3.34 (s, 4H), 6.92 (s, 2H), 7.42 (dd, *J*= 9.0, 6.1 Hz, 1H), 7.47-7.51 (m, 2H) ppm.

^{13}C NMR ($CDCl_3$, 75.5 MHz): δ 17.3 (CH_3), 22.5 (CH_2), 117.4 (C), 118.6 (q, *J*= 319.9 Hz, CF_3), 128.7 (CH), 129.5 (CH), 129.6 (C), 130.2 (CH), 133.4 (C), 136.7 (C), 139.4 (C), 146.8 (C) ppm.

^{19}F NMR ($CDCl_3$, 282.4 MHz): δ -73.72 (s, 3F) ppm.

HRMS (EI) calcd. for $C_{19}H_{16}F_3N_2O_3S$ [M+H$^+$]: 409.0828, found: 409.0815.

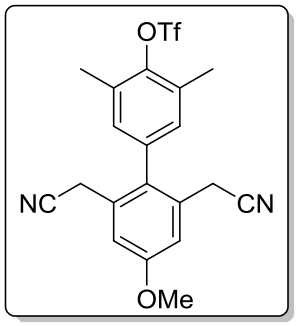

2',6'-Bis(cyanomethyl)-4'-methoxy-3,5-dimethyl-[1,1'-biphenyl]-4-yl trifluoromethanesulfonate, 4.38b

The crude mixture was purified *via* flash column chromatography using *n*-hexane:EtOAc (6:1) as the eluent, affording pure **4.38b** as a white solid (145 mg, 86%). The spectroscopic data were concordant with those reported in the literature.[308]

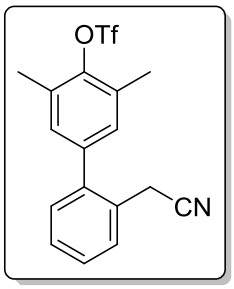

2'-(Cyanomethyl)-3,5-dimethyl-[1,1'-biphenyl]-4-yl trifluoromethanesulfonate, 4.46a

The crude mixture was purified *via* flash column chromatography using *n*-hexane:EtOAc (7:1) as the eluent, affording pure **4.46a** as a dense colourless oil (318 mg, 84%).

^{1}H NMR ($CDCl_3$, 300 MHz): δ 2.35 (s, 6H), 3.52 (s, 2H), 6.98 (s, 2H), 7.14-7.18 (m, 1H), 7.27-7.36 (m, 2H), 7.43-7.47 (m, 1H) ppm.

^{13}C NMR ($CDCl_3$, 75.5 MHz): δ 17.6 (CH_3), 22.5 (CH_2), 118.5 (C), 119.0 (q, *J*= 319.4 Hz, CF_3), 128.1 (C), 128.8 (CH), 129.1 (CH), 129.5 (CH), 130.7 (CH), 130.8 (CH), 132.4 (C), 140.2 (C), 140.6 (C), 146.8 (C) ppm.

^{19}F NMR ($CDCl_3$, 282.4 MHz): δ -73.86 (s, 3F) ppm.

HRMS (EI) calcd. for $C_{17}H_{18}F_3N_2O_3S$ [M+NH_4^+]: 387.0985, found: 387.0989.

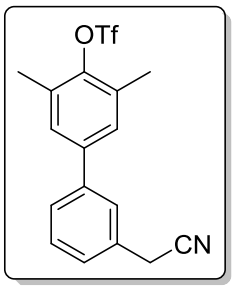

3'-(Cyanomethyl)-3,5-dimethyl-[1,1'-biphenyl]-4-yl trifluoromethanesulfonate, 4.46b

The crude mixture was purified *via* flash column chromatography using *n*-hexane:EtOAc (7:1) as the eluent, affording pure **4.46b** as a colourless oil (342 mg, 93%).

^{1}H NMR ($CDCl_3$, 300 MHz): δ 2.46 (s, 6H), 3.82 (s, 2H), 7.36-7.29 (m, 3H), 7.40-7.54 (m, 3H) ppm.

^{13}C NMR ($CDCl_3$, 75.5 MHz): δ 17.7 (CH_3), 24.0 (CH_2), 118.1 (C), 119.0 (q, *J*= 319.6 Hz, CF_3), 127.1 (CH), 127.3 (CH), 127.7 (CH), 129.0 (CH), 130.1 (CH), 131.0 (C), 132.4 (C), 140.5 (C), 141.1 (C), 147.0 (C) ppm.

^{19}F NMR ($CDCl_3$, 282.4 MHz): δ -73.87 (s, 3F) ppm.

HRMS (EI) calcd. for $C_{17}H_{18}F_3N_2O_3S$ [M+NH_4^+]: 387.0985, found: 387.0984.

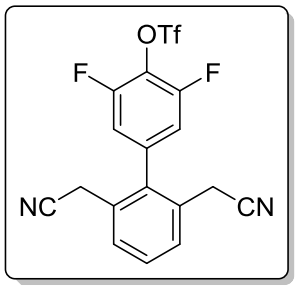

2',6'-Bis(cyanomethyl)-3,5-difluoro-[1,1'-biphenyl]-4-yl trifluoromethanesulfonate, 4.51

The crude mixture was purified *via* flash column chromatography using *n*-hexane:EtOAc (9:1) as the eluent, affording pure **4.51** as a yellow solid (170 mg, 76%) with a melting point of 96-98 °C.

^{1}H NMR ($CDCl_3$, 300 MHz): δ 3.43 (s, 4H), 6.97-7.05 (m, 2H), 7.50-7.63 (m, 3H) ppm.

^{13}C NMR ($CDCl_3$, 75.5 MHz): δ 22.8 (CH_2), 114.0-114.7 (m, CH), 117.2 (C), 119.0 (q, *J*= 321.7Hz, C), 129.7 (CH, C), 130.9 (CH), 137.6 (C), 138.5 (t, *J*= 8.3 Hz, C), 155.7 (d, *J*= 259.8 Hz, C) ppm.

^{19}F NMR ($CDCl_3$, 282.4 MHz): δ -73.30 (t, *J*= 6.4 Hz, 3F), -120.46 (q, *J*= 6.4 Hz, 2F) ppm.

HRMS (EI) calcd. for $C_{17}H_{13}F_5N_3O_3S$ [M+NH_4^+]: 434.0592, found: 434.0590.

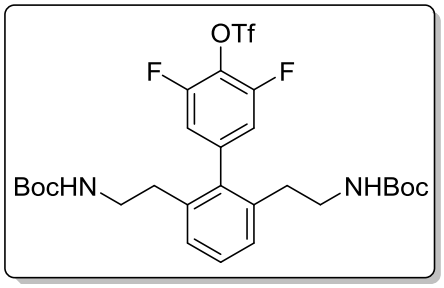

2',6'-Bis(2-((*tert*-butoxycarbonyl)amino)ethyl)-3,5-difluoro-[1,1'-biphenyl]-4-yl trifluoromethanesulfonate, 4.55

The crude mixture was purified *via* flash column chromatography using *n*-hexane:EtOAc (10:1) as the eluent, affording pure **4.55** as a colourless oil (166 mg, 86%).

^{1}H NMR ($CDCl_3$, 300 MHz): δ 1.41 (s, 18H), 2.51 (t, *J*= 7.1 Hz, 4H), 3.21 (dd, *J*= 13.5, 6.7 Hz, 4H), 4.46 (br s, 2H), 6.99 (d, *J*= 7.9 Hz, 2H), 7.20 (d, *J*= 7.6 Hz, 2H), 7.30-7.38 (m, 1H) ppm.

^{13}C NMR ($CDCl_3$, 75.5 MHz): δ 28.3, 34.0, 41.1, 79.4, 114.3 (d, *J*= 20.8 Hz, CH), 118.6 (q, *J*= 321.2 Hz, CF_3), 124.9, 127.8, 128.8, 136.8, 138.4, 141.9, 154.4 (d, *J*= 257.3 Hz, CF), 155.6 ppm.

^{19}F NMR ($CDCl_3$, 282.4 MHz): δ -72.99 (t, *J*= 6.4 Hz, 3F), -123.15 (br s, 2F) ppm.

HRMS (EI) calcd. for $C_{27}H_{34}F_5N_2O_7S$ [M+H^+]: 625.2001, found: 625.2018.

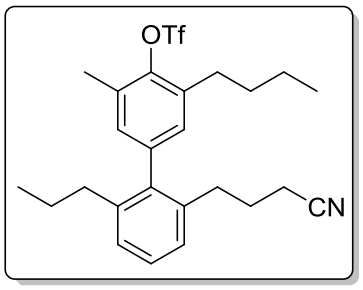

3-Butyl-2'-(3-cyanopropyl)-5-methyl-6'-propyl-[1,1'-biphenyl]-4-yl trifluoromethanesulfonate, 4.73

The crude mixture was purified *via* flash column chromatography using *n*-hexane:EtOAc (10:1) as the eluent, affording pure **4.73** as a colourless oil (128 mg, 89%).

^{1}H NMR ($CDCl_3$, 300 MHz): δ 0.78 (t, *J*= 7.3 Hz, 3H), 0.93 (t, *J*= 7.3 Hz, 3H), 1.29-1.50 (m, 4H), 1.59 (ddd, *J*= 11.5, 10.4, 5.0 Hz, 2H), 1.67-1.78 (m, 2H), 2.17 (t, *J*= 7.2 Hz, 3H), 2.21-2.30 (m, 2H), 2.43 (s, 3H), 2.45-2.52 (m, 2H), 2.77 (td, *J*= 7.3, 3.1 Hz, 2H), 6.93 (dd, *J*= 7.1, 1.9 Hz, 2H), 7.10 (dd, *J*= 7.5, 1.2 Hz, 1H), 7.16 (dd, *J*= 7.6, 1.2 Hz, 1H), 7.27 (t, *J*= 7.6 Hz, 1H) ppm.

^{13}C NMR ($CDCl_3$, 75.5 MHz): δ 13.8 (CH_3), 14.0 (CH_3), 16.7 (CH_2), 17.4 (CH_3), 22.3 (CH_2), 24.4 (CH_2), 26.6 (CH_2), 30.0 (CH_2), 32.1 (CH_2), 32.5 (CH_2), 35.7 (CH_2), 118.7 (q, *J*= 320.0 Hz, CF_3), 119.3 (C), 126.4 (CH), 127.3 (CH), 127.8 (CH), 129.9 (CH), 130.8 (CH), 131.6 (C), 136.1 (C), 137.7 (C), 139.7 (C), 139.9 (C), 141.1 (C), 145.3 (C) ppm.

^{19}F NMR ($CDCl_3$, 282.4 MHz): δ -73.44 (s, 3F) ppm.

HRMS (EI) calcd. for $C_{25}H_{34}F_3N_2O_3S$ [$M+NH_4^+$]: 499.2211, found: 499.2218.

4.9.3. Synthesis of terphenyls.

4.9.3.1. Suzuki cross coupling (Terphenyl).

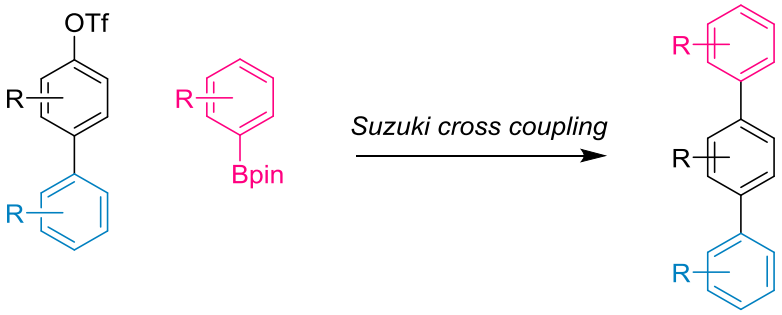

The required aryl bromide (or triflate) (1 equiv) was placed in a microwaveable vial along with the corresponding phenylboronic acid pinacol ester (1.1 equiv), and the mixture was dissolved in acetonitrile (0.2 M). Nitrogen gas was then bubbled through the solution for 5 minutes. Meanwhile, a solution of potassium phosphate tribasic (3 equiv) in degassed water (20% v/v of the required acetonitrile) was prepared. The aqueous solution was then added to the acetonitrile solution, followed by the addition of $Pd(OAc)_2$ (10 mol%) and triphenylphosphine (25 mol%), and the reaction vessel was sealed. The reaction was heated to 120 °C under microwave irradiation for 90 minutes, after which time the mixture was cooled to room temperature and extracted with ethyl acetate. The combined organic layers were dried over anhydrous sodium sulphate, filtered and concentrated. The crude mixture was purified *via* flash column chromatography using mixtures of *n*-hexane and ethyl acetate as the eluent. In some cases, it was necessary to use mixtures of toluene and ethyl acetate for the flash column chromatography in order to separate the terphenyl from the residual pinacol liberated in the reaction.

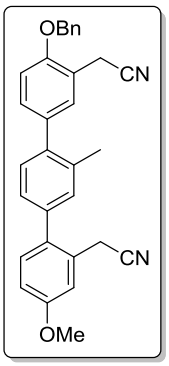

2,2'-(4''-(Benzyloxy)-4-methoxy-3'-methyl-[1,1':4',1''-terphenyl]-2,3''-diyl)diacetonitrile, 4.23a

The crude mixture was purified *via* flash column chromatography using *n*-hexane:EtOAc (3:1) as the eluent, affording pure **4.23a** as a pale brown solid (106 mg, 38%) with a melting point of 172-173 °C.

^{1}H NMR ($CDCl_3$, 300 MHz): δ 2.24 (s, 3H), 3.61 (s, 2H), 3.72 (s, 2H), 3.81 (s, 3H), 5.10 (s, 2H), 6.86 (dd, *J*= 8.5, 2.6 Hz, 1H), 6.96 (d, *J*= 8.4 Hz, 1H), 7.02 (d, *J*= 2.6 Hz, 1H), 7.03-7.07 (m, 1H), 7.09 (s, 1H), 7.16-7.19 (m, 2H), 7.23 (dd, *J*= 5.9, 2.7 Hz, 1H), 7.28-7.43 (m, 6H) ppm.

^{13}C NMR ($CDCl_3$, 75.5 MHz): δ 19.4, 21.0, 22.7, 55.9, 70.9, 111.9, 114.3, 114.6, 118.4, 118.7, 119.2, 127.1, 127.8, 128.6, 129.2, 129.3, 130.4, 130.5, 130.6, 131.7, 132.0, 134.4, 134.8, 136.2, 136.8, 139.1, 140.3, 155.4, 159.8 ppm.

HRMS (EI) calcd. for $C_{31}H_{30}N_3O_2$ [M+NH_4^+]: 476.2333, found: 476.2337.

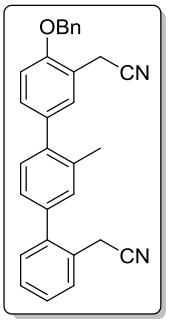

2,2'-(4''-(Benzyloxy)-3'-methyl-[1,1':4',1''-terphenyl]-2,3''-diyl)diacetonitrile, 4.23b

The crude mixture was purified *via* flash column chromatography using *n*-hexane:EtOAc (3:1) as the eluent, affording pure **4.23b** as a yellow solid (69 mg, 46%) with a melting point of 129-131 °C.

^{1}H NMR ($CDCl_3$, 300 MHz): δ 2.34 (s, 3H), 3.71 (s, 2H), 3.81 (s, 2H), 5.19 (s, 2H), 7.05 (d, *J*= 8.5 Hz, 1H), 7.16 (dd, *J*= 7.7, 1.5 Hz, 1H), 7.19-7.22 (m, 1H), 7.29 (d, *J*= 7.9 Hz, 1H), 7.31-7.52 (m, 10H), 7.56-7.60 (m, 1H) ppm.

^{13}C NMR ($CDCl_3$, 75.5 MHz): δ 19.4 (CH_2), 21.0 (CH_3), 22.5 (CH_2), 70.9 (CH_2), 111.9 (CH), 118.4 (C), 118.8 (C), 119.2 (C), 126.8 (CH), 127.8 (CH), 128.2 (C, C), 128.6 (2CH), 128.7 (CH), 129.15 (CH), 129.3 (CH), 130.5 (CH), 130.6 (CH), 130.9 (C, CH), 131.4 (CH), 134.7 (C), 136.3 (C), 136.8 (C), 139.3 (C), 140.6 (C), 142.0 (C), 155.5 (C) ppm.

HRMS (EI) calcd. for $C_{30}H_{28}N_3O$ [M+NH_4^+]: 446.2227, found: 446.2229.

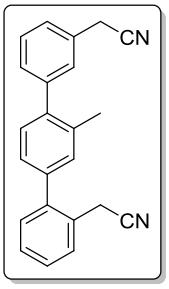

2,2'-(3'-Methyl-[1,1':4',1''-terphenyl]-2,3''-diyl)diacetonitrile, 4.23c

The crude mixture was purified *via* flash column chromatography using *n*-hexane:EtOAc (4:1) as the eluent, affording pure **4.23c** as a white solid (57 mg, 31%) with a melting point of 107-109 °C.

^{1}H NMR ($CDCl_3$, 300 MHz): δ 2.24 (s, 3H), 3.63 (s, 2H), 3.75 (s, 2H), 7.07-7.12 (m, 1H), 7.14 (dd, *J*= 1.2, 0.6 Hz, 1H), 7.21 (d, *J*= 7.7 Hz, 1H), 7.24-7.30 (m, 4H), 7.33-7.42 (m, 3H), 7.48-7.52 (m, 1H) ppm.

^{13}C NMR ($CDCl_3$, 75.5 MHz): δ 19.5, 21.1, 22.6, 116.8, 117.3, 125.4, 125.6, 126.8, 127.2, 127.7, 127.9, 127.9, 128.0, 128.9, 129.0, 129.4, 130.0, 134.7, 138.2, 139.4, 140.5, 141.4 ppm.

HRMS (EI) calcd. for $C_{23}H_{22}N_3$ [M+NH_4^+]: 340.1808, found: 340.1800.

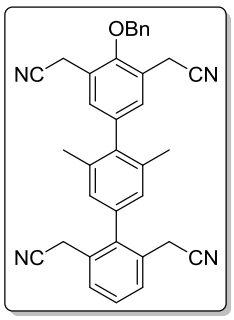

2,2',2'',2'''-(4''-(Benzyloxy)-3',5'-dimethyl-[1,1':4',1''-terphenyl]-2,3'',5'',6-tetrayl)tetraacetonitrile, 4.39a

The crude mixture was purified *via* flash column chromatography using *n*-hexane:EtOAc (3:1) as the eluent, affording pure **4.39a** as a white solid (117 mg, 54%) with a melting point of 173-176 °C.

^{1}H NMR ($CDCl_3$, 300 MHz): δ 2.02 (s, 6H), 3.45 (s, 4H), 3.67 (s, 4H), 4.94 (s, 2H), 6.86 (s, 2H), 7.27 (S, 2H), 7.33-7.44 (m, 6H), 7.51 (d, *J*= 7.3 Hz, 2H) ppm.

^{13}C NMR ($CDCl_3$, 75.5 MHz): δ 19.3, 21.4, 23.0, 117.9, 118.2, 125.7, 128.1, 128.5, 128.8, 129.4, 129.5, 130.1, 130.9, 135.9, 136.5, 137.9, 138.4, 140.3, 141.2, 153.5 ppm.

HRMS (EI) calcd. for $C_{35}H_{32}N_5O$ [M+NH_4^+]: 538.2601, found: 538.2586.

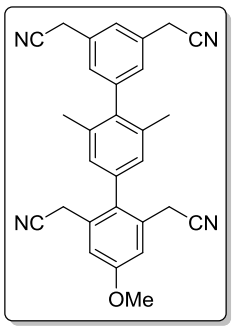

2,2',2'',2'''-(4-Methoxy-3',5'-dimethyl-[1,1':4',1''-terphenyl]-2,3'',5'',6-tetrayl)tetraacetonitrile, 4.39b

The crude mixture was purified *via* flash column chromatography using *n*-hexane:EtOAc (2:1) as the eluent, affording pure **4.39b** as a white solid (78 mg, 61%) with a melting point of 171-173 °C.

^{1}H NMR ($CDCl_3$, 300 MHz): δ 2.04 (s, 6H), 3.48 (s, 4H), 3.86 (s, 4H), 3.91 (s, 3H), 6.90 (s, 2H), 7.09 (s, 2H), 7.22 (d, *J*= 1.6 Hz, 2H), 7.31 (s, 1H) ppm.

^{13}C NMR ($CDCl_3$, 75.5 MHz): δ 19.9, 21.7, 22.5, 54.6, 112.9, 116.3, 116.7, 125.2, 127.3, 129.8, 130.6, 132.0, 135.0, 136.2, 139.1, 141.6, 158.6 ppm.

HRMS (EI) calcd. for $C_{29}H_{28}N_5O$ [M+NH_4^+]: 462.2300, found: 462.2260.

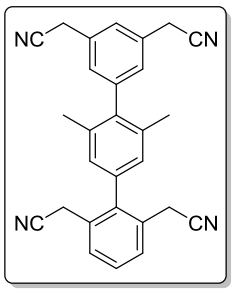

2,2',2'',2'''-(3',5'-Dimethyl-[1,1':4',1''-terphenyl]-2,3'',5'',6-tetrayl)tetraacetonitrile, 4.39c

The crude mixture was purified *via* flash column chromatography using *n*-hexane:EtOAc (2:1) as the eluent, affording pure **4.39c** as a white solid (312 mg, 65%) with a melting point of 176-178 °C.

^{1}H NMR ($CDCl_3$, 300 MHz): δ 2.05 (s, 6H), 3.51 (s, 4H), 3.86 (s, 4H), 6.93 (s, 2H), 7.22 (s, 2H), 7.32 (s, 1H), 7.46 (dd, *J*= 8.7, 6.7 Hz, 1H), 7.57 (d, *J*= 7.6 Hz, 2H) ppm.

^{13}C NMR ($CDCl_3$, 75.5 MHz): δ 20.9 (CH_3), 22.6 (CH_2), 23.5 (CH_2), 117.4 (C), 117.8 (C), 126.3 (CH), 127.7 (CH), 128.3 (CH), 128.4 (CH), 128.9 (CH), 129.6 (C), 131.7 (C), 136.1 (C), 137.3 (C), 140.2 (C), 140.8 (C), 142.5 (C) ppm.

HRMS (EI) calcd. for $C_{28}H_{23}N_4$ [M+H$^+$]: 415.1902, found: 415.1900.

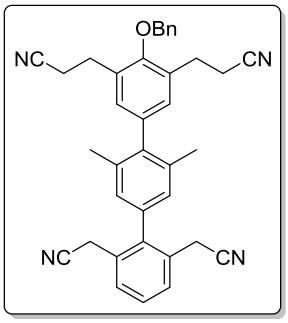

3,3'-(4-(Benzyloxy)-2'',6''-bis(cyanomethyl)-2',6'-dimethyl-[1,1':4',1''-terphenyl]-3,5-diyl)dipropanenitrile, 4.47a

The crude mixture was purified *via* flash column chromatography using *n*-hexane:EtOAc (2:1) as the eluent, affording pure **4.47a** as a white solid (75 mg, 46%) with a melting point of 110-112 °C.

^{1}H NMR ($CDCl_3$, 300 MHz): δ 2.11 (s, 6H), 2.69 (t, *J*= 7.2 Hz, 4H), 3.02 (t, *J*= 7.2 Hz, 4H), 3.51 (s, 4H), 4.98 (s, 2H), 6.90 (s, 2H), 7.07 (s, 2H), 7.39-7.49 (m, 6H), 7.57 (d, *J*= 7.7 Hz, 2H) ppm.

^{13}C NMR ($CDCl_3$, 75.5 MHz): δ 18.1 (CH_2), 21.0 (CH_3), 22.6 (CH_2), 26.6 (CH_2), 76.2 (CH_2), 117.9 (C), 119.0 (C), 127.5 (CH), 127.6 (CH), 128.4 (CH), 128.6 (CH), 128.9 (CH), 129.7 (CH), 130.1 (CH), 132.3 (C), 132.9 (C), 135.6 (C), 136.6 (C), 137.3 (C), 137.7 (C), 140.9 (C), 141.0 (C), 154.3 (C) ppm.

HRMS (EI) calcd. for $C_{37}H_{36}N_5O$ [M+NH_4^+]: 566.2914, found: 566.2908.

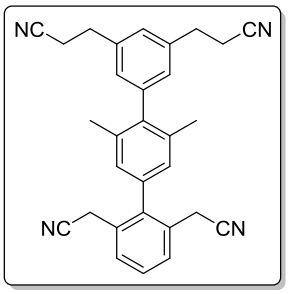

3,3'-(2'',6''-Bis(cyanomethyl)-2',6'-dimethyl-[1,1':4',1''-terphenyl]-3,5-diyl)dipropanenitrile, 4.47b

The crude mixture was purified *via* flash column chromatography using *n*-hexane:EtOAc (3:1) as the eluent, affording pure **4.47b** as a dense pale yellow oil (121 mg, 67%).

^{1}H NMR ($CDCl_3$, 300 MHz): δ 2.09 (s, 6H), 2.71 (t, *J*= 7.1 Hz, 4H), 3.04 (t, *J*= 7.1 Hz, 4H), 3.53 (s 4H), 6.92 (s, 2H), 7.06 (d, *J*= 1.5 Hz, 2H), 7.15 (s, 1H), 7.48 (dd, *J*= 8.6, 6.7 Hz, 1H), 7.59 (d, *J*= 7.6 Hz, 2H) ppm.

^{13}C NMR ($CDCl_3$, 75.5 MHz): δ 19.5, 20.9, 22.5, 31.4, 117.8, 118.9, 127.1, 127.5, 127.9, 128.4, 128.8, 129.6, 135.6, 137.5, 139.2, 141.0, 141.3, 141.6 ppm.

HRMS (EI) calcd. for $C_{30}H_{30}N_5$ [M+NH_4^+]: 460.2496, found: 460.2498.

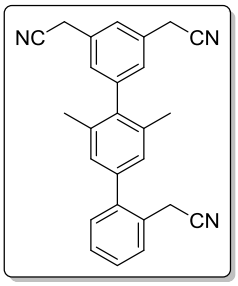

2,2',2''-(3',5'-Dimethyl-[1,1':4',1''-terphenyl]-2,3'',5''-triyl)triacetonitrile, 4.47c

The crude mixture was purified *via* flash column chromatography using *n*-hexane:EtOAc (3:1) as the eluent, affording pure **4.47c** as a white solid (127 mg, 61%) with a melting point of 139-140 °C.

^{1}H NMR ($CDCl_3$, 300 MHz): δ 2.06 (s, 6H), 3.71 (s, 2H), 3.85 (s, 4H), 7.04 (s, 2H), 7.20 (dd, *J*= 1.1, 0.6 Hz, 2H), 7.30-7.35 (m, 2H), 3.27-7.45 (m, 2H), 7.54-7.59 (m, 1H) ppm.

^{13}C NMR ($CDCl_3$, 75.5 MHz): δ 21.3 (CH_3), 22.5 (CH_2), 24.0 (CH_2), 117.8 (C), 118.8 (C), 126.5 (CH), 128.2 (C), 128.5 (CH), 128.6 (CH), 128.8 (CH), 129.3 (CH), 130.8 (CH), 131.9 (C), 136.6 (C), 139.7 (C), 139.8 (C), 142.0 (C), 143.4 (C) ppm.

HRMS (EI) calcd. for $C_{26}H_{25}N_4$ [M+NH_4^+]: 393.2074, found: 393.2072.

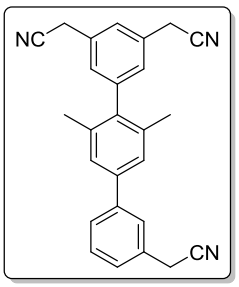

2,2',2''-(2',6'-Dimethyl-[1,1':4',1''-terphenyl]-3,3'',5-triyl)triacetonitrile, 4.47d

The crude mixture was purified *via* flash column chromatography using *n*-hexane:EtOAc (3:1) as the eluent, affording pure **4.47d** as a white solid (101 mg, 58%) with a melting point of 98-100 °C.

^{1}H NMR ($CDCl_3$, 300 MHz): δ 2.08 (s, 6H), 3.84 (s, 6H), 7.16 (d, *J*= 1.3 Hz, 2H), 7.30-7.35 (m, 4H), 7.43-7.49 (m, 1H), 7.59 (dd, *J*= 7.2, 1.0 Hz, 2H) ppm.

^{13}C NMR ($CDCl_3$, 75.5 MHz): δ 20.0 (CH_3), 22.5 (CH_2), 22.7 (CH_2), 116.3 (C), 116.8 (C), 125.0 (CH), 125.3 (CH), 125.6 (CH), 125.8 (CH), 125.9 (CH), 127.5 (CH), 128.6 (CH), 129.4 (C), 130.5 (C), 135.4 (C), 138.4 (C), 138.7 (C), 140.9 (C), 142.0 (C) ppm.

HRMS (EI) calcd. for $C_{26}H_{25}N_4$ [M+NH_4^+]: 393.2074, found: 393.2060.

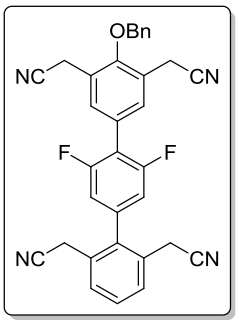

2,2',2'',2'''-(4''-(Benzyloxy)-3',5'-difluoro-[1,1':4',1''-terphenyl]-2,3'',5'',6-tetrayl)tetraacetonitrile, 4.52

The crude mixture was purified *via* flash column chromatography using *n*-hexane:EtOAc (3:1) as the eluent, affording pure **4.52** as a pale brown solid (31 mg, 38%). Unfortunately due to the small quantities obtained in this preliminary reaction and the failure of the subsequent reduction, we were unable to obtain an acceptable ^{13}C spectrum.

^{1}H NMR ($CDCl_3$, 300 MHz): δ 3.53 (s, 4H), 3.75 (s, 4H), 5.01 (s, 2H), 6.87-6.97 (m, 2H), 7.42-7.48 (m, 5H), 7.56 (d, *J*= 6.1 Hz, 1H), 7.59-7.65 (m, 4H) ppm.

^{19}F NMR ($CDCl_3$, 282.4 MHz): δ -111.17 (s, 2F) ppm.

HRMS (EI) calcd. for $C_{33}H_{26}F_2N_5O$ [M+NH_4^+]: 546.2100, found: 546.2094.

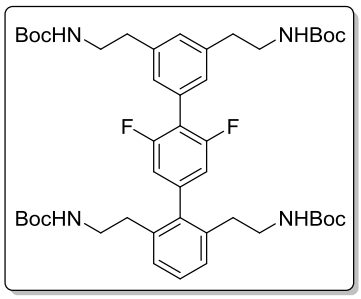

Tetra-*tert*-butyl ((3',5'-difluoro-[1,1':4',1''-terphenyl]-2,3'',5'',6-tetrayl)tetrakis(ethane-2,1-diyl))tetracarbamate, 4.56

The crude mixture was purified *via* flash column chromatography using *n*-hexane:EtOAc (5:1) as the eluent, affording pure **4.56** as a dense colourless oil (47 mg, 40%). Unfortunately due to the small quantities obtained in this preliminary reaction and the failure of the subsequent deprotection, we were unable to obtain an acceptable ^{13}C spectrum.

^{1}H NMR ($CDCl_3$, 300 MHz): δ 1.42 (s, 18H), 1.46 (s, 18H), 2.60 (t, *J*= 7.1 Hz, 4H), 2.87 (t, *J*= 7.1 Hz, 4H), 3.25 (dd, *J*= 12.4, 6.0 Hz, 4H), 3.45 (dd, *J*= 13.6, 7.8 Hz, 4H), 4.49 (br s, 2H), 4.66 (br s, 2H), 6.85 (d, *J*= 7.8 Hz, 2H), 7.11 (s, 1H), 7.18-7.28 (m, 4H), 7.30-7.41 (m, 1H) ppm.

^{19}F NMR ($CDCl_3$, 282.4 MHz): δ -113.39 (s, 2F) ppm.

HRMS (EI) calcd. for $C_{46}H_{68}F_2N_5O_8$ [M+NH_4^+]: 856.5002, found: 856.4997.

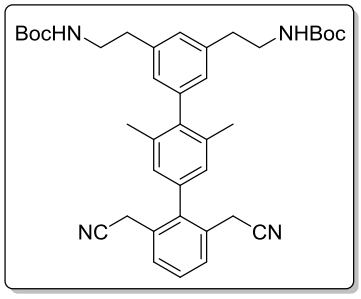

Di-*tert*-butyl ((2'',6''-bis(cyanomethyl)-2',6'-dimethyl-[1,1':4',1''-terphenyl]-3,5-diyl)bis(ethane-2,1-diyl))dicarbamate, 4.57

The crude mixture was purified *via* flash column chromatography using *n*-hexane:EtOAc (4:1) as the eluent, affording pure **4.57** as a colourless solid (154 mg, 62%) with a melting point of 145-147 °C.

^{1}H NMR ($CDCl_3$, 300 MHz): δ 1.42 (s, 18H), 2.06 (s, 6H), 2.83 (t, *J*= 7.1 Hz, 4H), 3.40 (t, *J*= 6.6 Hz, 4H), 3.50 (s, 4H), 4.59 (br s, 2H), 6.84-6.96 (m, 4H), 7.03 (s, 1H), 7.46 (dd, *J*= 8.6, 6.8 Hz, 1H), 7.57 (d, *J*= 7.6 Hz, 2H) ppm.

^{13}C NMR ($CDCl_3$, 75.5 MHz): δ 21.0, 22.5, 28.4, 29.7, 36.2, 42.0, 79.3, 117.8, 127.3, 127.5, 127.9, 128.3, 128.8, 129.7, 135.3, 137.4, 139.6, 140.6, 141.1, 142.0, 155.8 ppm.

HRMS (EI) calcd. for $C_{38}H_{47}N_4O_4$ [M+H$^+$]: 623.3592, found: 623.3588.

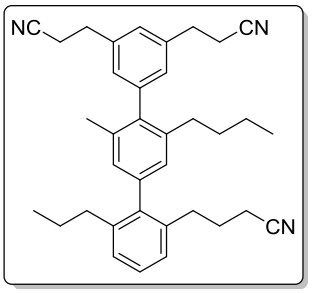

3,3'-(2'-Butyl-2''-(3-cyanopropyl)-6'-methyl-6''-propyl-[1,1':4',1''-terphenyl]-3,5-diyl)dipropanenitrile, 4.74

The crude mixture was purified *via* flash column chromatography using *n*-hexane:EtOAc (5:1) as the eluent, affording pure **4.74** as a pale brown oil (79 mg, 57%).

^{1}H NMR ($CDCl_3$, 300 MHz): δ 0.75 (t, *J*= 7.3 Hz, 3H), 0.83 (t, *J*= 7.3 Hz, 3H), 0.75 (t, *J*= 7.3 Hz, 2H), 1.15-1.20 (m, 2H), 1.31-1.43 (m, 2H), 1.44-1.54 (m, 2H), 1.70-1.83 (m, 2H), 2.03 (s, 3H), 2.21 (t, *J*= 7.1 Hz, 2H), 2.31-2.41 (m, 4H), 2.51-2.59 (m, 2H), 2.68 (t, *J*= 7.5 Hz, 4H), 3.02 (t, *J*= 7.4 Hz, 4H), 6.87 (d, *J*= 5.2 Hz, 2H), 7.06 (d, *J*= 1.6 Hz, 2H), 7.08-7.13 (m, 2H), 7.17 (dd, *J*= 7.6, 1.3 Hz, 1H), 7.22-7.28 (m, 1H) ppm.

^{13}C NMR ($CDCl_3$, 75.5 MHz): δ 13.9 (CH_3), 14.1 (CH_3), 16.8 (CH_2), 19.4 (CH_2), 19.5 (CH_2), 21.1 (CH_3), 22.3 (CH_2), 24.5 (CH_2), 26.8 (CH_2), 31.4 (CH_2), 31.5 (CH_2), 32.7 (CH_2), 33.1 (CH_2), 33.4 (CH_2), 35.7 (CH_2), 118.9 (C), 119.0 (C), 119.5 (C), 126.4 (CH), 126.7 (CH), 127.2 (CH), 127.3 (CH), 127.6 (CH), 128.2 (CH), 128.4 (CH), 128.6 (CH), 129.0 (CH), 135.7 (C), 138.0 (C), 138.6 (C), 138.7 (C), 139.2 (C), 140.3 (C), 141.3 (C), 141.5 (C), 142.2 (C) ppm.

HRMS (EI) calcd. for $C_{36}H_{45}N_4$ [M+NH_4^+]: 533.3639, found: 533.3622.

4.9.3.2. Synthesis of **Ter.1-14** and **Ter.25**.

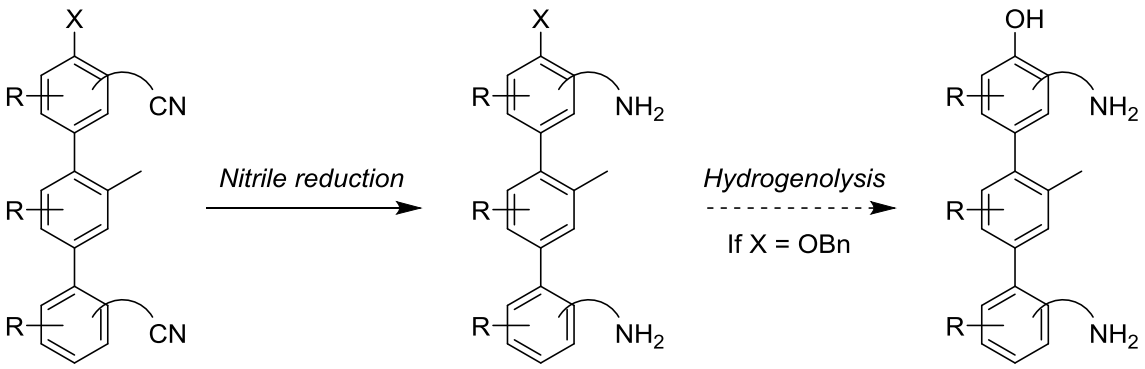

Nitrile reduction. The corresponding nitrile-bearing terphenyl (1 equiv) was placed in a sealable reaction vessel and dissolved in anhydrous THF (0.1 M). To this solution, BH_3·THF (1 M in THF) (5 equivalents for each nitrile group) was added and the reaction vessel was sealed and allowed to stir at 80 °C for 5 days. Subsequently, the reaction mixture was cooled to room temperature and aqueous HCl (3 M, 6 equivalents for each nitrile) was added carefully and the reaction was stirred for a further 2 hours open to air. Following this, the mixture was transferred to a round-bottomed flask washing with methanol and concentrated to dryness. The crude mixture was purified *via* flash column chromatography using mixtures of DCM and ammonia solution (7N in methanol) as eluents. The product was immediately dissolved in methanol (0.05 M) and treated with HCl (2N in Et_2O) to form the corresponding hydrochloride salt, and the solvent evaporated. The resulting residue was dissolved in the minimum amount of methanol and precipitated by adding diethyl ether. The supernatant was then decanted off to leave the pure products. In some cases the free amine was treated instead with methanesulfonic acid (1 equivalent for each amine) or *p*-toluenesulfonic acid to form the corresponding mesylate or tosylate salts.

O-Benzyl hydrogenolysis. The amine hydrochloride salt (1 equiv) was dissolved in anhydrous methanol (0.05 M) and palladium over charcoal (10-20% w/w) (10 mol%) was added. The reaction flask was purged 5 times with hydrogen gas from a gas bag and subsequently stirred vigorously for 18 hours. Following this, the reaction was filtered through a standard HPLC filter and concentrated to dryness, washing with extra methanol. No further purification was necessary.

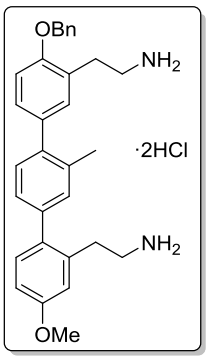

2,2'-(4''-(Benzyloxy)-4-methoxy-3'-methyl-[1,1':4',1''-terphenyl]-2,3''-diyl)bis(ethan-1-amine) hydrochloride salt, Ter.1

4.23a was subject to the previously described procedure for nitrile reduction. The crude mixture was purified *via* flash column chromatography using mixtures of DCM and ammonia solution (7 N in MeOH) (10:1) as the eluent, affording pure **Ter.1** as a pale brown solid (23 mg, 48%) with a melting point of 255-257 °C.

^{1}H NMR (CD_3OD, 300 MHz): δ 2.29 (s, 3H), 2.67-2.74 (m, 2H), 2.75-2.83 (m, 2H), 2.90 (h, *J*= 7.1 Hz, 4H), 3.82 (s, 3H), 6.80-6.89 (m, 2H), 7.09-7.22 (m, 7H), 7.32-7.43 (m, 3H), 7.49 (d, *J*= 7.3 Hz, 2H) ppm.

^{13}C NMR (CD_3OD, 75.5 MHz): δ 21.3 (CH_3), 35.5 (CH_2), 38.2 (CH_2), 43.2 (CH_2), 44.2 (CH_2), 56.1 (CH_3), 71.6 (CH_2), 113.0 (CH), 113.3 (CH), 116.6 (CH), 128.4 (CH), 128.9 (CH), 129.3 (CH), 129.4 (C), 129.9 (CH), 130.0 (CH), 131.1 (CH), 132.7 (CH), 132.9 (CH), 133.0 (CH), 136.0 (C), 136.4 (C), 136.7 (C), 139.3 (C), 139.9 (C), 141.8 (C), 142.1 (C), 157.6 (C), 160.9 (C) ppm.

HRMS (EI) calcd. for $C_{31}H_{35}N_2O_2$ [M+H$^+$]: 467.2693, found: 467.2671.

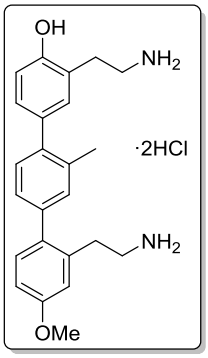

2'',3-Bis(2-aminoethyl)-4''-methoxy-2'-methyl-[1,1':4',1''-terphenyl]-4-ol hydrochloride salt, Ter.2

Ter.1 was subject to the previously described procedure for *O*-benzyl hydrogenolysis, affording pure **Ter.2** as a hygroscopic, dense brown oil (11 mg, 89%).

^{1}H NMR (CD_3OD, 300 MHz): δ 2.30 (s, 3H), 2.93-3.08 (m, 6H), 3.22 (t, *J*= 7.1 Hz, 2H), 3.84 (s, 3H), 6.90 (d, *J*= 8.3 Hz, 3H), 7.06-7.20 (m, 5H), 7.24 (d, *J*= 7.7 Hz, 1H) ppm.

^{13}C NMR (CD_3OD, 75.5 MHz): δ 21.3 (CH_3), 30.5 (CH_2), 32.8 (CH_2), 41.3 (CH_2), 41.7 (CH_2), 56.2 (CH_3), 113.9 (CH), 116.3 (CH), 116.6 (CH), 124.5 (C), 128.3 (CH), 130.8 (CH), 131.4 (CH), 132.7 (CH), 133.0 (CH), 133.2 (CH), 134.5 (C), 136.4 (C), 136.7 (C), 137.1 (C), 141.3 (C), 142.2 (C), 156.4 (C), 161.2 (C) ppm.

HRMS (EI) calcd. for $C_{24}H_{29}N_2O_2$ [M+H$^+$]: 377.2224, found: 377.2207.

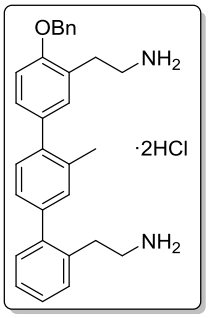

2,2'-(4''-(Benzyloxy)-3'-methyl-[1,1':4',1''-terphenyl]-2,3''-diyl)bis(ethan-1-amine) hydrochloride salt, Ter.3

4.23b was subject to the previously described procedure for nitrile reduction. The crude mixture was purified *via* flash column chromatography using mixtures of DCM and ammonia solution (7N in MeOH) (10:1) as the eluent, affording pure **Ter.3** as a pale brown solid (22 mg, 41%) with a melting point of 248-249 °C.

^{1}H NMR (CD_3OD, 300 MHz): δ 2.34 (s, 3H), 2.96-3.13 (m, 6H), 3.17-3.25 (m, 2H), 5.22 (s, 2H), 7.17-7.45 (m, 13H), 7.52 (d, *J*= 7.1 Hz, 2H) ppm.

^{13}C NMR (CD_3OD, 75.5 MHz): δ 21.3 (CH_3), 30.6 (CH_2), 32.6 (CH_2), 41.1 (CH_2), 41.8 (CH_2), 71.8 (CH_2), 113.6 (CH), 126.5 (C), 128.1 (CH), 128.7 (CH), 129.3 (CH), 129.5 (CH), 129.6 (CH), 130.2 (CH), 131.0 (CH), 131.1 (CH), 131.5 (CH), 132.0 (CH), 132.5 (CH), 133.1 (CH), 135.6 (C), 136.1 (C), 137.2 (C), 138.9 (C), 141.8 (C), 142.1 (C), 144.0 (C), 157.7 (C) ppm.

HRMS (EI) calcd. for $C_{30}H_{33}N_2O$ [M+H$^+$]: 437.2587, found: 437.2585.

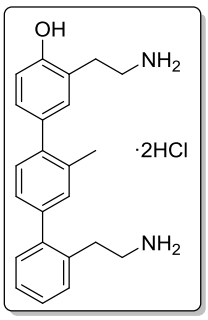

2'',3-Bis(2-aminoethyl)-2'-methyl-[1,1':4',1''-terphenyl]-4-ol hydrochloride salt, Ter.4

Ter.3 was subject to the previously described procedure for *O*-benzyl hydrogenolysis, affording pure **Ter.4** as a pale yellow solid (10 mg, 96%) with a melting point of 218-220 °C.

^{1}H NMR (CD_3OD, 300 MHz): δ 2.34 (s, 3H), 2.96-3.10 (m, 6H), 3.25 (t, *J*= 7.4 Hz, 2H), 6.94 (d, *J*= 8.2 Hz, 1H), 7.12-7.41 (m, 9H) ppm.

^{13}C NMR (CD_3OD, 75.5 MHz): δ 19.5, 28.7, 30.8, 39.5, 40.0, 114.5, 122.8, 126.2, 126.9, 127.6, 129.0, 129.2, 129.6, 130.2, 130.6, 131.2, 133.0, 133.7, 135.4, 139.7, 140.7, 142.2, 154.6 ppm.

HRMS (EI) calcd. for $C_{23}H_{27}N_2O$ [M+H$^+$]: 347.2118, found: 347.2122.

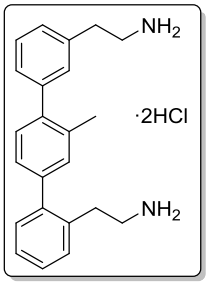

2,2'-(3'-Methyl-[1,1':4',1''-terphenyl]-2,3''-diyl)bis(ethan-1-amine) hydrochloride salt, Ter.5

4.23c was subject to the previously described procedure for nitrile reduction. The crude mixture was purified *via* flash column chromatography using mixtures of DCM and ammonia solution (7N in MeOH) (10:1) as the eluent, affording pure **Ter.5** as a pale yellow solid (18 mg, 54%) with a melting point of 171-175 °C.

^{1}H NMR (CD_3OD, 300 MHz): δ 2.31 (s, 3H), 2.91-3.11 (m, 6H), 3.20-3.26 (m, 2H), 7.20-7.49 (m, 11H) ppm.

^{13}C NMR (CD_3OD, 75.5 MHz): δ 21.1 (CH_3), 32.6 (CH_2), 35.0 (CH_2), 41.8 (CH_2), 42.4 (CH_2), 128.1 (CH), 128.8 (CH), 128.9 (CH), 129.5 (C), 129.6 (CH), 130.4 (CH), 131.1 (CH), 131.3 (CH), 132.0 (CH), 132.5 (CH), 135.5 (C), 137.1 (C), 138.5 (C), 142.1 (C), 142.4 (C), 143.9 (C), 144.0 (C) ppm.

HRMS (EI) calcd. for $C_{23}H_{27}N_2$ [M+H$^+$]: 331.2169, found: 331.2157.

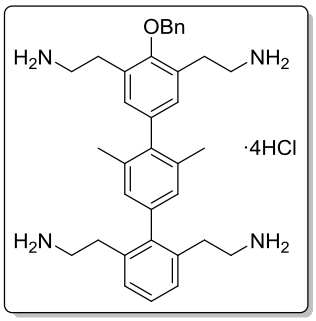

2,2',2'',2'''-(4''-(Benzyloxy)-3',5'-dimethyl-[1,1':4',1''-terphenyl]-2,3'',5'',6-tetrayl)tetrakis(ethan-1-amine) hydrochloride salt, Ter.6

4.39a was subject to the previously described procedure for nitrile reduction. The crude mixture was purified *via* flash column chromatography using mixtures of DCM and ammonia solution (7N in MeOH) (10:1) as the eluent, affording pure **Ter.6** as a white solid (17 mg, 34%) with a melting point of >300 °C.

^{1}H NMR (CD_3OD, 400 MHz): δ 2.08 (s, 6H), 2.61-2.68 (m, 8H), 2.68-2.76 (m, 4H), 2.76-2.80 (m, 4H), 4.96 (s, 2H), 6.93 (d, *J*= 10.3 Hz, 4H), 7.15-7.20 (m, 2H), 7.26 (dd, *J*= 8.5, 6.5 Hz, 1H), 7.34-7.47 (m, 3H), 7.52-7.56 (m, 2H) ppm.

^{13}C NMR (CD_3OD, 101 MHz): δ 20.1, 28.3, 32.3, 39.7, 40.1, 75.9, 127.9, 128.1, 128.1, 128.3, 130.6, 131.0, 135.4, 136.8, 136.9, 137.5, 137.6, 140.2, 142.1, 154.5 ppm.

HRMS (EI) calcd. for $C_{35}H_{45}N_4O$ [M+H$^+$]: 537.3588, found: 537.3585.

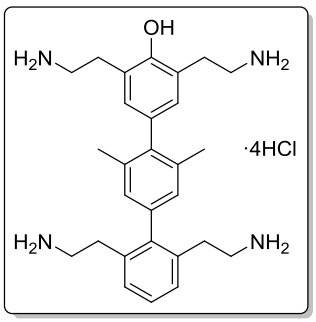

2'',3,5,6''-Tetrakis(2-aminoethyl)-2',6'-dimethyl-[1,1':4',1''-terphenyl]-4-ol hydrochloride salt, Ter.7

Ter.6 was subject to the previously described procedure for *O*-benzyl hydrogenolysis, affording pure **Ter.7** as a pale yellow solid (9 mg, 92%) with a melting point of >300 °C.

^{1}H NMR (CD_3OD, 300 MHz): δ 2.12 (s, 6H), 2.77-2.87 (m, 4H), 2.94-3.03 (m, 4H), 3.06-3.16 (m, 4H), 3.18-3.28 (m, 4H), 6.94-7.03 (m, 4H), 7.30-7.40 (m, 3H) ppm.

^{13}C NMR (CD_3OD, 75.5 MHz): δ 21.9 (CH_3), 30.4 (CH_2), 33.2 (CH_2), 41.3 (CH_2), 41.9 (CH_2), 127.1 (C), 129.7 (CH), 129.9 (CH), 130.0 (CH), 132.2 (CH), 135.1 (C), 137.2 (C), 138.8 (C), 139.0 (C), 142.4 (C), 144.0 (C), 153.8 (C) ppm.

HRMS (EI) calcd. for $C_{28}H_{39}N_4O$ [$M+H^+$]: 447.3118, found: 447.3104.

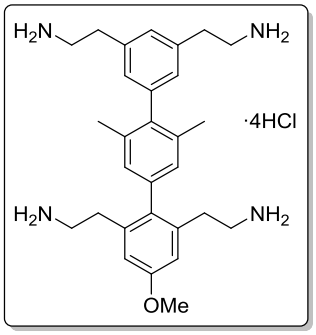

2,2',2'',2'''-(4-Methoxy-3',5'-dimethyl-[1,1':4',1''-terphenyl]-2,3'',5'',6-tetrayl)tetrakis(ethan-1-amine) hydrochloride salt, Ter.8

4.39b was subject to the previously described procedure for nitrile reduction. The crude mixture was purified *via* flash column chromatography using mixtures of DCM and ammonia solution (7N in MeOH) (8:1) as the eluent, affording pure **Ter.8** as a white solid (21 mg, 52%) with a melting point of >300 °C.

^{1}H NMR (CD_3OD, 300 MHz): δ 2.09 (s, 6H), 2.75-2.83 (m, 4H), 2.91-3.01 (m, 4H), 3.02-3.11 (m, 4H), 3.20-3.29 (m, 4H), 3.87 (s, 3H), 6.91 (s, 2H), 6.99 (s, 2H), 7.09 (s, 2H), 7.30 (s, 1H) ppm.

^{13}C NMR (CD_3OD, 75.5 MHz): δ 21.7 (CH_3), 33.4 (CH_2), 34.9 (CH_2), 41.8 (CH_2), 42.4 (CH_2), 56.3 (CH_3), 115.3 (CH), 129.3 (CH), 130.0 (CH), 130.4 (CH), 138.3 (C), 138.4 (C), 139.3 (C), 139.7 (C), 142.3 (C), 143.7 (C), 161.2 (C) ppm.

HRMS (EI) calcd. for $NaC_{29}H_{40}N_4O$ [M+Na^+]: 483.3094, found: 483.3090.

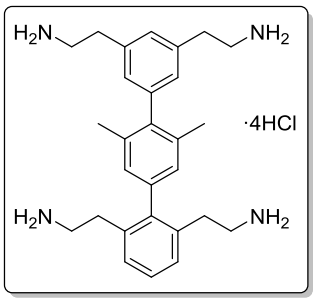

2,2',2'',2'''-(3',5'-Dimethyl-[1,1':4',1''-terphenyl]-2,3'',5'',6-tetrayl)tetrakis(ethan-1-amine) hydrochloride salt, Ter.9·Cl

4.39c was subject to the previously described procedure for nitrile reduction. The crude mixture was purified *via* flash column chromatography using mixtures of DCM and ammonia solution (7N in MeOH) (8:1) as the eluent, affording pure **Ter.9·Cl** as a white solid (153 mg, 51%) with a melting point of >300 °C.

^{1}H NMR (CD_3OD, 300 MHz): δ 2.10 (s, 6H), 2.78-2.87 (m, 4H), 2.93-3.03 (m, 4H), 3.03-3.12 (m, 4H), 3.21-3.30 (m, 4H), 7.01 (s, 2H), 7.11 (s, 2H), 7.28-7.43 (m, 4H) ppm.

^{13}C NMR (CD_3OD, 75.5 MHz): δ 21.7 (CH_3), 33.2 (CH_2), 34.9 (CH_2), 41.9 (CH_2), 42.4 (CH_2), 129.3 (CH), 129.8 (CH), 129.9 (CH), 130.0 (CH), 130.1 (CH), 137.1 (C), 138.4 (C), 139.4 (C), 139.7 (C), 142.4 (C), 143.6 (C), 143.9 (C) ppm.

MALDI (TOF) calcd. for $C_{28}H_{39}N_4$ [M+H^+]: 431.32, found 431.32. This sample failed to give the desired mass in HRMS electrospray ionisation sampling, although the major peak observed using MALDI coincided with the expected [M+H^+] value.

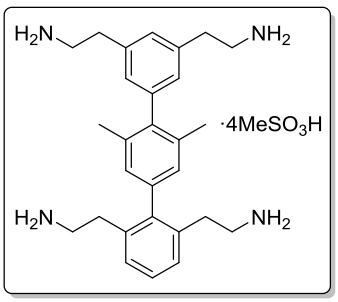

2,2',2'',2'''-(3',5'-Dimethyl-[1,1':4',1''-terphenyl]-2,3'',5'',6-tetrayl)tetrakis(ethan-1-amine) mesylate salt, Ter.9·Mes

Melting point = >300 °C

^{1}H NMR (CD_3OD, 300 MHz): δ 2.10 (s, 6H), 2.70 (s, 12H), 2.81 (dd, *J*= 10.0, 5.9 Hz, 4H), 2.99 (dd, *J*= 10.0, 6.2 Hz, 4H), 3.06 (dd, *J*= 9.7, 6.4 Hz, 4H), 3.25 (dd, *J*= 9.6, 6.5 Hz, 4H), 7.01 (s, 2H), 7.08 (d, *J*= 1.6 Hz, 2H), 7.28-7.44 (m, 4H) ppm.

^{13}C NMR (CD_3OD, 75.5 MHz): δ 21.6 (CH_3), 33.2 (CH_2), 34.9 (CH_2), 40.0 (CH_3), 41.8 (CH_2), 42.4 (CH_2), 129.3 (CH), 129.7 (CH), 129.8 (CH), 129.9 (CH), 130.0 (CH), 137.1 (C), 138.4 (C), 139.4 (C), 139.8 (C), 142.4 (C), 143.6 (C), 143.9 (C) ppm.

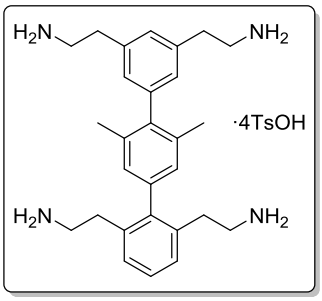

2,2',2'',2'''-(3',5'-Dimethyl-[1,1':4',1''-terphenyl]-2,3'',5'',6-tetrayl)tetrakis(ethan-1-amine) tosylate salt, Ter.9·Tos

Melting point = >300 °C

^{1}H NMR (CD_3OD, 300 MHz): δ 2.08 (s, 6H), 2.36 (s, 12H), 2.79 (dd, *J*= 9.9, 5.7 Hz, 4H), 2.97 (dd, *J*= 10.0, 6.2 Hz, 4H), 3.05 (dd, *J*= 9.6, 6.4 Hz, 4H), 3.23 (dd, *J*= 9.6, 6.3 Hz, 4H), 6.99 (s, 2H), 7.08 (d, *J*= 7.9 Hz, 2H), 7.22 (d, *J*= 7.9 Hz, 8H), 7.28-7.41 (m, 4H), 7.69 (d, *J*= 8.2 Hz, 8H) ppm.

^{13}C NMR (CD_3OD, 75.5 MHz): δ 21.6 (CH_3), 21.7 (CH_3), 33.2 (CH_2), 34.9 (CH_2), 41.9 (CH_2), 42.4 (CH_2), 127.3 (CH), 129.3 (CH), 129.7 (CH), 129.8 (CH), 129.9 (CH), 130.0 (CH), 130.3 (CH), 137.1 (C), 138.4 (C), 139.4 (C), 139.7 (C), 142.2 (C), 142.5 (C), 143.6 (c), 143.9 (C) ppm.

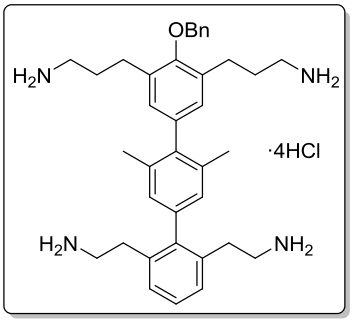

3,3'-(2'',6''-Bis(2-aminoethyl)-4-(benzyloxy)-2',6'-dimethyl-[1,1':4',1''-terphenyl]-3,5-diyl)bis(propan-1-amine) hydrochloride salt, Ter.10

4.47a was subject to the previously described procedure for nitrile reduction. The crude mixture was purified *via* flash column chromatography using mixtures of DCM and ammonia solution (7N in MeOH) (8:1) as the eluent, affording pure **Ter.10** as a white solid (31 mg, 37%) with a melting point of 251-252 °C.

^{1}H NMR (CD_3OD, 300 MHz): δ 1.78-1.89 (m, 4H), 2.07 (s, 6H), 2.52-2.67 (m, 8H), 2.68-2.73 (m, 4H), 2.74-2.83 (m, 4H), 4.95 (s, 2H), 6.91 (d, *J*= 10.3 Hz, 4H), 7.18 (d, *J*= 7.2 Hz, 2H), 7.25 (d, *J*= 6.5 Hz, 1H), 7.30-7.45 (m, 3H), 7.52 (d, *J*= 7.0 Hz, 2H) ppm.

^{13}C NMR (CD_3OD, 75.5 MHz): δ 21.2, 28.5, 35.0, 38.2, 42.1, 44.0, 77.0, 128.4, 128.5, 128.9, 129.1, 129.6, 129.7, 130.1, 136.7, 137.0, 137.1, 138.3, 139.1, 140.0, 141.8, 143.3, 155.5 ppm.

HRMS (EI) calcd. for $C_{37}H_{50}N_4O$ [M+2H$^+$]: 283.1987, found: 283.1984.

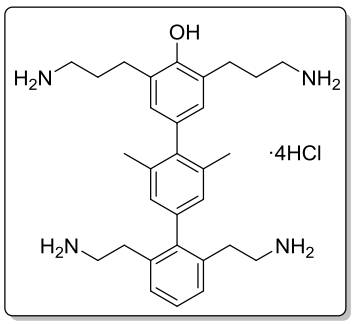

2'',6''-Bis(2-aminoethyl)-3,5-bis(3-aminopropyl)-2',6'-dimethyl-[1,1':4',1''-terphenyl]-4-ol hydrochloride salt, Ter.11

Ter.10 was subject to the previously described procedure for *O*-benzyl hydrogenolysis, affording pure **Ter.11** as a hygroscopic, dense pale yellow oil (14 mg, 90%).

^{1}H NMR (CD_3OD, 300 MHz): δ 1.97-2.08 (m, 4H), 2.11 (s, 6H), 2.77-2.87 (m, 8H), 2.93-3.04 (m, 8H), 6.87 (s, 2H), 6.98 (s, 2H), 7.29-7.44 (m, 3H) ppm.

^{13}C NMR (CD_3OD, 75.5 MHz): δ 21.8 (CH_3), 28.9 (CH_2), 29.5 (CH_2), 33.2 (CH_2), 41.0 (CH_2), 41.9 (CH_2), 129.6 (CH), 129.9 (CH), 130.7 (CH), 134.2 (C), 137.1 (C), 138.7 (C), 138.9 (C), 143.0 (C), 144.0 (C), 153.1 (C) ppm.

HRMS (EI) calcd. for $C_{30}H_{43}N_4O$ [M+H$^+$]: 475.3431, found: 475.4319.

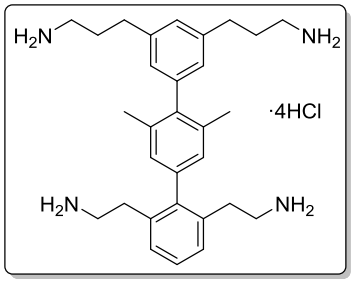

3,3'-(2'',6''-Bis(2-aminoethyl)-2',6'-dimethyl-[1,1':4',1''-terphenyl]-3,5-diyl)bis(propan-1-amine) hydrochloride salt, Ter.12

4.47b was subject to the previously described procedure for nitrile reduction. The crude mixture was purified *via* flash column chromatography using mixtures of DCM and ammonia solution (7N in MeOH) (8:1) as the eluent, affording pure **Ter.12** as a pale yellow solid (41 mg, 57%) with a melting point of 221-222 °C.

^{1}H NMR (CD_3OD, 300 MHz): δ 2.00-2.12 (m, 10H), 2.75-2.88 (m, 8H), 2.95-3.04 (m, 8H), 6.95-7.02 (m, 4H), 7.20 (s, 1H), 7.31-7.43 (m, 3H) ppm.

^{13}C NMR (CD_3OD, 75.5 MHz): δ 19.8 (CH_3), 29.0 (CH_2), 31.4 (CH_2), 32.1 (CH_2), 39.0 (CH_2), 40.1 (CH_2), 126.8 (CH), 126.9 (CH), 127.9 (CH), 128.0 (CH), 128.1 (CH), 135.3 (C), 136.5 (C), 137.4 (C), 141.1 (C), 141.2 (C), 141.3 (C), 142.1 (C) ppm.

HRMS (EI) calcd. for $C_{30}H_{42}N_4$ [M+H$^+$]: 459.3482, found: 459.3479.

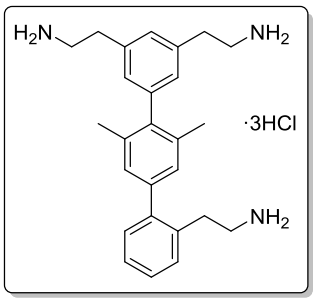

2,2',2''-(3',5'-Dimethyl-[1,1':4',1''-terphenyl]-2,3'',5''-triyl)tris(ethan-1-amine) hydrochloride salt, Ter.13·Cl

4.47c was subject to the previously described procedure for nitrile reduction. The crude mixture was purified *via* flash column chromatography using mixtures of DCM and ammonia solution (7N in MeOH) (8:1) as the eluent, affording pure **Ter.13** as a dense colourless oil (24 mg, 43%).

^{1}H NMR (CD_3OD, 300 MHz): δ 2.08 (s, 6H), 2.97-3.10 (m, 8H), 3.25 (dd, *J*= 9.4, 6.2 Hz, 4H), 7.03-7.09 (m, 4H), 7.23 (dd, *J*= 5.9, 2.3 Hz, 1H), 7.29-7.40 (m, 4H) ppm.

^{13}C NMR (CD_3OD, 75.5 MHz): δ 21.6 (CH_3), 32.6 (CH_2), 34.9 (CH_2), 41.8 (CH_2), 42.3 (CH_2), 128.7 (CH), 129.2 (CH), 129.4 (CH), 129.6 (CH), 130.0 (CH), 131.0 (CH), 132.0 (CH), 135.5 (C), 137.7 (C), 139.7 (C), 141.9 (C), 142.0 (C), 143.9 (C), 144.1 (C) ppm.

HRMS (EI) calcd. for $C_{26}H_{33}N_3$ [M+H$^+$]: 388.2747, found: 388.2737.

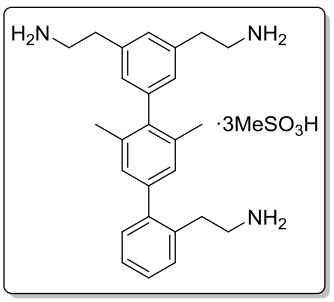

2,2',2''-(3',5'-Dimethyl-[1,1':4',1''-terphenyl]-2,3'',5''-triyl)tris(ethan-1-amine) mesylate salt, Ter.13·Mes

^{1}H NMR (CD_3OD, 300 MHz): δ 2.08 (s, 6H), 2.70 (s, 9H), 2.98-3.09 (m, 8H), 3.18-3.29 (m, 4H), 7.03-7.09 (m, 4H), 7.23 (dd, *J*= 6.0, 2.2 Hz, 1H), 7.29-7.40 (m, 4H) ppm.

^{13}C NMR (CD_3OD, 75.5 MHz): δ 21.6 (CH_3), 32.6 (CH_2), 34.9 (CH_2), 40.0 (CH_3), 41.8 (CH_2), 42.3 (CH_2), 128.7 (CH), 129.2 (CH), 129.4 (CH), 129.6 (CH), 130.0 (CH), 131.0 (CH), 132.0 (CH), 135.5 (C), 137.7 (C), 139.7 (C), 141.9 (C), 142.0 (C), 143.8 (C), 144.1 (C) ppm.

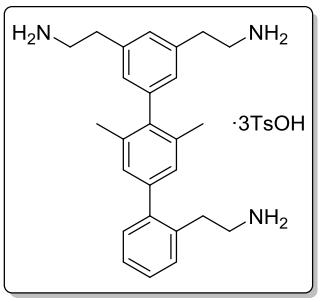

2,2',2''-(3',5'-Dimethyl-[1,1':4',1''-terphenyl]-2,3'',5''-triyl)tris(ethan-1-amine) tosylate salt, Ter.13·Tos

^{1}H NMR (CD_3OD, 300 MHz): δ 2.07 (s, 6H), 2.35 (s, 9H), 3.02 (dd, *J*= 10.1, 6.4 Hz, 8H), 3.17-3.27 (m, 4H), 7.00 (d, *J*= 1.4 Hz, 2H), 7.18-7.37 (m, 11H), 7.64-7.73 (m, 6H) ppm.

^{13}C NMR (CD_3OD, 75.5 MHz): δ 21.6 (CH_3), 21.7 (CH_3), 32.6 (CH_2), 34.9 (CH_2), 41.8 (CH_2), 42.4 (CH_2), 127.4 (CH), 128.7 (CH), 129.2 (CH), 129.4 (CH), 129.6 (CH), 130.0 (CH), 130.3 (CH), 131.1 (CH), 132.0 (CH), 135.6 (C), 137.7 (C), 139.7 (C), 141.9 (C), 142.0 (C), 142.3 (C), 143.8 (C), 143.9 (C), 144.1 (C) ppm.

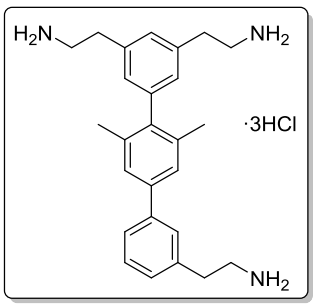

2,2',2''-(2',6'-Dimethyl-[1,1':4',1''-terphenyl]-3,3'',5-triyl)tris(ethan-1-amine) hydrochloride salt, Ter.14·Cl

4.47d was subject to the previously described procedure for nitrile reduction. The crude mixture was purified *via* flash column chromatography using mixtures of DCM and ammonia solution (7N in MeOH) (8:1) as the eluent, affording pure **Ter.14** as a dense colourless oil (27 mg, 48%).

^{1}H NMR (CD_3OD, 300 MHz): δ 2.10 (s, 6H), 3.04 (dd, *J*= 9.4, 6.5 Hz, 6H), 3.24 (dd, *J*= 10.1, 5.6 Hz, 6H), 7.04 (d, *J*= 1.3 Hz, 2H), 7.28 (d, *J*= 6.2 Hz, 2H), 7.39 (s, 2H), 7.44 (t, *J*= 7.4 Hz, 1H), 7.56 (d, *J*= 7.2 Hz, 2H) ppm.

^{13}C NMR (CD_3OD, 75.5 MHz): δ 21.6 (CH_3), 34.9 (CH_2), 35.1 (CH_2), 42.3 (CH_2), 42.4 (CH_2), 127.3 (CH), 127.5 (CH), 128.8 (CH), 129.0 (CH), 129.1 (CH), 130.0 (CH), 130.9 (CH), 137.9 (C), 138.6 (C), 138.9 (C), 139.6 (C), 141.4 (C), 143.5 (C), 144.0 (C) ppm.

LRMS (EI) calcd. for $C_{26}H_{34}N_3$ [M+H$^+$]: 388.2, found: 388.2. This sample failed to give the desired mass in HRMS electrospray ionisation sampling, although the major peak observed using LRMS coincided with the expected [M+H$^+$] value.

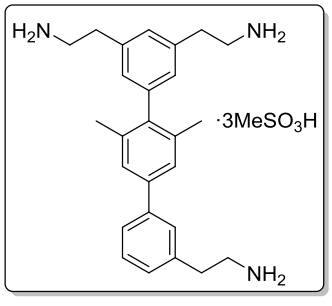

2,2',2''-(2',6'-Dimethyl-[1,1':4',1''-terphenyl]-3,3'',5-triyl)tris(ethan-1-amine) mesylate salt, Ter.14·Mes

^{1}H NMR (CD_3OD, 300 MHz): δ 2.10 (s, 6H), 2.71 (s, 9H), 3.04 (dd, *J*= 9.6, 6.3 Hz, 6H), 3.19-3.27 (m, 6H), 7.03 (d, *J*= 1.4 Hz, 2H), 7.27 (d, *J*= 5.7 Hz, 2H), 7.39 (s, 2H), 7.44 (t, *J*= 8.0 Hz, 1H), 7.56 (d, *J*= 6.8 Hz, 2H) ppm.

^{13}C NMR (CD_3OD, 75.5 MHz): δ 21.6 (CH_3), 34.9 (CH_2), 35.1 (CH_2), 39.9 (CH_3), 42.3 (CH_2), 42.4 (CH_2), 127.3 (CH), 127.5 (CH), 128.8 (CH), 129.0 (CH), 129.1 (CH), 130.0 (CH), 130.9 (CH), 137.9 (C), 138.6 (C), 138.9 (C), 139.6 (C), 141.4 (C), 143.5 (C), 144.0 (C) ppm.

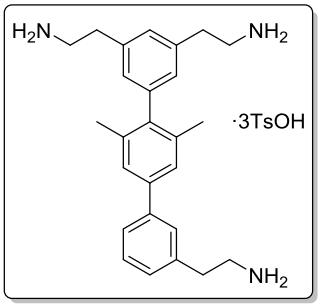

2,2',2''-(2',6'-Dimethyl-[1,1':4',1''-terphenyl]-3,3'',5-triyl)tris(ethan-1-amine) tosylate salt, Ter.14·Tos

^{1}H NMR (CD_3OD, 300 MHz): δ 2.08 (s, 6H), 2.35 (s, 9H), 3.03 (dt, *J*= 11.8, 5.8 Hz, 6H), 3.17-3.27 (m, 6H), 6.99 (s, 2H), 7.21 (d, *J*= 7.9 Hz, 6H), 7.26 (d, *J*= 6.8 Hz, 2H), 7.39 (s, 2H), 7.44 (t, *J*= 7.9 Hz, 1H), 7.56 (d, *J*= 1.8 Hz, 2H), 7.70 (d, *J*= 8.2 Hz, 6H) ppm.

^{13}C NMR (CD_3OD, 75.5 MHz): δ 21.6 (CH_3), 21.7 (CH_3), 34.9 (CH_2), 35.1 (CH_2), 42.3 (CH_2), 42.4 (CH_2), 127.3 (CH), 127.4 (CH), 127.5 (CH), 128.8 (CH), 129.1 (CH), 130.0 (CH), 130.3 (CH), 130.9 (CH), 137.9 (C), 138.9 (C), 139.6 (C), 141.4 (C), 142.2 (C), 143.4 (C), 143.8 (C), 143.9 (C) ppm.

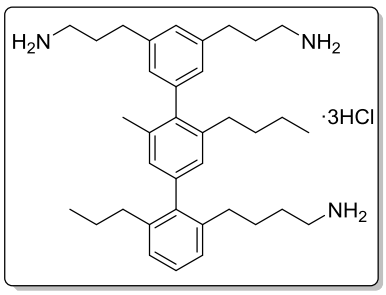

3,3'-(2''-(4-Aminobutyl)-2'-butyl-6'-methyl-6''-propyl-[1,1':4',1''-terphenyl]-3,5-diyl)bis(propan-1-amine) hydrochloride salt, Ter.25

4.74 was subject to the previously described procedure for nitrile reduction. The crude mixture was purified *via* flash column chromatography using mixtures of DCM and ammonia solution (7N in MeOH) (10:1) as the eluent, affording pure **Ter.25** as a dense pale brown oil (13 mg, 32%).

^{1}H NMR (CD_3OD, 300 MHz): δ 0.76 (t, *J*= 7.4 Hz, 3H), 0.80 (td, *J*= 7.4, 4.2 Hz, 3H), 1.11-1.20 (m, 2H), 1.27-1.52 (m, 9H), 1.67-1.76 (m, 1H), 1.89-1.98 (m, 3H), 2.04 (d, *J*= 5.5 Hz, 3H), 2.27-2.43 (m, 6H), 2.54 (td, *J*= 7.5, 4.3 Hz, 1H), 2.66-2.70 (m, 1H), 2.72-2.87 (m, 6H), 2.99 (td, *J*= 7.0, 2.1 Hz, 1H), 6.88 (s, 2H), 6.95 (d, *J*= 1.3 Hz, 1H), 6.97-7.04 (m, 1H), 7.09-7.25 (m, 4H) ppm.

^{13}C NMR (CD_3OD, 75.5 MHz): δ 16.7, 17.0, 19.6, 23.8, 25.9, 27.6, 28.3, 30.7, 31.9, 35.6, 36.3, 36.8, 37.4, 39.4, 43.8, 123.3, 130.0, 130.2, 130.3, 130.5, 130.7, 130.9, 131.2, 131.6, 131.8, 132.0, 132.1, 132.3, 139.4, 139.6, 142.2, 142.5, 143.0, 143.6, 144.1, 144.4, 144.6, 144.9, 145.1, 145.3, 145.4, 145.8 ppm.

HRMS (EI) calcd. for $C_{36}H_{50}N_3$ [M-2H_2+H^+]: 524.3999, found: 524.3975.

4.9.4. Further modifications.

4.9.4.1. Guanidine introduction and synthesis of **Ter.17-18**.

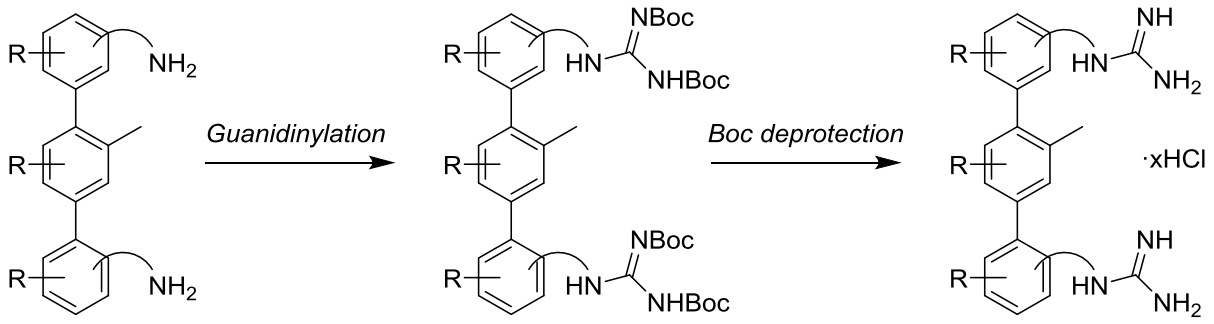

Guanidinylation. The corresponding amine hydrochloride salt (1 equiv) was suspended in anhydrous DCM (0.1 M) and dissolved with the minimum amount of anhydrous methanol. Triethylamine (1.5 equivalents for each amine) was added, followed by Goodman's reagent (1.5 equivalents for each amine). The mixture was stirred at room temperature for 16 hours, after which time water was added and the mixture transferred to a separating funnel. The organic phase was washed consecutively with water, saturated sodium bicarbonate solution and brine. The resulting organic phase was dried over anhydrous sodium sulphate, filtered and concentrated. The crude mixture was purified *via* flash column chromatography using mixtures of *n*-hexane and ethyl acetate as the eluent.

Boc deprotection (Version 1). The Boc-protected terphenyl was dissolved in an aqueous solution containing HCl (4N in water: 4N in 1,4-dioxane, 1:1, 0.05 M) and stirred for 16h at 40 °C. After this time, the mixture was cooled to room temperature and concentrated to dryness. The resulting residue was dissolved in the minimum amount of methanol and precipitated by adding diethyl ether. The supernatant was then decanted off to leave the pure products. No further purification was necessary.

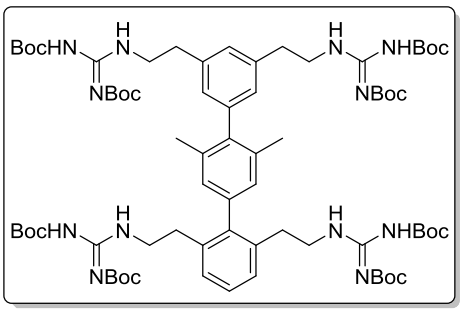

2,2',2'',2'''-(3',5'-Dimethyl-[1,1':4',1''-terphenyl]-2,3'',5'',6-tetrayl)tetrakis(ethan-1-di[*tert*-butyloxycarbonyl]guanidine), 4.59a

Ter.9 was subject to the previously described procedure for guanidinylation. The crude mixture was purified *via* flash column chromatography using mixtures of *n*-hexane:ethyl acetate (7:1) as the eluent, affording pure **4.59a** as a dense colourless oil (98 mg, 65%).

^{1}H NMR ($CDCl_3$, 300 MHz): δ 1.43-1.49 (m, 72H), 2.03 (s, 6H), 2.65 (t, *J*= 7.1 Hz, 4H), 2.90 (t, *J*= 6.7 Hz, 4H), 3.51 (dd, *J*= 11.6, 6.7 Hz, 4H), 3.74 (dd, *J*= 11.6, 6.4 Hz, 4H), 6.86 (s, 2H), 6.99 (d, *J*= 1.4 Hz, 2H), 7.09 (s, 1H), 7.18-7.29 (m, 4H), 8.20 (br s, 2H), 8.42 (br s, 2H) ppm.

^{13}C NMR ($CDCl_3$, 75.5 MHz): δ 21.0, 27.8, 28.0, 28.1, 28.3, 32.7, 35.2, 41.8, 42.2, 79.1, 127.4, 127.5, 127.6, 128.0, 128.1, 136.0, 136.9, 137.9, 139.1, 140.4, 141.7, 142.2, 153.0, 153.1, 156.0, 156.2, 163.5 ppm.

HRMS (EI) calcd. for $C_{72}H_{112}N_{12}O_{16}$ [M+2H$^+$]: 700.4154, found: 700.4175.

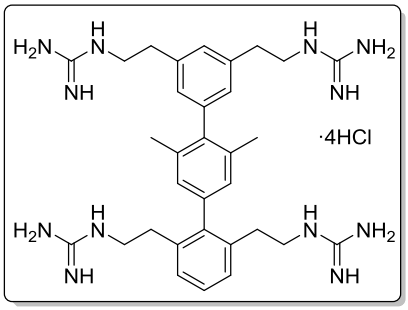

2,2',2'',2'''-(3',5'-Dimethyl-[1,1':4',1''-terphenyl]-2,3'',5'',6-tetrayl)tetrakis(ethan-1-guanidine) hydrochloride salt, Ter.17

4.59a was subject to the previously described procedure for Boc deprotection, affording pure **Ter.17** as a hygroscopic, dense, colourless oil (32 mg, 65%).

^{1}H NMR (CD_3OD, 300 MHz): δ 2.10 (s, 6H), 2.71 (t, *J*= 7.2 Hz, 4H), 2.98 (t, *J*= 6.8 Hz, 4H), 3.29 (t, *J*= 7.0 Hz, 4H), 3.57 (t, *J*= 6.8 Hz, 4H), 6.98 (s, 2H), 7.07 (s, 2H), 7.25-7.40 (m, 5H), 7.51 (t, *J*= 5.5 Hz, 1H) ppm.

^{13}C NMR (CD_3OD, 75.5 MHz): δ 19.9 (CH_3), 32.4 (CH_2), 34.6 (CH_2), 42.0 (CH_2), 42.5 (CH_2), 127.5 (CH), 127.6 (CH), 128.0 (CH), 128.1 (CH), 136.2 (C), 136.3 (C), 138.0 (C), 138.9 (C), 140.8 (C), 141.2 (C), 142.3 (C), 157.0 (C), 157.1 (C), 157.2 (C), 157.3 (C) ppm.

HRMS (EI) calcd. for $C_{32}H_{48}N_{12}$ [M+2H$^+$]: 300.2057, found: 300.2063.

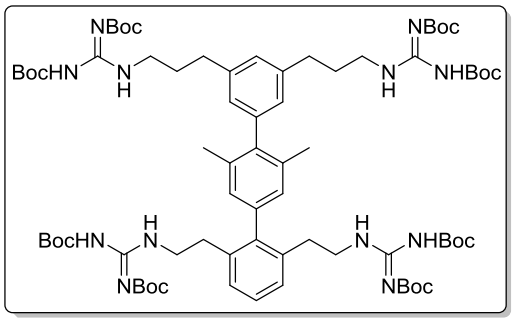

3,3'-(2'',6''-Bis(2-di[*tert*-butyloxycarbonyl]guanidinoethyl)-2',6'-dimethyl-[1,1':4',1''-terphenyl]-3,5-diyl)bis(propan-1-di[*tert*-butyloxycarbonyl]guanidine), 4.59b

Ter.12 was subject to the previously described procedure for guanidinylation. The crude mixture was purified *via* flash column chromatography using mixtures of *n*-hexane:ethyl acetate (7:1) as the eluent, affording pure **4.59b** as a dense colourless oil (61 mg, 71%).

^{1}H NMR ($CDCl_3$, 300 MHz): δ 1.42-1.52 (m, 72H), 1.90-2.10 (m, 10H), 2.61-2.74 (m, 8H), 3.44-3.57 (m, 8H), 6.87 (s, 2H), 6.91 (d, *J*= 1.3 Hz, 2H), 7.00 (s, 1H), 7.18-7.29 (m, 3H), 8.19 (t, *J*= 4.3 Hz, 2H), 8.39 (t, *J*= 4.9 Hz, 2H) ppm.

^{13}C NMR ($CDCl_3$, 75.5 MHz): δ 21.1, 28.1, 28.3, 30.7, 32.7, 40.6, 41.8, 53.4, 79.1, 79.3, 82.9, 83.1, 126.7, 126.9, 127.3, 127.5, 128.1, 135.9, 136.9, 137.8, 140.6, 141.2, 141.4, 142.2, 153.1, 153.3, 156.0, 156.2, 163.5, 163.6 ppm.

HRMS (EI) calcd. for $C_{74}H_{116}N_{12}O_{16}$ [M+2H$^+$]: 714.4311, found: 714.4314.

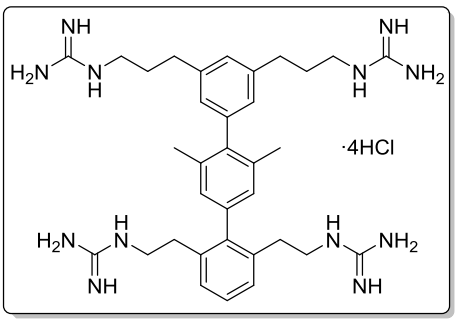

3,3'-(2'',6''-Bis(2-guanidinoethyl)-2',6'-dimethyl-[1,1':4',1''-terphenyl]-3,5-diyl)bis(propan-1-guanidine), Ter.18

4.59b was subject to the previously described procedure for Boc deprotection, affording pure **Ter.18** as a hygroscopic, dense, colourless oil (18 mg, 59%).

^{1}H NMR (CD_3OD, 300 MHz): δ 1.91-2.04 (m, 4H), 2.09 (s, 6H), 2.67-2.83 (m, 8H), 3.21-3.33 (m, 8H), 6.98 (s, 4H), 7.16 (s, 1H), 7.27-7.38 (m, 3H) ppm.

^{13}C NMR (CD_3OD, 75.5 MHz): δ 19.9 (CH_3), 30.4 (CH_2), 32.2 (CH_2), 32.4 (CH_2), 40.6 (CH_2), 41.9 (CH_2), 126.8 (CH), 126.9 (CH), 127.5 (CH), 127.6 (CH), 128.1 (CH), 136.2 (C), 136.3 (C), 137.9 (C), 140.9 (C), 141.1 (C), 141.7 (C), 142.3 (C), 157.1 (C), 157.3 (C) ppm.

HRMS (EI) calcd. for $C_{34}H_{52}N_{12}$ [M+2H$^+$]: 314.2213, found: 314.2220.

*4.9.4.2. Intermediates towards **Ter.19**.*

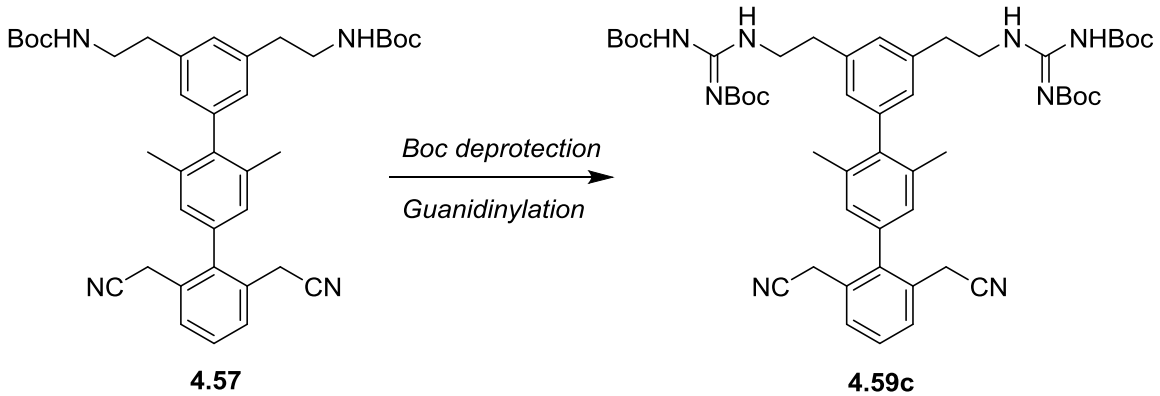

Boc deprotection (Version 2). Previously synthesised **4.57** (62 mg, 0.1 mmol) was dissolved in anhydrous DCM (4 ml) and trifluoroacetic acid (1 ml) was added slowly at room temperature. The

resulting mixture was stirred for 16h and, following this, the mixture was basified with saturated sodium bicarbonate solution, diluted with DCM (5 ml) and transferred to a separating funnel. The mixture was washed consecutively with saturated sodium bicarbonate solution (3 x 5 ml), and brine (5 ml). The organic phase was then dried over anhydrous sodium sulphate, filtered and concentrated to dryness. The residue was then used directly in the next step without further purification.

Guanidinylation. The crude product of the previous deprotection was subjected to the aforementioned guanidinylation conditions (*see Guanidinylation, Section 4.9.4.1*).

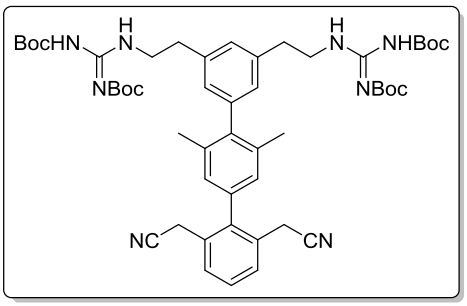

2,2'-(3'',5''-Bis(2-guanidinoethyl)-3',5'-dimethyl-[1,1':4',1''-terphenyl]-2,6-diyl)diacetonitrile, 4.59c

The crude mixture was purified *via* flash column chromatography using mixtures of *n*-hexane:EtOAc (5:1) as the eluent, affording **4.59c** as a white solid (50 mg, 55% from **4.57**). An unknown impurity was observed upon characterisation of this compound, and unfortunately we were unable to obtain an acceptable ^{13}C spectrum.

^{1}H NMR ($CDCl_3$, 300 MHz): δ 1.35-1.53 (m, 36H), 1.95-2.12 (m, 6H), 2.85-3.10 (m, 4H), 3.48-3.56 (m, 4H), 3.70-3.95 (m, 4H), 6.82-7.01 (m, 4H), 7.48-7.63 (m, 4H) ppm.

HRMS (EI) calcd. for $C_{50}H_{67}N_8O_8$ [M+H$^+$]: 907.5076, found: 907.5061.

4.9.4.3. Intermediates towards **Ter.20**.

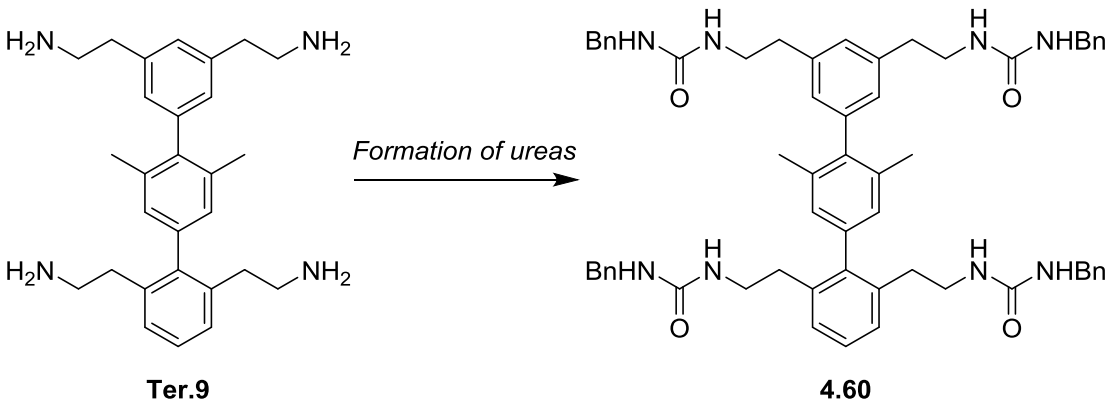

Ter.9 **4.60**

Ter.9 (25 mg, 0.06 mmol) was suspended in anhydrous DCM (3 ml) and benzyl isocyanate (0.08 ml, 0.6 mmol) was added at room temperature. The mixture was stirred for 16 hours at room temperature and after this time the solvent was decanted away, washing twice with methanol (2 x 3 ml). The resulting solid (44 mg, 77%) was difficult to handle and was insoluble in most common solvents, although we found it was slightly soluble in DMSO. For this reason, only the most characteristic NMR signals are listed below.

^{1}H NMR (DMSO-d_6, 300 MHz): δ 1.98 (s, 6H), 2.35-2.49 (m, 4H), 2.61-2.79 (m, 4H), 3.04-3.17 (m, 4H), 3.20-3.35 (m, 4H), 4.09-4.24 (m, 8H), 5.85 (t, *J*= 6.0 Hz, 1H), 5.97 (t, *J*= 6.0 Hz, 1H), 6.28 (t, *J*= 6.2 Hz, 1H), 6.42 (t, *J*= 6.2 Hz, 1H), 6.88 (d, *J*= 12.0 Hz, 4H), 7.04 (s, 1H), 7.10-7.29 (m, 22H) ppm.

HRMS (EI) calcd. for $C_{60}H_{67}N_8O_4$ [M+H$^+$]: 963.5280, found: 963.5298.

4.9.4.4. Synthesis of **Ter.21**.

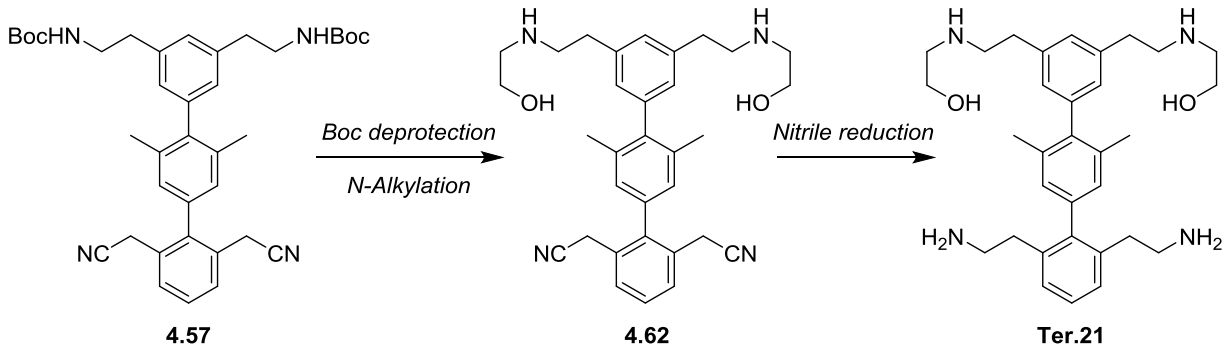

Boc deprotection (Version 2). Terphenyl **4.57** (200 mg, 0.32 mmol) was subjected to the same conditions as described previously for the Boc deprotection (*see Boc deprotection (Version 2), section 4.9.4.2*). The crude product was subject to the next step without further purification.

N-Alkylation. The crude product of the previous step was dissolved in acetonitrile (5 ml) in a sealable reaction vessel, and triethylamine (0.18 ml, 1.24 mmol) and 2-iodoethanol (0.12 ml, 1.6 mmol) were added. The reaction vessel was then sealed and the reaction was heated at 80 °C for 20h. After this time, the reaction was cooled to room temperature and the reaction was neutralised with saturated ammonium chloride solution. The mixture was transferred to a separating funnel and the mixture was extracted with ethyl acetate (2 x 10 ml). The combined organic layers were washed with saturated sodium bicarbonate solution (3 x 5 ml), dried over anhydrous sodium bicarbonate, filtered and concentrated to dryness. Further purification was unnecessary, and the desired **4.62** was obtained as a yellow oil (76 mg, 47% from **4.57**).

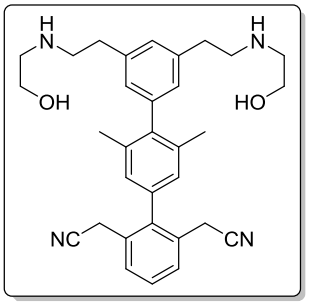

2,2'-(3'',5''-Bis(2-((2-hydroxyethyl)amino)ethyl)-3',5'-dimethyl-[1,1':4',1''-terphenyl]-2,6-diyl)diacetonitrile, 4.62

^{1}H NMR (CD_3OD, 300 MHz): δ 2.10 (s, 6H), 3.04-3.17 (m, 5H), 3.22-3.28 (m, 5H), 3.35-3.44 (m, 3H), 3.62 (s, 4H), 3.82-3.88 (m, 3H), 6.92-7.18 (m, 4H), 7.35-7.59 (m, 4H) ppm.

^{13}C NMR (CD_3OD, 75.5 MHz): δ 19.8, 21.4, 27.6, 31.7, 33.1, 40.5, 49.4, 56.5, 118.0, 127.7, 128.1, 128.4, 128.5, 130.2, 135.7, 136.3, 137.0, 137.7, 137.9, 141.3, 141.5, 141.7, 141.9 ppm.

HRMS (EI) calcd. for $C_{32}H_{39}N_4O_2$ [M+H$^+$]: 511.3068, found: 511.3058.

Nitrile reduction. Hydroxyethylamine derivative **4.62** (51 mg, 0.1 mmol) was subjected to the same conditions as previously described (*see Nitrile reduction, section 4.9.3.2*).

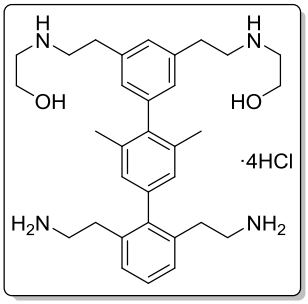

2,2'-(((2'',6''-Bis(2-aminoethyl)-2',6'-dimethyl-[1,1':4',1''-terphenyl]-3,5-diyl)bis(ethane-2,1-diyl))bis(azanediyl))bis(ethan-1-ol), Ter.21

The crude mixture was purified *via* flash column chromatography using mixtures of DCM and ammonia solution (7N in MeOH) (4:1-2:1) as the eluent, affording pure **Ter.21** as a dense yellow oil (18 mg, 35%).

^{1}H NMR (CD_3OD, 300 MHz): δ 2.10 (s, 6H), 2.83 (dd, *J*= 9.9, 5.8 Hz, 4H), 2.99 (dd, *J*= 10.0, 5.8 Hz, 4H), 3.05-3.20 (m, 4H), 3.22-3.30 (m, 6H), 3.35-3.56 (m, 3H), 3.82-3.99 (3H), 7.00 (s, 2H), 7.12 (d, *J*= 7.3 Hz, 2H), 7.30-7.44 (m, 4H) ppm.

^{13}C NMR (CD_3OD, 75.5 MHz): δ 19.9, 31.3, 31.7, 33.0, 40.1, 40.6, 49.4, 56.6, 127.6, 127.9, 128.1, 128.2, 135.3, 136.6, 137.5, 137.7, 137.9, 140.6, 141.8, 142.1 ppm.

HRMS (EI) calcd. for $C_{32}H_{47}N_4O_2$ [M+H$^+$]: 519.3694, found: 519.3686.